DEVELOPMENT OF SYNTHETIC METHODS TO ENABLE THE SYNTHESIS OF PYRROLOIMINOQUINONE ALKALOIDS

Thesis by

Samir Peter Rezgui

In Partial Fulfillment of the Requirements for

the Degree of

Doctor of Philosophy

CALIFORNIA INSTITUTE OF TECHNOLOGY

Pasadena, California

2026

(Defended June 9th, 2025)

© 2025

Samir Rezgui

ORCID: 0000-0003-4080-9835

All Rights Reserved

To my parents and grandparents

ACKNOWLEDGEMENTS

I have had a tremendous amount of support during (and before) my time at Caltech and I am very grateful to all of those who have helped me along the way. First, I need to thank Prof. Brian Stoltz for allowing me to conduct research under his supervision—it has truly been an intellectual journey of a lifetime. Brian is a fantastic chemist whose rigor, creativity, and genuine passion for organic chemistry is contagious, which has been extremely motivating even in times of failure and frustration. Brian has had countless suggestions that have helped overcome many synthetic challenges, while importantly, still allowing us the freedom and creativity to conceive and pursue the ideas we are most excited about; I believe this second point has been the biggest factor for my development as a chemist. However, I believe the defining trait of Brian, something that probably every graduate of this group feels, is his unconditional support and kindness. I've learned just as much about being a good human being as I have about chemistry from Brian Stoltz, and for that, I am forever grateful.

Additionally, I have enjoyed getting to know Brian's family— Erna, Harry, and Teddy, who have always welcomed us with open arms to their home where we've had many excellent group parties. They all share the same kindness as Brian, and I think serve as a "role model" family. It is really special to witness the love that they have for each other.

Next, I would like to thank my committee chair, Prof. Sarah Reisman, for all of her invaluable guidance and support. Sarah takes her role as chair seriously, something that I have truly appreciated, and has offered many insightful suggestions that have helped propel projects forward. For example, during the development of the Larock chemistry, Sarah was kind enough to meet with me one on one several ocassions, and takeaways from

these discussions were instrumental in the reaction investigation process. It has also been a pleasure to get to know Sarah outside of chemistry, and the small instances where Sarah will stop and check in with me speak to her character. I also am grateful for my other committee members, Prof. Bill Goddard and Prof. Greg Fu, who have also been extremely supportive throughout my PhD.

I next need to acknowledge Dr. Scott Virgil. I feel very lucky that I have been able to spend so much time with Scott; I think anyone would agree that he is perhaps the most intelligent person they have personally met. What is more commendable however, is his willingness to drop anything he is doing to offer a helping hand— literally and figuratively. Some of my best memories of graduate school are the hours spent at the prep HPLC with Scott, having countless discussion about chemistry and life in general. He is another person whose passion for organic chemistry is infectious, and it was an absolute pleasure to serve as his TA for the graduate NMR class. I'd also like to thank his wife, Silva Virgil, who is perhaps one of the kindest people I have ever met. The annual Christmas parties at the Virgil household is something I will surely miss.

I of course have to thank the rest of the staff at Caltech, including NMR facility director Dr. David Vander Velde for assistance with a number of NMR experiments, X-Ray crystallography facility director Dr. Mike Takase for his assistance in solving X-Ray structures, former mass spectrometry director Dr. Mona Shagholi for assistance with mass spectrometry data, and Alison Ross, Beth Marshall, Tomomi Kano, Raul Elizarraras, Joe Drew, Greg Rolette, Armando Villasenor, Rebecca Fox, Grace Liang-Franco, Elyse Garlock, and Leslie Corado for administrative and practical support they provide to the CCE division.

This experience has been so wonderful in part due to the people I've shared it with. I have to thank Dr. Zack Sercel who served as my mentor when I joined the lab. Zack is a brilliant chemist and it was a pleasure working alongside him on the aleutianamine project. Zack is also an incredibly genuine and kind person, who has become a good friend. I also have to thank Hao who was another project partner and instrumental in completing the aleutianamine synthesis. Hao is an actual organic chemistry textbook, and I've been lucky to learn so much from him. Also, thanks to Jonathan who has been a great project partner and hood mate, I'm excited to see what he accomplishes. Several of the older students were also influential when I first joined the lab. Dr. Nick Hafeman, my first hood mate, has become a close friend and I have to thank him for everything he has taught me. I also have to thank Dr. Tyler Fulton, again someone who has taught me so much and who later became a good friend. I have to give thanks to Dr. Stephen Sardini Jr. and Dr. Veronica Hubble who were postdocs in the lab for my first three years— they provided countless support and were some of my closest friends. I'll always remember the Caltech Cornhole League. Dr. Chris Cooze was a post doc who joined in my third year, and has become one of my closest friends— thanks for all the good times and rounds of golf buddy. I have to thank Dr. Alex Cusumano, and Dr. Tyler Casselman, all of whom served as role models as well as friends and special thanks to Dr. Alexia Kim who is a close friend. Thanks to Dr. Ally Stanko for your bright personality and infectious positivity, something that was really important during times of frustration, and thanks to Dr. Melinda Chan who holds the same traits and is a close friend. I of course have to thank the rest of my class mates, Dr. Kali Flesh, Elliot Hicks, Jay Barbor, Kevin Gonzalez, Farbod Moghadam, and Adrian Samkian. This experience would not have been the same without their support and close friendship. I am extremely excited to see how

we all end up, and I'm sure we'll all stay in close contanct. Special thanks to Elliot, whom I worked with in the satellite lab in Crellin for close to year— I had a blast over there with you and that experience is something I'll never forget. Also, special thanks to Kali, whom I owe a significant amount of money to for all of therapy sessions, and who will always be close friend. Special thanks to Kevin; our countless conversations about chemistry will be cherished, and I look forward to remaining close when we are both in the bay. The students below us, Christian Strong, Cami Saurez, Marva Tariq, Ruby Chen, Ben Gross, Adrian de Almenara, Chloe Cerione, Bryce Gaskins, Sara Siddiqui, and Eli Gonzalez have also been important in establishing such a positive and welcoming lab culture. Special thanks to Cami who has also become a close friend. Thank you to all of the people in the Reisman lab, especially Simon, Jordan, and Emily, whose friendship I hold dearly. Finally, my support system Caltech outside of the Stoltz group has been extremely important. Enric Adillon, Madeline Hicks, Skylar Osler, and Helena Awad have been some of my best friends over the last five years, and I'm excited that I'll have these people for the rest of my life.

I next need to highlight some individuals at the University of Denver; I went to college to study international business, and without the influential professors and peers I met, I would have never made the switch to organic chemistry. Prof. Alex Huffman served as my academic advisor and my first research mentor; he enlightened me about the possibility of going to graduate school during my freshman year, something that had never crossed my mind. He was a fantastic mentor and support system, and without him I wouldn't have had this experience— thank you. Prof. Balasingmam Murugaverl was my first sophomore organic chemistry professor; his class was the reason I fell in love with organic chemistry, and I am eternally indebted to him for that. Prof, Brian Cowen was also a fantastic organic

chemistry professor and further solidified my decision on pursuing studies this field. I need to give significant thanks to Prof. Brian Michel, who allowed me to join his lab at the end of my sophomore year. Brian pushed me and held high expectations and was instrumental in building my foundation as a researcher, which certainly helped me get into graduate school. I did not even consider applying to Caltech until Brian told me to— for that I thank you. I also have to thank all of my peers/good friends from DU: Mitchell, Max, Andres, and Morgan were lab mates that turned into good friends. Luke, Teddy, Steven, Sam, Will, and Jimmy were great friends whom I spent countless hours with in the library. Myles, Zach, Grace, and Cori were very important people at DU, and I owe them thanks for their friendship.

I of course have to thank all of the people in my life outside of academics. First, thank you to my loving girlfriend Sydney Harvard. Your unconditional love and support over the last two years have helped me finish off graduate school strong. You've also kept me grounded, and helped remind me there are important things in life besides chemistry. I love you deeply, and am beyond excited to start our life together in San Francisco. Also, thanks to Sydney's family, Vanessa, Tracy, Austin, and the other countless family members who have taken me in as their own.

I need to give extreme thanks to my best friends from Colorado: Cody, Matt, Keith, Mario, Romeo, Naose, Ray, and Cody. I've been best friends with these guys since 6th grade, and consider them brothers at this point. The friendship we hold is rare, and I wouldn't have made it through life, let alone graduate school, without all of you. I love you all.

Finally, words can’t describe the gratitude I have to my parents Ali and Leslie, and my grandparents Jim and Jane. Thank you for raising the man I am today. I wouldn’t be where I am without your continued love and support.

ABSTRACT

Natural product total synthesis continues to serve as a driving force for inventions in organic chemistry, and is an essential paradigm in the Stoltz group. The content of this thesis reflects this central objective. Chapter 1 focuses on the total synthesis of aleutianamine— a new pyrroloiminoquinone alkaloid natural product that possesses an unprecedented structure and potent anti-tumor activity. Herein is described a non-biomimetic synthesis that hinges upon the development of a dearomative thiophene arylation to construct the unique [3.3.1] ring system of the natural product. An unconventional ketone installation was then developed to install the alkenyl bromide, and finally, an oxidative amination/thioaminal formation protocol was developed to complete the synthesis. Additionally, a novel Larock/Buchwald–Hartwig annulation/cyclization was developed to access the core of the natural product.

Chapter 2 focuses on leveraging the Larock/Buchwald–Hartwig annulation/cyclization developed en route to aleutianamine to access several pyrroloiminoquinone alkaloids in a divergent manner. This strategy led to the shortest synthetic sequences at the time of four pyrroloiminoquinone alkaloids, and the first synthesis of another.

Chapter 3 describes the progress toward the total synthesis of atkamine, another pyrroloiminoquinone that has yet to be synthesized, by further leveraging of the Larock/Buchwald–Hartwig annulation/cyclization. The development of additional reaction

methodologies were investigated to try and rapidly access the complex bicyclic ring system of this natural product.

Finally, Chapter 4 describes the synthesis of authentic standards to enable investigations of pinene secondary organic aerosols. Access to these standards allowed for the identification and formation mechanism of dimer esters in pinene organic aerosols, which has been a long-standing challenge in the field.

PUBLISHED CONTENT AND CONTRIBUTIONS

1. Yu, H.‡; Zercel, Z. P.‡; Rezgui, S. P.; Farhi, J.; Virgil, S. C.; Stoltz, B. M. Total Synthesis of Aleutianamine. *J. Am. Chem. Soc.* **2023**, *145*, 25533–25537. DOI: 10.1021/jacs.3c10212

   S.P.R participated in conceiving and performing experimental work, data analysis, and manuscript preparation.

2. Rezgui, S. P.; Farhi, J.; Yu, H.; Sercel, S. P.; Virgil, S. C.; Stoltz, B. M. Divergent total syntheses of pyrroloiminoquinone alkaloids enabled by the development of a Larock/Buchwald–Hartwig annulation/cyclization. *Chem. Sci.* **2024**, *15*, 12284–12290. DOI: 10.1039/d4sc02981j.

   S.P.R conceived of and performed experimental work, data analysis, and manuscript preparation.

3. Kenseth, C. M.; Hafeman, N. J.; Rezgui, S. P. Chen, J.; Huang, Y.; Dalleska, N. F.; Kjaergaard, H. G.; Stoltz, B. M.; Seinfeld, J. H.; Wennberg, P. O. Particle-phase accretion forms dimer esters in pinene secondary organic aerosol. *Science* **2023**, *382*, 787–792. DOI: 10.1126/science.adi0857

   S.P.R participated in experimental work, data analysis, and manuscript preparation.

TABLE OF CONTENTS

Dedication iii
Acknowledgements iv
Abstract x
Published Content and Contributions xii
Table of Contents xiii
List of Figures xviii
List of Schemes xxix
List of Tables xxxiv
List of Abbreviations xxxvii

CHAPTER 1 **1**
Total Synthesis of Aleutianamine

1.1 Introduction 1
1.2 Retrosynthetic Analysis 8
1.3 Synthesis of the Simplified Tricycle and the Development of a Novel Dearomative Thiophene Arylation 11
1.4 Synthesis of the Amino Tricycle Enabled by the Development of a Larock/Buchwald–Hartwig Annulation/Cyclization 14
1.5 Attempted Dearomative Thiophene Arylation on the Amino Tricycle 21
1.6 Formation of the Full Ring System of Aleutianamine and Failed Late-Stage Bromination 25
1.7 Completion of the Total Synthesis of Aleutianamine 31
1.8 Preliminary Biological Studies 34
1.9 Conclusion 35

1.10 Experimental Section 36
1.10.1 Materials and Methods 36
1.10.2 Experimental Procedures 38
1.10.3 Comparison of Synthetic Aleutianamine to Published Data 101
1.11 References and Notes 104

APPENDIX 1 **114**
Synthetic Summary for Chapter 1

APPENDIX 2 **117**
Spectra Relevant to Chapter 1

APPENDIX 3 **217**
X-Ray Crystallography Reports Relevant to Chapter 1

APPENDIX 4 **286**
Additional Strategies Toward the Total Synthesis of Aleutianamine

A4.1 Introduction 286
A4.2 Alternative Protecting Groups on the Amino Tricycle System 286
A4.3 Failed Advancement of *N*-Ac Thioimidate **74** 289
A4.4 Attempted Development of an Intramolecular Dearomative 2,5-Difunctionalization of Thiophenene 290
A4.5 Failed Late-Stage Vinyl Bromide Installation Strategies 292
A4.6 Attempted Synthesis of a Thiophene Fragment Containing a Pre-Installed Functional Handle for Alkenyl Bromide Installation 294
A4.7 Preliminary Efforts Toward an Asymmetric Synthesis of Aleutianamine 297
A4.8 References and Notes 301

APPENDIX 4 **302**
Full Investigation of the Larock/Buchwald–Hartwig Annulation/Cyclization

CHAPTER 2 ***305***
Divergent Total Syntheses of Pyrroloiminoquinone Alkaloids Enabled by the Development of a Larock/Buchwald–Hartwig Annulation/Cyclization

2.1 Introduction 305
2.2 Total Synthesis of Makaluvamine C 308
2.3 Total Synthesis of Makaluvamine A 309
2.4 Total Synthesis of Makaluvamine D 309
2.5 Total Synthesis of Isobatzelline B 310
2.6 Total Synthesis of Makaluvamine N 312
2.7 Preliminary Investigation of Biological Activities 313
2.8 Conclusion 314
2.9 Experimental Section 316
2.9.1 Materials and Methods 316
2.9.2 Experimental Procedures 318
2.9.3 Comparison of Synthetic Makaluvamine N to Published Data 332
2.10 References and Notes 334

APPENDIX 6 ***339***
Synthetic Summary for Chapter 2

APPENDIX 7 ***342***
Spectra Relevant to Chapter 2

CHAPTER 3 ***367***
Progress Toward the Total Synthesis of Atkamine

3.1 Introduction 367
3.2 1st Generation Retrosynthetic Analysis 369

3.3 Failed Synthesis of the Dearomative Cyclization Substrate..... 372

3.4 Design of the Modified Dearomative Cyclization Substrate 373

3.5 Synthesis of the Modified Dearomative Cyclization Substrate and Failed Dearomative Cyclization.....378

3.6 Experimental Section.....676

3.6.1 Materials and Methods.....378

3.5.2 Experimental Procedures.....380

3.7 References and Notes.....391

APPENDIX 8 ***393***

Spectra Relevant to Chapter 3

APPENDIX 9 ***404***

Additional Investigations Into the Dearomative Furan Coupling

A9.1 Introduction 404

A9.2 Synthesis and Investigation of Model System **291** 404

A9.3 Synthesis and Investigation of Model System **298** 406

A9.4 Progress Toward the Fully Substituted Larock/Dearomative Furan Coupling Substrate.....408

A9.5 References and Notes.....410

APPENDIX 10 ***411***

Additional Strategies and Tactics Toward the Total Synthesis of Atkamine

A10.1 Introduction 411

A10.2 Ring-Closing Metathesis Strategy.....411

A10.3 [3+2] Dipolar Cycloaddition Strategy.....416

A10.4 References and Notes.....421

CHAPTER 4 ***423***

Synthesis of Authentic Standards to Enable Investigations of Pinene Secondary Organic Aerosols

4.1 Introduction 423

4.2 Synthesis of Primary Dimer Esters.....425

4.3 Synthesis of Secondary Dimer Esters 427

4.4 Determination of Dimer Ester Structures in Pinene Secondary Organic Aerosol 428

4.5 Formation Mechanism of Dimer Esters.....429

4.6 Conclusion.....433

4.7 Experimental Section.....434

4.7.1 Materials and Methods.....434

4.7.2 Experimental Procedures.....435

4.8 References and Notes.....466

APPENDIX 11 ***470***

Spectra Relevant to Chapter 4

ABOUT THE AUTHOR ***507***

LIST OF FIGURES

CHAPTER 1
Total Synthesis of Aleutianamine

Figure 1.1.1 Pyrroloiminoquinone Alkaloids.....1

Figure 1.1.2 Aleutianamine (**15**).....4

Figure 1.8.1 Preliminary biological studies 35

Figure 1.10.2.1 Preliminary X-Ray Structure of benzoaxazole **109** 75

APPENDIX 2
Spectra Relevant to Chapter 1

Figure A2.1 ^{1}HNMR (400MHz, $CDCl_3$) of compound **62**.....119

Figure A2.2 Infrared spectrum (Thin Film, NaCl) of compound **62**.....120

Figure A2.3 ^{13}CNMR (100MHz, $CDCl_3$) of compound **62**.....120

Figure A2.4 ^{1}HNMR (400MHz, $CDCl_3$) of compound **63**.....121

Figure A2.5 Infrared spectrum (Thin Film, NaCl) of compound **63**.....122

Figure A2.6 ^{13}CNMR (100MHz, $CDCl_3$) of compound **63**.....122

Figure A2.7 ^{1}HNMR (400MHz, $CDCl_3$) of compound **64**.....123

Figure A2.8 Infrared spectrum (Thin Film, NaCl) of compound **64**.....124

Figure A2.9 ^{13}CNMR (100MHz, $CDCl_3$) of compound **64**.....124

Figure A2.10 ^{1}HNMR (400MHz, $CDCl_3$) of compound **65**.....125

Figure A2.11 Infrared spectrum (Thin Film, NaCl) of compound **65**.....126

Figure A2.12 ^{13}CNMR (100MHz, $CDCl_3$) of compound **65**.....126

Figure A2.13 ^{1}HNMR (400MHz, $CDCl_3$) of compound **66**.....127

Figure A2.14 Infrared spectrum (Thin Film, NaCl) of compound **66**.....128

Figure A2.15 ^{13}CNMR (100MHz, $CDCl_3$) of compound **66**.....128

Figure A2.16 ^{1}HNMR (400MHz, DMSO) of compound **69** 129
Figure A2.17 Infrared spectrum (Thin Film, NaCl) of compound **69** 130
Figure A2.18 ^{13}CNMR (100MHz, DMSO) of compound **69** 130
Figure A2.19 ^{1}HNMR (400MHz, C_6D_6) of compound **70** 131
Figure A2.20 Infrared spectrum (Thin Film, NaCl) of compound **70** 132
Figure A2.21 ^{13}CNMR (100MHz, C_6D_6) of compound **70** 132
Figure A2.22 ^{1}HNMR (400MHz, C_6D_6) of compound **73** 133
Figure A2.23 Infrared spectrum (Thin Film, NaCl) of compound **73** 134
Figure A2.24 ^{13}CNMR (100MHz, C_6D_6) of compound **73** 134
Figure A2.25 ^{1}HNMR (400MHz, C_6D_6) of compound **74** 135
Figure A2.26 Infrared spectrum (Thin Film, NaCl) of compound **74** 136
Figure A2.27 ^{13}CNMR (100MHz, C_6D_6) of compound **74** 136
Figure A2.28 ^{1}HNMR (400MHz, $CDCl_3$) of compound **83** 137
Figure A2.29 Infrared spectrum (Thin Film, NaCl) of compound **83** 138
Figure A2.30 ^{13}CNMR (100MHz, $CDCl_3$) of compound **83** 138
Figure A2.31 ^{1}HNMR (400MHz, $CDCl_3$) of compound **84** 139
Figure A2.32 Infrared spectrum (Thin Film, NaCl) of compound **84** 140
Figure A2.33 ^{13}CNMR (100MHz, $CDCl_3$) of compound **84** 140
Figure A2.34 ^{1}HNMR (400MHz, $CDCl_3$) of compound **85** 141
Figure A2.35 Infrared spectrum (Thin Film, NaCl) of compound **85** 142
Figure A2.36 ^{13}CNMR (100MHz, DMSO) of compound **85** 142
Figure A2.37 ^{1}HNMR (400MHz, DMSO) of compound **86** 143
Figure A2.38 Infrared spectrum (Thin Film, NaCl) of compound **86** 144
Figure A2.39 ^{13}CNMR (100MHz, DMSO) of compound **86** 144
Figure A2.40 ^{1}HNMR (400MHz, $CDCl_3$) of compound **89** 145
Figure A2.41 Infrared spectrum (Thin Film, NaCl) of compound **89** 146
Figure A2.42 ^{13}CNMR (100MHz, $CDCl_3$) of compound **89** 146
Figure A2.43 ^{1}HNMR (400MHz, MeOD) of compound **90** 147

Figure A2.44 Infrared spectrum (Thin Film, NaCl) of compound **90**..... 148
Figure A2.45 ^{13}CNMR (100MHz, MeOD) of compound **90** 148
Figure A2.46 ^{1}HNMR (400MHz, DMSO) of compound **91** 149
Figure A2.47 Infrared spectrum (Thin Film, NaCl) of compound **91**.....150
Figure A2.48 ^{13}CNMR (100MHz, DMSO) of compound **91** 150
Figure A2.49 ^{1}HNMR (400MHz, $CDCl_3$) of compound **151** 151
Figure A2.50 Infrared spectrum (Thin Film, NaCl) of compound 1**51**.....152
Figure A2.51 ^{13}CNMR (100MHz, $CDCl_3$) of compound **151** 152
Figure A2.52 ^{1}HNMR (400MHz, $CDCl_3$) of compound **153** 153
Figure A2.53 Infrared spectrum (Thin Film, NaCl) of compound 1**53**.....154
Figure A2.54 ^{13}CNMR (100MHz, $CDCl_3$) of compound **153** 154
Figure A2.55 ^{1}HNMR (400MHz, MeOD) of compound **154**.....155
Figure A2.56 Infrared spectrum (Thin Film, NaCl) of compound 1**54**.....156
Figure A2.57 ^{13}CNMR (100MHz, MeOD) of compound **154** 156
Figure A2.58 ^{1}HNMR (400MHz, $CDCl_3$) of compound **92** 157
Figure A2.59 Infrared spectrum (Thin Film, NaCl) of compound **92**.....158
Figure A2.60 ^{13}CNMR (100MHz, $CDCl_3$) of compound **92** 158
Figure A2.61 ^{1}HNMR (400MHz, $CDCl_3$) of compound **93** 159
Figure A2.62 Infrared spectrum (Thin Film, NaCl) of compound **93**.....160
Figure A2.63 ^{13}CNMR (100MHz, $CDCl_3$) of compound **93** 160
Figure A2.64 ^{1}HNMR (400MHz, MeOD) of compound **94**.....161
Figure A2.65 Infrared spectrum (Thin Film, NaCl) of compound **94**.....162
Figure A2.66 ^{13}CNMR (100MHz, MeOD) of compound **94** 162
Figure A2.67 ^{1}HNMR (400MHz, MeOD) of compound **95** 163
Figure A2.68 Infrared spectrum (Thin Film, NaCl) of compound **95**.....164
Figure A2.69 ^{13}CNMR (100MHz, MeOD) of compound **95** 164
Figure A2.70 ^{1}HNMR (400MHz, $CDCl_3$) of compound **96** 165
Figure A2.71 Infrared spectrum (Thin Film, NaCl) of compound **96**.....166

Figure A2.72 ^{13}CNMR (100MHz, $CDCl_3$) of compound **96** 166
Figure A2.73 ^{1}HNMR (400MHz, MeOD) of compound **97** 167
Figure A2.74 Infrared spectrum (Thin Film, NaCl) of compound **97**.....168
Figure A2.75 ^{13}CNMR (100MHz, MeOD) of compound **97** 168
Figure A2.76 ^{1}HNMR (400MHz, C_6D_6) of compound **98** 169
Figure A2.77 Infrared spectrum (Thin Film, NaCl) of compound **98**.....170
Figure A2.78 ^{13}CNMR (100MHz, C_6D_6) of compound **98**.....170
Figure A2.79 ^{1}HNMR (400MHz, C_6D_6) of compound **100** 171
Figure A2.80 Infrared spectrum (Thin Film, NaCl) of compound **100**.....172
Figure A2.81 ^{13}CNMR (100MHz, C_6D_6) of compound **100**.....172
Figure A2.82 ^{1}HNMR (400MHz, acetone-d6) of compound **102** 173
Figure A2.83 Infrared spectrum (Thin Film, NaCl) of compound **102**.....174
Figure A2.84 ^{13}CNMR (100MHz, acetone-d6) of compound **102**.....174
Figure A2.85 ^{1}HNMR (400MHz, $CDCl_3$) of compound **106** 175
Figure A2.86 Infrared spectrum (Thin Film, NaCl) of compound **106**.....176
Figure A2.87 ^{13}CNMR (100MHz, $CDCl_3$) of compound **106** 176
Figure A2.88 ^{1}HNMR (400MHz, $CDCl_3$) of compound **107** 177
Figure A2.89 Infrared spectrum (Thin Film, NaCl) of compound **107**.....178
Figure A2.90 ^{13}CNMR (100MHz, $CDCl_3$) of compound **107** 178
Figure A2.91 ^{1}HNMR (400MHz, $CDCl_3$) of compound **108** 179
Figure A2.92 Infrared spectrum (Thin Film, NaCl) of compound **108**.....180
Figure A2.93 ^{13}CNMR (100MHz, $CDCl_3$) of compound **108** 180
Figure A2.94 ^{1}HNMR (400MHz, $CDCl_3$) of compound **155** 181
Figure A2.95 Infrared spectrum (Thin Film, NaCl) of compound **155**.....182
Figure A2.96 ^{13}CNMR (100MHz, $CDCl_3$) of compound **155** 182
Figure A2.97 ^{1}HNMR (400MHz, $CDCl_3$) of compound **117** 183
Figure A2.98 Infrared spectrum (Thin Film, NaCl) of compound **117**.....184
Figure A2.99 ^{13}CNMR (100MHz, $CDCl_3$) of compound **117** 184

Figure A2.100 ^{1}HNMR (400MHz, $CDCl_3$) of compound **118** 185
Figure A2.101 Infrared spectrum (Thin Film, NaCl) of compound **118** 186
Figure A2.102 ^{13}CNMR (100MHz, $CDCl_3$) of compound **118**.....186
Figure A2.103 ^{1}HNMR (400MHz, CD_2Cl_2) of compound **114** 187
Figure A2.104 Infrared spectrum (Thin Film, NaCl) of compound **114** 188
Figure A2.105 ^{13}CNMR (100MHz, CD_2Cl_2) of compound **114**.....188
Figure A2.106 ^{1}HNMR (400MHz, $CDCl_3$) of compound **119** 189
Figure A2.107 Infrared spectrum (Thin Film, NaCl) of compound **119** 190
Figure A2.108 ^{13}CNMR (100MHz, $CDCl_3$) of compound **119**.....190
Figure A2.109 ^{1}HNMR (400MHz, C_6D_6) of compound **115**.....191
Figure A2.110 Infrared spectrum (Thin Film, NaCl) of compound **115** 192
Figure A2.111 ^{13}CNMR (100MHz, C_6D_6) of compound **115** 192
Figure A2.112 ^{1}HNMR (400MHz, C_6D_6) of compound **121**.....193
Figure A2.113 Infrared spectrum (Thin Film, NaCl) of compound **121** 194
Figure A2.114 ^{13}CNMR (100MHz, C_6D_6) of compound **121** 194
Figure A2.115 ^{1}HNMR (400MHz, C_6D_6) of compound **122**.....195
Figure A2.116 ^{1}HNMR (400MHz, C_6D_6) of compound **124**.....196
Figure A2.117 ^{1}HNMR (400MHz, C_6D_6) of compound **130**.....197
Figure A2.118 Infrared spectrum (Thin Film, NaCl) of compound **130** 198
Figure A2.119 ^{13}CNMR (100MHz, C_6D_6) of compound **130** 198
Figure A2.120 ^{1}HNMR (400MHz, MeOD) of compound **134** 199
Figure A2.121 Infrared spectrum (Thin Film, NaCl) of compound **134** 200
Figure A2.122 ^{13}CNMR (100MHz, MeOD) of compound **134**.....200
Figure A2.123 ^{1}HNMR (400MHz, MeOD) of compound **147** 201
Figure A2.124 Infrared spectrum (Thin Film, NaCl) of compound **147** 202
Figure A2.125 ^{13}CNMR (100MHz, MeOD) of compound **147**.....202
Figure A2.126 ^{1}HNMR (400MHz, C_6D_6) of compound **137**.....203
Figure A2.127 Infrared spectrum (Thin Film, NaCl) of compound **137** 204

Figure A2.128 ^{13}CNMR (100MHz, C_6D_6) of compound **137** 204
Figure A2.129 ^{1}HNMR (400MHz, CD_2Cl_2) of compound **141** 205
Figure A2.130 Infrared spectrum (Thin Film, NaCl) of compound **141** 206
Figure A2.131 ^{13}CNMR (100MHz, CD_2Cl_2) of compound **141**.....206
Figure A2.131 ^{1}HNMR (400MHz, C_6D_6) of compound **142**.....207
Figure A2.133 Infrared spectrum (Thin Film, NaCl) of compound **142** 208
Figure A2.134 ^{13}CNMR (100MHz, C_6D_6) of compound **142**.....208
Figure A2.135 ^{1}HNMR (400MHz, C_6D_6) of compound **145**.....209
Figure A2.136 Infrared spectrum (Thin Film, NaCl) of compound **145** 210
Figure A2.137 ^{13}CNMR (100MHz, C_6D_6) of compound **145** 210
Figure A2.138 ^{1}HNMR (400MHz, C_6D_6) of compound **135**.....211
Figure A2.139 Infrared spectrum (Thin Film, NaCl) of compound **135** 212
Figure A2.140 ^{13}CNMR (100MHz, C_6D_6) of compound **135** 212
Figure A2.141 ^{1}HNMR (400MHz, C_6D_6) of compound **136**.....213
Figure A2.142 Infrared spectrum (Thin Film, NaCl) of compound **136** 214
Figure A2.143 ^{13}CNMR (100MHz, C_6D_6) of compound **136** 214
Figure A2.144 ^{1}HNMR (400MHz, MeOD) of aleutianamine (**15**) 215
Figure A2.142 Infrared spectrum (Thin Film, NaCl) of aleutianamine (**15**) 216
Figure A2.143 ^{13}CNMR (100MHz, MeOD) of aleutianamine (**15**) 216

APPENDIX 3

X-Ray Crystallography Reports Relevant to Chapter 1

Figure A3.1.1 X-Ray Crystal Structure of *N*-Ac thioimidate **74**.....218
Figure A3.2.1 X-Ray Crystal Structure of *dienone* **130** 242
Figure A3.3.1 X-Ray Crystal Structure of *allylic alcohol* **137**.....268

APPENDIX 4

Additional Strategies Toward the Total Synthesis of Aleutianamine

Figure A4.4.1 Ideal intramolecular dearomative 2,5-difunctionalizaiton 290

CHAPTER 2

Divergent Total Syntheses of Pyrroloiminoquinone Alkaloids Enabled by the Development of a Larock/Buchwald–Hartwig Annulation/Cyclization

Figure 2.1.1 Common synthetic strategy to pyrroloiminoquinone alkaloids.....305

Figure 2.7.1 Preliminary biological activities of simpler pyrroloiminoquinones...314

APPENDIX 7

Spectra Relevant to Chapter 2

Figure A7.1 ^{1}HNMR (400MHz, MeOD) of compound **227** 343

Figure A7.2 Infrared spectrum (Thin Film, NaCl) of compound **227** 344

Figure A7.3 ^{13}CNMR (100MHz, MeOD) of compound **227** 345

Figure A7.4 ^{1}HNMR (400MHz, DMSO) of makaluvamine C (**228**) 345

Figure A7.5 ^{1}HNMR (400MHz, MeOD) of makaluvamine C (**228**) 346

Figure A7.6 Infrared spectrum (Thin Film, NaCl) of makaluvamine C (**228**) 347

Figure A7.7 ^{13}CNMR (100MHz, DMSO) of makaluvamine C (**228**).....347

Figure A7.8 ^{13}CNMR (100MHz, MeOD) of makaluvamine C (**228**).....348

Figure A7.9 ^{1}HNMR (400MHz, MeOD) of compound **229** 349

Figure A7.10 Infrared spectrum (Thin Film, NaCl) of compound **229** 350

Figure A7.11 ^{13}CNMR (100MHz, MeOD) of compound **229** 350

Figure A7.12 ^{1}HNMR (400MHz, DMSO) of makaluvamine A (**230**) 351

Figure A7.13 ^{1}HNMR (400MHz, MeOD) of makaluvamine A (**230**) 352

Figure A7.14 Infrared spectrum (Thin Film, NaCl) of makaluvamine A (**230**) 353

Figure A7.15 ^{13}CNMR (100MHz, DMSO) of makaluvamine A (**230**).....353

Figure A7.16 ^{1}HNMR (400MHz, MeOD) of makaluvamine D (**10**) 354

Figure A7.17 Infrared spectrum (Thin Film, NaCl) of makaluvamine D (**10**).....355

Figure A7.18 ^{13}CNMR (100MHz, MeOD) of makaluvamine D (**10**) 355

Figure A7.19 ^{1}HNMR (400MHz, MeOD) of compound **235** 356

Figure A7.20 Infrared spectrum (Thin Film, NaCl) of compound **235**.....357
Figure A7.21 ^{13}CNMR (100MHz, MeOD) of compound **235** 357
Figure A7.22 ^{1}HNMR (400MHz, 1:1 MeOD:$CDCl_3$) of isobatzelline B (**237**).....358
Figure A7.23 ^{1}HNMR (400MHz, MeOD) of isobatzelline B (**237**).....359
Figure A7.24 Infrared spectrum (Thin Film, NaCl) of isobatzelline B (**237**).....360
Figure A7.25 ^{13}CNMR (100MHz, MeOD) of of isobatzelline B (**237**) 360
Figure A7.26 ^{1}HNMR (400MHz, 1:1 MeOD:$CDCl_3$) of isobatzelline A (**1**).....361
Figure A7.27 Infrared spectrum (Thin Film, NaCl) of isobatzelline A (**1**).....362
Figure A7.28 ^{13}CNMR (100MHz,1:1 MeOD:$CDCl_3$) of isobatzelline A (**1**) 362

CHAPTER 3

Progress Toward the Total Synthesis of Atkamine

Figure 3.1.1 Atkamine (**241**) 367

APPENDIX 8

Spectra Relevant to Chapter 3: Progress Toward the Total Synthesis of Atkamine

Figure A8.1 ^{1}HNMR (400MHz, $CDCl_3$) of compound **263** 394
Figure A8.2 Infrared spectrum (Thin Film, NaCl) of compound **263**.....395
Figure A8.3 ^{13}CNMR (100MHz, $CDCl_3$) of compound **263** 395
Figure A8.4 ^{1}HNMR (400MHz, $CDCl_3$) of compound **265** 396
Figure A8.5 Infrared spectrum (Thin Film, NaCl) of compound **265**.....397
Figure A8.6 ^{13}CNMR (100MHz, $CDCl_3$) of compound **265** 397
Figure A8.7 ^{1}HNMR (400MHz, $CDCl_3$) of compound **281** 398
Figure A8.8 Infrared spectrum (Thin Film, NaCl) of compound **281**.....399
Figure A8.9 ^{13}CNMR (100MHz, $CDCl_3$) of compound **281** 399
Figure A8.10 ^{1}HNMR (400MHz, $CDCl_3$) of compound **284** 400
Figure A8.11 Infrared spectrum (Thin Film, NaCl) of compound **284**.....401

Figure A8.12 ^{13}CNMR (100MHz, $CDCl_3$) of compound **284** 401
Figure A8.13 ^{1}HNMR (400MHz, $CDCl_3$) of compound **285** 402
Figure A8.14 Infrared spectrum (Thin Film, NaCl) of compound **285**.....403
Figure A8.15 ^{13}CNMR (100MHz, $CDCl_3$) of compound **285** 403

CHAPTER 4

Synthesis of Authentic Standards to Enable Investigations of Pinene Secondary Organic Aerosols

Figure 4.1.1 Structure's of secondary dimer esters in pinene SOA remain unknown 424
Figure 4.1.2 Synthetic targets for this study 425
Figure 4.4.1 Dimer ester identification.....429
Figure 4.5.1 Formation of ^{18}O dimer ester IV 431
Figure 4.5.2 Enone **285** and enal **284** ozonolysis experiments 433

APPENDIX 11

Spectra Relevant to Chapter 4

Figure A11.1 ^{1}HNMR (400MHz, $CDCl_3$) of compound **364** 471
Figure A11.2 Infrared spectrum (Thin Film, NaCl) of compound **364**.....472
Figure A11.3 ^{13}CNMR (100MHz, $CDCl_3$) of compound **364** 472
Figure A11.4 ^{1}HNMR (400MHz, $CDCl_3$) of compound **365** 473
Figure A11.5 Infrared spectrum (Thin Film, NaCl) of compound **365**.....474
Figure A11.6 ^{13}CNMR (100MHz, $CDCl_3$) of compound **365** 474
Figure A11.7 ^{1}HNMR (400MHz, $CDCl_3$) of compound **366** 475
Figure A11.8 Infrared spectrum (Thin Film, NaCl) of compound **366**.....476
Figure A11.9 ^{13}CNMR (100MHz, $CDCl_3$) of compound **366** 476
Figure A11.10 ^{1}HNMR (400MHz, $CDCl_3$) of compound **367** 477
Figure A11.11 Infrared spectrum (Thin Film, NaCl) of compound **367**.....478

Figure A11.12 ^{13}CNMR (100MHz, $CDCl_3$) of compound **367** 478
Figure A11.13 ^{1}HNMR (400MHz, $CDCl_3$) of compound **368**.....479
Figure A11.14 Infrared spectrum (Thin Film, NaCl) of compound **368**.....480
Figure A11.15 ^{13}CNMR (100MHz, $CDCl_3$) of compound **368** 480
Figure A11.16 ^{1}HNMR (400MHz, $CDCl_3$) of compound **369**.....481
Figure A11.17 Infrared spectrum (Thin Film, NaCl) of compound **369**.....482
Figure A11.18 ^{13}CNMR (100MHz, $CDCl_3$) of compound **369** 482
Figure A11.19 ^{1}HNMR (400MHz, $CDCl_3$) of compound **370**.....483
Figure A11.20 Infrared spectrum (Thin Film, NaCl) of compound **370**.....484
Figure A11.21 ^{13}CNMR (100MHz, $CDCl_3$) of compound **370** 484
Figure A11.22 ^{1}HNMR (400MHz, $CDCl_3$) of compound **371**.....485
Figure A11.23 Infrared spectrum (Thin Film, NaCl) of compound **371**.....486
Figure A11.24 ^{13}CNMR (100MHz, $CDCl_3$) of compound **371** 486
Figure A11.25 ^{1}HNMR (400MHz, $CDCl_3$) of compound **373**.....487
Figure A11.26 Infrared spectrum (Thin Film, NaCl) of compound **373**.....488
Figure A11.27 ^{13}CNMR (100MHz, $CDCl_3$) of compound **373** 488
Figure A11.28 ^{1}HNMR (400MHz, $CDCl_3$) of compound **374**.....489
Figure A11.29 Infrared spectrum (Thin Film, NaCl) of compound **374**.....490
Figure A11.30 ^{13}CNMR (100MHz, $CDCl_3$) of compound **374** 490
Figure A11.31 ^{1}HNMR (400MHz, $CDCl_3$) of compound **375**.....491
Figure A11.32 Infrared spectrum (Thin Film, NaCl) of compound **375**.....492
Figure A11.33 ^{13}CNMR (100MHz, $CDCl_3$) of compound **375** 492
Figure A11.34 ^{1}HNMR (400MHz, $CDCl_3$) of compound **387**.....493
Figure A11.35 Infrared spectrum (Thin Film, NaCl) of compound **387**.....494
Figure A11.36 ^{13}CNMR (100MHz, $CDCl_3$) of compound **387** 494
Figure A11.37 ^{1}HNMR (400MHz, $CDCl_3$) of compound **360**.....495
Figure A11.38 Infrared spectrum (Thin Film, NaCl) of compound **360**.....496
Figure A11.39 ^{13}CNMR (100MHz, $CDCl_3$) of compound **360** 496

Figure A11.40 ^{1}HNMR (400MHz, $CDCl_3$) of compound **376**..... 497
Figure A11.41 Infrared spectrum (Thin Film, NaCl) of compound **376**.....498
Figure A11.42 ^{13}CNMR (100MHz, $CDCl_3$) of compound **376**.....498
Figure A11.43 ^{1}HNMR (400MHz, $CDCl_3$) of compound **380**.....499
Figure A11.44 Infrared spectrum (Thin Film, NaCl) of compound **380**.....500
Figure A11.45 ^{13}CNMR (100MHz, $CDCl_3$) of compound **380**.....500
Figure A11.46 ^{1}HNMR (400MHz, $CDCl_3$) of compound **381**.....501
Figure A11.47 Infrared spectrum (Thin Film, NaCl) of compound **381**.....502
Figure A11.48 ^{13}CNMR (100MHz, $CDCl_3$) of compound **381**.....502
Figure A11.49 ^{1}HNMR (400MHz, $CDCl_3$) of compound **382**.....503
Figure A11.50 Infrared spectrum (Thin Film, NaCl) of compound **382**.....504
Figure A11.51 ^{13}CNMR (100MHz, $CDCl_3$) of compound **382**.....504
Figure A11.52 ^{1}HNMR (400MHz, $CDCl_3$) of compound **383**.....505
Figure A11.53 Infrared spectrum (Thin Film, NaCl) of compound **383**.....506
Figure A11.54 ^{13}CNMR (100MHz, $CDCl_3$) of compound **383**.....506

LIST OF SCHEMES

CHAPTER 1
Total Synthesis of Aleutianamine

Scheme 1.1.1 Proposed biosynthesis of pyrroloiminoquinone alkaloids.....2
Scheme 1.1.2 Kita's biomimetic synthesis of makaluvamine F (**2**).....3
Scheme 1.1.3 Proposed biosynthesis of aleutianamine (**15**).....5
Scheme 1.1.4 Tokuyama's biomimetic synthesis of aleutianamine (**15**).....6
Scheme 1.1.5 Wood's total synthesis of aleutianamine (**15**) 8
Scheme 1.2.1 Key retrosynthetic disconnections for a non-biomimetic synthesis 9
Scheme 1.2.2 Retrosynthetic analysis of aleutianamine (**15**).....10
Scheme 1.3.1 Synthesis of simplified tricycle **66**.....12
Scheme 1.3.2 Synthesis of aminothiophene **71**.....12
Scheme 1.3.3 Synthesis of dearomative thiophene arylation substrate **72**.....13
Scheme 1.3.4 Successful dearomative thiophene arylation.....13
Scheme 1.3.5 Proposed mechanism of the dearomative thiophene arylation 14
Scheme 1.4.1 Retrosynthetic analysis of amino tricycle **77**.....14
Scheme 1.4.2 Synthesis of the requisite Larock/Buchwald–Hartwig annulation/cyclization substrate **86** and **89** 16
Scheme 1.4.3 Selected substrate scope.....21
Scheme 1.5.1 Full synthetic sequence to amino tricycle **90**.....22
Scheme 1.5.2 Elaboration of amino tricycle **90** and failed reductive amination.....22
Scheme 1.5.3 Failed synthesis of the desired dearomative thiophene arylation substrate 23
Scheme 1.5.4 Failed dearomative thiophene arylation on the amino tricycle system 24

Scheme 1.6.1 Remaining challenges to complete the synthesis of aleutianamine (**15**) 25
Scheme 1.6.2 Failed elaboration of *N*-Ac thioimidate **74** 26
Scheme 1.6.3 Synthesis of *N*-Ts thioimidate **119** 27
Scheme 1.6.4 Failed 1,2 reduction of thiobutenolide **121** 28
Scheme 1.6.5 Failed elaboration of saturated thiobutenolide **115** 29
Scheme 1.6.6 Synthesis of *N*-tosyl des-bromoaleutianamine (**134**) and failed late-stage bromination.....30
Scheme 1.7.1 Alternative strategy for alkenyl bromide installation (**15**) 31
Scheme 1.7.2 Synthesis of allylic alcohol **137** and failed oxidation.....32
Scheme 1.7.3 Successful synthesis of diketone **145** 33
Scheme 1.7.4 Completion of the total synthesis of aleutianamine (**15**) 34

APPENDIX 1

Synthetic Summary for Chapter 1: Total Synthesis of Aleutianamine

Scheme A1.1 Synthesis of tricycle **66**.....115
Scheme A1.2 Synthesis of ketothiophene **116**.....115
Scheme A1.3 Synthesis of *N*-Ts thioimidate **119** 116
Scheme A1.4 Synthesis of aleutianamine (**15**) 117

APPENDIX 4

Additional Strategies Toward the Total Synthesis of Aleutianamine

Scheme A4.2.1 Failed deprotection of *N*-Ac **107** and **108** 287
Scheme A4.2.2 Failed halogenation of arene **160** under standard conditions 288
Scheme A4.2.3 Undesired Bromination of arene **160** 288
Scheme A4.3.1 Failed thioaminal formation from thioimidate **74** 289
Scheme A4.4.1 Failed dearomative 2,5-difunctionalization 291
Scheme A4.5.1 Failed bromination of arene **181** 293

Scheme A4.5.2 Failed hydrolysis of **183** to **145** 293

Scheme A4.6.1 Strategy for pre-installed functional handle for alkenyl bromide installation.....294

Scheme A4.6.2 Failed synthesis of a thiophene fragment containing a nitrile as the functional handle 295

Scheme A4.6.3 Failed synthesis of a thiophene fragment containing a methyl ester as the functional handle 296

Scheme A4.7.1 Failed indium-mediated asymmetric reductive amination 297

Scheme A4.7.2 Failed attempts at the preparation of chiral amine **210**.....298

Scheme A4.7.3 Failed attempts at the preparation of enamine **219**.....300

CHAPTER 2

Divergent Total Syntheses of Pyrroloiminoquinone Alkaloids Enabled by the Development of a Larock/Buchwald–Hartwig Annulation/Cyclization

Scheme 2.1.1 Approaches to common intermediate **220** 307

Scheme 2.1.2 Our divergent strategy to access pyrroloiminoquinones 308

Scheme 2.2.1 Total Synthesis of makaluvamine C (**228**).....308

Scheme 2.3.1 Total Synthesis of makaluvamine A (**230**).....309

Scheme 2.4.1 Total Synthesis of makaluvamine D (**10**) 310

Scheme 2.5.1 Non-selective thiomethylation of tricycle **97** 310

Scheme 2.5.2 Total synthesis of isobatzelline B (**237**).....311

Scheme 2.5.3 Alternative reaction conditions to access isobatzelline B (**237**) 312

Scheme 2.6.1 Failed synthesis of bromoarene **238** 313

Scheme 2.6.2 Total synthesis of makaluvamine N (**240**).....313

Scheme 2.8.1 Vanderwal's improved sequence to common intermediate **13**.....315

Scheme 2.8.2 Vanderwal's divergent synthesis of pyrroloiminoquinones from common intermediate **13** 316

APPENDIX 6

Synthetic Summary for Chapter 2: Divergent Total Syntheses of Pyrroloiminoquinone Alkaloids Enabled by the Development of a Larock/Buchwald–Hartwig Annulation/Cyclization

Scheme A6.1 Synthesis of bromoarene **86** 340

Scheme A6.2 Synthesis of alkyne **89** 340

Scheme A6.3 Divergent synthesis of pyrroloiminoquinone alkaloids 341

CHAPTER 3

Progress Toward the Total Synthesis of Atkamine

Scheme 3.1.1 Zhang's progress toward the total synthesis of atkamine (**241**) 368

Scheme 3.2.1 1st generation retrosynthesis.....370

Scheme 3.2.2 Previous studies on dearomative furan arylations 372

Scheme 3.3.1 Failed synthesis of dearomative substrate **267** 373

Scheme 3.4.1 Design of the modified dearomatization substrate **273**.....374

Scheme 3.5.1 Synthesis of carbamate **276** 376

Scheme 3.5.2 Synthesis of trianiline **281**.....377

Scheme 3.5.3 Failed dearomative furan arylation 378

APPENDIX 9

Additional Investigations Into the Dearomative Furan Coupling

Scheme A9.2.1 Synthesis of model substrate **291**.....405

Scheme A9.3.1 Synthesis of dearomative-Heck substrate **298**.....407

Scheme A9.4.1 Synthesis of fully substituted arene **306**.....409

APPENDIX 10

Additional Strategies and Tactics Toward the Total Synthesis of Atkamine

Scheme A10.2.1 Ring-closing metathesis strategy 412

Scheme A10.2.2 Failed deprotection of amidine **312**..... 413
Scheme A10.2.3 Failed ring closing metathesis of hemiaminal **318**.....414
Scheme A10.2.4 Altered ring-closing metathesis strategy.....414
Scheme A10.2.5 Synthesis of acrylamide **328**.....415
Scheme A10.3.1 [3+2] dipolar cycloaddition strategy.....417
Scheme A10.3.2 Failed [3+2] cycloaddition of hydrazone **334**.....418
Scheme A10.3.3 Successful [3+2] cycloaddition employing hydrazone **336** 419
Scheme A10.3.4 Proposed mechanism of oxindole **338** formation 419
Scheme A10.3.5 Proposed mechanism for the formation of adduct **339** 420
Scheme A10.3.6 Failed [3+2] cycloaddition with benzothiophene-based dipolarophiles 420

CHAPTER 4

Synthesis of Authentic Standards to Enable Investigations of Pinene Secondary Organic Aerosols

Scheme 4.2.1 Retrosynthetic analysis for primary ester dimer target **355**.....426
Scheme 4.2.2 Synthesis of divergent acid **368**.....426
Scheme 4.2.3 Synthesis of dimer esters **369-371** 427
Scheme 4.3.1 Retrosynthetic analysis for secondary ester dimer target **356**.....427
Scheme 4.3.2 Synthesis of secondary dimer esters **373-376** 428
Scheme 4.5.1 Synthesis of ^{18}O labeled OH-pinonic acid (**380**).....430
Scheme 4.5.2 Synthesis of enal **384** and enone **385** 432

LIST OF TABLES

CHAPTER 1
Total Synthesis of Aleutianamine

Table 1.4.1 Investigation of the Larock/Buchwald–Hartwig annulation/cyclization 17
Table 1.4.2 Ligand stoichiometry effects on the tandem transformation.....18
Table 1.4.3 Investigation of the individual steps of the tandem annulation/cyclization process.....20
Table 1.10.3.1 ^{1}H NMR comparison table for aleutianamine (**15**).....101
Table 1.10.3.2 ^{13}C NMR comparison table for aleutianamine (**15**) 102

APPENDIX 3
X-Ray Crystallography Reports Relevant to Chapter 1

Table A3.1.1 Experimental Details 219
Table A3.1.2 Crystal Data of **74**.....220
Table A3.1.3 Atomic Coordinates of **74**.....221
Table A3.1.4 Full Bond Distances and Angles of **74**.....223
Table A3.1.5 Anisotropic Displacement Parameters of **74**.....233
Table A3.1.6 Hydrogen Atomic Coordinates of **74**.....235
Table A3.1.7 Torsion Angles of **74** 237
Table A3.2.1 Experimental Details 243
Table A3.2.2 Crystal Data of **130** 244
Table A3.2.3 Atomic Coordinates of **130** 246
Table A3.2.4 Full Bond Distances and Angles of **130**.....249
Table A3.2.5 Anisotropic Displacement Parameters of **130**.....259
Table A3.2.6 Hydrogen Atomic Coordinates of **130**.....261

Table A3.2.7 Torsion Angles of **130** 263
Table A3.3.1 Experimental Details 269
Table A3.3.2 Crystal Data of **137** 270
Table A3.3.3 Atomic Coordinates of **137** 271
Table A3.3.4 Full Bond Distances and Angles of **137** 273
Table A3.3.5 Anisotropic Displacement Parameters of **137** 279
Table A3.3.6 Hydrogen Atomic Coordinates of **137** 281
Table A3.3.7 Torsion Angles of **137** 282

APPENDIX 4
Additional Strategies Toward the Total Synthesis of Aleutianamine

Table A4.5.1 Failed allylic oxidation of **129** 292

CHAPTER 2
Divergent Total Syntheses of Pyrroloiminoquinone Alkaloids Enabled by the Development of a Larock/Buchwald–Hartwig Annulation/Cyclization

Table 2.9.3.1 ^{1}H NMR comparision table for makaluvamine N (**240**) 332

CHAPTER 3
Progress Toward the Total Synthesis of Atkamine

Table 3.5.1 Investigation of the Buchwald–Hartwig amination of aryl chloride **262** 375

APPENDIX 9
Additional Investigations Into the Dearomative Furan Coupling

Table A9.2.1 Investigation of the dearomative furan coupling on **291**..... 406

Table A9.3.1 Investigation of the dearomative Heck reaction on **298** 408

APPENDIX 10

Additional Strategies and Tactics Toward the Total Synthesis of Atkamine

Table A10.2.1 Preliminary investigation into the ring-closing metathesis of **328** ..416

LIST OF ABBREVIATIONS

$[\alpha]_D$	specific rotation at wavelength of sodium D line
ºC	degrees Celsius
Å	Angstrom
λ	wavelength
μ	micro
Ac	acyl
Aq	aqueous
Ar	aryl
atm	atmosphere
Bn	benzyl
Boc	*tert*-butyloxycarbonyl
bp	boiling point
br	broad
Bz	benzoyl
c	concentration for specific rotation measurements
calc'd	calculated
cm^{-1}	wavenumer(s)
d	doublet
D	deuterium
dba	dibenzylideneacetone
DIBAL	diisobutylaluminum hydride

DMAP	4-dimethylaminopyridine
DMF	*N,N*-dimethylformamide
dr	diastereomeric ratio
D*t*-BPF	1,1'-Bis(di-*tert*-butylphosphino)ferrocene
e.g.	for example (Latin exempli gratia)
ee	enantiomeric excess
EI+	electron impact
equiv	equivalent(s)
ESI	electrospray ionization
Et	ethyl
EtOAc	ethyl acetate
G	grams
GC	gas chromatography
h	hours
HPLC	high-performance liquid chromatography
HRMS	high-resolution mass spectrometry
Hz	hertz
i.e.	that is (Latin id est)
IPA	isopropanol
i-Pr	*iso*-propyl
IR	infrared (spectroscopy)
J	coupling constant (NMR), exchange coupling constant (diradicals)
K	Kelvin (absolute temperature)

kcal	kilocalorie
KHMDS	potassium hexamethyldisilazide
L	liter; ligand
LDA	lithium diisopropylamide
LHMDS	lithium hexamethyldisilazide
M	multiplet, milli, molarity
m/z	mass to charge ratio
m-CPBA	*meta*-chloroperoxybenzoic acid
Me	methyl
MeCN	acetonitrile
MeOH	methanol
mg	milligram(s)
MHz	megahertz
min	minutes
mol	mole(s)
n-Bu	*n*-butyl
NMR	nuclear magnetic resonance
OAc	acetate
Pd/C	palladium on carbon
Ph	phenyl
ppm	parts per million
PTSA	*para*-toluenesulfonic acid
q	quartet

R	generic for any atom or functional groups
S	singlet
SCF	self-consistent field
SFC	supercritical fluid chromatography
t	triplet
TBS	*tert*-butyldimethylsilyl
t-Bu	*tert*-butyl
TES	triethylsilyl
TFA	trifluoroacetic acid
THF	tetrahydrofuran
TLC	thin-layer chromatography
*t*R	retention time
Ts	tosyl
UV	ultraviolet
X	anionic ligand or electronegative element
XPhos	2-Dicyclohexylphosphino-2',4',6'-triisopropylbiphenyl

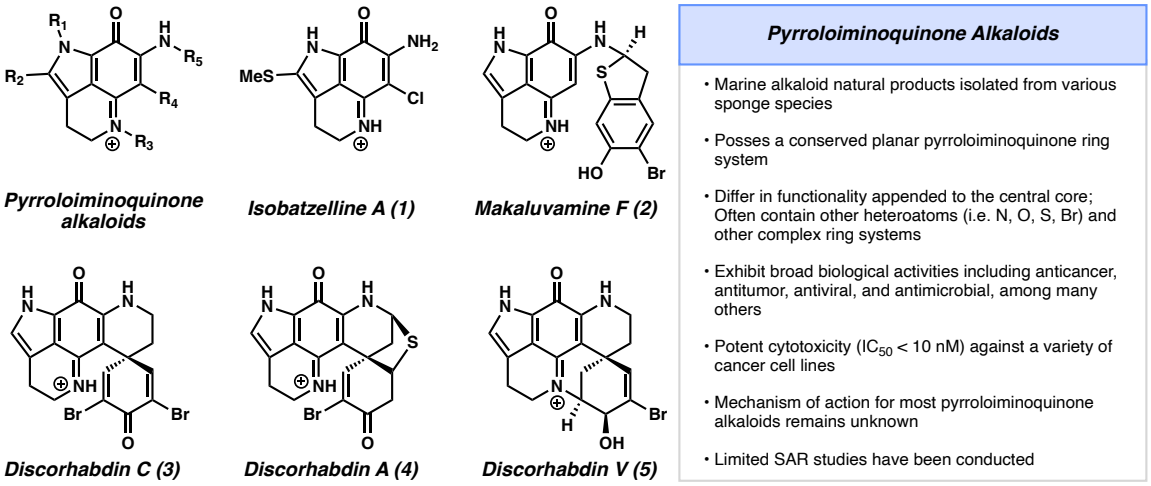
CHAPTER 1

Total Synthesis of Aleutianamine[†]

1.1 INTRODUCTION

Pyrroloiminoquinone alkaloids are a large class of marine sponge- and fungal-derived natural products defined by their conserved pyrrolo[4,3,2-de]quinoline ring system (Figure 1.1.1).[1] Members of the class differ in the functionality appended to this central ring and typically posses other complex ring systems and a variety of heteroatoms, as exemplified by Discorhabdin A (**4**). Efforts to isolate novel pyrroloiminoquinones have

Figure 1.1.1 *Pyrroloiminoquinone Alkaloids.*



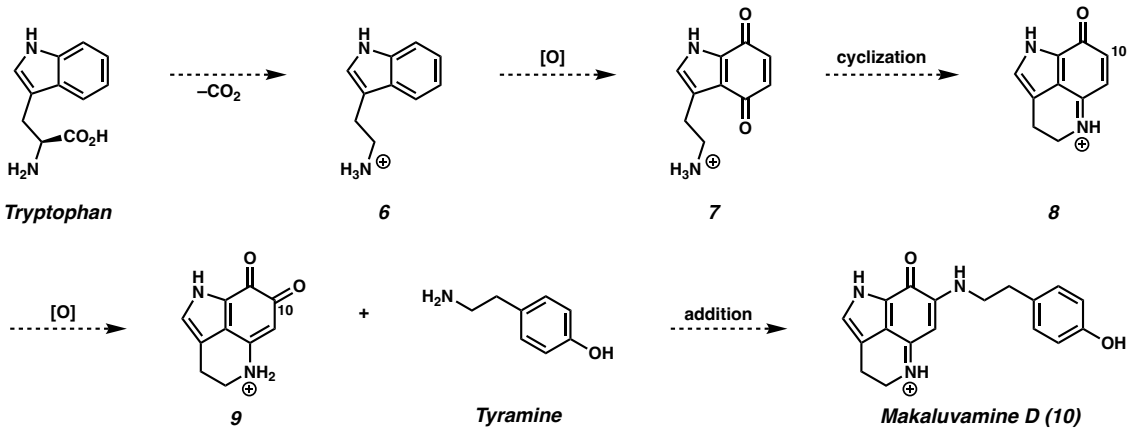
progressed over the last 40 years and have been largely motivated by the fact that these alkaloids display a wide range of biological activities ranging from antiviral, antimicrobial, and immunomodulatory activities.[2] However, most attention has been directed toward their

[†]This research was performed in collaboration with Zachary Sercel, Hao Yu, and Jonathan Farhi. Portions of this chapter are reproduced with permission from Stoltz, et al. *J. Am. Chem. Soc.* **2023**, *145*, 25533–25537; and Stoltz, et al. *Chem. Sci.* **2024**, *15*, 12284–12290.

antitumor activities as several of these alkaloids display significant potency to a variety of human cancer cells, with some members possessing IC_{50} values in the low nanomolar range. Despite significant research efforts, a common mechanism of action for their displayed antitumor activity has remained elusive. For example, members of the makaluvamine subtype (*i.e.* makaluvamine F (**2**)) have been shown to inhibit topoisomerase II in contrast to the discorhabdins (*i.e.* discorhabdin C (**3**)), which do not, despite displaying high potency against tumor cells.[1,2]

Biosynthetically, pyrroloiminoquinones are thought to arise from tryptophan via a decarboxylation and subsequent oxidation of the central arene to provide quinone **7** (Scheme 1.1.1).[3] Cyclization of the tethered amine followed by oxidation at C10 would then yield pyrroloiminoquinone **9** that is thought to be the precursor of most pyrroloiminoquinone natural products. For example, addition of tyramine into the C10 position would yield makaluvamine D (**10**).

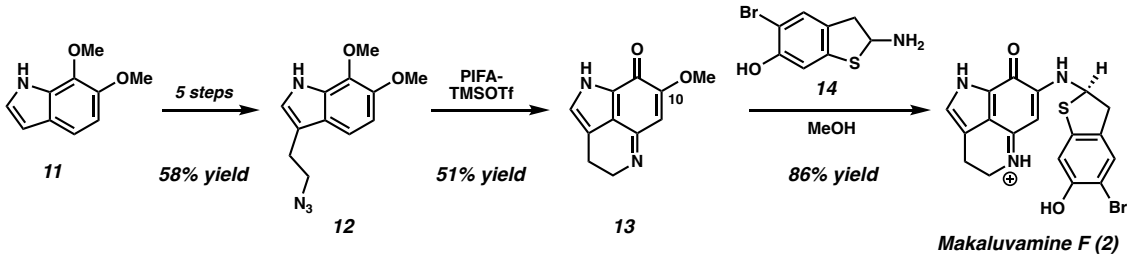
Scheme 1.1.1 *Proposed biosynthesis of pyrroloiminoquinone alkaloids.*



Given their complex molecular frameworks and numerous biological activities, pyrroloiminoquinones have received significant attention from the synthetic community over the last thirty years.[4,5] Apart from a few unique approaches, most syntheses of

pyrroloiminoquinones have employed a biomimetic strategy, as exemplified by Kita's synthesis of makaluvamine F (**2**).[4j] Indole **11** was elaborated to azide **12** over five steps, which was then converted to pyrroloiminoquinone **13** via a PIFA-mediated oxidative cyclization (Scheme 1.1.2). It should be noted that C10 oxygenated pyrroloiminoquinone **13** is a common intermediate employed in a number of other syntheses. Addition of thioaminal **14** (prepared in twelve steps) then yielded makaluvamine F (**2**).

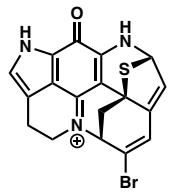
Scheme 1.1.2 *Kita's biomimetic synthesis of makaluvamine F (**2**).*



This overall sequence of oxidative cyclization to form the pyrroloiminoquinone core and subsequent addition of an amine nucleophile parallels the proposed biosynthesis of pyrroloiminoquinone alkaloids. Although commonly employed, biomimetic strategies have been effective in preparing even the most complex members of pyrroloiminoquinone natural products, and despite certain redundancies in strategy design, the arena of pyrroloiminoquinone total synthesis has inspired the development of numerous reaction methodologies.[4j,k,5b]

In 2019, Hamann and coworkers reported the isolation of aleutianamine (**15**, Figure 1.1.2), a novel pyrroloiminoquinone alkaloid, from the sea sponge *Latrunculia (Latrunculia) austini* found off the coast of the Aleutian Islands.[6] This compound was found to possess potent cytotoxicity against several human solid tumor cell lines, with

Figure 1.1.2 *Aleutianamine (**15**).*



Aleutianamine (15)

Aleutianamine

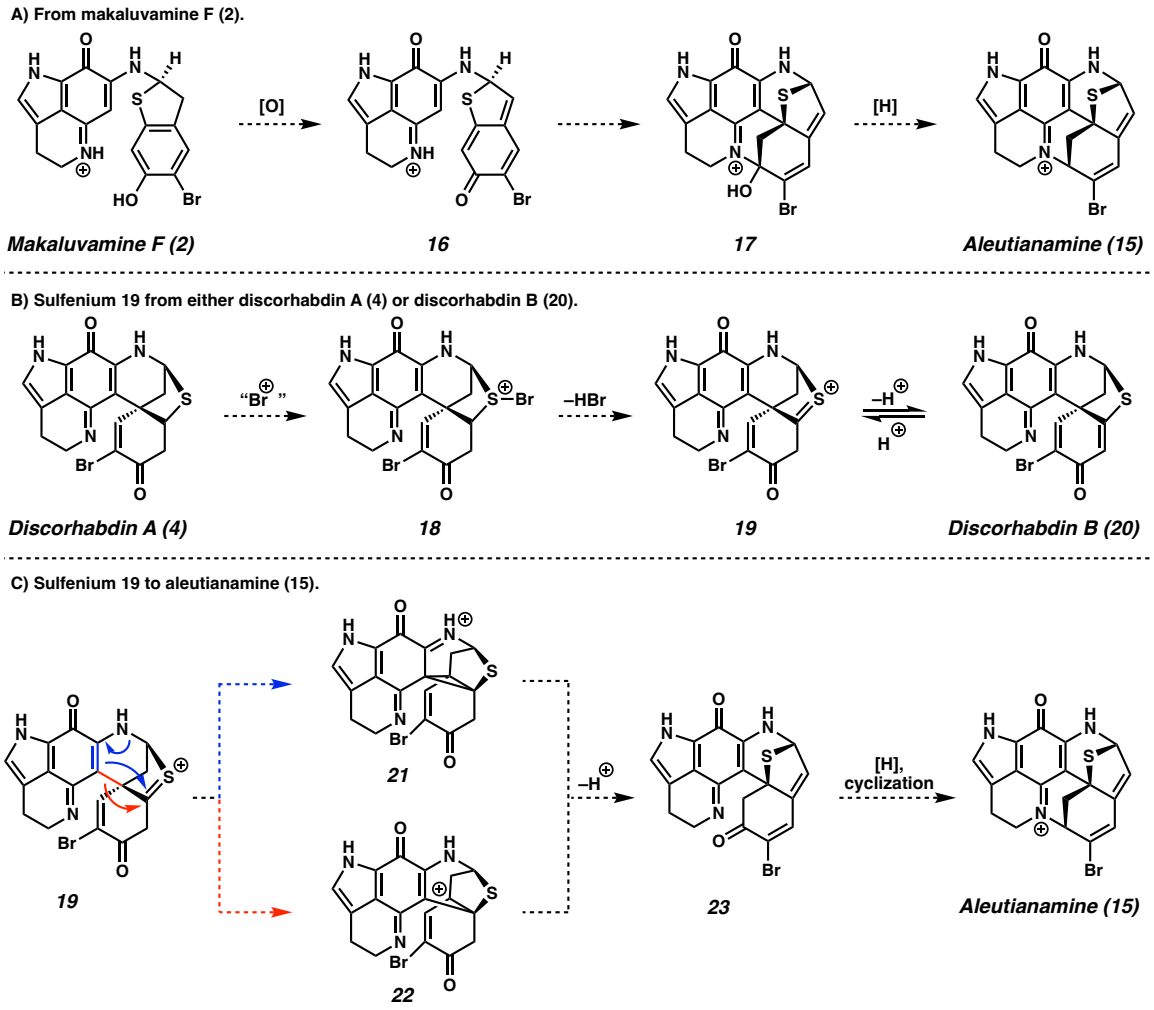
- Isolated from *Latrunculia (Latrunculia) austini*
- Identified using mass spectrometry, NMR spectroscopy, and molecular ion networking (MoIN)
- Structural assignment accomplished via spectroscopic and computational methods
- Contains planar pyrroloiminoquinone core with appended azabicyclo[3.3.1]nonane ring system
- The highly strained bicycle, bridging tertiary sulfide, thioaminal linkage, and alkenyl bromide represent significant synthetic challenges
- Potent and selective cytotoxicity against human PANC-1 pancreatic cancer cells (IC_{50} = 25 nM)

exceptional selectivity for a particular pancreatic cancer cell line (IC_{50} = 25 nM against PANC-1). The structure of aleutianamine (**15**) was elucidated by unusual combinations of spectroscopic and density functional theory methods. Structurally, aleutianamine (**15**) bears the conserved pyrroloiminoquinone moiety but posses some unique structural features such as the fused heptacyclic ring system, a bridging azabicyclo[3.3.1]nonane ring system, another bridging thioaminal linkage, a congested tertiary sulfide, and lone alkenyl bromide, all of which make aleutianamine (**15**) a considerable synthetic challenge. Additionally, the multi-bridged ring system of the natural product bears three stereocenters and is highly strained due to extensive unsaturation. The unusual structure of aleutianamine (**15**), coupled with its potent biological activity, makes this compound an attractive target for a synthetic effort.

Aleutianamine is proposed to biosynthetically arise from one of three related pyrroloiminoquinone alkaloids: makaluvamine F (**2**), discorhabdin A (**4**), or discorhabdin B (**20**). Mechanistically, makaluvamine F (**2**) could undergo oxidation to *p*-quinone methide **16** that could then cyclize to hemiaminal **17** (Scheme 1.1.3A). Reduction would lead to aleutianamine (**15**). Alternatively, either *S*-bromination of discorhabdin A (**4**)

followed by HBr elimination or protonation of discorhabdin B (**20**) would lead to sulfenium intermediate **19** (Scheme 1.1.3B). Then, enamine-like reactivity (blue) would lead to

Scheme 1.1.3 *Proposed biosynthesis of aleutianamine (**15**).*

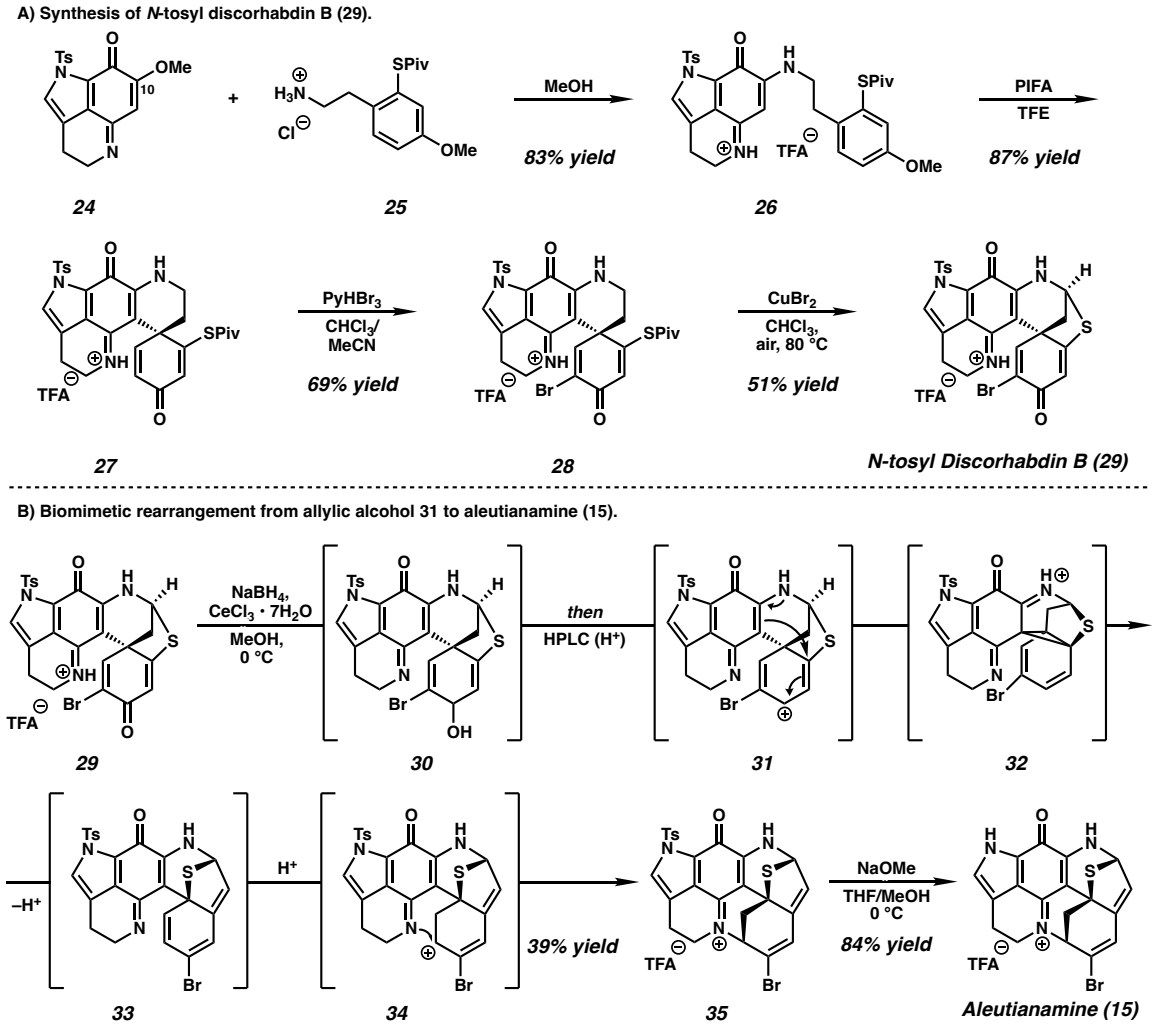


cyclopropane **21**, or a σ-bond shift (red) would afford tertiary carbocation **22** (Scheme 1.1.3C). Both **21** and **22** could undergo an elimination reaction to yield **23**. Finally, a cyclization and reduction would form aleutianamine (**15**).

Throughout the first three years of our synthetic studies toward aleutianamine (**15**) there had been no reported syntheses of the natural product, but this feat was first achieved by Tokuyama and coworkers in 2023 through a biomimetic approach.[7] Briefly,

pyrroloiminoquinone **24** was coupled to tyramine derivative **25** (each prepared in seven steps) that then underwent a PIFA-mediated oxidative spirocyclization to afford pentacycle **27** (Scheme 1.1.4A). A regioselective bromination was then achieved followed by an oxidative thioaminal formation yielding *N*-tosyl discorhabdin B (**29**).

Scheme 1.1.4 *Tokuyama's biomimetic synthesis of aleutianamine (**15**).*

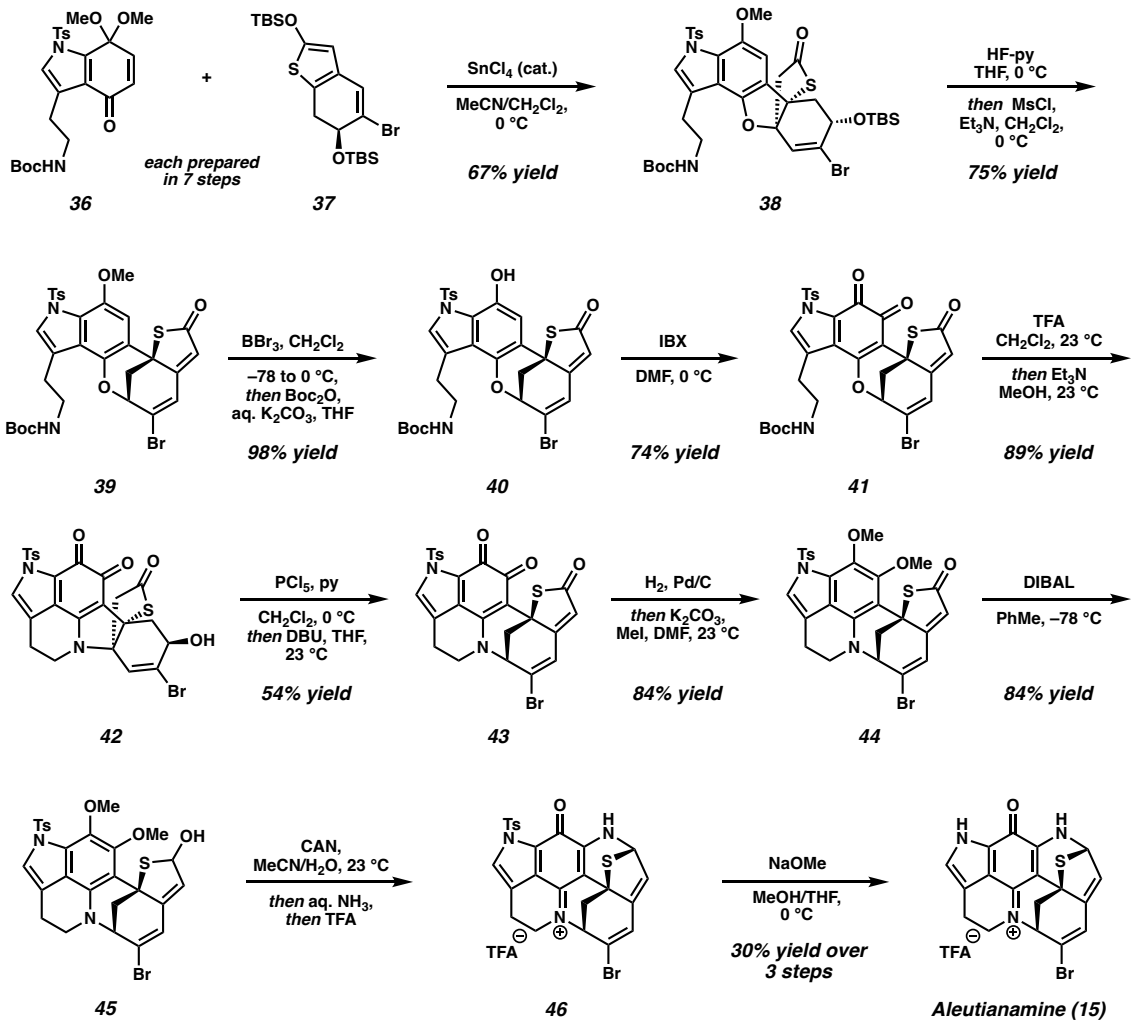


When attempting to access discorhabdin B (**20**) analogs, they observed an unexpected rearrangement: a selective 1,2 reduction of the enone moiety on *N*-tosyl discorhabdin B (**29**) under Luche conditions afforded intermediate allylic alcohol **30** (Scheme 1.1.4B). While attempting to purify **30** via preparatory HPLC using an acidic mobile phase, they

were surprised to isolate *N*-tosyl aleutianamine (**35**) out of the purification. They hypothesize that allylic alcohol **30** undergoes an acid-mediated biomimetic rearrangement to yield the heptacyclic ring system of aleutianamine (**15**, see Scheme 1.1.3). Finally, deprotection of the tosyl group affords aleutianamine (**15**). This elegant synthesis corroborated the proposed biosynthetic pathway and showcased that a biomimetic approach could concisely produce aleutianamine (**15**).

After our synthetic studies were disclosed, Wood and coworkers published a non-biomimetic synthesis of aleutianamine (**15**).[8] Their strategy utilized a convergent coupling approach wherein siloxythiophene **37** underwent an intermolecular vinylogous Mukaiyama-Michael reaction with pyrroloquinone monoketal **36** to form the central C–C bond found in aleutianamine (**15**), which occurred with concomitant intramolecular oxa-Michael addition into the thiobutenolide moiety to provide [4.3.3]-thioaxapropellane **38** (Scheme 1.1.5). Then, they developed a one-step protocol to rearrange the propellane ring system of **38** to **39** that contains the desired [3.3.1] ring system, albeit embedded with an undesired ether linkage. To ablate the ether linkage and access the desired [3.3.1] aza-bicycle, **39** was converted to *o*-quinone **41** via a two-step deprotection/oxidation sequence. Treatment of *o*-quinone **41** with TFA removed the Boc group and subsequent exposure to Et_3N affected an intramolecular substitution and aza-Michael addition furnishing *aza*-propellane **42**. Another rearrangement was achieved via a one-pot chlorination/retro-*aza*-Michael/substitution sequence that provided **43** containing the desired *aza*-[3.3.1] ring system. To complete the synthesis, *o*-quinone **43** was first reduced and methylated to provide anisole **44**. Finally, they implemented our end-game strategy (*vide infra*) consisting of thiobutenolide reduction/oxidative-amination/ring closure/and

Scheme 1.1.5 *Wood's total synthesis of aleutianamine (**15**).*



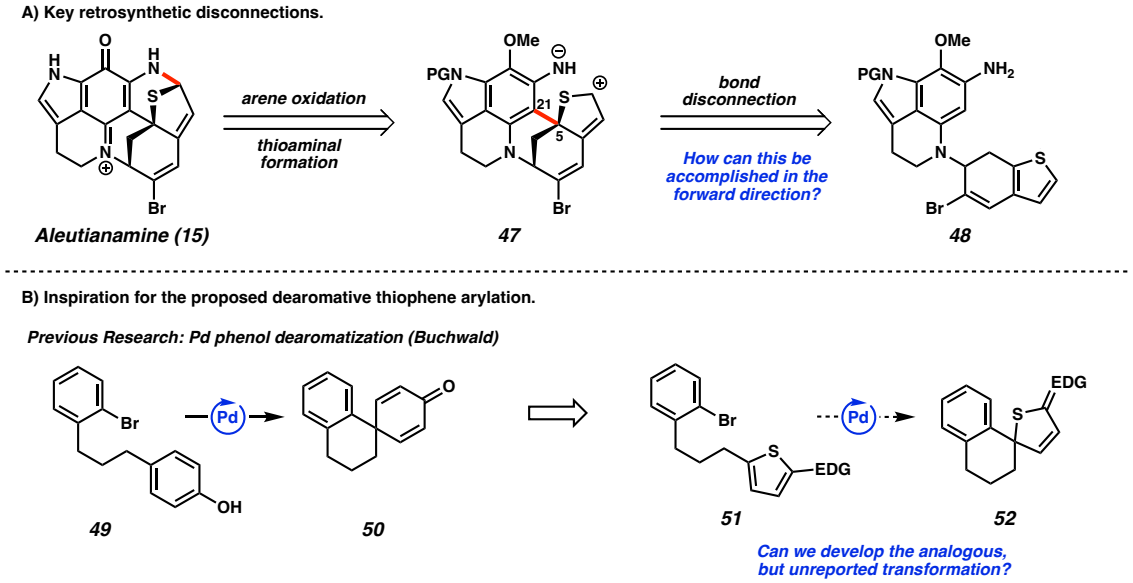
Ts-deprotection to yield aleutianamine **15** in sixteen steps (LLS). The series of intriguing skeletal rearrangements highlight the challenges and unique reactivates associated with the densely functionalized ring system found in aleutianamine **15**, and the overall unique approach employing initial central C–C bond formation adds to the paradigm of pyrroloiminoquinone alkaloid synthesis at large

1.2 RETROSYNTHETIC ANALYSIS

At the onset of our synthetic studies, we were interested in employing a non-biomimetic approach as a it would advance the field of pyrroloiminoquinone synthesis at

large, as well as provide the opportunity for novel methods development. With an abiotic strategy in mind, key disconnections were performed that would inform a full retrosynthetic strategy. The first key disconnection was adjustment of the arene oxidation state to the reduced anisole system (Scheme 1.2.1A). We hypothesized that carrying

Scheme 1.2.1 *Key retrosynthetic disconnections for a non-biomimetic synthesis.*

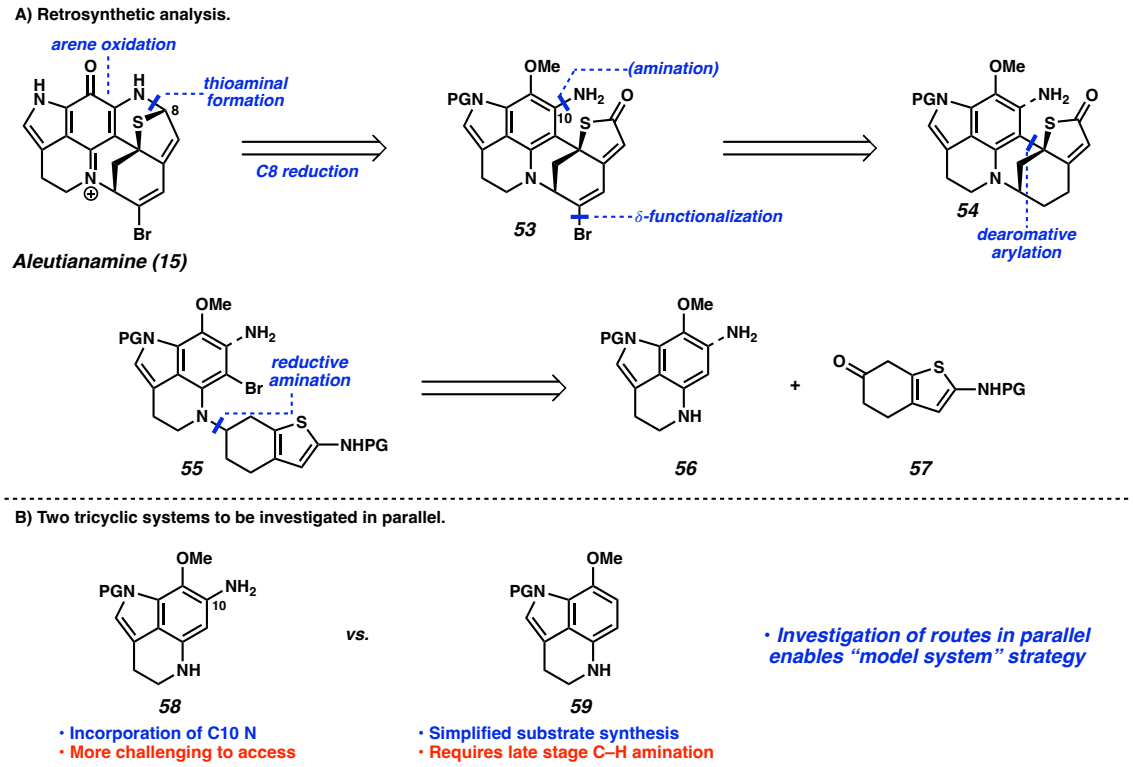


neutral intermediates in the anisole oxidation state through the synthesis would simplify practical aspects, as charged iminoquinone species are notoriously difficult to isolate. Additionally, we envisaged that advanced intermediates bearing the anisole oxidation state would be more amenable for late-stage functionalization to access analogs for future structure-activity relationship studies. The next key disconnection was cleavage of the thioaminal as we hypothesized this motif would likely be labile and difficult to advance through multiple synthetic steps. The final key disconnection was cleavage of the C21-C5 bond (i.e. **47** to **48**). This was viewed as an ideal bond disconnection as it simplified the congested tertiary sulfide and bridging azabicyclic ring system. However, we were unaware of existing synthetic methodology that would accomplish this in the forward

direction. This was viewed as a fantastic opportunity for reaction development and we were inspired by palladium-mediated dearomative phenol arylations reported by Buchwald and coworkers (Scheme 1.2.1B).[9] We wondered if this same type of reactivity could be applied to thiophenes containing an electron-donating group at the C2 position as it would construct the desired C(sp^2)–C(sp^3) bond in addition to forming the tertiary sulfide. With these key disconnections in hand, the following full retrosynthetic analysis was devised.

First, adjustment of the arene oxidation state, cleavage of the thioaminal linkage, and redox manipulation of C8 would lead back to aminoanisole **53** (Scheme 1.2.2).

Scheme 1.2.2 *Retrosynthetic analysis of aleutianamine (**15**).*



Next, we considered disconnecting the C10 nitrogen, but recognized that a late-stage C–H amination could be a challenging tactic to execute in the forward direction, so installation of the C10 nitrogen atom at an earlier stage was also envisaged. At this point the alkenyl bromide was also cleaved, wherein we hypothesized that a δ-functionalization of

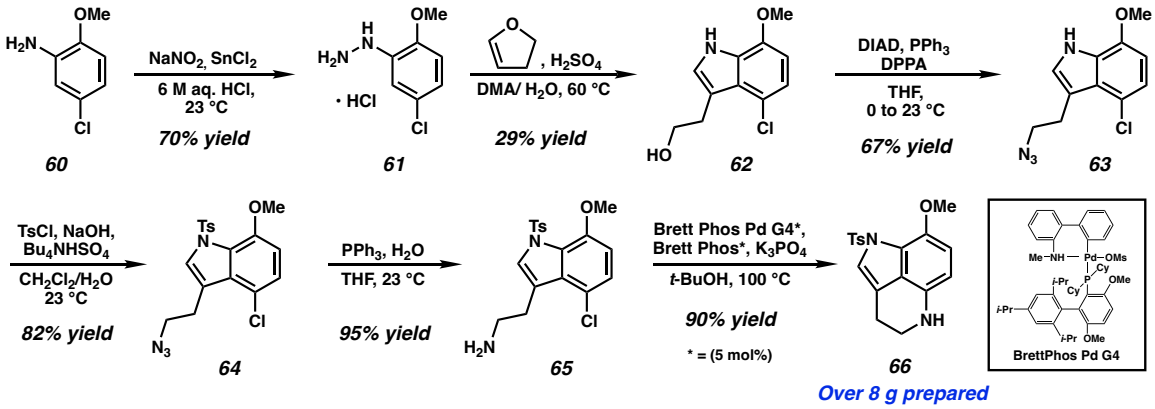
thiobutenolide **54** could serve to install this moiety. From thiobutenolide **54**, disconnection of the central C(sp^2)–C(sp^3) bond would yield aryl bromide **55**; this C–C bond formation could be accomplished via the development of a dearomative thiophene arylation. Finally, cleavage of the C–N bond would reveal two fragments (**56** and **57**) that could be coupled in a convergent fashion.

This leads back to two possible tricyclic coupling partners **58** and **59** that differ by the presence of the C10 nitrogen (Scheme 1.2.2B). Incorporation of the C10 nitrogen atom at an early stage would circumvent the potentially challenging late-stage C–H amination, but it was recognized that **58** would be more challenging to access. The simplified tricyclic substrate **59** would likely be easier to synthesize, but does pose the challenge of a late-stage C–H amination. By investigating both routes in parallel, a "model system" type approach could be employed, wherein the simplified substrate **59** could be quickly accessed to investigate the dearomative thiophene arylation, while simultaneously investigating the synthesis of the amino tricycle **58**. After establishing the dearomative thiophene arylation, it could be applied to **58**. However, in contrast to traditional model systems, simplified tricycle **59** could also potentially be elaborated to aleutianamine (**15**).

1.3 SYNTHESIS OF THE SIMPLIFIED TRICYCLE AND THE DEVELOPMENT OF A NOVEL DEAROMATIVE THIOPHENE ARYLATION

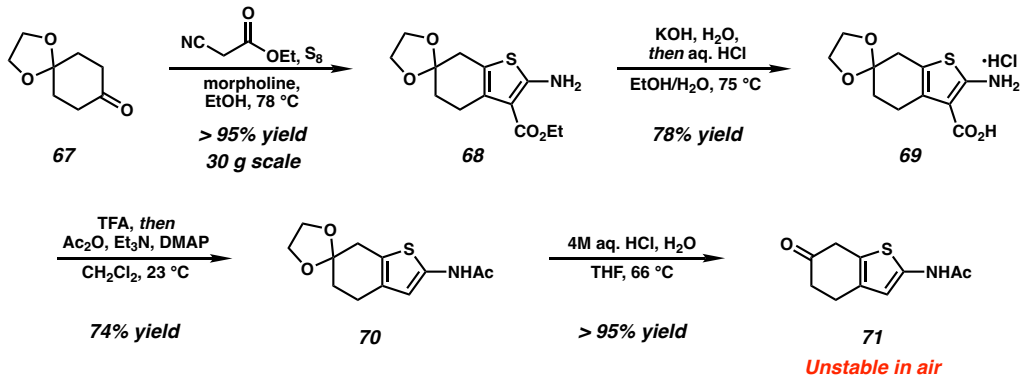
Our studies commenced with preparation of known arylhydrazine **61**[10] followed by Fischer indolization with dihydrofuran which provided tryptophol **62** (Scheme 1.3.1).[11] A three-step sequence involving a Mitsunobu reaction with DPPA, subsequent *N*-tosylation, and Staudinger reduction yielded protected tryptamine **65**. Finally, intramolecular Buchwald−Hartwig amination provided tricyclic aniline **66**.[12]

Scheme 1.3.1 *Synthesis of simplified tricycle* ***66***.



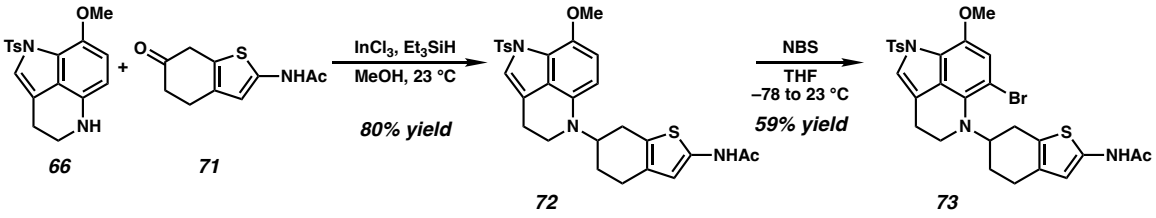
The synthesis of thiophene coupling fragment **71** began with aminothiophene **68**, which was prepared in one step from 1,4-cyclohexanedione monoethylene ketal (**67**) via Gewald aminothiophene synthesis (Scheme 1.3.2).[13] Saponification and decarboxylation served to remove the ester group, and the resulting amine was readily protected as the acetamide. Subsequent ketal cleavage afforded the ketothiophene coupling partner **71**.[14]

Scheme 1.3.2 *Synthesis of aminothiophene* ***71***.



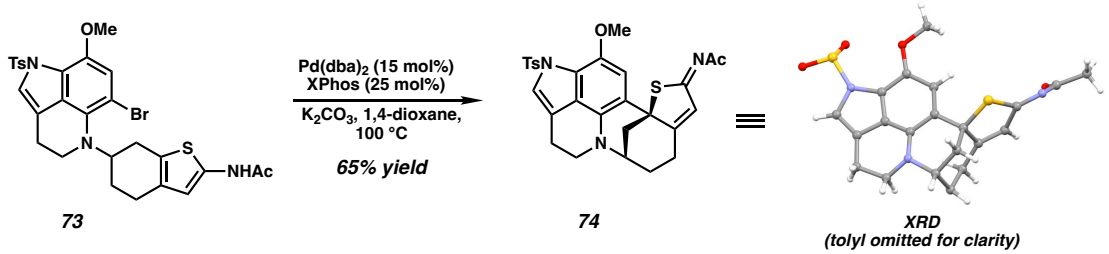
Coupling of tricyclic aniline **66** with ketothiophene **71** was achieved by employing indium hydride-mediated reductive amination conditions developed by Yang[15] (Scheme 1.3.3). Subsequent bromination yielded the desired dearomative thiophene arylation substrate **72**.[16]

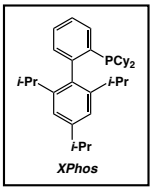
Scheme 1.3.3 *Synthesis of dearomative thiophene arylation substrate* ***72***.



Gratifyingly, treatment of bromoaniline **73** with $Pd(dba)_2$ and XPhos in the presence of K_2CO_3 led to the desired dearomative cyclization which provided thioimidate **74** in an outstanding 70% yield (Scheme 1.3.4).[17] In addition to completing the carbon skeleton of aleutianamine (**15**) and assembling the tertiary alkyl sulfide, this reaction constitutes the first dearomative arylation of a thiophene derivative to date.[18]

Scheme 1.3.4 *Successful dearomative thiophene arylation.*

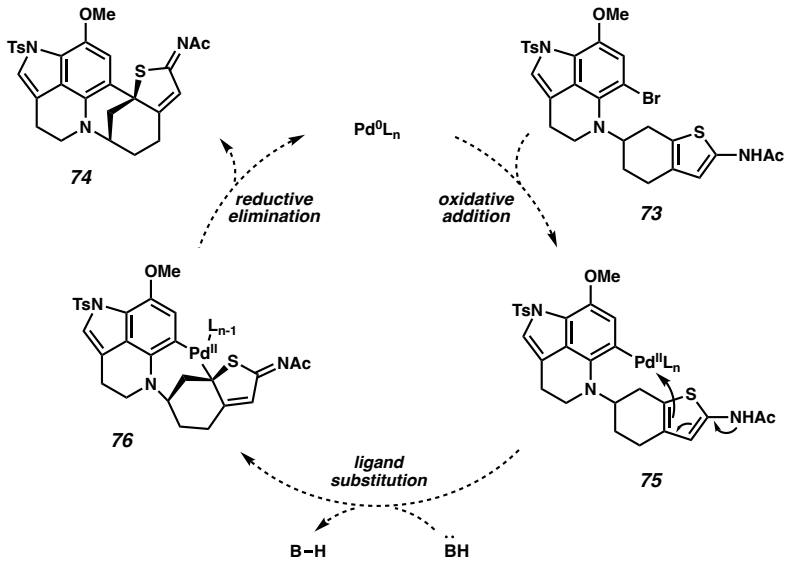




- *First example of dearomative thiophene coupling*
- *Successful installation of tertiary bridgehead sulfide*
- *Rapid construction of [3.3.1] bicyclic core*
- *Entire carbon skeleton of aleutianamine established*

Mechanistically, we hypothesize that after oxidative addition, ligand substitution mediated by nucleophilic attack of the thiophene onto palladium could yield palladacycle **76** that could then undergo reductive elimination to yield desired thioimidate **74** (Scheme 1.3.5). However, this is a tentative mechanistic hypothesis, and a dearomative Heck-type mechanism cannot be ruled out. With this exciting result in hand, we then turned our attention toward applying it to the amino tricycle containing the C10 nitrogen.

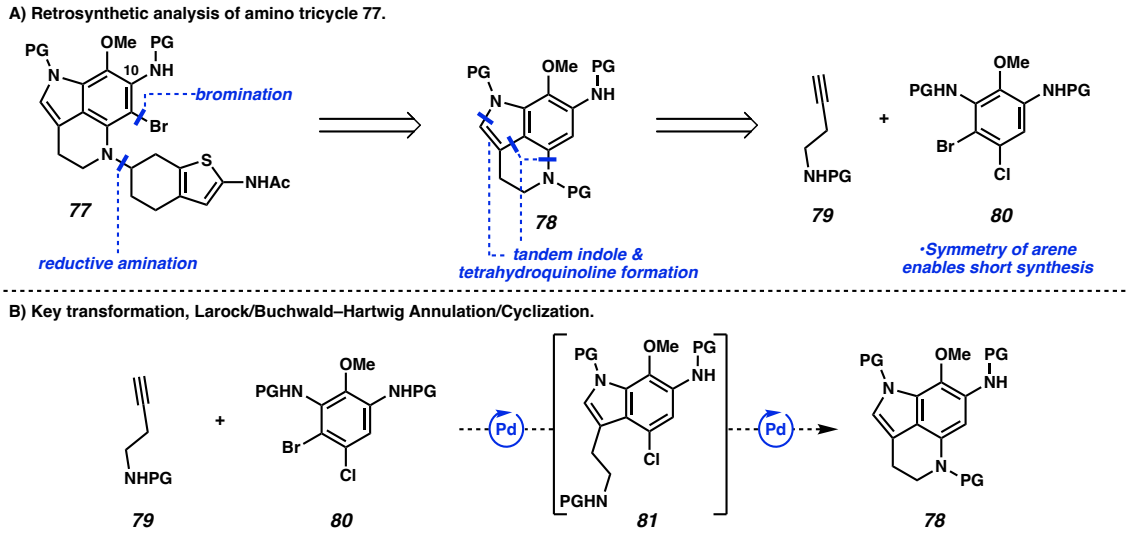
Scheme 1.3.5 *Proposed mechanism of the dearomative thiophene arylation.*



1.4 SYNTHESIS OF THE AMINO TRICYCLE ENABLED BY THE DEVELOPMENT OF A LAROCK/BUCHWALD–HARTWIG ANNULATION/CYCLIZATION

The requisite dearomative substrate containing the C10 nitrogen atom (**77**) was hypothesized to arise from an analogous reductive amination/bromination sequence, leading back to amino tricycle **78**— the core of the pyrroloiminoquinone alkaloids bearing a reduced arene oxidation state (Scheme 1.4.1A). We recognized a pseudosymmetric

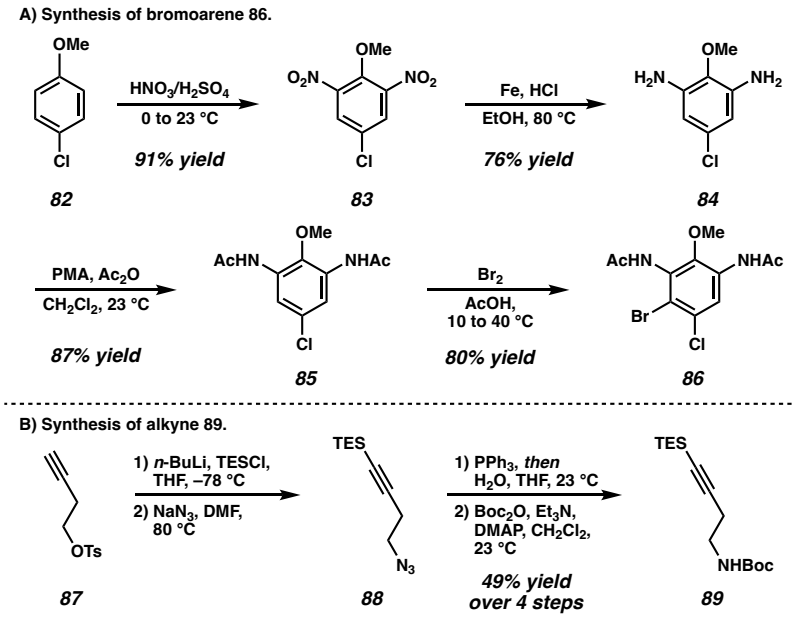
Scheme 1.4.1 *Retrosynthetic analysis of amino tricycle **77**.*



mirror plane through the central arene of amino tricycle **78**; this inspired the disconnection of both the indole and tetrahydroquinoline ring systems, revealing pseudosymmetric arene **80**. We imagined that the symmetry of this highly substituted arene would simplify its synthesis, precluding the need for a lengthy synthetic sequence that is typical of highly substituted arenes. Critical to the success of this strategy is the indolization/ tetrahydroquinoline formation step. We envisioned that the development of a tandem Larock/Buchwald–Hartwig annulation/cyclization could enable this approach (Scheme 1.4.1B). While both the Larock indole synthesis and Buchwald–Hartwig amination are well documented independently,[19,20] to the best of our knowledge a tandem Larock/Buchwald–Hartwig annulation/cyclization has yet to be reported. To this end, we set out to access the Larock/Buchwald–Hartwig annulation/cyclization substrates.

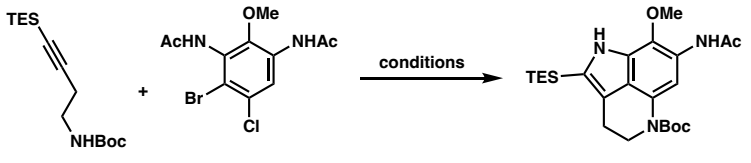
Dinitration of 4-chloroanisole (**82**) proceeded smoothly to provide dinitro arene **83**, which underwent reduction to the corresponding dianiline (**84**) (Scheme 1.4.2A). Phosphomolybdic acid (PMA)-mediated acetylation [21] then yielded diacetanilide **85**. Finally, monobromination served as the desymmetrizing step to provide the first Larock/Buchwald–Hartwig cyclization substrate **86** in just four steps. The synthesis of the alkyne coupling partner commenced from commercially available alkyne **87**, which was silylated followed by substitution of the tosyl group with NaN_3 to afford azide **88** (Scheme 1.4.2B). Azide **88** was then converted to the amine via Staudinger reduction, which was subsequently Boc protected to provide alkyne coupling partner **89** in four total steps.

Scheme 1.4.2 *Synthesis of the requisite Larock/Buchwald–Hartwig annulation/cyclization substrates* ***86*** *and* ***89****.*



We next turned our attention to the development of the key Larock/Buchwald–Hartwig annulation/cyclization. Since Larock's original disclosure of the palladium-mediated indolization of alkynes and *o*-iodoanilines, the scope has been expanded to *o*-bromoanilines through catalyst and ligand design.[20] Despite these efforts, examples of substrates bearing bis *ortho* substitution with respect to the halide are rare, so we anticipated that this would be a difficult transformation to realize. We first tested the conditions reported by Reisman and coworkers,[22] which employ Pd[P(*t*-Bu)$_3$]$_2$ as the catalyst and ligand source along with a soluble amine base (Cy_2NMe), but these led to no detectable product formation and primarily protodebromination of arene **86** (Table 1.4.1, entry 1). We next evaluated conditions reported by Boger and coworkers,[23] which again utilize a Pd (0) precatalyst, now in combination with the electron-rich 1,10 -bis(di-tert-butylphosphino)ferrocene (D*t*-BPF) ligand and Et_3N as the base, but protodebromination was similarly observed with no desired product formation (entry 2). Utilizing modified

Table 1.4.1 *Investigation of the Larock/Buchwald–Hartwig annulation/cyclization.*



89 ***86*** ***90***

Entry	Catalyst	Ligand	Base	Solvent	Temp/Time	Yield
1[a]	$Pd[P(t\text{-}Bu)_3]_2$ (10 mol %)	-	Cy_2NMe	1,4-dioxane	80 °C, 24 h	0%
2[a]	$Pd_2(dba)_3$ (10 mol %)	D*t*-BPF (20 mol %)	Et_3N	DMF	130 °C, 30 h	0%
3[a]	$Pd(OAc)_2$ (5 mol %)	D*t*-BPF (10 mol %)	K_2CO_3	NMP	110 °C, 24 h	15%
4[b]	$Pd(OAc)_2$ (15 mol %)	D*t*-BPF (30 mol %)	K_2CO_3	NMP	110 °C, 24 h	32%
5[c]	$Pd(OAc)_2$ (15 mol %)	D*t*-BPF (15 mol %) + XPhos (15 mol%)	K_2CO_3	NMP	90 °C, 24 h	69%

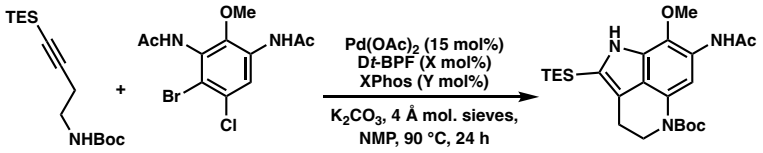
Reactions performed on a 0.1 mmol scale at 0.1 M. Yields refer to isolated yields. [a]*2.0 equiv of alkyne* ***89****, 2.5 equiv of base.* [b]*5.0 equiv of alkyne* ***89****, 5.0 equiv of freshly dried powdered* K_2CO_3. [c]*0.44 mmol scale, 5.0 equiv of alkyne* ***89****, 5.0 equiv of freshly dried granular* K_2CO_3*, freshly activated 4Å mol. sieves.*

conditions reported by Senanayake and coworkers[24] that implement a Pd(II) precatalyst and D*t*-BPF as the ligand, now using an inorganic base (K_2CO_3), we were encouraged to isolate 15% yield of desired tricycle **90** (entry 3). This represents a powerful transformation, as 3 bonds and 2 rings are formed in a single synthetic step. This yield could be improved to 32% by increasing the catalyst and ligand loading, using greater equivalents of alkyne **89**, and freshly drying the K_2CO_3 (entry 4). After extensive investigation, we discovered that the addition of another ligand (XPhos) to the system improved the yield to 69% (entry 5, see Appendix A5 for additional optimization details). Lastly, the addition of 4 Å molecular sieves addressed issues with reproducibility, likely caused by the presence of water. Overall, this transformation represents the first example of a tandem Larock/Buchwald–Hartwig annulation/cyclization and provides access to the key amino

tricycle **90**— the core of the pyrroloiminoquinone alkaloids– in a longest linear sequence (LLS) of just five steps, which to the best of our knowledge is the shortest synthetic sequence to such a tricyclic intermediate.

Given our success with the development of the Larock/Buchwald–Hartwig annulation/cyclization we were interested to gain insight on how the dual ligand system was uniquely effective in this transformation. First, we investigated the effects of the ligand stoichiometry under the optimal reaction conditions. The ratio of D*t*-BPF:XPhos was varied, while keeping the total ligand percentage at 30 mol% (2 equivalents with respect to Pd). If an excess of D*t*-BPF was used in respect to XPhos, the efficiency of the annulation/cyclization was diminished (Table 1.4.2, entries 1–3). In these cases, a large portion of the remaining mass balance was the intermediate indole product (*vide infra*). Efficient formation of tricyclic product **90** was restored under the optimal reaction conditions consisting of a 1:1 D*t*-BPF:XPhos ratio (entry 4). Interestingly, a 1:2

Table 1.4.2 *Ligand stoichiometry effects on the tandem transformation.*



89 ***86*** ***90***

Entry	D*t*-BPF mol %	XPhos mol%	Yield[a]
1	30	0	3%
2	25	5	8%
3	20	10	10%
4	15	15	72%
5	10	20	64%
6	5	25	47%
7	0	30	36%

[a]*Yields were determined by LC/MS using 1,3,5-trimethoxy benzene as an internal standard.*

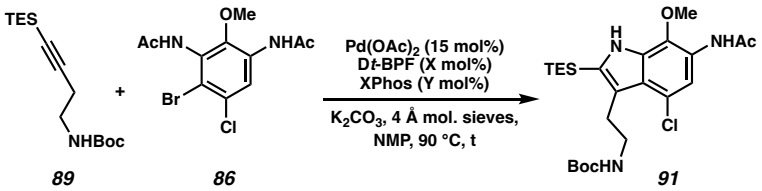
D*t*-BPF:XPhos mixture was also effective, providing **90** in a 64% yield (entry 5). However, once a larger excess of XPhos was employed the yield of **90** decreased (entries 6 and 7). In these cases, the reaction profile was more complicated with unidentifiable side/decomposition products leading to lower yields of **90**.

To gain further insight, we studied each step of the tandem process individually while adjusting the ligand stoichiometry. We first studied the Larock indolization process by monitoring the consumption of bromoarene **86** by LC/MS. We found that either D*t*-BPF or XPhos on their own could facilitate the Larock indolization with similar efficiencies, although a significant reaction rate difference was observed (Table 1.4.3A, entries 1 and 3). Interestingly, the yield of indole **91** was increased when a 1:1 D*t*-BPF:XPhos ratio was employed, suggesting a synergistic effect of the dual ligand system on the Larock indolization process (entry 2). The lower yield of just the Larock indolization process (Table 1.4.3A, entry 2) compared to the tandem process (Table 1.4.1, entry 5) is likely due to quenching of intermediates on the catalytic cycle, as the reaction was stopped as soon as bromoarene **86** was consumed.[25]

We next studied the Buchwald–Hartwig step by subjecting indole **91** to different ligand mixtures. D*t*-BPF on its own only provided a 20% yield of tricycle **90** (Table 1.4.3B, entry 1). However, the addition of XPhos formed **90** in an 87% yield (entry 2). A similar result was obtained when XPhos was used on its own, however the rate of product formation was faster compared to the 1:1 D*t*-BPF:XPhos mixture (entry 3). These results suggest that XPhos facilitates the Buchwald–Hartwig amination step of the tandem annulation/cyclization process.

Table 1.4.3 *Investigation of the individual steps of the tandem annulation/cyclization process.*

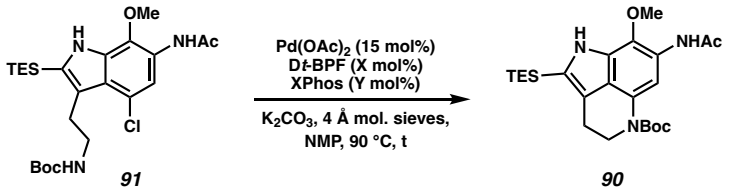
A) Investigation of the Larock indolization step.



89 ***86*** ***91***

Entry	D*t*-BPF mol %	XPhos mol%	Time	Yield[a]
1	30	0	20 h	45%
2	15	15	8 h	62%
3	0	30	11 h	44%

B) Investigation of the Buchwald–Hartwig cyclization step



91 ***90***

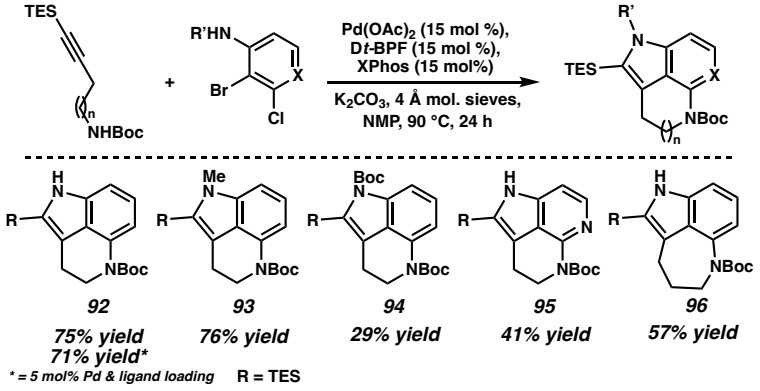
Entry	D*t*-BPF mol %	XPhos mol%	Time	Yield[a]
1	30	0	24 h	20%
2	15	15	16 h	87%
3	0	30	8 h	88%[b]

[a]Yields were determined by LC/MS using 1,3,5-trimethoxy benzene as an internal standard. [b]Isolated yield.

Taken together, we hypothesize that under the optimal reaction conditions a dynamic ligand exchange process between D*t*-BPF and XPhos on the palladium center gives rise to a synergistic effect on the Larock indolization, a phenomenon that has been well documented for mixed ligand systems in palladium catalysis.[26] Additionally, the ligand exchange allows for XPhos to facilitate the Buchwald–Hartwig amination step efficiently. This transformation highlights the utility of mixed ligand systems in palladium catalysis and suggests it should be explored more generally in reaction optimization.

With these results in hand, we were interested to see if this method could be applied more generally. Using commercially available 2-bromo-3-chloroaniline resulted in a 75% yield of tricycle **92** (Scheme 1.4.3). Additionally, the catalyst and ligand loading could

Scheme 1.4.3 *Selected substrate scope of the Larock/Buchwald–Hartwig annulation/cyclization.*

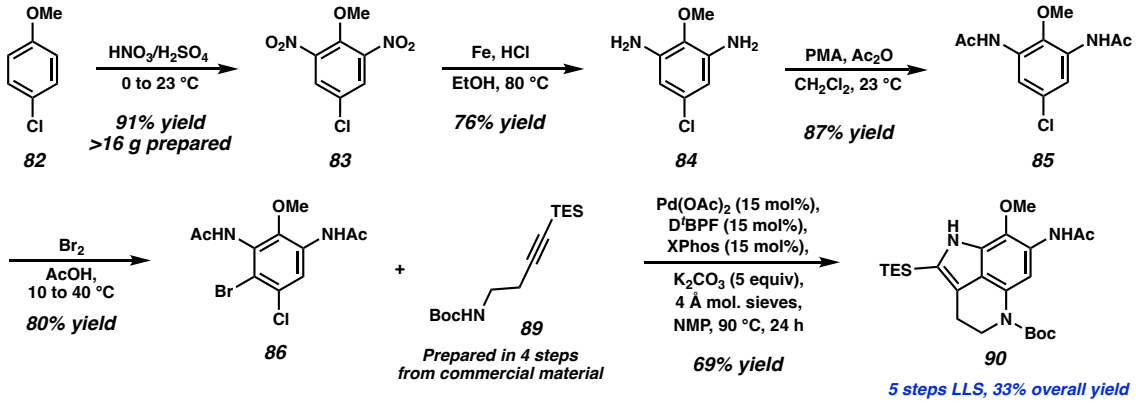


be lowered to 5 mol% without a significant decrease in yield (*i.e.*, 71% yield). *N*-Substitution on the aniline was tolerated, providing both *N*-Me (**93**) and *N*-Boc (**94**) cyclization products. Excitingly, employing 3-bromo-2- chloropyridine resulted in a 41% yield of azaindole derivative **95**, demonstrating the compatibility of heterocyclic substrates in the transformation. Finally, an alkyne coupling partner with a longer carbon chain could be used to provide the 5,6,7-tricyclic product **96** in 57% yield.

1.5 ATTEMPTED DEAROMATIVE THIOPHENE ARYLATION ON THE AMINO TRICYCLE

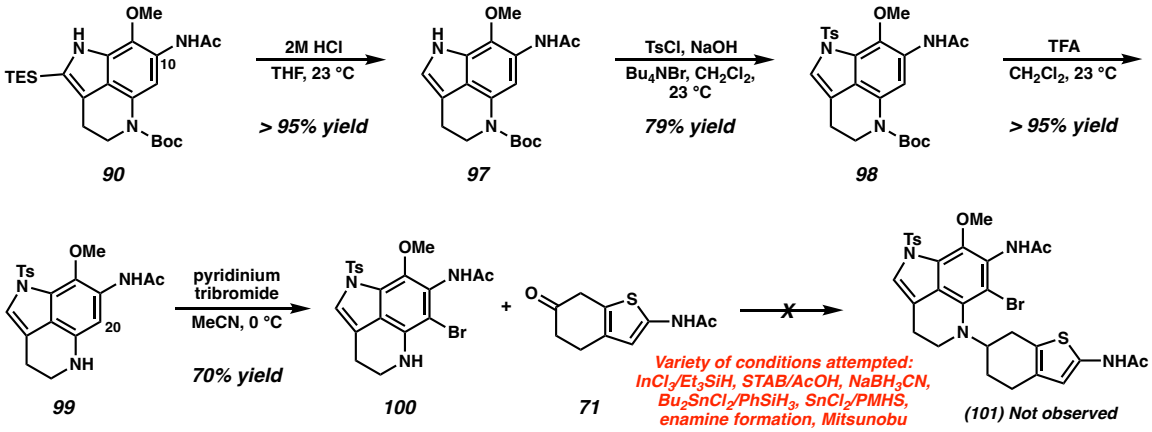
Having successfully developed a concise route to amino tricycle **90** enabled by the novel Larock/Buchwald–Hartwig annulation/cyclization (Scheme 1.5.1), we focused our efforts toward preparing the requisite dearomative thiophene arylation substrate containing

Scheme 1.5.1 *Full synthetic sequence to amino tricycle* ***90***.



the C10 nitrogen. This commenced with first desilylation of tricycle **90** followed by protection of the indole nitrogen as the sulfonamide yielding *N*-Ts tricycle **98** (Scheme 1.5.2). The Boc group on the secondary aniline was then removed under standard conditions and was followed by selective bromination of the C20 position which afforded aryl bromide **100**. Unfortunately, despite extensive investigation, the reductive amination between aryl bromide **100** and ketothiophene **71** proved unsuccessful; in most cases unreacted starting material (**100**) was obtained.[27] We hypothesize that because the secondary aniline nitrogen is confined to the plane of the aromatic system, unfavorable steric interactions caused by the bulky *o*-bromide substituent prevent engagement between

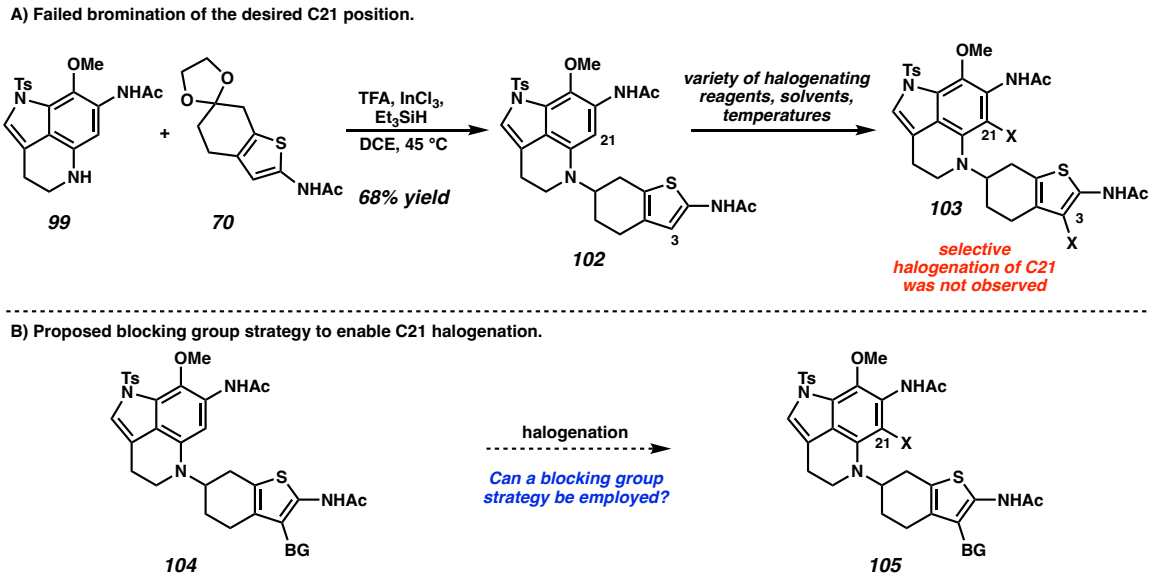
Scheme 1.5.2 *Elaboration of amino tricycle* ***90*** *and failed reductive amination.*



aniline **100** and ketothiophene **71**.[28] When attempting to employ more forcing conditions (i.e. high temperatures), decomposition of either starting material was typically observed.

Fortunately, the reductive amination between aminotricycle **99** without the *o*-bromide present proceeded smoothly to deliver **102** (Scheme 1.5.3A). Slightly modified reaction conditions were necessary; employing the reductive amination conditions used for the simplified tricycle (see Section 1.3, Scheme 1.3.3), which used methanol as the solvent

Scheme 1.5.3 *Failed synthesis of the desired dearomative thiophene arylation substrate.*

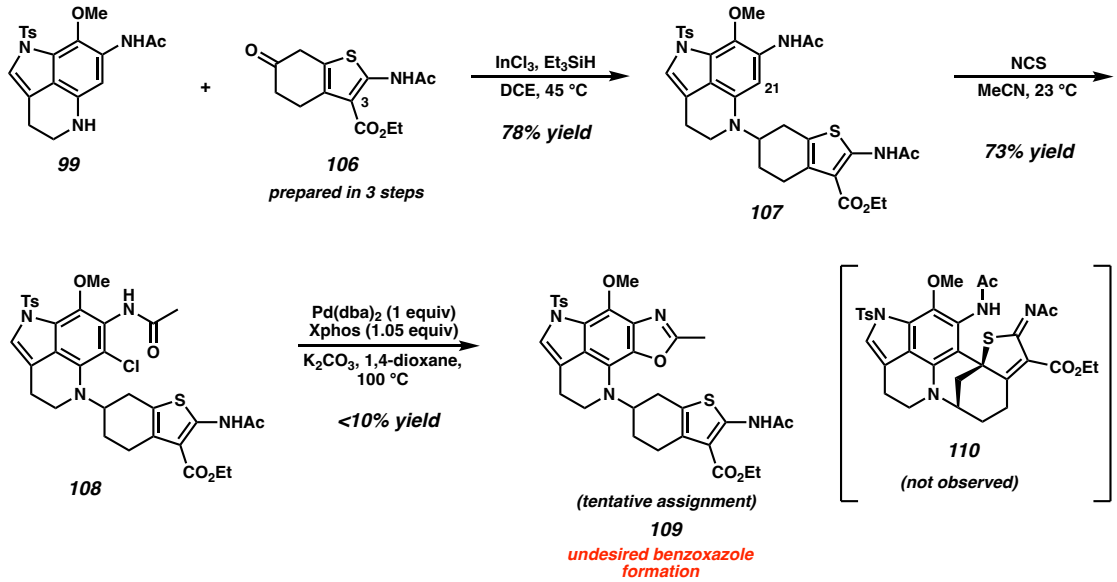


at ambient temperatures, lead to no desired product and instead formation of the dimethyl acetal on ketothiophene **71** was observed, highlighting the differences in reactivity of the aminotricycle compared to the simplified system. With coupled product **102** in hand, efforts were focused on affecting the selective halogenation of the C21 position. Despite a thorough investigation of halogenation conditions (i.e. various electrophilic iodine, bromine, and chlorine sources under a variety of solvents and temperatures), the desired C21 halogenation product was not observed. In most cases, dihalogenation product **103**

was obtained in which the C3 position of the thiophene was also halogenated. Attempting to carefully control the stoichiometry of the halogenating reagent typically resulted in selective halogenation of the C3 thiophene position. Additionally, attempting to employ different protecting groups on the C10 nitrogen to alter the electronics of the arene lead to similar results. To circumvent this challenge, we were interested in employing a blocking group strategy to prevent competitive halogenation at the C3 position of the thiophene (Scheme 1.5.3B). Critical to the success of this approach is the selection of a blocking group that could be removed later in the synthetic sequence: we elected to pursue an ester and hypothesized that a hydrolysis and subsequent decarboxylation sequence could be employed later in the synthesis.

Ketothiophene **106**, containing an ethyl ester at the C3 postion, was prepared using an analogous Gewald sequence (Scheme 1.5.4). Coupling of **106** and aminotricycle **99** under the previously employed reductive amination conditions afforded coupled product **107**. Excitingly, with the C3 thiophene position of **107** blocked, selective chlorination of

Scheme 1.5.4 *Failed dearomative thiophene arylation on the amino tricycle system.*

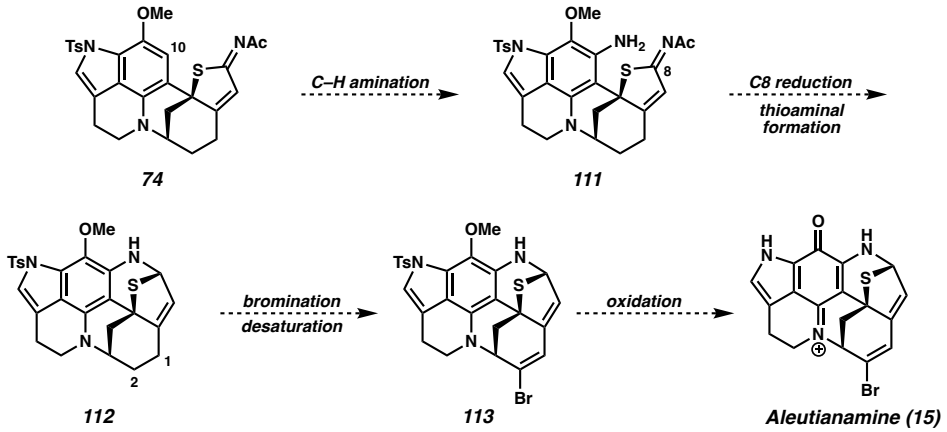


the C21 position was achieved yielding aryl chloride **108**.[29] Subjecting aryl chloride **108** to stoichiometric dearomative thiophene arylation conditions yielded benzoxazole **109** (resulting from oxygen insertion of the acetamide), and unfortunately, no desired thiophene arylation product **110** was observed. We believe that the addition of an electron-withdrawing group on the thiophene (i.e. the C3 ester) decreases its nucleophilicity and prevents the nucleophilic ligand substitution step of the dearomative thiophene arylation.[30] In an attempt to promote the desired thiophene arylation on this system, alternative C3 thiophene blocking groups and C10 nitrogen protecting groups underwent preliminary investigations, but ultimately these efforts proved unfruitful (see Appendix A4). Given the challenges faced in advancing the aminotricycle, efforts were returned toward advancing the simplified system.

1.6 FORMATION OF THE FULL RING SYSTEM OF ALEUTIANAMINE AND FAILED LATE-STAGE BROMINATION

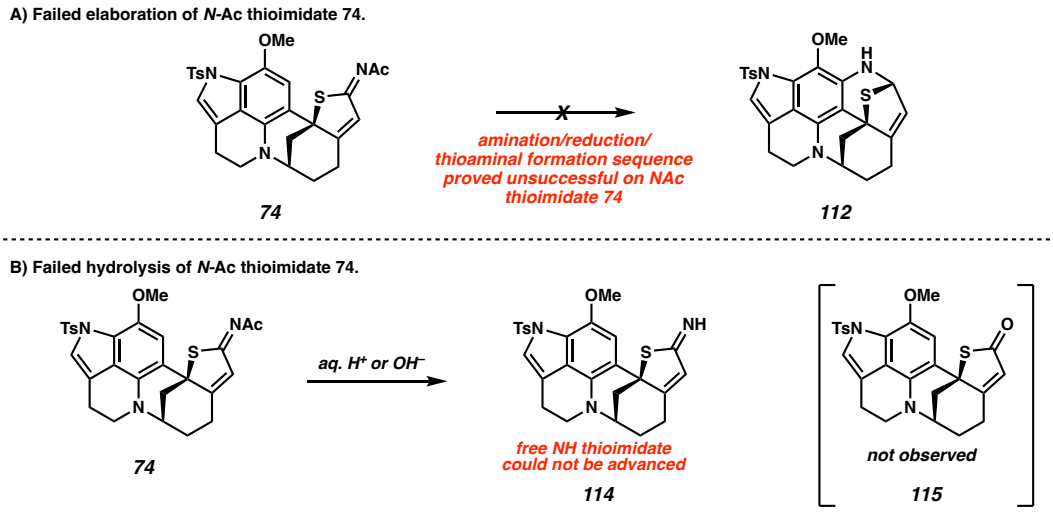
From previously accessed thioimidate **74**, several challenges remained in the synthesis of aleutianamine (**15**): installation of the C10 nitrogen, reduction of C8 and subsequent thioaminal formation, installation of the alkenyl bromide, and final oxidation

Scheme 1.6.1 *Remaining challenges to complete the synthesis of aleutianamine (**15**).*



of the central arene (Scheme 1.6.1). The order of events was unclear *a priori*, but we decided to first focus on the amination/reduction/thioaminal formation sequence. Despite extensive efforts, *N*-Ac thioimidate **74** could not be advanced through this sequence (Scheme 1.6.2A); undesired reactivity of the *N*-Ac group proved to be a major challenge (See appendix A4 for details). Additionally, there was no clear path to affect the desaturation of the C1-C2 position on *N*-Ac thioimidate **74**; thus, we were interested in exploring an

Scheme 1.6.2 *Failed elaboration of N-Ac thioimidate* ***74***.

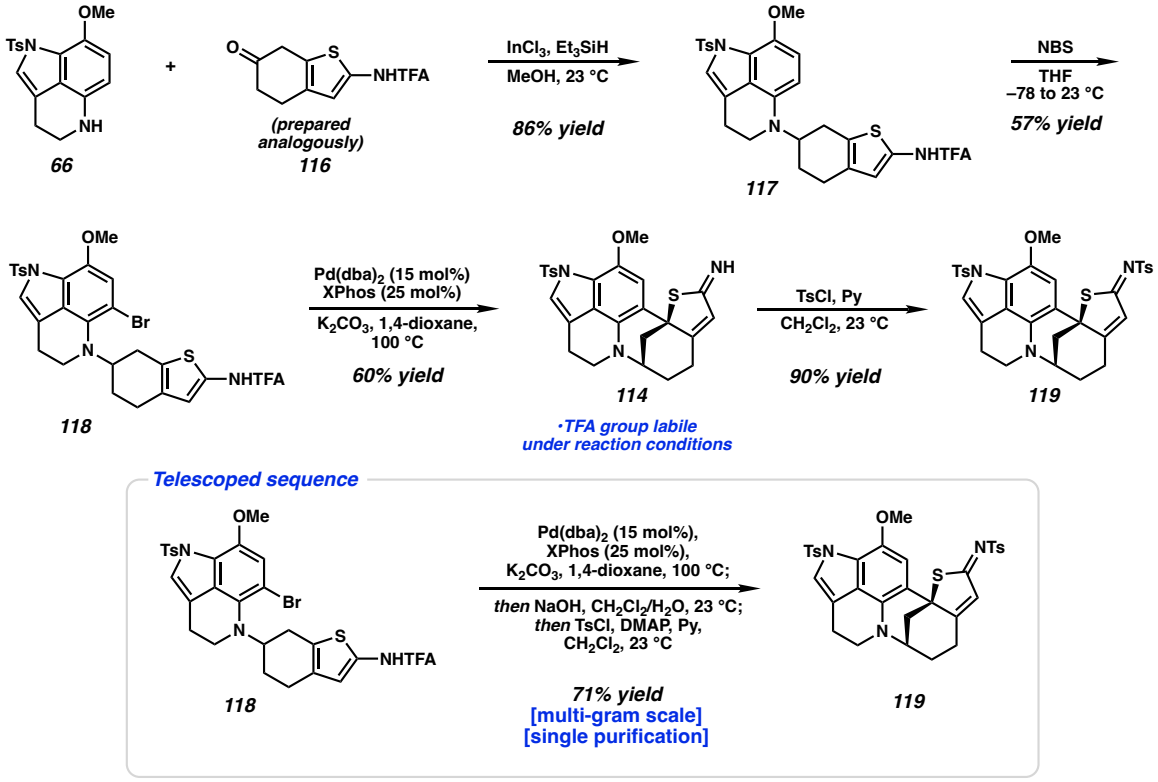


alternative thiobutenolide system. However, hydrolysis of *N*-Ac thioimidate under a variety of acidic or basic conditions yielded free *N*-H thioimidate **114** and desired thiobutenolide **115** was not observed (Scheme 1.6.2B). Moreover, the amination/reduction/thioaminal formation sequence failed on free *N*-H thioimidate **114**.

We hypothesized that a more electron-withdrawing thioimidate protecting group could facilitate the desired hydrolysis. Therefore, *N*-TFA ketothiophene **116** was prepared analogously and was successfully carried through the reductive amination/bromination sequence to yield aryl bromide **118** (Scheme 1.6.3). This substrate proved competent in the

dearomative arylation, although this occurred with concomitant cleavage of the trifluoroacetamide which yielded free *N*-H thiomidate **114**. The product of

Scheme 1.6.3 *Synthesis of N-Ts thioimidate* ***119***.

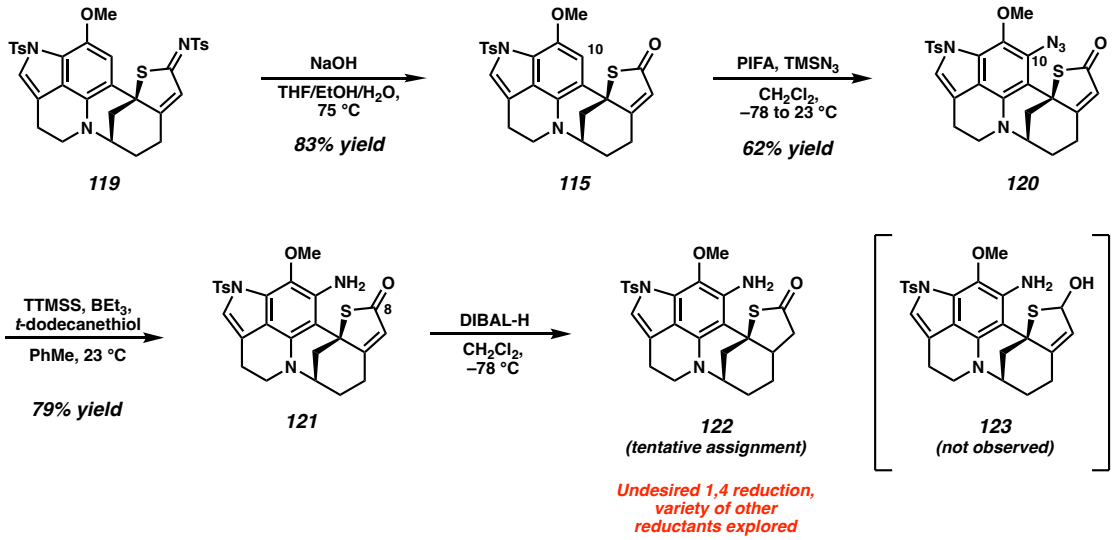


this coupling (**114**) was then *N*-tosylated to provide thioimidate **119**. To circumvent the challenging purification of free thioimidate **114**, the dearomative arylation and tosylation steps were telescoped to provide an improved yield of *N*-tosyl thioimidate **119** on multigram scale.

Excitingly, subjection of intermediate **119** to aqueous alkaline conditions led to the hydrolysis of the tosyl thioimidate, yielding thiobutenolide **115** (Scheme 1.6.4). Although canonical electrophilic amination strategies failed, installation of the C10 nitrogen atom was achieved utilizing conditions previously reported by Kita and coworkers[31]; treatment

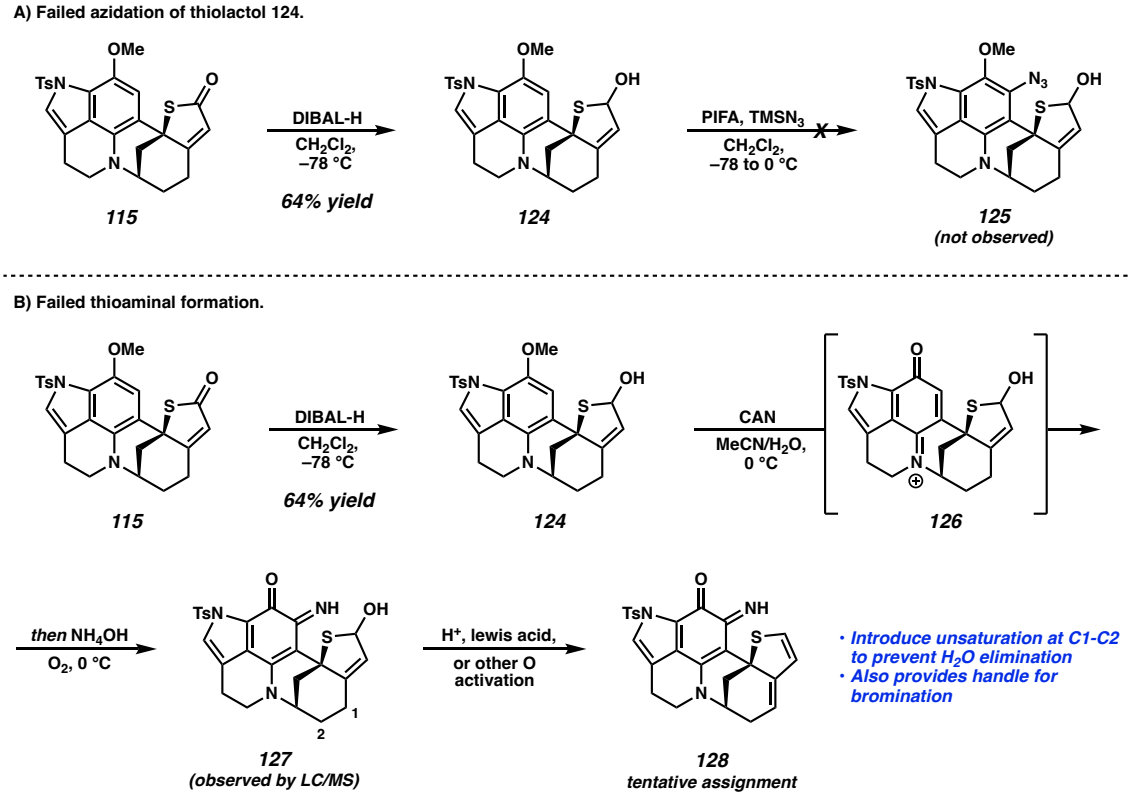
of **115** with PIFA and $TMSN_3$ affected an oxidative azidation which provided aryl azide **120**.

Scheme 1.6.4 *Failed 1,2 reduction of thiobutenolide* ***121***.



Reduction of the azide to the aniline proved challenging, but eventually radical-based reduction conditions reported by Zanardi and coworkers[32] afforded desired aniline **121**. Our next focus was the reduction of C8 on thiobutenolide **121** to enable eventual thioaminal formation. Treatment of aniline **121** with DIBAL lead to undesired 1,4 reduction and the formation of saturated thiobutenolide **122**, and unfortunately, no desired 1,2 reduction (i.e. **123**) was observed. Formation of an aluminate complex with the free aniline likely occurs, which interestingly, favors 1,4-reduction. Similar results were obtained when employing a variety of other reductants.

Scheme 1.6.5 *Failed elaboration of saturated thiobutenolide* ***115***.

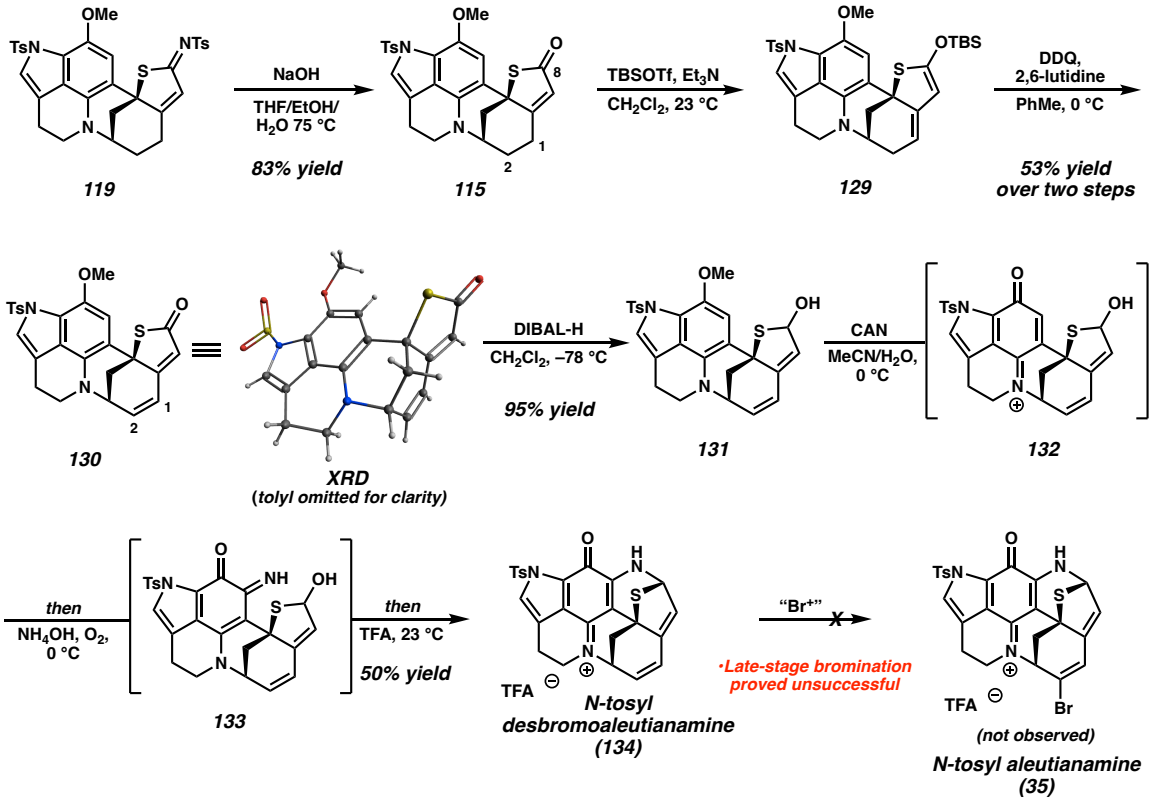


An alternative order of events was employed to address this challenge. Selective 1,2 reduction of thiobutenolide **115** prior to C10 nitrogen installation proceeded smoothly to yield thiolactol **124** as a mixture of diastereomers (Scheme 1.6.5A). Surprisingly, oxidative azidation of thiolactol **124** failed and instead lead to a complex mixture of unidentified products. Utilizing the same oxidative amination logic, treatment of thiolactol **124** with CAN oxidized the arene to pyrroloiminoquinone **126**, and subsequent addition of aqueous ammonia affected amination and aerobic oxidation to deliver pyrroloiminoquinone **127** (observed via LC/MS, Scheme 1.6.5B).[33] However, thioaminal formation was unsuccessful at this stage: attempting to affect this transformation under a variety of Bronsted or Lewis acidic conditions, or other oxygen activation methods (i.e. mesylation) led to tentatively assigned diene **128** resulting from dehydration. At this point

we recognized that introducing desaturation at the C1-C2 position would prevent dehydration. Additionally, an olefin at the C1-C2 position would provide a functional handle for bromination.

While a variety of standard conditions failed to promote vinylogous desaturation of this intermediate (**115**), soft enolization with TBSOTf afforded an intermediate silyl ketene thioacetal that was treated with DDQ to provide diene **130**, the structure of which was

Scheme 1.6.6 *Synthesis of N-tosyl des-bromoaleutianamine (**134**) and failed late-stage bromination.*



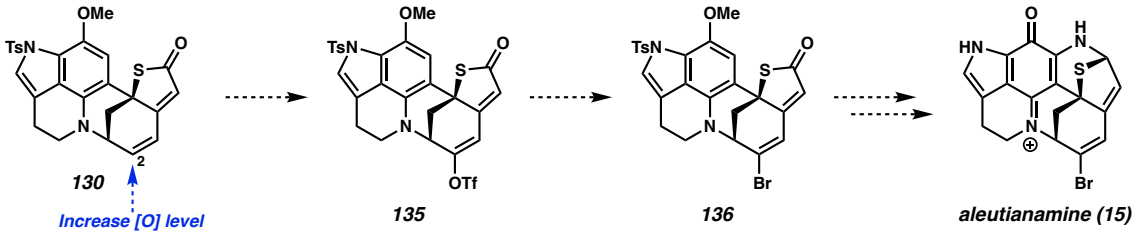
confirmed by X-ray crystallography. Reasoning that the electronics of diene **130** would promote bromination at the undesired C1 position, we opted to delay the installation of the alkenyl bromide until the final stage of the synthesis. Thus, DIBAL reduction of the thiolactone smoothly provided thiolactol **131**. At this point, the same amination strategy

was realized: treatment with CAN oxidized the arene to the desired pyrroloiminoquinone **132**, and addition of aqueous ammonia affected amination and aerobic oxidation to deliver pyrroloiminoquinone **133**. Gratifyingly, the addition of TFA led to dehydrative cyclization to yield thioaminal **134**, which bears the full ring system of aleutianamine (**15**). Unfortunately, direct bromination of *N*-tosyl des- bromoaleutianamine (**134**) was unsuccessful in our hands; all surveyed bromination conditions led to decomposition or undesired regioselectivity.

1.7 COMPLETION OF THE TOTAL SYNTHESIS OF ALEUTIANAMINE

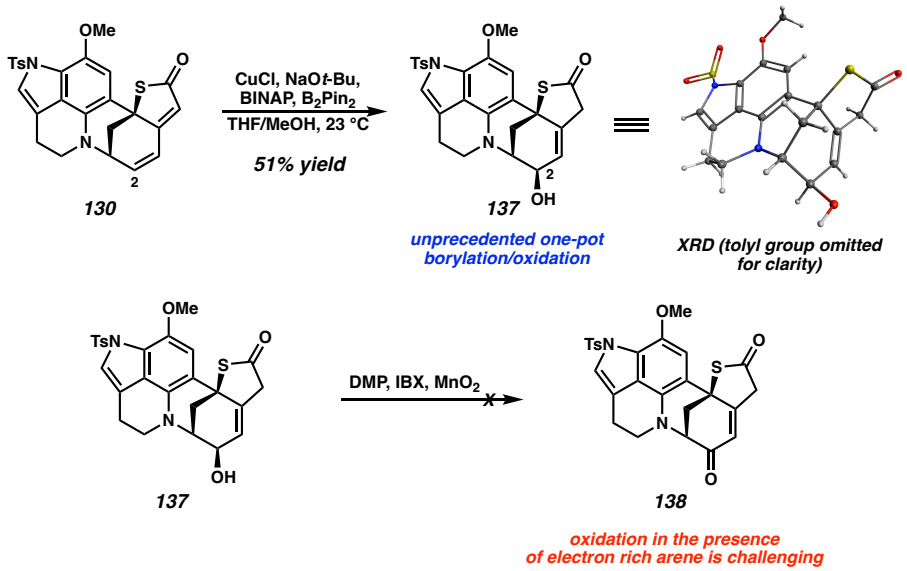
To circumvent the unsuccessful late-stage bromination, we attempted to increase the oxidation state at C2 on diene **130**, which would provide an alternative functional handle for bromination (Scheme 1.7.1).

Scheme 1.7.1 *Alternative strategy for alkenyl bromide installation.*



However, the incorporation of a suitable functional handle proved to be a significant challenge. Installation of a ketone or an equivalent thereof at the C2 position was attempted by allylic oxidation of **129**, thia-Michael addition and Pummerer Rearrangement of **130**, and organosilane 1,6- addition of **130**. Additionally, incorporation of an oxidation handle into aminothiophene coupling fragment **116** proved unsuccessful (See Appendix A4). After extensive experimentation, it was discovered that a 1,6-conjugate borylation could affect the desired C2 functionalization. Treatment of thiobutenolide **130** with modified conjugate-borylation conditions reported by Fernández

Scheme 1.7.2 *Synthesis of allylic alcohol* ***137*** *and failed oxidation.*

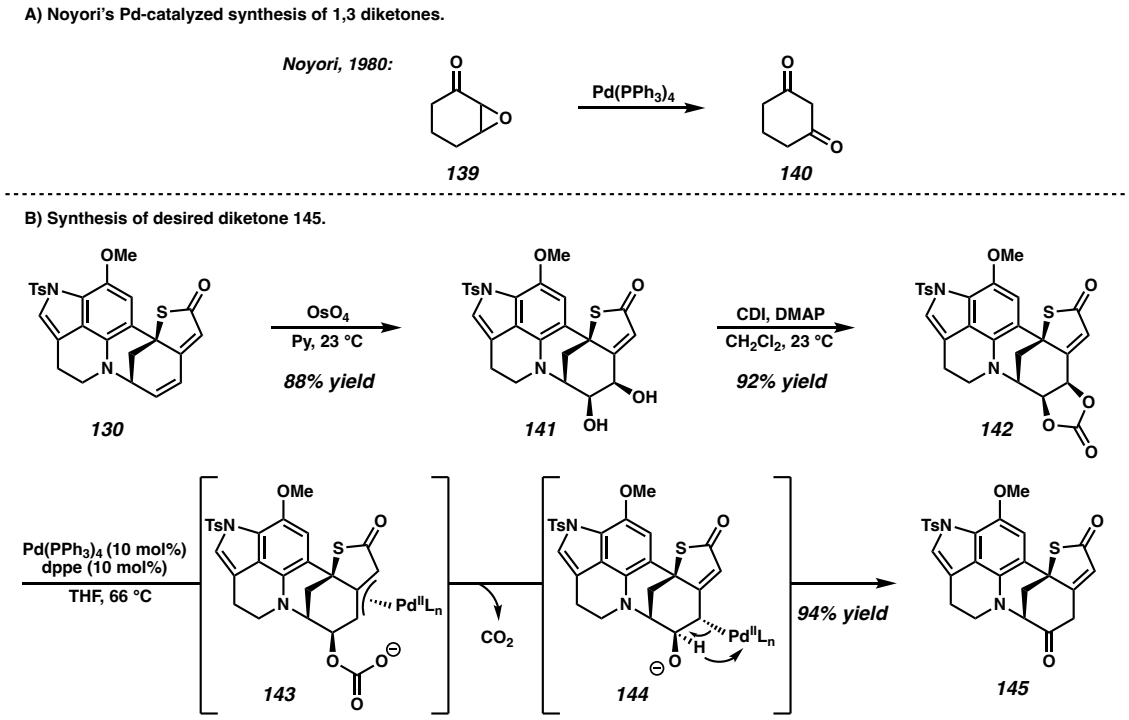


and coworkers[34] resulted in the formation of allylic alcohol **137**, the structure of which was confirmed by X-Ray crystallography (Scheme 1.7.2). This surprising result represents an unprecedented one-pot borylation/oxidation transformation, notably, without the addition of an oxidant to the system. We hypothesize that trace oxygen forms hydrogen peroxide under the reaction conditions that facilitates the oxidation of the intermediate boronic ester, although this is a working hypothesis and mechanistic experiments were not conducted. Nonetheless, for the first time a suitable functional handle had been successfully installed at the C2 position. Unfortunately, limited attempts at oxidizing allylic alcohol **137** to the desired ketone **138** proved unsuccessful. Employing canonical oxidants resulted in either oxidation of the central arene and/or non-specific decomposition, suggesting that performing an alcohol oxidation in the presence of the electron rich arene would prove challenging.

This led us to pursue alternative ketone installation methods that did not employ strong oxidants and inspiration was taken from Noyori and coworkers[35] where they

demonstrated that 1,3 diketones could be accessed from the Pd(0)-catalyzed rearrangement of α,β-epoxy ketones (Scheme 1.7.3A). This method was particularly attractive as the

Scheme 1.7.3 *Successful synthesis of diketone* ***145***.



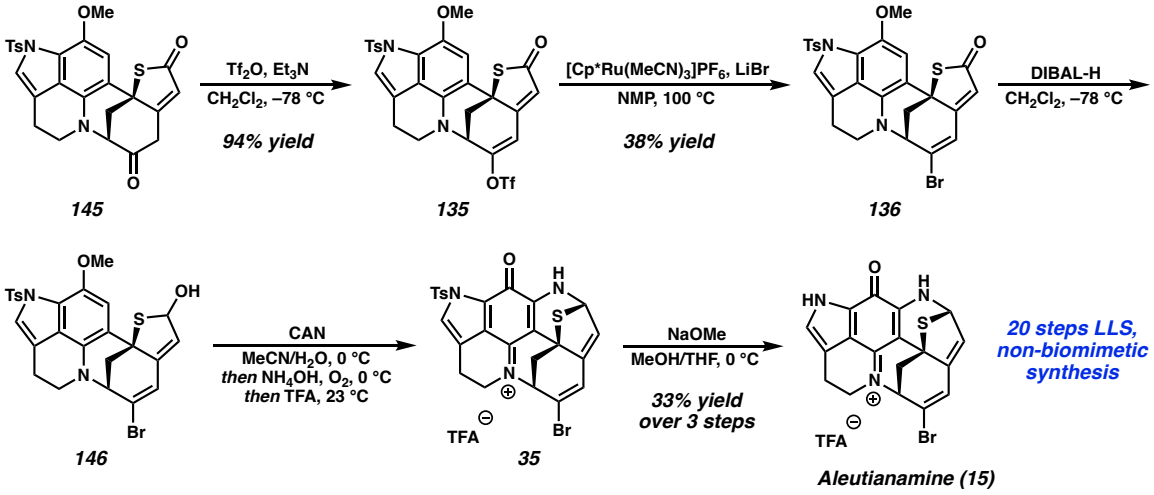
desired oxidation pattern could be accessed under mild reaction conditions without the use of a strong oxidant. Although the analogous γ,δ-epoxide could not be prepared[36], we hypothesized that a γ,δ-cyclic carbonate could serve as an alternative ionizable functionality for the Pd-catalyzed rearrangement.

Beginning with diene **130**, γ,δ- dihydroxylation with OsO4 provided diol **141**, which was readily advanced to carbonate **142** (Scheme 1.7.3B). Treatment with Pd(0) and dppe[37] led to a decarboxylative pinacol-type rearrangement, presumably via putative π-allyl Pd(II) intermediate **143**, which could undergo decarboxylation to afford **144**, and subsequent β-hydride elimination and tautomerization to afford the desired ketone **145**. To

the best of our knowledge, this represents the first palladium-catalyzed decarboxylative pinacol-type rearrangement of allylic carbonates.

With this exciting result of installing the C2 ketone, we focused our efforts toward completing the synthesis of aleutianamine (**15**). Conversion of ketone **145** to enol triflate **135** was followed by Shirakawa and Hayashi's Ru-catalyzed triflate–halogen exchange to provide desired alkenyl bromide **136** (Scheme 1.7.4).[38] Finally, in an analogous fashion to the synthesis of des-bromo compound **134**, 1,2-reduction with DIBAL followed by oxidative amination and cyclization yielded penultimate intermediate **35**, and tosyl group cleavage with NaOMe afforded aleutianamine (**15**) in a longest linear sequence of 20 steps.[39]

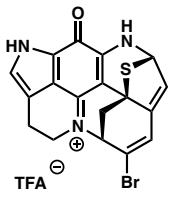
Scheme 1.7.4 *Completion of the total synthesis of aleutianamine (**15**).*



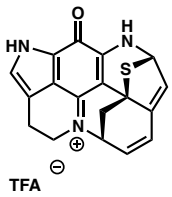
1.8 PRELIMINARY BIOLOGICAL STUDIES

With aleutianamine (**15**) and other synthetic intermediates in hand, we initiated a collaboration with the Chou lab at Caltech to further assess the preliminary biological activity of these molecules against five different human cancer cell lines (Figure 1.8.1). Aleutianamine (**15**) was highly active against all five cancer cell lines tested.[40] Remarkably,

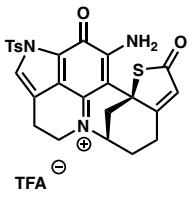
Figure 1.8.1 *Preliminary biological studies.*



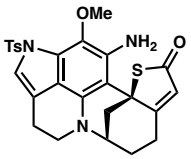
Aleutianamine (15)



des-bromo Aleutianamine (147)



Thiolactone 148



anisole-thiolactone 121

Cell line:	IC50 (μM):	IC50 (μM):	IC50 (μM):	IC50 (μM):
HCT116	0.07	0.24	0.38	>55
PANC1	0.09	0.21	0.6	>55
MCF7	0.001	0.2	0.3	>55
LNCaP	0.084	0.24	0.59	>55
PC3	0.00004	0.1	0.3	>55
DU145	0.095	0.82	1.2	>55

aleutianamine (**15**) displayed extreme potency against human prostate cell line PC3 with an IC_{50} = 40 pM. This is in contrast to *des*-bromoaleutianamine (**147**), which showed only moderate activity across the cell lines, highlighting the importance of the alkenyl bromide or other substitution at the C2 position for bioactivity. Interestingly, thiolactone **148** also showed weak activity despite sharing some structural features with aleutianamine (**15**, i.e. the oxidized pyrroloiminoquinone core and C10 nitrogen). Additionally, anisole-thiolactone **121**, possessing an unoxidized central ring, showed no activity implying the iminoquinone moiety is crucial for biological activity. These exciting preliminary results necessitate an investigation into the mechanism of action of the pyrroloiminoquinone biological activity against human cancer cells, which will then inform rational design in structure-activity-relationship (SAR) studies.

1.9 CONCLUSION

In conclusion, this total synthesis represents the first nonbiomimetic synthetic approach to aleutianamine (**15**). Key to the completion of the synthesis was the development of the Pd-catalyzed intramolecular dearomative arylation of an aminothiophene, the development of an unusual ketone installation by the Pd-catalyzed

pinacol-type rearrangement of a cyclic carbonate, and the development of a late- stage arene oxidative amination/thioaminal formation. Additionally, a Larock/Buchwald–Hartwig annulation/cyclization was developed to quickly access amino tricycle **90**, representing the core of pyrroloiminoquinone alkaloids, in just five steps. This synthesis highlights that ambitious retrosynthetic disconnections can facilitate the development of novel reaction methodology, which ultimately can enable the successful synthesis of the desired target. With authentic material in hand, novel biological activities of aleutianamine (**15**) were discovered; with its extreme potency to prostate cancer cells, aleutianamine (**15**) could potentially serve as a novel prostate cancer therapeutic. Efforts to prepare analogues of aleutianamine (**15**) with related sequences, establish a structure−activity relationship against biologically relevant cancer cell lines, and uncover its mechanism of action are ongoing.

1.10 EXPERIMENTAL SECTION

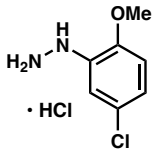
1.10.1 MATERIALS AND METHODS

Unless otherwise stated, reactions were performed in flame-dried glassware under an argon or nitrogen atmosphere using dry, deoxygenated solvents. Solvents were dried by passage through an activated alumina column under argon.[41] NBS was recrystallized from boiling water prior to use, amines and TMSCl were distilled under nitrogen prior to use, and K_2CO_3 was flame-dried under vacuum and stored in a nitrogen-filled glovebox prior to use. 4Å molecular sieves were activated via microwave heating (1100 W, full power, 45 s X 4), cooled under N_2, and stored in a N_2 filled glovebox. All other reagents were purchased from commercial sources and used as received unless otherwise indicated. Reaction temperatures were controlled by an IKAmag temperature modulator. Reaction

progress was monitored by thin-layer chromatography (TLC) or Agilent 1290 UHPLC-MS. TLC was performed using E. Merck silica gel 60 F254 precoated glass plates (0.25 mm) and visualized by UV fluorescence quenching, $KMnO_4$ staining, or *p*-anisaldehyde staining. Silicycle SiliaFlash® P60 Academic Silica gel (particle size 40–63 nm) was used for flash chromatography. Preparative HPLC was performed on an Agilent 1100 Series HPLC system using a 9.4 x 250 mm Agilent Eclipse XDB-C18 column, or on an Agilent 1200 Series HPLC system using a 9.4 x 250 mm Agilent Zorbax Rx-SIL column. ^{1}H NMR spectra were recorded on Varian Inova 500 MHz, Varian 600 MHz, and Bruker 400 MHz spectrometers and are reported relative to residual $CHCl_3$ (δ 7.26 ppm), C_6D_6 (δ 7.16 ppm), DMSO-d_6 (δ 2.50 ppm), CD_2Cl_2 (δ 5.32 ppm), or CD_3OD (δ 3.31 ppm). ^{13}C NMR spectra were recorded on a Bruker 400 MHz spectrometer (100 MHz) and are reported relative to $CHCl_3$ (δ 77.16 ppm), C_6D_6 (δ 128.06 ppm), DMSO-d_6 (δ 39.52 ppm), CD_2Cl_2 (δ 53.84 ppm), or CD_3OD (δ 49.00 ppm). Data for ^{1}H NMR are reported as follows: chemical shift (δ ppm) (multiplicity, coupling constant (Hz), integration). Multiplicities are reported as follows: s = singlet, d = doublet, t = triplet, q = quartet, p = pentet, sept = septuplet, m = multiplet, br s = broad singlet, br d = broad doublet. Data for ^{13}C NMR are reported in terms of chemical shifts (δ ppm). Some reported spectra include minor solvent impurities of water, ethyl acetate, diethyl ether, methylene chloride, acetone, grease, and/or silicon grease, which do not impact product assignments. IR spectra were obtained by use of a Perkin Elmer Spectrum BXII spectrometer using thin films deposited on NaCl plates and reported in frequency of absorption (cm^{-1}). High resolution mass spectra (HRMS) were obtained from an Agilent 6230 LC/TOF with an Agilent Jet Stream ion source in electrospray ionization (ESI+ or ESI–) mode, from the Caltech Mass Spectrometry

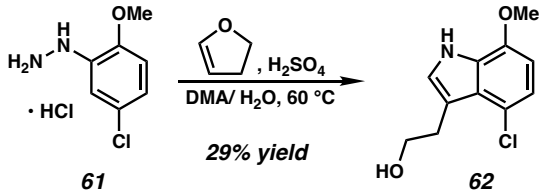
Laboratory using a JEOL JMS-T2000GC AccuTOFTM GC-Alpha in field desorption (FD+) mode, or from a JEOL JMS-600H High Resolution Mass Spectrometer in fast atom bombardment (FAB+), GC field ionization (GCFI+), or electron ionization (EI+) mode.

1.10.2 EXPERIMENTAL PROCEDURES



61

Hydrazine 61: Prepared according to the procedure of Thibeault and coworkers from 4-chloro-2-methoxyaniline.[13] All characterization data matched those reported in the literature.



61 *62*

Tryptophol 62: To a 250 mL round bottom flask were added (5-chloro-2-methoxyphenyl)hydrazine hydrochloride (**61**, 8.60 g, 41.1 mmol, 1.0 equiv), DMA (65 mL), H_2O (65 mL), and 25% (v/v) aq. H_2SO_4 (11.0 mL, 51.4 mmol, 1.25 equiv). 2,3-dihydrofuran (3.42 mL, 45.2 mmol, 1.1 equiv) was added slowly with stirring, resulting in a slow color change to yellow, whereafter the flask was equipped with an air-cooled reflux condenser and heated to 60 °C in an oil bath for 6 h. The reaction mixture was then allowed to cool to 23 °C and transferred to a separatory funnel containing 1:1 saturated aq. $NaHCO_3$/brine (250 mL). The mixture was then extracted with EtOAc (4x100 mL), and the combined organic extracts were washed with water, dried over Na_2SO_4, and

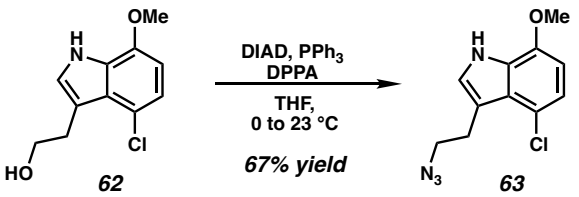
concentrated under reduced pressure. The crude product was purified by silica gel flash chromatography (60% EtOAc/hexanes) to afford the title compound as a thick, red-brown syrup that slowly crystallized upon storage at –20 °C (2.66 g, 11.79 mmol, 29% yield).

^{1}H NMR (400 MHz, $CDCl_3$): δ 8.54 (br s, 1H), 7.00 (d, *J* = 2.2 Hz, 1H), 6.96 (d, *J* = 8.2 Hz, 1H), 6.50 (d, *J* = 8.2 Hz, 1H), 3.94 (t, *J* = 6.4 Hz, 2H), 3.91 (s, 3H), 3.23 (td, *J* = 6.4, 0.8 Hz, 2H).

^{13}C NMR (100 MHz, $CDCl_3$): δ 145.2, 128.4, 124.8, 123.8, 120.2, 118.2, 113.1, 102.4, 63.7, 55.7, 29.5.

IR (Neat Film, NaCl): 3416, 2935, 2580, 1786, 1703, 1626, 1571, 1494, 1452, 1339, 1230, 1115, 1052, 937, 789, 736, 694, 628 cm^{-1}.

HRMS (FD+): *m/z* calc'd for $C_{11}H_{13}ClNO_2$ $[M+H]^+$: 225.0557, found 225.0552.



Indole azide 63: To a 250 mL round bottom flask was added tryptophol **62** (3.36 g, 14.89 mmol, 1.0 equiv). Traces of water were azeotropically removed by addition of three portions of benzene followed by rotary evaporation. PPh_3 (4.69 g, 17.87 mmol, 1.2 equiv) was added, and the headspace of the flask was evacuated and backfilled with nitrogen. THF (60 mL) was added, and the reaction mixture was cooled to 0 °C. Then, DIAD (3.52 mL, 17.87 mmol, 1.2 equiv) was added dropwise over 4 min. The reaction mixture was stirred at 0 °C for an additional 15 min, after which DPPA (3.85 mL, 17.87 mmol, 1.2 equiv) was added rapidly and the reaction mixture was allowed to warm to 23 °C. The reaction mixture became cloudy over several minutes. TLC analysis after 16 h indicated a high degree of

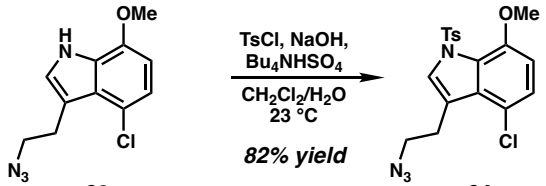
conversion to product. Stirring for another 24 h led to no change in the reaction profile by TLC analysis. The reaction mixture was concentrated under reduced pressure and purified by automated silica gel flash chromatography (Teledyne ISCO, 0→40% EtOAc/hexanes) to afford an intermediate azide as an orange-brown solid (2.50 g, 9.97 mmol, 67% yield).

^{1}H NMR (600 MHz, $CDCl_3$): δ 8.34 (s, 1H), 7.26 (s, 0H), 7.05 (d, *J* = 2.4 Hz, 1H), 6.98 (d, *J* = 8.2 Hz, 1H), 6.53 (d, *J* = 8.2 Hz, 1H), 3.93 (s, 3H), 3.59 (t, *J* = 7.2 Hz, 2H), 3.27 (td, *J* = 7.1, 0.8 Hz, 2H).

^{13}C NMR (100 MHz, $CDCl_3$): δ 145.2, 128.2, 124.5, 123.5, 120.3, 117.9, 113.2, 102.5, 55.6, 52.8, 25.9, 14.2.

IR (Neat Film, NaCl): 3890, 3864, 3668, 3316, 3132, 3084, 3008, 2938, 2876, 2588, 2492, 2352, 2204, 2106, 1768, 1652, 1630, 1574, 1494, 1464, 1450, 1434, 1380, 1332, 1294, 1272, 1236, 1194, 1172, 1154, 1130, 1070, 1034, 958, 930, 864, 830, 808, 782, 760, 740, 708, 684, 670, 662, 632, cm^{-1}.

HRMS (ESI+): *m/z* calc'd for $C_{11}H_{12}ClN_2O$ $[M+H]^+$: 223.0638, found 223.0630.



63 ***64***

Tosyl indole 64: To a 250 mL round bottom flask under air were added azide **63** (5.11 g, 20.4 mmol, 1.0 equiv), CH_2Cl_2 (41 mL), and Bu_4NHSO_4 (69 mg, 0.204 mmol, 1 mol %), followed by 50% w/v aq. NaOH (14 mL). After stirring for 5 min, TsCl (7.78 g, 40.8 mmol, 2.0 equiv) was added in a single portion. The reaction mixture was subjected to vigorous magnetic stirring for 10 min, then diluted with H_2O (100 mL) and CH_2Cl_2 (30 mL). The layers were separated, and the aqueous phase was extracted with CH_2Cl_2 (3x50 mL). The

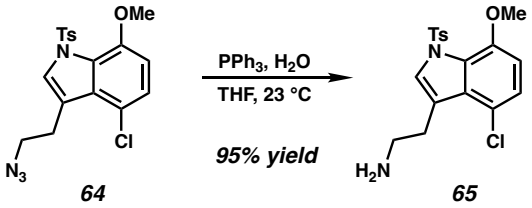
combined organic phases were washed with brine, dried over Na_2SO_4, and concentrated under reduced pressure. The crude product was purified by automated silica gel flash chromatography (Teledyne ISCO, 0→45% EtOAc/hexanes) to afford an intermediate tosyl indole as a white solid (6.77 g, 16.7 mmol, 82% yield).

^{1}H NMR (400 MHz, $CDCl_3$): δ 7.74 (s, 1H), 7.71 (d, *J* = 8.4 Hz, 2H), 7.29 – 7.26 (m, 2H), 7.08 (d, *J* = 8.5 Hz, 1H), 3.64 (s, 3H), 3.62 (d, *J* = 7.1 Hz, 2H), 3.26 (td, *J* = 7.1, 1.0 Hz, 2H), 2.40 (s, 3H).

^{13}C NMR (100 MHz, $CDCl_3$): δ 146.9, 144.9, 137.6, 129.9, 129.6, 128.6, 127.6, 126.7, 125.0, 118.5, 116.7, 108.0, 56.1, 52.2, 26.7, 22.1.

IR (Neat Film, NaCl): 3992, 3892, 3854, 3752, 3630, 3620, 3608, 3586, 3402, 3116, 2926, 2514, 2368, 2098, 1598, 1572, 1540, 1518, 1488, 1464, 1362, 1294, 1252, 1234, 1192, 1172, 1146, 1120, 1092, 1058, 994, 910, 858, 846, 808, 798, 772, 736, 702, 676, 662, 632, 624 cm^{-1}.

HRMS (ESI+): m/z calc'd for $C_{18}H_{17}ClN_4O_3SNa$ $[M+Na]^+$: 427.0608, found 427.0603.



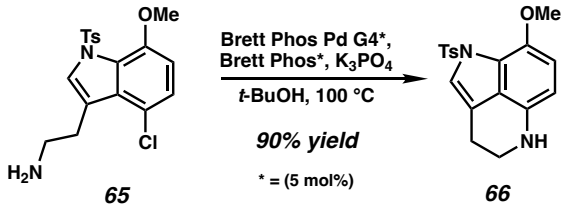
Tryptamine 65: To a 500 mL round bottom flask under air were added tosyl azide **64** (11.73 g, 28.97 mmol, 1.0 equiv), PPh_3 (9.88 g, 37.66 mmol, 1.3 equiv), and THF (190 mL). The reaction mixture was stirred at 23 °C for 15 h, whereafter deionized water (9.5 mL) was added. After an additional 30 h, the reaction mixture was concentrated under reduced pressure and purified by silica gel flash chromatography (10% MeOH/CH_2Cl_2 + 1% Et_3N) to afford the title compound as a white solid (10.41 g, 27.48 mmol, 95% yield).

^{1}H NMR (400 MHz, $CDCl_3$): δ 7.72 – 7.65 (m, 3H), 7.29 – 7.23 (m, 2H), 7.05 (d, *J* = 8.5 Hz, 1H), 6.56 (d, *J* = 8.5 Hz, 1H), 3.62 (s, 3H), 3.14 – 3.00 (m, 4H), 2.39 (s, 3H).

^{13}C NMR (100 MHz, $CDCl_3$): δ 146.5, 144.4, 137.4, 129.7, 129.5, 127.4, 127.2, 126.5, 124.6, 118.5, 118.1, 107.5, 55.8, 42.9, 30.7, 21.7.

IR (Neat Film, NaCl): 2938, 2686, 2595, 2515, 2363, 1574, 1487, 1366, 1290, 1237, 1171, 1092, 1052, 997, 937, 809, 662 cm^{-1}.

HRMS (ESI+): *m/z* calc'd for $C_{18}H_{20}ClN_2O_3S$ $[M+H]^+$: 379.0878, found 379.0877.



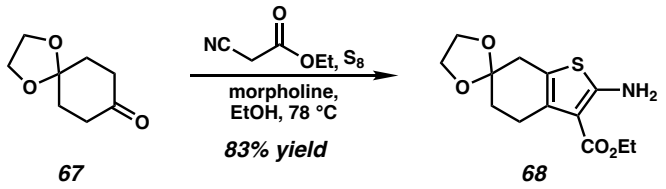
Tricycle 66: A 20 mL glass vial containing tryptamine **65** (1.0 g, 2.64 mmol, 1.0 equiv) was brought into a nitrogen-filled glovebox. To this vial were added BrettPhos Pd G4 (121 mg, 0.132 mmol, 5 mol %), BrettPhos (71 mg, 0.132 mmol, 5 mol %), and K_3PO_4 (784 mg, 3.70 mmol, 1.4 equiv), followed by *t*-BuOH (6.6 mL). The vial was sealed with a PTFE-lined cap and electrical tape, removed from the glovebox, and stirred at 100 °C in a metal heating block. After 3 days, the reaction mixture was partitioned between CH_2Cl_2 and water and the layers were separated. The aqueous phase was extracted with CH_2Cl_2 (3x), and the combined organic phases were concentrated under reduced pressure. The crude product was purified by silica gel flash chromatography (40% EtOAc/hexanes) to afford the title compound as a beige foam (816 mg, 2.38 mmol, 90% yield).

^{1}H NMR (400 MHz, $CDCl_3$): δ 7.79 (d, *J* = 8.4 Hz, 2H), 7.32 (s, 1H), 7.23 (d, *J* = 7.9 Hz, 2H), 6.56 (d, *J* = 8.1 Hz, 1H), 6.27 (d, *J* = 8.1 Hz, 1H), 3.70 (s, 3H), 3.37 (t, *J* = 5.9 Hz, 2H), 2.91 (t, *J* = 5.2 Hz, 2H), 2.36 (s, 3H).

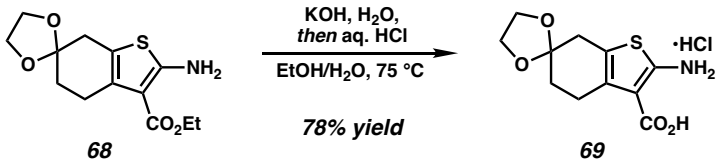
^{13}C NMR (100 MHz, $CDCl_3$): δ 144.1, 140.5, 137.1, 135.8, 129.4, 127.7, 124.0, 122.6, 120.2, 115.2, 110.7, 105.0, 57.5, 43.0, 22.8, 21.7.

IR (Neat Film, NaCl): 3384, 2956, 2834, 1595, 1512, 1421, 1356, 1260, 1170, 1103, 1035, 977, 937, 795, 664 cm^{-1}.

HRMS (ESI+): m/z calc'd for $C_{18}H_{19}N_2O_3S$ $[M+H]^+$: 343.1111, found 343.1127.



Aminothiophene 68: Prepared according to the procedure of Andersen, Møller, and coworkers from 1,4- cyclohexandione monoethylene ketal (**67**).[13] To a 500 mL round bottom flask were added 1,4- cyclohexanedione monoethylene ketal (**67**, 20 g, 128 mmol, 1.0 equiv), S_8 (4.1 g, 128 mmol, 1.0 equiv), ethyl cyanoacetate (14 mL, 128 mmol, 1.0 equiv), morpholine (11 mL, 128 mmol, 1.0 equiv), and EtOH (250 mL). The mixture was refluxed for 12 h, at which point TLC analysis showed full conversion. The reaction mixture was cooled to 23 °C and concentrated under reduced pressure until the amount of solution became approximately half. Then, the product was collected by vacuum filtration to afford aminothiophene **68** as a light-yellow solid (30.3 g, 107 mmol, 83% yield). All characterization data matched those reported in the literature.



Amino acid hydrochloride 69: To a 350 mL glass pressure vessel under air were added aminothiophene **68** (22.2 g, 78.35 mmol, 1.0 equiv), KOH (17.6 g, 313.4 mmol, 4.0 equiv), EtOH (165 mL), and water (33 mL). The flask was sealed, and the reaction mixture was

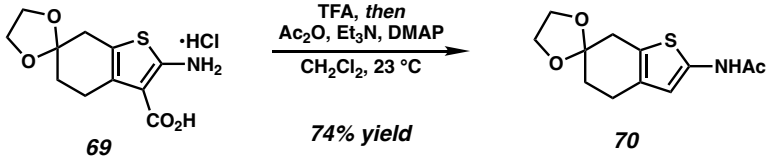
stirred at 75 °C in an oil bath for 12 h. The reaction mixture was subsequently transferred to an Erlenmeyer flask and cooled to 0 °C in an ice bath. The solution was acidified with 1 N aq. HCl (375 mL), resulting in the formation of a thick precipitate. The product was collected by vacuum filtration and washed with water. The resulting clay-like material was transferred to a round bottom flask with MeOH. The solvent was removed under reduced pressure and the product was dried under high vacuum to afford the title compound as a cream-colored powder (17.95 g, 61.53 mmol, 79% yield assuming complete conversion to hydrochloride). **Note**: Conducting this transformation in a vessel with increased headspace generally leads to lower yields, likely due to atmospheric oxidation.

^{1}H NMR (400 MHz, DMSO): δ 11.81 (br s, 1H), 7.20 (br s, 2H), 3.90 (s, 4H), 2.72 (t, J = 6.4 Hz, 2H), 2.59 (s, 2H), 1.75 (t, J = 6.5 Hz, 2H).

^{13}C NMR (100 MHz, DMSO): δ 166.7, 163.4, 130.9, 112.4, 107.6, 102.6, 63.9, 34.3, 31.0, 25.1.

IR (Neat Film, NaCl): 3409, 2890, 1635, 1580, 1474, 1451, 1353, 1294, 1267, 1105, 1054, 1036, 926, 642 cm^{-1}.

HRMS (ESI–): *m/z* calc'd for $C_{11}H_{12}NO_4S$ [M–H]$^-$: 254.0493, found 254.0494.



Acetamidothiophene 70: To a 500 mL round bottom flask containing hydrochloride salt **69** (10.78 g, 37.0 mmol, 1.0 equiv) were added CH_2Cl_2 (186 mL) and TFA (8.6 mL, 111 mmol, 3.0 equiv). After stirring for 2 h at 23 °C, DMAP (230 mg, 1.86 mmol, 5 mol %) and Et_3N (26 mL, 185 mmol, 5.0 equiv) were added rapidly, followed by acetic anhydride (5.25 mL, 56.0 mmol, 1.5 equiv). After an additional 4 h, the reaction mixture was

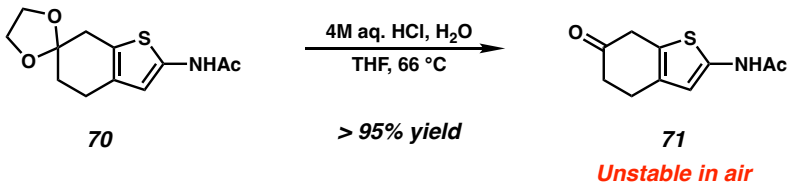
concentrated under reduced pressure and purified by silica gel flash chromatography (35% acetone/hexanes) to afford a crude product. Repurification by silica gel flash chromatography (30% acetone/hexanes) provided the title compound as a cream-colored solid (6.95 g, 27.4 mmol, 74% yield).

^{1}H NMR (400 MHz, C_6D_6): δ 6.64 (br s, 1H), 6.14 (s, 1H), 3.52 – 3.40 (m, 4H), 2.85 (s, 2H), 2.74 (tt, J = 6.5, 1.6 Hz, 2H), 1.86 (t, J = 6.5 Hz, 2H), 1.39 (s, 3H).

^{13}C NMR (100 MHz, C_6D_6): δ 165.7, 137.5, 130.9, 125.4, 111.7, 108.9, 64.5, 35.1, 34.9, 32.5, 32.4, 24.4, 22.7.

IR (Neat Film, NaCl): 3260, 3089, 3046, 2931, 2892, 1650, 1583, 1434, 1370, 1301, 1263, 1114, 1060, 986, 946, 837, 737 cm^{-1}.

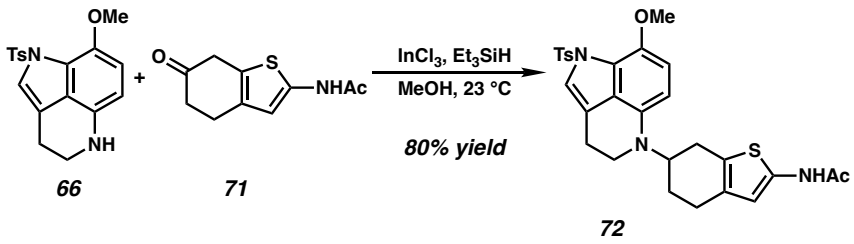
HRMS (ESI+): *m/z* calc'd for $C_{12}H_{16}NO_3S$ $[M+H]^+$: 254.0845, found 254.0847.



70 ***> 95% yield*** ***71***

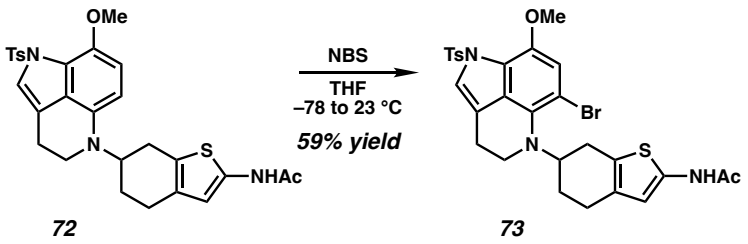
Unstable in air

Ketothiophene 71: To a 100 mL round bottom flask containing thiophene-ketal **70** (1.64 g, 5.34 mmol, 1.5 equiv) under nitrogen and equipped with a reflux condenser were added THF (27 mL) and 4 N aq. HCl (5.3 mL, 21.2 mmol, 4.0 equiv w.r.t. ketal). The reaction mixture was heated to reflux and stirred for 1.5 h, then allowed to cool and quenched with saturated aq. $NaHCO_3$ (100 mL). The resulting mixture was extracted with CH_2Cl_2 (3x40 mL). The combined organic extracts were washed with brine, and the brine phase was back-extracted once with CH_2Cl_2. The combined organic phases were dried over Na_2SO_4 and $MgSO_4$ and concentrated under reduced pressure to afford crude ketone **71** as an orange solid that was used directly without further purification**.**



Arene 72: To a 20 mL glass vial were added tricycle **66** (182 mg, 0.532 mmol, 1.0 equiv), the crude ketone prepared from ketal **70** (144 mg, 0.692 mmol, 1.3 equiv assuming a pure compound), and $InCl_3$ (235 mg, 1.06 mmol, 2.0 equiv). The headspace of the vial was evacuated and backfilled with nitrogen. Dry MeOH (3.6 mL) and triethylsilane (0.26 mL, 1.6 mmol, 3.0 equiv) were added by syringe and the reaction mixture was allowed to stir at 23 °C for 19 h. At this point, additional triethylsilane (0.26 mL, 1.6 mmol, 3.0 equiv) was added. After 2 more days, additional triethylsilane (0.26 mL, 1.6 mmol, 3.0 equiv) and intermediate ketone **71** (50 mg, 0.24 mmol, 0.45 equiv assuming a pure compound) were added. After stirring for an additional 21 h at 23 °C, the reaction mixture was diluted with saturated aq. $NaHCO_3$ and extracted with CH_2Cl_2 (3x). The combined organic extracts were dried over Na_2SO_4, concentrated under reduced pressure, and purified by silica gel flash chromatography (35% acetone/hexanes) to afford an intermediate tertiary aniline as an off-white foam (231 mg, 0.431 mmol, 80% yield).

^{1}H NMR (400 MHz, C_6D_6): δ 7.95 – 7.87 (m, 2H), 7.48 (s, 1H), 6.64 (d, J = 8.1 Hz, 2H), 6.50 (d, J = 8.3 Hz, 1H), 6.19 (s, 1H), 6.04 (d, J = 8.4 Hz, 1H), 3.90 – 3.74 (m, 1H), 3.56 (s, 3H), 2.79 – 2.61 (m, 3H), 2.57 – 2.40 (m, 5H), 1.73 (s, 3H), 1.71 – 1.64 (m, 1H), 1.62 – 1.56 (m, 1H), 1.55 (s, 3H).



72 *73*

Bromoarene 73: To a 50 mL round bottom flask was added this intermediate tertiary aniline (**72**, 103.4 mg, 0.193 mmol, 1.0 equiv), and the headspace of the flask was evacuated and backfilled with nitrogen. THF (5 mL) was added, and the flask was cooled to –78 °C. Subsequently, a solution of NBS (34.3 mg, 0.193 mmol, 1.0 equiv) was added by syringe pump over a period of 1 h with rapid stirring. After completion of the addition, the cooling bath was removed, and the reaction mixture was allowed to warm to 23 °C. The reaction mixture was concentrated under reduced pressure and purified by silica gel flash chromatography (30% acetone/hexanes) to afford the title compound as an off-white foam of sufficient purity for use in the next step (70 mg, 0.114 mmol, 59% yield); a nearly pure sample for analysis was obtained by preparative HPLC (SiO_2 column, 30→100% acetone/hexanes over 18 min at 12 mL/min).

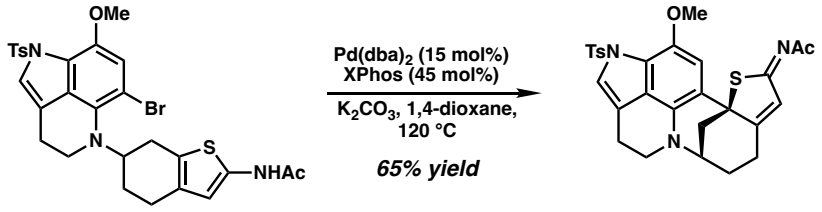
^{1}H NMR (400 MHz, C_6D_6): δ 7.86 – 7.80 (m, 2H), 7.52 (s, 1H), 7.35 (s, 1H), 6.75 (s, 1H), 6.65 (d, *J* = 8.1 Hz, 2H), 6.28 (s, 1H), 4.24 (ddq, *J* = 13.9, 7.9, 2.6 Hz, 1H), 3.21 (s, 3H), 3.05 – 2.91 (m, 2H), 2.86 (ddd, *J* = 13.9, 7.8, 4.9 Hz, 1H), 2.72 (ddd, *J* = 14.5, 11.3, 2.4 Hz, 1H), 2.55 – 2.36 (m, 2H), 2.35 – 2.18 (m, 2H), 1.87 – 1.69 (m, 1H), 1.76 (s, 3H), 1.59 – 1.49 (m, 1H), 1.56 (s, 3H).

^{13}C NMR (100 MHz, C_6D_6): δ 166.1, 144.0, 142.8, 137.9, 137.6, 134.8, 131.1, 129.5, 128.0, 127.7, 126.8, 123.1, 122.3, 115.4, 114.3, 112.2, 106.1, 59.9, 56.4, 43.1, 29.6, 28.8, 26.3, 22.8, 22.6, 21.1. Additional peaks in the ^{1}H NMR spectrum at 1.60 ppm and in the

^{13}C NMR spectrum at 29.2 and 176.8 ppm arise from an unknown impurity; correlations to the resonances of bromoarene **73** are not observed in a ^{1}H/^{13}C HMBC experiment.

IR (Neat Film, NaCl): 3256, 2932, 2842, 1713, 1582, 1487, 1347, 1288, 1228, 1169, 1112, 804, 684 cm^{-1}.

HRMS (ESI+): *m/z* calc'd for $C_{28}H_{29}BrN_3O_4S_2$ $[M+H]^+$: 614.0777, found 614.0786.



73 ***74***

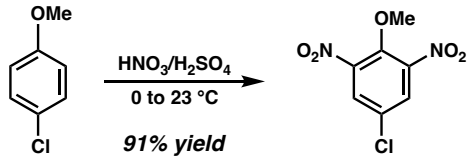
Thioimidate 74: To a 1-dram glass vial in a nitrogen-filled glovebox were added bromoarene **73** (18 mg, 0.0293 mmol, 1.0 equiv), 1,4-dioxane (0.3 mL), and K_2CO_3 (6.1 mg, 0.0441 mmol, 1.5 equiv). $Pd(dba)_2$ (2.5 mg, 0.0043 mmol, 0.15 equiv) and XPhos (3.5 mg, 0.0132 mmol, 0.45 equiv) were added as a stock solution in 1,4-dioxane (0.44 mL, prestirred for 10 min at 28 °C). The vial was sealed with a PTFE-lined cap, removed from the glovebox, and stirred at 120 °C in a metal heating block for 6 h. Then, the reaction mixture was allowed to cool to 23 °C and concentrated under reduced pressure. The crude product was purified by preparative TLC on silica gel (100% EtOAc) to afford the title compound as a brown solid (11.2 mg of material containing 10 wt % EtOAc by ^{1}H NMR analysis, 0.0189 mmol, 65% yield).

^{1}H NMR (400 MHz, C_6D_6): δ 7.87 – 7.82 (m, 2H), 7.47 (s, 1H), 6.86 (s, 1H), 6.62 – 6.56 (m, 2H), 6.11 (d, *J* = 1.4 Hz, 1H), 3.24 (s, 3H), 2.74 (p, *J* = 2.9 Hz, 1H), 2.72 – 2.55 (m, 2H), 2.51 – 2.42 (m, 2H), 2.38 (dt, *J* = 12.3, 2.7 Hz, 1H), 2.33 (s, 3H), 1.91 (dt, *J* = 13.9, 6.5 Hz, 1H), 1.72 (s, 3H), 1.69 – 1.58 (m, 3H), 0.84 – 0.70 (m, 1H).

^{13}C NMR (100 MHz, C_6D_6): δ 184.5, 183.6, 175.0, 143.8, 140.1, 137.9, 133.4, 129.4, 124.3, 123.2, 121.9, 120.9, 114.4, 112.4, 109.1, 63.5, 57.2, 52.9, 47.1, 40.3, 31.5, 27.6, 25.1, 23.0, 21.1 (an additional ^{13}C resonance associated with the tosyl group is likely obscured by the solvent signal).

IR (Neat Film, NaCl): 2924, 1665, 1503, 1362, 1285, 1234, 1172, 1106, 1004, 672 cm^{-1}.

HRMS (ESI+): *m/z* calc'd for $C_{28}H_{28}N_3O_4S_2$ $[M+H]^+$: 534.1516, found 534.1524.



82 ***83***

Dinitroarene 83: *Caution! Fuming nitric acid is extremely corrosive and oxidizing. Standard latex and nitrile gloves should not be used when using fuming nitric acid. Wear neoprene based gloves. All operations using fuming nitric acid should be conducted behind a safety shield.*

Behind a safety shield, a flame dried 500 mL 3-neck round-bottom flask equipped with a 100 mL additional funnel was charged with fuming nitric acid (40 mL) and brought to 5 °C. 4-chloroanisole (**82**, Combi-Blocks, 20.0 g, 140.27 mmol, 1.0 equiv) was added dropwise such that the temperature was kept below 30 °C (~ 30 min). The reaction mixture was then brought to 0 °C and concentrated sulfuric acid (20 mL) was added dropwise such that the temperature was kept below 20 °C (~ 30 min). The reaction mixture was then brought to 5 °C and fuming nitric acid (20 mL) was added dropwise such that the temperature was kept below 20 °C (~ 20 min). The reaction mixture was then stirred for 10 min at 23 °C. The reaction mixture was then poured onto ice (100 mL) and the yellow precipitate was collected via vacuum filtration. The yellow solid was rinsed with cold water and dried

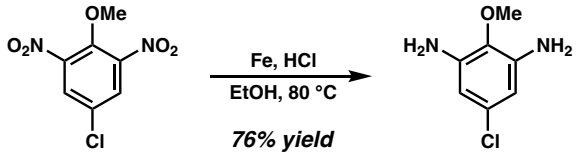
under vacuum for 16 h. This yellow solid was taken forward without additional purification. A small sample was purified by column chromatography (SiO_2, 5% EtOAc/Hexanes) for analytical characterization.

^{1}H NMR (400 MHz, $CDCl_3$): δ 8.04 (s, 2H), 4.07 (s, 3H).

^{13}C NMR (100 MHz, $CDCl_3$): δ 146.5, 145.7, 129.6, 129.3, 65.2.

IR (Neat Film, NaCl): 3082, 2964, 2324, 1608, 1531, 1475, 1421, 1401, 1363, 1254, 1172, 1097, 976, 922, 888, 806, 778, 754, 721 cm^1.

HRMS (GCFI+): *m/z* calc'd for $C_7H_5ClN_2O_5$ $[M]^{+\bullet}$: 231.9887, found 231.9876.



83 ***84***

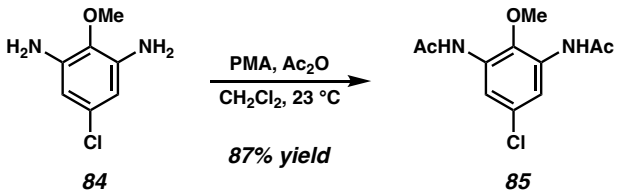
Dianiline 84: A flame dried 500 mL 3-neck round-bottom flask equipped with a reflux condenser was charged with dinitro arene **83** (15.0 g, 64.5 mmol, 1.0 equiv) in EtOH (184 mL, 0.35 M) and 1.5% aq. HCl (64.5 mL, 1 M). Iron (21.6 g, 387.0 mmol, 6 equiv) was added in 5 portions over 5 minutes. The reaction mixture was heated to 80 °C for 6 h, at which point TLC indicated consumption of the starting material. The crude reaction mixture was pushed through a pad of celite with EtOAc (200 mL). The filtrate was diluted with water (300 mL) and the product was extracted with EtOAc (3 x 300 mL). The combined organic layers were washed with brine, dried over Na_2SO_4, filtered, and concentrated under reduced pressure. The crude product was purified by column chromatography (SiO_2, 40%-50%-75% EtOAc/Hexanes) to afford the title compound (8.44 g, 76% yield) as an off white solid.

^{1}H NMR (400 MHz, $CDCl_3$): δ 6.15 (s, 2H), 3.78 – 3.72 (m, 7H).

^{13}C NMR (100 MHz, $CDCl_3$): δ 140.9, 133.0, 130.1, 106.2, 58.6.

IR (Neat film, NaCl): 3308, 2361, 1675, 1598, 1504, 1435, 1292, 1237, 991, 683 cm^{1}.

HRMS (ESI+): *m/z* calc'd for $C_7H_{10}ClN_2O$ $[M+H]^+$: 173.0476, found 173.0478.



84 ***85***

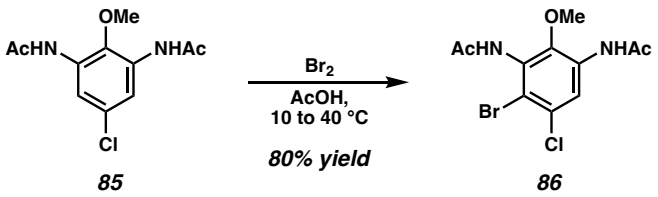
Diacetamide 85: Prepared using a modified literature procedure.[21] A flame dried 100 mL round-bottom flask was charged with dianline **84** (2.0 g, 11.6 mmol, 1.0 equiv) in CH_2Cl_2 (23 mL, 0.5 M). Acetic anhydride (2.4 mL, 25.52 mmol, 2.2 equiv) and phosphomolybdic acid (PMA, 423.0 mg, 0.23 mmol, 0.02 equiv) were then added. The reaction mixture was stirred at 23 °C for 3 h, at which point TLC indicated complete consumption of the starting material. The reaction mixture was diluted with water (100 mL) and ethyl acetate (150 mL) and the product was extracted with EtOAc (3 x 100 mL). The combined organic layers were washed with brine, dried over Na_2SO_4, filtered, and concentrated under reduced pressure to afford the title compound (2.57 g, 87% yield) as a brown solid which was taken forward without additional purification**.**

^{1}H NMR (400 MHz, $CDCl_3$): δ 8.08 (s, 2H), 7.47 (s, 2H), 3.77 (s, 3H), 2.23 (s, 6H).

^{13}C NMR (100 MHz, DMSO-d_6): δ 169.3, 139.4, 132.9, 127.1, 116.8, 60.5, 23.9.

IR (Neat film, NaCl): 3413, 3342, 3317, 3220, 2979, 1635, 1592, 1505, 1442, 1322, 1227, 1150, 1023, 985, 889, 816, 763, 714, 678 cm^{1}.

HRMS (ESI+): *m/z* calc'd for $C_{11}H_{14}ClN_2O_3$ $[M+H]^+$: 257.0687, found 257.0689.



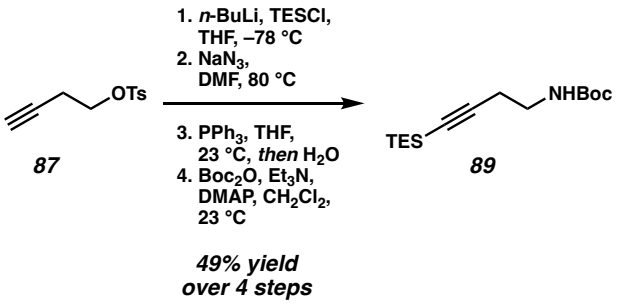
Bromoarene 86: A flame dried 50 mL round-bottom flask was charged with diacetamide **85** (2.57 g, 10.0 mmol, 1.0 equiv) in glacial acetic acid (14.0 mL, 0.73M). The solution was cooled to 10 °C and Br_2 (0.77 mL, 30.0 mmol, 3.0 equiv) was added dropwise over 2 min. The reaction mixture was warmed to 23 °C over 1 h and was then heated to 40 °C for 16 h, at which point LC/MS analysis indicated complete consumption of the starting material. The reaction mixture was poured into ice water (50 mL) and the precipitate was collected via vacuum filtration. The crude product was purified by column chromatography (SiO_2, 100% EtOAc) to afford the title compound (2.7 g, 80% yield) as a brown solid.

^{1}H NMR (600 MHz, DMSO-d_6): δ 9.74 (s, 1H), 9.60 (s, 1H), 8.31 (s, 1H), 3.67 (s, 3H), 2.14 (s, 3H), 2.07 (s, 3H).

^{13}C NMR (100 MHz, DMSO-d_6): δ 169.5, 168.6, 146.7, 132.4, 132.4, 128.0, 120.9, 117.9, 60.9, 23.9, 22.6.

IR (Neat film, NaCl): 3902, 3735**,** 3182, 3002, 2335,1665, 1583, 1514, 1458, 1399, 1370, 1267, 1227, 1165, 1086, 995, 911, 871, 835, 817, 770, 755, 700, 680, 612 cm^1.

HRMS (ESI+): *m/z* calc'd for $C_{11}H_{13}BrClN_2O_3$ $[M+H]^+$: 334.9793, found 334. 9794.



Alkyne 89: A flame dried 250 mL round-bottom flask was charged with but-3-yn-1-yl 4-methylbenzenesulfonate (**87**, 7.35 g, 32.77 mmol, 1.0 equiv) and THF (82.5 mL, 0.4 M). The solution was cooled to –78 °C and *n*-BuLi (15.73 mL, 39.33 mmol, 1.2 equiv) was added dropwise over 10 min. The solution was stirred at –78 °C for 30 min, at which point TESCl (6.6 mL, 39.33 mmol, 1.2 equiv) was added dropwise over 5 min. The reaction was stirred at –78 °C for 2 h, at which point TLC analysis indicated consumption of the starting material. The reaction mixture was warmed to 23 °C and saturated aq. NH_4Cl (100 mL) and EtOAc (100 mL) were added. The product was extracted with EtOAc (3 x 150 mL), the combined organic layers were washed with brine, dried over Na_2SO_4, filtered, and concentrated under reduced pressure to afford the intermediate silylated alkyne (10.27 g, 93% yield) as a yellow oil which was taken forward without additional purification. A small sample was purified via column chromatography (SiO_2, 5% EtOAc/Hexanes) for characterization.

^{1}H NMR (600 MHz, $CDCl_3$): δ 7.80 (d, J = 8.4 Hz, 2H), 7.35 (d, J = 8.0 Hz, 2H), 4.10 (t, J = 7.3 Hz, 2H), 2.62 (t, J = 7.3 Hz, 2H), 2.45 (s, 3H), 0.94 (t, J = 7.9 Hz, 9H), 0.54 (q, J = 7.9 Hz, 6H).

^{13}C NMR (100 MHz, $CDCl_3$): δ 145.0, 133.1, 130.0, 128.1, 101.5, 84.9, 67.8, 21.8, 20.9, 7.5, 4.4.

IR (Neat film, NaCl): 3859, 3552, 2955, 2911, 2875, 2732, 2178, 1598, 1494, 1458, 1413, 1367, 1307, 1290, 1237, 1189, 1179, 1097, 1062, 1018, 984, 905, 814, 763, 737, 686, 665 cm^{1}.

HRMS (GCFI+): *m/z* calc'd for $C_{17}H_{27}O_3SSi$ $[M+H]^+$: 339.1450, found 339.1450.

A flame dried 100 mL round-bottom flask was charged with the intermediate silylated alkyne (not shown, 10.27 g, 30.34 mmol, 1.0 equiv), DMF, (30.34 mL, 1.0 M), and NaN_3 (2.96 g, 45.5 mmol, 1.5 equiv). The reaction mixture was heated at 80 °C for 5h, at which point TLC analysis indicated consumption of the starting material. The reaction mixture was diluted with Et_2O (100 mL) and H_2O (200 mL). The product was extracted with Et_2O (3 x 150 mL), the combined organic layers were washed with 1M aq. LiCl (5 x 50 mL), dried over Na_2SO_4, filtered, and concentrated under reduced pressure to near dryness to afford an intermediate azide in a solution of Et_2O (~15 mL), which was taken forward to the next step without additional purification.

A flame dried 250 mL round-bottom flask was charged with a solution of the intermediate azide in Et_2O (15 mL, not shown) and THF (90 mL, 0.3 M). PPh_3 (11.94 g, 45.5 mmol, 1.5 equiv) was added in 5 portions over 5 min at 23 °C. The reaction mixture was stirred for 2 h at 23 °C, at which point ^1H NMR analysis indicated consumption of the azide. H_2O (6 mL, 5 M) was added and the reaction mixture was further stirred at 23 °C for 12 h. The reaction mixture was diluted with Et_2O (100 mL) and H_2O (200 mL). The product was extracted with Et_2O (3 x 150 mL), the combined organic layers were washed with brine, dried over Na_2SO_4, filtered, and concentrated under reduced pressure to near dryness to afford the title compound in a solution of Et_2O (~15 mL), which was taken forward to the next step without additional purification.

A flame dried 250 mL round-bottom flask was charged with a solution of the intermediate primary amine in Et_2O (15 mL, not shown), Boc_2O (7.28 g, 33.37 mmol, 1.1 equiv), CH_2Cl_2 (90 mL, 0.3 M), Et_3N (6.3 mL, 45.5 mmol, 1.5 equiv), and DMAP (366.0 mg, 3 mmol, 0.1 equiv). The reaction mixture was stirred at 23 °C for 12 h, at which point TLC analysis indicated consumption of the primary amine. The reaction mixture was diluted with Et_2O (200 mL) and H_2O (200 mL). The product was extracted with Et_2O (3 x 150 mL), the combined organic layers were washed with brine, dried over Na_2SO_4, filtered, and concentrated under reduced pressure. The crude product was purified by column chromatography (SiO_2, 5% EtOAc/Hexanes) to afford the title compound (4.56 g, 53% yield over 3 steps) as a yellow oil.

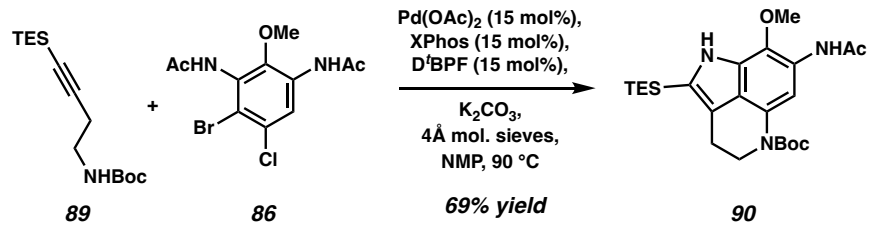
Additionally, we found that after isolation, another drying process of alkyne **89** led to better yields in the subsequent cyclization/annulation. This was achieved by first dissolving alkyne **89** in EtOAc and adding $MgSO_4$. This solution was then passed through a short plug of basic alumina followed by concentration under reduced pressure.

^{1}H NMR (600 MHz, $CDCl_3$): δ 4.81 (br s, 1H), 3.27 (q, J = 6.5 Hz, 2H), 2.43 (t, J = 6.6 Hz, 2H), 1.44 (s, 9H), 0.98 (t, J = 7.9 Hz, 9H), 0.58 (q, J = 7.9 Hz, 6H).

^{13}C NMR (100 MHz, $CDCl_3$): δ 155.9, 105.3, 83.8, 79.5, 39.5, 28.5, 21.4, 7.6, 4.6.

IR (Neat film, NaCl): 3354, 2954, 2912, 2875, 2173, 1696, 1520, 1458, 1391, 1365, 1248, 1176, 1072, 1004, 971, 870, 719, 738, cm^1.

HRMS (GCFI+): *m/z* calc'd for $C_{15}H_{30}NO_2Si$ $[M+H]^+$: 284.2046, found 284.2041.



General procedure A: Larock/Buchwald–Hartwig annulation/cyclization.

Note: This reaction was found to be water sensitive. It is critical to use freshly flame-dried K_2CO_3, freshly activated 4Å molecular sieves, and anhydrous NMP (Sigma-Aldrich, item# 328634).

Aminotricycle 90: In a nitrogen filled glovebox, to a flame dried 8 mL vial equipped with a magnetic stir bar was sequentially added K_2CO_3 (granular, freshly flame-dried, 303.4 mg, 2.2 mmol, 5.0 equiv), 4Å molecular sieves (powdered, freshly activated, 150 mg, 50 wt% with respect to K_2CO_3), $Pd(OAc)_2$ (Strem, 14.8 mg, 0.066 mmol, 0.15 equiv), XPhos (Combi Blocks, 31.4 mg, 0.066 mmol, 0.15 equiv), D*t*BPF (TCI, 31.3 mg, 0.066 mmol, 0.15 equiv), aryl bromide **86** (147.7 mg, 0.44 mmol, 1.0 equiv), alkyne **89** (622.6 mg, 2.2 mmol, 5.0 equiv), and NMP (4.4 mL, 0.1 M). The vial was sealed with a PTFE cap, removed from the glovebox, stirred at 1000 rpm, and heated at 90 °C for 24 h at which point LC/MS indicated consumption of the starting material. The reaction mixture was pushed through a short pad of celite with EtOAc (20 mL) and was diluted with 1 M aq. LiCl (30 mL). The product was extracted with EtOAc (5 x 30 mL). The combined organic layers were washed with 1M aq. LiCl (x3, 30 mL), dried over Na_2SO_4, filtered, and concentrated under reduced pressure. The crude product was purified by column chromatography (SiO_2, 50%-60-70% EtOAc/Hexanes) to afford the title compound (139.7 mg, 69% yield) as a brown solid. Additionally, unreacted alkyne **89** could be recovered in the first few collected fractions (483 mg, 90% recovery).

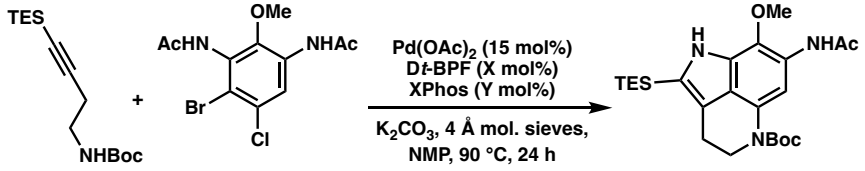
^{1}H NMR (600 MHz, CD_3OD): δ 10.10 (s, 1H), 7.54 (s, 1H), 3.98 (t, J = 5.7 Hz, 2H), 3.89 (s, 3H), 2.99 (t, J = 5.6 Hz, 2H), 2.18 (s, 3H), 1.56 (s, 9H), 1.00 (t, J = 7.7 Hz, 9H), 0.91 (q, J = 8.0 Hz, 6H).

Note: Two carbon signals are observed as a doublet due to hindered rotation about the C–N bond of the carbamate.

^{13}C NMR (100 MHz, CD_3OD): δ 172.3, 155.4, 136.0, 131.2 (d, J = 15.0 Hz), 129.8 (d, J = 16.7 Hz), 128.9, 125.0, 123.2, 121.7, 109.2, 82.4, 61.3, 46.8, 28.7, 25.6, 23.3, 7.7, 4.4.

IR (Neat film, NaCl): 3307, 2952, 2930, 2873, 2485, 1667, 1622, 1539, 1516, 1456, 1388, 1368, 1312, 1364, 1160, 1077, 1050, 1003, 977, 855, 737 cm^{1}.

HRMS (ESI+): *m/z* calc'd for $C_{24}H_{38}N_3O_4Si$ $[M+H]^+$: 460.2626, found 460.2625.



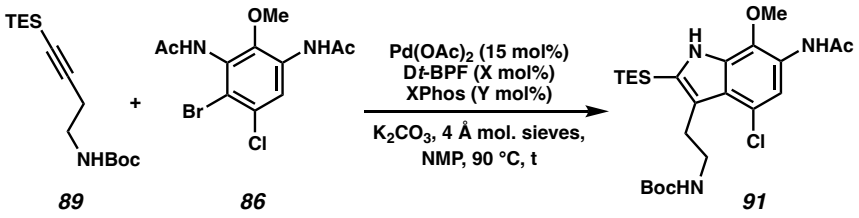
89 ***86*** ***90***

Entry	D*t*-BPF mol %	XPhos mol%	Yield[a]
1	30	0	3%
2	25	5	8%
3	20	10	10%
4	15	15	72%
5	10	20	64%
6	5	25	47%
7	0	30	36%

Ligand stoichiometry experiments: The reactions were set up according to general procedure A on 0.05 mmol scale, using the following modifications: A stock solution of XPhos was prepared in CH_2Cl_2 and the necessary amount was added to each vial via Hamilton syringe. The CH_2Cl_2 was evaporated by blowing air into the vial using a pipette.

After the CH_2Cl_2 was evaporated, the vial was charged with K_2CO_3 and 4 Å mol. sieves. Stock solutions of bromoarene **86**, D*t*-BPF, and $Pd(OAc)_2$ were prepared in NMP, and added to the reaction vial via Hamilton syringe. Alkyne **89** was then added. After 24 h, 0.05 mmol of 1,3,5-trimethoxybenzene was added to the reaction vial. It was sealed and stirred for 20 seconds to ensure mixing. A pipette tip of the reaction mixture was then added to an LC/MS vial which was further diluted with 1 mL of MeCN. Yields were calculated based on the areas under the curve at 230 nM using calibration curves.

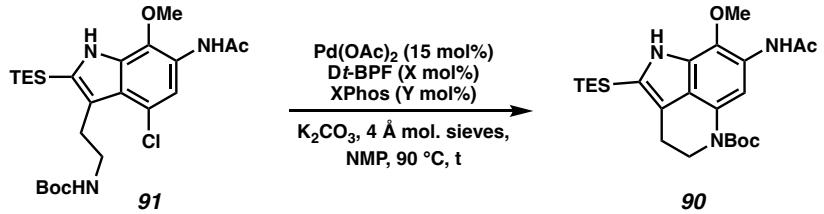
A) Investigation of the Larock indolization step.



89 ***86*** ***91***

Entry	D*t*-BPF mol %	XPhos mol%	Time	Yield[a]
1	30	0	20 h	45%
2	15	15	8 h	62%
3	0	30	11 h	44%

B) Investigation of the Buchwald–Hartwig cyclization step

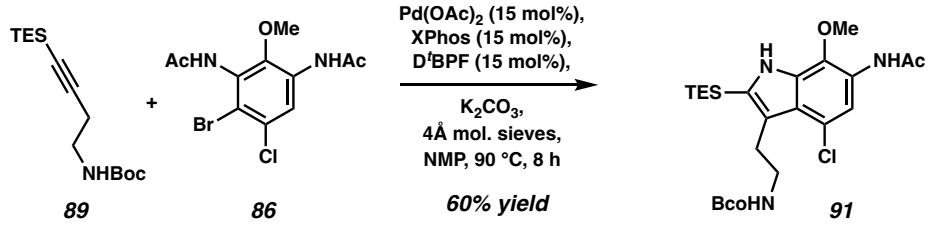


91 ***90***

Entry	D*t*-BPF mol %	XPhos mol%	Time	Yield[a]
1	30	0	24 h	20%
2	15	15	16 h	87%
3	0	30	8 h	88%[b]

Ligand stoichiometry experiments of each individual step of the tandem annulation/cyclization: These experiments were set up following the procedure described on the previous page with the following modification: Reaction vials were sealed with a red septa cap and connected to a nitrogen line. Aliquots were taken every 1 h until

bromoarene **86** was fully consumed, at which point the reaction vial was opened to air and yields were obtained as described on the previous page.



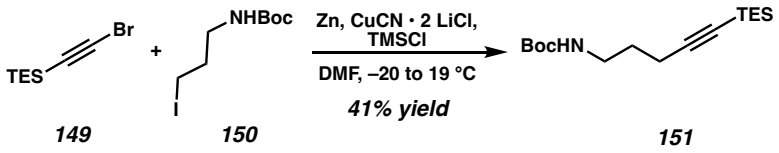
Indole 91: Prepared according to general procedure A, except the reaction was monitored by LC/MS every hour until bromo arene **86** was consumed. Purification by column chromatography (SiO_2, 40-50-60% ethyl acetate/hexanes) afforded the title compound (60% yield) as an off-white foam.

^{1}H NMR (400 MHz, DMSO-d$_6$): δ 10.61 (s, 1H), 9.40 (s, 1H), 7.43 (s, 1H), 6.97 (t, J = 5.6 Hz, 1H), 3.78 (s, 3H), 3.17 3.11 (m, 2H), 3.01 – 2.97 (m, 2H), 2.10 (s, 3H), 1.38 (s, 9H), 0.94 – 0.92 (m, 15H).

^{13}C NMR (100 MHz DMSO-d$_6$): δ 168.7, 155.5, 136.2, 134.2, 133.4, 124.6, 123.3, 122.5, 118.3, 116.4, 77.3, 60.6, 43.5, 28.3, 26.8, 23.6, 7.4, 3.1.

IR (Neat film, NaCl): 3298, 2954, 2874, 2173, 1693, 1618, 1585, 1506, 1366, 1249, 1169, 1062, 1002, 962, 856, 734, 683 cm[1].

HRMS (ESI+): *m/z* calc'd for $C_{20}H_{31}ClN_3O_4Si$ $[M+H]^+$: 440.1767, found 440.1773.



Alkyne 151: Alkyl iodide **150** and bromo alkyne **149** were prepared as previously described[42,43], then coupled by the conditions by Baran and coworkers.[43] Briefly, a flame-dried flask was charged with zinc dust (235 mg, 3.6 mmol, 3.6 equiv), DMF (1.5 mL), and 1,2-dibromoethane (0.017 mL, 0.2 mmol, 0.2 equiv). The suspension was heated at 80 °C

for 30 minutes. After cooling to 19 °C, trimethylsilylchloride (0.013 mL, 0.1 mmol, 0.1 equiv, freshly distilled over CaH_2) was added and the suspension was stirred an additional 30 minutes at 19 °C. To this suspension was slowly added (ca. 2 min) a DMF solution of the alkyl iodide **150** (285.1 mg, 1 mmol, 1 equiv, 0.1 mL DMF) which resulted in an exotherm. After returning to 19 °C, stirring was ceased and the alkyl zinc reagent was transferred dropwise via cannula to a cooled (–20 °C) DMF solution of CuCN (80.6 mg, 0.9 mmol, 0.9 equiv) and LiCl (76.3 mg, 1.8 mmol, 1.8 equiv) in DMF (2.5 mL; 0.25 M, total volume relative to alkyl iodide).

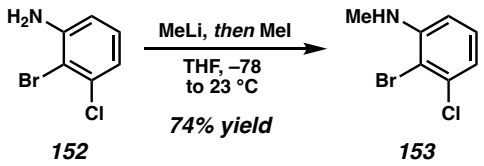
After a period of 15 minutes, neat bromo acetylene **149** (306.6 mg, 1.4 mmol, 1.4 equiv) was added dropwise to the reaction mixture at –20 °C. The reaction mixture was then allowed to slowly warm to 19 °C over a 3 hour period, and was further stirred at that temperature for an additional 8 hours. At this time the reaction was quenched by the addition of brine (20 mL) and extracted with Et_2O (4 × 50 mL). The organic extracts were washed with brine (5 x 100 mL), dried over $MgSO_4$, filtered, and concentrated under reduced pressure. The product was purified using silica gel flash column chromatography (5 to 15% EtOAc/hexanes) to afford the title compound (168 mg, 41 %) as a light-yellow oil.

^{1}H NMR (400 MHz, $CDCl_3$): δ 4.78 (s, 1H), 3.23 (q, J = 6.5 Hz, 2H), 2.29 (t, J = 6.9 Hz, 2H), 1.74 – 1.67 (m, 2H), 1.43 (s, 9H), 0.97 (t, J = 7.9 Hz, 9H), 0.56 (q, J = 7.9 Hz, 6H);

^{13}C NMR (100 MHz, $CDCl_3$): δ 156.1, 107.6, 82.7, 79.3, 40.0, 28.9, 28.5, 17.7, 7.6, 4.6;

IR (Neat film, NaCl): 3351, 2925, 2171, 1684, 1404, 1298, 1169, 1112, 983, 739 cm^1.

HRMS (GCFI+): *m/z* calc'd for $C_{16}H_{32}NO_2Si$ $[M+H]^+$: 298.2202, found 298.2200.



152 ***153***

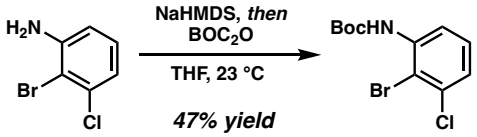
***N*-methyl aniline 153:** A flame dried round-bottom flask was charged with 2-bromo-3-chloroaniline (**152,** 300.0 mg, 1.45 mmol, 1.0 equiv) in THF (14.5 mL, 0.1 M). The solution was cooled to –78 °C and MeLi (3.1 M in diethoxymethane, 4.68 mL, 1.45 mmol, 1.0 equiv) was added dropwise over 1 h. The resultant solution was stirred for 30 min at –78 °C, at which point MeI (0.118 mL, 1.89 mmol, 1.3 equiv) in THF (0.63 mL) was added dropwise over 1 min. The resultant solution was stirred for 1 h at –78 °C, and was then warmed to 23 °C. The reaction was diluted with EtOAc (50 mL) and water (50 mL) and the product was extracted with EtOAc (3 x 50 mL). The combined organic layers were washed with brine, dried over Na_2SO_4, filtered, and concentrated under reduced pressure. The crude product was purified by column chromatography (SiO_2, 5%-10% EtOAc/Hexanes) to afford the title compound (234.5 mg, 74% yield) as a yellow oil.

^{1}H NMR (400 MHz, MeOD): δ 7.13 (t, *J* = 8.1 Hz, 1H), 6.75 (dd, *J* = 7.9, 1.4 Hz, 1H), 6.54 (dd, *J* = 8.3, 1.4 Hz, 1H), 2.85 (s, 3H).

^{13}C NMR (100 MHz, MeOD): δ 149.6, 135.7, 129.8, 118.2, 109.5, 109.4, 30.8.

IR (Neat film, NaCl): 3423, 3075, 2988, 2934, 2901, 2821, 1906, 1715, 1595, 1508, 1457, 1426, 1390, 1319, 1281, 1171, 1135, 1100, 1070, 1019,862, 762, 718, 697 cm[1].

HRMS (ESI+): m/z calc'd for C_7H_8BrClN [M+H$^+$]: 219.9523, found 219.9517.



152 ***154***

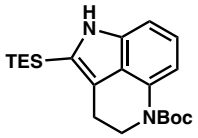
***N*-Boc aniline 154:** A flame dried round-bottom flask was charged with 2-bromo-3-chloroaniline (**152,** 300.0 mg, 1.45 mmol, 1.0 equiv) in THF (10.0 mL, 0.145 M). NaHMDS (531.0 mg, 2.9 mmol, 2.0 equiv) in THF (3.0 mL) was added dropwise over 2 min at 23 °C. The resulting solution was allowed to stir for 20 min. Boc_2O (348.0 mg, 1.6 mmol, 1.1 equiv) in THF (2 mL) was then added dropwise over 2 min, and the reaction mixture was stirred for 2 h. The reaction was diluted with EtOAc (50 mL) and water (50 mL) and the product was extracted with EtOAc (3 x 50 mL). The combined organic layers were washed with brine, dried over Na_2SO_4, filtered, and concentrated under reduced pressure. The crude product was purified by column chromatography (SiO_2, 1-2-3-5% EtOAc/Hexanes) to afford the title compound (207.2 mg, 47% yield) as an orange solid.

^{1}H NMR (400 MHz, MeOD): δ 7.73 (dd, *J* = 7.2, 2.4 Hz, 1H), 7.33 – 7.22 (m, 2H), 1.52 (s, 9H).

^{13}C NMR (100 MHz, MeOD): δ 154.8, 139.9, 135.9, 129.5, 126.6, 122.9, 117.3, 82.0, 28.5.

IR (Neat film, NaCl): 3140, 3106, 2997, 2930, 1849, 1721, 1570, 1520, 1453, 1400, 1368, 1329, 1297, 1232, 1178, 1165, 1063, 1024, 878, 772, 758, 697, 622 cm^1.

HRMS (GCFI+): m/z calc'd for $C_{11}H_{13}NO_2ClBr$ $[M]^{+\bullet}$: 304.9818, found 304.9805.



92

Tricycle 92: Prepared according to general procedure A using 2-bromo-3-chloroaniline **152**(Combi Blocks, 20.6 mg, 0.1 mmol) and alkyne **89**. Purification by column chromatography (SiO_2, 2-5% EtOAc/Hexanes) afforded the title compound (27.6 mg, 75% yield) as a white solid.

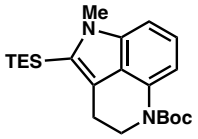
Additionally, this compound could be prepared according to general procedure A with only 5 mol% catalyst and ligand loading to afford the title compound in 71% yield (26.5 mg).

^{1}H NMR (600 MHz, $CDCl_3$): δ 7.82 (s, 1H), 7.29 (s, 1H), 7.11 (t, J = 7.9 Hz, 1H), 7.02 (d, J = 8.1 Hz, 1H), 4.10 – 4.06 (m, 2H), 3.05 – 3.03 (m, 2H), 1.58 (s, 9H), 1.00 (t, J = 7.8 Hz, 9H), 0.85 (q, J = 7.8 Hz, 6H).

^{13}C NMR (100 MHz, MeOD): δ 155.6, 139.4, 133.7, 128.4, 123.6, 122.9, 120.5, 110.0, 107.1, 82.2, 46.9, 28.7, 25.7, 7.7, 4.5.

IR (Neat film, NaCl): 3356, 2953, 2877, 2505, 1673, 1594, 1391, 1313, 1232, 1210, 1165, 1005, 9811, 845, 765, 737, 720 cm^1.

HRMS (ESI+): *m/z* calc'd for $C_{21}H_{33}N_2O_2Si$ $[M+H]^+$: 373.2306, found 373.2303.



93

***N*-Me tricycle 93:** Prepared according to general procedure A using 2-bromo-3-chloro-*N*-methylaniline (**153**, 22.0 mg, 0.1 mmol) and alkyne **89**. Purification by column chromatography (SiO_2, 2-4-6-8% EtOAc/Hexanes), followed by preparative TLC (10% EtOAc/Hexanes) afforded the title compound (29.4 mg, 76% yield) as a white solid.

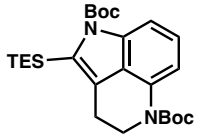
^{1}H NMR (400 MHz, MeOD): δ 7.22 (m, 1H), 7.08 (t, *J* = 7.9 Hz, 1H), 6.96 (d, *J* = 8.2, 1H), 3.98 (t, *J* = 5.6 Hz, 2H), 3.78 (s, 3H), 3.03 (t, *J* 5.7 Hz, 2H), 1.55 (s, 9H), 1.01 – 0.91 (m, 15H).

Note: The product was observed as a mixture of rotamers in the ^{13}C NMR.

^{13}C NMR (100 MHz, MeOD): δ 169.3, 155.4, 140.6, 133.9, 133.6, 132.4, 130.6, 129.8, 124.1, 122.4, 122.2, 110.1, 105.0, 82.3, 69.1, 46.8, 40.1, 33.6, 31.6, 30.1, 28.7, 26.2, 24.9, 24.0, 14.4, 11.4, 7.8, 5.2.

IR (Neat film, NaCl): 2952, 2926, 2874, 1694, 1598, 1463, 1454, 1388, 1352, 1316, 1293, 1227, 1162, 1129, 103, 938, 834, 811, 779, 764, 734.

HRMS (ESI+): *m/z* calc'd for $C_{18}H_{21}N_2O_2Si$ (- *t*-Bu) $[M+H]^+$: 331.1836, found 331.1835.



94

***N*-Boc tricycle 94:** Prepared according to general procedure A using *tert*-butyl (2-bromo-3-chlorophenyl)carbamate (arene **154**, 30.6 mg, 0.1 mmol) and alkyne **89**. Purification by column chromatography (SiO_2, 2% to 3% to 5% ethyl acetate/hexanes) afforded the title compound (13.5 mg, 29% yield) as a white solid.

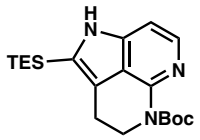
^{1}H NMR (400 MHz, MeOD): δ 7.53 (d, *J* = 8.2 Hz, 1H), 7.44 (d, *J* = 7.9 Hz, 1H), 7.20 (t, *J* = 8.1 Hz, 1H), 4.00 – 3.93 (m, 2H), 3.04 (dd, *J* = 6.4, 5.3 Hz, 2H), 1.70 (s, 9H), 1.57 (s, 9H), 0.96 – 0.93 (m, 15H).

Note: The product was observed as a mixture of rotamers in the ^{13}C NMR.

^{13}C NMR (100 MHz, MeOD): δ 155.0, 153.1, 137.9, 134.3, 132.4, 131.5, 129.9, 129.2, 126.5, 124.3, 114.6, 111.4, 84.9, 82.7, 69.1, 46.2, 40.2, 28.6, 28.5, 8.3, 5.9.

IR (Neat film, NaCl): 3124, 3052, 2932, 2856, 1726, 1595, 1508, 1449, 1365, 1265, 1147, 1107, 1056, 996, 739, 703, 661 cm[1].

HRMS (ESI+): *m/z* calc'd for $C_{22}H_{33}N_2O_4Si$ (- *t*-Bu) $[M+H]^+$: 417. 2204, found 417.2200.



95

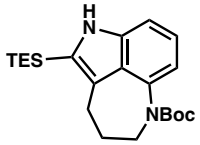
Azaindole 95: Prepared according to general procedure A using 4-amino-3-bromo-2-chloropyridine (Combi Blocks, 20.7 mg, 0.1 mmol) and alkyne **89**. Purification by column chromatography (SiO_2, 4% acetone/hexanes) afforded the title compound (15.1 mg, 41% yield) as a brown solid.

^{1}H NMR (600 MHz, $CDCl_3$): δ 8.11 (s, 1H) 8.09 (d, *J* = 5.8 Hz, 1H), 6.94 (d, *J* = 5.9 Hz, 1H), 4.14 (t, *J* = 5.7 Hz, 2H), 3.02 (t, *J* = 5.7 Hz, 2H), 1.57 (s, 9H), 0.99 (t, *J* = 7.9 Hz, 9H), 0.85 (q, *J* = 7.8 Hz, 6H).

^{13}C NMR (100 MHz, $CDCl_3$): δ 152.7, 148.2, 141.1, 140.9, 128.5, 121.9, 117.4, 102.7, 81.4, 47.0, 28.5, 24.5, 7.5, 3.6.

IR (Neat film, NaCl): 3302, 2954, 1700, 1600, 1380, 1311, 1244, 1153, 1052, 1007, 982, 906, 729 cm[1].

HRMS (ESI+): *m/z* calc'd for $C_{16}H_{24}N_3O_2Si$ (- *t*-Bu) $[M+H]^+$: 318.1632, found 318.1646.



96

Tricycle 96: Prepared according to general procedure A using 2-bromo-3-chloroaniline (**152**, 20.6 mg, 0.1 mmol) and alkyne **151**. Purification by column chromatography (SiO_2, 4% acetone/hexanes) afforded the title compound (22.0 mg, 57% yield) as a white solid.

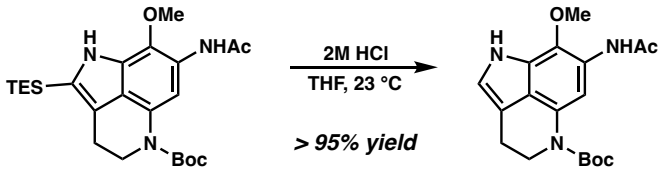
^{1}H NMR (600 MHz, $CDCl_3$): δ 7.84 (s, 1H), 7.14 – 7.05 (m, 2H), 7.01 (d, J = 7.5 Hz, 1H), 3.87 (t, J = 6.2 Hz, 2H), 3.01 (t, J = 6.9 Hz, 2H), 2.17 (tt, J = 6.9, 6.2 Hz, 2H), 1.52 (s, 9H), 1.01 (t, J = 7.8 Hz, 9H), 0.87 (q, J = 7.8 Hz, 6H).

Note: This compound was observed as a mixture of rotamers in the ^{13}C NMR spectrum.

^{13}C NMR (100 MHz, MeOD): δ 156.5, 141.7, 141.6, 137.4, 131.1, 131.0, 126.3, 126.2, 124.7, 124.6, 115.8, 109.5, 109.5, 81.5, 50.9, 29.5, 24.9, 7.8, 4.6.

IR (Neat film, NaCl): 3344, 2952, 2874, 2496, 1667, 1609, 1581, 1453, 1392, 1366, 1324, 1219, 1172, 1107, 1003, 982, 735 cm^{1}.

HRMS (ESI+): *m/z* calc'd for $C_{18}H_{27}N_2O_2Si$ (- *t*-Bu) $[M+H]^+$: 331.1836, found 331.1836.



90 ***97***

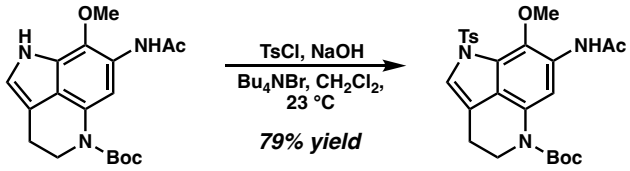
Desilylated amino tricycle 97: To a 20 mL vial under an ambient atmosphere was added tricycle **90** (134.0 mg, 0.29 mmol, 1.0 equiv), THF (2.9 mL, 0.1 M), and 2 M aq. HCl (2.9 mL, 0.1 M). The reaction mixture was stirred at 23 °C for 4 h, at which point LC/MS analysis indicated complete consumption of the starting material. Aq. saturated $NaHCO_3$ (10 mL) was added, and the reaction mixture was transferred to a separatory funnel with EtOAc. The mixture was further diluted with EtOAc (30 mL) and water (30 mL). The product was extracted with EtOAc (3 x 30 mL), the combined organic layers were washed with brine, dried over Na_2SO_4, filtered, and concentrated under reduced pressure to afford the title compound (97.1 mg, quantitative yield) as a brown solid, which was taken directly forward without further purification.

^{1}H NMR (400 MHz, CD_3OD) δ 7.54 (s, 1H), 6.88 (s, 1H), 3.97 (t, J = 5.6 Hz, 2H), 3.92 (s, 3H), 2.92 (t, J = 5.7 Hz, 2H), 2.17 (s, 3H), 1.56 (s, 9H).

^{13}C NMR (100 MHz, CD_3OD): δ 172.3, 155.4, 136.4, 128.9, 127.7, 124.2, 122.5, 119.4, 111.2, 109.6, 82.4, 60.9, 46.6, 28.7, 23.8, 23.3.

IR (Neat film, NaCl): 3317, 2972, 2929, 2444, 1668, 1510, 1389, 1367, 1326, 1264, 1247, 1206, 1160, 1125, 1037, 969, 873 cm[1].

HRMS (ESI+): *m/z* calc'd for $C_{14}H_{16}N_3O_4$ (loss of *t*Bu) $[M+H]^+$: 290.1135, found 290.1135.



97 ***98***

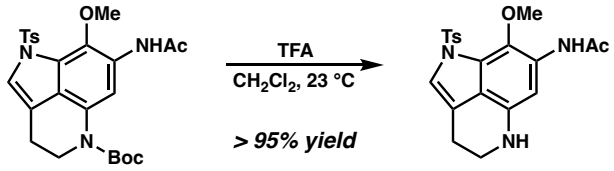
Tosylated amino tricycle 98: A flame-dried 1 dram vial was charged with indole **97** (25 mg, 0.0724 mmol, 1.0 equiv), TsCl (28 mg, 0.145 mmol, 2.0 equiv), Bu_4NBr (2.4 mg, 0.00724 mmol, 0.1 equiv), and powdered KOH (13 mg, 0.217 mmol, 3.0 equiv). The vial was evacuated and backfilled with nitrogen, then CH_2Cl_2 (0.72 mL, 0.1M) was added, and the resulting suspension was stirred at 23 °C for 30 min. The reaction was diluted with CH_2Cl_2 (5 mL) and water (5 mL) and the layers were separated. The aqueous layer was extracted with CH_2Cl_2 (3x3 mL), the combined organic extracts were dried with Na_2SO_4, and concentrated under reduced pressure. The crude product was purified by silica gel flash chromatography (15% EtOAc/hexanes to 50% EtOAc/hexanes) to afford the title compound (28.5 mg, 0.0571 mmol, 79%) as a yellow solid.

^{1}H NMR (400 MHz, C_6D_6): δ 9.11 (s, 1H), 7.85 (d, J = 8.3 Hz, 2H), 7.33 – 7.20 (m, 2H), 6.65 (d, J = 8.3 Hz, 2H), 3.76 (t, J = 5.7 Hz, 2H), 3.66 (s, 3H), 2.29 (m, 2H), 1.67 (s, 3H), 1.64 – 1.46 (m, 12H).

^{13}C NMR (100 MHz, C_6D_6): δ 167.1, 153.5, 144.4, 144.3, 136.6, 132.8, 130.9, 130.5, 129.7, 125.8, 121.7, 121.6, 117.0, 110.5, 81.8, 61.6, 44.3, 28.5, 24.3, 22.5, 21.1.

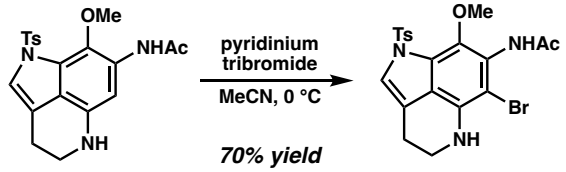
IR (Neat film, NaCl): 3301, 3133, 2978, 2933, 1693, 1681, 1613, 1530, 1470, 1370, 1328, 1306, 1271, 1168, 1094, 849, 800, 766, 735, 703, 681, 667 cm[1].

HRMS (FD+): *m/z* calc'd for $C_{25}H_{29}N_3O_6S$ $[M+H]^+$: 500.1855, found 500.1866.



98 ***99***

Deprotected amino tricycle 99: A flame-dried 1 dram vial was charged with indole **98** (28.5 mg, 0.0571 mmol, 1.0 equiv), CH_2Cl_2 (0.57 mL, 0.1M), and TFA (0.13 mL, 1.71 mmol, 30 equiv). The resulting mixture was stirred at 23 °C for 2 h, at which point LC/MS analysis showed full consumption of starting material. The reaction was diluted with CH_2Cl_2 (7 mL), washed with sat. $NaHCO_3$ (3x5 mL), and dried over Na_2SO_4, and concentrated under reduced pressure afford the intermediate secondary aniline which was used directly without further purification.



99 ***100***

Brominated amino tricycle 100: A 20 mL flame-dried vial containing intermediate secondary aniline (**99**, *ca.*0.0571 mmol, 1.0 equiv) was charged with MeCN (4.0 mL,

0.14M). The resulting solution was cooled to 0 °C with ice/water bath, and pyridinium tribromide ($PyHBr_3$, 16.4 mg, 0.0514 mmol, 0.9 equiv) in MeCN (1.7 mL) was then added. The mixture was stirred at 0 °C for 30 min, at which point LC/MS indicated near full consumption of the starting material. The reaction mixture was concentrated under reduced pressure, and resulting residue was purified by preparatory TLC (100% EtOAc) to afford the title compound (19.3 mg, 0.0404 mmol, 70% over 2 steps) as a brown oil.

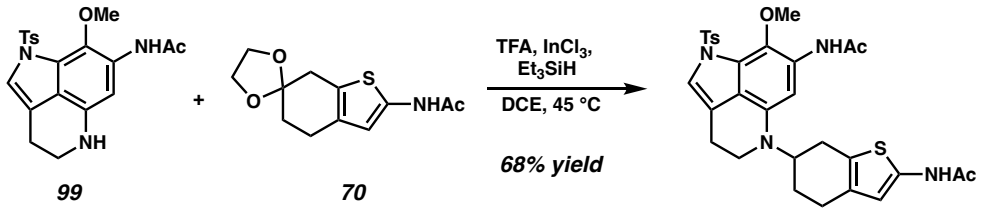
Note: This compound was observed as a mixture of rotamers due to hindered rotation about the amide C–N bond.

^{1}H NMR (400 MHz, C_6D_6): δ 7.97 – 7.79 (m, 2H), 7.31 (s, 1H), 6.73 – 6.57 (m, 2H), 3.87 (s, 1H), 3.79 – 3.71 (m, 3H), 2.66 – 2.52 (m, 2H), 2.32 – 2.44 (m, 2H), 1.74 – 1.61 (m, 6H).

^{13}C NMR (100 MHz, C_6D_6): δ 172.5, 168.0, 144.3, 137.7, 137.4, 136.8, 136.1, 129.7, 129.6, 126.2, 122.0, 121.7, 121.2, 115.5, 115.0, 100.9, 99.8, 62.1, 61.8, 42.0, 22.9, 22.2, 21.0.

IR (Neat film, NaCl): 2919, 1813, 1688, 1504, 1353, 1288, 1167, 1138, 1106, 1055, 814, 665 cm^1.

HRMS (FD+): *m/z* calc'd for $C_{20}H_{21}BrN_3O_4S$ $[M+H]^+$: 478.0436, found 478.0441.



Amino tricycle 102: A flame-dried 1 dram vial was charged with ketal **70** (25.3 mg, 0.1 mmol, 2.0 equiv). The vial was evacuated and backfilled with N_2 (x3). Then, DCE (0.5 mL, 0.1M) and TFA (0.1mL, 0.5M) were added and the resulting solution was heated to 45 °C for 7 hours, at which point LC/MS analysis indicated complete consumption of ketal **70**.

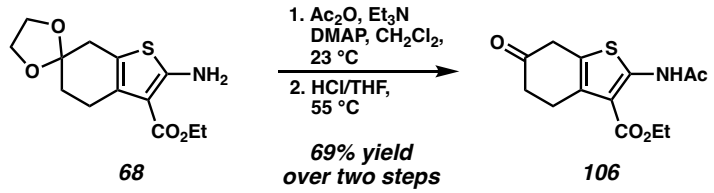
The reaction mixture was cooled to 23 °C and tricycle **99** (20.0 mg, 0.05 mmol, 1.0 equiv) in DCE (0.5 mL, 0.1 M) was then added. The vial septa was briefly removed and $InCl_3$ (22.1 mg, 0.1 mmol, 2.0 equiv) was added rapidly. The reaction vial was then rapidly evacuated and refilled with nitrogen (x10) such that solvent boiling was not observed. Et_3SiH (0.016 mL, 0.1 mmol, 2.0 equiv) was added and the resulting solution was heated to 45 °C for 16 h, at which point LC/MS analysis showed incomplete consumption of tricycle **99**. Additional Et_3SiH (0.016 mL, 0.1 mmol, 2.0 equiv) was added and the reaction was stirred at 45 °C for an additional 8 hours, at which point LC/MS analysis showed complete consumption of tricycle **99**. A small amount of silica gel was added directly to the reaction vial and the reaction mixture was concentrated under reduced pressure. The resulting free flowing silica mixture was purified by column chromatography (SiO_2, 40 to 45 to 50% acetone/hexanes) afforded the title compound (20.3 mg, 68% yield) as a brown film.

^{1}H NMR (400 MHz, Acetone-d6): δ 10.03 (s, 1H), 8.59 (s, 1H), 7.81 (d, J = 8.4 Hz, 2H), 7.43 (s, 1H), 7.42 – 7.20 (m, 2H), 7.22 (s, 1H), 6.32 (s, 1H), 4.04 (m, 1H), 3.71 (s, 3H), 3.43 – 3.31 (m, 1H), 3.26 (m, 1H), 2.99 – 2.87 (m, 2H), 2.84 (d, J = 7.8 Hz, 2H), 2.69 (m, 2H), 2.36 (s, 3H), 2.15 (s, 3H), 1.96 (s, 2H). *Note: a NAc Me group is obscured by the solvent signal- this was determined by HSQC analysis.*

^{13}C NMR (100 MHz, Acetone-d6): δ 145.5, 138.7, 137.0, 131.6, 130.5, 128.3, 127.0, 125.5, 119.9, 117.8, 111.2, 100.4, 61.7, 54.6, 42.7, 27.7, 26.4, 26.2, 23.8, 22.8, 21.4.

IR (Neat film, NaCl): 3255, 2927, 2356, 1712, 1647, 1582, 1554, 1297 cm^1.

HRMS (FD+): *m/z* calc'd for $C_{30}H_{33}N_4O_5S_2$ $[M+H]^+$: 593.1887, found 593.1887.



Ketothiophene 106: To a 250 mL round bottom flask containing ketal **68** (2.98 g, 10.5 mmol, 1.0 equiv) were added CH_2Cl_2 (105 mL, 0.1M) and DMAP (122.0 mg, 1.0 mmol, 0.095 equiv). The resulting solution was sparged with N_2 for 10 minutes, and Et_3N (5.8 mL, 42.0 mmol, 4.0 equiv) and Ac_2O (20.0 mL, 210 mmol, 20.0 equiv) were subsequently added. The resulting solution was stirred at 23 °C for 16 h, at which point TLC analysis indicated incomplete consumption of the starting material. Another 10 mL of Ac_2O was added, and the reaction mixture was stirred at 23 °C for an additional 3 h, at which point TLC analysis indicated complete consumption of the starting material. The reaction was diluted with CH_2Cl_2 (150 mL) and water (250 mL) and the layers were separated. The aqueous layer was extracted with CH_2Cl_2 (3x100 mL), the combined organic extracts were dried with Na_2SO_4, and concentrated under reduced pressure. The crude product was purified by silica gel flash chromatography (25 to 40 to 50% acetone/hexanes) to afford the title compound (3.46 g, quantitative) as an orange solid.

^{1}H NMR (500 MHz, $CDCl_3$): δ 11.25 (s, 1H), 4.32 (q, J = 7.1 Hz, 2H), 4.03 (s, 4H), 3.03 – 2.96 (m, 2H), 2.87 (s, 2H), 2.26 (s, 3H), 1.94 (t, J = 6.6 Hz, 2H), 1.38 (t, J = 7.1 Hz, 3H).

To a 250 mL round bottom flask containing the intermediate acylated ketal (not shown, 3.4 g, 10.4 mmol, 1.0 equiv) under nitrogen was added THF (52 mL, 0.2 M) and 3M HCl (38.5 mL, 0.27 M). The resulting solution was stirred at 55 °C for 5 hours, at which point LC/MS analysis indicated complete consumption of the starting material. The reaction was diluted with EtOAc (150 mL) and water (100 mL) and the layers were separated. The aqueous layer was extracted with EtOAc (3x75 mL), the combined organic

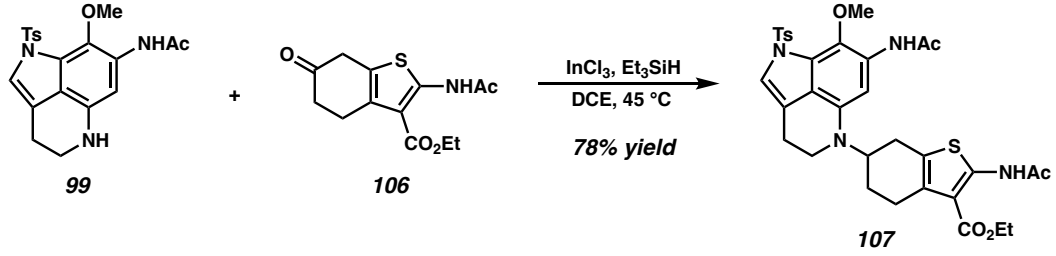
extracts were dried with Na_2SO_4, and concentrated under reduced pressure to yield the titled compound (2.06 g, 69% yield over two steps) as a yellow solid. The crude product was stored in a nitrogen filled glovebox to limit aerobic oxidation, and was used crude in subsequent transformations.

^{1}H NMR (400 MHz, $CDCl_3$): δ 11.25 (s, 1H), 4.35 (q, J = 7.1 Hz, 2H), 3.54 – 3.47 (m, 2H), 3.32 – 3.14 (m, 2H), 2.65 (t, J = 6.9 Hz, 2H), 2.27 (s, 3H), 1.39 (t, J = 7.1 Hz, 3H).

^{13}C NMR (100 MHz, $CDCl_3$): δ 207.7, 167.3, 166.2, 149.3, 130.3, 122.8, 110.5, 61.0, 38.8, 38.7, 25.6, 23.8, 14.4.

IR (Neat film, NaCl): 3270, 2973, 1704, 1655, 1565, 1535, 1404, 1247, 1208, 1036, 784, 701 cm^1.

HRMS (FD+): Oxidation to the phenol was observed using FD+ ionization. *m/z* calc'd for $C_{13}H_{14}NO_4S$ $[M+H]^+$: 280.0638, found 280.0634.



Aminotricycle 107: A flame dried 1 dram vial was charged with tricycle **99** (10.0 mg, 0.025 mmol, 1.0 equiv), ketothiophene **106** (14.2 mg, 0.05 mmol, 2.0 equiv), and $InCl_3$ (11.1 mg, 0.05 mmol, 2.0 equiv). The vial was evacuated and backfilled with N_2 (x3). Then, DCE (0.5 mL, 0.1M) and Et_3SiH (0.008 mL, 0.05 mmol, 2.0 equiv) were added. The resulting solution was stirred at 45 °C for 6 h, at which point LC/MS analysis indicated incomplete consumption of tricycle **99**. Another 0.008 mL of Et_3SiH was added, and the reaction was further stirred at 45 °C for 16 h, at which point LC/MS analysis indicated complete consumption of tricycle **99**. The resulting free flowing silica mixture was purified

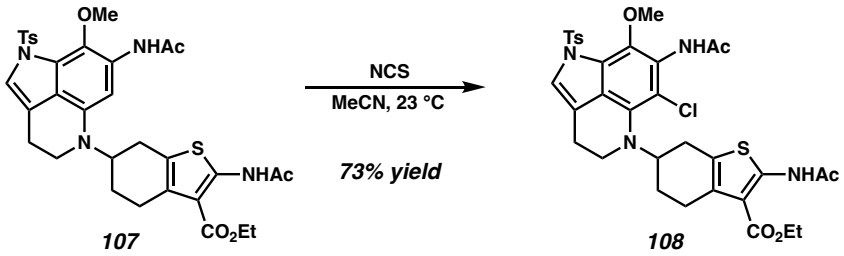
by column chromatography (SiO_2, 35 to 40 % acetone/hexanes) to afford the title compound (13.0 mg, 78% yield) as a white solid.

^{1}H NMR (400 MHz, $CDCl_3$): δ 11.19 (s, 1H), 7.68 (d, J = 8.3 Hz, 2H), 7.58 (s, 1H), 7.44 (s, 1H), 7.16 – 6.99 (m, 3H), 4.26 (q, J = 7.1 Hz, 2H), 4.01 (m, 1H), 3.72 (s, 3H), 3.18 (m, 2H), 3.12 – 2.97 (m, 1H), 2.88 – 2.71 (m, 5H), 2.28 (s, 3H), 2.19 (s, 3H), 2.12 (s, 3H), 1.31 (t, J = 7.2 Hz, 3H).

^{13}C NMR (100 MHz, $CDCl_3$): δ 168.3, 167.0, 166.5, 148.5, 144.3, 137.9, 135.7, 130.4, 130.2, 129.6, 129.1, 127.5, 125.9, 124.7, 119.3, 118.9, 116.9, 110.8, 98.0, 61.9, 52.8, 41.8, 26.7, 26.3, 25.0, 23.7, 23.2, 21.6, 14.4.

IR (Neat film, NaCl): 3268, 3052, 2934, 2853, 1664, 1560, 1532, 1478, 1415, 1369, 1330, 1248, 1209, 1173, 1096, 1035, 811, 783, 735, 668 cm^1.

HRMS (FD+): *m/z* calc'd for $C_{33}H_{37}N_4O_7S_2$ $[M+H]^+$: 665.2098, found 655.2091.



Chloro aminotricycle 107: A flame dried 1 dram vial was charged with tricycle **107** (14.4 mg, 0.022 mmol, 1.0 equiv). The vial was evacuated and backfilled with N_2 (x3). MeCN (1.1 mL, 0.02M), and NCS (2.9 mg, 0.022 mmol, 1.0 equiv) in MeCN (0.1 mL) were then added. The resulting mixture was stirred at 23°C for 16 h, at which point LC/MS analysis indicated full consumption of the starting material. The reaction was diluted with EtOAc (1 mL) and saturated aqueous $Na_2S_2O_3$ solution (1 mL). The aqueous layer was extracted with EtOAc (3x1 mL), the combined organic extracts were dried with Na_2SO_4, and concentrated under reduced pressure. The crude mixture was purified by preparatory thin

layer chromatography (55% acetone/hexanes) to afford the titled compound (11.2 mg, 73% yield) as an off-white solid.

Note: This compound was observed as a mixture of rotamers in the ^{1}H NMR spectrum.

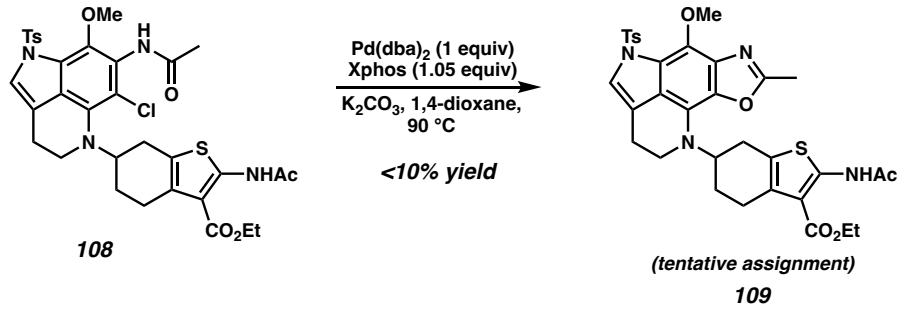
^{1}H NMR (400 MHz, $CDCl_3$): δ 11.22 (s, 1H), 8.38 (s, 1H), 7.80 – 7.76 (m, 2H), 7.43 – 7.36 (m, 1H), 7.24 – 7.20 (m, 2H), 6.99 – 6.95 (m, 1H), 4.43 – 4.19 (m, 2H), 4.16 – 4.08 (m, 1H), 3.78 – 3.74 (m, 3H), 3.44 – 3.41 (m, 1H), 3.32 – 3.20 (m, 1H), 3.14 – 2.99 (m, 1H), 3.00 – 2.84 (m, 2H), 2.81 – 2.75 (m, 5H), 2.35 – 2.34 (m, 3H), 2.28 – 2.07 (m, 4H), 2.08 – 2.04 (m, 1H), 1.92 – 1.87 (m, 1H), 1.39 – 1.32 (m, 3H).

Note: This compound was observed as a mixture of rotamers in the ^{13}C NMR spectrum.

^{13}C NMR (100 MHz, $CDCl_3$): δ 177.4, 173.8, 169.6, 167.2, 166.5, 148.5 (d, J = 10.3 Hz), 144.8 (d, J = 17.1 Hz), 138.8, 135.9, 135.6, 130.1, 129.8, 129.7 (d, J = 3.2 Hz), 127.8, 127.7, 127.2, 126.4, 125.5, 125.2, 124.8, 122.9, 122.5, 116.7, 115.7, 110.9, 62.1, 60.7, 58.2, 44.8, 42.8, 29.7, 29.5, 28.6, 27.0, 23.8, 23.5, 22.8, 21.7, 14.4.

IR (Neat film, NaCl): 3262, 2929, 1664, 1565, 1533, 1474, 1407, 1369, 1247, 1209, 1176, 1096, 1034, 832, 733, 648 cm^{1}.

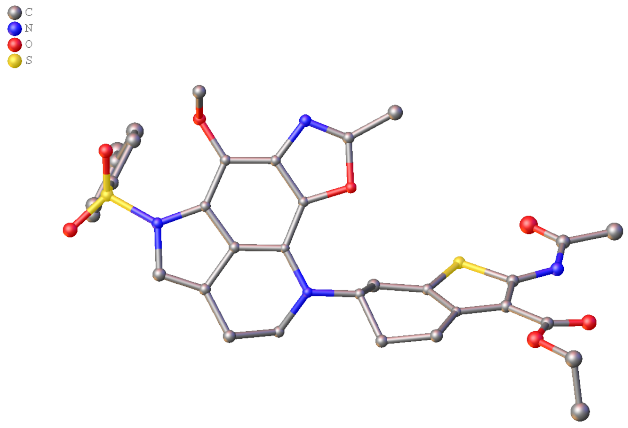
HRMS (FD+): *m/z* calc'd for $C_{33}H_{36}ClN_4O_7S_2$ $[M+H]^+$: 699.1708, found 699.1706.



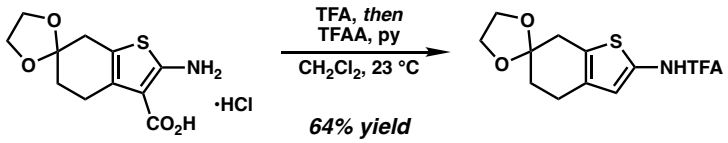
Benzoxazole 109: To a 1-dram glass vial in a nitrogen-filled glovebox were added chloroarene **108** (11.2 mg, 0.016 mmol, 1.0 equiv), K_2CO_3 (8.5 mg, 0.06 mmol, 3.8 equiv),

$Pd(dba)_2$ (9.2 mg, 0.016 mmol, 1.0 equiv), XPhos (8.0, 0.0168 mmol, 1.05 equiv), and 1,4-dioxane (0.3 mL, 0.05M). The vial was sealed with a PTFE-lined cap, removed from the glovebox, and stirred at 90 °C in a metal heating block for 16 h. Then, the reaction mixture was allowed to cool to 23 °C and was pushed through a short pad of celite with CH_2Cl_2. The resulting solution was concentrated under reduced pressure. The crude product was purified by preparative TLC on silica gel (45% acetone/hexanes) to afford the title compound (1.2 mg, <10% yield) as an off-white solid. Crystals suitable for X-Ray diffraction were obtained via layer diffusion with CH_2Cl_2 and hexanes.

Figure 1.10.2.1*Preliminary X-Ray structure of benzoxazole* ***109.***



The structure of benzoxazole **109** was elucidated via a preliminary X-Ray diffraction structure (Figure 1.10.2.1). However, refined X-Ray data was not obtained. Thus, benzoxazole **109** is reported as a tentative assignment.



69 ***155***

Trifluoroacetamidothiophene 155: To a 500 mL round bottom flask was added hydrochloride salt **69** (14.29 g, 48.98 mmol, 1.0 equiv). Traces of water were azeotropically

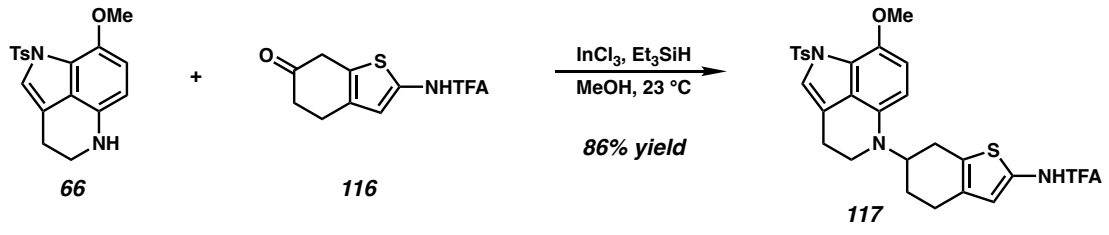
removed by addition of three portions of benzene followed by rotary evaporation. Then, the headspace of the flask was evacuated and backfilled with nitrogen, and CH_2Cl_2 (150 mL) and TFA (11.2 mL, 146.9 mmol, 3.0 equiv) were added. After 15 min, additional CH_2Cl_2 (50 mL) was added to reduce the viscosity of the mixture. The reaction mixture was stirred for 2.5 h at 23 °C, whereafter it was cooled to 0 °C in an ice bath and pyridine (19.7 mL, 244.9 mmol, 5.0 equiv) was added rapidly. TFAA (10.2 mL, 73.47 mmol, 1.5 equiv) was then added, and the ice bath was removed. After stirring for an additional 16 h at 23 °C, silica gel was added, and the reaction mixture was concentrated under reduced pressure and purified by silica gel flash chromatography (33% EtOAc/hexanes) to afford the title compound as an orange solid (9.67 g, 31.47 mmol, 64% yield).

^{1}H NMR (400 MHz, $CDCl_3$): δ 8.72 (s, 1H), 6.59 (s, 1H), 4.06 – 3.98 (m, 4H), 2.91 (d, *J* = 1.5 Hz, 2H), 2.74 (tt, *J* = 6.5, 1.6 Hz, 2H), 1.94 (t, *J* = 6.5 Hz, 2H).

^{13}C NMR (100 MHz, $CDCl_3$): δ 154.2, 153.8, 153.4, 153.0, 133.4, 131.8, 127.9, 120.1, 117.2, 116.1, 114.4, 111.5, 108.5, 64.8, 34.9, 31.7, 24.0.

IR (Neat Film, NaCl): 3248, 3097, 2894, 1713, 1589, 1434, 1362, 1250, 1169, 1060, 946, 905, 842, 739 cm^{-1}.

HRMS (ESI+): *m/z* calc'd for $C_{12}H_{13}F_3NO_3S$ $[M+H]^+$: 308.0563, found 308.0561.



Arene 117: To a 100 mL round bottom flask containing thiophene-ketal **155** (1.64 g, 5.34 mmol, 1.5 equiv) under nitrogen and equipped with a reflux condenser were added THF (27 mL) and 4 N aq. HCl (5.3 mL, 21.2 mmol, 4.0 equiv w.r.t. ketal). The reaction mixture

was heated to reflux and stirred for 1.5 h, then allowed to cool and quenched with saturated aq. $NaHCO_3$ (100 mL). The resulting mixture was extracted with CH_2Cl_2 (3x40 mL). The combined organic extracts were washed with brine, and the brine phase was back-extracted once with CH_2Cl_2. The combined organic phases were dried over Na_2SO_4 and $MgSO_4$ and concentrated under reduced pressure to afford crude ketone **116** as an orange solid that was used directly without further purification**.**

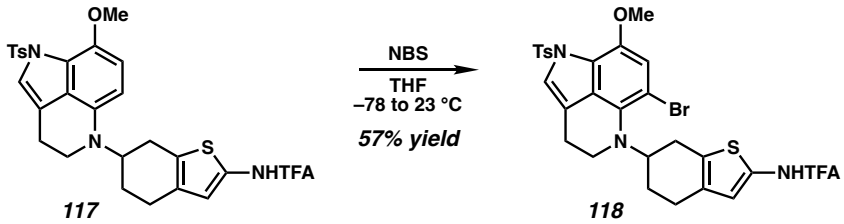
To a 50 mL round bottom flask were added tricyclic aniline **66** (1.22 g, 3.56 mmol, 1.0 equiv), the crude ketone **116** resulting from hydrolysis of ketal **155** (th. 5.34 mmol), and $InCl_3$ (1.57 g, 7.12 mmol, 2.0 equiv). The headspace of the flask was evacuated and replaced with nitrogen. MeOH (12 mL) and Et_3SiH (5.7 mL, 35.6 mmol, 10 equiv) were added and the reaction mixture was stirred at 23 °C for 24 h, whereafter it was transferred to a separatory funnel containing saturated aq. $NaHCO_3$ (200 mL). The resulting suspension was extracted with CH_2Cl_2 (3x70 mL). The combined organic extracts (still containing a significant quantity of water and indium salts) were dried over Na_2SO_4, concentrated under reduced pressure, and purified by automated silica gel flash chromatography (Teledyne ISCO, 0→60% EtOAc/hexanes) to afford the title compound as a golden-colored foam of sufficient purity for use in the next step (1.80 g, 3.05 mmol, 86% yield). A sample for analysis was obtained by preparative TLC on silica gel (33% EtOAc/hexanes).

^{1}H NMR (400 MHz, $CDCl_3$): δ 8.40 (br s, 1H), 7.82 – 7.75 (m, 2H), 7.34 (t, *J* = 1.5 Hz, 1H), 7.26 – 7.21 (m, 2H), 6.60 (s, 1H), 6.58 (d, *J* = 8.3 Hz, 1H), 6.30 (d, *J* = 8.8 Hz, 1H), 4.15 – 4.01 (m, 1H), 3.68 (s, 3H), 3.33 (dt, *J* = 11.0, 5.4 Hz, 1H), 3.21 (dt, *J* = 11.5, 6.2 Hz, 1H), 2.99 – 2.92 (m, 3H), 2.91 – 2.66 (m, 3H), 2.37 (s, 3H), 2.07 – 1.98 (m, 2H).

^{13}C NMR (100 MHz, $CDCl_3$): δ 153.8, 153.4, 144.2, 140.0, 137.1, 136.3, 133.2, 132.4, 129.5, 129.4, 127.7, 124.2, 123.2, 119.7, 117.2, 116.5, 115.4, 114.4, 110.3, 102.7, 57.3, 53.5, 42.2, 27.0, 26.0, 25.9, 23.5, 21.7.

IR (Neat Film, NaCl): 3281, 3126, 3058, 2935, 2841, 1714, 1588, 1510, 1442, 1356, 1251, 1169, 1108, 1056, 996, 903, 739, 663 cm^{-1}.

HRMS (ESI+): *m/z* calc'd for $C_{28}H_{27}F_3N_3O_4S_2$ $[M+H]^+$: 590.1390, found 590.1404.



Bromoarene 118: To a 250 mL round bottom flask was added tertiary aniline **117** (1.78 g, 3.02 mmol, 1.0 equiv). Traces of water were azeotropically removed by addition of three portions of benzene followed by rotary evaporation, and the headspace of the flask was evacuated and backfilled with nitrogen. The starting material was taken up in THF (50 mL), and the flask was cooled to –78 °C and protected from light. A solution of NBS (484 mg, 2.72 mmol, 0.9 equiv) in THF (50 mL) was added as a slow stream with rapid stirring. Following addition, the reaction mixture was allowed to stir at –78 °C for 5 additional minutes, whereafter the cooling bath was removed and the reaction mixture allowed to warm to 23 °C. The reaction mixture was concentrated under reduced pressure and purified by automated silica gel flash chromatography (Teledyne ISCO, 0→50% EtOAc/hexanes) to afford the title compound as a brown foam (1.16 g, 1.74 mmol, 57% yield from tertiary aniline **117** or 64% from NBS).

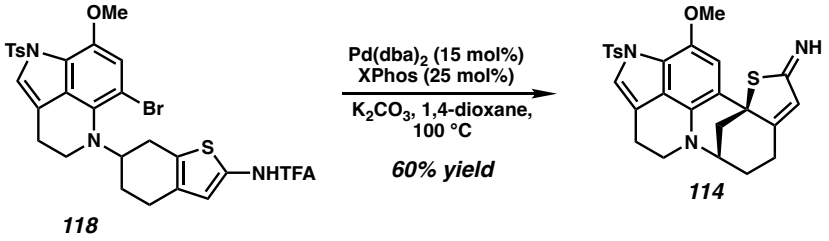
^{1}H NMR (400 MHz, C_6D_6): δ 7.83 (d, J = 8.3 Hz, 2H), 7.54 (s, 1H), 6.75 (s, 1H), 6.64 (d, J = 8.2 Hz, 2H), 6.01 (s, 1H), 4.17 (dddd, J = 13.7, 11.3, 5.3, 2.6 Hz, 1H), 3.19 (s, 3H),

2.99 – 2.75 (m, 3H), 2.58 (tdd, J = 11.7, 3.9, 2.0 Hz, 1H), 2.36 – 2.09 (m, 4H), 1.80 – 1.71 (m, 4H), 1.76 (s, 3H), 1.45 (tdd, J = 12.2, 10.7, 6.7 Hz, 1H).

^{13}C NMR (100 MHz, C_6D_6): δ 153.6, 153.2, 144.1, 143.0, 137.8, 134.6, 133.6, 131.9, 129.6, 129.5, 128.0, 127.7, 123.1, 122.4, 117.7, 116.6, 116.2, 115.2, 114.2, 106.2, 59.5, 56.3, 43.0, 29.5, 28.5, 26.0, 22.6, 21.1.

IR (Neat Film, NaCl): 3295, 2931, 1714, 1588, 1490, 1438, 1347, 1251, 1172, 1111, 908, 804, 737, 665 cm^{-1}.

HRMS (ESI+): *m/z* calc'd for $C_{28}H_{26}BrF_3N_3O_4S_2$ $[M+H]^+$: 668.0495, found 668.0502.



118 *114*

***N*-H thioimidate 114:** To a 40 mL glass vial was added bromoarene **118** (331 mg, 0.495 mmol, 1.0 equiv). Traces of water were azeotropically removed by addition of three portions of benzene followed by rotary evaporation, the vial was transferred to a nitrogen-filled glovebox, and K_2CO_3 (96 mg, 0.695 mmol, 1.4 equiv) was added. In a separate vial, a stock solution of $Pd(dba)_2$ (46.2 mg) and XPhos (64.2 mg) in 1,4-dioxane (13.3 mL) was prepared and stirred at 28 °C for 10 min. Then, 12.4 mL of this solution were transferred to the vial containing bromoarene **118** (for 43 mg $Pd(dba)_2$ (0.0748 mmol, 15 mol %) and 59.1 mg XPhos (0.124 mmol, 25 mol %)). The vial was sealed with a PTFE/silicone septum cap and electrical tape, removed from the glovebox, and stirred at 100 °C for 6 h. The reaction mixture was then allowed to cool and passed through a PTFE syringe filter, which was subsequently rinsed with EtOAc. The solution was concentrated under reduced

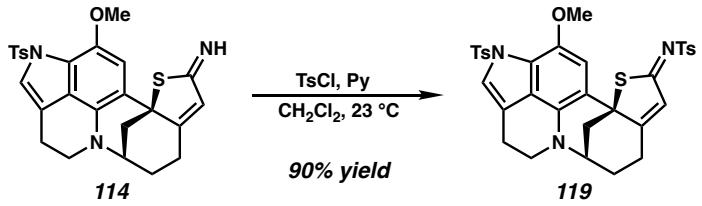
pressure and purified by silica gel flash chromatography (100% EtOAc → 100% acetone) to afford the title compound as an off-white solid (145 mg, 0.295 mmol, 60% yield).

^{1}H NMR (400 MHz, CD_2Cl_2): δ 7.81 – 7.72 (m, 2H), 7.32 – 7.24 (m, 3H), 6.81 (s, 1H), 5.78 (d, *J* = 1.7 Hz, 1H), 3.64 (s, 3H), 3.59 (p, *J* = 2.7 Hz, 1H), 3.35 (ddd, *J* = 11.1, 9.7, 5.7 Hz, 1H), 3.25 (ddd, *J* = 11.1, 4.8, 3.5 Hz, 1H), 3.04 – 2.94 (m, 2H), 2.65 (dt, *J* = 12.5, 2.9 Hz, 1H), 2.54 – 2.47 (m, 1H), 2.40 (qd, *J* = 5.3, 3.1 Hz, 1H), 2.37 (s, 3H), 2.33 (dd, *J* = 12.5, 2.9 Hz, 1H), 2.06 – 1.97 (m, 1H), 1.61 (tdd, *J* = 13.7, 5.3, 2.9 Hz, 1H).

^{13}C NMR (100 MHz, CD_2Cl_2): δ 178.5, 168.3, 144.9, 139.3, 137.2, 133.5, 129.7, 128.0, 123.5, 122.3, 121.7, 120.6, 115.2, 114.5, 109.1, 63.5, 57.4, 47.6, 41.9, 31.9, 24.8, 23.2, 21.7 (the bridgehead methine ^{13}C resonance is obscured by the solvent peak).

IR (Neat Film, NaCl): 2925, 2851, 1595, 1503, 1462, 1349, 1284, 1226, 1174, 1106, 1011, 898, 808, 738, 704, 672 cm^{-1}.

HRMS (ESI+): *m/z* calc'd for $C_{26}H_{26}N_3O_3S_2$ $[M+H]^+$: 492.1410, found 492.1410.



114 ***119***

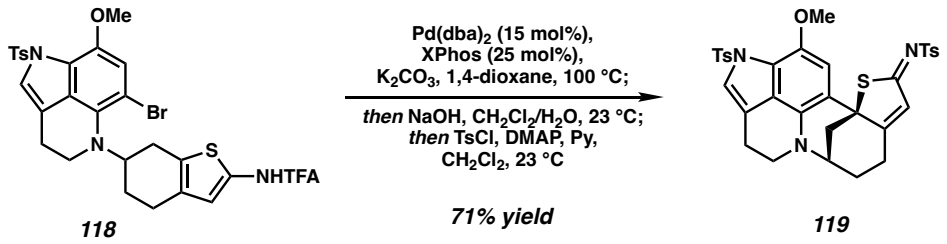
***N*-tosyl thiomidiate 119:** To a 1-dram glass vial containing TsCl (16 mg, 0.0814 mmol, 2.0 equiv) under nitrogen was added thioimidate **114** (20 mg, 0.0407 mmol, 1.0 equiv) as a stock solution in CH_2Cl_2 (1 mL), followed by pyridine (10 µL, 0.122 mmol, 3.0 equiv). The reaction mixture was stirred at 23 °C for 3 days, after which it was concentrated under reduced pressure and purified by silica gel flash chromatography (50% EtOAc/hexanes) to afford the title compound as an orange film (23.7 mg, 0.0367 mmol, 90% yield).

^{1}H NMR (400 MHz, $CDCl_3$): δ 7.93 (d, *J* = 8.1 Hz, 2H), 7.83 – 7.74 (m, 2H), 7.36 – 7.28 (m, 3H), 7.28 – 7.22 (m, 2H), 6.49 (s, 1H), 5.97 (d, *J* = 1.6 Hz, 1H), 3.65 – 3.61 (m, 1H), 3.59 (s, 3H), 3.37 (dt, *J* = 10.9, 7.6 Hz, 1H), 3.27 (dt, *J* = 11.1, 4.2 Hz, 1H), 3.06 – 2.97 (m, 2H), 2.83 (dt, *J* = 12.6, 2.8 Hz, 1H), 2.68 – 2.58 (m, 1H), 2.49 – 2.44 (m, 1H), 2.43 (s, 3H), 2.38 (s, 3H), 2.21 – 2.04 (m, 2H), 1.59 – 1.51 (m, 1H).

^{13}C NMR (100 MHz, $CDCl_3$): δ 184.5, 175.3, 144.4, 144.0, 139.4, 137.3, 136.9, 133.1, 129.6, 129.5, 127.9, 127.6, 123.6, 122.7, 121.6, 120.7, 114.2, 111.1, 107.8, 65.4, 57.2, 53.0, 47.4, 40.4, 31.7, 25.4, 23.0, 21.7.

IR (Neat Film, NaCl): 2924, 2850, 1596, 1519, 1449, 1286, 1228, 1167, 1107, 1010, 867, 813, 734, 664 cm^{-1}.

HRMS (ESI+): *m/z* calc'd for $C_{33}H_{32}N_3O_5S_3$ $[M+H]^+$: 646.1499, found 646.1500.

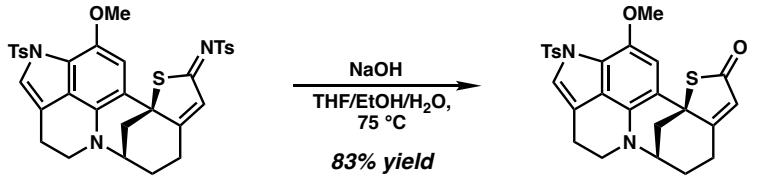


Procedure for the direct preparation of *N*-tosylthioimidate 119: To a 500 mL Schlenk bomb in a nitrogen-filled glovebox was added bromoarene **118** (3.88 g, 5.80 mmol, 1.0 equiv) as a solution in a minimal amount of benzene. The benzene was removed under reduced pressure, and K_2CO_3 (1.12 g, 8.12 mmol, 1.4 equiv) and 1,4-dioxane (110 mL) were added. In a separate vial, $Pd(dba)_2$ (500 mg, 0.870 mmol, 15 mol %) and XPhos (691 mg, 1.45 mmol, 25 mol %) were combined. 1,4-dioxane (35 mL) was added and the mixture was stirred at 28 °C for 10 min. Then, the Pd/ligand solution was transferred by pipette to the Schlenk bomb. The vessel was sealed, removed from the glovebox, and

stirred at 100 °C for 7 h. The reaction mixture was allowed to cool, filtered through a Celite plug with EtOAc, and concentrated under reduced pressure.

The residue was taken up in CH_2Cl_2 (70 mL). 1 N aq. NaOH was added, and the biphasic mixture was subjected to vigorous magnetic stirring for 1 h. The layers were separated, and the aqueous phase was extracted with CH_2Cl_2 (3x20 mL). The combined organic phases were dried over Na_2SO_4 and concentrated under reduced pressure in a 500 mL round bottom flask.

Traces of water were azeotropically removed by addition of three portions of $PhCH_3$ followed by rotary evaporation. DMAP (71 mg, 0.58 mmol, 10 mol %) was added and the headspace of the flask was evacuated and replaced with nitrogen. CH_2Cl_2 (115 mL) was added, followed by pyridine (1.4 mL, 17.4 mmol, 3.0 equiv). TsCl (2.21 g, 11.6 mmol, 2.0 equiv) was added in a single portion under a stream of nitrogen. The reaction mixture was stirred at 23 °C for 58 h, then concentrated under reduced pressure. The crude product was purified by automated silica gel flash chromatography (Teledyne ISCO, 0→40→75% EtOAc/hexanes) to afford *N*-tosylthioimidate **119** as an orange foam that crystallized upon standing (2.66 g, 4.12 mmol, 71% yield). For characterization data, see above.



119 ***115***

Thiobutenolide 115: To a 250 mL round bottom flask were added thioimidate **119** (940 mg, 1.46 mmol, 1.0 equiv), THF (30 mL), water (10 mL), degassed ethanol (50 mL), and 2 N aq. NaOH (6 mL, 12 mmol, 8.2 equiv). The headspace of the vial was purged with nitrogen and the vial was sealed with a PTFE/silicone septum. The reaction mixture was

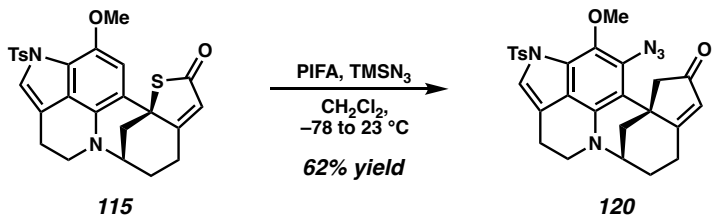
stirred at 80 °C for 1 hour, at which point the solution became homogenous and was immediately removed from the oil bath and allowed to cool to 23 °C. The reaction mixture was quenched with glacial acetic acid (2 mL) and partitioned between water and EtOAc. The layers were separated, and the aqueous phase was extracted with EtOAc (3x). The combined organic phases were dried over Na_2SO_4 and concentrated *in vacuo* to afford the crude product. Purification by silica gel flash chromatography (0→2% EtOAc/CH_2Cl_2) afforded the title compound (591 mg, 1.21 mmol, 83% yield).

^{1}H NMR (400 MHz, C_6D_6): δ 7.86 (d, *J* = 8.2 Hz, 2H), 7.47 (d, *J* = 1.6 Hz, 1H), 6.89 (t, *J* = 1.3 Hz, 1H), 6.67 – 6.59 (m, 2H), 5.50 (d, *J* = 1.7 Hz, 1H), 3.32 (s, 3H), 2.87 – 2.78 (m, 1H), 2.78 – 2.59 (m, 2H), 2.59 – 2.45 (m, 2H), 2.40 (dt, *J* = 12.4, 2.8 Hz, 1H), 1.91 – 1.81 (m, 1H), 1.81 – 1.76 (m, 1H), 1.74 (s, 3H), 1.73 – 1.66 (m, 1H), 1.66 – 1.56 (m, 1H), 0.97 – 0.81 (m, 1H).

^{13}C NMR (100 MHz, C_6D_6): δ 196.3, 177.3, 143.9, 140.0, 137.8, 133.5, 129.4, 124.2, 121.9, 121.7, 121.0, 114.6, 112.8, 108.9, 60.8, 60.8, 57.0, 53.0, 47.1, 40.9, 31.4, 24.8, 23.0, 21.1 (an additional ^{13}C resonance associated with the tosyl group is likely obscured by the solvent signal).

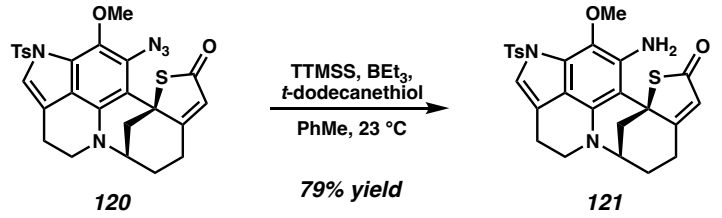
IR (Neat Film, NaCl): 2931, 2851, 1682, 1504, 1348, 1284, 1227, 1169, 1107, 1011, 897, 851, 814, 738, 662 cm^{-1}.

HRMS (ESI+): *m/z* calc'd for $C_{26}H_{25}N_2O_4S_2$ $[M+H]^+$: 493.1250, found 493.1251.



115 ***120***

Aryl azide 120: To a 1-dram glass vial containing thiolactone **115** (22.6 mg, 0.0459 mmol, 1.0 equiv) under nitrogen were added CH_2Cl_2 (2.3 mL) and $TMSN_3$ (30 μL, 0.23 mmol, 5.0 equiv). The reaction mixture was cooled to –78 °C and a solution of PIFA (18.8 mg, 0.0437 mmol, 0.95 equiv) in CH_2Cl_2 (0.5 mL) was added dropwise. After stirring for 10 min at –78 °C, the reaction mixture was allowed to warm to 23 °C, concentrated under reduced pressure, and purified by preparative TLC on silica gel (90% Et_2O/hexanes, eluted twice) to afford an intermediate aryl azide as a brown film (15.3 mg, 0.0287 mmol, 62% yield); ^{1}H NMR (600 MHz, C_6D_6) δ 7.95 – 7.91 (m, 2H), 7.34 (s, 1H), 6.56 (d, J = 8.2 Hz, 2H), 5.66 (d, J = 1.6 Hz, 1H), 3.81 (s, 3H), 2.61 – 2.56 (m, 2H), 2.53 – 2.46 (m, 1H), 2.41 – 2.32 (m, 2H), 2.24 (dt, J = 12.7, 2.8 Hz, 1H), 1.82 – 1.77 (m, 1H), 1.63 (dd, J = 12.7, 3.1 Hz, 1H), 1.58 (s, 3H), 1.54 – 1.43 (m, 2H), 0.79 (tdd, J = 13.0, 5.7, 3.2 Hz, 1H).



120 ***121***

Primary aniline 121: To a ½-dram glass vial under air was added intermediate aryl azide **120** (7.3 mg, 0.0137 mmol, 1.0 equiv) as a stock solution in CH_2Cl_2. The solvent was removed by blowing a stream of nitrogen over the surface of the solution. Then, $PhCH_3$ (0.36 mL), tris(trimethylsilyl)silane (21 μL, 0.0684 mmol, 5.0 equiv), *tert*-dodecanethiol (1.6 μL, 0.0069 mmol, 0.5 equiv), and triethylborane (1 M in hexanes, 41 μL, 0.0411 mmol, 3.0 equiv) were added under air. After 5 min, the reaction mixture was concentrated under

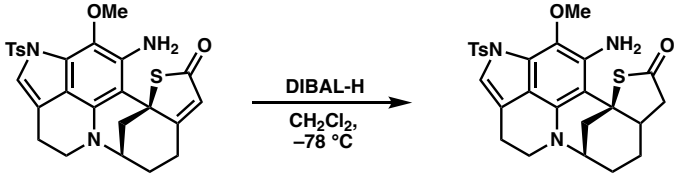
reduced pressure and purified by preparative TLC on silica gel (100% EtOAc) to afford the title compound as a brown film (5.5 mg, 0.0108 mmol, 79% yield).

^{1}H NMR (400 MHz, C_6D_6): δ 8.02 – 7.97 (m, 2H), 7.26 (d, *J* = 1.6 Hz, 1H), 6.59 – 6.54 (m, 2H), 5.60 (d, *J* = 1.5 Hz, 1H), 4.53 (s, 2H), 3.77 (s, 3H), 2.63 – 2.50 (m, 3H), 2.42 – 2.34 (m, 3H), 1.75 – 1.67 (m, 2H), 1.65 (s, 3H), 1.58 – 1.53 (m, 2H), 0.75 – 0.63 (m, 1H).

^{13}C NMR (100 MHz, C_6D_6): δ 194.9, 175.9, 143.9, 139.9, 136.8, 136.6, 129.6, 127.5, 127.2, 122.7, 117.8, 116.5, 112.2, 100.0, 60.3, 60.3, 52.8, 48.0, 44.0, 30.9, 25.2, 22.9, 21.0 (an additional ^{13}C resonance associated with the tosyl group is likely obscured by the solvent signal).

IR (Neat Film, NaCl): 3440, 3347, 2921, 2854, 1682, 1486, 1367, 1294, 1177, 1136, 1094, 967, 828, 738, 683 cm^{-1}.

HRMS (ESI+): *m/z* calc'd for $C_{26}H_{26}N_3O_4S_2$ $[M+H]^+$: 508.1359, found 508.1374.

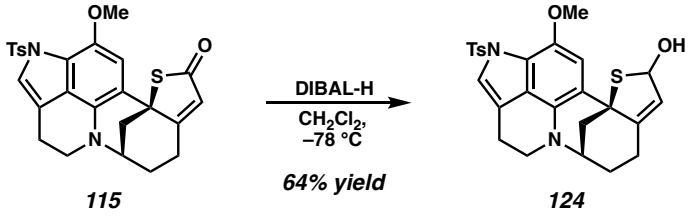


121 ***122*** ***(tentative assignment)***

Saturated thiobutenolide 122: To a 20 mL glass vial containing primary aniline **121** (0.5 mg, 0.00098 mmol, 1.0 equiv) under nitrogen was added CH_2Cl_2 (0.15 mL). The solution was cooled to –78 °C in a dry ice/acetone bath. To the resulting mixture was added DIBAL (100 μL, 0.0049 mmol, 5.0 equiv) as a freshly prepared solution in CH_2Cl_2 (0.049M). The reaction was quenched at –78 °C by the addition of 2 mL saturated aqueous Rochelle's salt solution immediately following the addition of DIBAL. The resulting mixture was allowed to warm up to 23 °C and was stirred vigorously for 45 min. The layers were then separated, and the aqueous phase was extracted with CH_2Cl_2 (3 × 2 mL). The combined organic

phases were dried over Na_2SO_4 and concentrated *in vacuo* to afford crude saturated thiobutenolide **122** (ca. 0.3 mg) as a yellow oil. This tentative assignment was made based on the disappearance of ^1H resonances in the alkenyl (5.0-7.0 ppm) region in the ^1H spectrum.

^1H NMR (400 MHz, C_6D_6): δ 8.01 (d, *J* = 8.3 Hz, 2H), 7.28 (s, 1H), 6.58 (d, *J* = 8.1 Hz, 2H), 4.62 (s, 2H), 3.85 (s, 3H), 2.81 – 2.32 (m, 6H), 2.16 (dd, *J* = 17.3, 13.4 Hz, 2H), 2.07 – 1.91 (m, 2H), 1.65 (s, 3H). Full characterization data was not acquired due to the insufficient quantities of material.

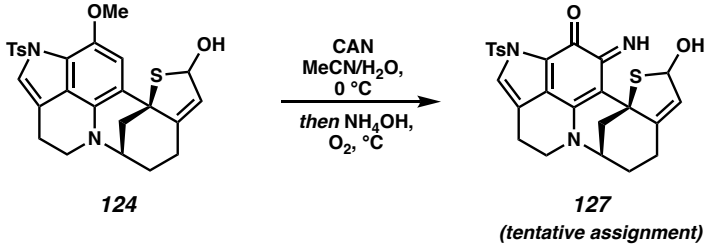


115 ***124***

Thiolactol 124: To a 20 mL glass vial containing thiobutenolide **115** (10.0 mg, 0.02 mmol, 1.0 equiv) under nitrogen was added CH_2Cl_2 (1.0 mL). The solution was cooled to –78 °C in a dry ice/acetone bath. To the resulting mixture was added DIBAL (0.1 μL, 0.024 mmol, 1.2 equiv) as a freshly prepared solution in CH_2Cl_2 (0.24M). The reaction was quenched at –78 °C by the addition of 2 mL saturated aqueous Rochelle's salt solution immediately following the addition of DIBAL. The resulting mixture was allowed to warm up to 23 °C and was stirred vigorously for 45 min. The layers were then separated, and the aqueous phase was extracted with CH_2Cl_2 (3 × 2 mL). The combined organic phases were dried over Na_2SO_4 and concentrated *in vacuo* to afford crude thiolactol **124** (6.4 mg, 64% yield) as a yellow oil (single diastereomer).

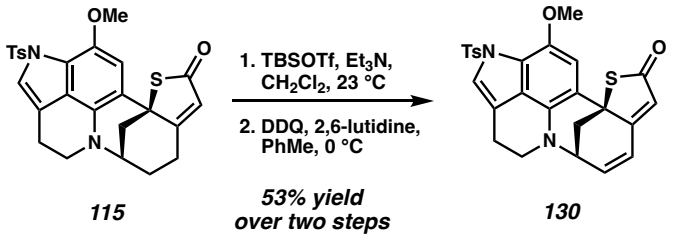
^1H NMR (400 MHz, C_6D_6): δ 7.97 – 7.88 (m, 2H), 7.48 (s, 1H), 7.35 (s, 1H), 6.77 – 6.51 (m, 2H), 6.08 – 5.86 (m, 1H), 5.07 (dd, J = 2.7, 1.8 Hz, 1H), 3.57 (s, 3H), 2.90 (t, J = 3.0

Hz, 1H), 2.81 – 2.73 (m, 1H), 2.64 (m, 1H), 2.58 – 2.44 (m, 3H), 1.96 – 1.82 (m, 2H), 1.80 – 1.74 (m, 1H), 1.71 (s, 3H).



124 ***127***
(tentative assignment)

Iminoquinone 127: To a 20 mL vial containing thiolactol **124** (0.5 mg, 0.001 mmol, 1.0 equiv) under nitrogen was added MeCN (0.15 mL). The vial was cooled to 0 °C in an ice bath and CAN (0.55 mg, 0.001 mmol, 1.0 equiv) was added dropwise as a freshly prepared solution in 0.05 mL water. The resulting mixture was stirred at 0 °C for 5 min, after which aqueous ammonia (27% w/w, 5 μL) was added. The reaction vessel was flushed with O_2, and the resulting mixture was stirred for 7 min under an O_2 atmosphere at 0 °C. The reaction mixture was warmed to 23 °C and was diluted with EtOAc (5 mL) and water (3 mL). The layers were separated, and the aqueous phase was extracted with EtOAc (4x4 mL). The combined organic phases were dried over Na_2SO_4 and concentrated in vacuo. LC/MS analysis indicated formation of iminoquinone **127**. Attempting to effect thioaminal formation with this intermediate via acidic (i.e. TFA) or oxygen activation (i.e. acylation or mesylation of the thiolactol) methods led to dehydration as observed by LC/MS analysis, supporting the tentative assignment of diene **128**.



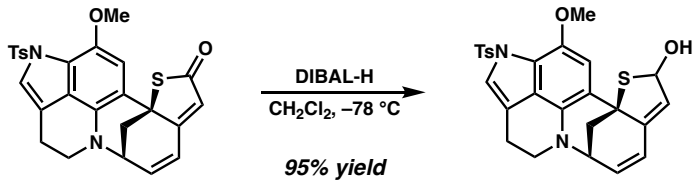
Diene 130: To a 20 mL glass vial containing thiobutenolide **115** (50 mg, 0.102 mmol, 1.0 equiv) under nitrogen was added CH_2Cl_2 (1 mL), triethylamine (0.15 mL, 1.02 mmol, 10 equiv), and TBSOTf (0.16 mL, 0.711 mmol, 7.0 equiv). The reaction mixture was stirred at 23 °C for 14 hours before being loaded on to a silica gel column. The column was flushed with 10% EtOAc/hexanes (200 mL), followed by 40% EtOAc/hexanes (150 mL) to afford an intermediate silyl ketene thioacetal and starting material (12.7 mg, 0.0258 mmol, 25% recovery). The silyl ketene thioacetal was transferred to an 8 mL vial, which was evacuated and backfilled 3 times with N_2, and PhMe (0.76 mL) was added. The resulting mixture was cooled to 0 °C in an ice bath, whereafter 2,6-lutidine (17.5 μL, 0.152 mmol, 2.0 equiv) and DDQ (17.3 mg, 0.0761 mmol, 1.0 equiv, as a solution in 0.76 mL PhMe) were sequentially added. The reaction mixture was stirred at 0 °C and the reaction was monitored by LC/MS. Upon the completion of the reaction (*ca*. ~5 min), the reaction mixture was loaded directly onto silica gel. Purification by silica gel flash chromatography (0→35% EtOAc/hexanes) afforded diene **130** (26.3 mg, 0.0537 mmol, 53% over 2 steps) as an orange solid.

^{1}H NMR (400 MHz, C_6D_6): δ 7.83 – 7.78 (m, 2H), 7.44 (d, *J* = 1.6 Hz, 1H), 6.92 (s, 1H), 6.62 – 6.53 (m, 2H), 5.87 (ddd, *J* = 9.7, 1.9, 0.9 Hz, 1H), 5.52 (s, 1H), 5.46 – 5.38 (m, 1H), 3.29 (s, 3H), 3.19 (dtt, *J* = 4.7, 3.3, 2.0 Hz, 1H), 2.67 – 2.55 (m, 3H), 2.40 – 2.32 (m, 2H), 1.93 (dd, *J* = 12.3, 3.9 Hz, 1H), 1.71 (s, 3H).

^{13}C NMR (100 MHz, C_6D_6): δ 196.1, 171.8, 143.8, 141.3, 137.8, 132.8, 131.8, 129.4, 128.0, 125.1, 124.1, 123.4, 121.6, 121.2, 114.3, 113.6, 108.7, 58.2, 56.8, 53.0, 47.9, 37.6, 23.0, 21.1.

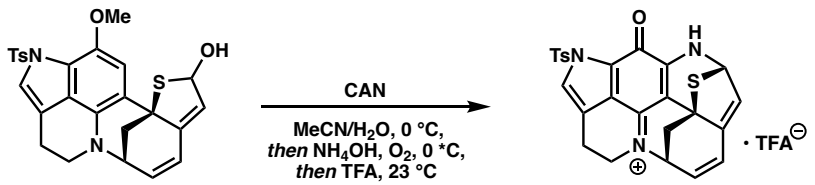
IR (Neat Film, NaCl): 3060, 2934, 2841, 1681, 1622, 1504, 1347, 1287, 1226, 1177, 1106, 1016, 967, 898, 856, 813, 732, 662, 623 cm^{-1}.

HRMS (ESI+): *m/z* calc'd for $C_{26}H_{23}N_2O_4S_2$ $[M+H]^+$: 491.1094, found 491.1098.



130 ***131***

Thiolactol 131: To a 20 mL glass vial containing diene **130** (20 mg, 0.0408 mmol, 1.0 equiv) under nitrogen was added CH_2Cl_2 (1.9 mL). The solution was cooled to –78 °C in a dry ice/acetone bath. To the resulting mixture was added DIBAL (70 μL, 0.408 mmol, 10 equiv) as a freshly prepared solution in CH_2Cl_2 (1 mL). The reaction was quenched at –78 °C by the addition of 2 mL saturated aqueous Rochelle's salt solution immediately following the addition of DIBAL. The resulting mixture was allowed to warm up to 23 °C and was stirred vigorously for 45 min. The layers were then separated, and the aqueous phase was extracted with CH_2Cl_2 (3 × 2 mL). The combined organic phases were dried over Na_2SO_4 and concentrated *in vacuo* to afford crude thiolactol **131** as a yellow oil, which was used immediately in the next step without further purification.



131 ***50% yield*** ***N-tosyl desbromoaleutianamine (134)***

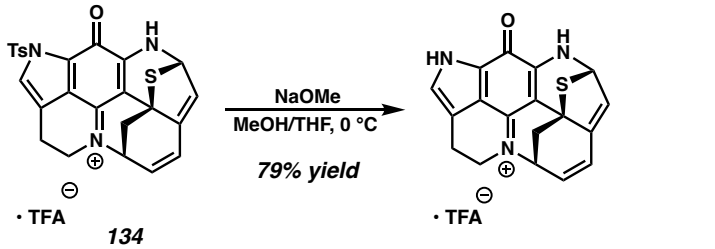
***N*-tosyl desbromoaleutianamine (134):** To a 20 mL vial containing thiolactol **131** (20 mg, 0.0408 mmol, 1.0 equiv) under nitrogen was added MeCN (2.7 mL). The vial was cooled to 0 °C in an ice bath and CAN (44.8 mg, 0.0816 mmol, 2.0 equiv) was added dropwise as a freshly prepared solution in 1.3 mL water. The resulting mixture was stirred at 0 °C for 5 min, after which aqueous ammonia (27% w/w, 34 μL, 0.408 mmol, 10 equiv) was added. The reaction vessel was flushed with O_2, and the resulting mixture was stirred for 7 min under an O_2 atmosphere at 0 °C. The reaction mixture was warmed to 23 °C and was diluted with EtOAc (5 mL) and water (3 mL). The layers were separated, and the aqueous phase was extracted with EtOAc (4x4 mL). The combined organic phases were dried over Na_2SO_4 and concentrated *in vacuo*. The residue was taken up in TFA (4 mL), and the mixture was allowed to stand at 23 °C for 10 min before being concentrated by rotary evaporation. The crude *N*-tosyl desbromoaleutianamine (**134**) was purified by preparative reverse phase HPLC (Eclipse XDB-C18, 5 μm, 9.4 x 250 mm, MeCN-H_2O (0.1% TFA) = 32.5:67.5 to 100:0, linear gradient for 6 min, flow rate = 5 mL/min) to afford *N*-tosyl desbromoaleutianamine (**134**) as the TFA salt (12 mg, 0.0204 mmol, 50% yield).

^{1}H NMR (400 MHz, CD_3OD): δ 8.09 – 8.01 (m, 2H), 7.78 (d, *J* = 1.4 Hz, 1H), 7.42 (d, *J* = 8.0 Hz, 2H), 6.72 (d, *J* = 9.4 Hz, 1H), 6.16 (dd, *J* = 9.5, 5.9 Hz, 1H), 5.94 (d, *J* = 3.3 Hz, 1H), 5.31 (d, *J* = 3.3 Hz, 1H), 4.95 (dt, *J* = 6.0, 2.9 Hz, 1H), 4.26 – 4.16 (m, 1H), 4.15 – 3.97 (m, 1H), 3.22 (td, *J* = 15.4, 7.1 Hz, 1H), 3.16 – 3.04 (m, 1H), 2.51 – 2.31 (m, 5H).

^{13}C NMR (100 MHz, MeOD): δ 167.4, 148.7, 147.4, 141.9, 140.7, 134.6, 131.1, 130.1, 129.3, 127.8, 124.4, 123.7, 118.8, 112.3, 102.5, 64.8, 57.6, 51.9, 50.9, 30.9, 21.7, 20.3. (one of the ^{13}C signal overlapped with other)

IR (Neat Film, NaCl): 3136, 2932, 1682, 1622, 1524, 1442, 1420, 1378, 1346, 1268, 1194, 1180, cm^{-1}.

HRMS (ESI+): *m/z* calc'd for $C_{25}H_{20}N_3O_3S_2$ $[M+H]^+$: 474.0941, found 474.0959.



134 ***Desbromoaleutianamine (147)***

Desbromoaleutianamine (147): To a 4 mL vial containing *N*-tosyl desbromoaleutianamine (**134**, 12 mg, 0.0204 mmol, 1.0 equiv) under nitrogen was added THF (1.2 mL). The resulting mixture was cooled to 0 °C with an ice water bath, and 0.2 M NaOMe in MeOH (0.72 mL, 0.14 mmol, 7.0 equiv) was added. The reaction mixture was stirred at 0 °C for 10 min, after which 0.2 M TFA in MeOH (0.72 mL, 0.144 mol, 7.0 equiv) was added. The reaction mixture was allowed to warm to 23 °C. The mixture was then concentrated *in vacuo* and the residue was purified by preparative reverse-phase HPLC (Eclipse XDB-C18, 5 μm, 9.4 x 250 mm, MeCN-H_2O (0.1% TFA) = 0:100 to 100:0, linear gradient for 6 min, flow rate = 5 mL/min) to afford desbromoaleutianamine (**147**) as the TFA salt (7 mg, 0.0162 mmol, 79% yield).

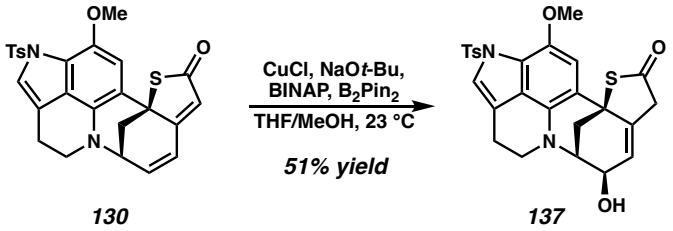
^{1}H NMR (600 MHz, CD_3OD): δ 7.06 (d, *J* = 1.0 Hz, 1H), 6.74 (d, *J* = 9.4 Hz, 1H), 6.23 (dd, *J* = 9.5, 5.9 Hz, 1H), 5.95 (d, *J* = 3.4 Hz, 1H), 5.35 (d, *J* = 3.4 Hz, 1H), 4.92 (dt, *J* = 6.0, 2.9 Hz, 1H), 4.18 (ddd, *J* = 14.2, 7.3, 2.0 Hz, 1H), 4.04 (td, *J* = 14.1, 6.4 Hz, 1H), 3.22

(dddd, J = 15.4, 14.0, 7.2, 1.2 Hz, 1H), 3.06 (ddd, J = 16.4, 6.4, 2.0 Hz, 1H), 2.52 (ddd, J = 12.7, 2.8, 1.5 Hz, 1H), 2.43 (dd, J = 12.7, 3.0 Hz, 1H).

^{13}C NMR (100 MHz, CD_3OD): δ 169.0, 149.2, 142.0, 141.5, 127.4, 126.3, 125.7, 124.3, 122.6, 119.0, 112.3, 102.0, 64.8, 56.8, 52.4, 51.1, 31.4, 20.9.

IR (Neat Film, NaCl): 3106, 2930, 1672, 1620, 1580, 1556, 1520, 1486, 1436, 1412, 1376, 1342,1270, 1202, 1132, 1034, 1000, 964, 824, 798, 720, 676, cm^{-1}.

HRMS (ESI+): *m/z* calc'd for $C_{18}H_{14}N_3OS$ $[M+H]^+$: 320.0852, found 320.0857.



130 ***137***

Allylic alcohol 137: To a flame dried 1 dram vial in a nitrogen filled glove box was added CuCl (1.5 mg, 0.0155 mmol, 0.38 equiv), BINAP (9.65 mg, 0.0155 mmol, 0.38 equiv), NaO*t*-Bu (1.5 mg, 0.0155 mmol, 0.38 equiv) and THF (1 mL, 0.04 M). The vial was sealed and stirred for 10 min at 23 °C. Then, dienone **130** (20.0 mg, 0.04 mmol, 1.0 equiv) and B_2Pin_2 (81.3 mg, 0.32 mmol, 8.0 equiv) as a solution in THF (1 mL, 0.04M) were added to the CuCl solution. The vial was sealed with a septa cap and removed for the glovebox. MeOH (0.024 mL, 0.6 mmol, 15.0 equiv) was then added, and the reaction mixture was stirred for 10 min at 23 °C, at which point LC/MS analysis indicated complete consumption of the starting material. The reaction mixture was diluted with EtOAc (5 mL) and a saturated solution of NH_4Cl (3 mL). The layers were separated, and the aqueous phase was extracted with EtOAc (4x4 mL). The combined organic phases were dried over Na_2SO_4 and concentrated in vacuo. The crude solid was purified by preparatory TLC (60%

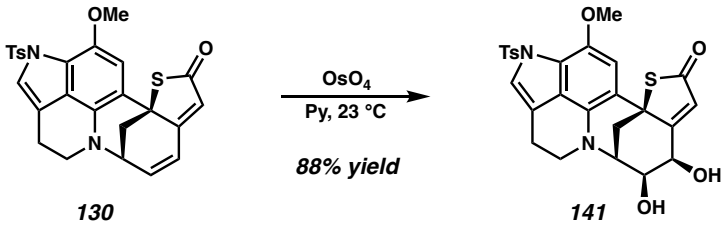
EtOAc/hexanes) to afford the titled compound (10.3 mg, 50% yield) as a yellow solid. Suitable crystals for X-Ray diffraction were grown via layer diffusion (CH_2Cl_2/hexanes)

^{1}H NMR (400 MHz, C_6D_6): δ 7.88 (d, J = 8.4 Hz, 2H), 7.40 (s, 1H), 7.00 (s, 1H), 6.79 – 6.47 (m, 2H), 4.92 (ddd, J = 3.9, 2.6, 1.2 Hz, 1H), 3.72 (s, 1H), 3.46 (s, 3H), 3.23 (td, J = 2.7, 1.2 Hz, 1H), 2.99 (dt, J = 19.4, 2.7 Hz, 1H), 2.80 – 2.58 (m, 2H), 2.56 (s, 1H), 2.49 – 2.27 (m, 2H), 2.15 (dd, J = 12.0, 2.5 Hz, 1H), 1.80 (dd, J = 12.1, 4.0 Hz, 1H), 1.71 (s, 3H).

^{13}C NMR (100 MHz, C_6D_6): δ 201.2, 143.8, 141.4, 139.8, 137.8, 130.0, 129.4, 121.8, 121.0, 120.9, 114.4, 114.3, 108.7, 66.1, 59.9, 58.1, 56.1, 47.6, 45.6, 32.4, 30.7, 22.8, 21.1.

IR (Neat Film, NaCl): 3315, 2919, 1712, 1503, 1355, 1286, 1173, 1104,

HRMS (ESI+): *m/z* calc'd for $C_{26}H_{25}N_2O_5S_2$ $[M+H]^+$: 509.1199, found 509.1196.



130 ***141***

Diol 141: To a 20 mL glass vial equipped with a septum cap was added diene **130** (20 mg, 0.041 mmol, 1.0 equiv), and the vial was evacuated and backfilled with nitrogen 3 times. Freshly distilled pyridine (1 mL) was added, followed by OsO_4 (11.4 mg, 0.0449mmol, 1.1 equiv) as a solution in pyridine (0.3 mL). The reaction mixture was stirred at 23 °C for 30 min, after which LC/MS analysis indicated complete consumption of the starting material. The reaction was quenched by addition of saturated aqueous Na_2SO_3 (0.5 mL) and water (5 mL). The mixture was extracted with EtOAc (4x5 mL), and the combined organic layers were dried over Na_2SO_4, filtered, and concentrated *in vacuo*. The crude osmate ester was dissolved in THF (1.5 mL), then saturated aqueous Na_2SO_3 (0.5 mL) and water (1 mL)

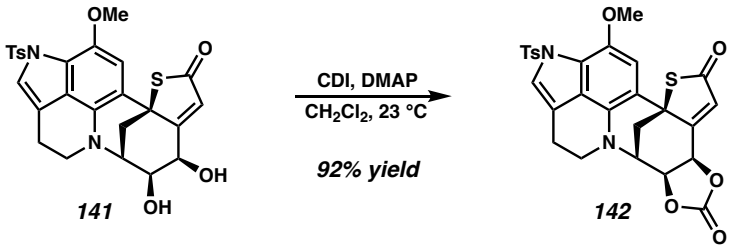
were sequentially added. The resulting mixture was vigorously stirred for 15 h before water (5 mL) was added. The mixture was extracted with EtOAc (3x7 mL), dried with Na_2SO_4, filtered, and concentrated in vacuo. The crude product was purified by silica gel flash chromatography (40→80% EtOAc/hexanes) to afford diol **141** as a light-yellow foam (18.9 mg, 0.0361 mmol, 88% yield).

^{1}H NMR (400 MHz, CD_2Cl_2): δ 7.75 (d, *J* = 8.4 Hz, 2H), 7.31 (s, 1H), 7.27 (d, *J* = 7.7 Hz, 2H), 6.77 (s, 1H), 5.98 (d, *J* = 2.0 Hz, 1H), 4.37 (t, *J* = 3.8 Hz, 1H), 4.26 (dd, *J* = 4.3, 1.9 Hz, 1H), 3.72 (t, *J* = 3.3 Hz, 1H), 3.62 (s, 3H), 3.42 (t, *J* = 5.8 Hz, 2H), 3.00 (tdd, *J* = 6.3, 4.2, 1.6 Hz, 2H), 2.83 (br, 1H), 2.58 (dd, *J* = 12.7, 3.0 Hz, 1H), 2.45 (ddd, *J* = 12.7, 3.0, 1.0 Hz, 1H), 2.37 (s, 3H), 1.64 (br, 1H).

^{13}C NMR (100 MHz, CD_2Cl_2): δ 197.1, 178.6, 145.1, 139.7, 137.0, 131.6, 129.8, 127.9, 123.7, 123.1, 122.1, 121.1, 114.7, 112.4, 108.4, 73.7, 69.2, 60.3, 58.1, 57.2, 48.4, 34.6, 23.3, 21.7.

IR (Neat Film, NaCl): 2920, 1832, 1814, 1690, 1504, 1440, 1404, 1354, 1288, 1230, 1168, 1138, 1106, 1056, 838, 814, 666 cm^{-1}.

HRMS (ESI+): *m/z* calc'd for $C_{26}H_{25}N_2O_6S_2$ $[M+H]^+$: 525.1154, found 525.1144.



Cyclic carbonate 142: To a 20 mL glass vial equipped with a septum cap was added diol **141** (20.8 mg, 0.0397 mmol, 1.0 equiv) and DMAP (0.1 mg, 0.8 μmol, 0.02 equiv). The vial was evacuated and backfilled with nitrogen three times. CDI (18.6 mg, 0.119 mmol,

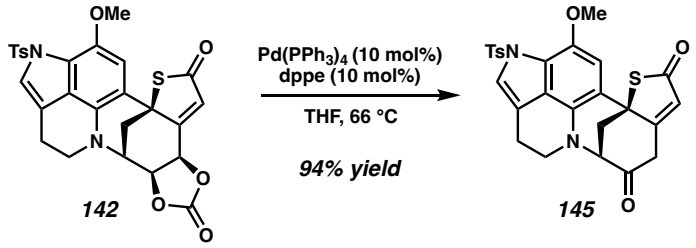
3.0 equiv) was added as a solution in CH_2Cl_2 (4 mL). The reaction mixture was stirred at 23°C for 30 min, after which TLC analysis indicated full consumption of starting material. The reaction mixture was washed with 5% aqueous citric acid (3x5 mL), dried with Na_2SO_4, and concentrated *in vacuo*. The crude product was purified by silica gel flash chromatography (0→35% EtOAc/hexanes) to afford cyclic carbonate **142** as a yellow foam (20 mg, 0.0363 mmol, 92%).

^{1}H NMR (400 MHz, C_6D_6): δ 7.88 – 7.80 (m, 2H), 7.46 (d, *J* = 1.2 Hz, 1H), 6.64 – 6.62 (m, 2H), 6.61 (s, 1H), 5.97 (d, *J* = 2.0 Hz, 1H), 3.73 (dt, *J* = 6.7, 1.8 Hz, 1H), 3.59 (ddd, *J* = 6.6, 2.1, 0.7 Hz, 1H), 3.28 (s, 3H), 2.92 (q, *J* = 2.8 Hz, 1H), 2.49 – 2.27 (m, 4H), 1.96 (ddd, *J* = 13.4, 2.7, 1.4 Hz, 1H), 1.74 (dd, *J* = 13.4, 3.5 Hz, 1H), 1.70 (s, 3H).

^{13}C NMR (100 MHz, C_6D_6): δ 193.9, 170.4, 152.1, 144.3, 141.2, 137.5, 130.7, 129.5, 124.8, 124.3, 122.5, 121.5, 113.6, 109.5, 108.3, 75.9, 73.3, 57.8, 56.7, 53.0, 47.4, 34.1, 22.7, 21.1.

IR (Neat Film, NaCl): 3442, 2920, 1832, 1814, 1690, 1504, 1440, 1404, 1354, 1288, 1230, 1168, 1138, 1106, 1056, 838, 814, 666 cm^{-1}.

HRMS (ESI+): *m/z* calc'd for $C_{27}H_{23}N_2O_7S_2$ $[M+H]^+$: 551.0947, found 551.0937.



Diketone 145: Procedure adapted from a report by Noyori.[35] A 20 mL glass vial containing cyclic carbonate **142** (20.6 mg, 0.0375 mmol, 1.0 equiv) was transferred to a nitrogen-filled glovebox. In a separate vial, a stock solution of $Pd(PPh_3)_4$ (7.7 mg) and dppe (2.7 mg) in THF (2.6 mL) was prepared and stirred at 28 °C for 10 min. Then, 1.5 mL of the catalyst

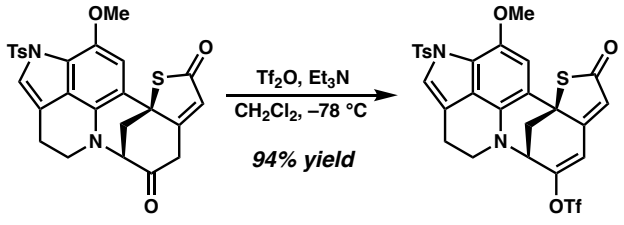
solution was transferred to the vial containing cyclic carbonate **142** (for 4.4 mg of $Pd(PPh_3)_4$ [0.00375 mmol, 10 mol %] and 1.5 mg dppe [0.00375 mmol, 10 mol %]). The vial was sealed with a PTFE/silicone septum cap and electrical tape, removed from the glovebox, and stirred at 66 °C for 5 h. The reaction mixture was concentrated *in vacuo* and purified by silica gel flash chromatography (0→40% EtOAc/hexanes) to afford diketone **145** as a yellow oil (18 mg, 0.036, 94% yield).

^{1}H NMR (400 MHz, C_6D_6): δ 7.88 – 7.79 (m, 2H), 7.42 (s, 1H), 6.80 (s, 1H), 6.62 (d, *J* = 8.1 Hz, 2H), 5.20 (d, *J* = 2.2 Hz, 1H), 3.29 (s, 3H), 3.17 – 3.10 (m, 1H), 2.86 (dd, *J* = 17.0, 1.6 Hz, 1H), 2.73 – 2.64 (m, 1H), 2.60 – 2.43 (m, 2H), 2.38 – 2.25 (m, 2H), 2.11 (dd, *J* = 17.0, 2.4 Hz, 1H), 1.72 (s, 3H), 1.51 (dd, *J* = 13.3, 3.2 Hz, 1H).

^{13}C NMR (100 MHz, C_6D_6): δ 198.5, 195.5, 172.9, 144.1, 141.3, 137.7, 130.3, 129.4, 124.4, 122.9, 122.6, 121.7, 113.8, 112.0, 108.0, 62.9, 58.7, 56.7, 48.1, 43.9, 35.2, 22.6, 21.1. (An additional ^{13}C resonance associated with the tosyl group is obscured by the solvent signal.)

IR (Neat Film, NaCl): 2920, 1832, 1814, 1690, 1504, 1440, 1404, 1354, 1288, 1230, 1168, 1138, 1106, 1056, 838, 814, 666 cm^{-1}.

HRMS (ESI+): *m/z* calc'd for $C_{26}H_{23}N_2O_5S_2$ $[M+H]^+$: 507.1048, found 507.1051.



145 ***135***

Enol triflate 135: To a 20 mL glass vial containing diketone **145** (12 mg, 0.024 mmol, 1.0 equiv) under nitrogen was added CH_2Cl_2 (2.4 mL). The mixture was cooled to -78 °C in a

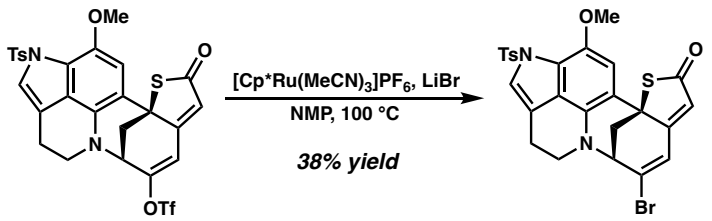
dry ice/acetone bath, then triethyl amine (34 μL, 0.24 mmol, 10 equiv) and triflic anhydride (20 μL, 0.12 mmol, 5 equiv) were sequentially added. The reaction mixture was stirred at -78 °C and the reaction progress was monitored by LC–MS. The reaction was quenched by addition of water (2 mL) at -78 °C upon completion (*ca*. 5-10 min). The resulting mixture was allowed to warm up to 23 °C, then the layers were separated. The organic phase was washed with water (2x2 mL), dried with Na_2SO_4, and concentrated *in vacuo*. The crude product was purified by silica gel flash chromatography (0→10% EtOAc/CH_2Cl_2) to afford enol triflate **135** as a red film (14.2 mg, 0.0222 mmol, 94% yield).

^{1}H NMR (400 MHz, C_6D_6): δ 7.83 – 7.75 (m, 2H), 7.41 (d, *J* = 1.7 Hz, 1H), 6.75 (s, 1H), 6.61 – 6.53 (m, 2H), 5.71 (s, 1H), 5.28 (s, 1H), 3.49 (ddd, *J* = 3.8, 2.5, 1.1 Hz, 1H), 3.29 (s, 3H), 2.82 – 2.72 (m, 2H), 2.52 (dddd, *J* = 15.7, 10.8, 6.7, 2.0 Hz, 1H), 2.31 (dt, *J* = 15.7, 2.9 Hz, 1H), 2.15 (dd, *J* = 12.5, 2.5 Hz, 1H), 1.79 (dd, *J* = 12.5, 3.9 Hz, 1H), 1.67 (s, 3H).

^{13}C NMR (100 MHz, C_6D_6): δ 195.1, 144.1, 141.9, 137.5, 130.4, 129.4, 128.0, 124.8, 124.3, 123.5, 121.8, 118.9 (q, *J* = 322.2 Hz), 116.3, 114.1, 112.1, 108.1, 56.8, 56.5, 49.2, 36.4, 22.8, 21.0. (Bridgehead sulfide carbon has the same chemical shift as the anisole methyl carbon, as shown in HSQC.)

IR (Neat Film, NaCl): 2920, 1832, 1814, 1690, 1504, 1440, 1404, 1354, 1288, 1230, 1168, 1138, 1106, 1056, 838, 814, 666 cm^{-1}.

HRMS (ESI+): *m/z* calc'd for $C_{27}H_{22}F_3N_2O_7S_3$ $[M]^+$: 638.0463, found 638.0547.



135 *136*

Alkenyl bromide 136: A 4 mL vial containing enol triflate **135** (18 mg, 0.028 mmol, 1.0 equiv) was brought to a nitrogen-filled glovebox. In a separate vial, a stock solution of $[Cp^*Ru(MeCN)_3]PF_6$ (10.2 mg) and LiBr (17.7 mg) in NMP (2.3 mL) was prepared and stirred at 28 °C for 10 mins. Then, 0.94 mL of the catalyst solution was transferred to the vial containing enol triflate **135** (for 4.3 mg of $[Cp^*Ru(MeCN)_3]PF_6$ [0.00852 mmol, 30 mol %] and 7.3 mg LiBr [0.0852 mmol, 3 equiv]). The vial was sealed with a PTFE/silicone septum cap and electrical tape, removed from glovebox, and stirred at 100 °C for 5 h. Then the reaction mixture was diluted with Et_2O (2 mL) and water (2 mL) and filtered through a PTFE syringe filter. The layers were separated, and the aqueous layer was extracted with Et_2O (4x2 mL). The combined organic phased were dried over Na_2SO_4 and concentrated *in vacuo*. The crude product was purified by silica gel flash chromatography (100% hexanes→100% CH_2Cl_2) to afford alkenyl bromide **136** (6.8 mg, 0.012 mmol, 38% yield) as an orange film.

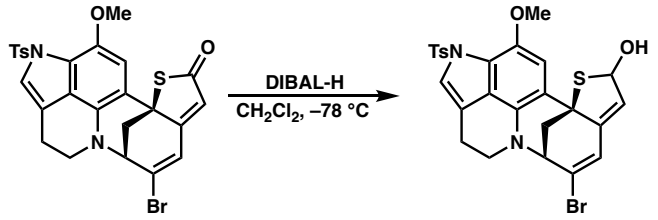
^{1}H NMR (400 MHz, C_6D_6): δ 7.84 – 7.76 (m, 2H), 7.41 (d, *J* = 1.7 Hz, 1H), 6.83 (s, 1H), 6.61 – 6.53 (m, 2H), 6.15 (s, 1H), 5.34 (s, 1H), 3.48 – 3.42 (m, 1H), 3.29 (s, 3H), 3.17 (ddd, *J* = 12.2, 11.1, 3.7 Hz, 1H), 2.90 (ddd, *J* = 11.1, 4.9, 2.5 Hz, 1H), 2.55 (dddd, *J* = 15.6, 12.1, 4.9, 1.9 Hz, 1H), 2.40 (dt, *J* = 15.6, 3.2 Hz, 1H), 2.14 (dd, *J* = 12.3, 2.5 Hz, 1H), 1.83 – 1.73 (m, 1H), 1.70 (s, 3H).

^{13}C NMR (100 MHz, C_6D_6): δ 195.5, 170.3, 143.9, 141.6, 137.7, 130.7, 129.4, 127.6, 124.3, 123.3, 121.4, 121.1, 114.2, 112.1, 108.4, 61.4, 56.8, 56.5, 49.7, 38.3, 23.2, 21.1. (A

^{13}C resonance associated with the tosyl group and the ^{13}C resonance associated with alkenyl bromide carbon are obscured by the solvent signal.)

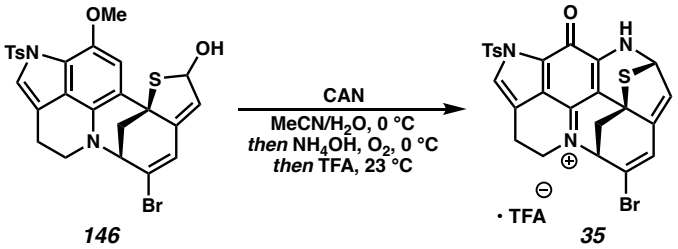
IR (Neat Film, NaCl): 2920, 1832, 1814, 1690, 1504, 1440, 1404, 1354, 1288, 1230, 1168, 1138, 1106, 1056, 838, 814, 666, cm^{-1}.

HRMS (ESI+): *m/z* calc'd for $C_{26}H_{22}BrN_2O_4S_2$ $[M+H]^+$: 571.0184, found 571.0154.

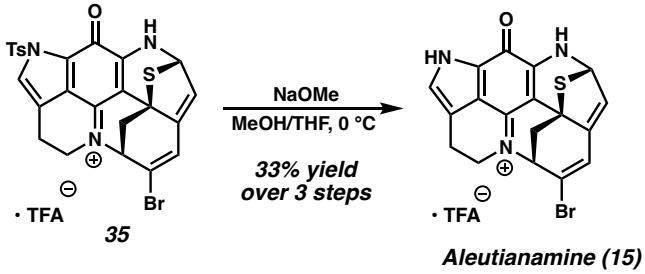


136 ***146***

Thiolactol 146: To an 8 mL vial containing alkenyl bromide **146** (6.8 mg, 0.0120 mmol, 1.0 equiv) under nitrogen was added CH_2Cl_2 (0.9 mL). The resulting mixture was cooled to –78 °C in a dry ice/acetone bath, then DIBAL (21 μL, 0.12 mmol, 10 equiv) was added as a freshly prepared solution in CH_2Cl_2 (0.3 mL, 0.4 M). The reaction was quenched at –78 °C by addition of 1 mL saturated aqueous Rochelle's salt solution immediately after the addition of DIBAL. The resulting mixture was allowed to warm up to 23 °C and was stirred vigorously for 45 min. The layers were separated, and the aqueous phase was extracted with CH_2Cl_2 (3x1 mL). The combined organic phases were dried over Na_2SO_4 and concentrated *in vacuo* to afford crude thiolactol **146** as a yellow oil, which was used directly in the next step without further purification.



***N*-tosylaleutianamine (35):** To an 8 mL vial containing thiolactol **146** (6.8 mg, 0.012 mmol, 1.0 equiv) under nitrogen was added MeCN (0.8 mL). The resulting solution was cooled to 0 °C in an ice water bath, and CAN (13.2 mg, 0.024 mmol, 2.0 equiv) was added dropwise as a freshly prepared solution in 0.3 mL water. The resulting mixture was stirred at 0 °C for 5 min, whereafter concentrated aqueous ammonia (27% w/w, 35 μL, 0.42 mmol, 35 equiv) was added. The reaction vessel was flushed with O_2, and the resulting mixture was stirred for 7 min under an O_2 atmosphere at 0 °C. The reaction mixture was then warmed to 23 °C and was diluted with EtOAc (2 mL) and water (1.5 mL). The layers were separated, and the aqueous phase was extracted with EtOAc (4x2 mL). The combined organic phases were dried over Na_2SO_4 and concentrated *in vacuo*. The residue was taken up in TFA (1 mL), and the mixture was allowed to stand at 23 °C for 10 min before being concentrated *in vacuo*. The crude N-tosyl aleutianamine (**35**) was used directly in the next step without further purification.



Aleutianamine (15): Procedure adapted from a report by Kita.[5f] To a 4 mL vial containing *N*-tosyl aleutianamine (**35**, 0.012 mmol, 1.0 equiv) under nitrogen was added THF (0.78

mL). The resulting mixture was cooled to 0 °C in an ice bath and 0.2 M NaOMe in MeOH (0.42 mL, 0.084 mmol, 7.0 equiv) was added. The reaction mixture was stirred at 0 °C for 10 min, after which 0.2 M TFA in MeOH (0.42 mL) was added and the reaction mixture was allowed to warm to 23 °C. The mixture was concentrated *in vacuo* and the residue was purified by preparative reverse-phase HPLC (Eclipse XDB-C18, 5 μm, 9.4 x 250 mm, MeCN-H_2O (0.1% TFA) = 0:100 to 100:0, linear gradient for 6 min, flow rate = 5 mL/min) to afford aleutianamine (**15**) as the TFA salt (2 mg, 0.00391 mmol, 33%).

^{1}H NMR (500 MHz, CD_3OD): δ 7.14 (s, 1H), 7.08 (d, *J* = 1.1 Hz, 1H), 5.97 (d, *J* = 3.4 Hz, 1H), 5.43 – 5.38 (m, 1H), 5.13 (t, *J* = 3.0 Hz, 1H), 4.29 – 4.22 (m, 2H), 3.29 – 3.18 (m, 1H), 3.14 – 3.05 (m, 1H), 2.67 (dd, *J* = 12.8, 3.1 Hz, 1H), 2.57 (ddd, *J* = 12.8, 3.0, 1.2 Hz, 1H).

^{13}C NMR (100 MHz, CD_3OD): δ 168.6, 149.8, 142.9, 142.2, 129.2, 126.5, 125.8, 122.7, 119.3, 118.1, 112.5, 101.8, 65.4, 64.9, 54.1, 49.8, 32.5, 21.2.

IR (Neat film, NaCl): 3106, 2928, 1674, 1616, 1520, 1410, 1342, 1170, 996, 800, 720, cm^{-1}.

HRMS (ESI+): *m/z* calc'd for $C_{18}H_{13}BrN_3OS$ $[M+H]^+$: 399.9937, found 399.9945.

1.10.3 COMPARISON OF SYNTHETIC ALEUTIANAMINE TO PUBLISHED DATA

Table 1.10.3.1 *^{1}H NMR comparison table for aleutianamine (**15**).*

	Natural aleutianamine TFA salt[6] (600 MHz, CD_3OD)	**Reported Synthetic aleutianamine TFA salt[7] (600 MHz, CD_3OD)**	**Synthetic aleutianamine TFA salt, this work, (500 MHz, CD_3OD)**
H-1	7.12 (s, 1H)	7.14 (s, 1H)	7.14 (s, 1H)
H-14	7.07 (s, 1H)	7.09 (s, 1H)	7.08 (d, J = 1.1 Hz, 1H)
H-8	5.96 (d, J = 3.3 Hz, 1H)	5.97 (d, J = 3.0 Hz, 1H)	5.97 (d, J = 3.4 Hz, 1H)

H-7	5.40 (d, J = 3.2 Hz, 1H)	5.41 (d, J = 3.0 Hz, 1H)	5.43 – 5.38 (m, 1H)
H-3	5.12 (t, J = 2.9 Hz, 1H)	5.13 (t, J = 3.0 Hz, 1H)	5.13 (t, J = 3.0 Hz, 1H)
H-17A	4.26 (dd, J = 10.5, 4.3 Hz, 1H)	4.28–4.23 (m, 2H)	4.29 – 4.22 (m, 2H)
H-17B	4.24 (dd, J = 10.5, 4.3 Hz, 1H)		
H-16A	3.22 (m, 1H)	3.25–3.18 (m, 1H)	3.29 – 3.18 (m, 1H)
H-16B	3.10 (dt, J = 16.2, 4.2 Hz, 1H)	3.12–3.06 (m, 1H)	3.14 – 3.05 (m, 1H)
H-4A	2.65 (dd, J = 12.7, 2.2 Hz, 1H)	2.66 (dd, J = 12.6, 3.0 Hz, 1H)	2.67 (dd, J = 12.8, 3.1 Hz, 1H)
H4B	2.54 (dd, J = 12.7, 3.0 Hz, 1H)	2.56 (dd, J = 12.6, 3.0 Hz, 1H)	2.57 (ddd, J = 12.8, 3.0,1.2 Hz, 1H)

Table 1.10.3.2 *^{13}C NMR comparison table for aleutianamine (**15**).*

	Natural aleutianamine TFA salt[6] (600 MHz, CD_3OD)	**Reported Synthetic aleutianamine TFA salt,[7] (600 MHz, CD_3OD)**	**Synthetic aleutianamine TFA salt, this work, (500 MHz, CD_3OD)**
C-11	167.2	168.6	168.6
C-19	148.3	148.8	149.8
C-6	141.5	142.9	142.9
C-10	140.8	142.2	142.2
C-1	127.8	129.2	129.2
C-14	125.2	126.5	126.5
C-12	124.3	125.8	125.8
C-15	121.2	122.7	122.7
C-20	118.0	119.3	119.3
C-2	116.7	118.1	118.1
C-7	111.1	112.5	112.5
C-21	100.3	101.8	101.8
C-8	64.0	65.4	65.4
C-3	63.4	64.9	64.9

C-17	52.6	54.1	54.1
C-5	48.5	49.8	49.8
C-4	31.1	32.5	32.5
C-16	19.8	21.2	21.2

Note: The small difference in ^{13}C NMR shifts between the synthetic and natural sample is likely due to incorrect referencing of the solvent signal in the original isolation report.

1.11 REFERENCES AND NOTES

(1) For representative reviews of pyrroloiminoquinones see (a) Antunes, E. M.; Copp, B. R.; Davies-Coleman, M. T.; Samaai, T. Pyrroloiminoquinone and related metabolites from marine sponges. *Nat. Prod. Rep.* **2005**, *22*, 62–72. (b) Hu, J.; Fan, H.; Xiong, J.; Wu, S. Discorhabdins and Pyrroloiminoquinone-Related Alkaloids. *Chem. Rev.* **2011**, *111*, 5465– 5491.

(2) (a) J.-C. J. Kalinski, A. Polyzois, S. C. Waterworth, X. S. Noundou and R. A. Dorrington. Current Perspectives on Pyrroloiminoquinones: Distribution, Biosynthesis and Drug Discovery Potential. *Molecules*, **2022**, *27*, 8724; (b) L. R. Barrows, D. C. Radisky, B. R. Copp, D. S. Swaffar, R. A. Kramer, R. L. Warters and C. M. Ireland. Makaluvamines, marine natural products, are active anti-cancer agents and DNA topo II inhibitors. *Anti-Cancer Drug Des.*, **1993**, *8*, 333–347. Also see refs. 1a and b.

(3) Lill, R. E.; Major, D. A.; Blunt, J. W.; Munro, H.G. M.; Battershill, C. N.; McLean, M. G.; Baxter, R. L. Studies on the Biosynthesis of Discorhabdin B in the New Zealand Sponge *Lantruculia* SP. B. *J. Nat. Prod.* **1995**, *58*, 306–311.

(4) For representative syntheses of simpler pyrroloiminoquinones see: (a) X. L. Tao, S. Nishiyama and S. Yamamura, Total Syntheses of Batzelline C and Isobatzelline C, the Novel Pyrroloquinoline Alkaloids Isolated from the Marine Sponge *Batzella* Sp. *Chem. Lett*., **1991**, *20*, 1785–1786; (b) J. D. White, K. M. Yager and T. Yakura, Synthetic Studies of the Pyrroloquinoline Nucleus of the Makaluvamine Alkaloids. Synthesis of the Topoisomerase II Inhibitor Makaluvamine D. *J. Am. Chem. Soc.*,

1994, *116*, 1831–1838; (c) T. Izawa, S. Nishiyama and S. Yamamura, Total syntheses of makaluvamines A, B, C, D and E, cytotoxic pyrroloiminoquinone alkaloids isolated from marine sponge bearing inhibitory activities against topoisomerase II. *Tetrahedron*, **1994**, *50*, 13593–13600; (d) D. Roberts, L. Venemalm, M. Alvarez and J. A. Joule, Synthesis of damirones A and B from a quinoline. *Tetrahedron Lett*., **1994**, *35*, 7857–7860; (e) E. V. Sadanandan, S. K. Pillai, M. V. Lakshmikantham, A. D. Billimoria, J. S. Culpepper and M. P. Cava, Efficient Syntheses of the Marine Alkaloids Makaluvamine D and Discorhabdin C: The 4,6,7-Trimethoxyindole Approach. *J. Org. Chem.*, **1995**, *60*, 1800–1805; (f) A. J. Peat and S. L. Buchwald, Novel Syntheses of Tetrahydropyrroloquinolines: Applications to Alkaloid Synthesis. *J. Am. Chem. Soc.*, **1996**, *118*, 1028–1030; (g) D. Roberts, J. A. Joule, M. A. Bros and M. Alvarez, Synthesis of Pyrrolo[4,3,2-de]quinolines from 6,7-Dimethoxy-4-methylquinoline. Formal Total Syntheses of Damirones A and B, Batzelline C, Isobatzelline C, Discorhabdin C, and Makaluvamines A−D. *J. Org. Chem.*, **1997**, *62*, 568–577; (h) M. Iwao, O. Motoi, T. Fukuda and F. Ishibashi, New synthetic approach to pyrroloiminoquinone marine alkaloids. Total synthesis of makaluvamines A, D, I, and K. *Tetrahedron*, **1998**, *54*, 8999–9010; (i) M. Alvarez, M. A. Bros, G. Gras, W. Ajana and J. A. Joule, Syntheses of Batzelline A, Batzeline B, Isobatzelline A, and Isobatzelline B. *Eur. J. Org Chem.*, **1999**, 1173–1183; (j) Y. Kita, M. Egi and H. Tohma, Total synthesis of sulfur-containing pyrroloiminoquinone marine product, (±)-makaluvamine F using hypervalent iodine(III)-induced reactions. *Chem. Commun*.,

1999, 143–144; (k) T. Oshiyama, T. Satoh, K. Okano and H. Tokuyama, Total synthesis of batzelline C and isobatzelline C. *RSC Adv*., **2012**, *2*, 5147–5149; (l) T. Oshiyama, T. Satoh, K. Okano and H. Tokuyama, Total synthesis of makaluvamine A/D, damirone B, batzelline C, makaluvone, and isobatzelline C featuring one-pot benzyne-mediated cyclization- functionalization. *Tetrahedron*, **2012**, *68*, 9376–9383; (m) J. Backenköhler, S. Spindler and P. Spiteller, Total Synthesis of Damirone C, Makaluvamine O, Makaluvone, Batzelline C and Batzelline D. *ChemistrySelect*, **2017**, *2*, 2589–2592; (n) Y. Yamashita, L. Poignant, J. Sakata and H. Tokuyama, Divergent Total Syntheses of Isobatzellines A/B and Batzelline A. *Org. Lett*., **2020**, *22*, 6239–6243; (o) J. An, R. K. Jackson III, J. P. Tuccinardi and J. L. Wood, Pyrroloiminoquinone Alkaloids: Total Synthesis of Makaluvamines A and K. *Org. Lett.*, **2023**, *25*, 1868–1871; and references therein.

(5) For representative syntheses of complex pyrroloiminoquinones see: (a) S. Nishiyama, J.-F. Cheng, X. L. Tao and S. Yamamura, Synthetic studies on novel sulfur-containing alkaloids, prianosins and discorhabdins: total synthesis of discorhabdin C. *Tetrahedron Lett*., **1991**, *32*, 4151–4154; (b) Y. Kita, H. Tohma, M. Inagaki, K. Hatanaka and T. Yakura, Total synthesis of discorhabdin C: a general aza spiro dienone formation from O-silylated phenol derivatives using a hypervalent iodine reagent. *J. Am. Chem. Soc*., **1992**, *114*, 2175–2180; (c) X. L. Tao, J.-F. Cheng, S. Nishiyama and S. Yamamura, Synthetic studies on tetrahydropyrroloquinoline-containing natural products: Syntheses of discorhabdin C, batzelline C and isobatzelline C. *Tetrahedron*, **1994**, *50*, 2017–2028; (d) K. M.

Aubart and C. H. Heathcock, A Biomimetic Approach to the Discorhabdin Alkaloids: Total Syntheses of Discorhabdins C and E and Dethiadiscorhabdin D. *J. Org. Chem.*, **1999**, *64*, 16–22; (e) H. Tohma, Y. Harayama, M. Hashizume, M. Iwata, M. Egi and Y. Kita, Synthetic Studies on the Sulfur-Cross-Linked Core of Antitumor Marine Alkaloid, Discorhabdins: Total Synthesis of Discorhabdin A. *Angew. Chem., Int. Ed*., **2002**, *41*, 348–350; (f) H. Tohma, Y. Harayama, M. Hashizume, M. Iwata, Y. Kiyono, M. Egi and Y. Kita, The first total synthesis of discorhabdin A. *J. Am. Chem. Soc.*, **2003**, *125*, 11235–11240; (g) M. W. Smith, I. D. Falk, H. Ikemoto and N. Z. Burns, A Convenient C-H Functionalization Platform for Pyrroloiminoquinone Alkaloid Synthesis. *Tetrahedron*, **2019**, *75*, 3366–3370; (h) T. Noro, J. Sakata and H. Tokuyama, Synthetic studies on discorhabdin V: Construction of the A–F hexacyclic framework. *Tetrahedron Lett*., **2021**, *81*, 153333; (i) B. C. Derstine, A. J. Cook, J. D. Collings, J. Gair, J. Saurí, E. E. Kwan and N. Z. Burns, Total Synthesis of (+)-Discorhabdin V. *Angew. Chem., Int. Ed*., **2024**, *63*, e202315284; and references therein.

(6) Zou, Y.; Wang, X.; Sims, J.; Wang, B.; Pandey, P.; Welsh, C. L.; Stone, R. P.; Avery, M. A.; Doerksen, R. J.; Ferreira, D.; Anklin, C.; Valeriote, F. A.; Kelly, M.; Hamann, M. T. Computationally Assisted Discovery and Assignment of a Highly Strained and PANC-1 Selective Alkaloid from Alaska's Deep Ocean. *J. Am. Chem. Soc.* **2019**, *141*, 4338–4344.

(7) Shimomura, M.; Ide, K.; Sakata, J.; Tokuyama, H. Unified Divergent Total Synthesis of Discorhabdin B, H, K, and Aleutianamine via the Late-Stage Oxidative N,S-Acetal Formation. *J. Am. Chem. Soc.* **2023**, *145*, 18233−18239.

(8) Tuccinardi, J. P.; Wood, J. L. Convergent Total Synthesis of Aleutianamine. *J. Am. Chem. Soc.* **2025**, *147*, 5736–5742.

(9) Rousseaux, S.; García-Fortanet, J.; Sanchez, M. A. D. A.; Buchwald, S. L. Palladium(0)-Catalyzed Arylative Dearomatization of Phenols. *J. Am. Chem. Soc.* **2011**, *133*, 9282–9285.

(10) Thibeault, C.; Clark, C. G.; DeLucca, I.; Hu, C. H.; Jeon, Y.; Lam, P. Y. S.; Qiao, J. X.; Yang, W.; Wang, Y.; Wang, T. C. 7-hydroxy- spiropipiperidine indolinyl antagonists of p2y1 receptor. U.S. Patent US9428504B2, August 30, 2016.

(11) Campos, K. R.; Woo, J. C. S.; Lee, S.; Tillyer, R. D. A General Synthesis of Substituted Indoles from Cyclic Enol Ethers and Enol Lactones. *Org. Lett.* **2004**, *6*, 79−82.

(12) Surry, S. D.; Buchwald, L. S. Dialkylbiaryl phosphines in Pd-catalyzed amination: a user's guide. *Chem. Sci.* **2011**, *2*, 27−50.

(13) Andersen, H. S; Olsen, O. H.; Iversen, L. F.; Sørensen, A. L. P.; Mortensen, S. B.; Christensen, M. S.; Branner, S.; Hansen, T. K.; Lau, J. F.; Jeppesen, L.; Moran, E. J.; Su, J.; Bakir, F.; Judge, L.; Shahbaz, M.; Collins, T.; Vo, T.; Newman, M. J.; Ripka, W. C.; Møller, N. P. H. Discovery and SAR of a Novel Selective and Orally Bioavailable Nonpeptide Classical Competitive Inhibitor Class of Protein-Tyrosine Phosphatase 1B. *J. Med. Chem.* **2002**, *45*, 4443−4459.

(14) Ketothiophene coupling partner **71** had to be prepared freshly and used immediately in the subsequent reductive amination due to its propensity to undergo autoxidation to the resulting phenol under ambient conditions (*i.e*. prolonged storage at –20 ºC).

(15) Lee, O.; Law, K.; Ho, C.; Yang, D. Highly Chemoselective Reductive Amination of Carbonyl Compounds Promoted by $InCl_3$/ Et_3SiH/MeOH System. *J. Org. Chem.* **2008**, *73*, 8829−8837.

(16) Small amounts of undesired dibromination were also observed (tentatively bromination of the thiophene C3 position); THF was found to be the optimal solvent to suppress this by product, although it was still observed under the optimized reaction conditions. Additionally, it should be noted that if bromination is first performed, the subsequent reductive amination failed to produce the coupled product **73**.

(17) These reaction conditions were derived from the conditions reported by Buchwald, see ref. 9.

(18) Intermolecular radical-based dearomative arylations of thiophene have been reported utilizing thiophene as a solvent. See: a) Crich, D.; Patel, M. Facile Dearomatizing Radical Arylation of Furan and Thiophene. *Org. Lett.* **2005**, *7*, 3625–3628. b) Crich, D.; Patel, M. Radical dearomatization of arenes and heteroarenes. *Tetrahedron* **2006**, *62*, 7824–7837.

(19) For reviews of the Buchwald–Hartwig cyclization see: (a) P. Ruiz-Castillo and S. L. Buchwald*, Chem. Rev.*, **2016**, *116*, 12564–12649; (b) P. A. Forero-Cort´es and A. M. Haydl, *Org. Process Res. Dev*., **2019**, *23*, 1478–1483; and references therein.

(20) (a) R. C. Larock and E. K. Yum, *J. Am. Chem. Soc*., **1991**, *113*, 6689–6690. 3,4-fused tricyclic indoles have been prepared using an intramolecular Larock indolization. See (b) D. Shan, Y. Gao and T. Jia, *Angew. Chem., Int. Ed.*, **2013**, *52*, 4902–4905; (c) Y. Gao, D. Shan and Y. Jia, *Tetrahedron*, **2014**, *70*, 5136– 5141.

(21) S. T. Kadam and S. S. Kim, *Synthesis*, **2008**, *2*, 267–271.

(22) K. V. Chuang, M. E. Kieffer and S. E. Reisman, *Org. Lett.*, **2016**, *18*, 4750–4753.

(23) S. P. Breazzano, Y. B. Poudel and D. L. Boger, *J. Am. Chem. Soc*., **2013**, *135*, 1600–1606.

(24) M. Shen, G. Li, B. Z. Lu, A. Hossain, F. Roschangar, V. Farina and C. H. Senanayake, *Org. Lett*., **2004**, *6*, 4129–4132.

(25) This is supported by observation of large amounts of protodebromination (*i.e*. **85**) and other unidentifiable by-products in the LC/MS trace, which is not the case when the reaction is allowed to proceed for 24 h (*i.e*. optimized conditions).

(26) (a) W.-M. Cheng, R. Shang and Y. Fu, *Nat. Commun.*, **2018**, *9*, 5215; (b) B. Zhao, R. Shang, G.-Z. Wang, S. Wang, H. Chen and Y. Fu, *ACS Catal.*, **2020**, *10*, 1334–1343; (c) G. Meng, Z. Wang, H. S. S. Chan, N. Chekshin, Z. Li, P. Wang and J.-Q. Yu, *J. Am. Chem. Soc*., **2023**, *145*, 8198–8208; (d) M. Wakioka, K. Hatakeyama, S. Sakai, T. Seki, K.-I. Tada, Y. Mizuhata, T. Nakazato, S. Koguchi, Y. Shibuya, Y. Maruyama and M. Ayabe, *Organometallics*, **2023**, *42*, 3454–3465; (e) Y. Fan, M. Cong and L. Peng, *Chem.–Eur. J*., **2014**, *20*, 2698–2702.

(27) Nitrogen alkylation was also attempted with (Csp^3) thiophene electrophiles.

(28) It should be noted that no reactivity was also observed in the simplified tricyclic system with the *o*-bromide present (see section 1.3).

(29) Bromination of this substrate proved unsuccessful; decomposition or oxidized arene products were typically observed.

(30) Similarly, no dearomative thiophene arylation product was obtained when employing the C3 ester thiophene fragment on the simplified tricycle, supporting the hypothesis that decreased nucleophilicity of the thiophene prevents dearomative arylation.

(31) Kita, Y.; Tohma, H.; Hatanaka, K.; Takada, T.; Fujita, S.; Mitoh, S.; Sakurai, H.; Oka, S. Hypervalent Iodine-Induced Nucleophilic Substitution of *para*-Substituted Phenol Ethers. Generation of Cation Radicals as Reactive Intermediates. *J. Am. Chem. Soc*. **1994**, *116*, 3684–3691.

(32) Benati, L.; Bencivenni, G.; Leardini, R.; Minozzi, M.; Nanni, D.; Scialpi, R.; Spagnolo, P.; Zanardi, G. Radical Reduction of Aromatic Azides to Amines with Triethylsilane. *J. Org. Chem.* **2006**, *71*, 5822–5825.

(33) White, J. D.; Yager, K. M.; Yakura, T. Synthetic Studies of the Pyrroloquinoline Nucleus of the Makaluvamine Alkaloids. Synthesis of the Topoisomerase II Inhibitor Makaluvamine D. *J. Am. Chem. Soc*. **1994**, *116*, 1831−1838.

(34) Solé, C.; Tatla, A.; Mata, J. A.; Whiting, A.; Gulyás, H.; Fernádez, E. Catalytic 1,3-Difunctionalisation of Organic Backbones through a Highly Stereoselective, One-

Pot, Boron Conjugate-Addition/Reduction/Oxidation Process. *Chem. Eur. J.* **2011**, *17*, 14248–14257.

(35) Suzuki, M.; Watanabe, A.; Noyori, R. Palladium(0)-Catalyzed Reaction of α,β-Epoxy Ketones Leading to β-Diketones. *J. Am. Chem. Soc.* **1980**, *102*, 2095–2096.

(36) Attempts to affect an epoxidation of thiobutenolide **130** resulted in either central arene oxidation and/or non-specific decomposition, again highlighting the sensitivity of the system to oxidants.

(37) Reaction conditions adopted from Noyori and coworkers. See reference 35.

(38) Imazaki, Y.; Shirakawa, E.; Ueno, R.; Hayashi, T. Ruthenium- Catalyzed Transformation of Aryl and Alkenyl Triflates to Halides. *J. Am. Chem. Soc*. **2012**, *134*, 14760−14763. Utilizing the reaction conditions reported my Reisman and coworkers led to lower yields and more complex reaction profiles. See: Hofstra, J. L.; Poremba, K. E.; Shimozono, A. M.; Reisman, S. E. Nickel-Catalyzed Conversion of Enol Triflates into Alkenyl Halides. *Angew. Chem. Int. Ed.* **2019**, *58*, 14901–14905.

(39) Tosyl group cleavage conditions were adapted from Kita. See reference 5f.

(40) Our results were largely in agreement with those obtained by Hamann and coworkers (see reference 6) in which aleutianamine (**15**) was highly potent against cancer cells. Of the same cell lines in which IC_{50} values were reported, only small discrepancies were observed: They reported an IC_{50} of 1μM and 25 nM against HCT-116 and PANC-1, respectively. We observed IC_{50} values of 70 and 90 nM against the same two cell lines, respectively.

(41) Pangborn, A. M.; Giardello, M. A.; Grubbs, R. H.; Rosen, R. K.; Timmers, F. J. Safe and Convenient Procedure for Solvent Purification. *Organometallics* **1996**, *15*, 1518–1520

(42) D. Crich, Md. Y. Rahaman, Thiomaleic Anhydride: A Convenient Building Block for the Synthesis of α-Substituted γ- and δ-Lactones through Free-Radical Addition, Nucleophilic Ring Opening, and Subsequent Thiocarboxylate Manipulation. *J. Org. Chem.* **2009**, *74*, 6792–6796.

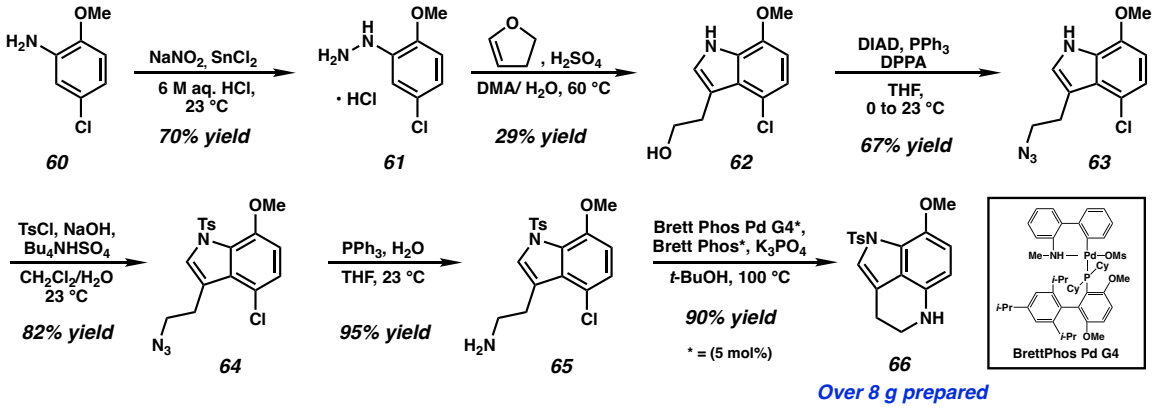
(43) T. Newhouse, C. A. Lewis, P. S. Baran, Enantiospecific Total Syntheses of Kapakahines B and F. *J. Am. Chem. Soc.* **2009**, *131*, 6360–6361.

Appendix 1

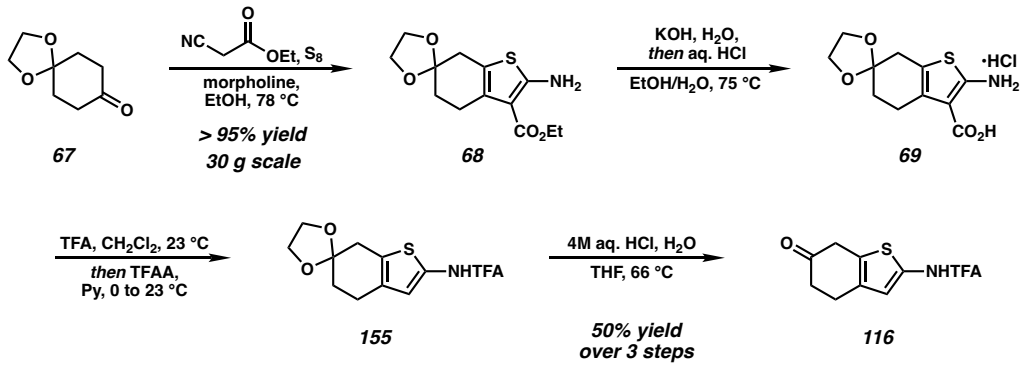
Synthetic Summary for Chapter 1:

Total Synthesis of Aleutianamine

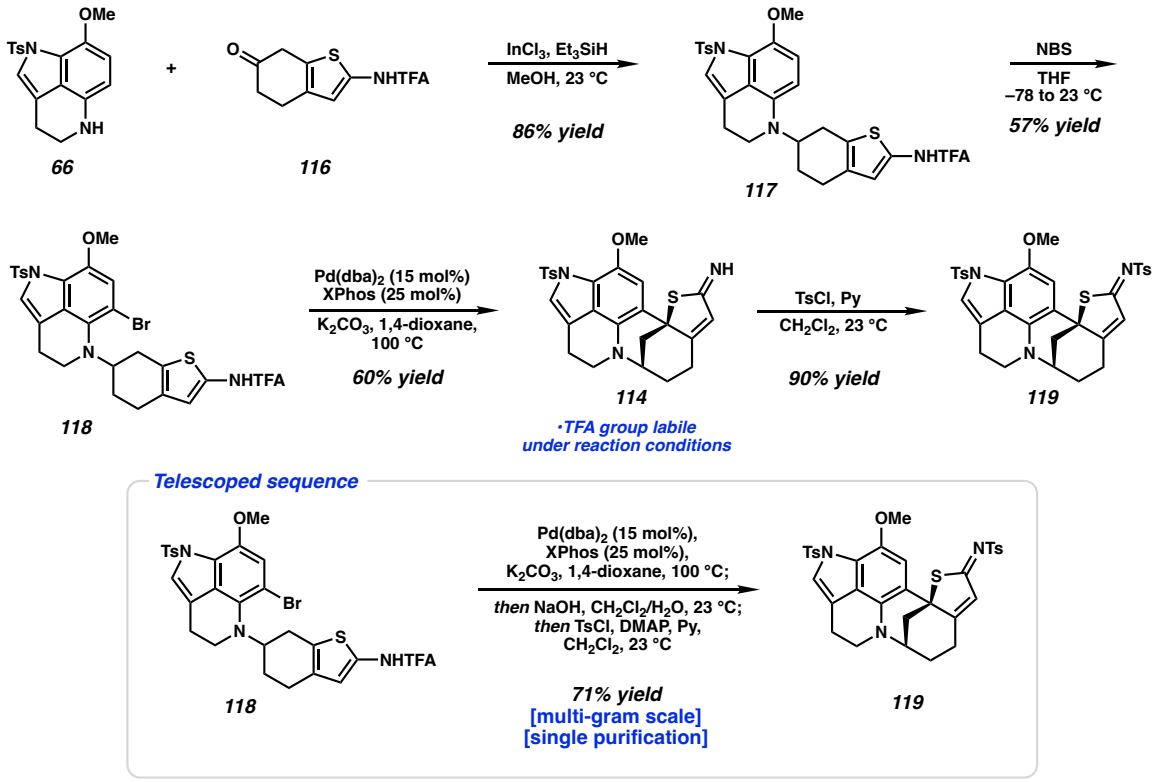
Scheme A1.1 *Synthesis of tricycle* ***66.***



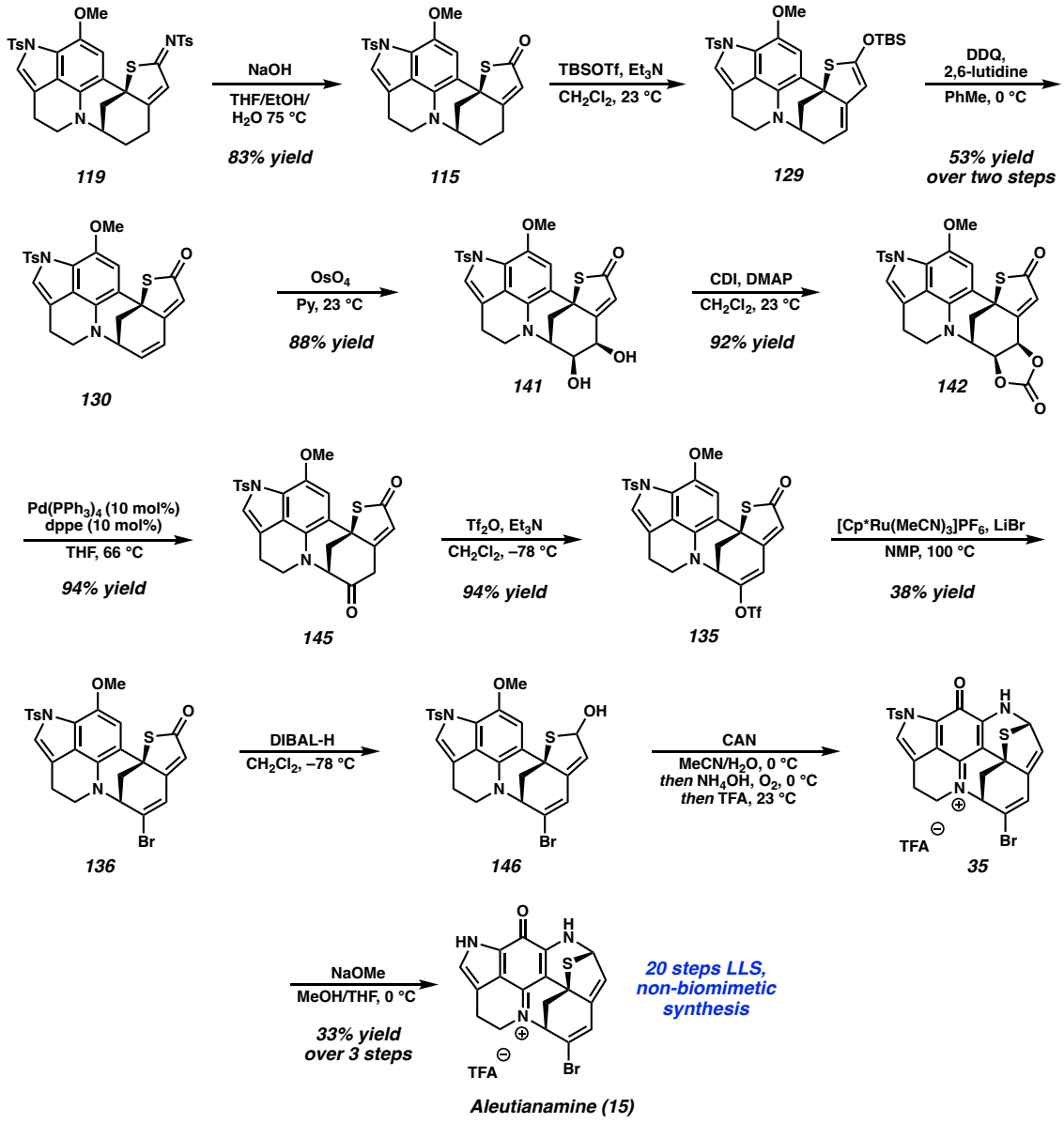
Scheme A1.2 *Synthesis of ketothiophene* ***116***.



Scheme A1.3 *Synthesis of N-Ts thioimidate* ***119***.



Scheme A1.4 *Synthesis of aleutianamine (**15**).*



Appendix 2

Spectra Relevant to Chapter 1:

Total Synthesis of Aleutianamine

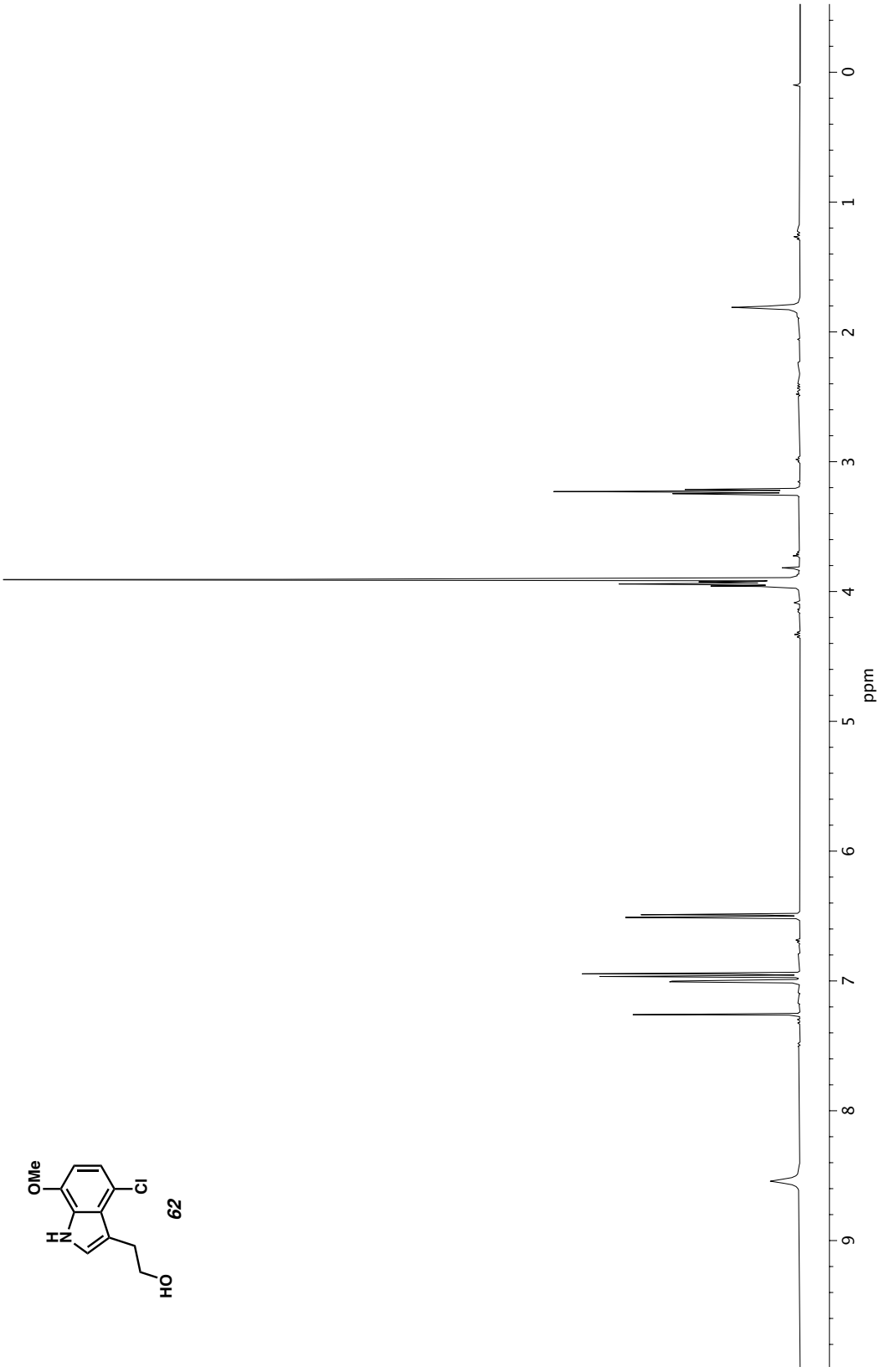


Figure A2.1. ^{1}H NMR (400 MHz, $CDCl_3$) of compound **62**.

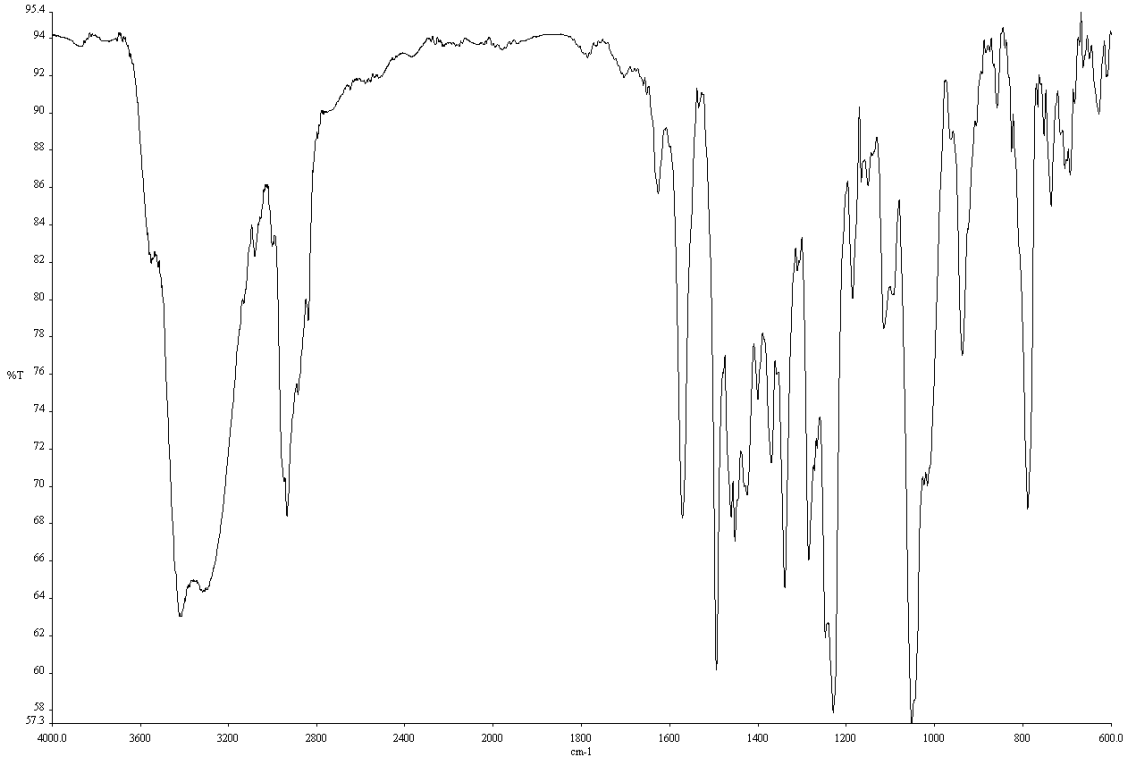


Figure A2.2. Infrared spectrum (Thin Film, NaCl) of compound **62**.

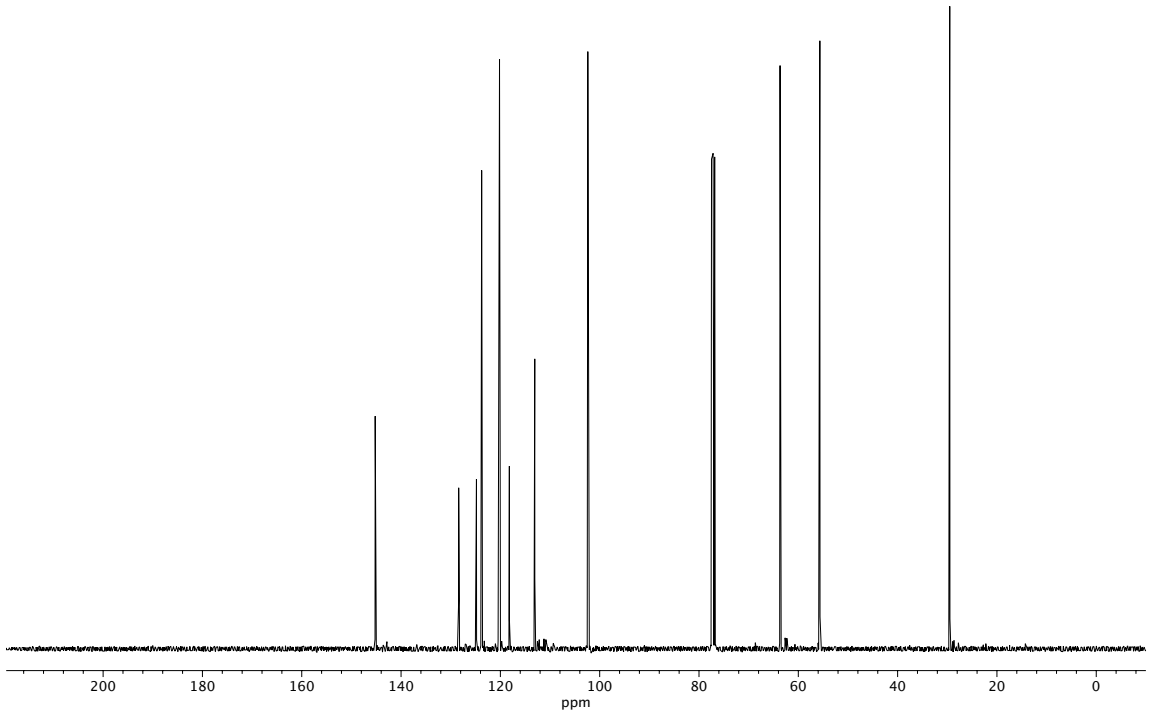


Figure A2.3. ^{13}C NMR (100 MHz, $CDCl_3$) of compound **62**.

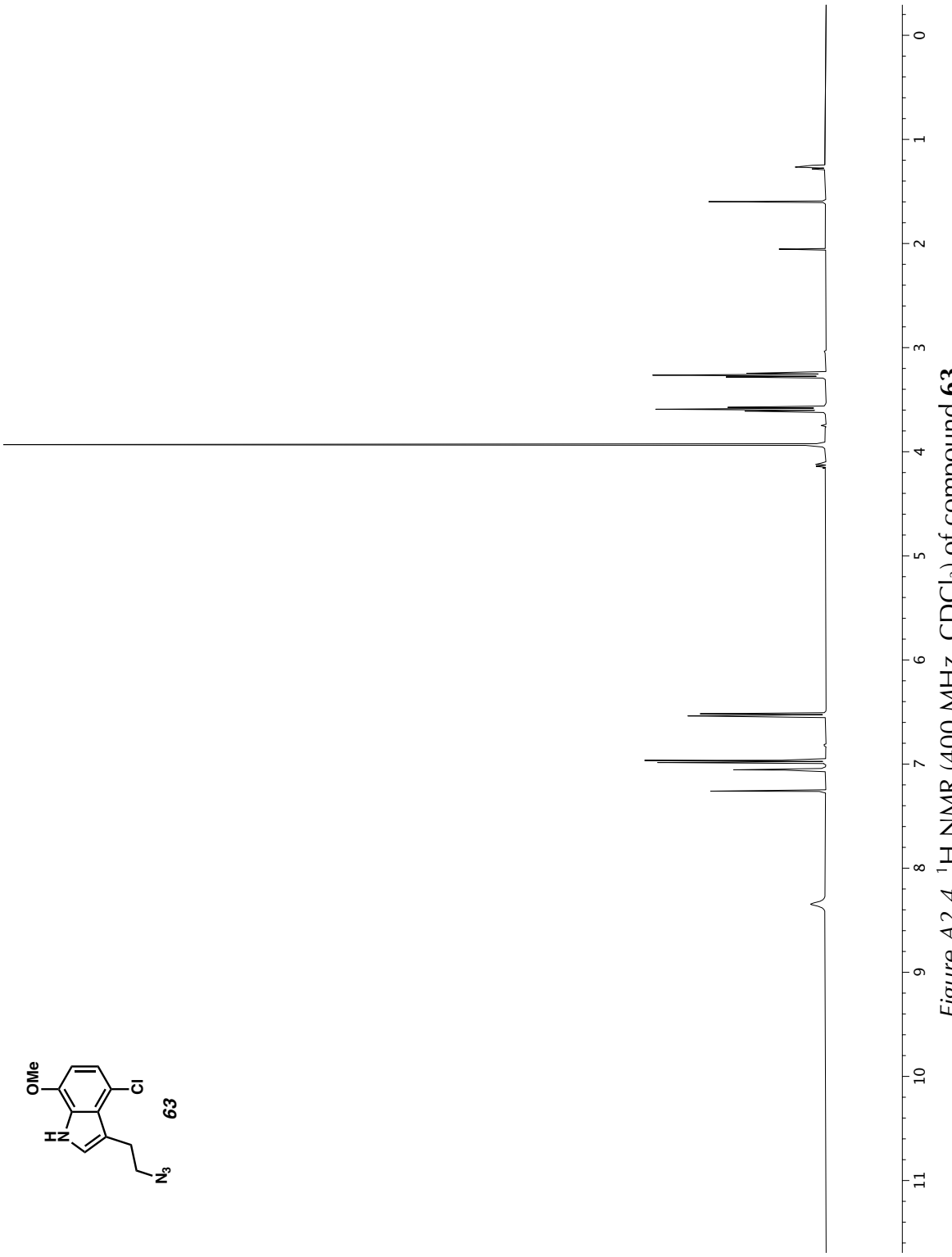


Figure A2.4. ^{1}H NMR (400 MHz, $CDCl_3$) of compound **63**.

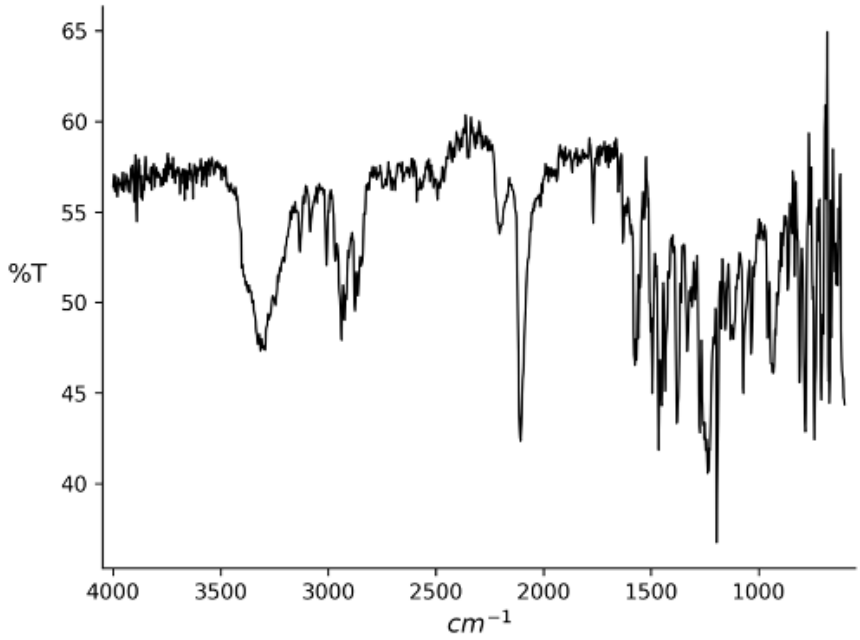


Figure A2.5 Infrared spectrum (Thin Film, NaCl) of compound **63**.

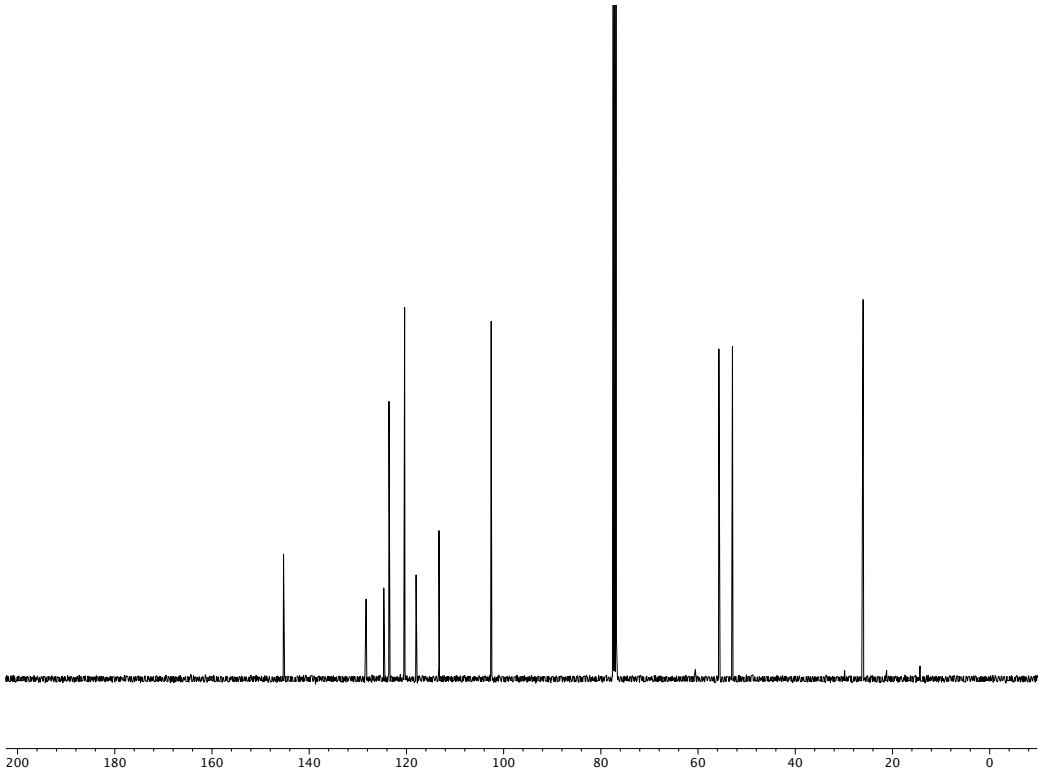


Figure A2.6 ^{13}C NMR (100 MHz, $CDCl_3$) of compound **63**.

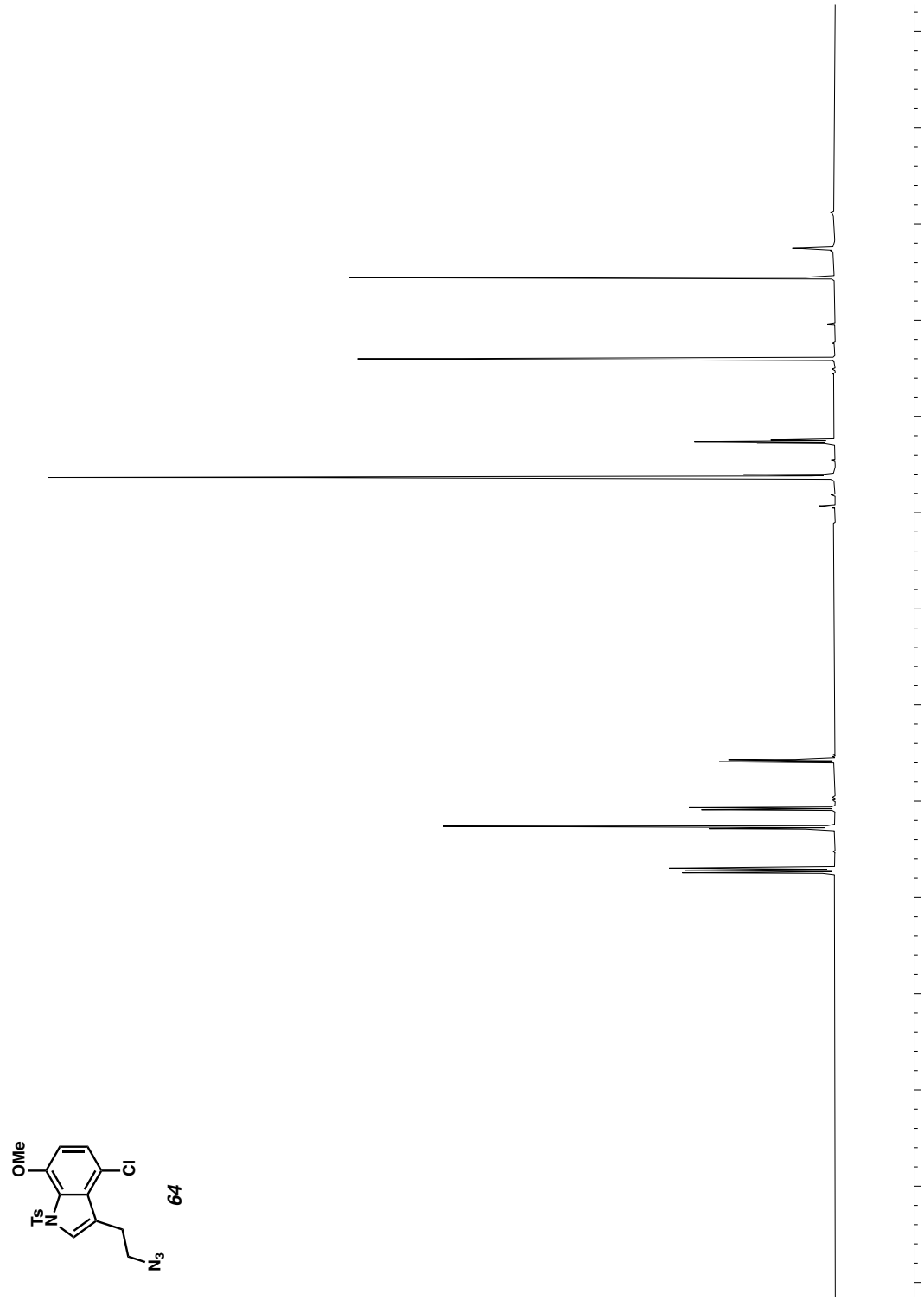


Figure A2.7. ^{1}H NMR (400 MHz, $CDCl_3$) of compound **64**.

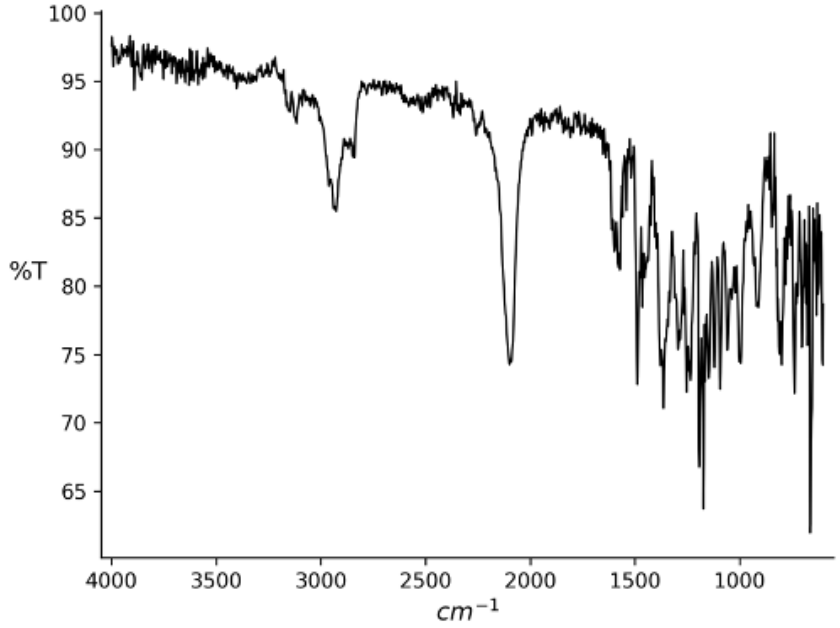


Figure A2.8 Infrared spectrum (Thin Film, NaCl) of compound **64**.

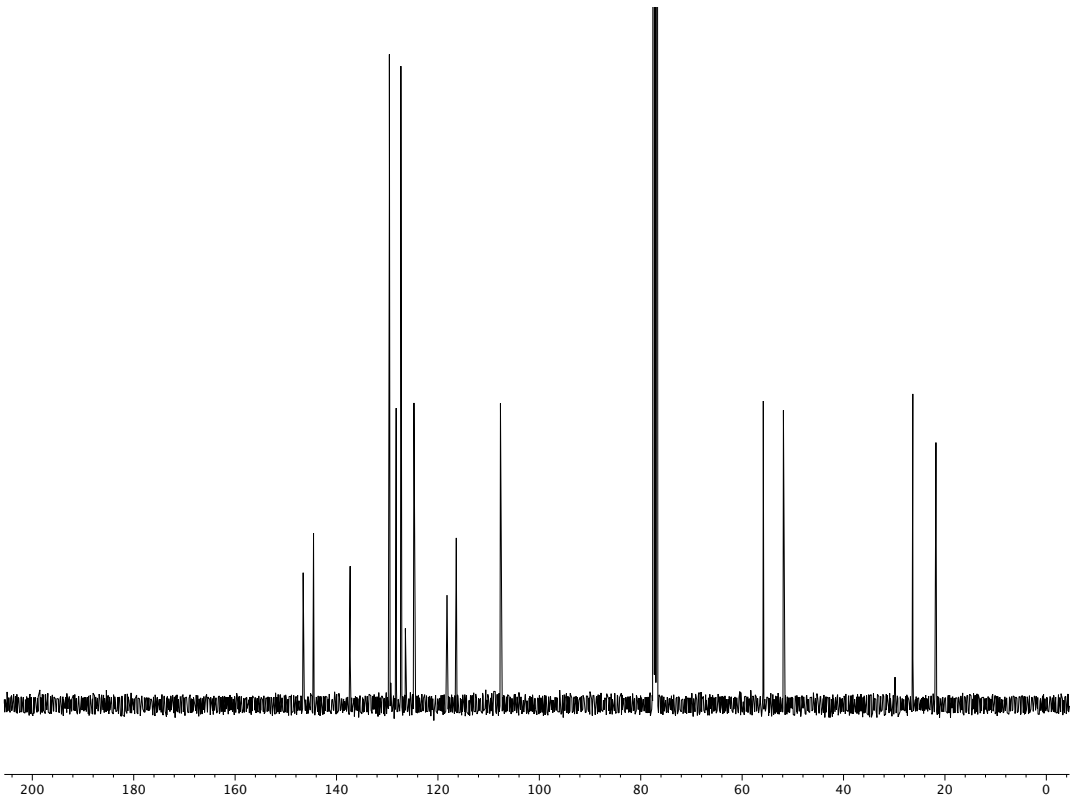


Figure A2.9 ^{13}C NMR (100 MHz, $CDCl_3$) of compound **64**.

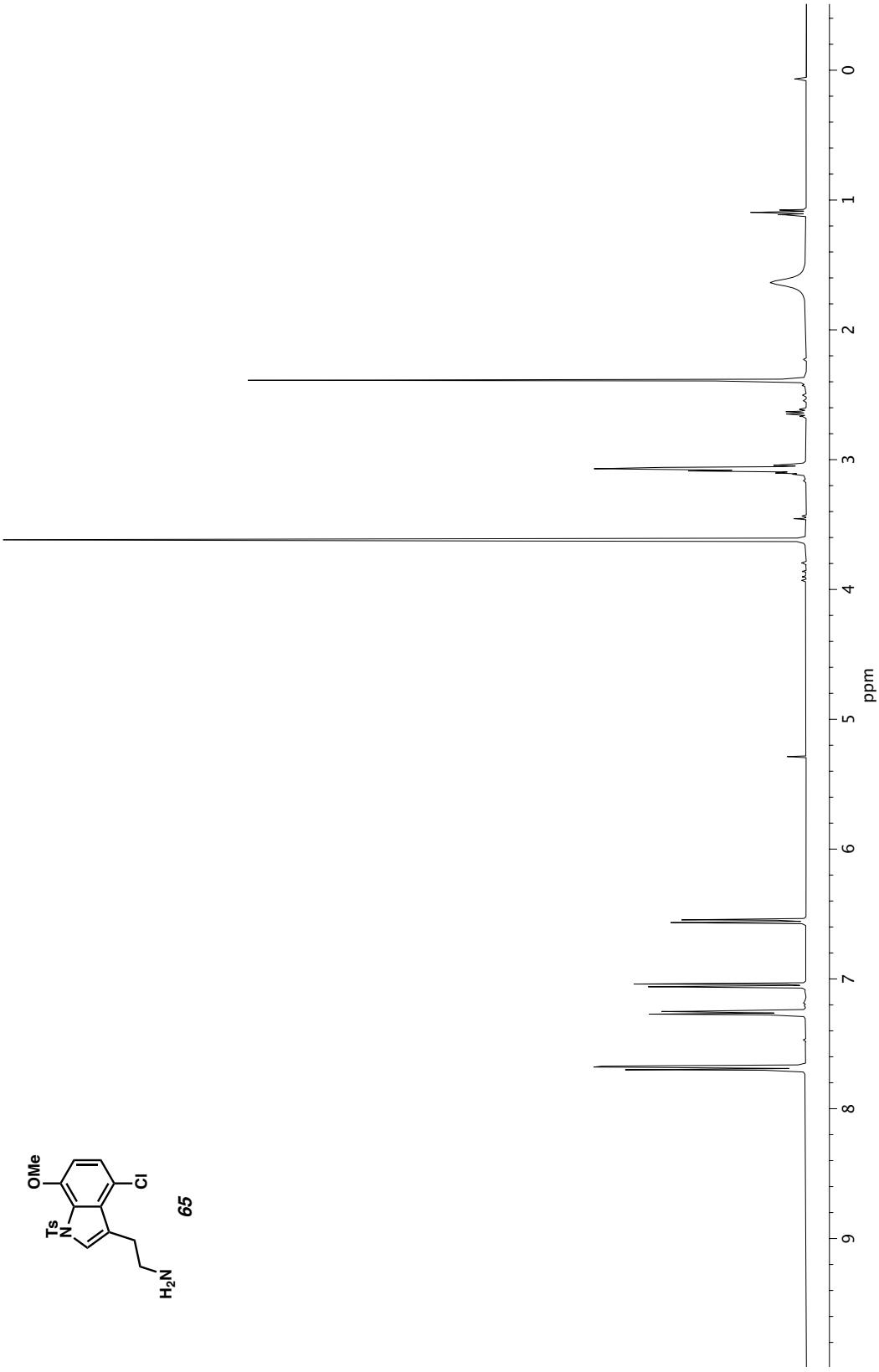


Figure A2.10. ^{1}H NMR (400 MHz, $CDCl_3$) of compound **65**.

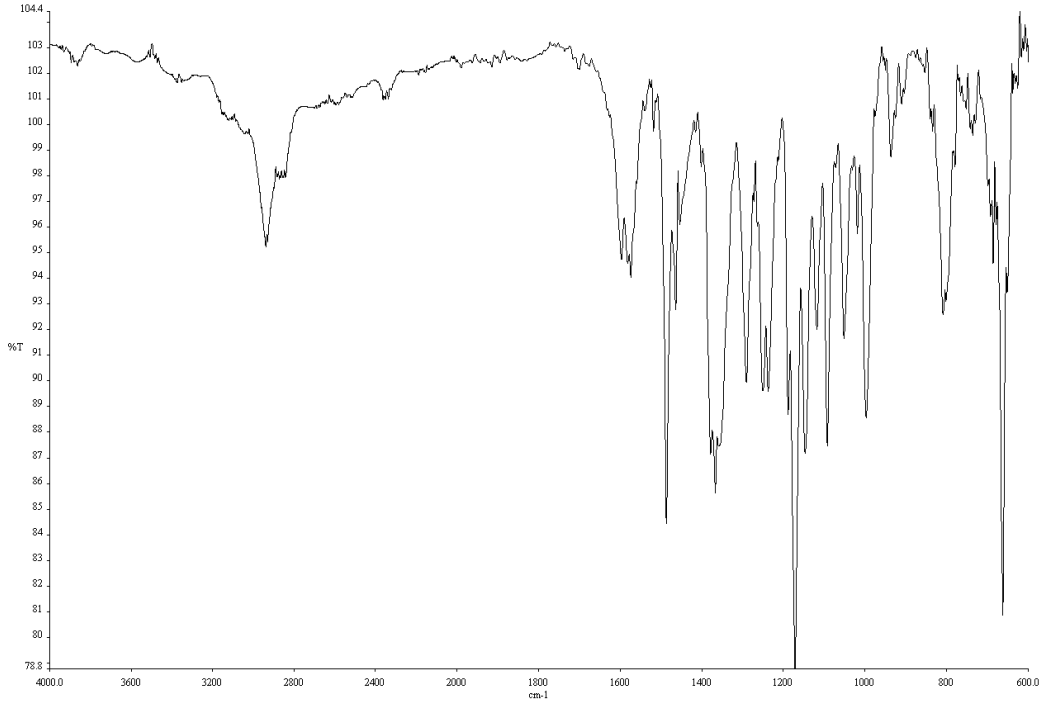


Figure A2.11 Infrared spectrum (Thin Film, NaCl) of compound **65**.

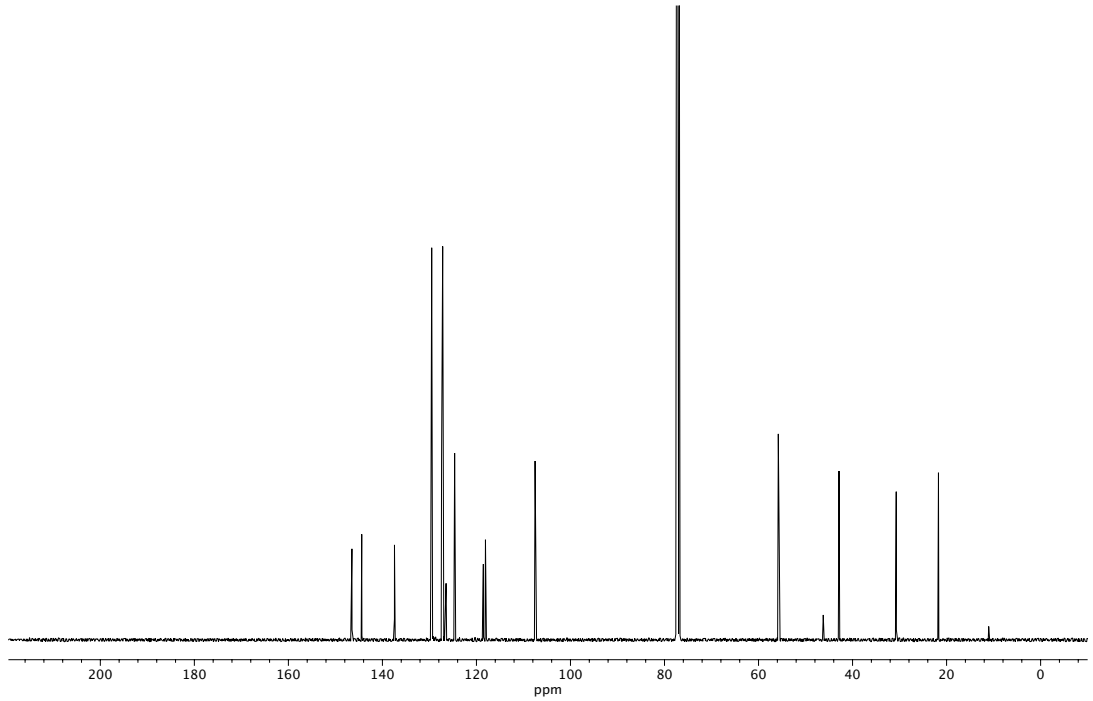


Figure A2.12 ^{13}C NMR (100 MHz, $CDCl_3$) of compound **65**.

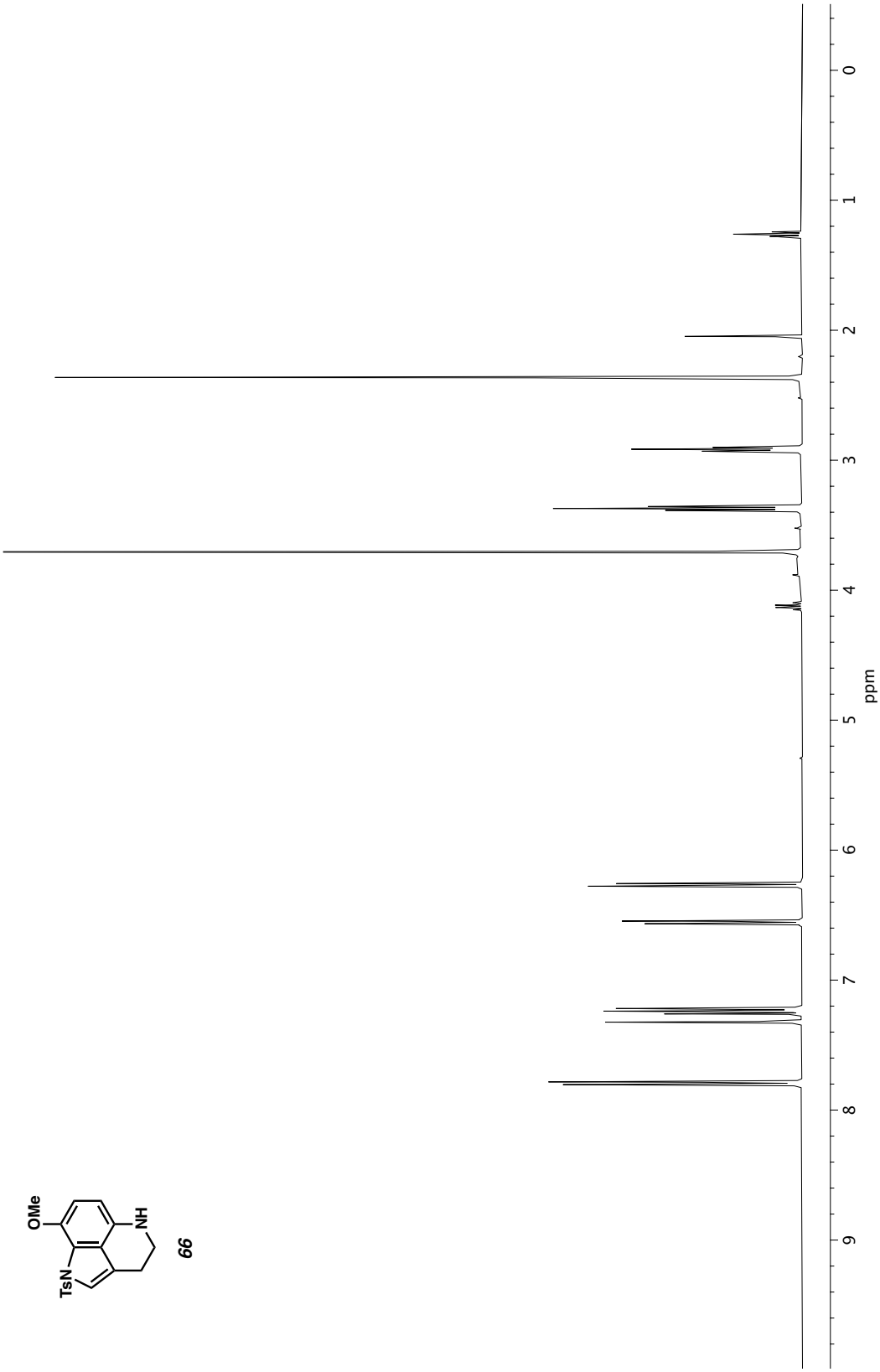


Figure A2.13. ^{1}H NMR (400 MHz, $CDCl_3$) of compound **66**.

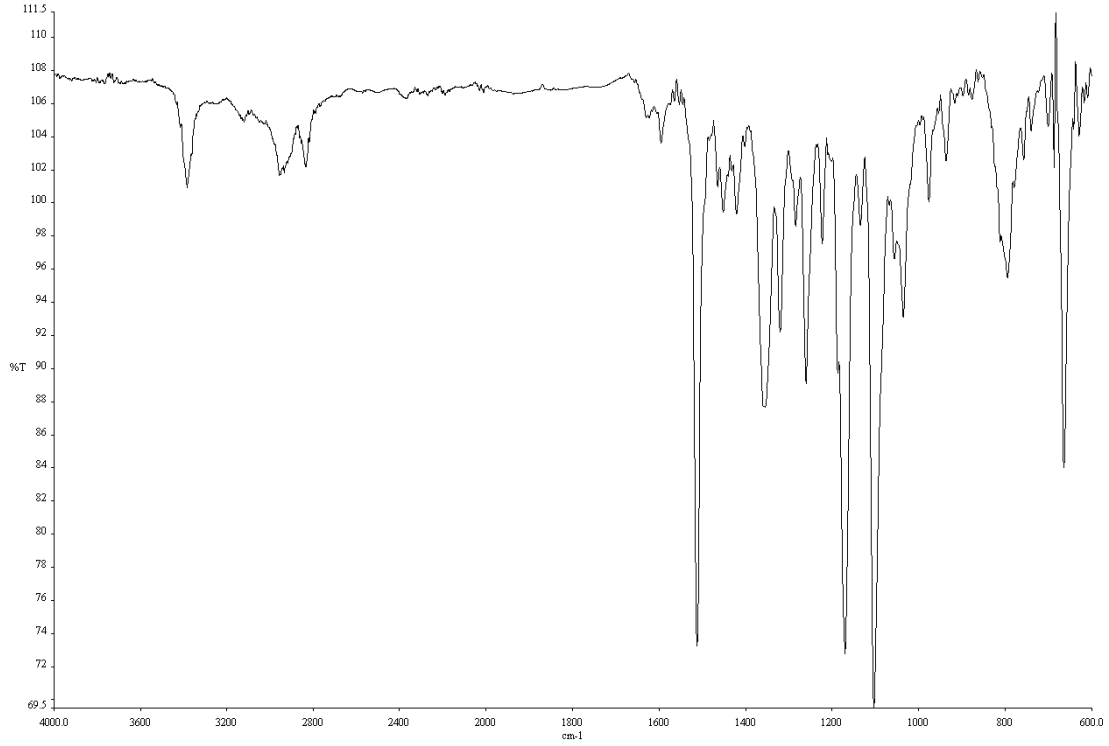


Figure A2.14 Infrared spectrum (Thin Film, NaCl) of compound **66**.

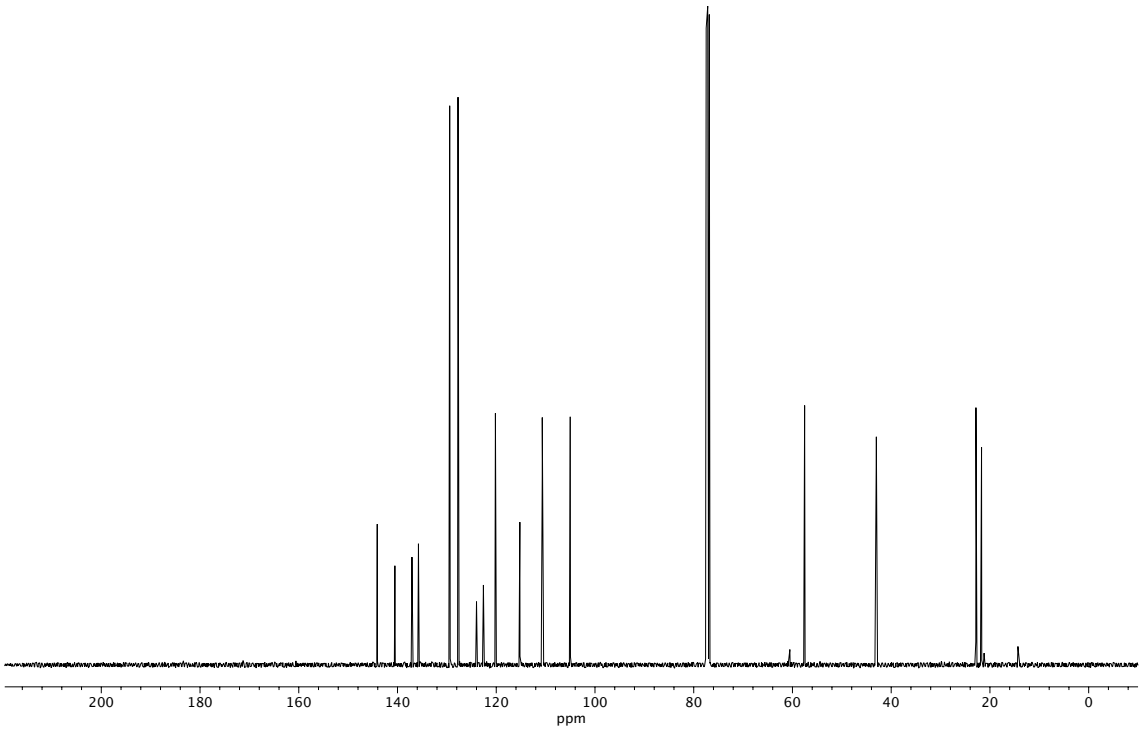
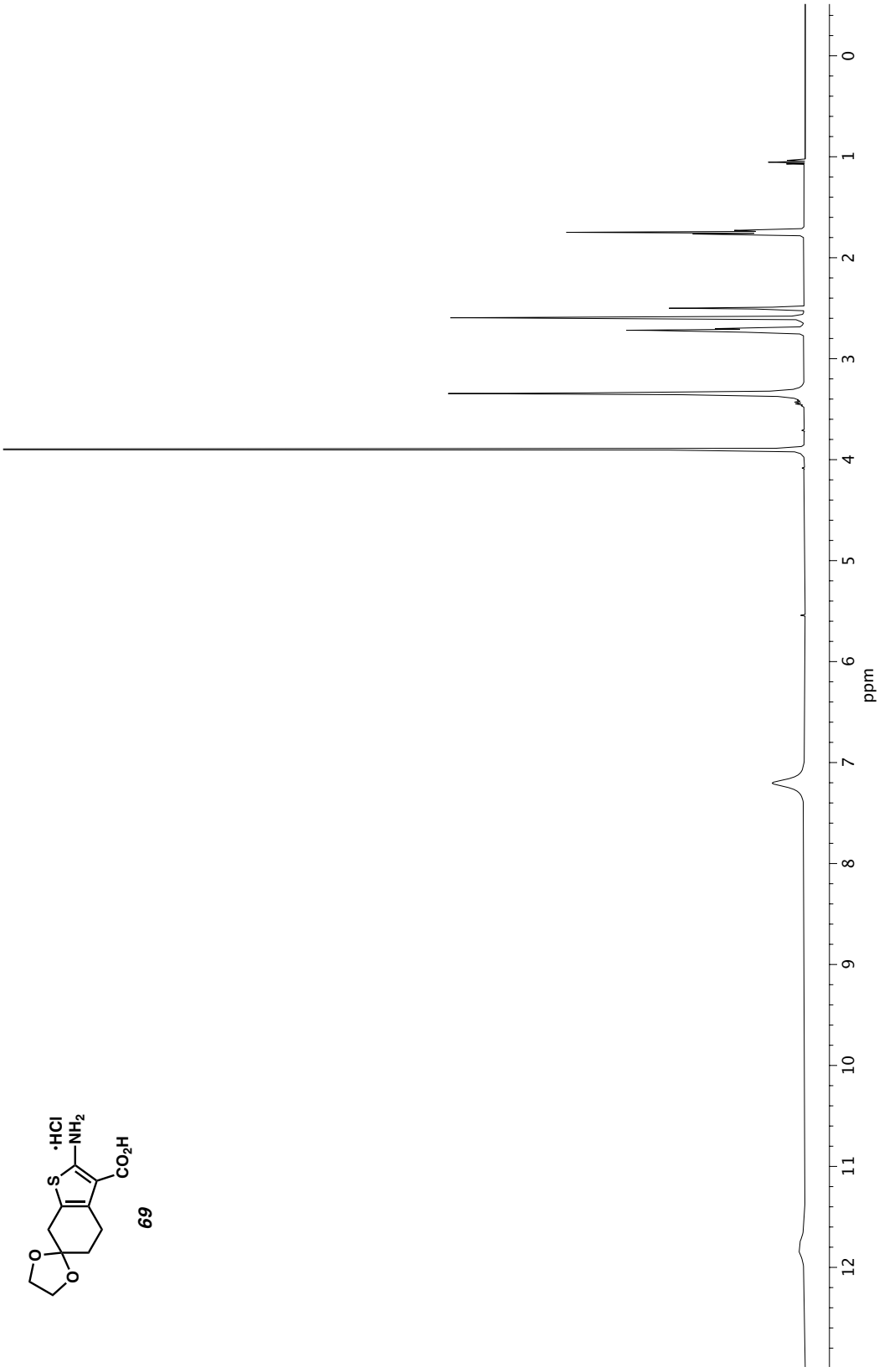


Figure A2.15 ^{13}C NMR (100 MHz, $CDCl_3$) of compound **66**.



69

Figure A2.16. ^{1}H NMR (400 MHz, DMSO) of compound **69**.

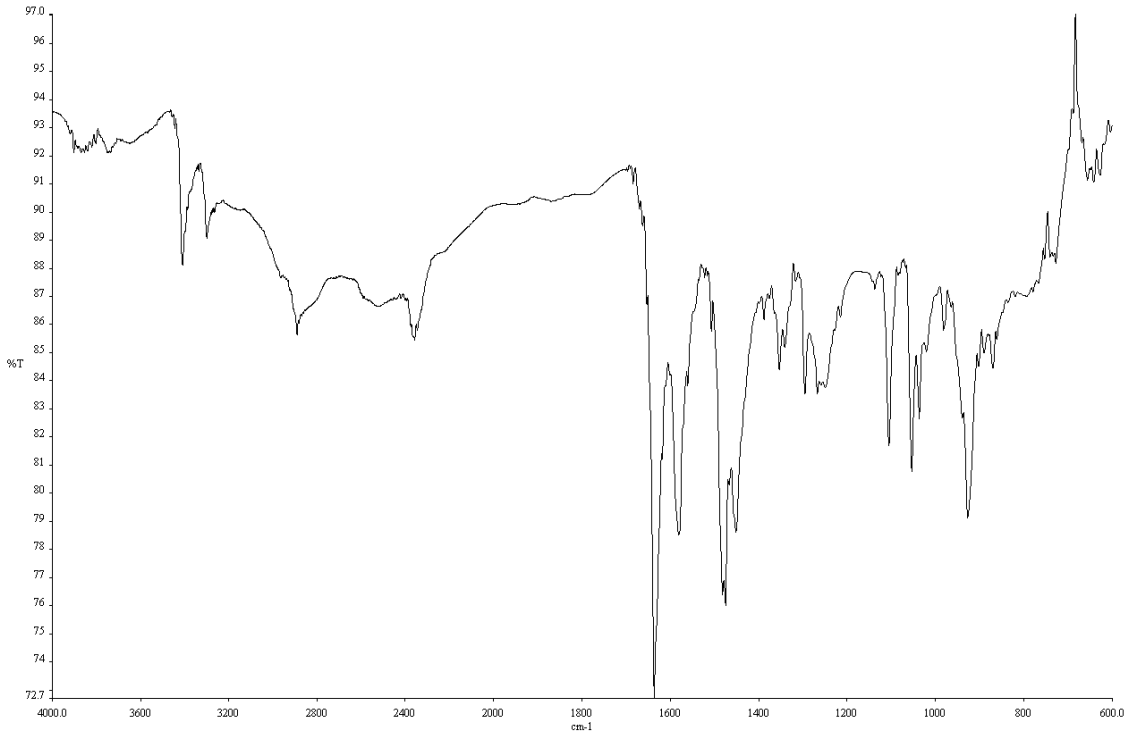


Figure A2.17 Infrared spectrum (Thin Film, NaCl) of compound **69**.

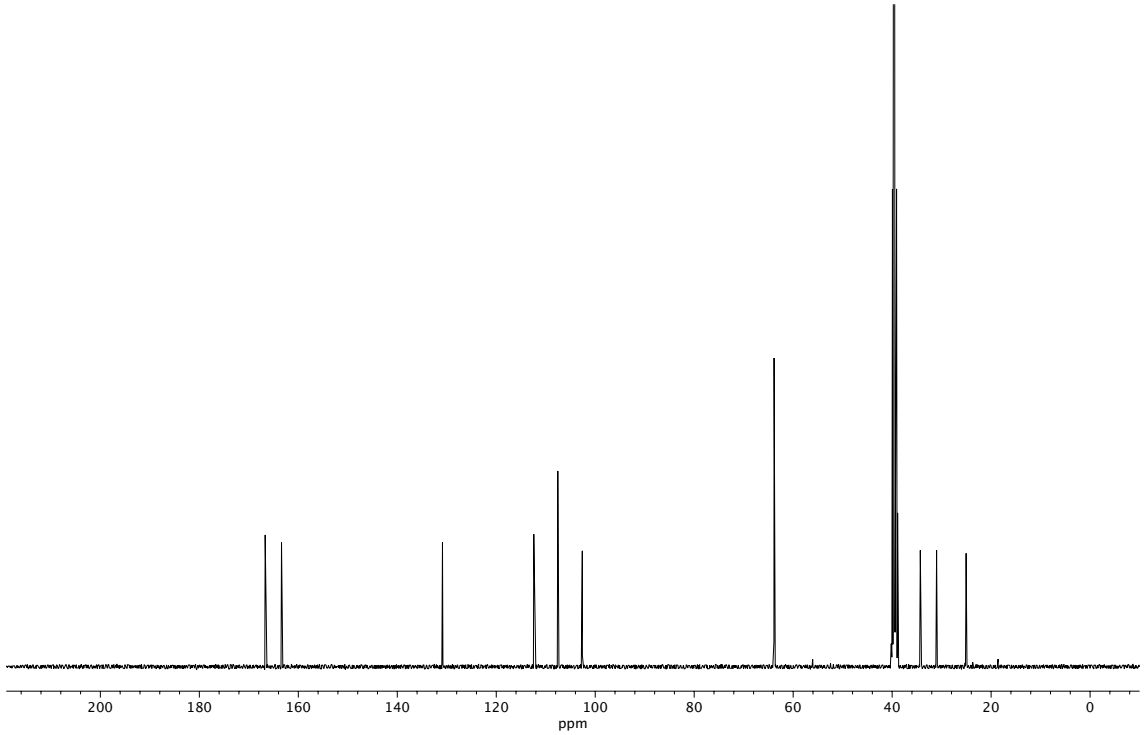


Figure A2.18 ^{13}C NMR (100 MHz, DMSO) of compound **69**.

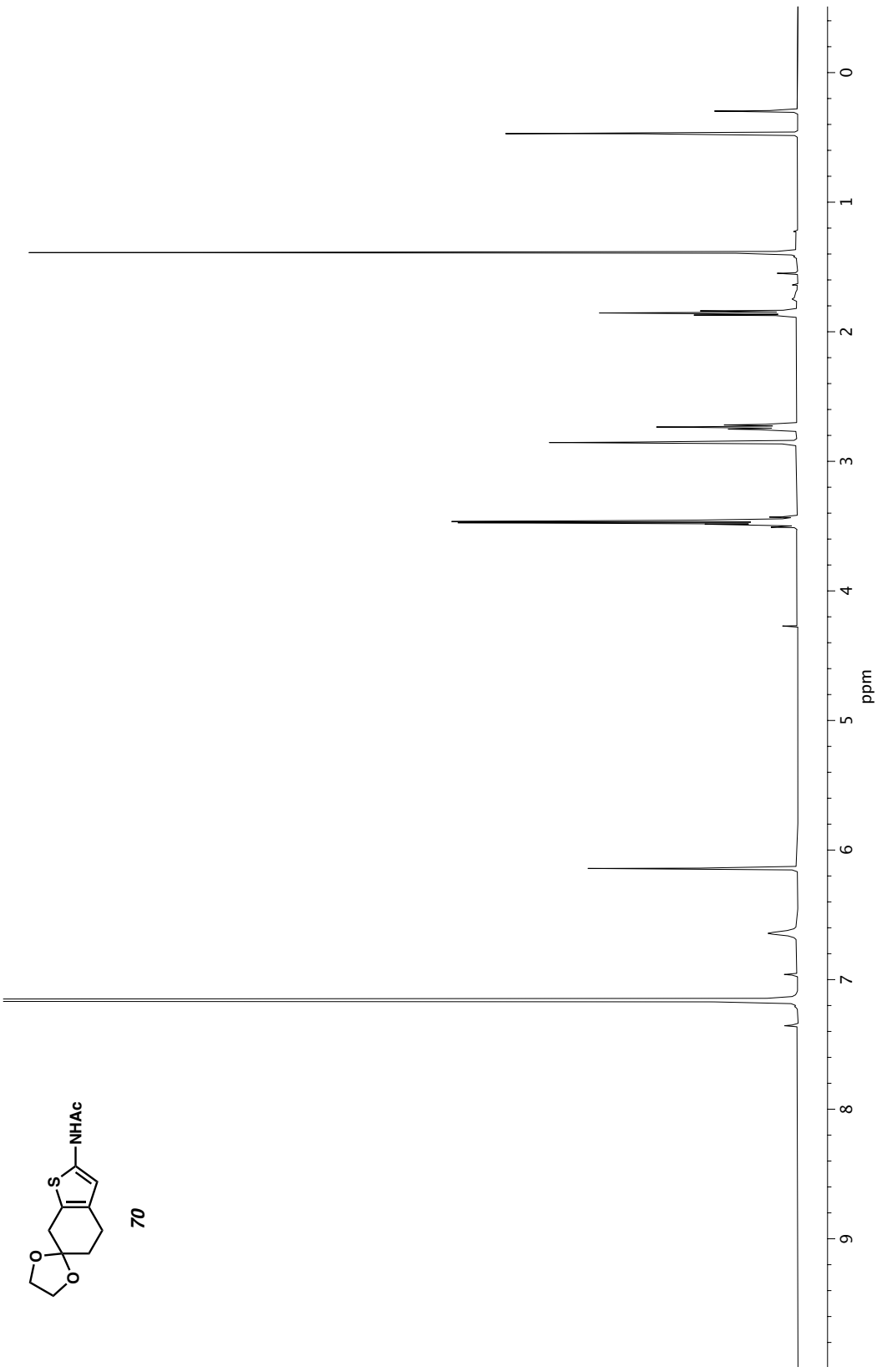


Figure A2.19. ^{1}H NMR (400 MHz, C_6D_6) of compound **70**.

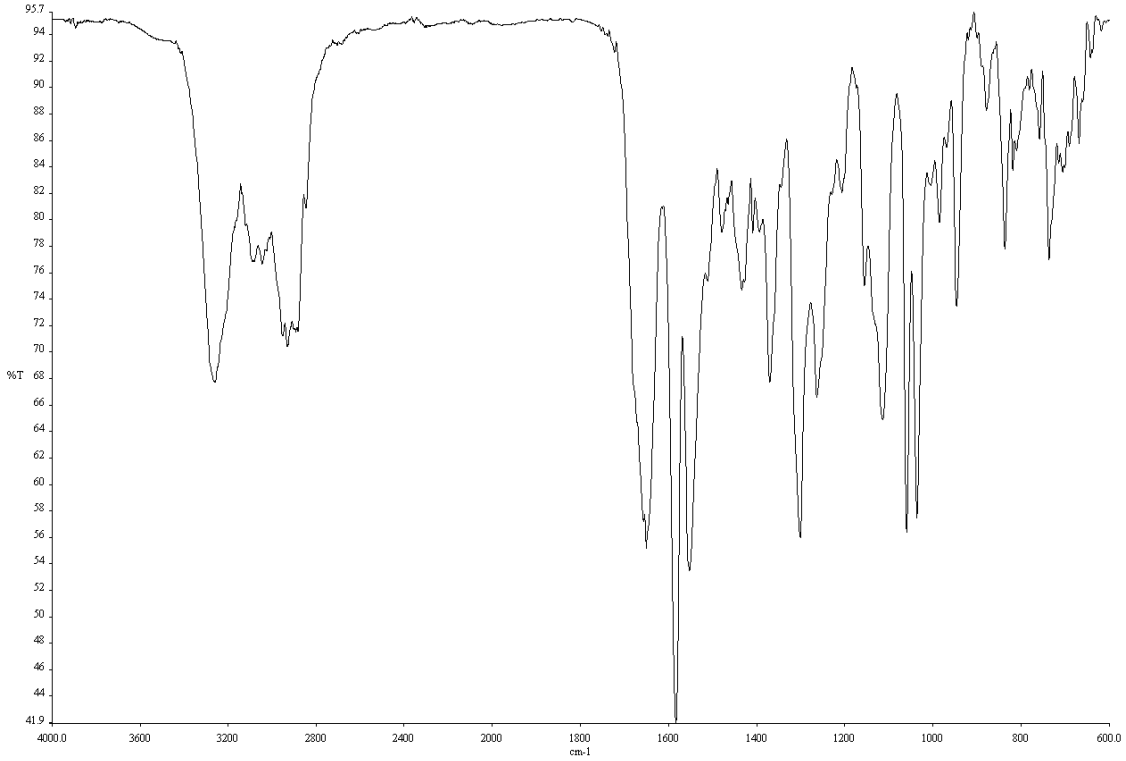


Figure A2.20 Infrared spectrum (Thin Film, NaCl) of compound **70**.

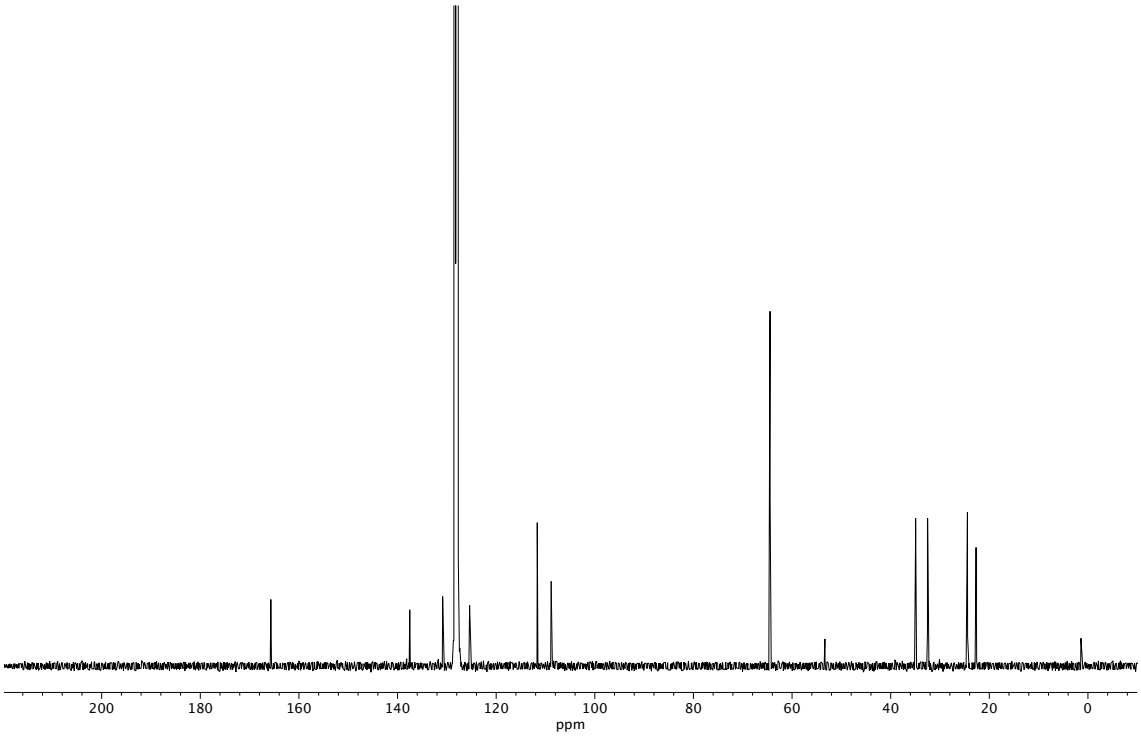


Figure A2.21 ^{13}C NMR (100 MHz, C_6D_6) of compound **70**.

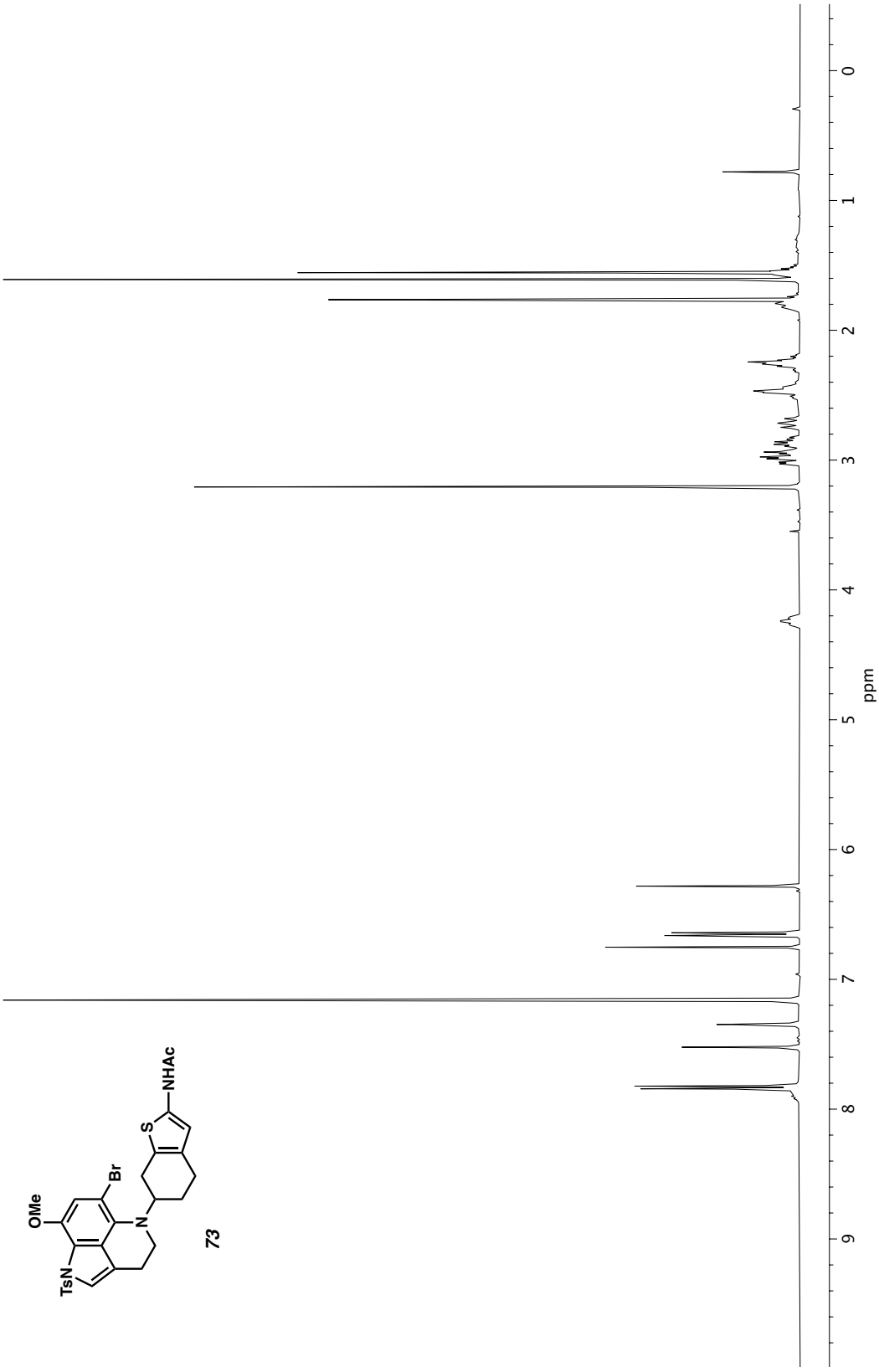


Figure A2.22. ^{1}H NMR (400 MHz, C_6D_6) of compound **73**.

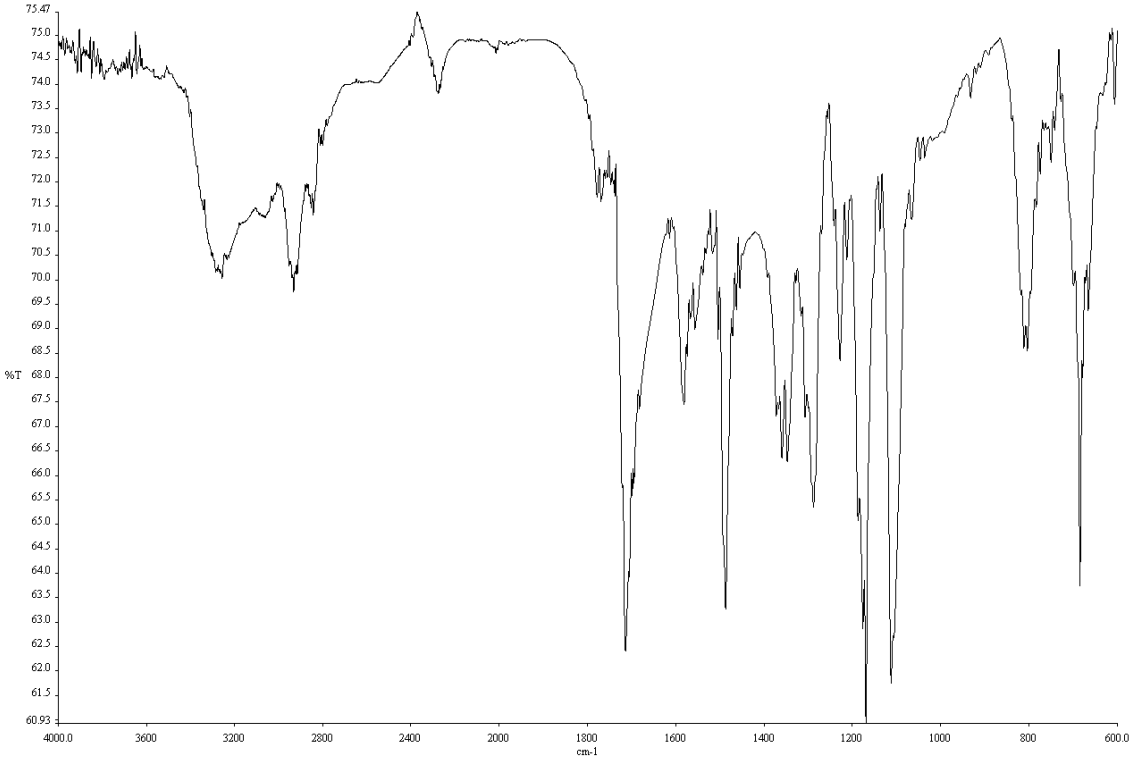


Figure A2.23 Infrared spectrum (Thin Film, NaCl) of compound **73**.

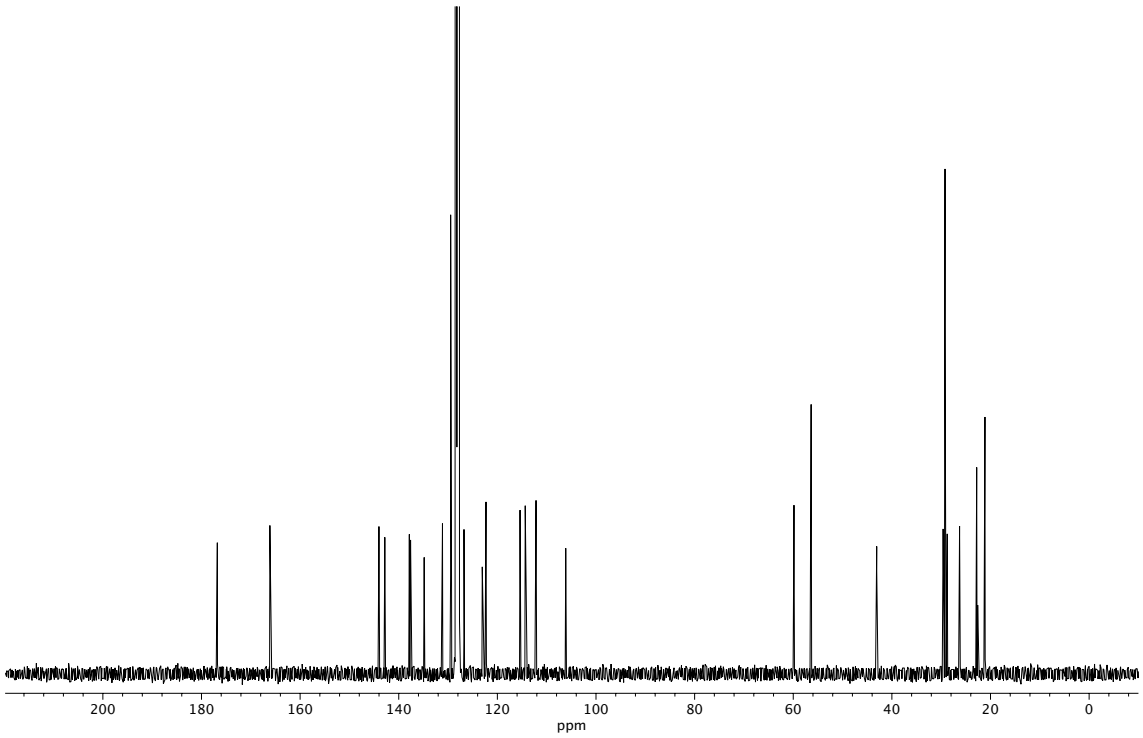


Figure A2.24 ^{13}C NMR (100 MHz, C_6D_6) of compound **73**.

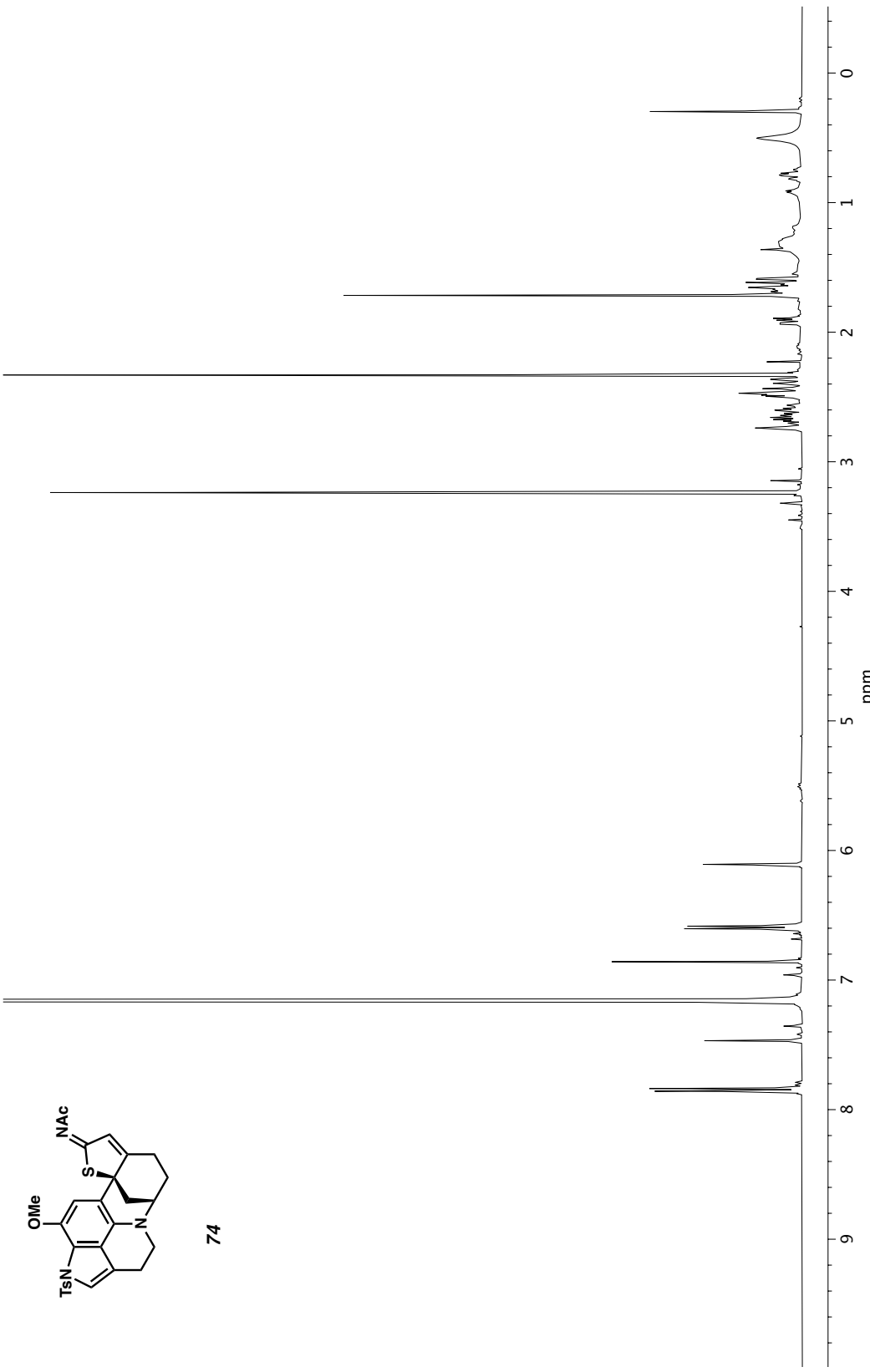


Figure A2.25. ^{1}H NMR (400 MHz, C_6D_6) of compound **74**.

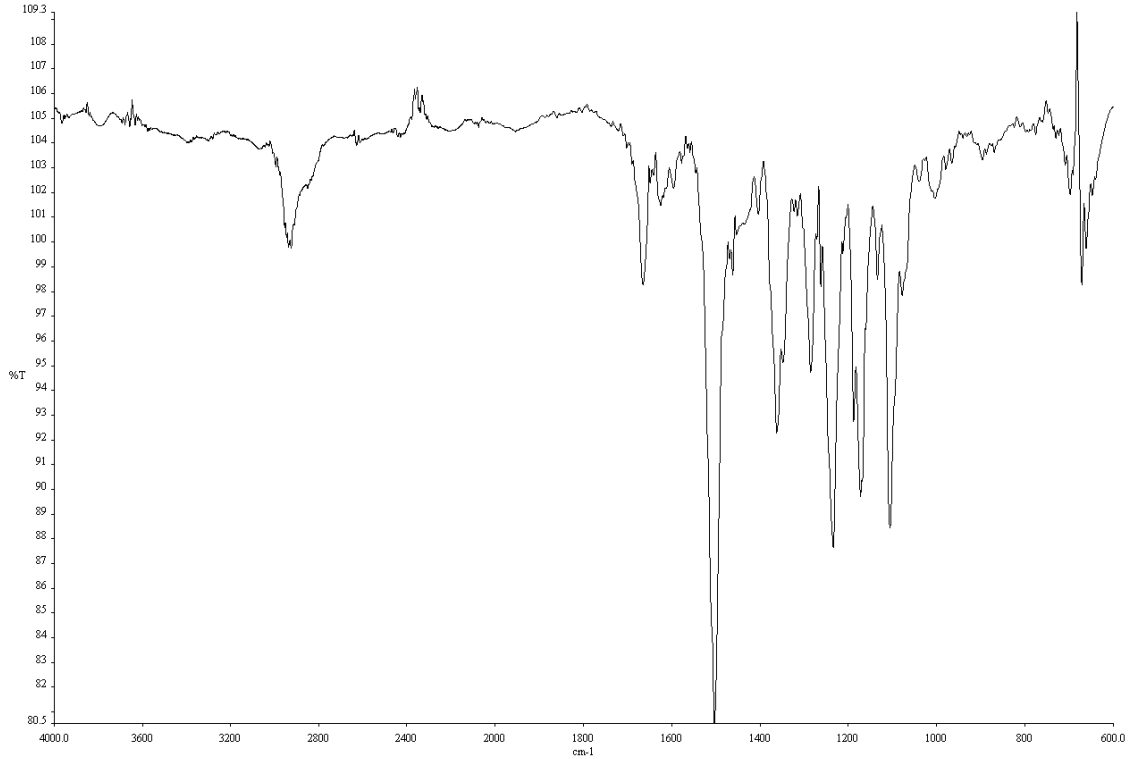


Figure A2.26 Infrared spectrum (Thin Film, NaCl) of compound **74**.

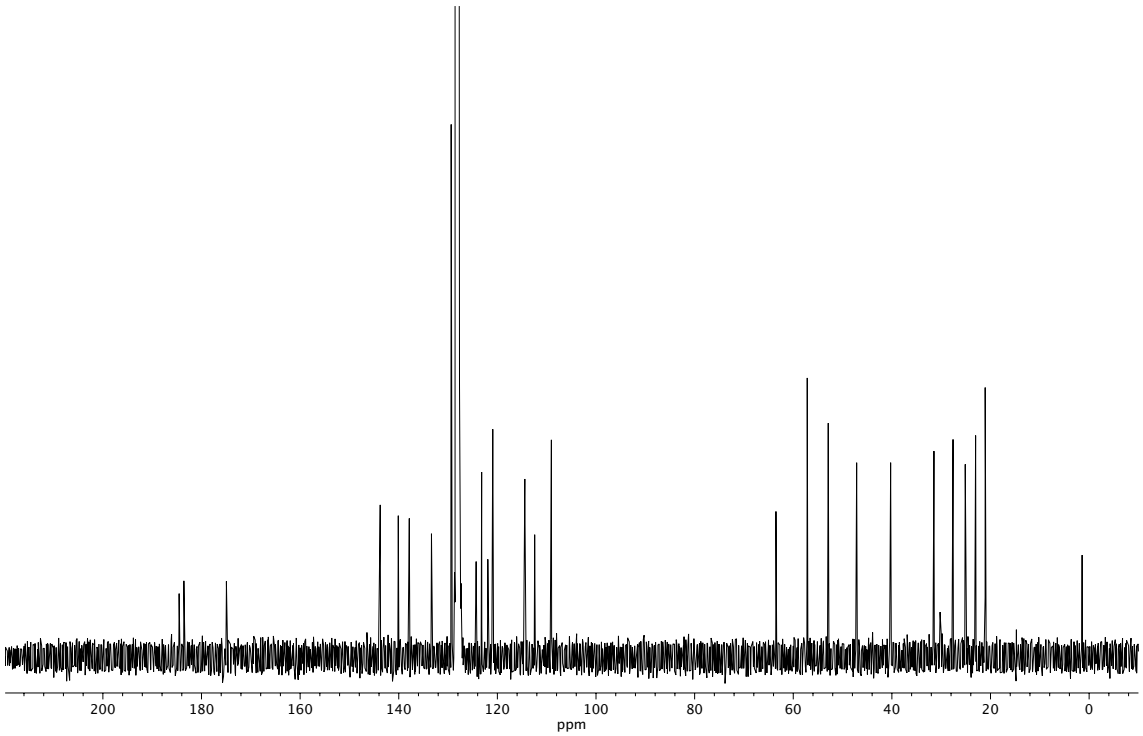


Figure A2.27 ^{13}C NMR (100 MHz, C_6D_6) of compound **74**.

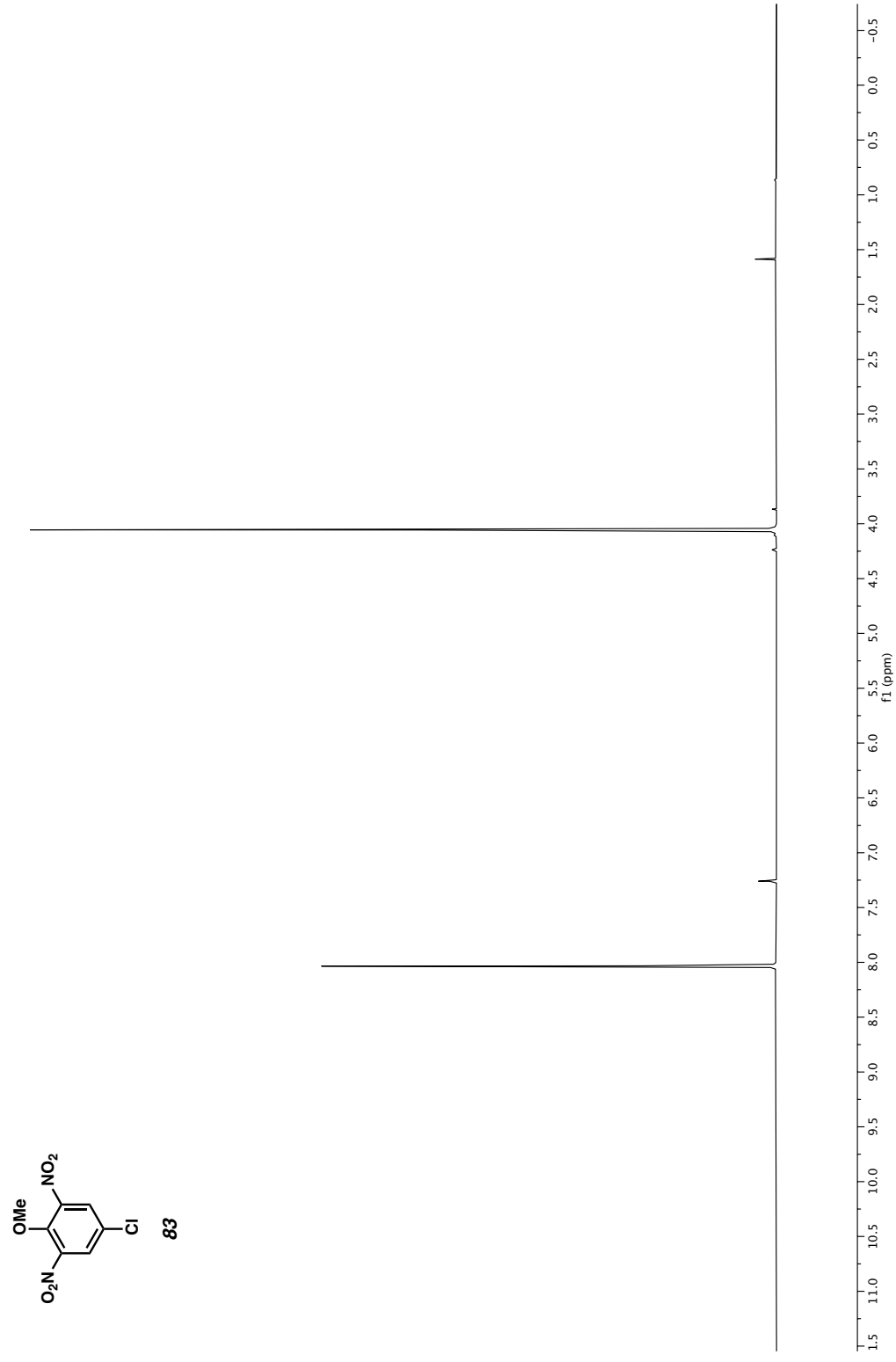


Figure A2.28. ^{1}H NMR (400 MHz, $CDCl_3$) of compound **83**.

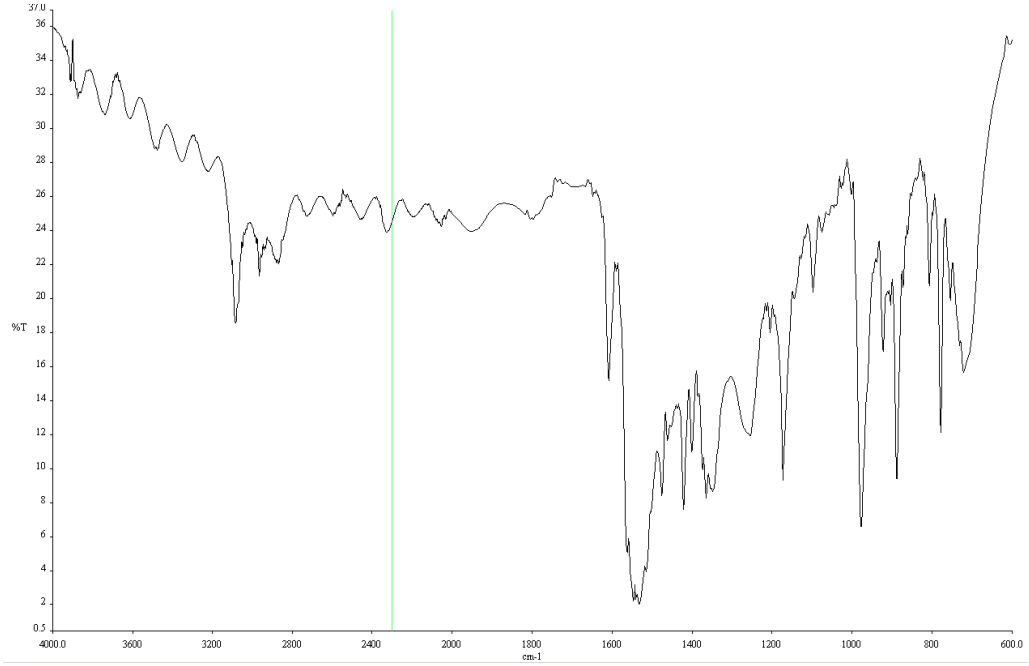


Figure A2.29 Infrared spectrum (Thin Film, NaCl) of compound **83**.

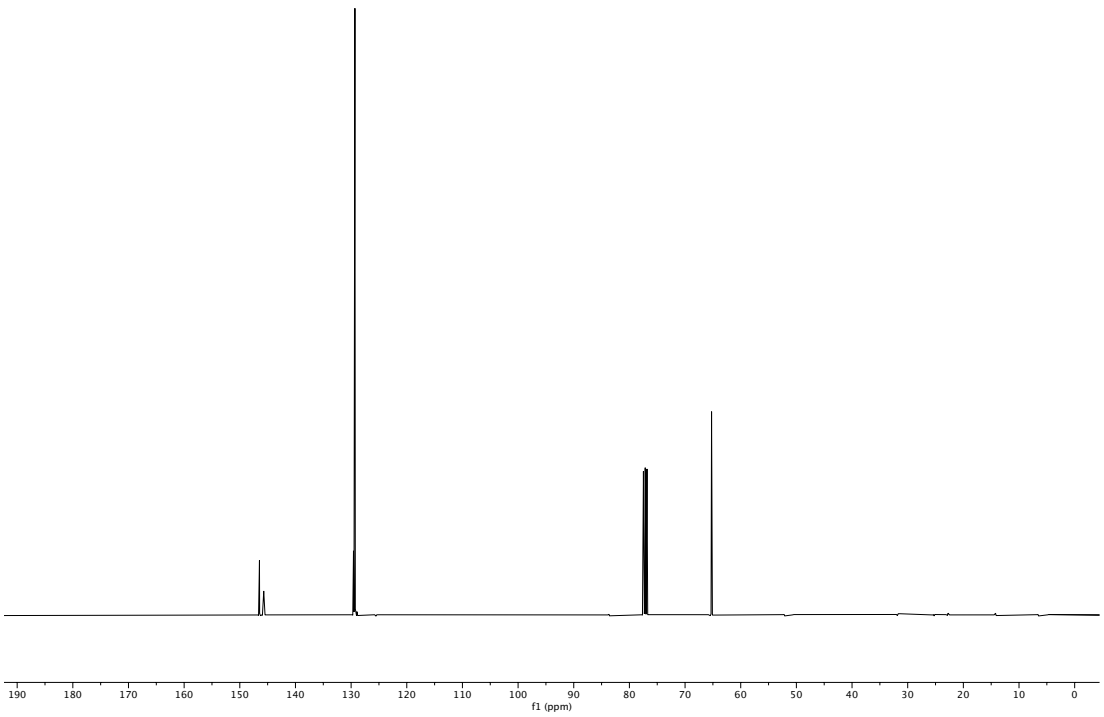


Figure A2.30 ^{13}C NMR (100 MHz, $CDCl_3$) of compound **83**.

Figure A2.31. ^{1}H NMR (400 MHz, $CDCl_3$) of compound **84**.

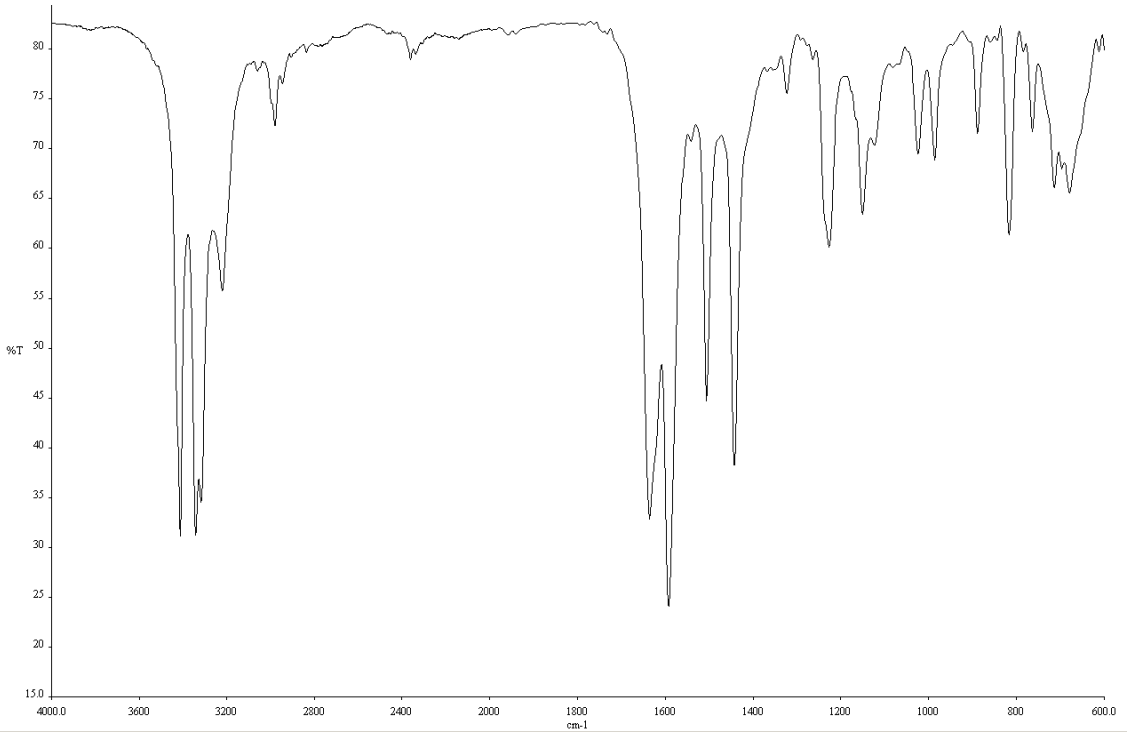


Figure A2.32 Infrared spectrum (Thin Film, NaCl) of compound **84**.

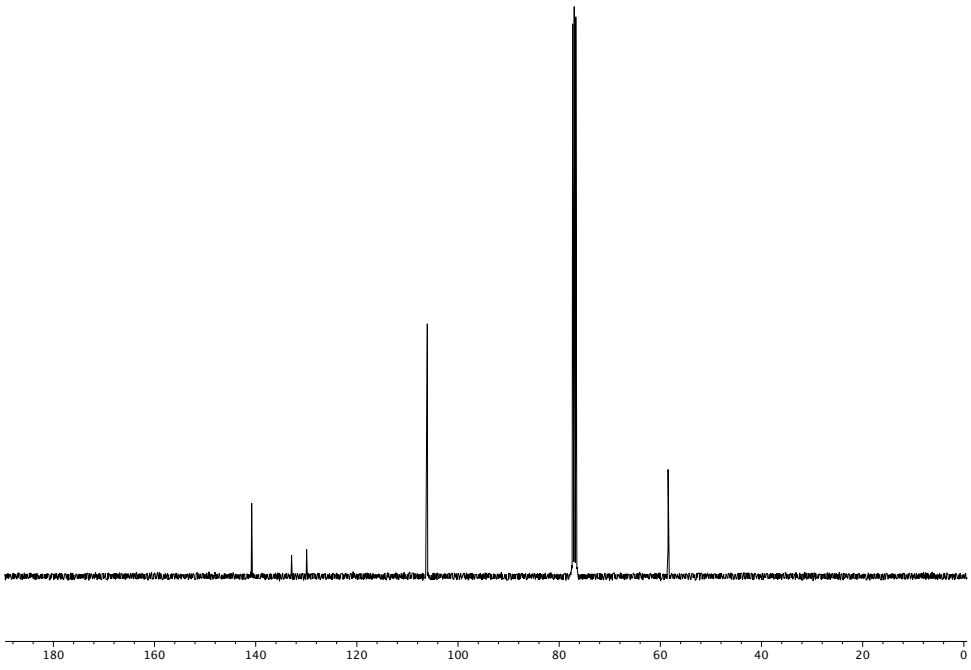


Figure A2.33 ^{13}C NMR (100 MHz, $CDCl_3$) of compound **84**.

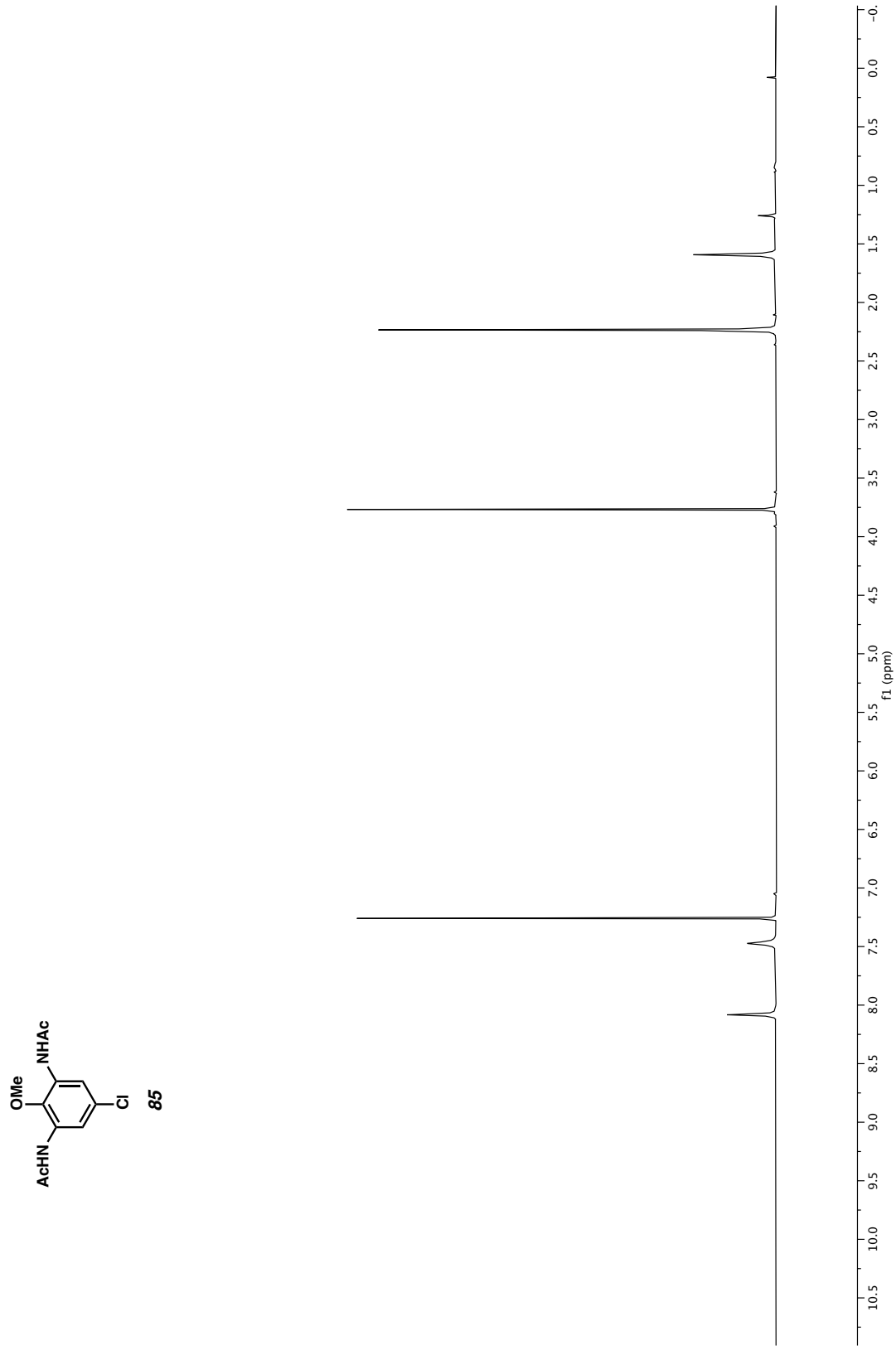


Figure A2.34. ^{1}H NMR (400 MHz, C_6D_6) of compound **85**.

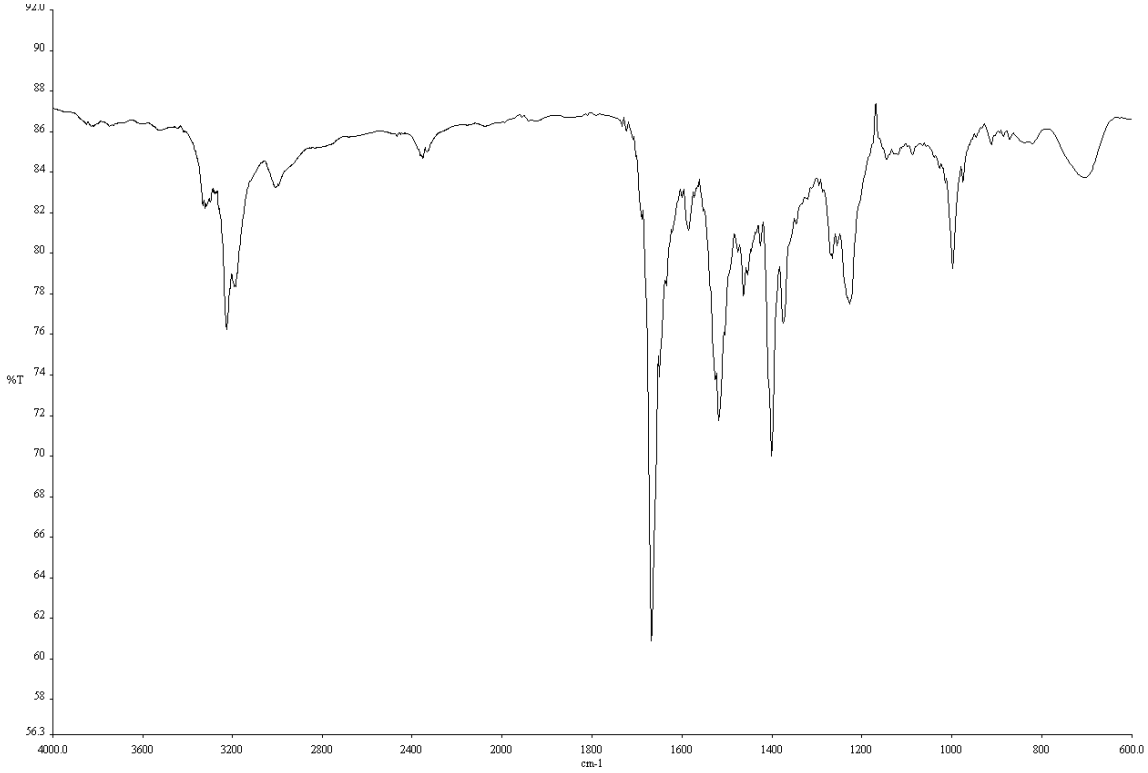


Figure A2.35 Infrared spectrum (Thin Film, NaCl) of compound **85**.

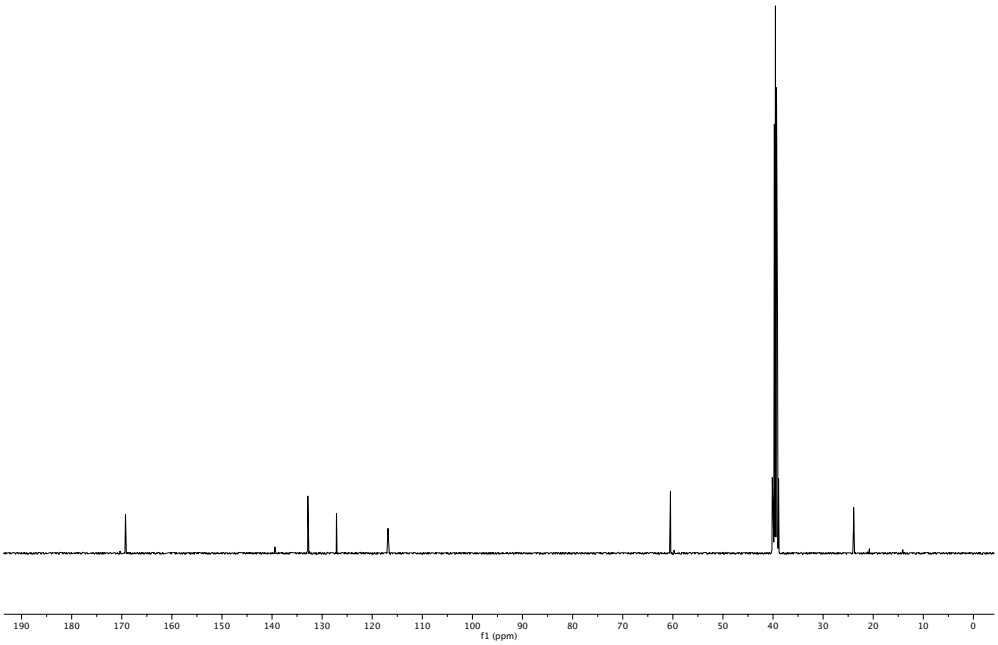


Figure A2.36 ^{13}C NMR (100 MHz, DMSO) of compound **85**.

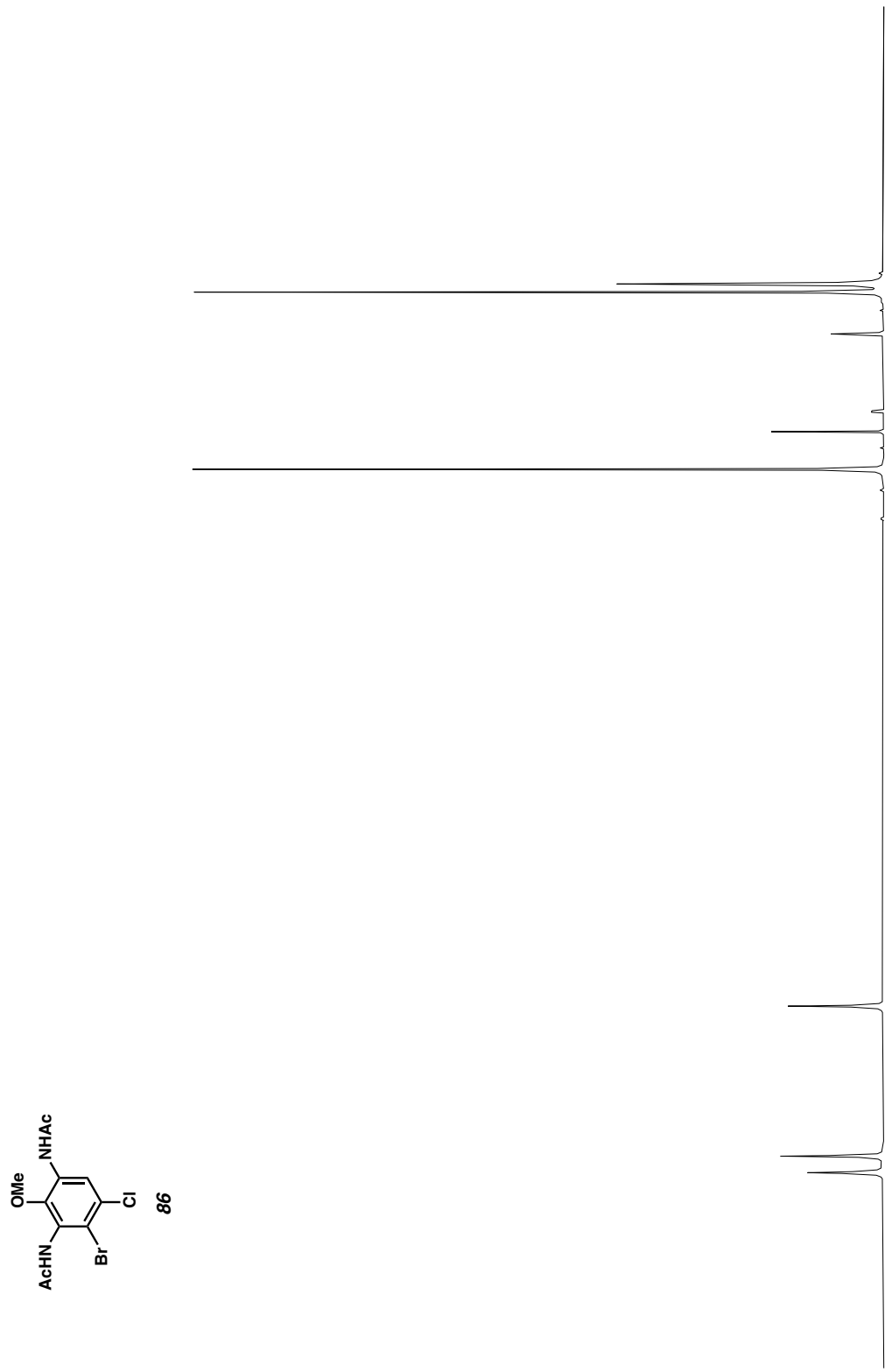


Figure A2.37. ^{1}H NMR (400 MHz, DMSO) of compound **86**.

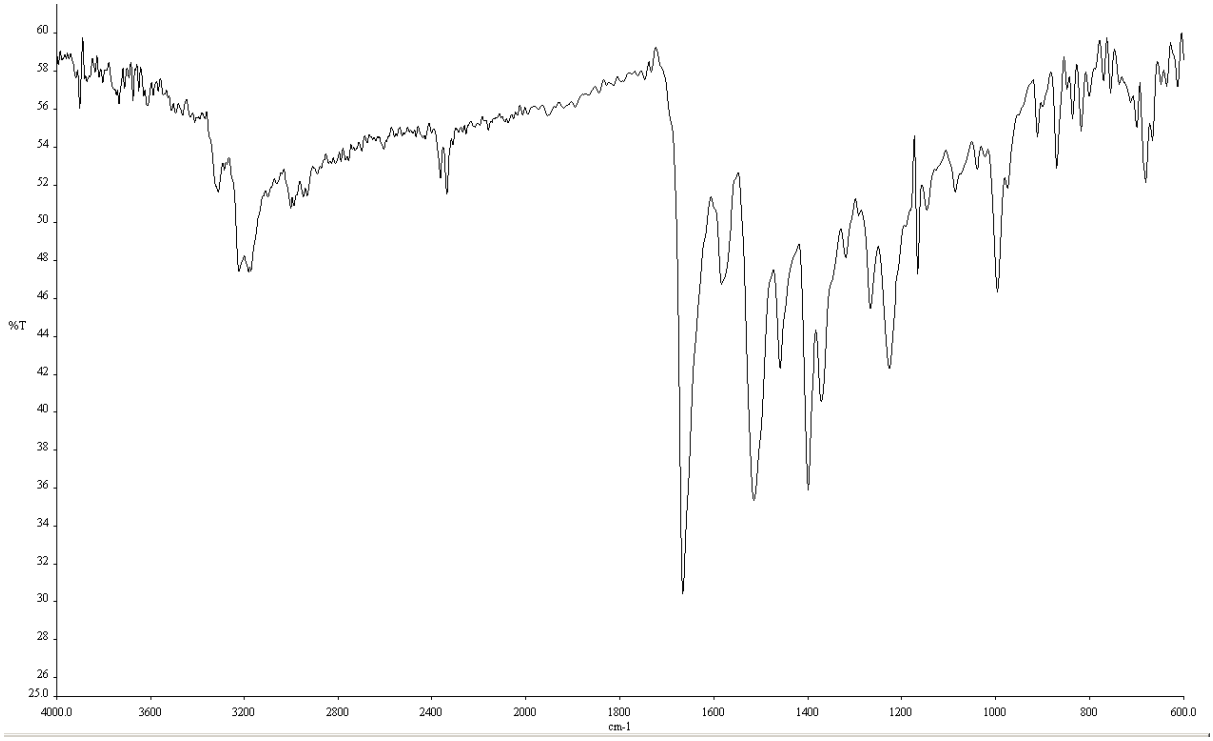


Figure A2.38 Infrared spectrum (Thin Film, NaCl) of compound **86**.

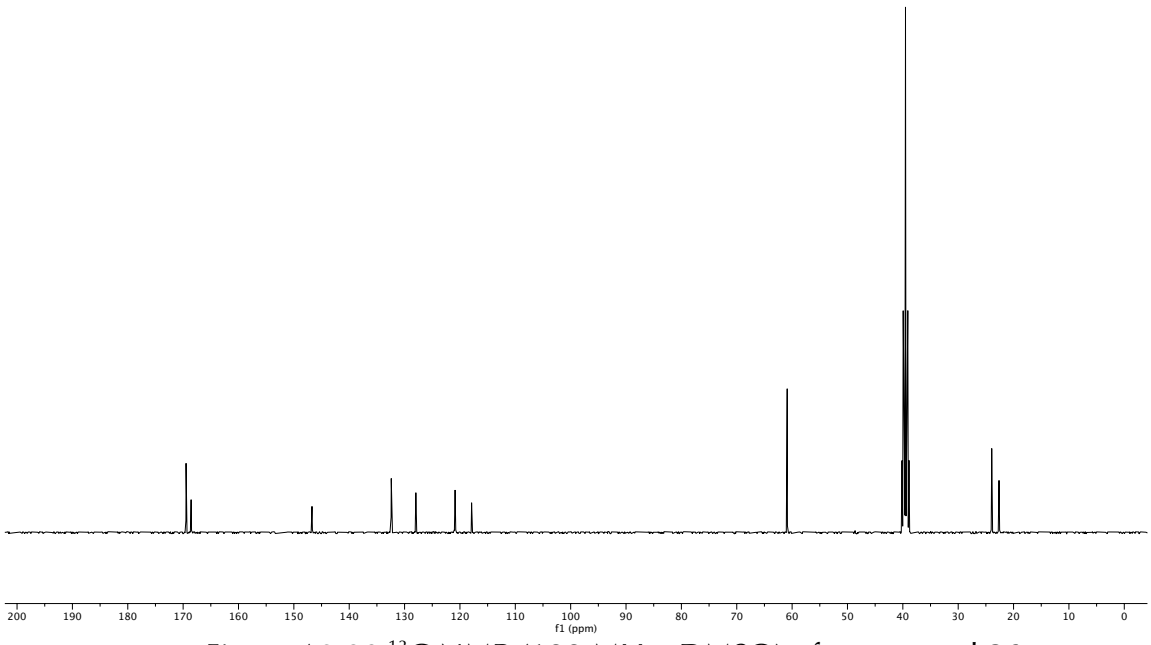


Figure A2.39 ^{13}C NMR (100 MHz, DMSO) of compound **86**.

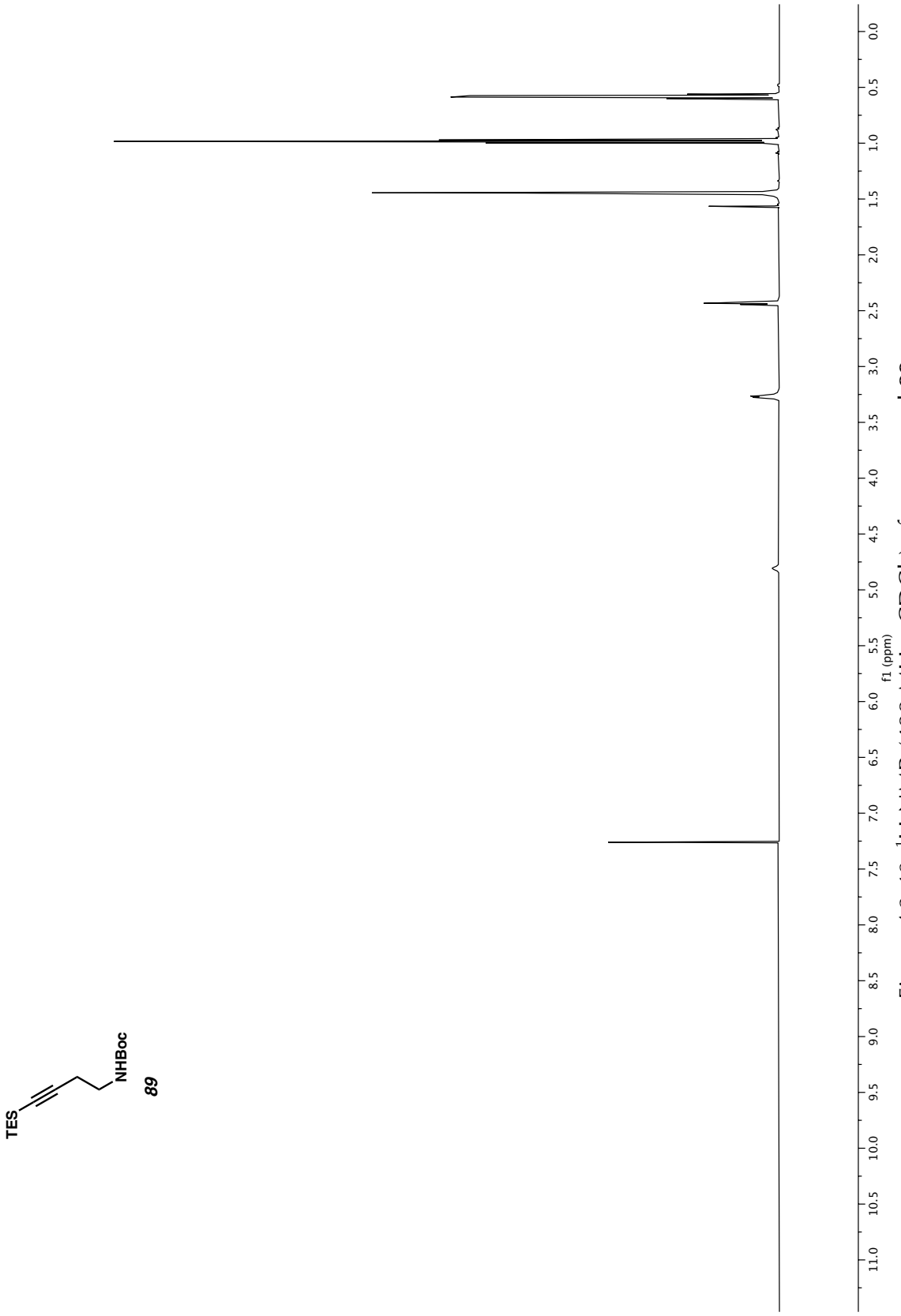


Figure A2.40. ^{1}H NMR (400 MHz, $CDCl_3$) of compound **89**.

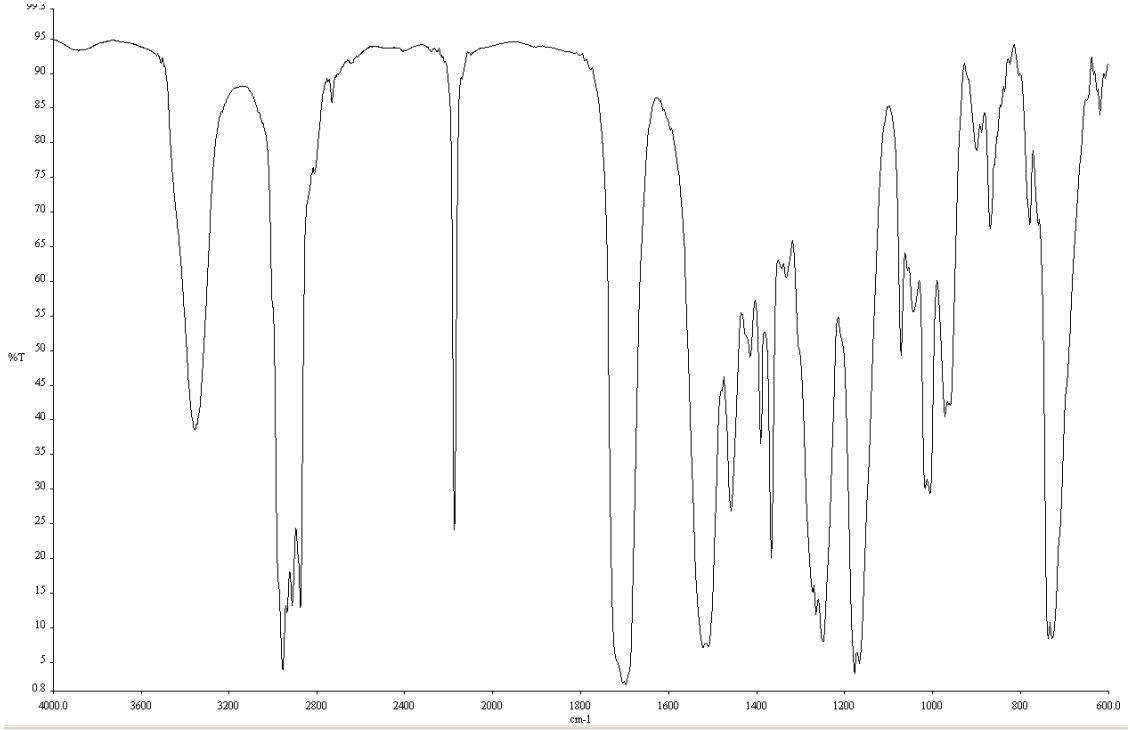


Figure A2.41 Infrared spectrum (Thin Film, NaCl) of compound **89**.

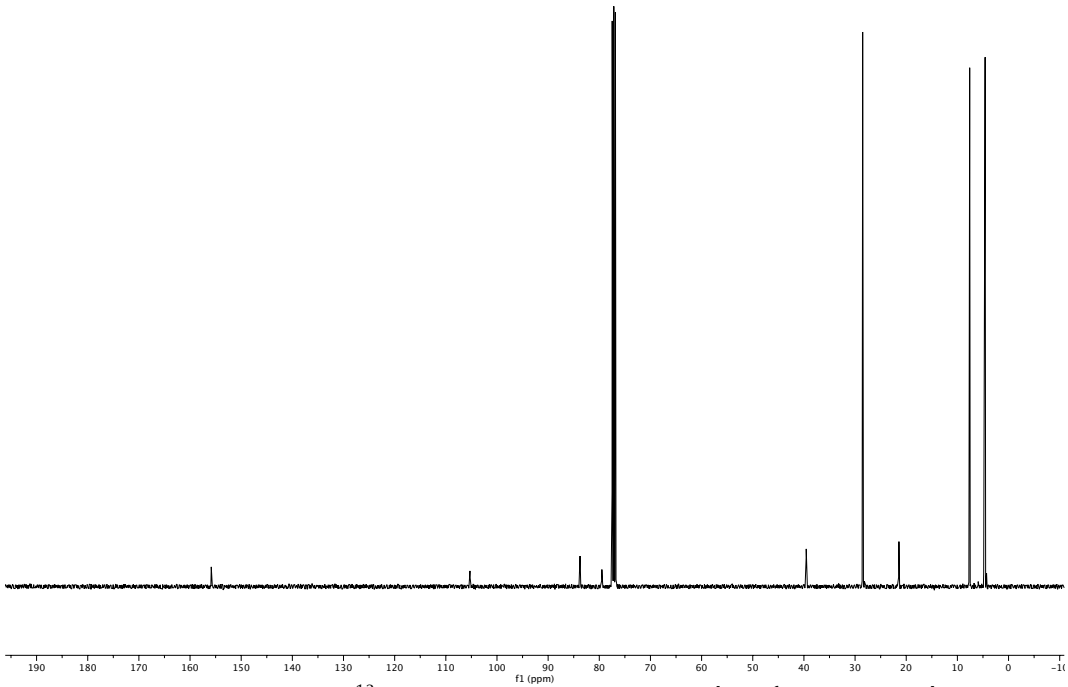
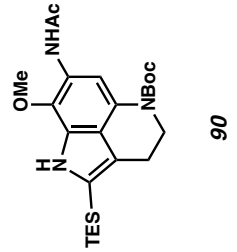


Figure A2.42 ^{13}C NMR (100 MHz, $CDCl_3$) of compound **89**.



90

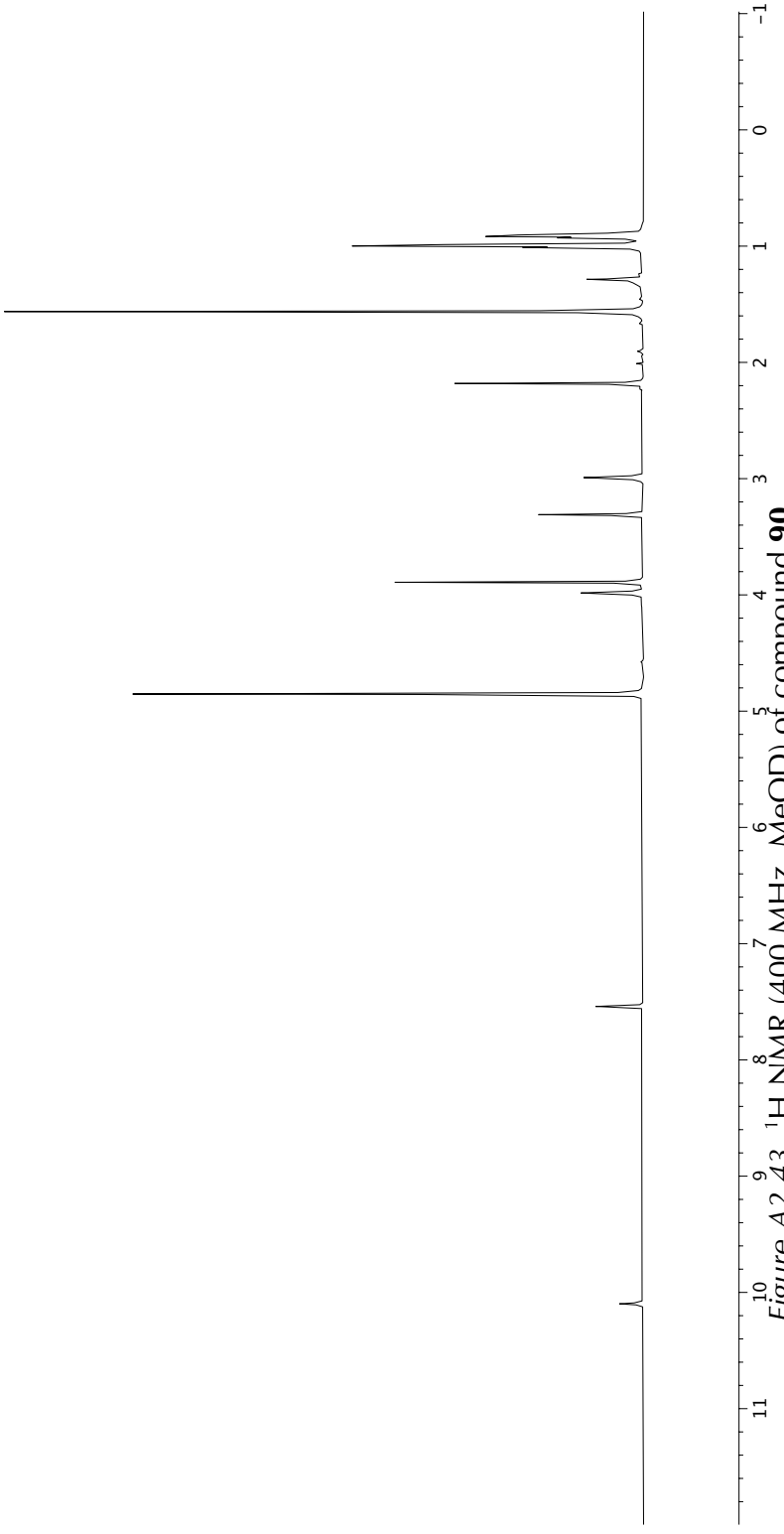


Figure A2.43. ^{1}H NMR (400 MHz, MeOD) of compound **90**.

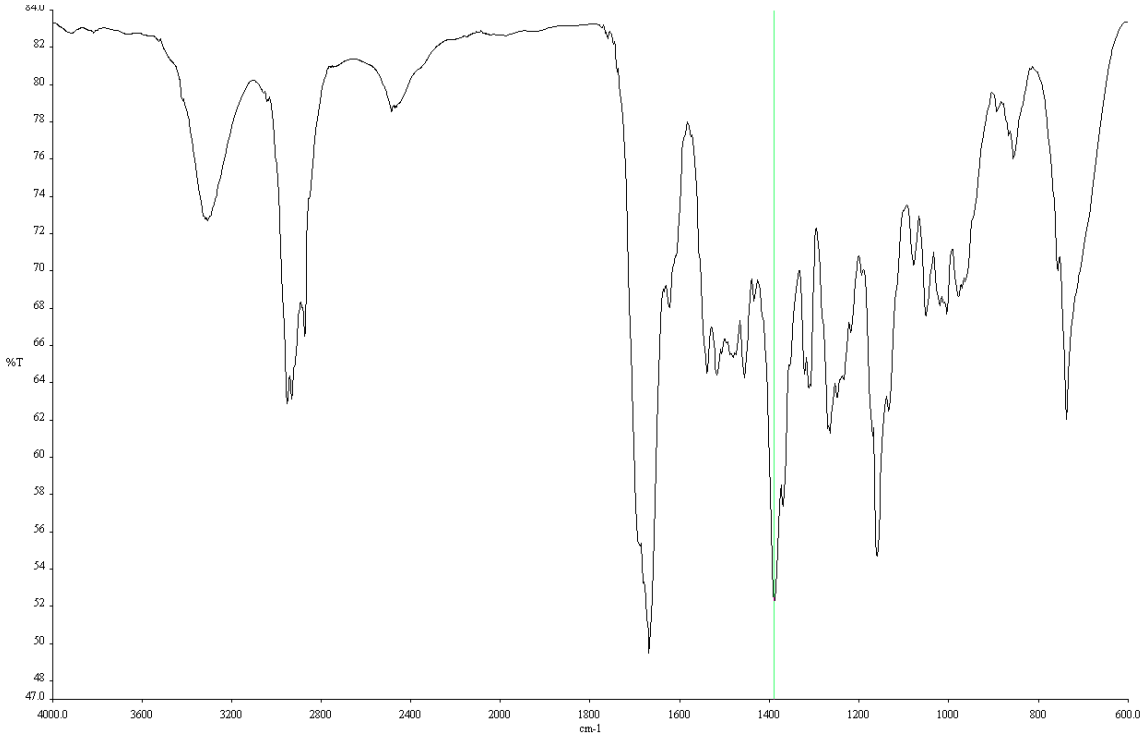


Figure A2.44 Infrared spectrum (Thin Film, NaCl) of compound **90**.

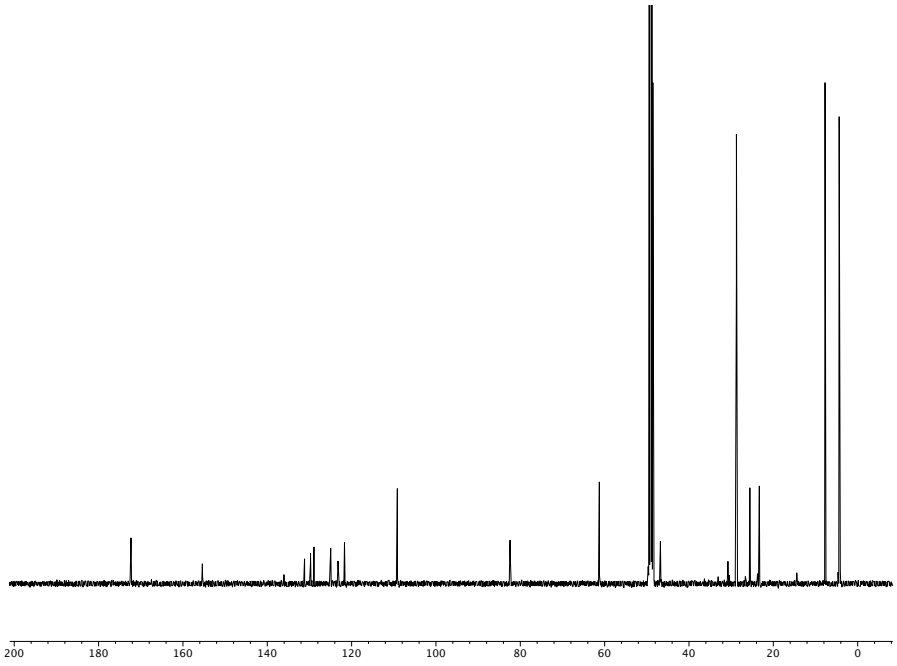


Figure A2.45 ^{13}C NMR (100 MHz, MeOD) of compound **90**.

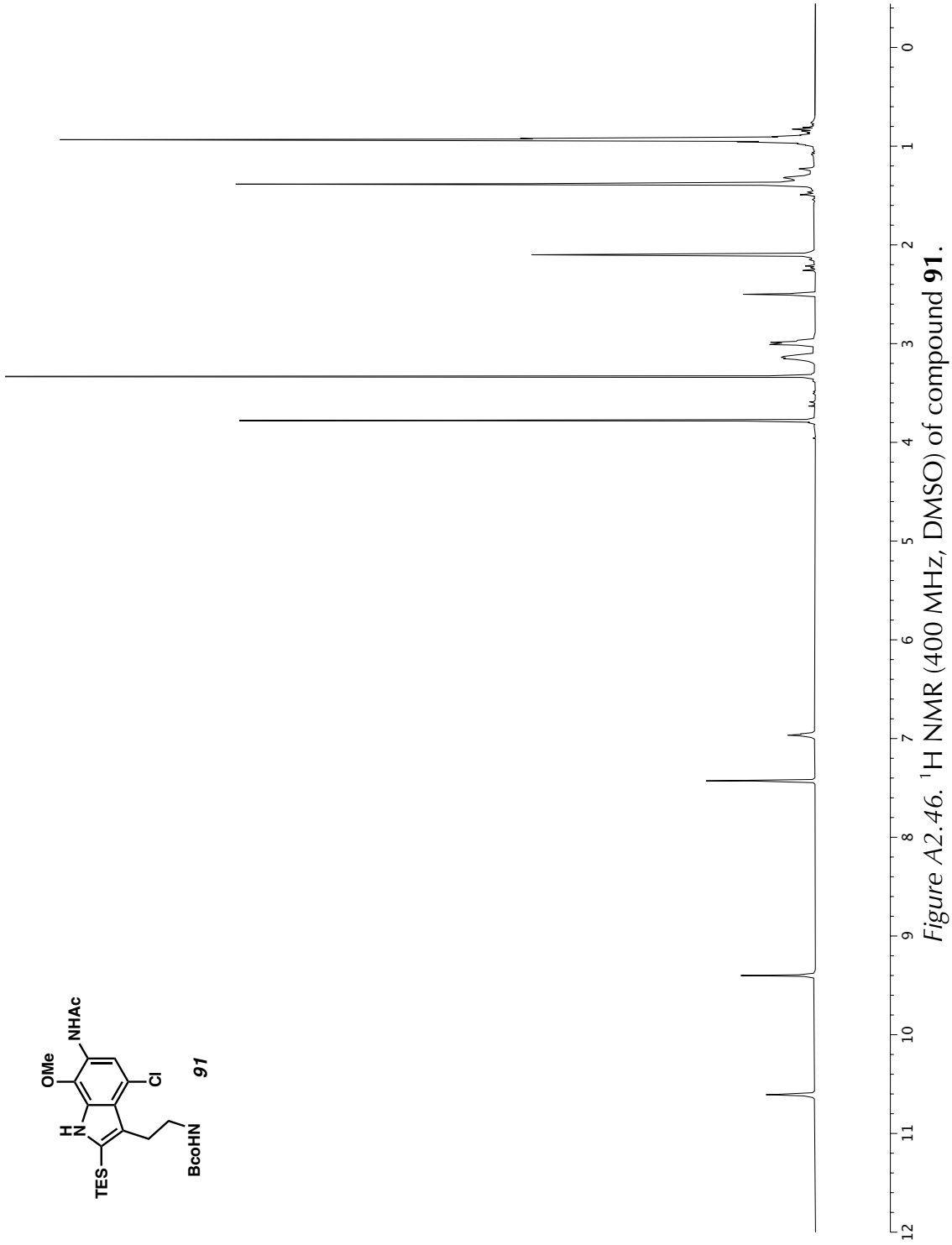


Figure A2.46. ^{1}H NMR (400 MHz, DMSO) of compound **91**.

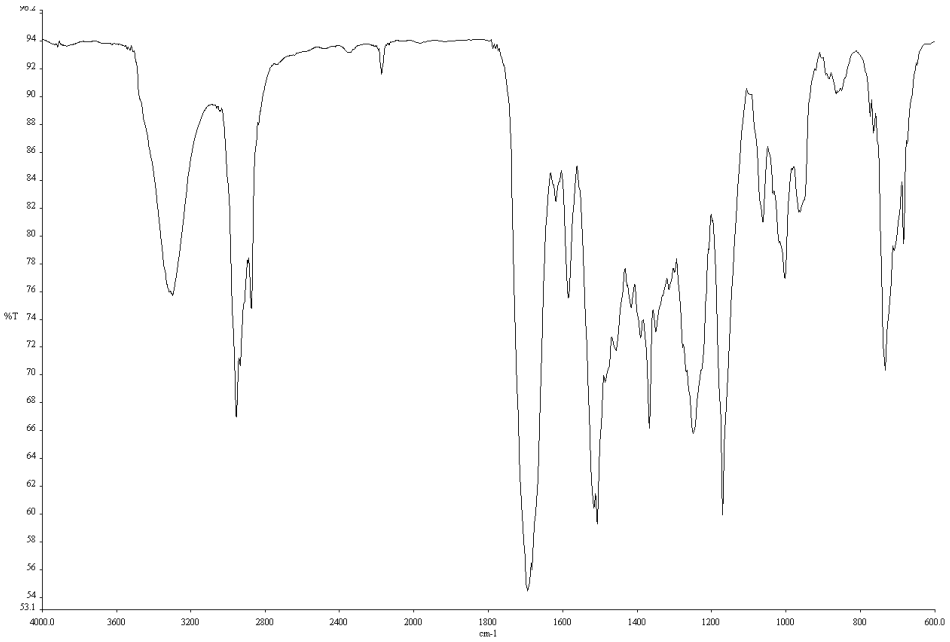


Figure A2.47 Infrared spectrum (Thin Film, NaCl) of compound **91**.

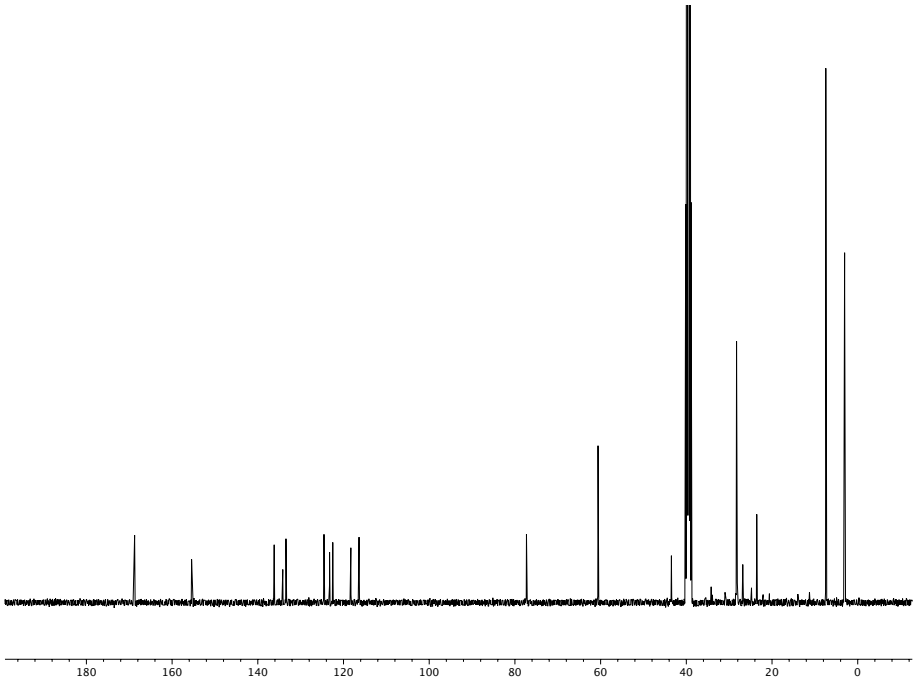


Figure A2.48 ^{13}C NMR (100 MHz, DMSO) of compound **91**.

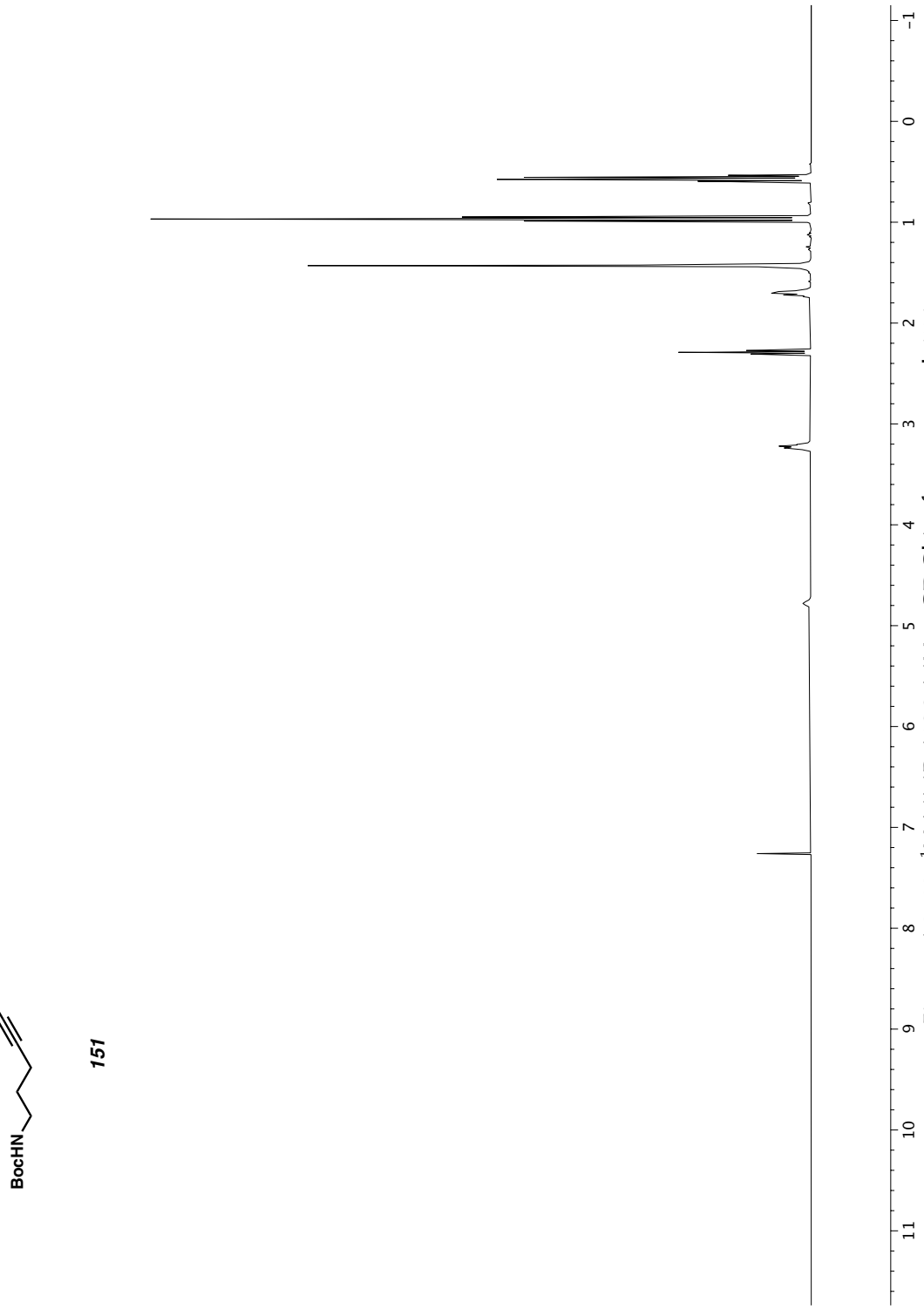


Figure A2.49. ^{1}H NMR (400 MHz, $CDCl_3$) of compound **151**.

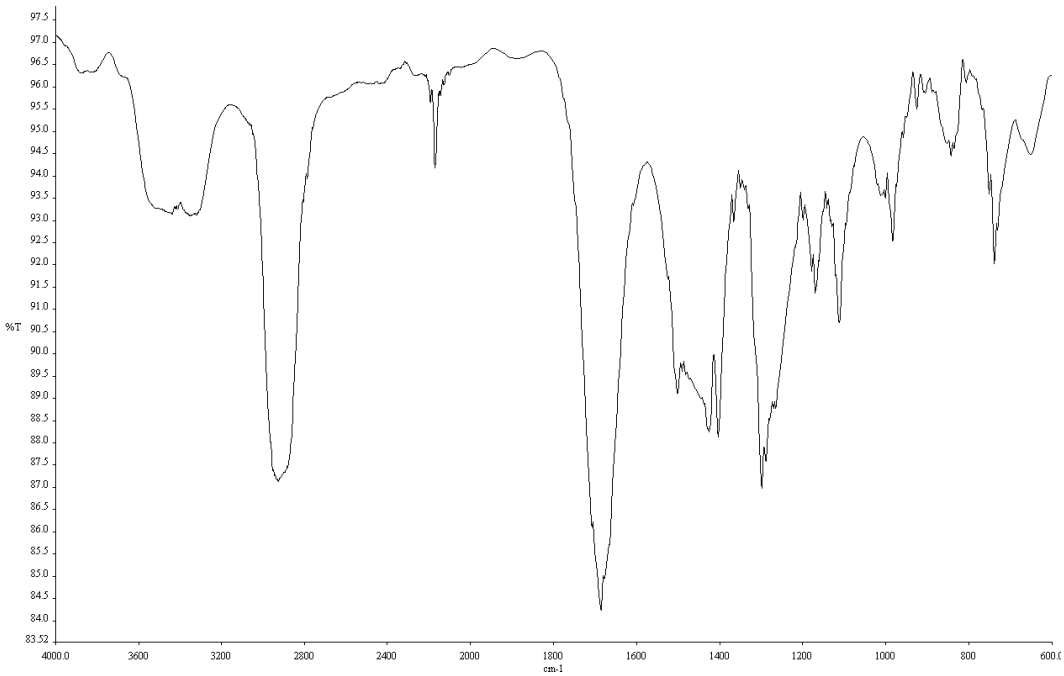


Figure A2.50 Infrared spectrum (Thin Film, NaCl) of compound **151**.

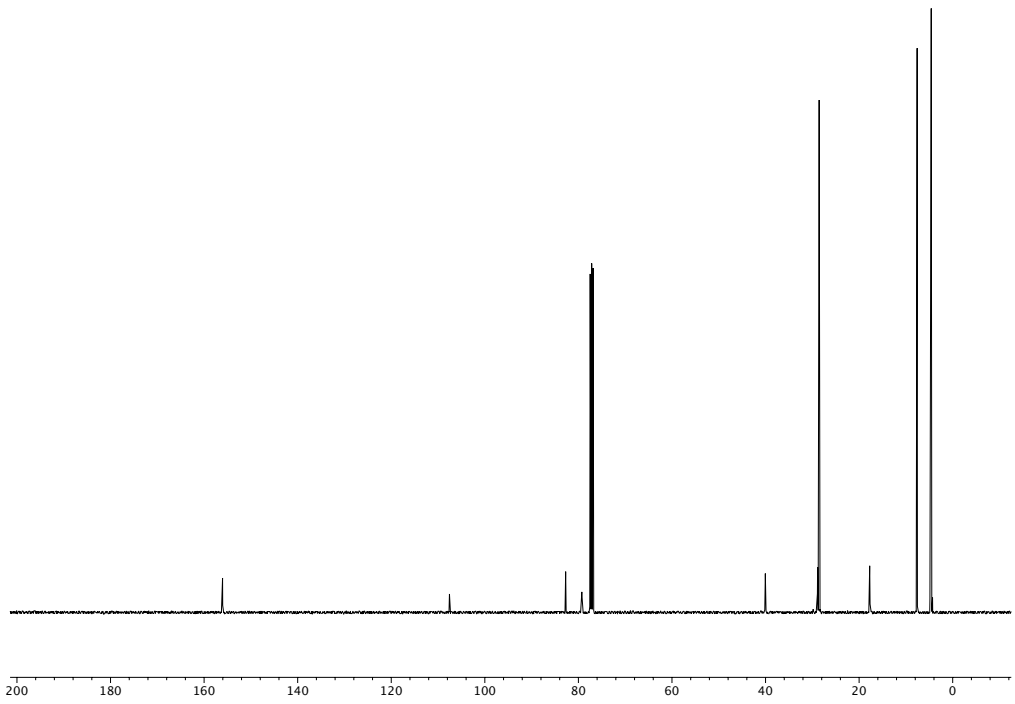


Figure A2.51 ^{13}C NMR (100 MHz, $CDCl_3$) of compound **151**.

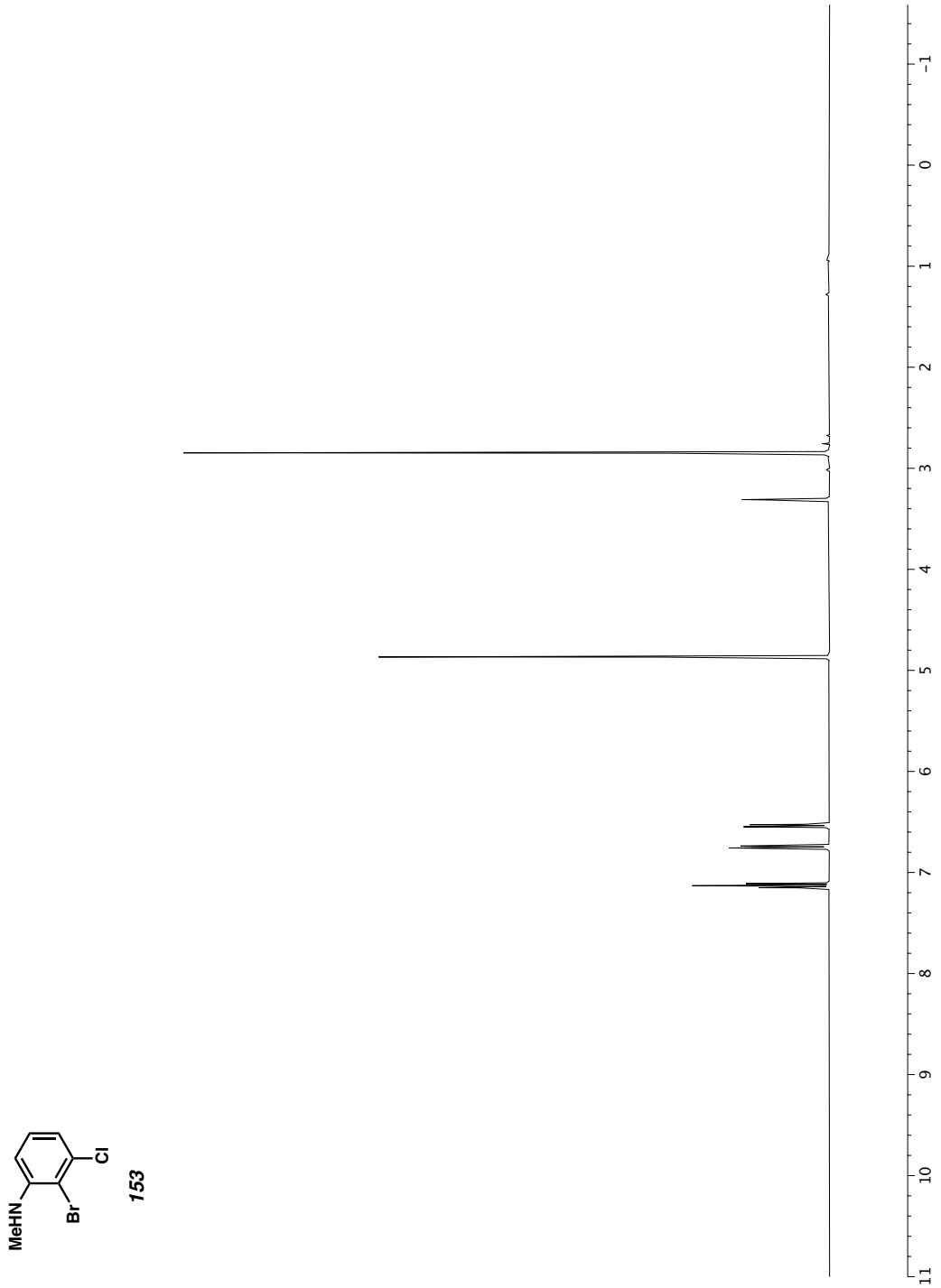


Figure A2.52. ^{1}H NMR (400 MHz, MeOD) of compound **153**.

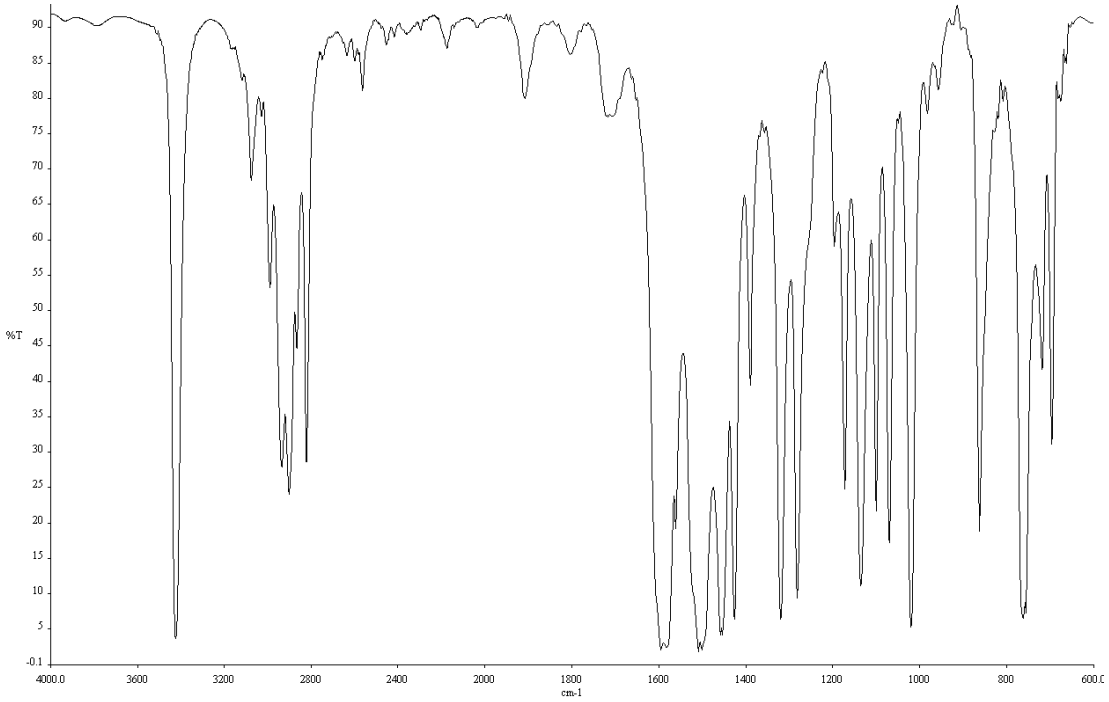


Figure A2.53 Infrared spectrum (Thin Film, NaCl) of compound **153**.

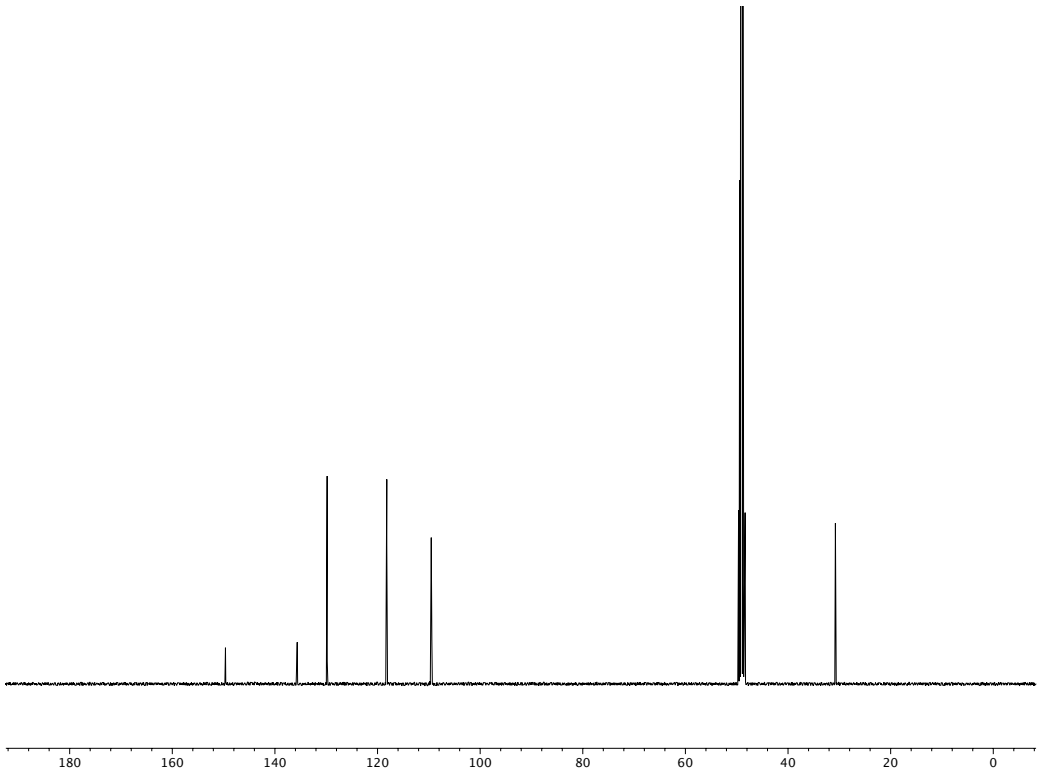


Figure A2.54 ^{13}C NMR (100 MHz, MeOD) of compound **153**.

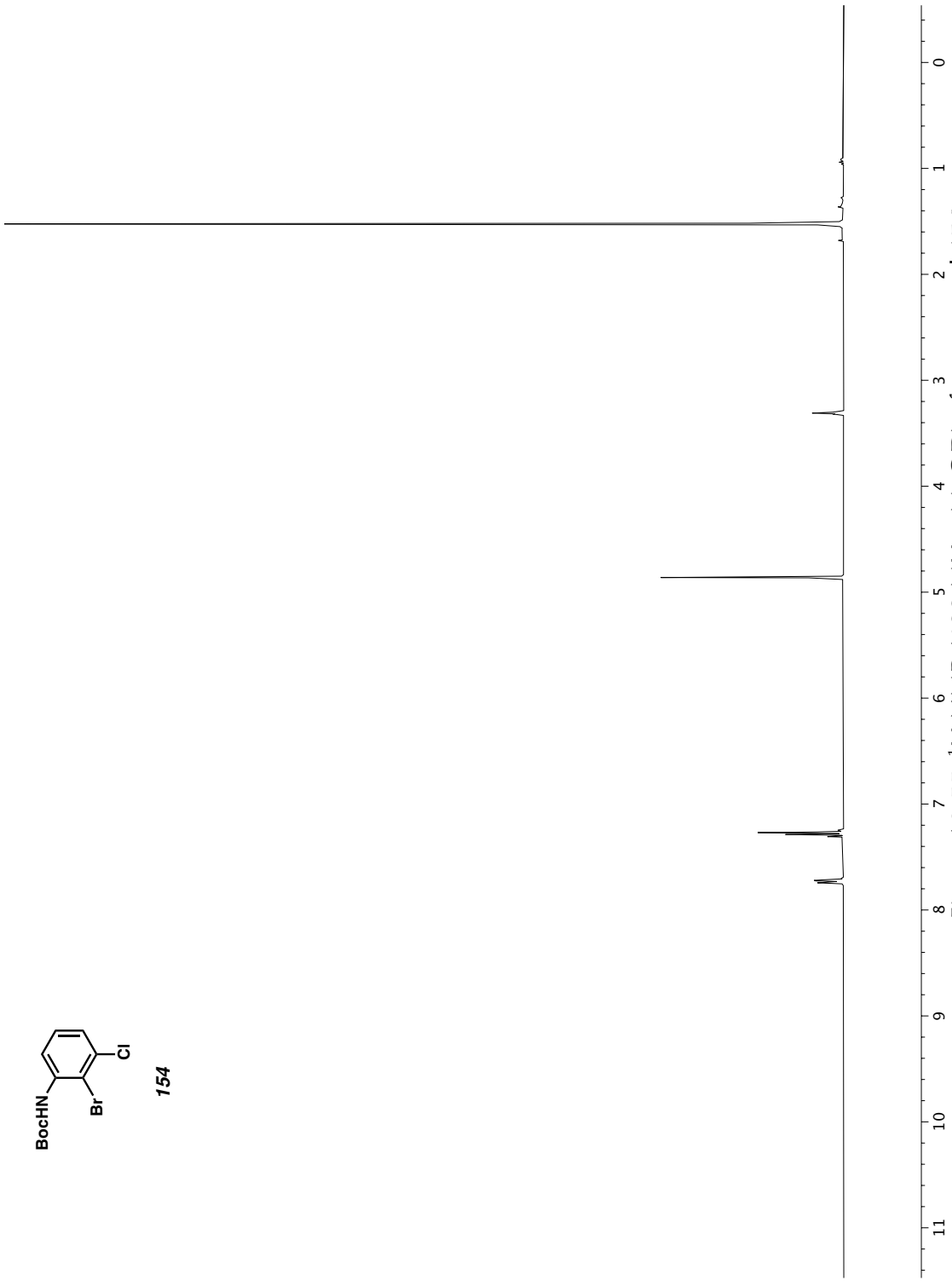


Figure A2.55. ^{1}H NMR (400 MHz, MeOD) of compound **154**.

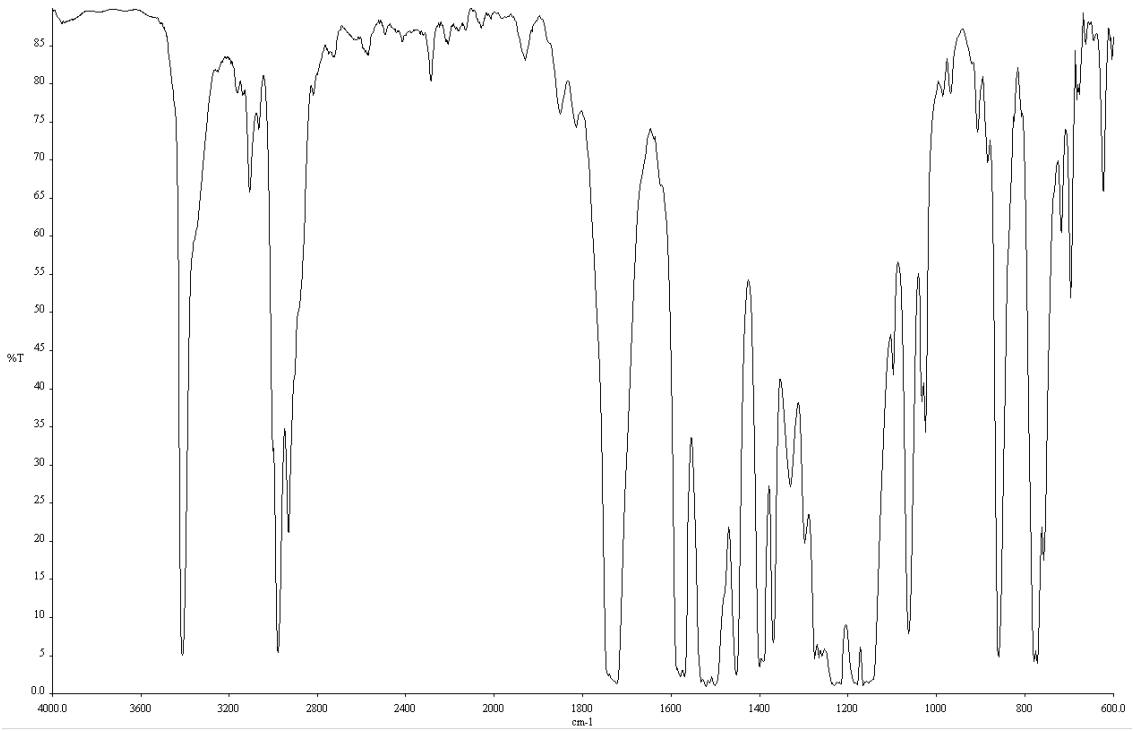


Figure A2.56 Infrared spectrum (Thin Film, NaCl) of compound **154**.

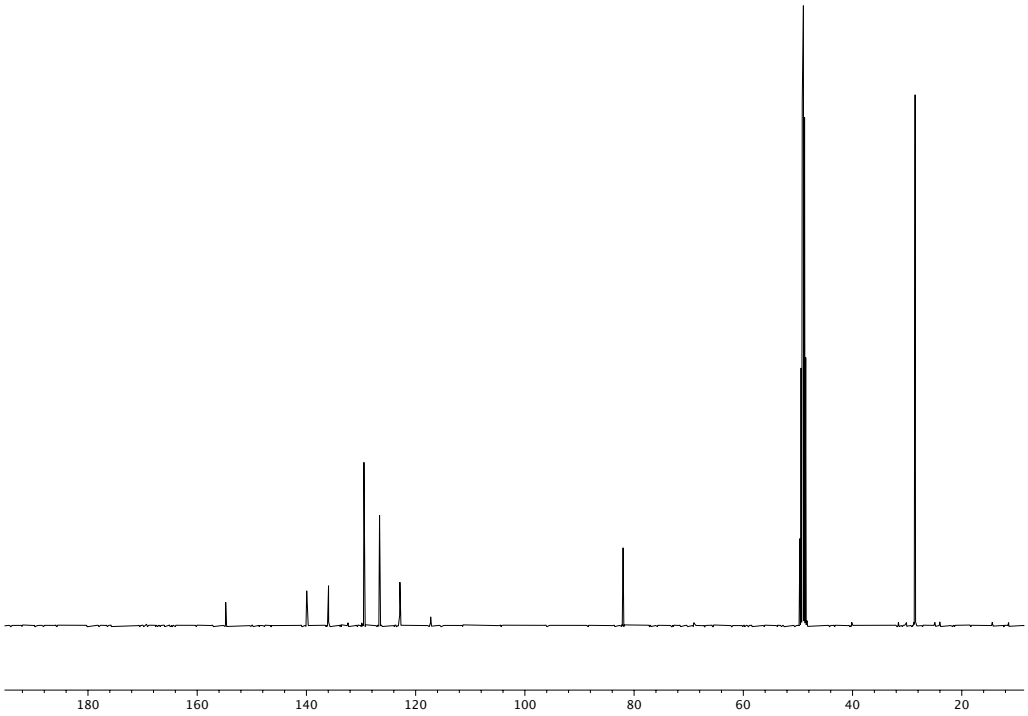


Figure A2.57 ^{13}C NMR (100 MHz, MeOD) of compound **154**.

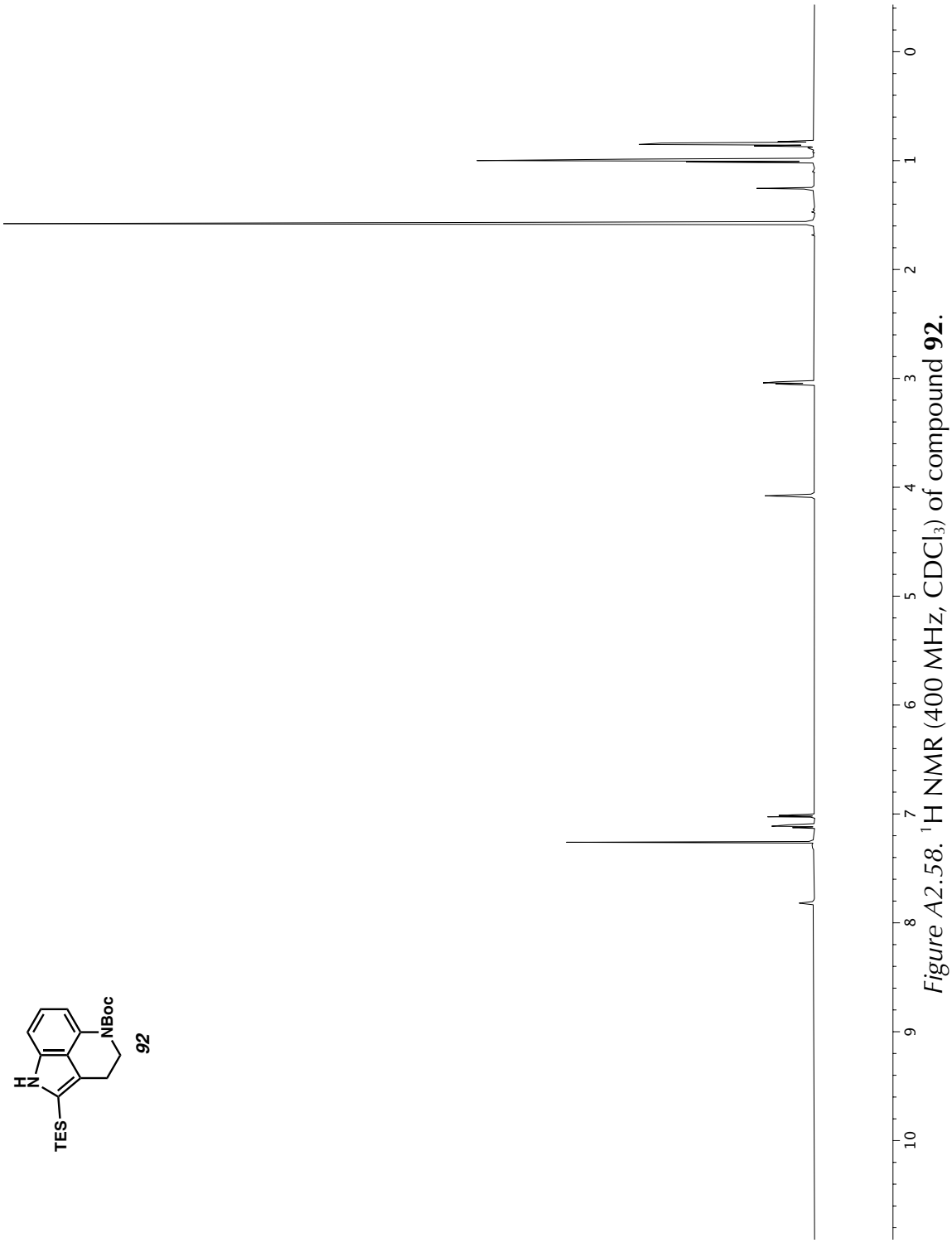


Figure A2.58. ^{1}H NMR (400 MHz, $CDCl_3$) of compound **92**.

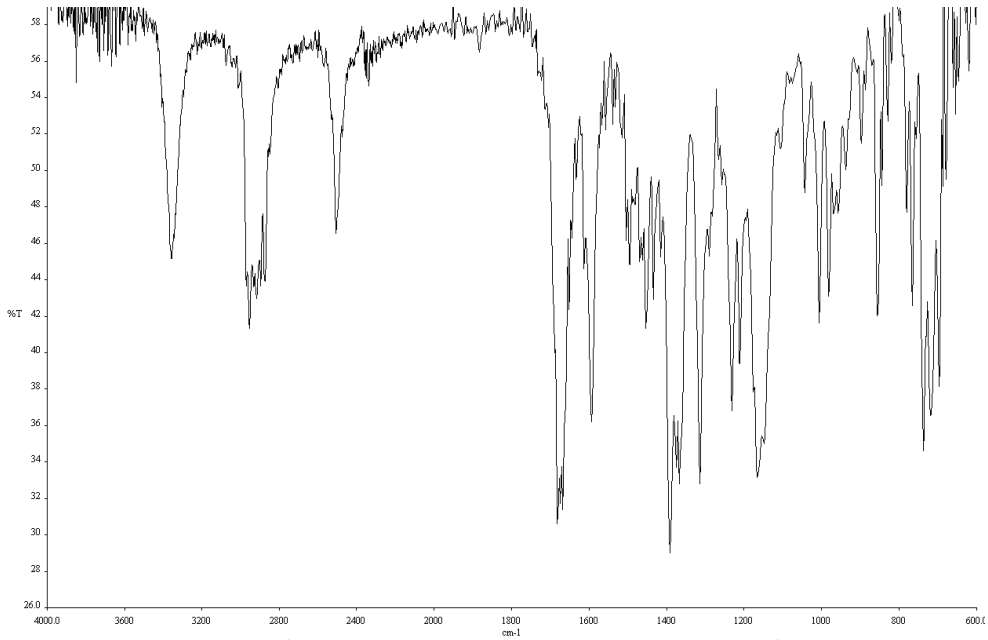


Figure A2.59 Infrared spectrum (Thin Film, NaCl) of compound **92**.

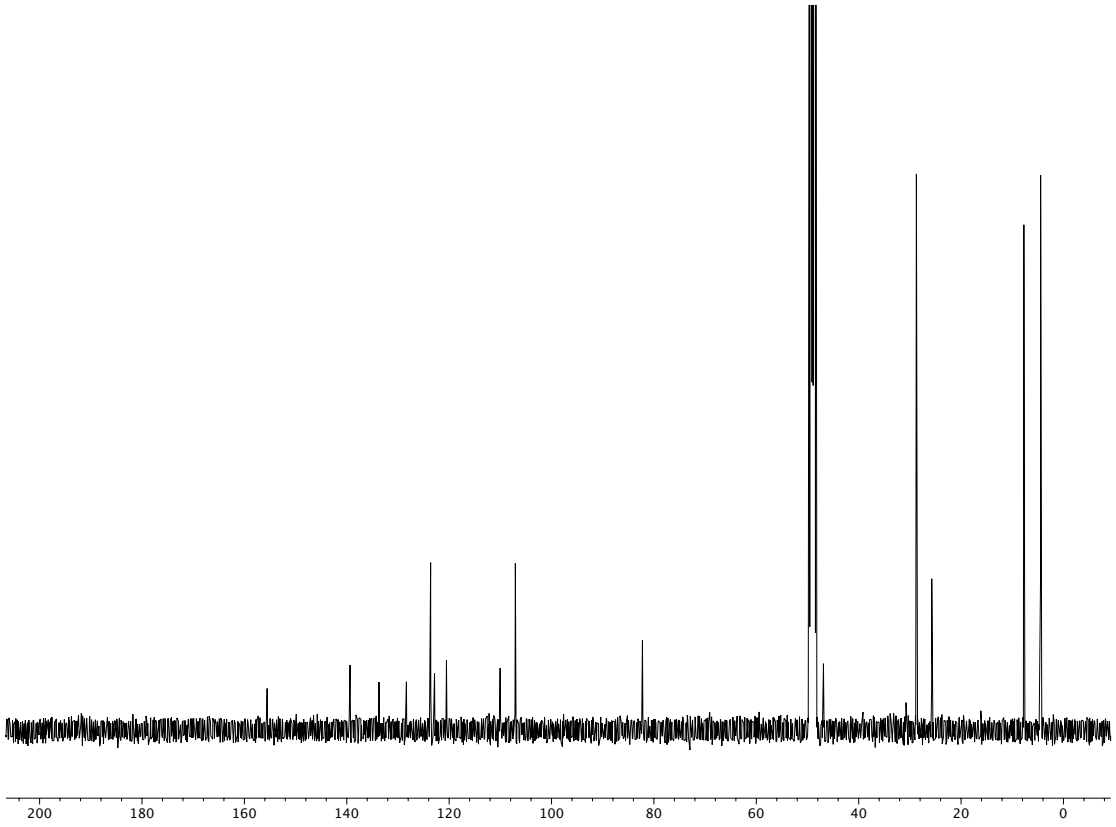


Figure A2.60 ^{13}C NMR (100 MHz, MeOD) of compound **92**.

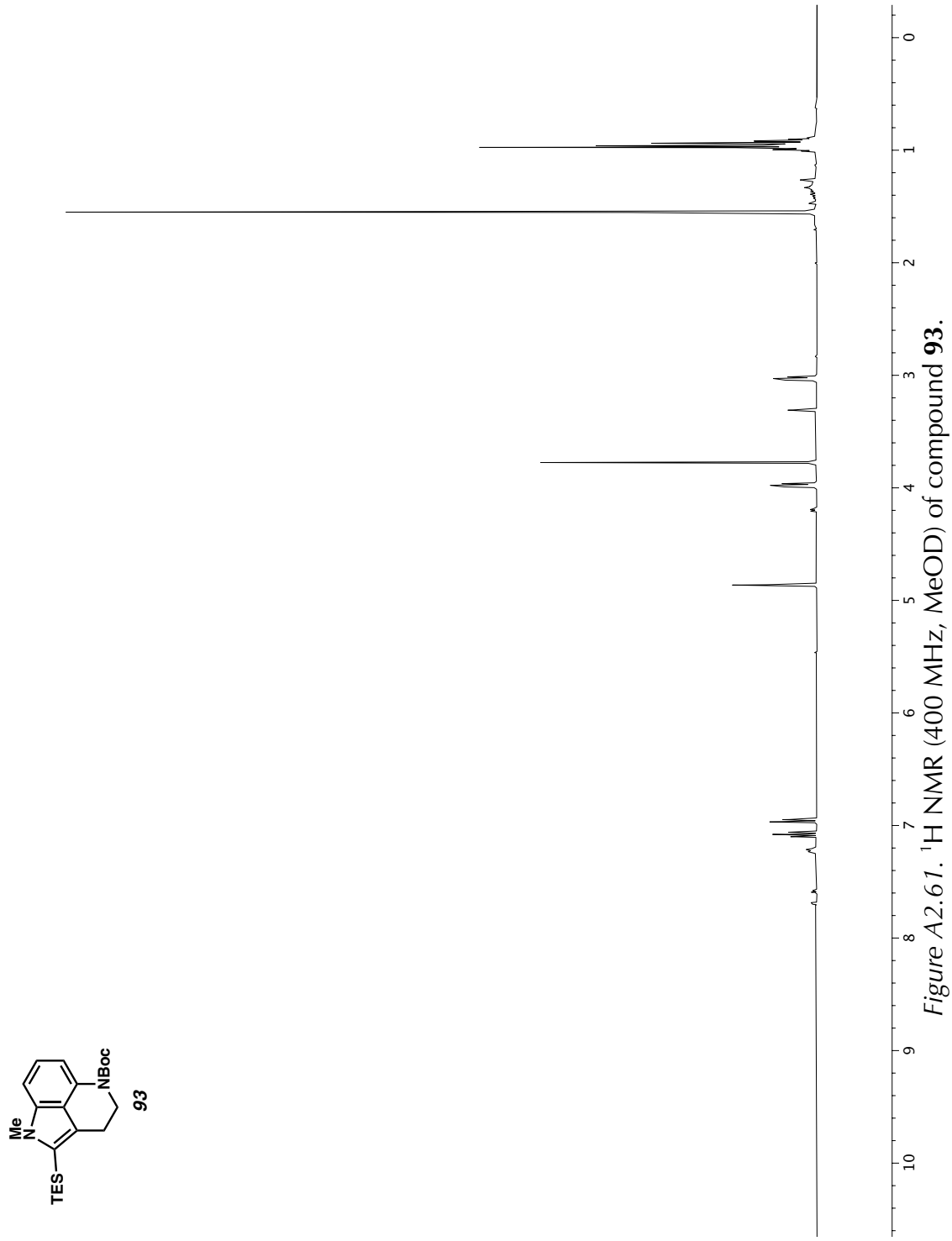


Figure A2.61. ^{1}H NMR (400 MHz, MeOD) of compound **93**.

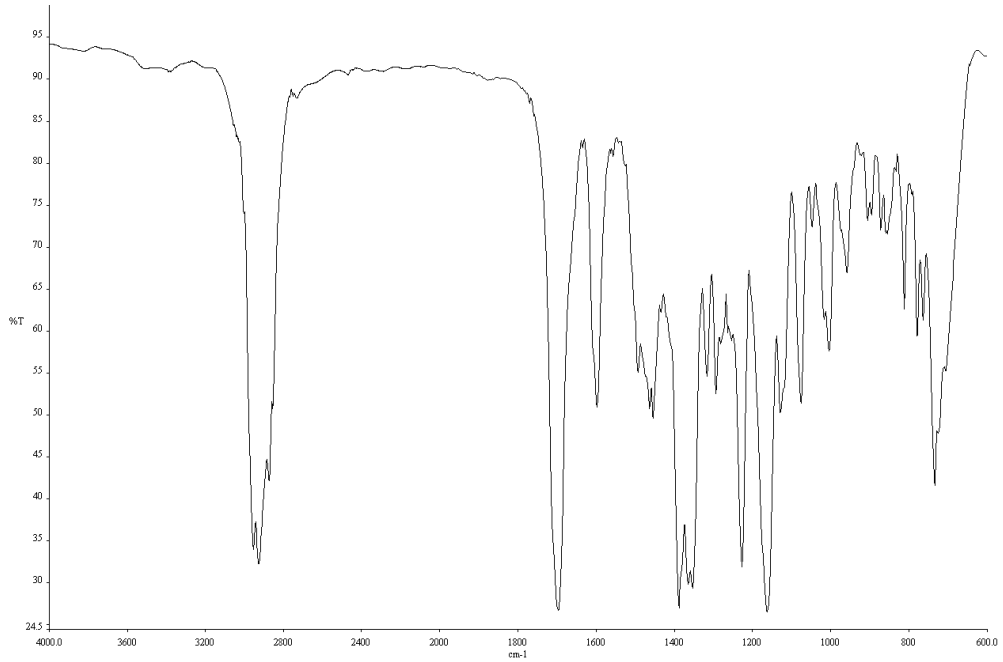


Figure A2.62 Infrared spectrum (Thin Film, NaCl) of compound **93**.

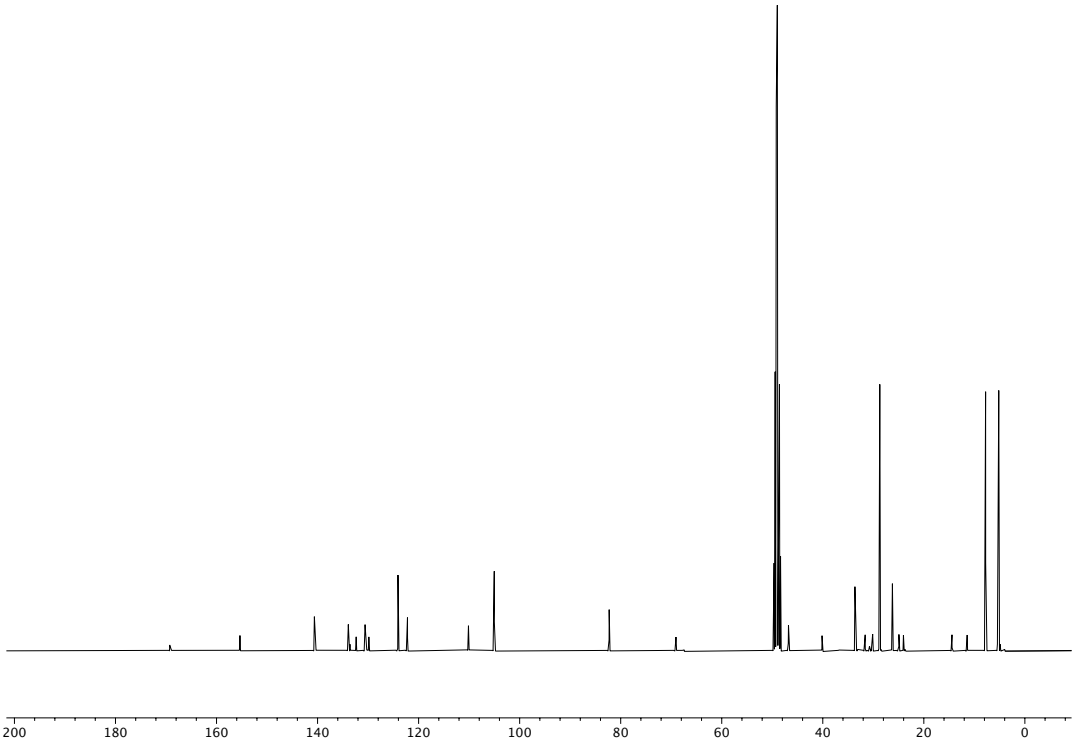


Figure A2.63 ^{13}C NMR (100 MHz, MeOD) of compound **93**.

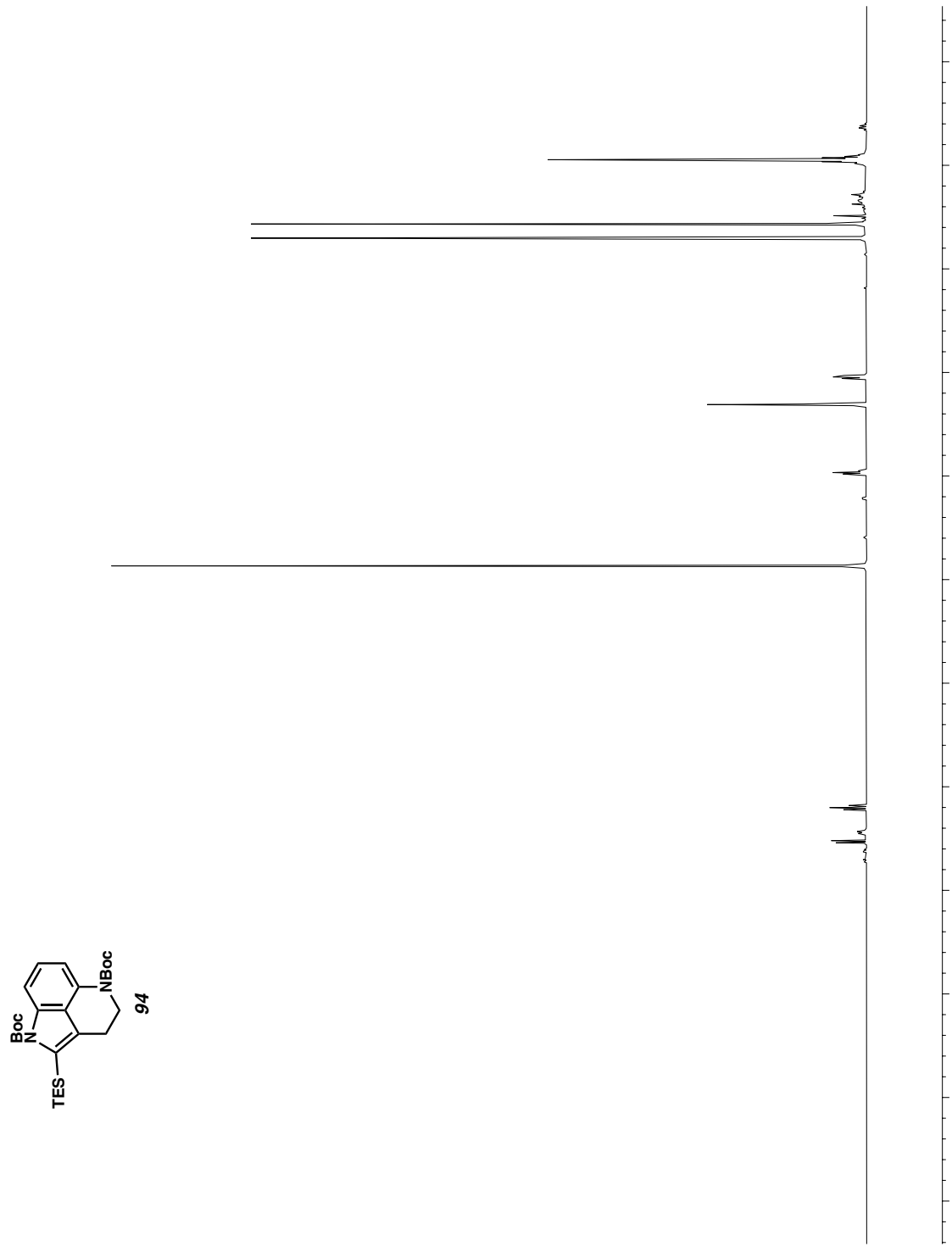


Figure A2.64. ^{1}H NMR (400 MHz, MeOD) of compound **94**.

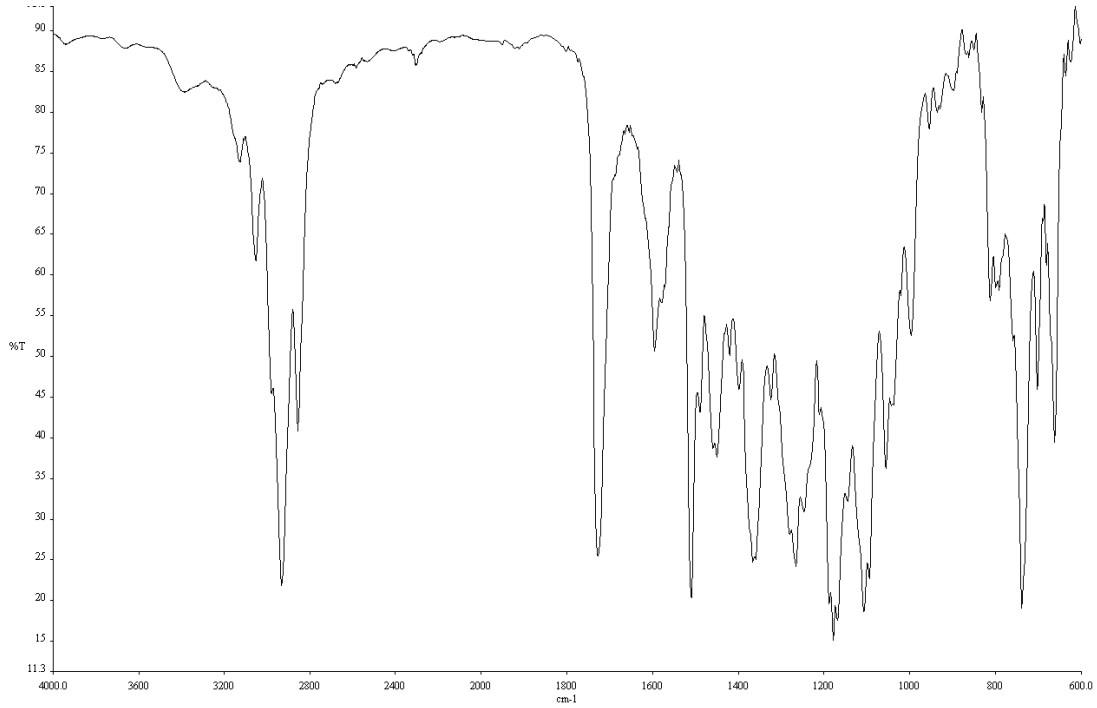


Figure A2.65 Infrared spectrum (Thin Film, NaCl) of compound **94**.

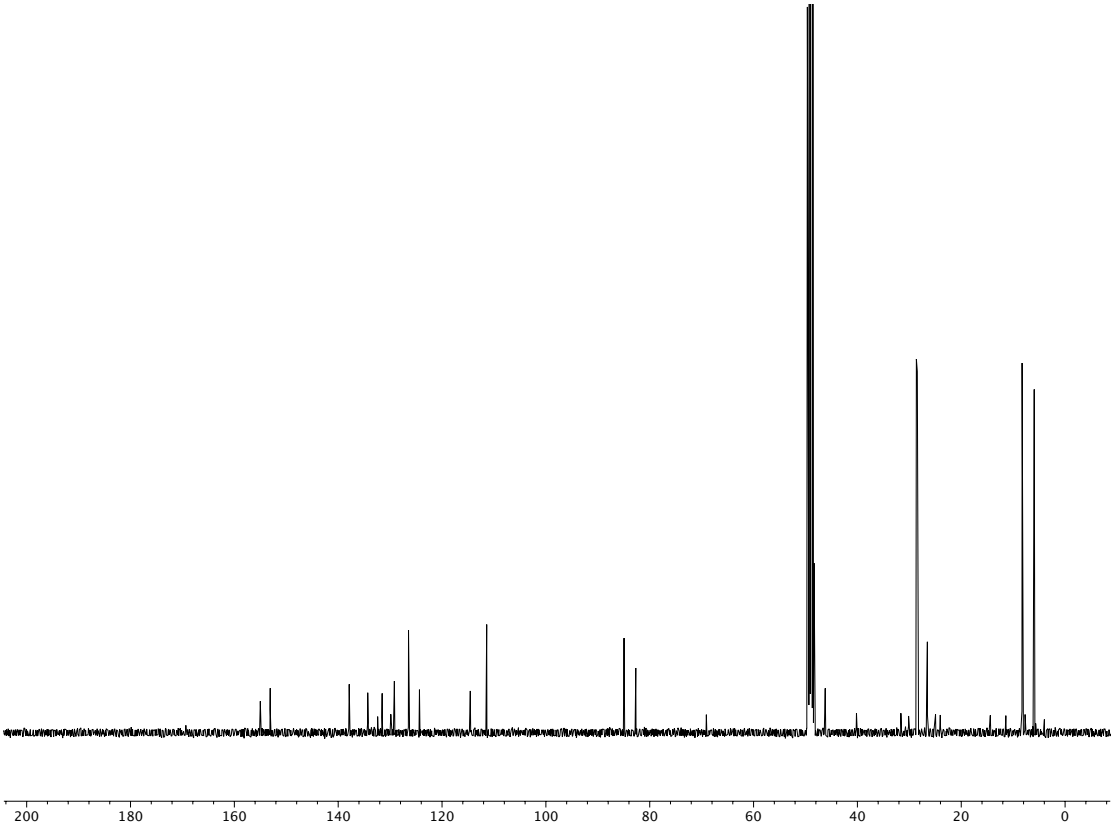


Figure A2.66 ^{13}C NMR (100 MHz, MeOD) of compound **94**.

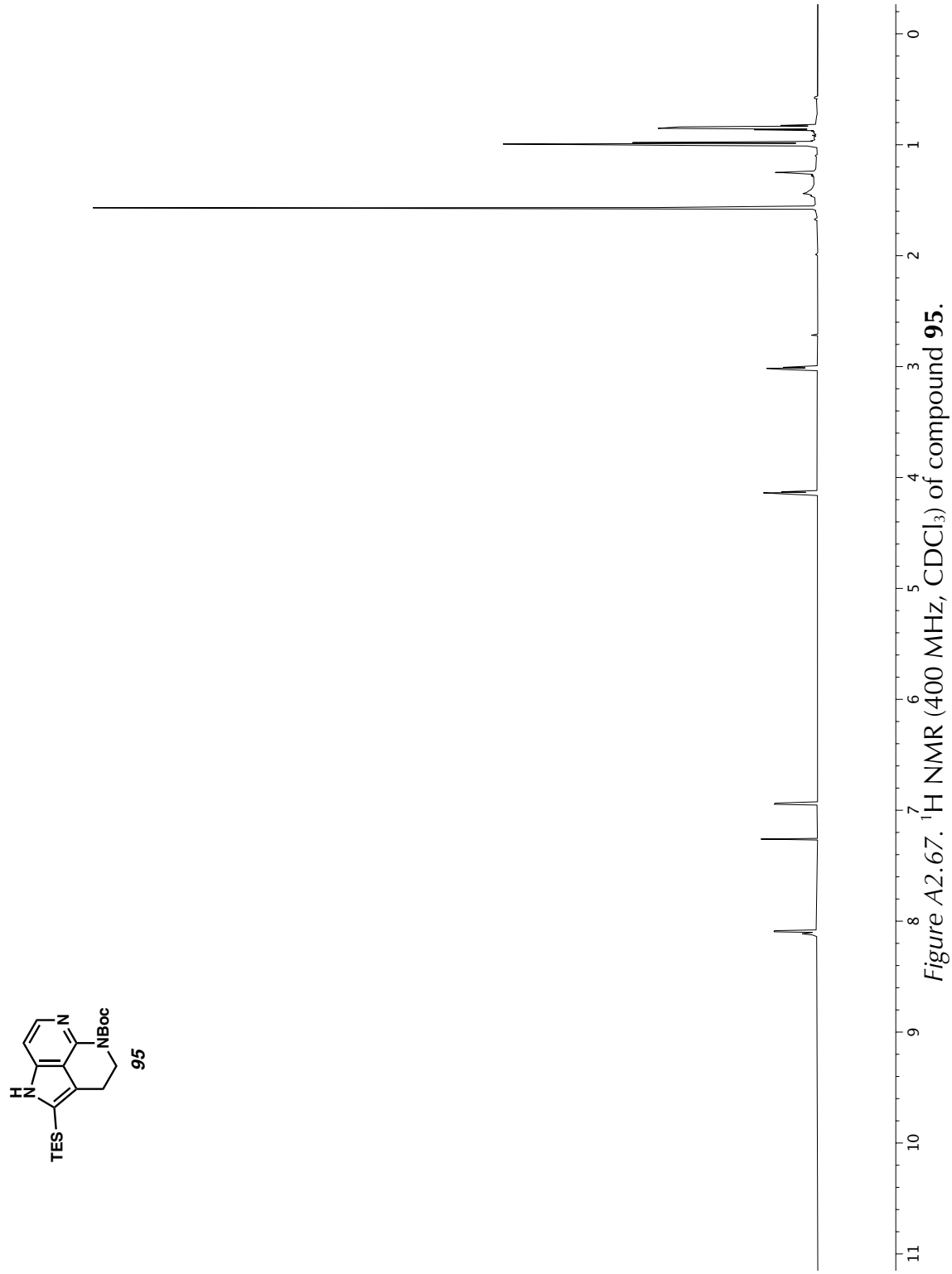


Figure A2.67. ^{1}H NMR (400 MHz, $CDCl_3$) of compound **95**.

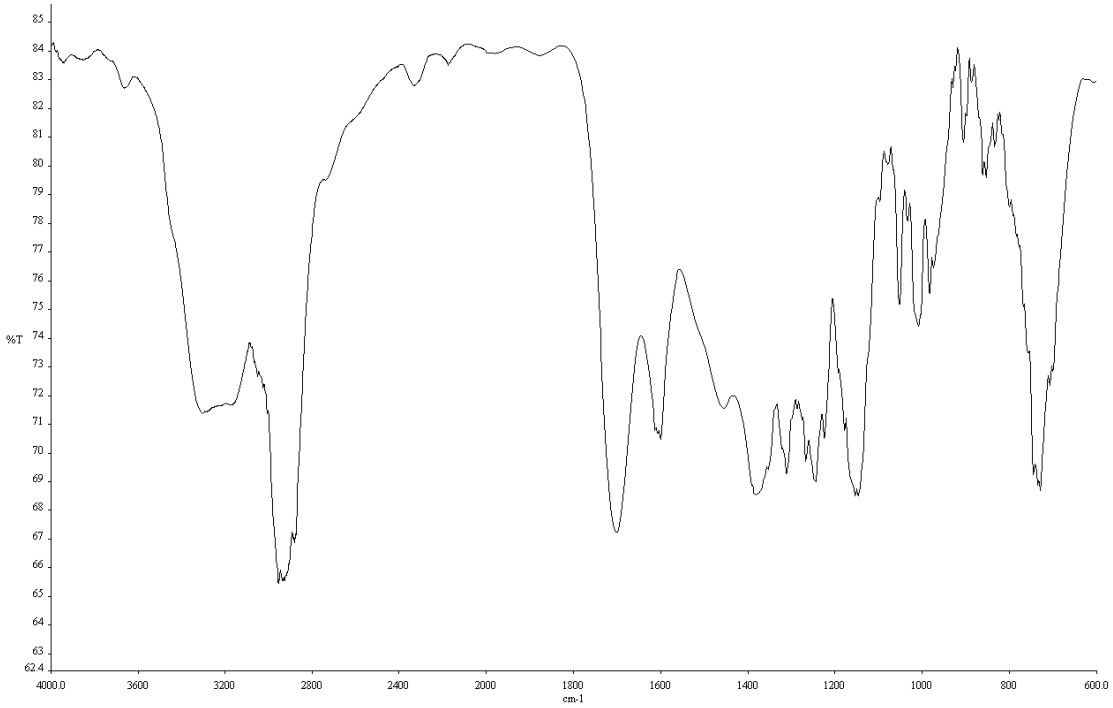


Figure A2.68 Infrared spectrum (Thin Film, NaCl) of compound **95**.

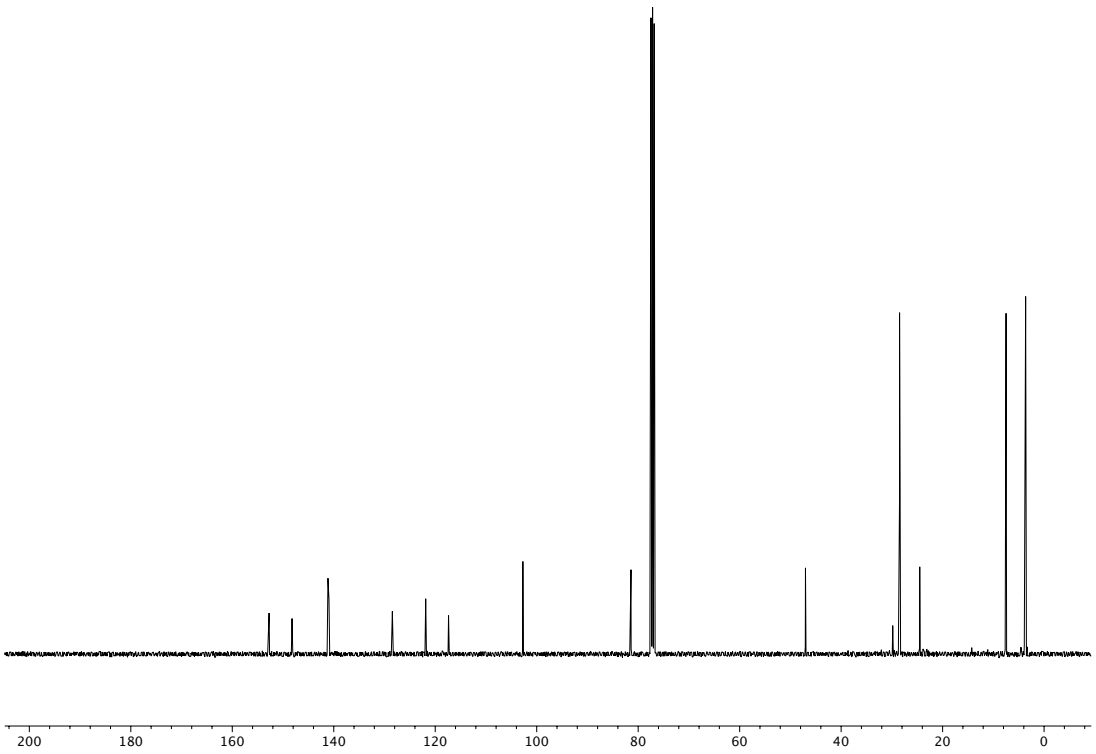


Figure A2.69 ^{13}C NMR (100 MHz, $CDCl_3$) of compound **95**.

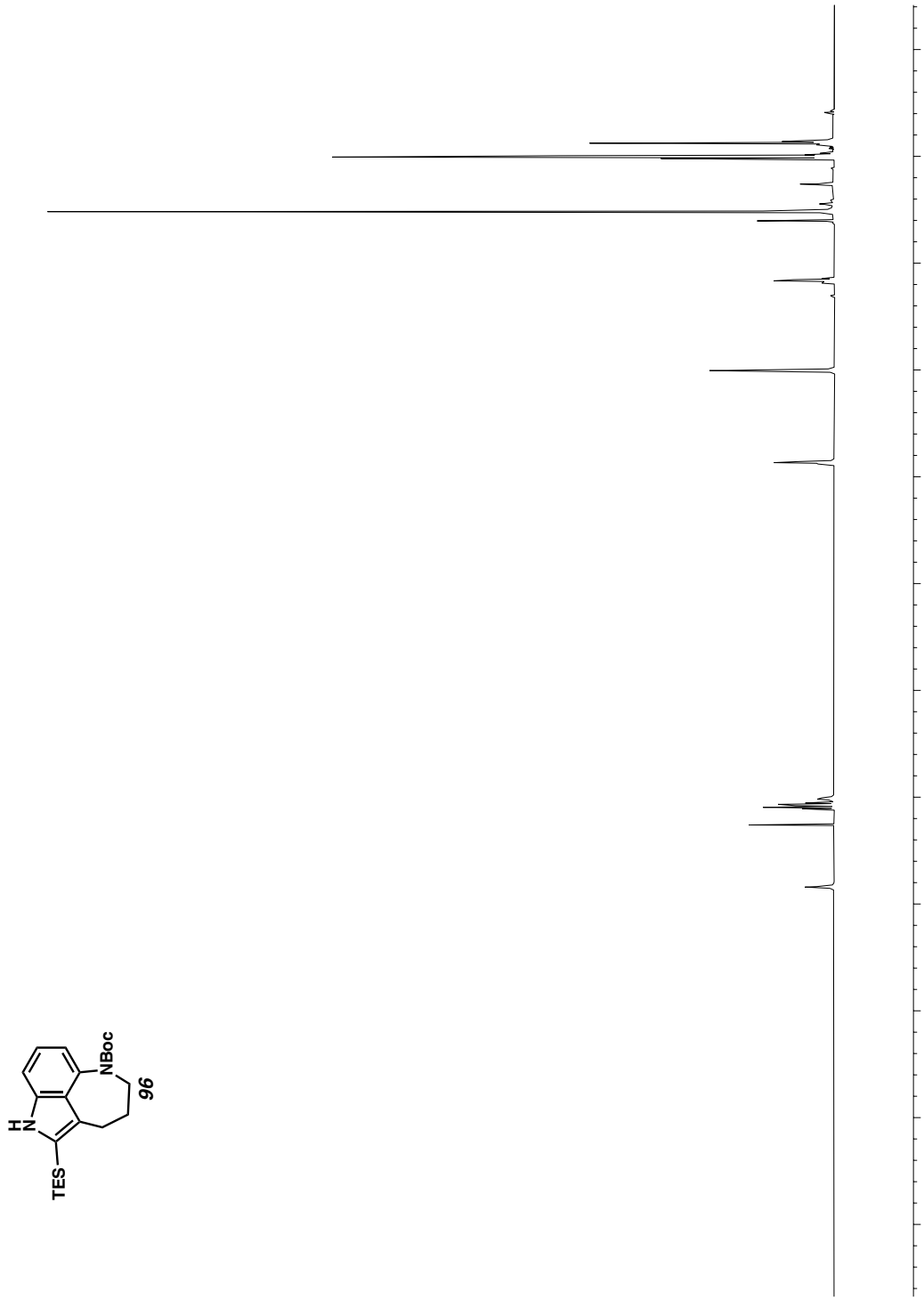


Figure A2.70. ^{1}H NMR (400 MHz, $CDCl_3$) of compound **96**.

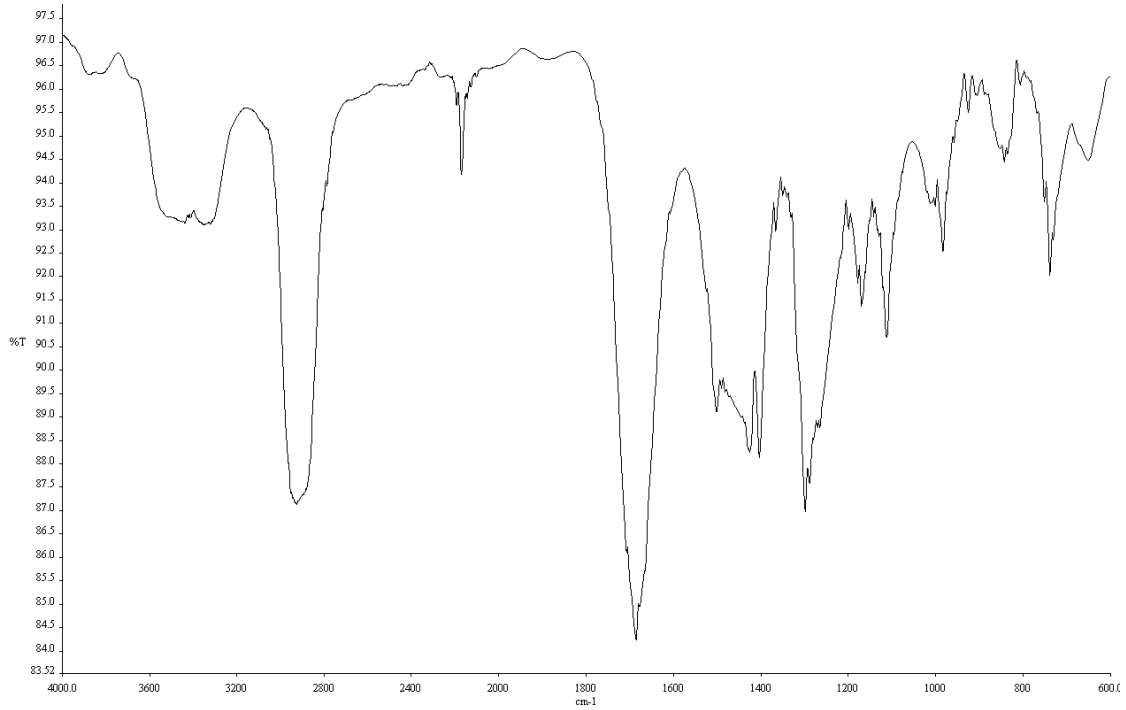


Figure A2.71 Infrared spectrum (Thin Film, NaCl) of compound **96**.

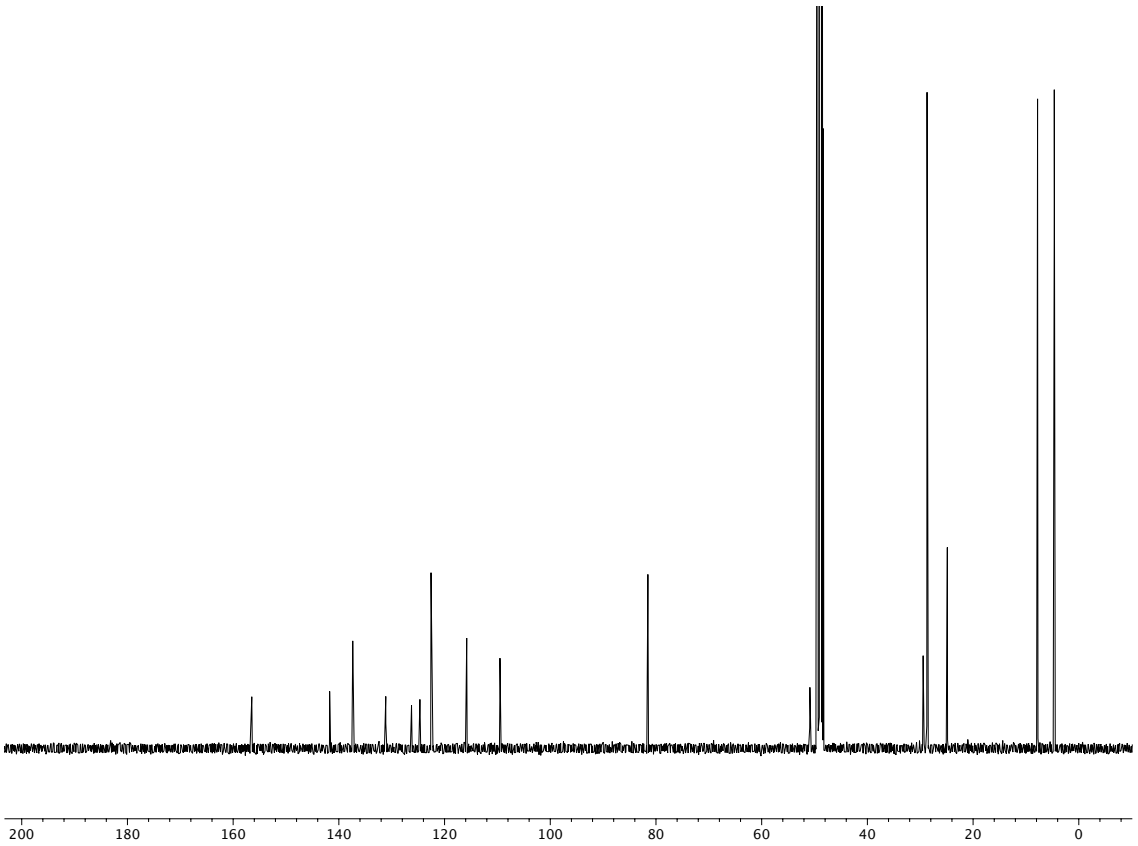


Figure A2.72 ^{13}C NMR (100 MHz, MeOD) of compound **96**.

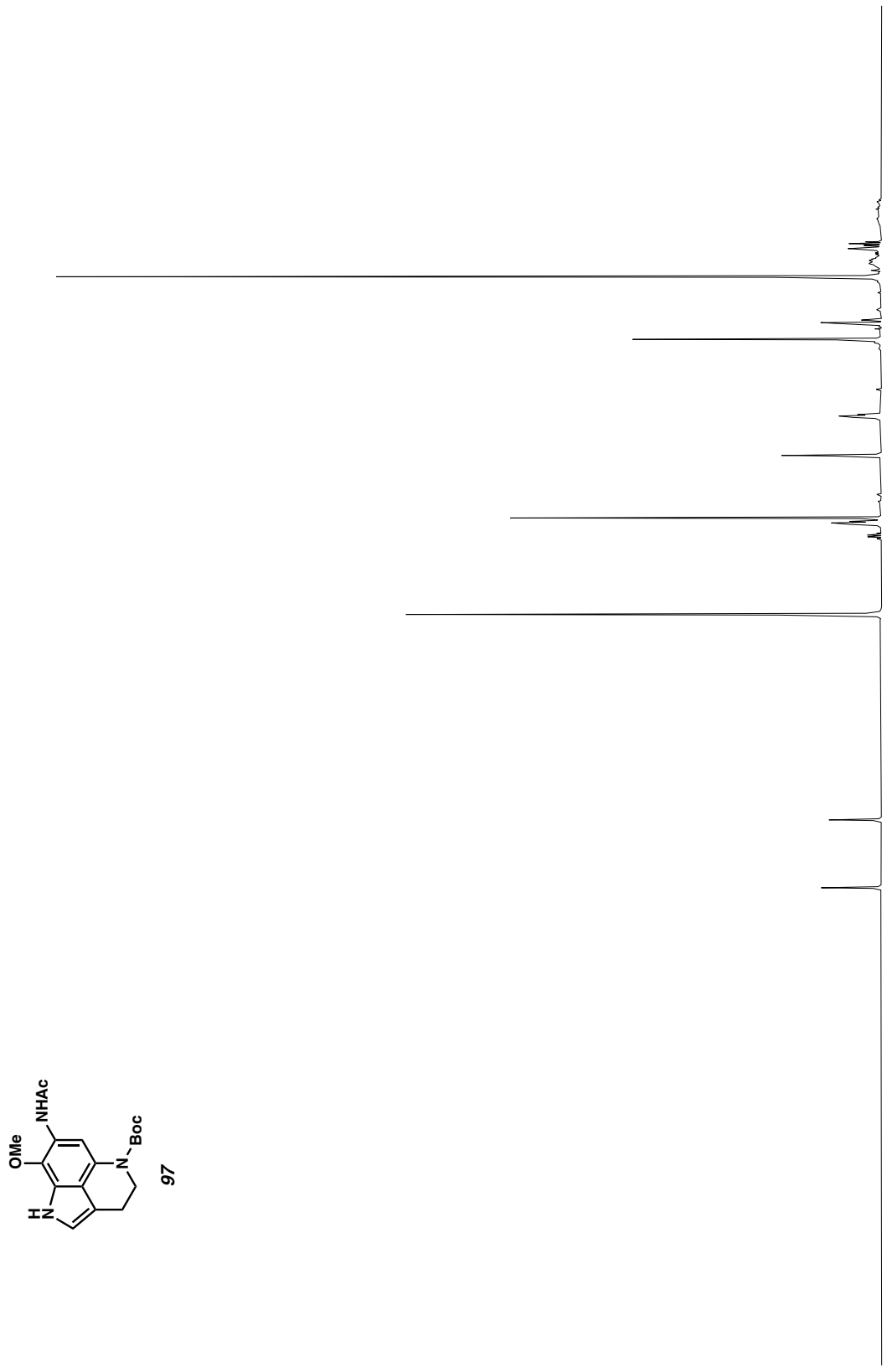


Figure A2.73. ^{1}H NMR (400 MHz, MeOD) of compound **97**.

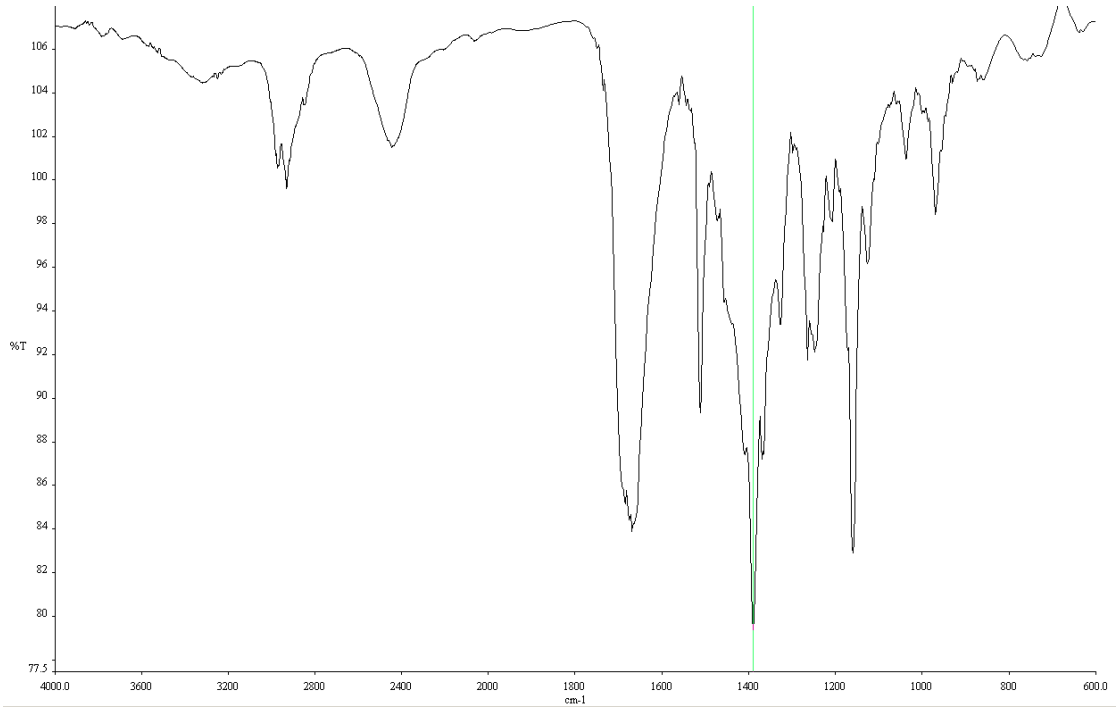


Figure A2.74 Infrared spectrum (Thin Film, NaCl) of compound **97**.

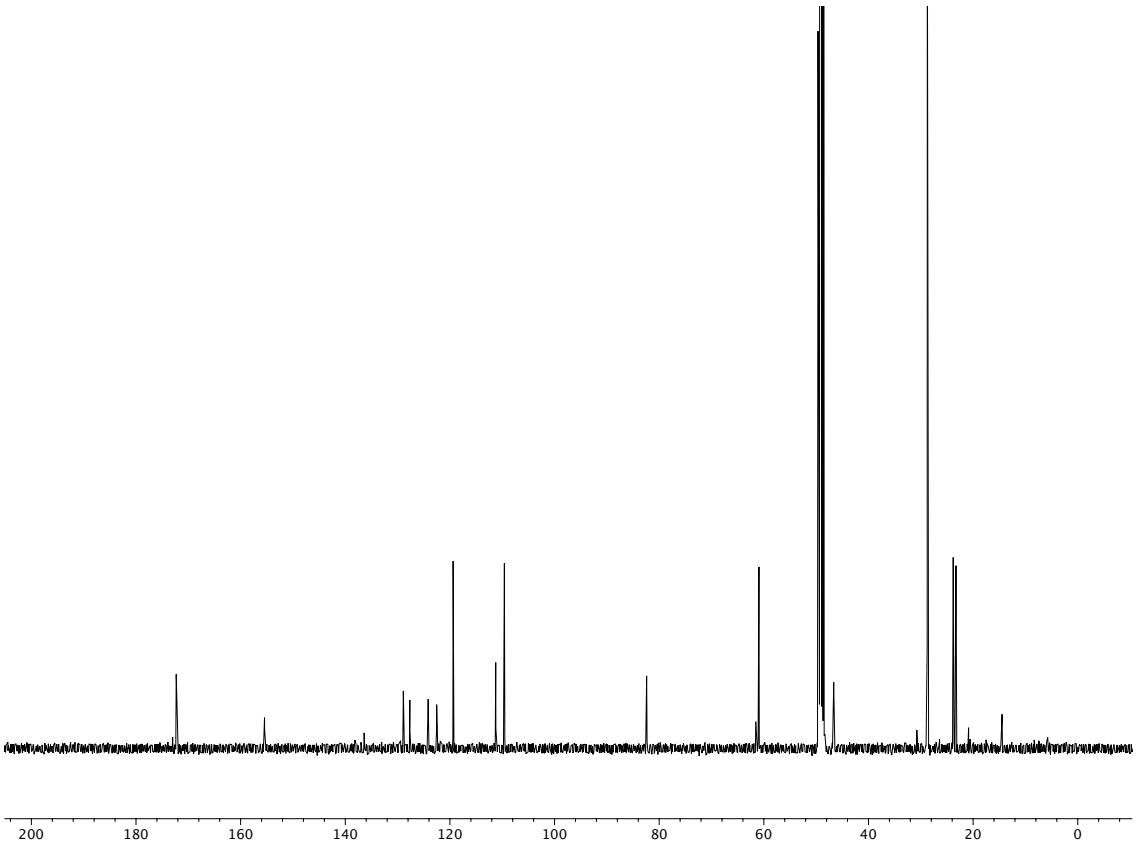


Figure A2.75 ^{13}C NMR (100 MHz, MeOD) of compound **97**.

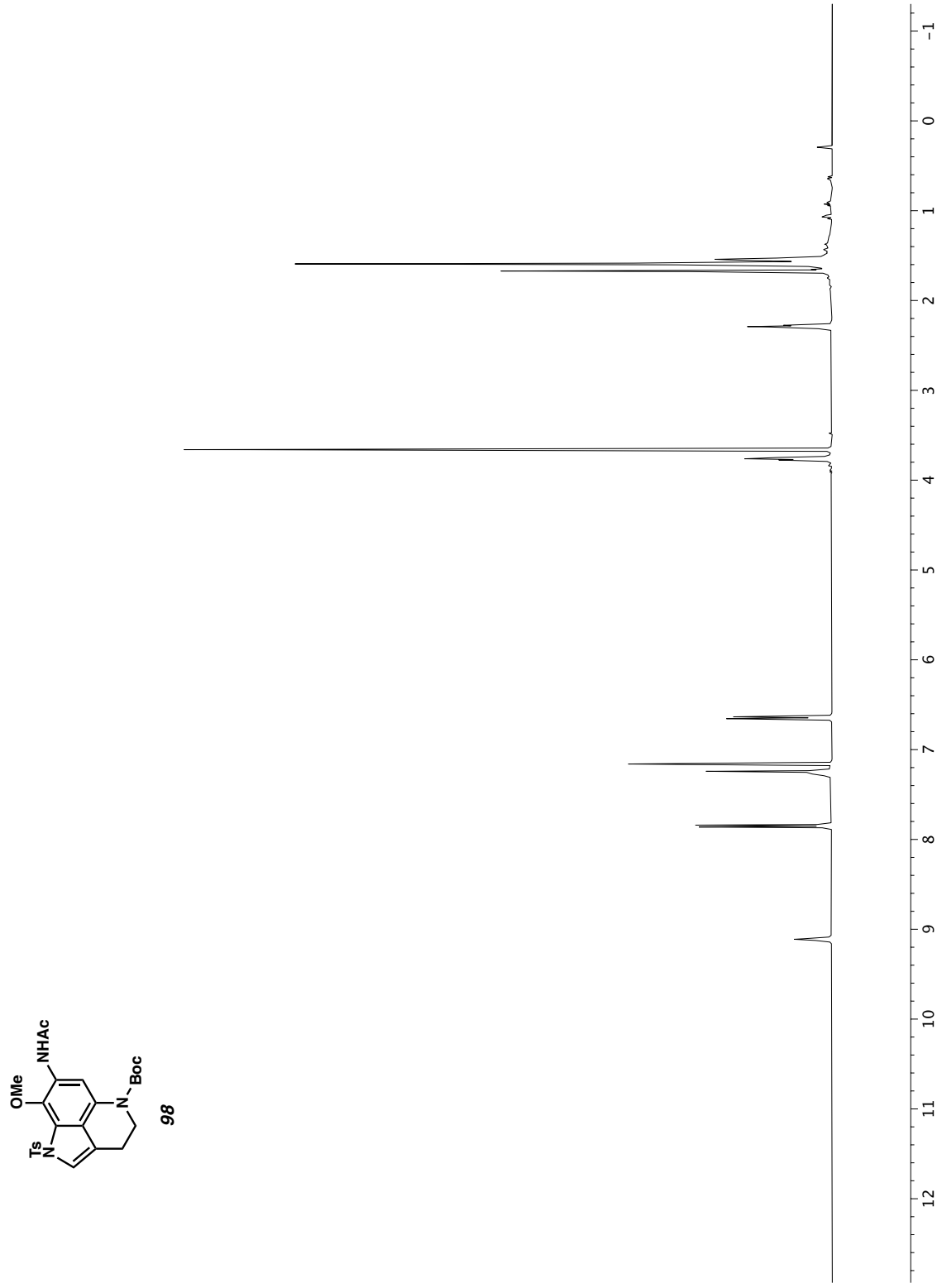


Figure A2.76. ^{1}H NMR (400 MHz, C_6D_6) of compound **98**.

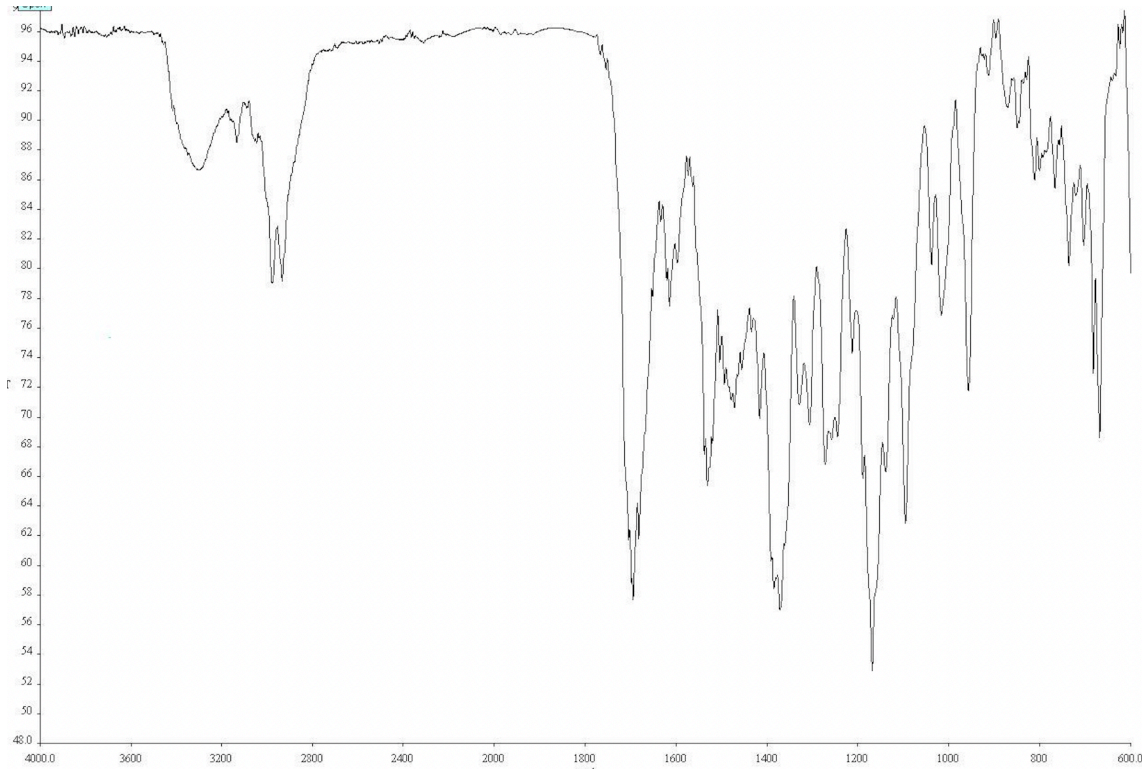


Figure A2.77 Infrared spectrum (Thin Film, NaCl) of compound **98**.

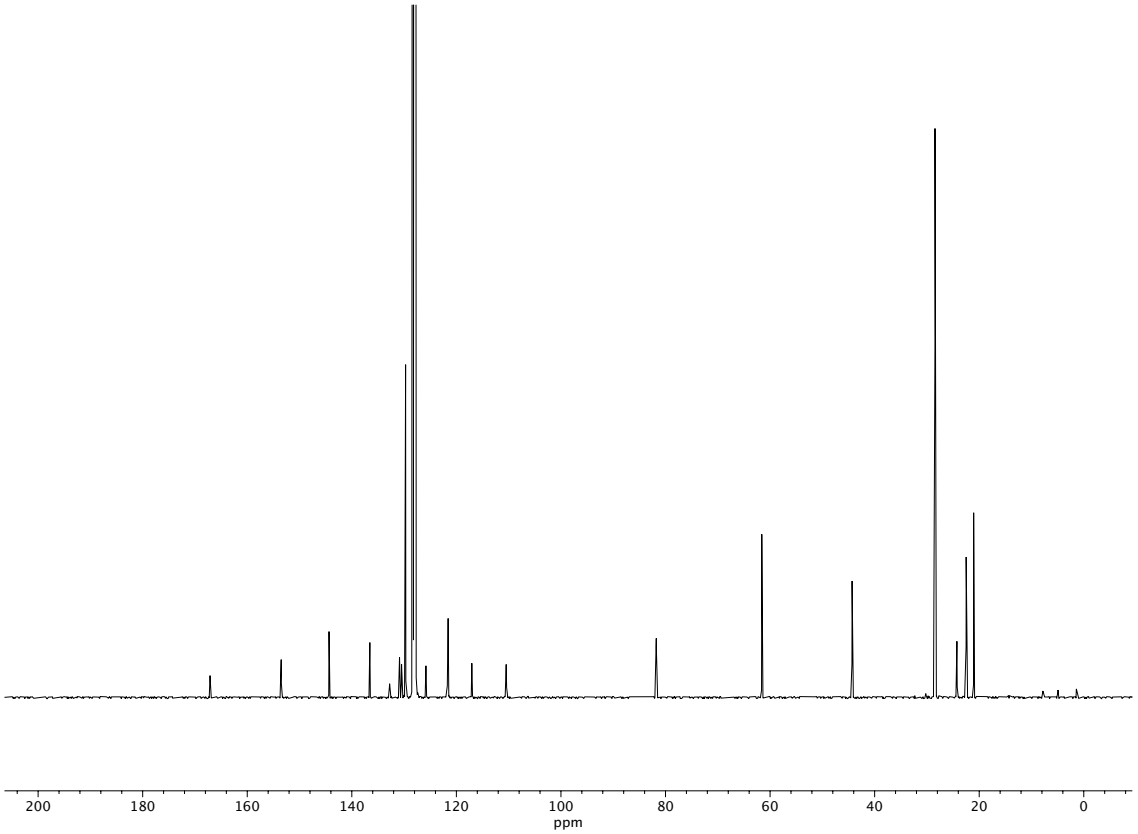


Figure A2.78 ^{13}C NMR (100 MHz, C_6D_6) of compound **98**.

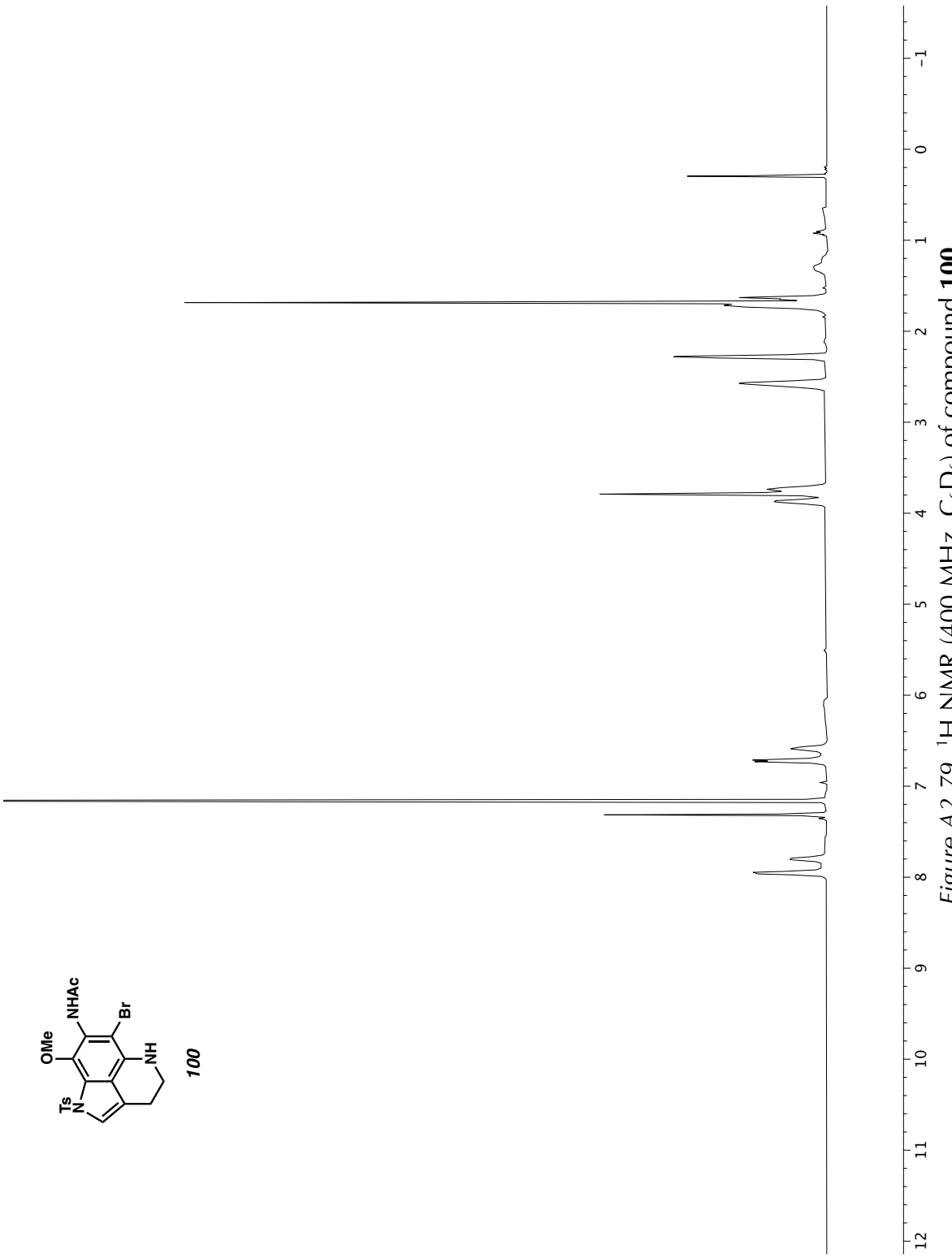


Figure A2.79. ^{1}H NMR (400 MHz, C_6D_6) of compound **100**.

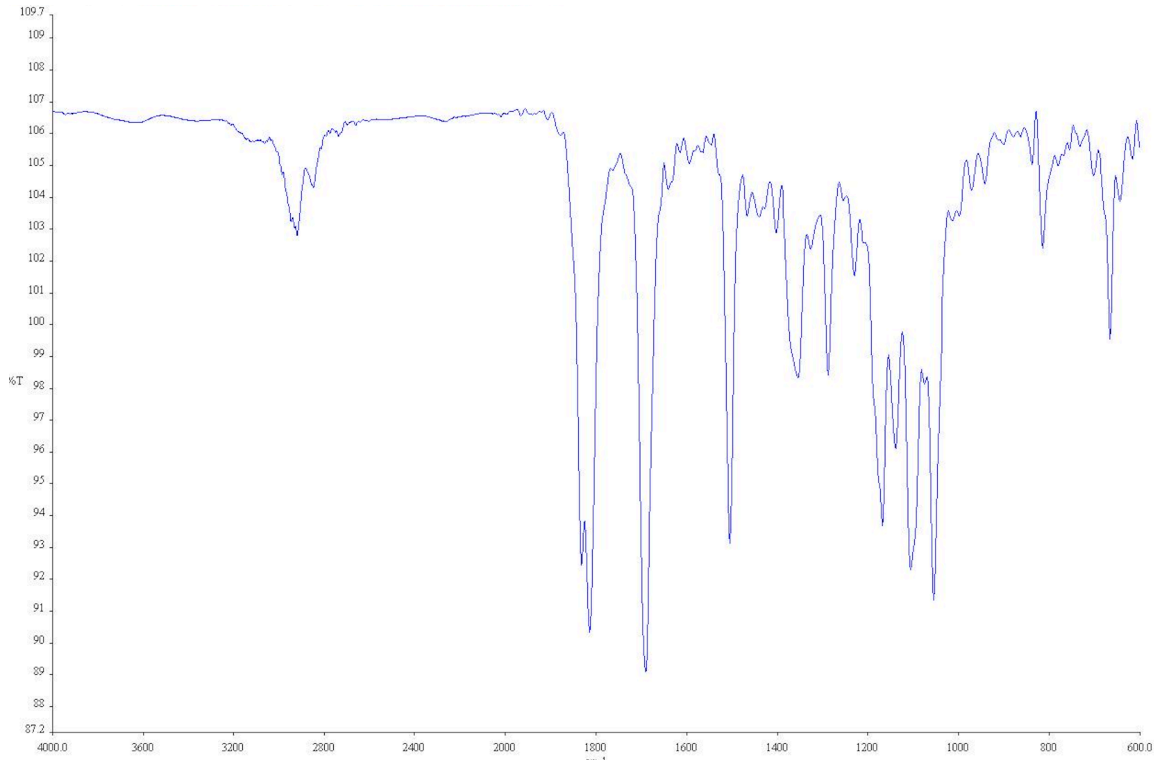


Figure A2.80 Infrared spectrum (Thin Film, NaCl) of compound **100**.

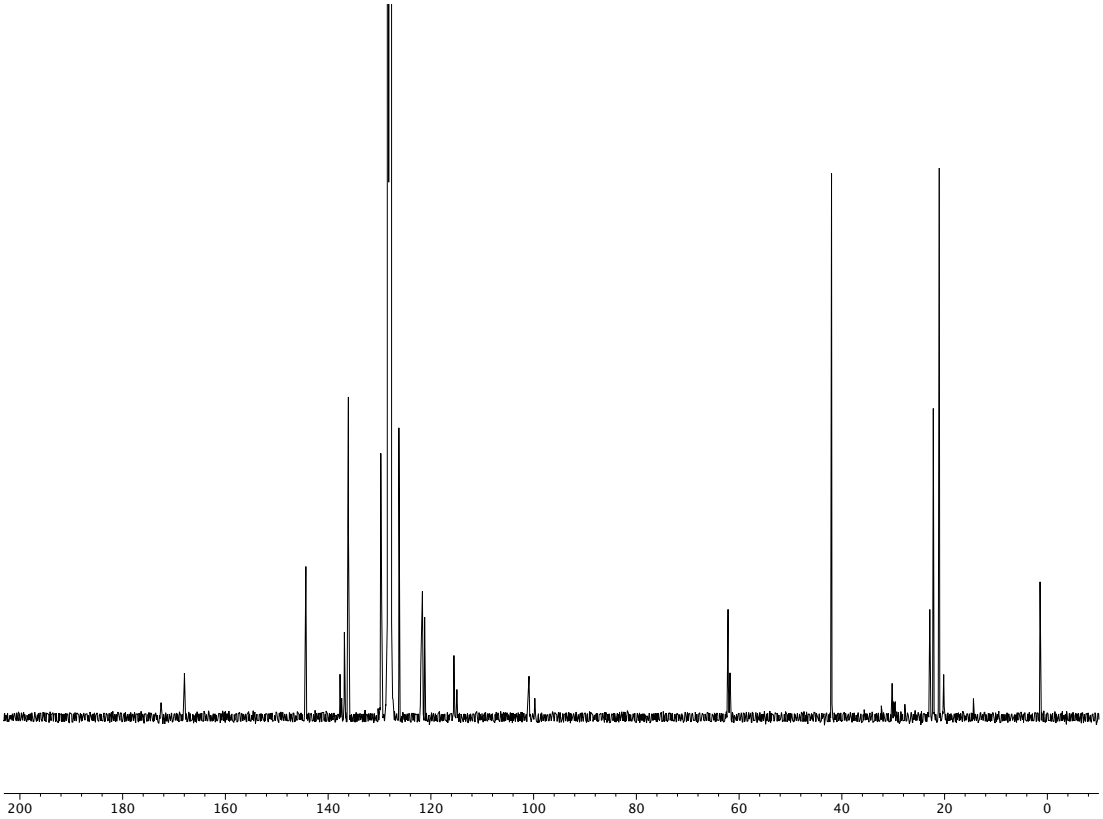


Figure A2.81 ^{13}C NMR (100 MHz, C_6D_6) of compound **101**.

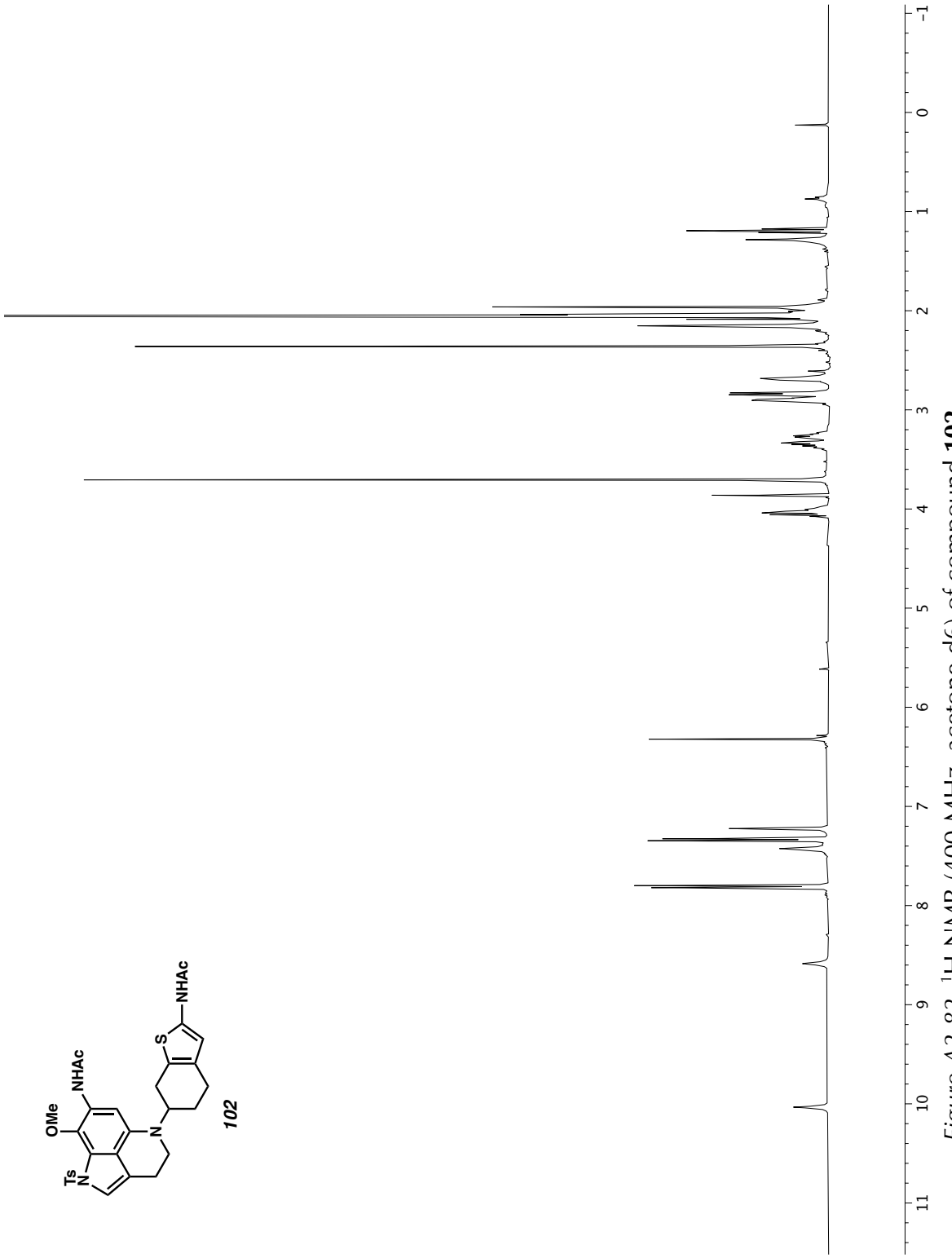


Figure A2.82. ^{1}H NMR (400 MHz, acetone-d6) of compound **102**.

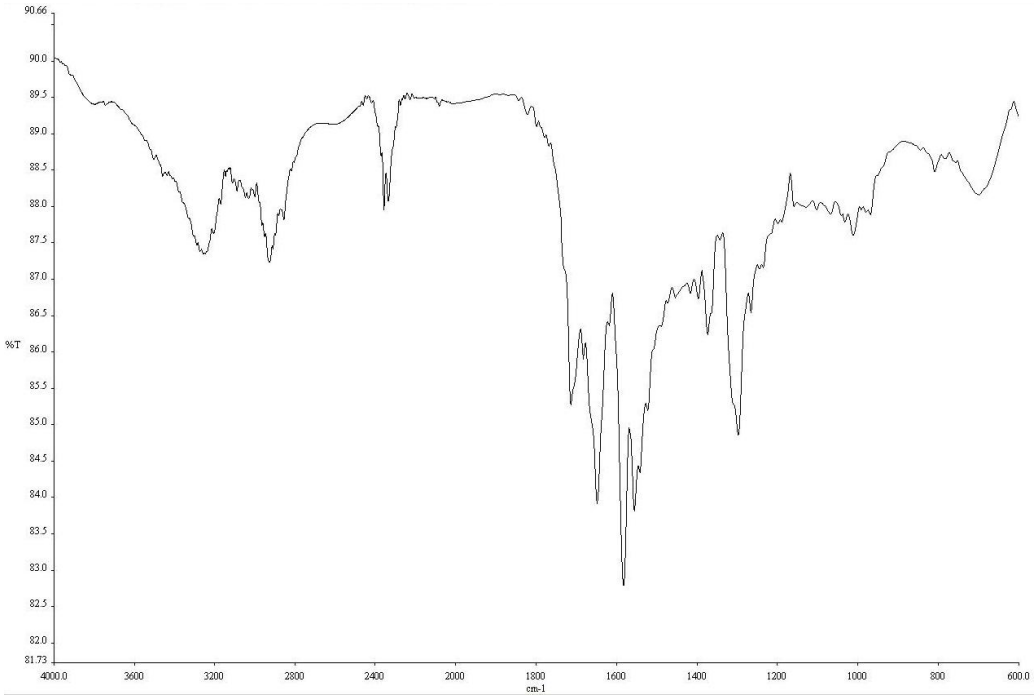


Figure A2.83 Infrared spectrum (Thin Film, NaCl) of compound **102**.

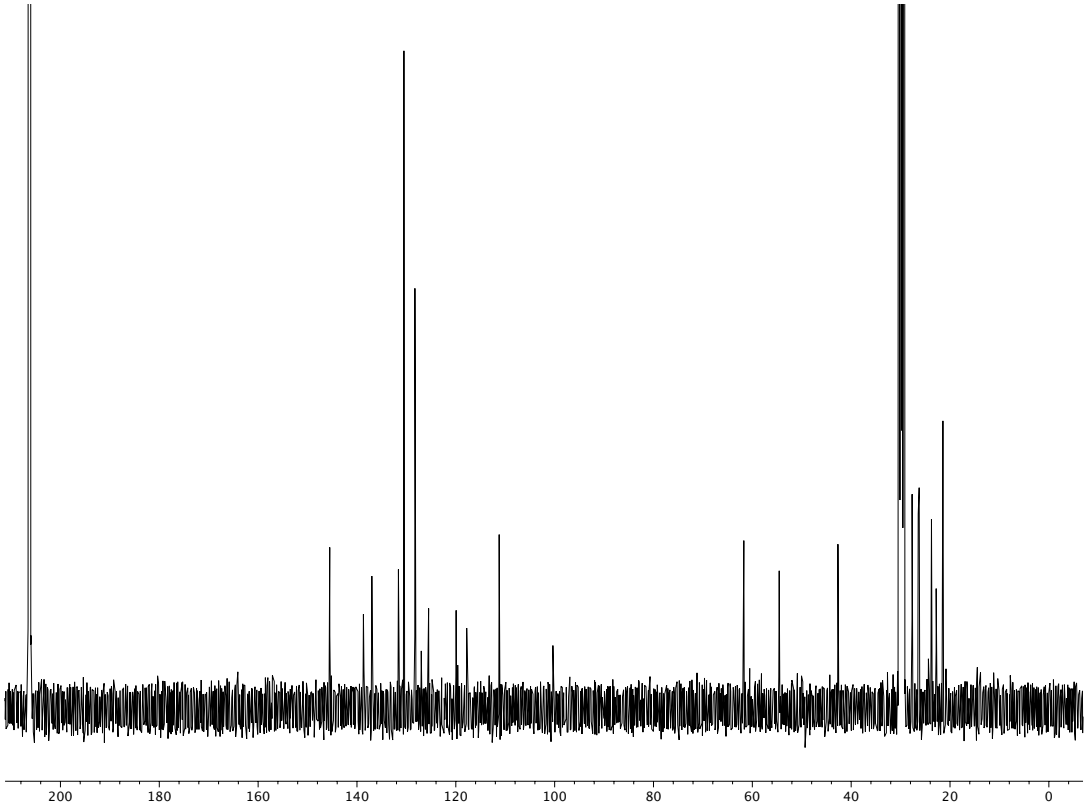


Figure A2.84 ^{13}C NMR (100 MHz, acetone-d6) of compound **102**.

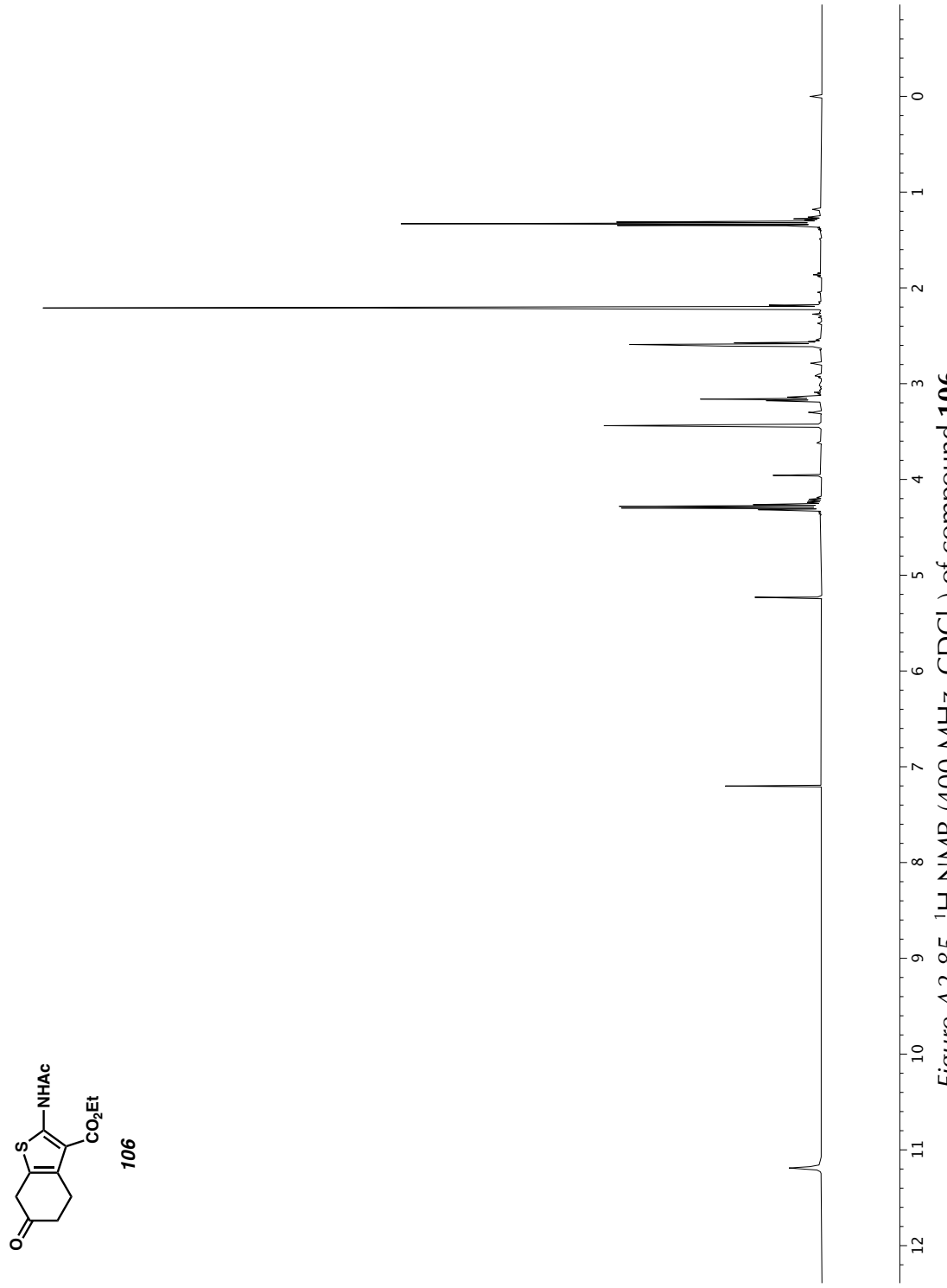


Figure A2.85. ^{1}H NMR (400 MHz, $CDCl_3$) of compound **106**.

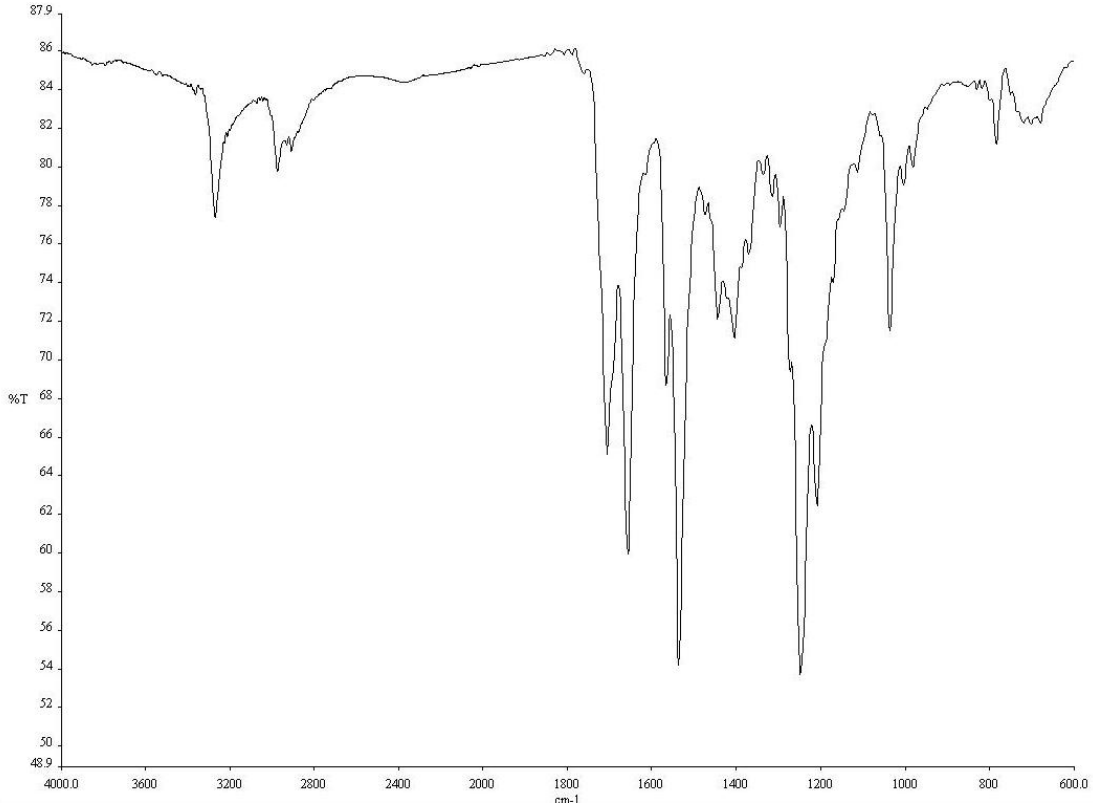


Figure A2.86 Infrared spectrum (Thin Film, NaCl) of compound **106**.

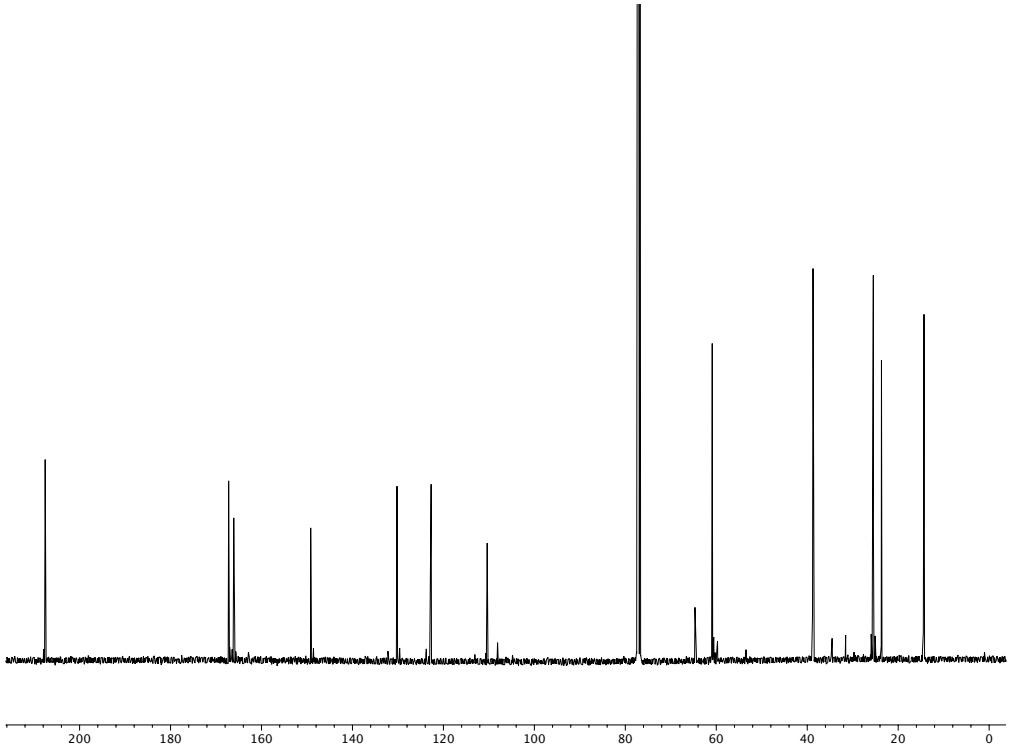


Figure A2.87 ^{13}C NMR (100 MHz, $CDCl_3$) of compound **106**.

Figure A2.88. ^{1}H NMR (400 MHz, $CDCl_3$) of compound **107**.

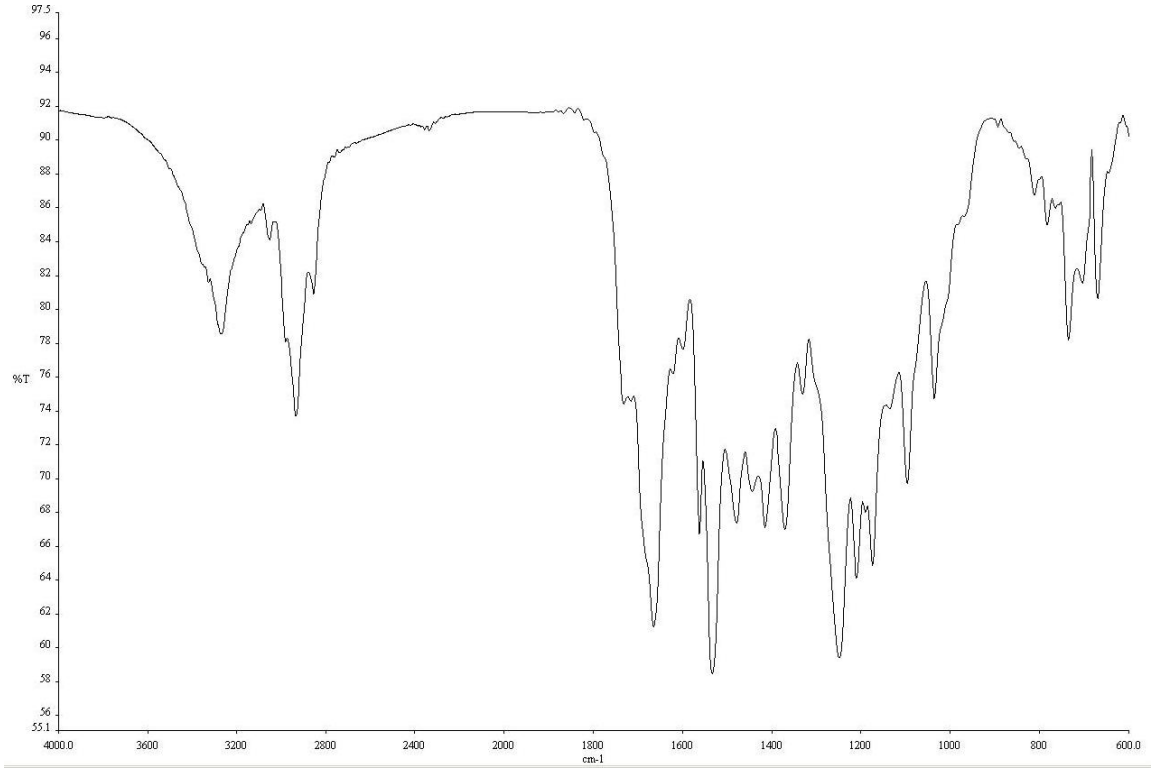


Figure A2.89 Infrared spectrum (Thin Film, NaCl) of compound **107**.

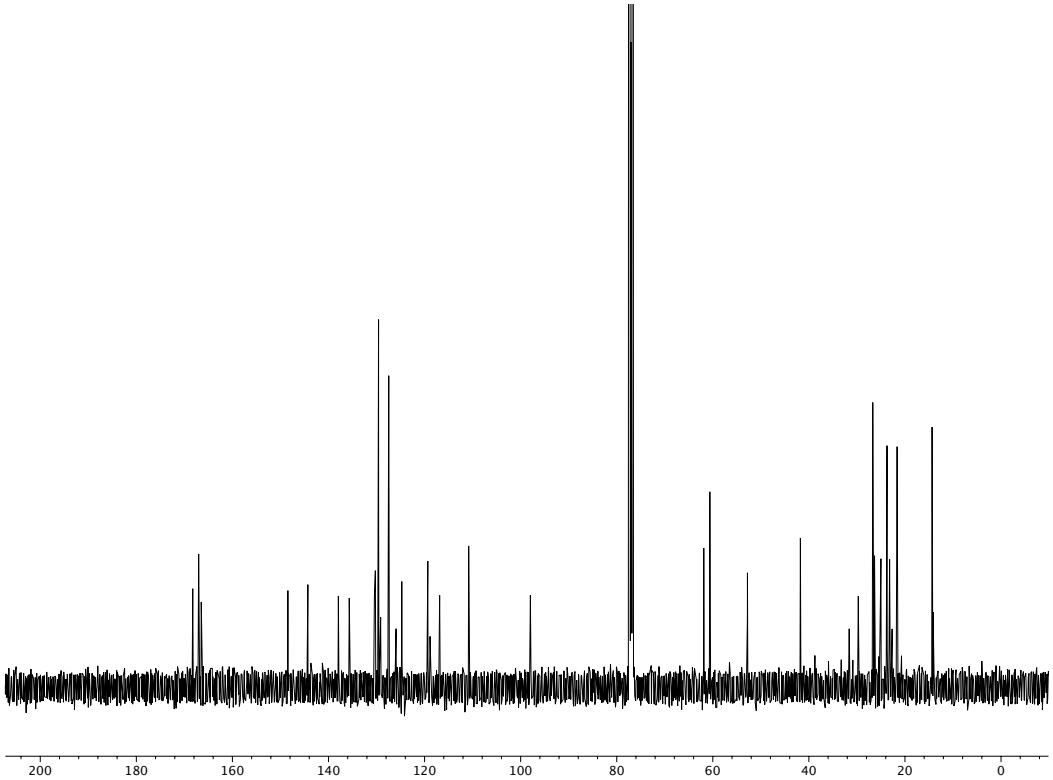


Figure A2.90 ^{13}C NMR (100 MHz, $CDCl_3$) of compound **107**.

Figure A2.91. ^{1}H NMR (400 MHz, $CDCl_3$) of compound **108**.

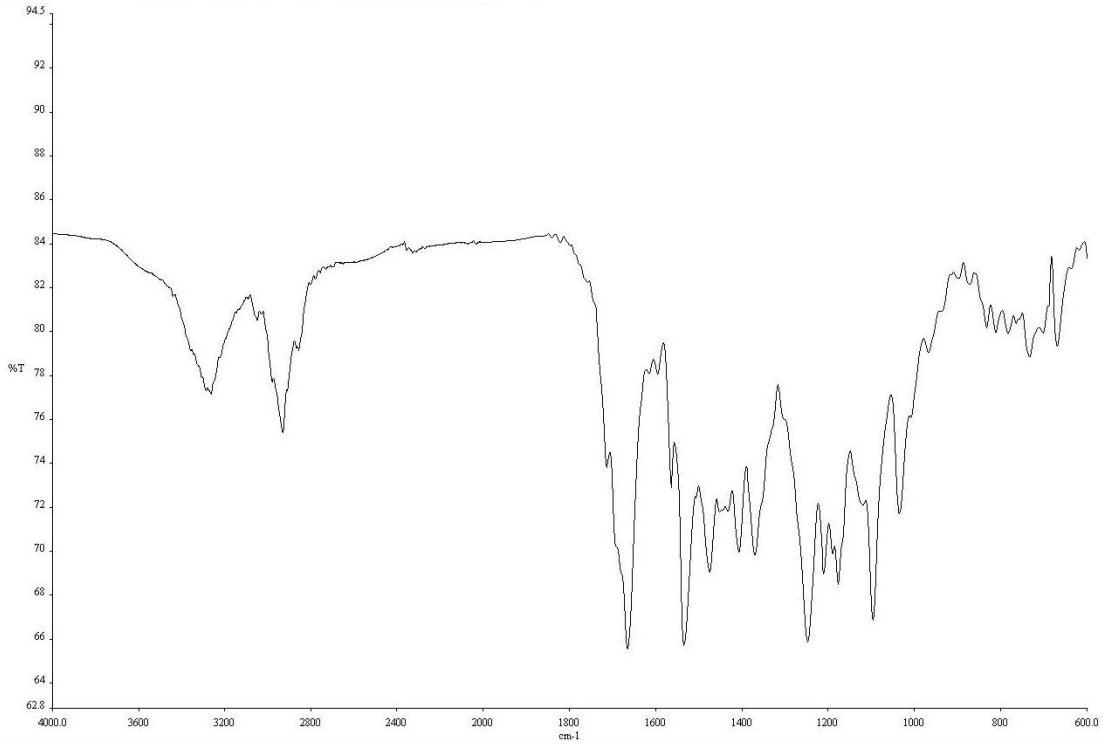


Figure A2.92 Infrared spectrum (Thin Film, NaCl) of compound **108**.

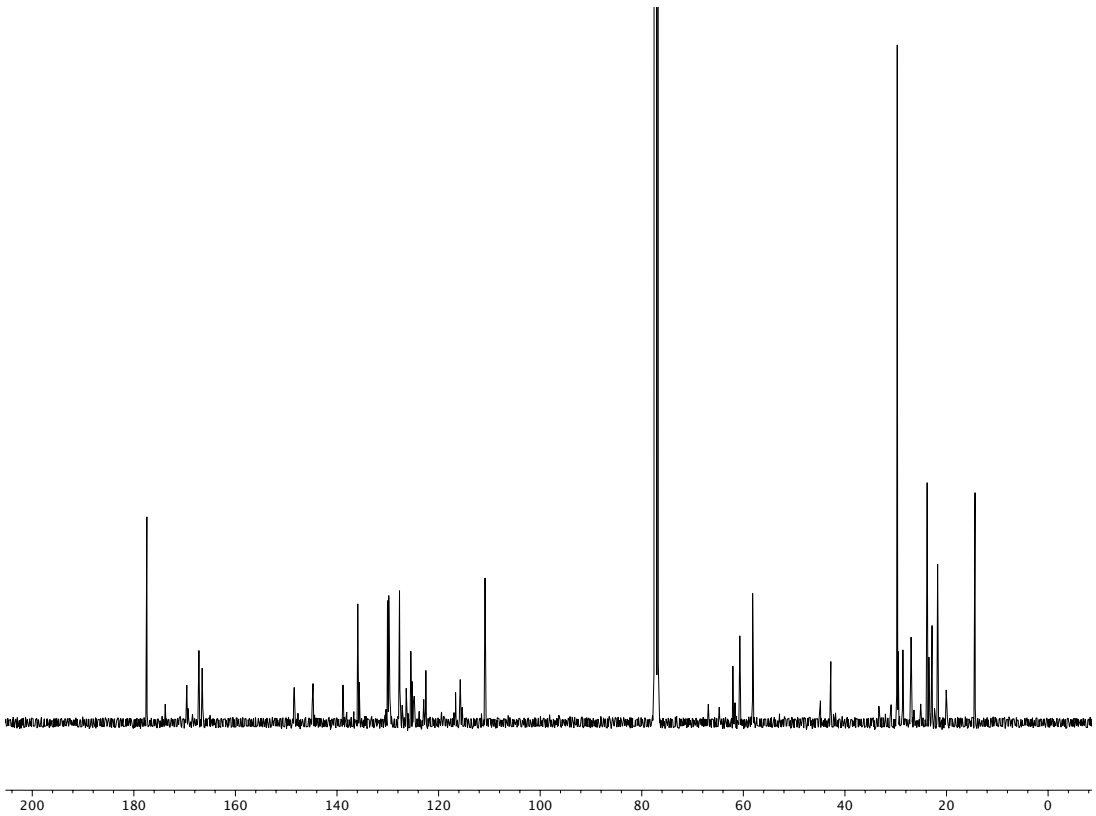


Figure A2.93 ^{13}C NMR (100 MHz, $CDCl_3$) of compound **108**.

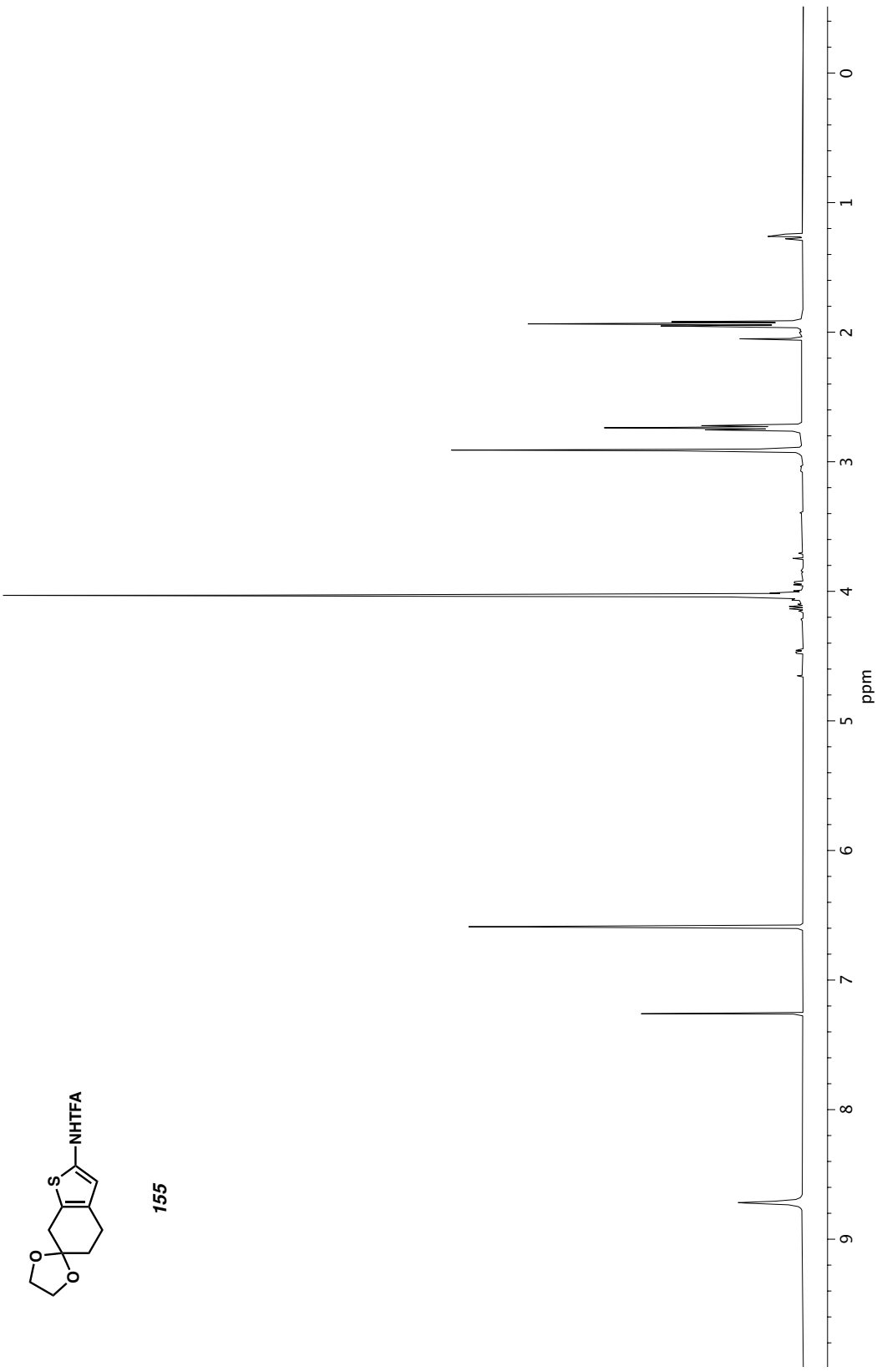


Figure A2.94. ^{1}H NMR (400 MHz, $CDCl_3$) of compound **155**.

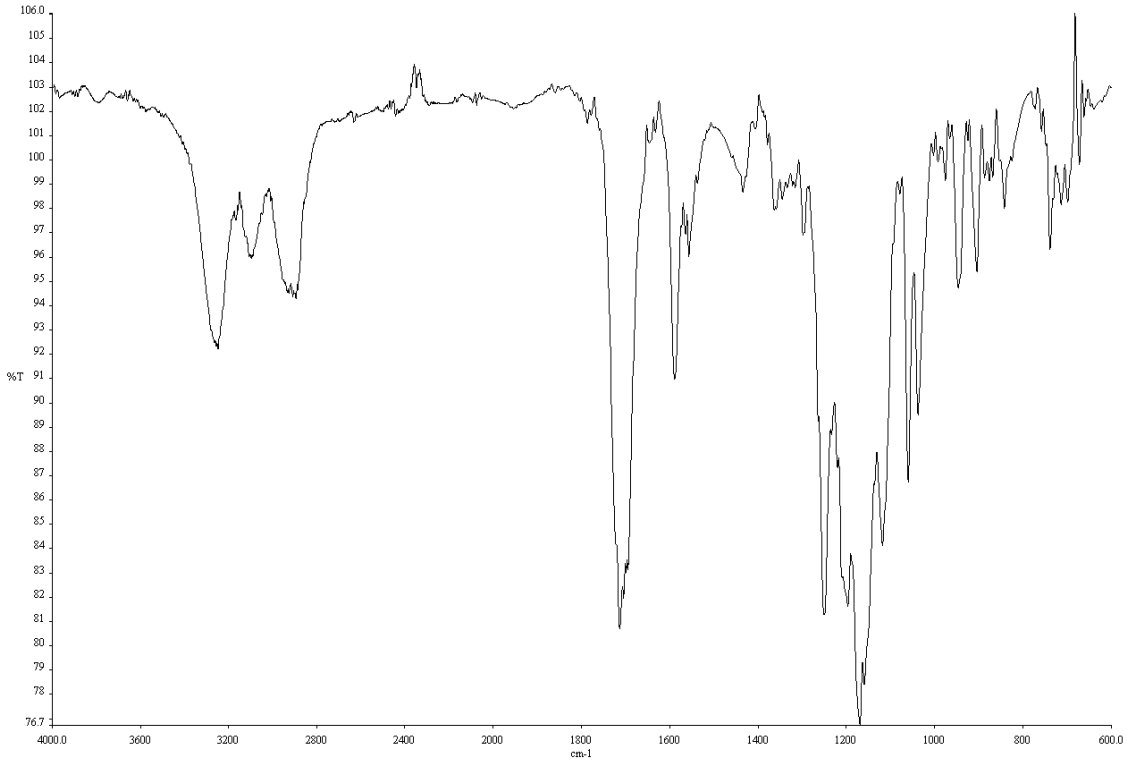


Figure A2.95 Infrared spectrum (Thin Film, NaCl) of compound **155**.

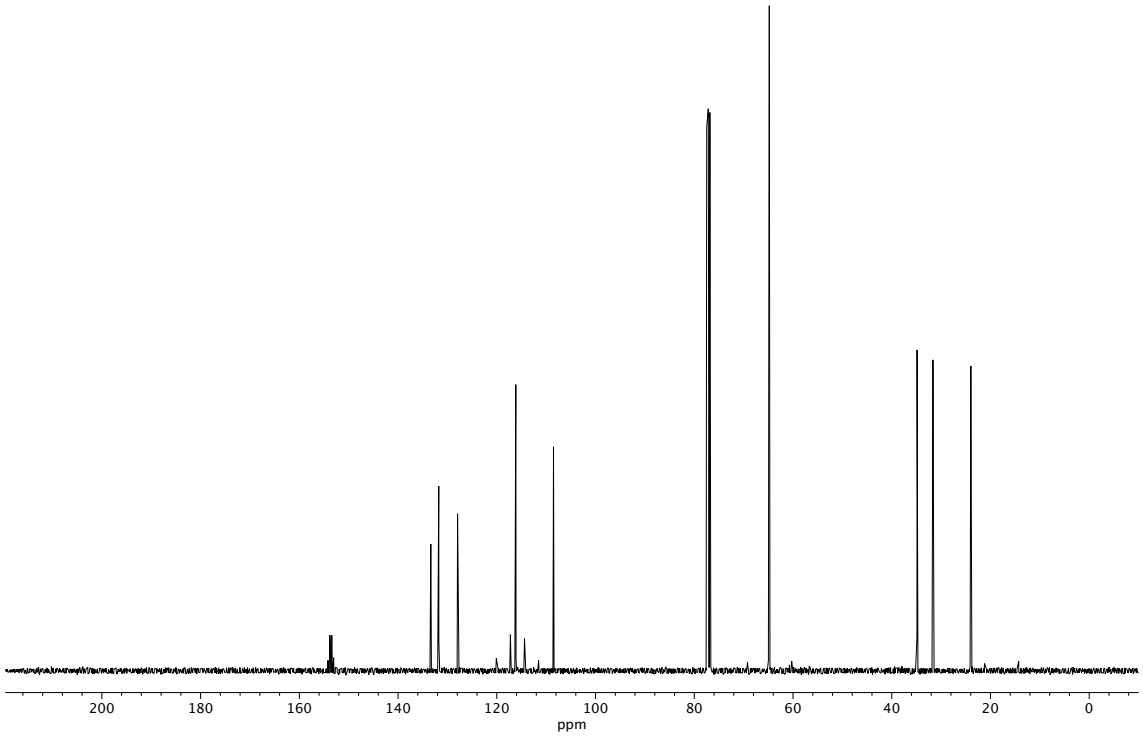


Figure A2.96 ^{13}C NMR (100 MHz, $CDCl_3$) of compound **155**.

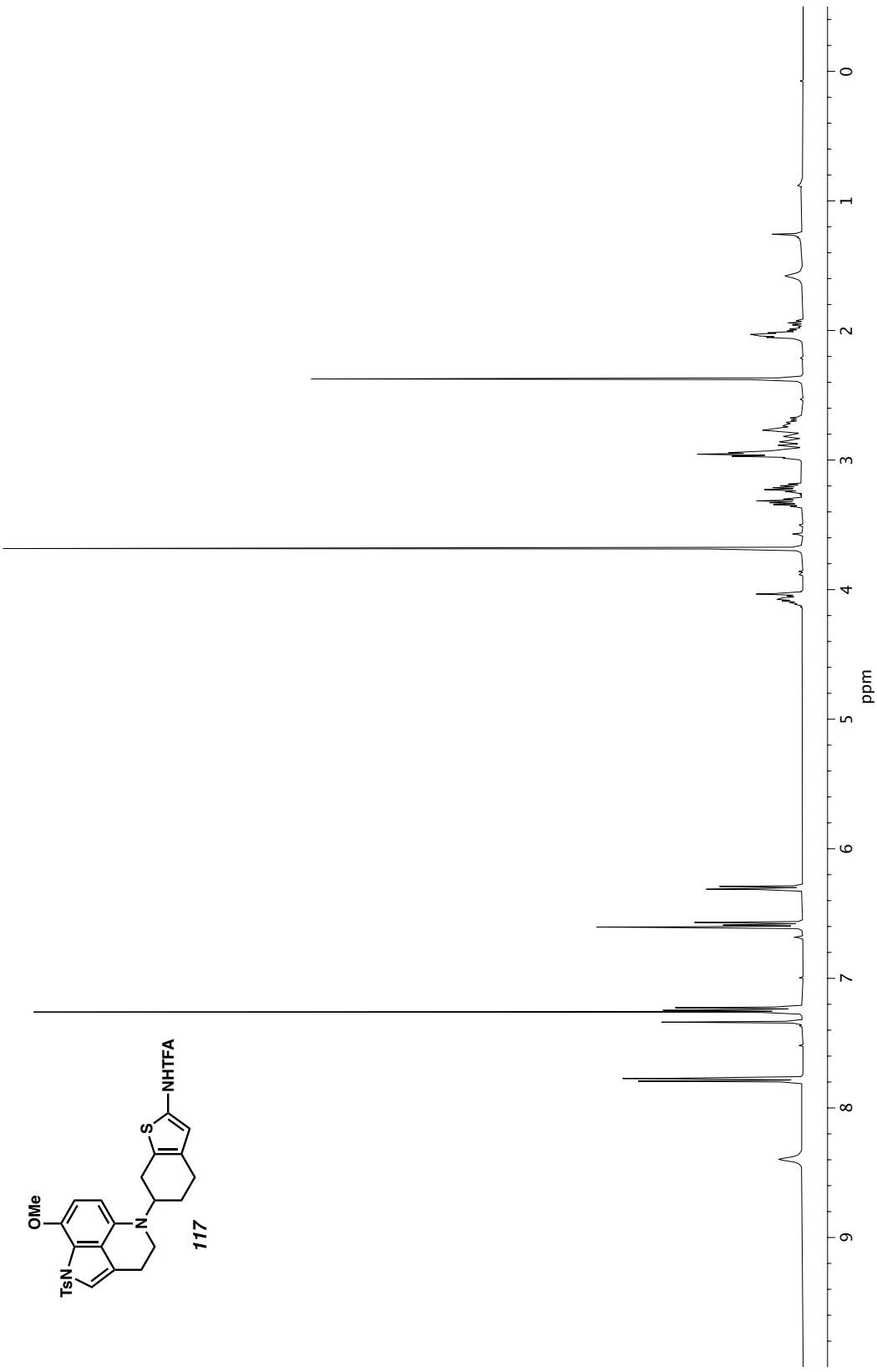


Figure A2.97. ^{1}H NMR (400 MHz, $CDCl_3$) of compound **117**.

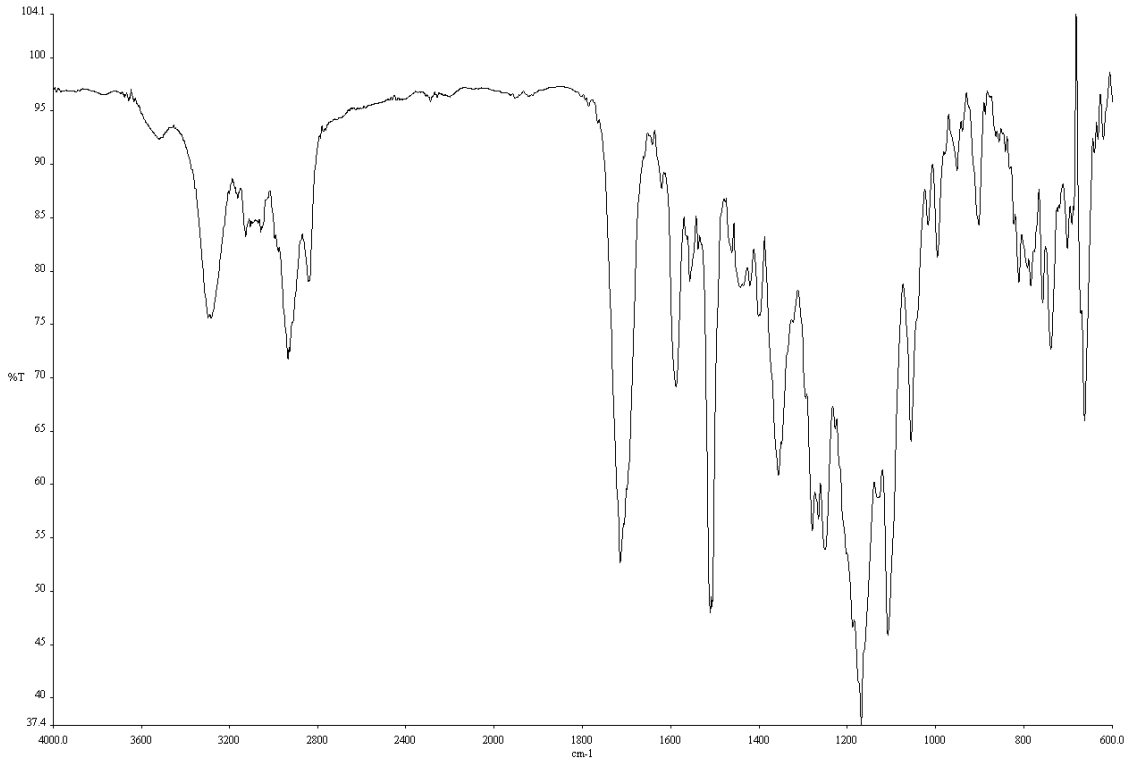


Figure A2.98 Infrared spectrum (Thin Film, NaCl) of compound **117**.

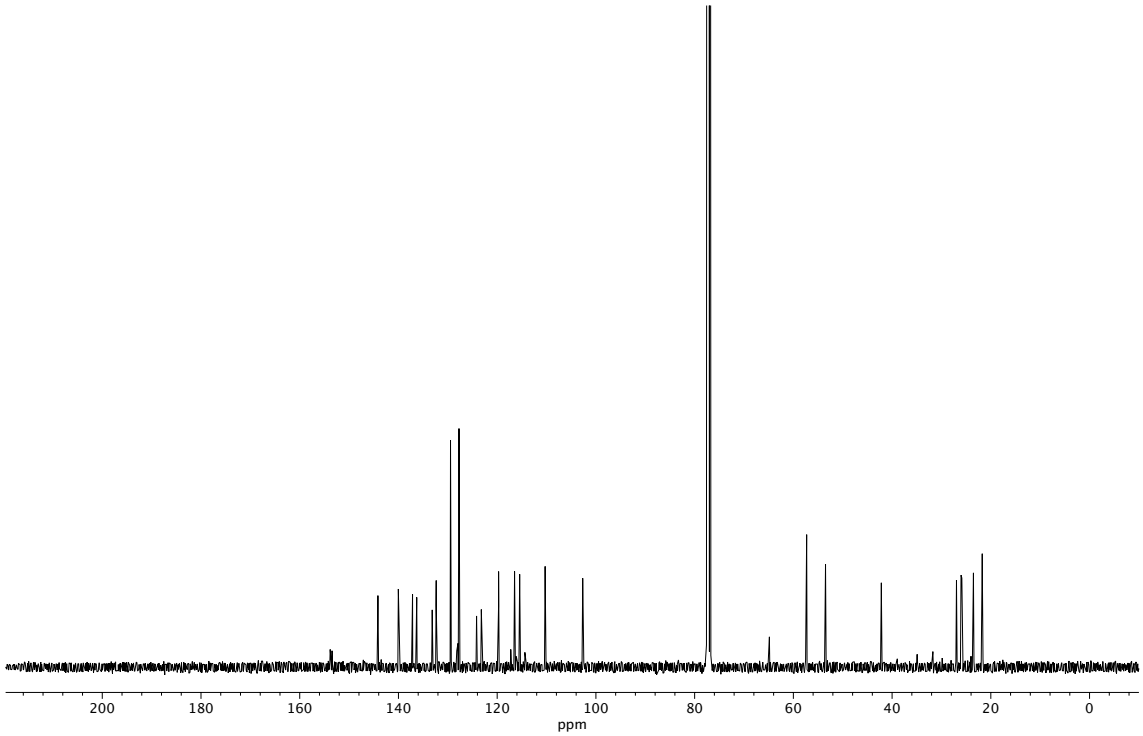


Figure A2.99 ^{13}C NMR (100 MHz, $CDCl_3$) of compound **117**.

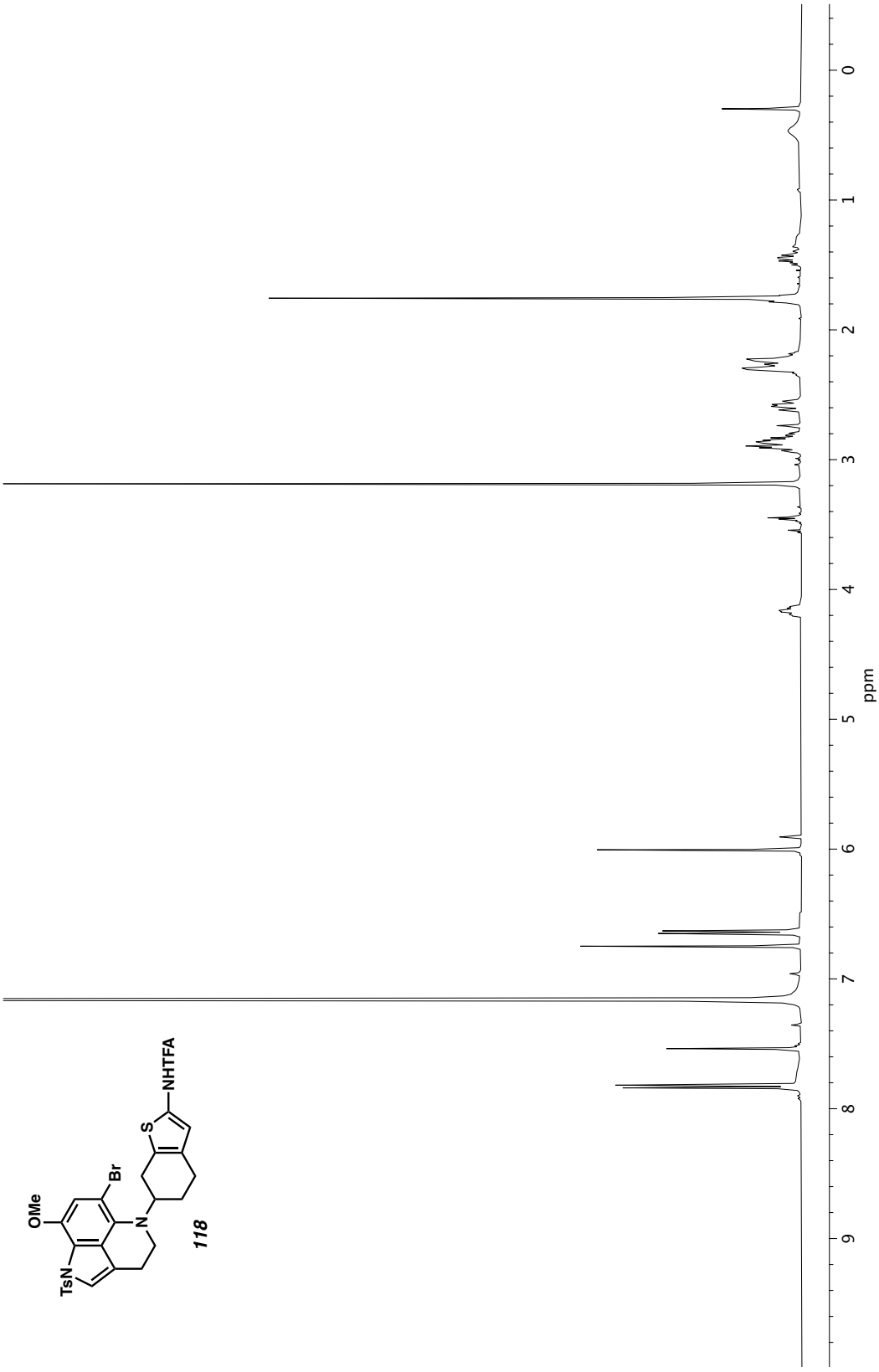


Figure A2.100. ^{1}H NMR (400 MHz, C_6D_6) of compound **118**.

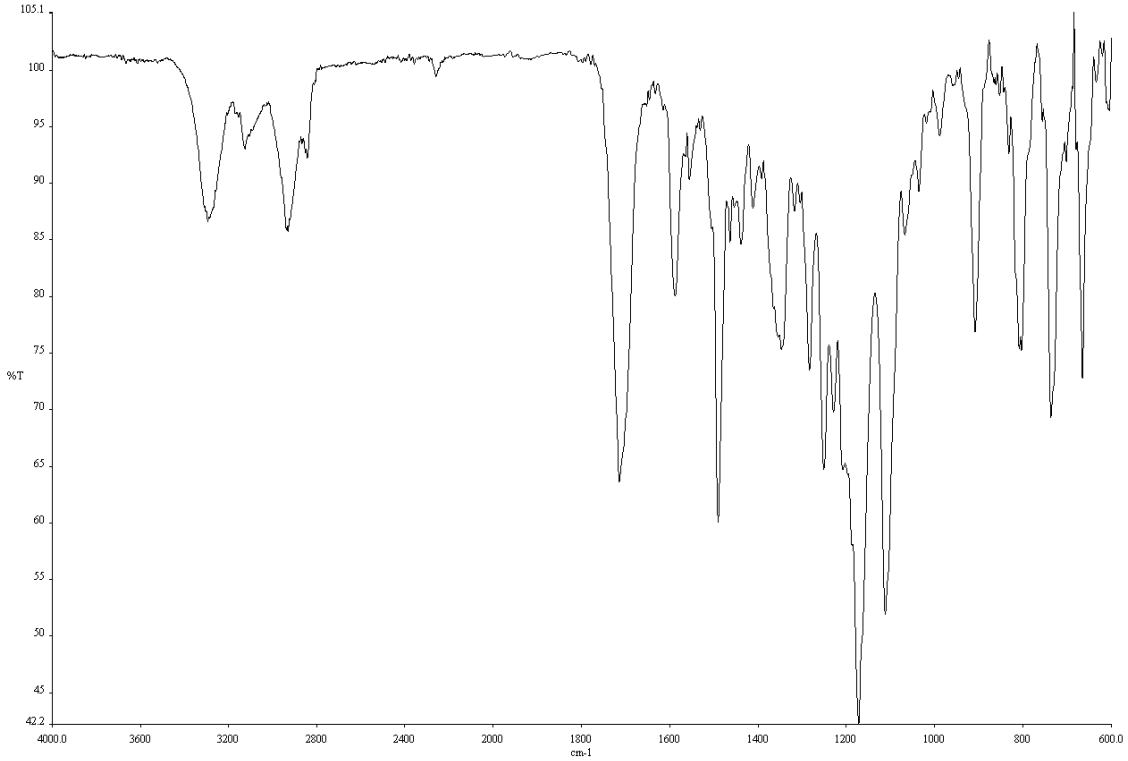


Figure A2.101 Infrared spectrum (Thin Film, NaCl) of compound **118**.

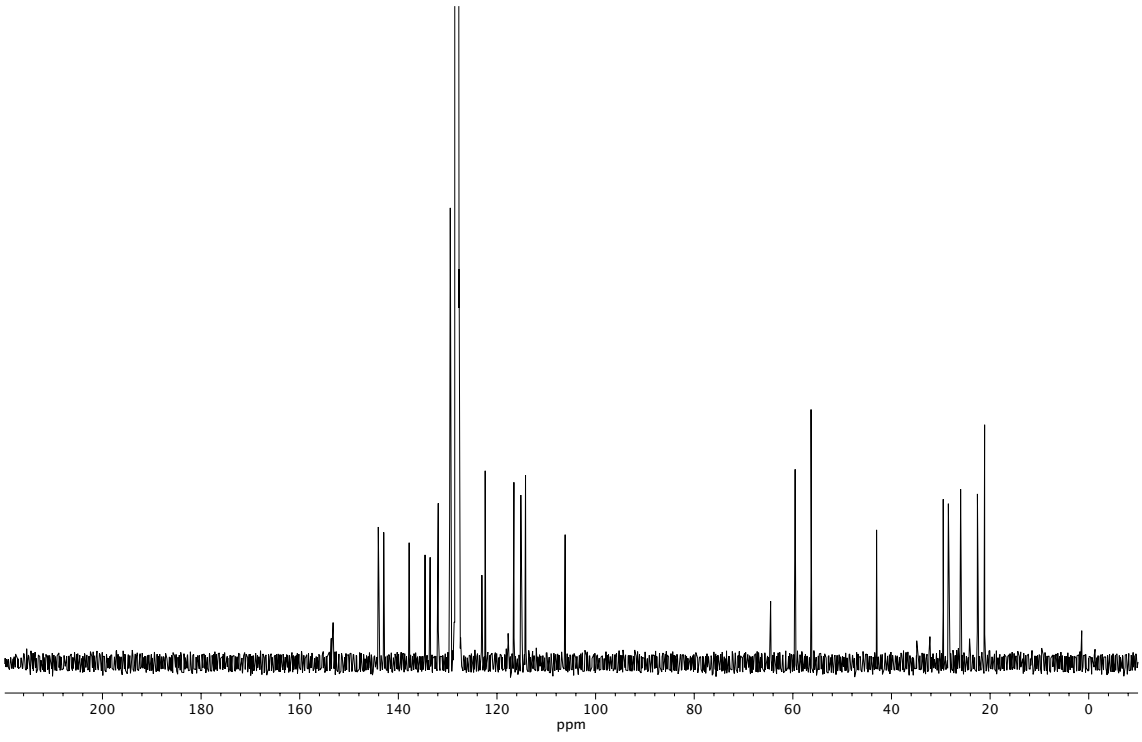


Figure A2.102 ^{13}C NMR (100 MHz, $CDCl_3$) of compound **118**.

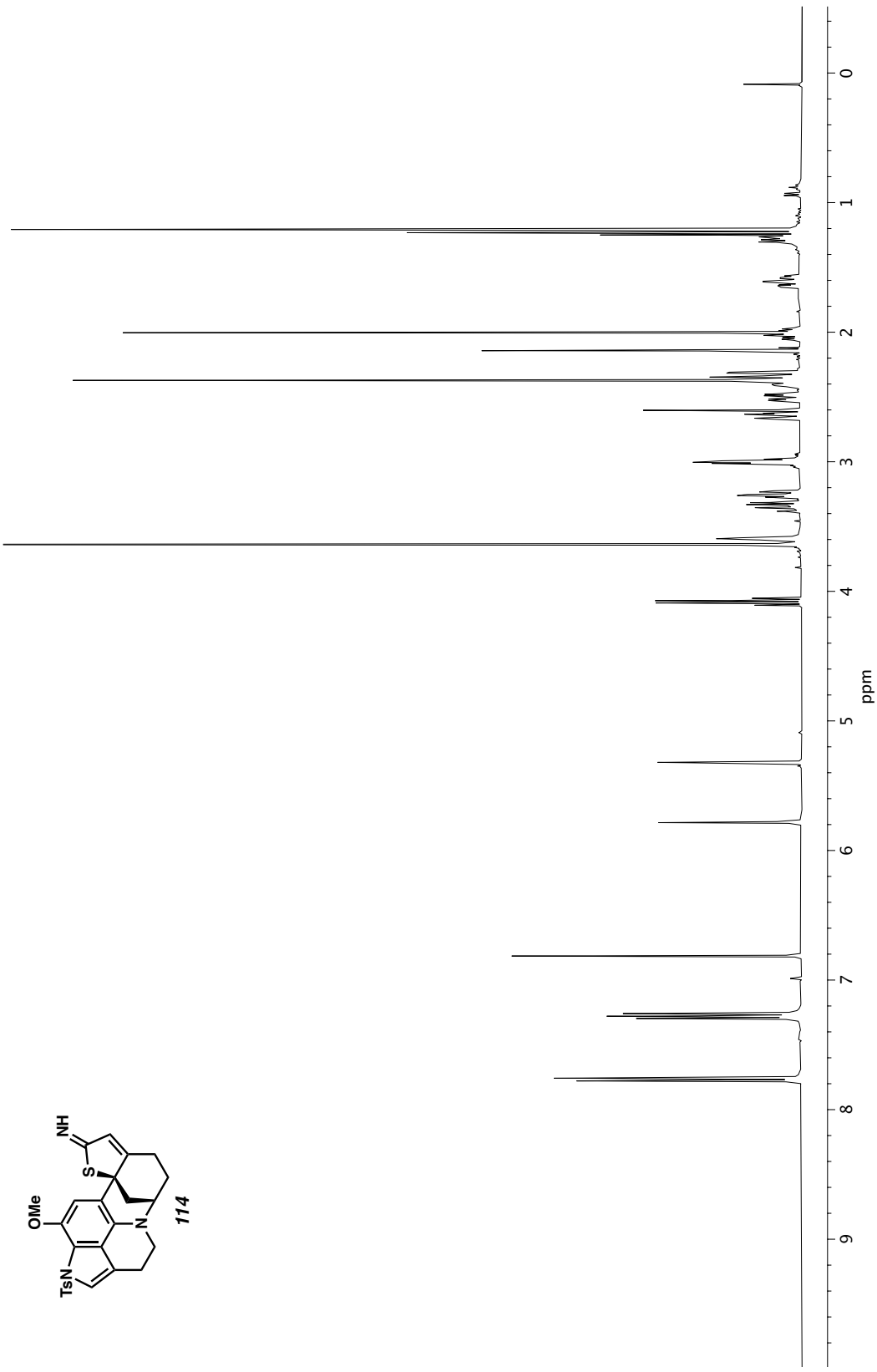


Figure A2.103. ^{1}H NMR (400 MHz, CD_2Cl_2) of compound **114**.

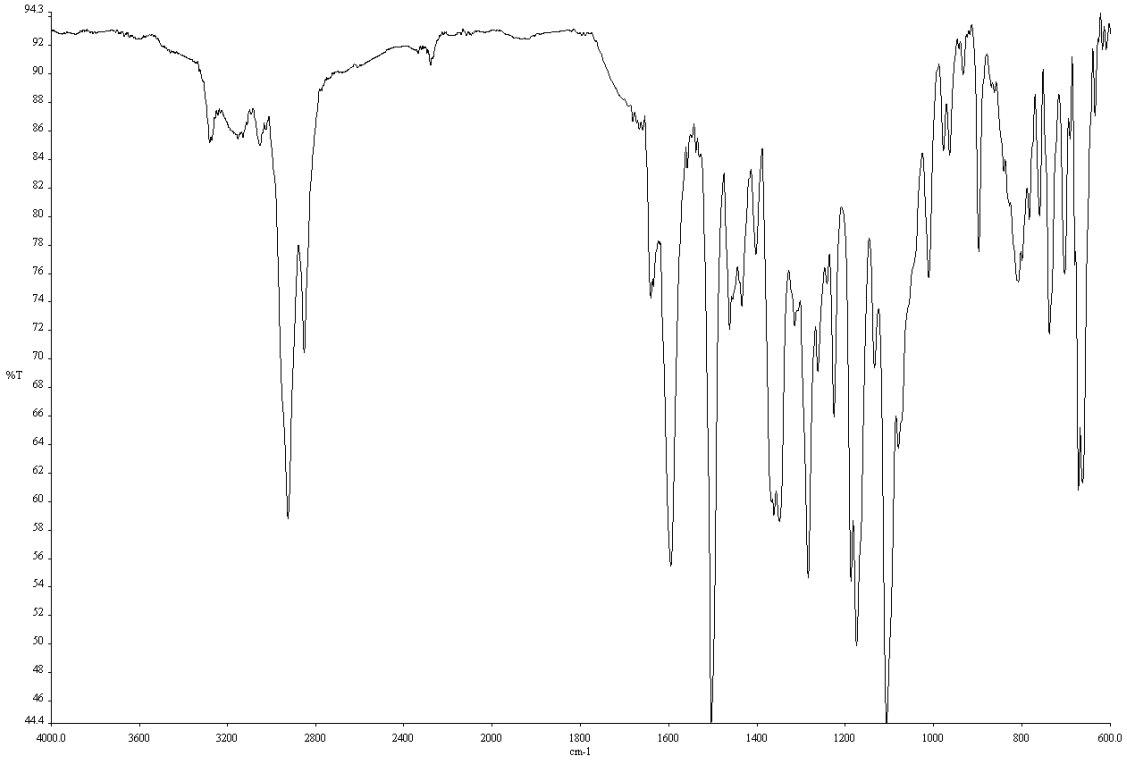


Figure A2.104 Infrared spectrum (Thin Film, NaCl) of compound **114**.

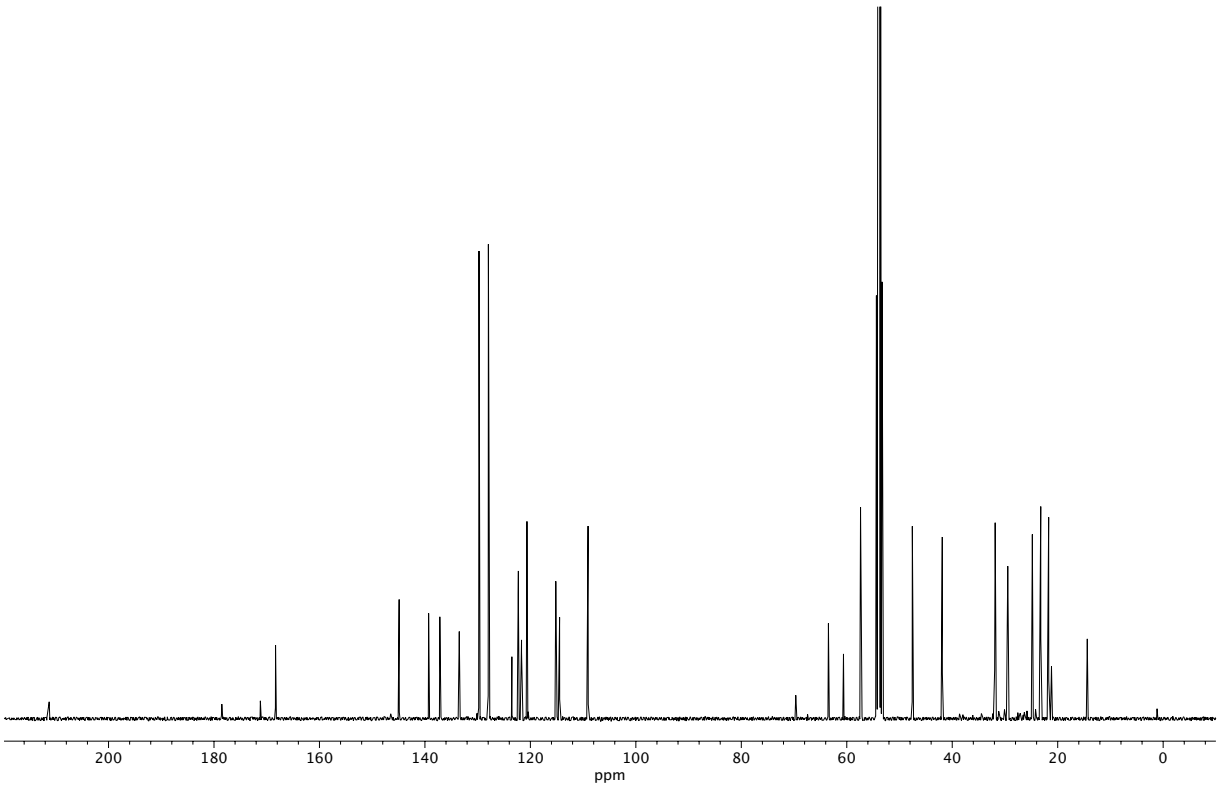


Figure A2.105 ^{13}C NMR (100 MHz, CD_2Cl_2) of compound **114**.

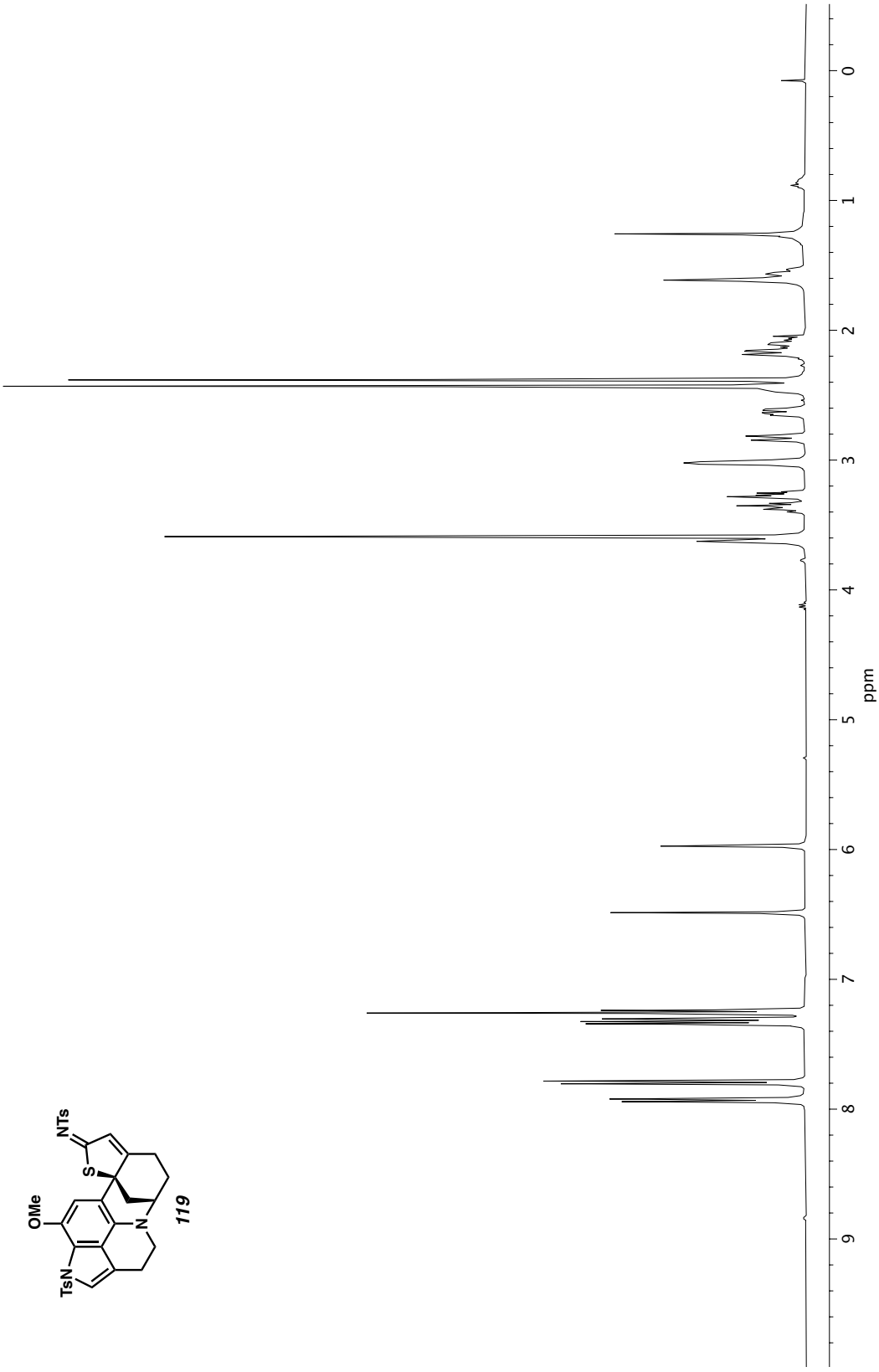


Figure A2.106. ^{1}H NMR (400 MHz, $CDCl_3$) of compound **119**.

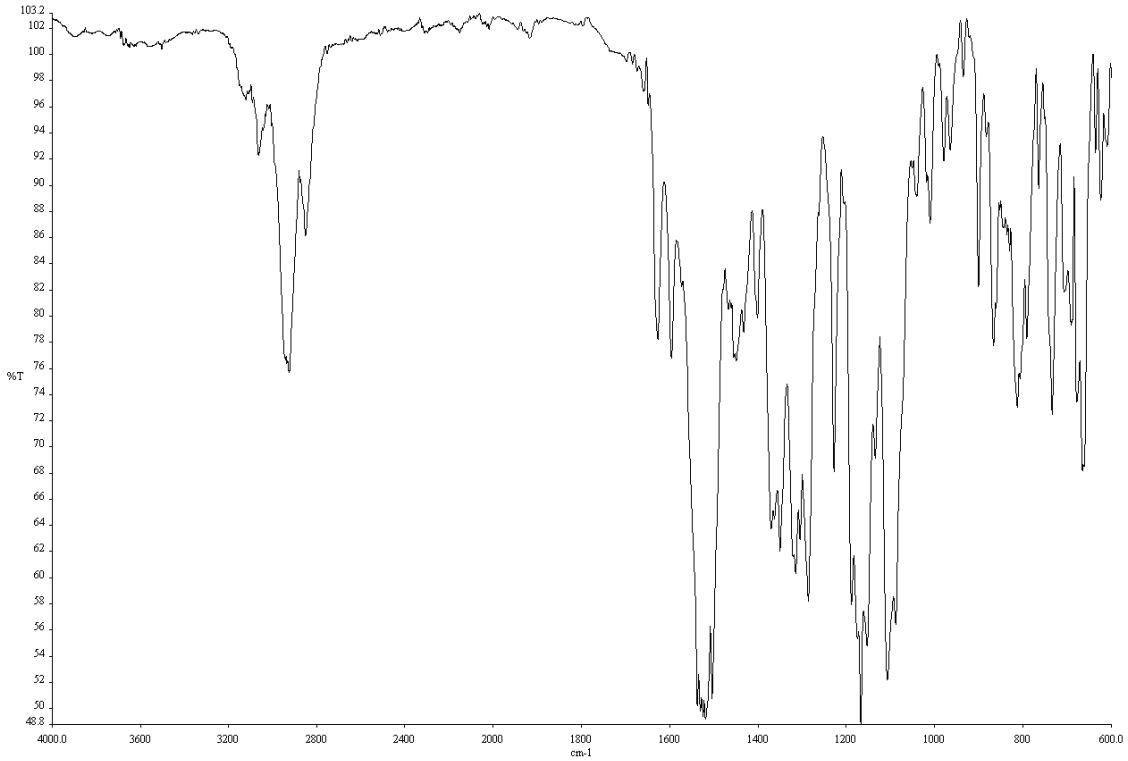


Figure A2.107 Infrared spectrum (Thin Film, NaCl) of compound **119**.

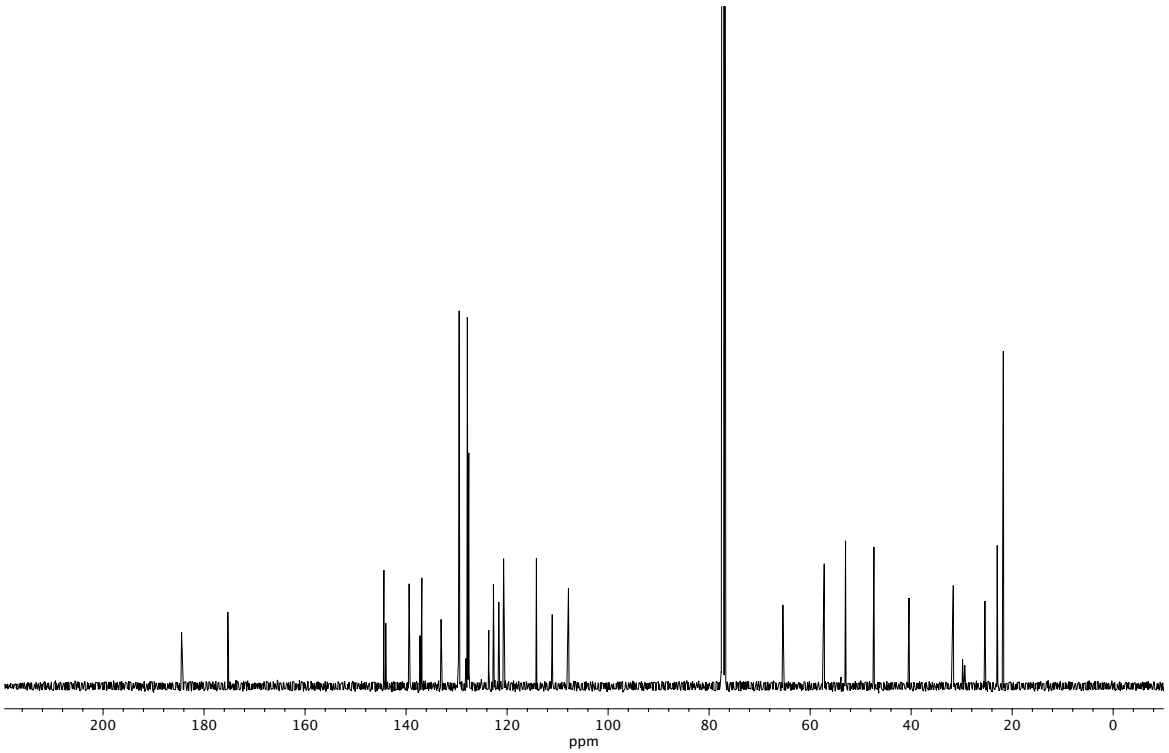


Figure A2.108 ^{13}C NMR (100 MHz, $CDCl_3$) of compound **119**.

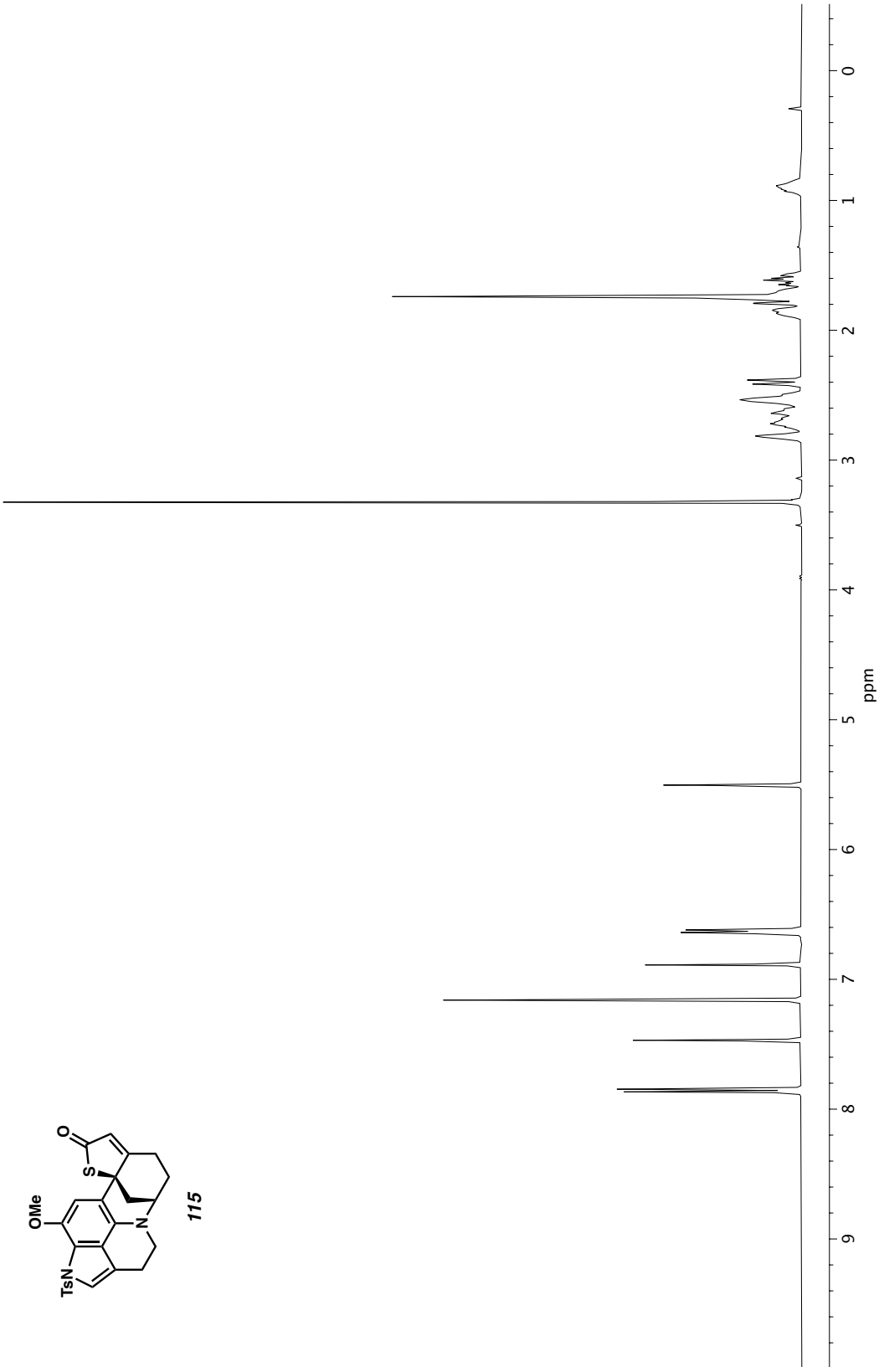


Figure A2.109. ^{1}H NMR (400 MHz, C_6D_6) of compound **115**.

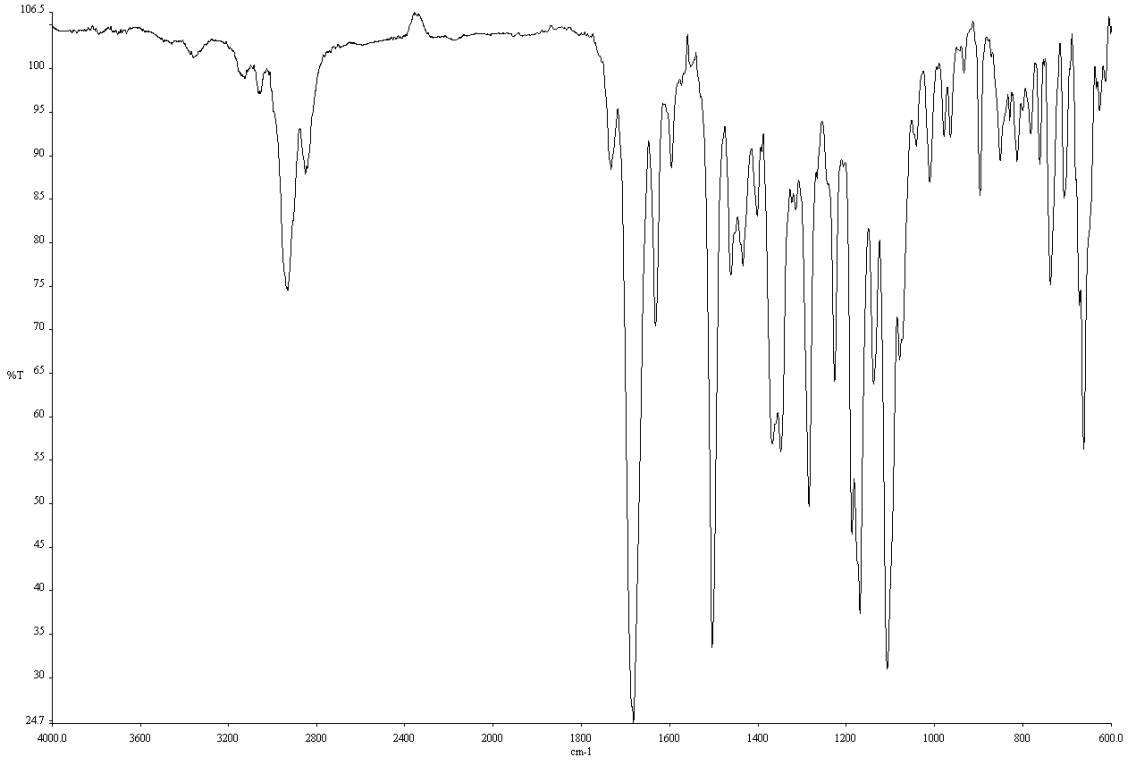


Figure A2.110 Infrared spectrum (Thin Film, NaCl) of compound **115**.

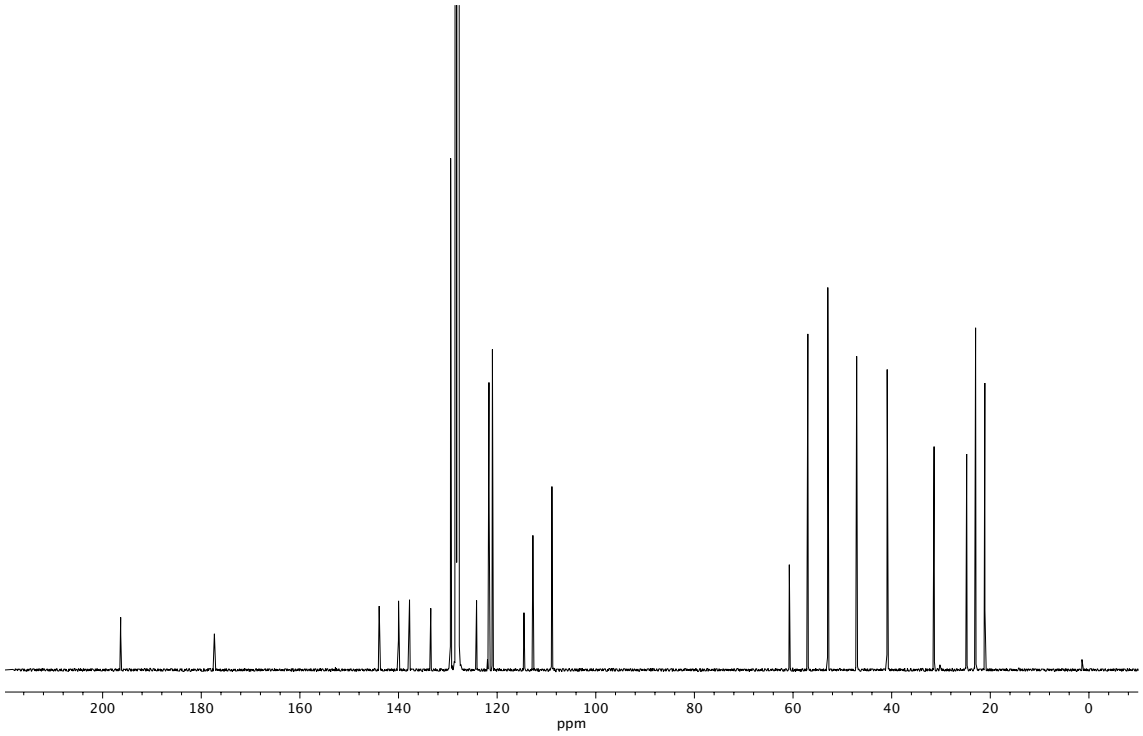


Figure A2.111 ^{13}C NMR (100 MHz, C_6D_6) of compound **115**.

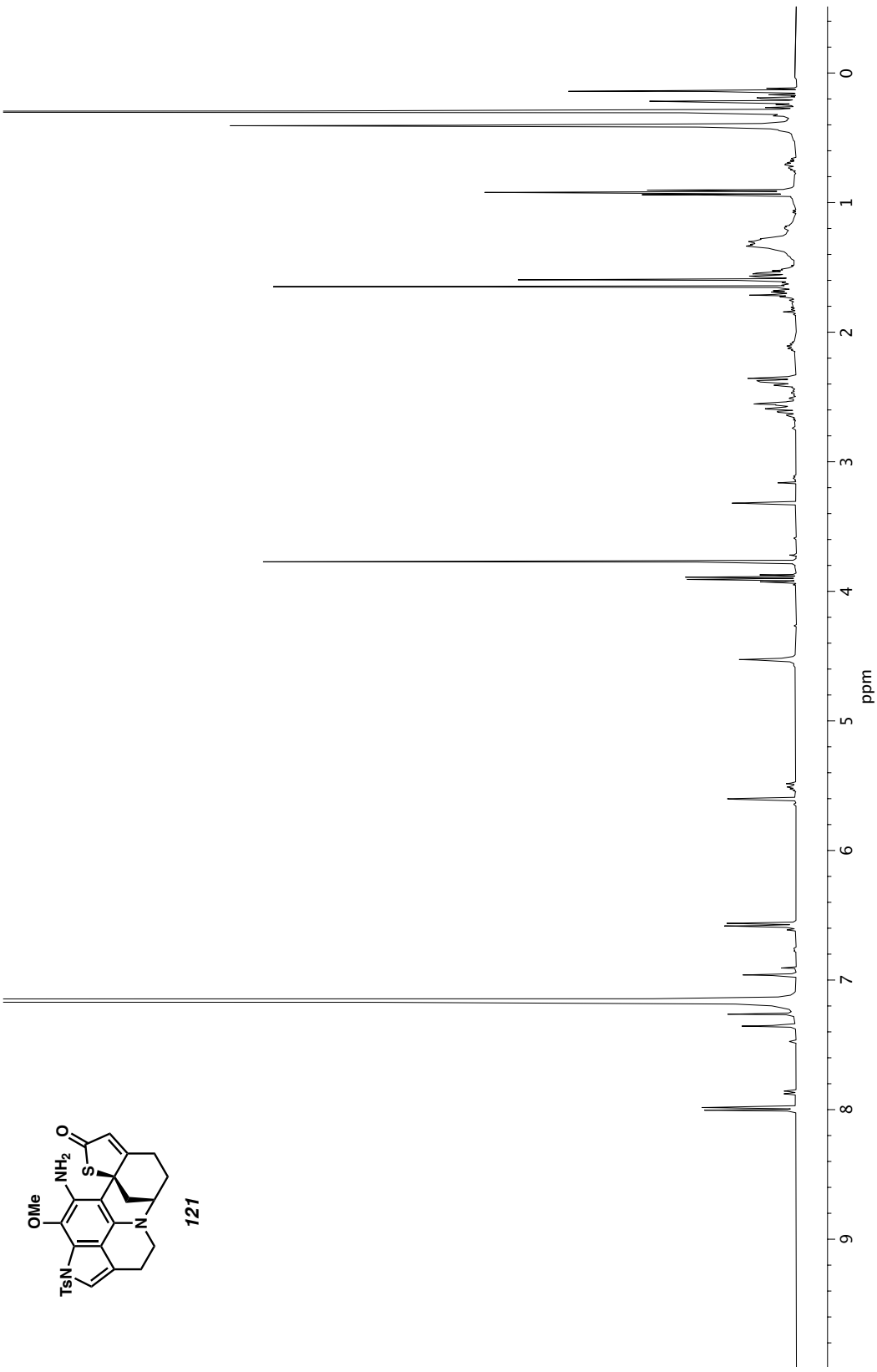


Figure A2.112. ^{1}H NMR (400 MHz, C_6D_6) of compound **121**.

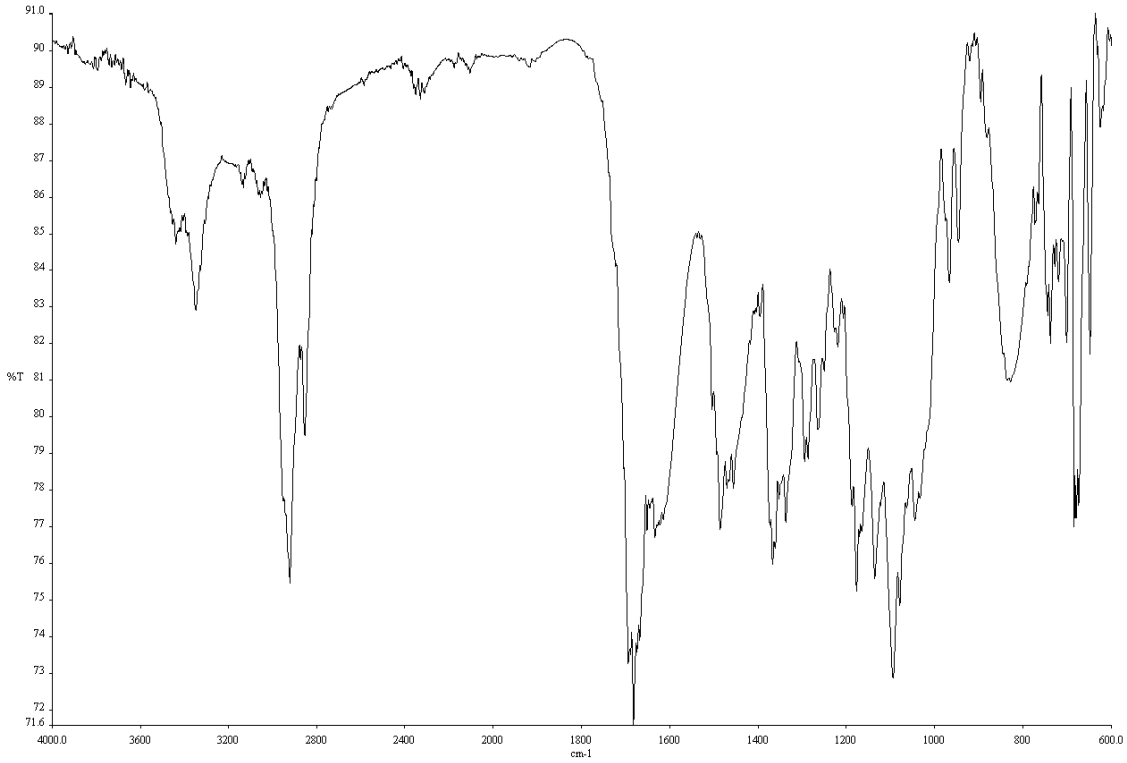


Figure A2.113 Infrared spectrum (Thin Film, NaCl) of compound **121**.

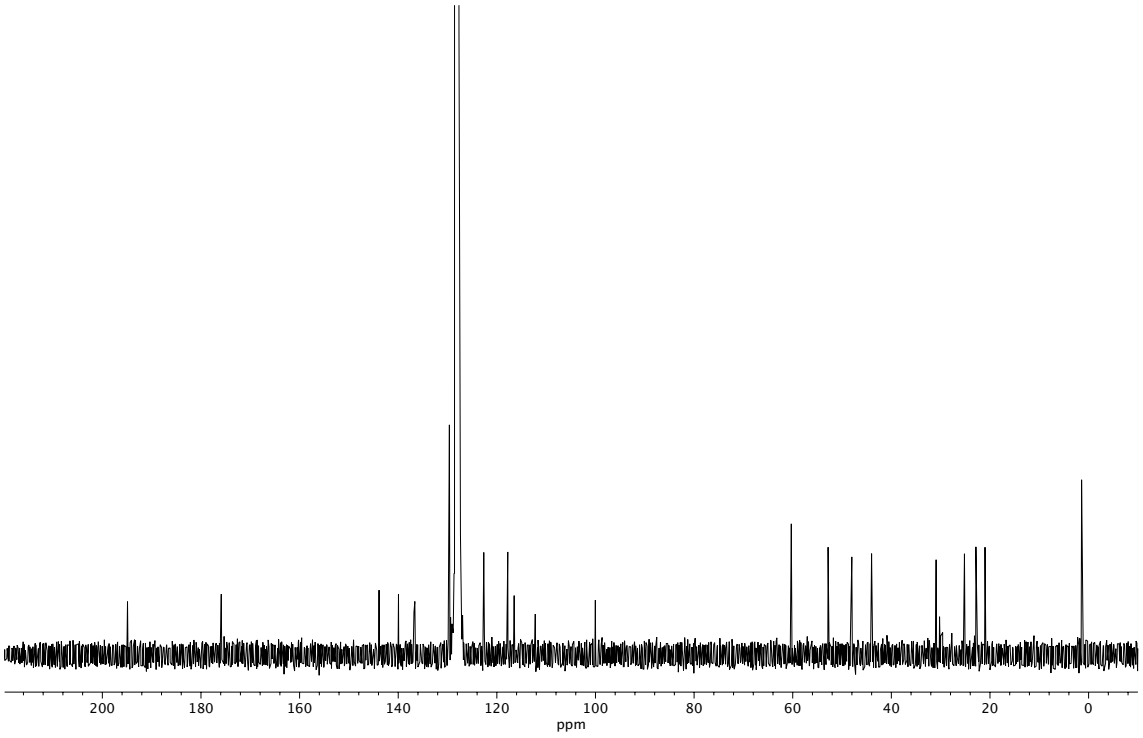


Figure A2.114 ^{13}C NMR (100 MHz, C_6D_6) of compound **121**.

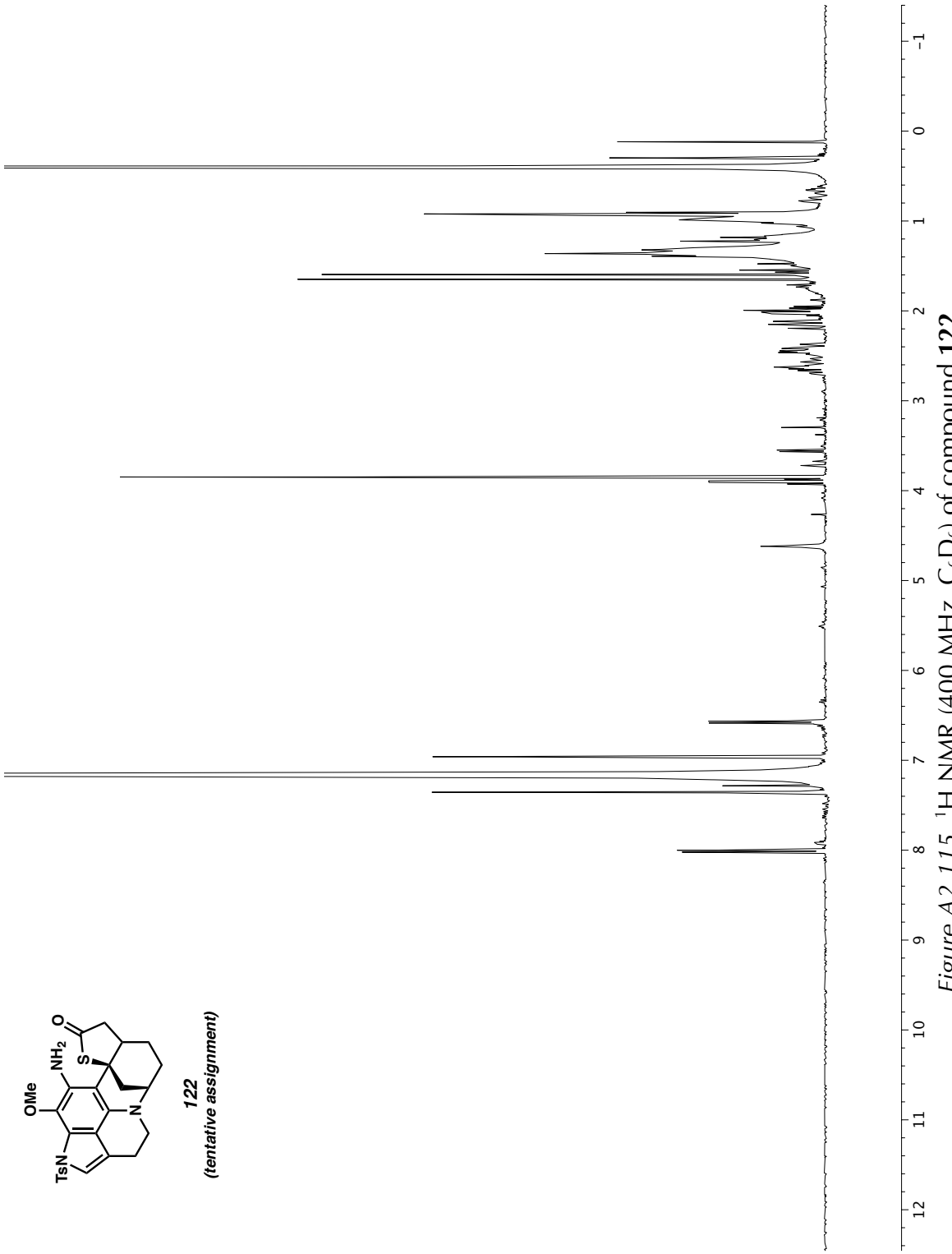


Figure A2.115. ^{1}H NMR (400 MHz, C_6D_6) of compound **122**.

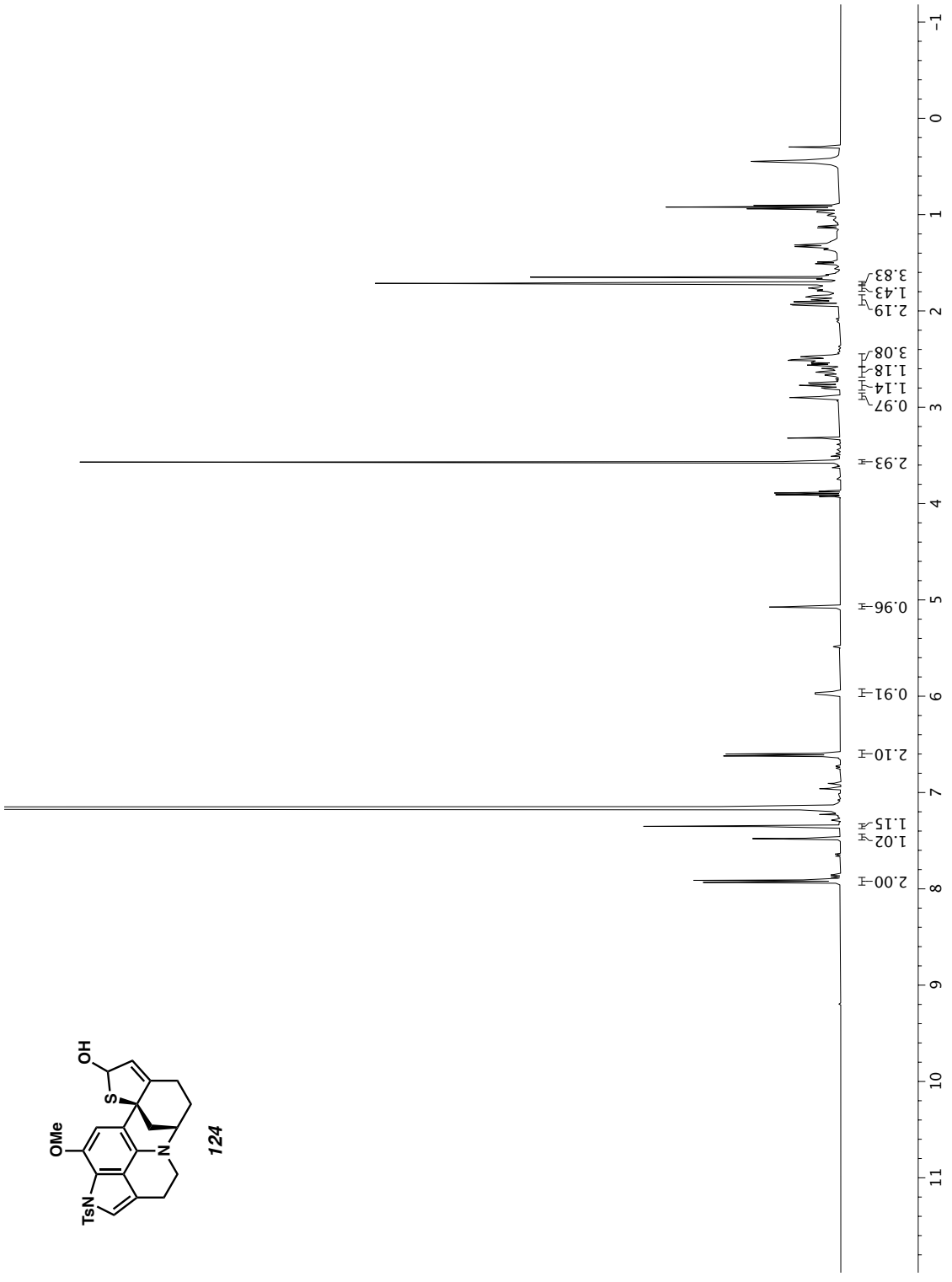


Figure A2.116. ^{1}H NMR (400 MHz, C_6D_6) of compound **124**.

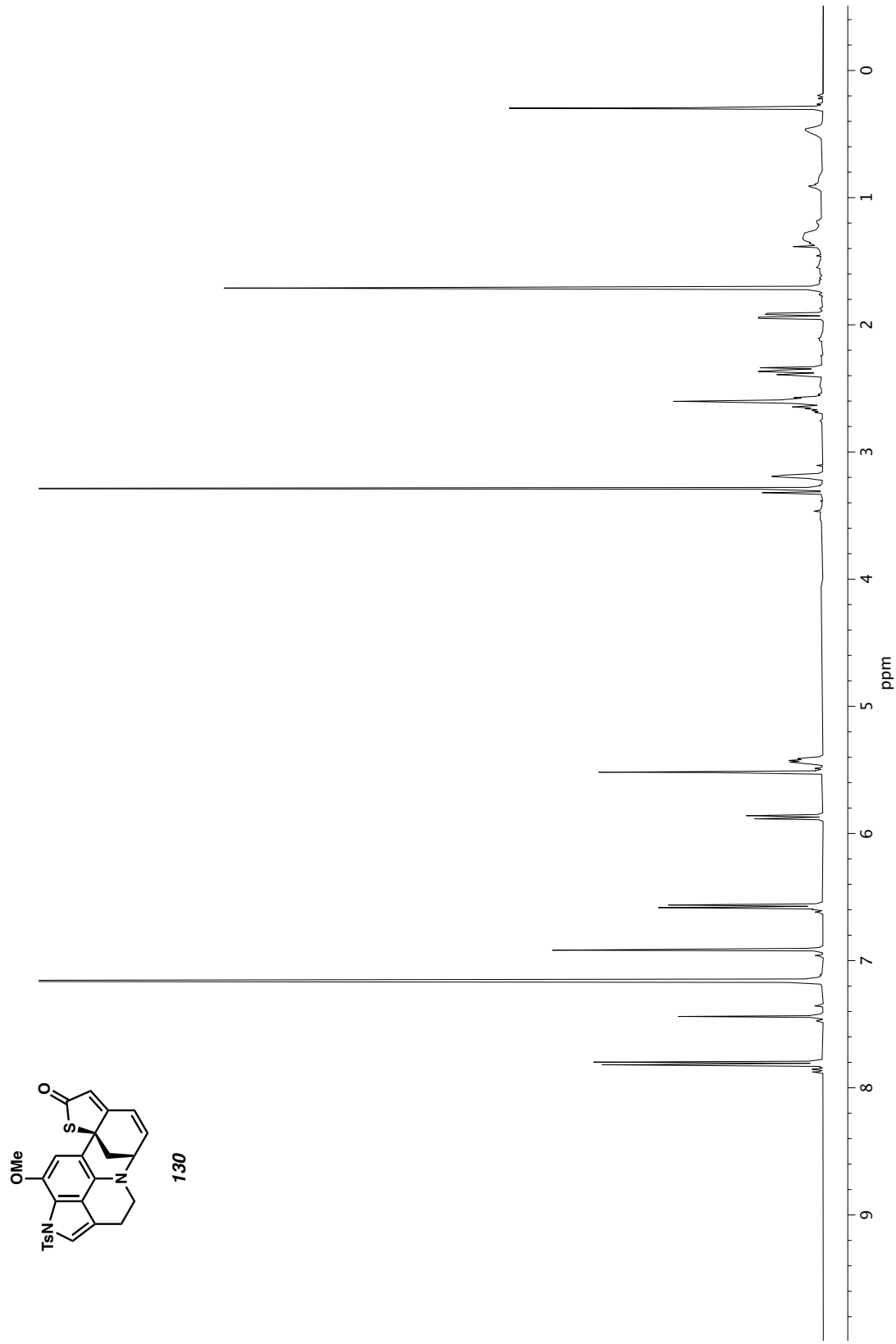


Figure A2.117. ^{1}H NMR (400 MHz, C_6D_6) of compound **130**.

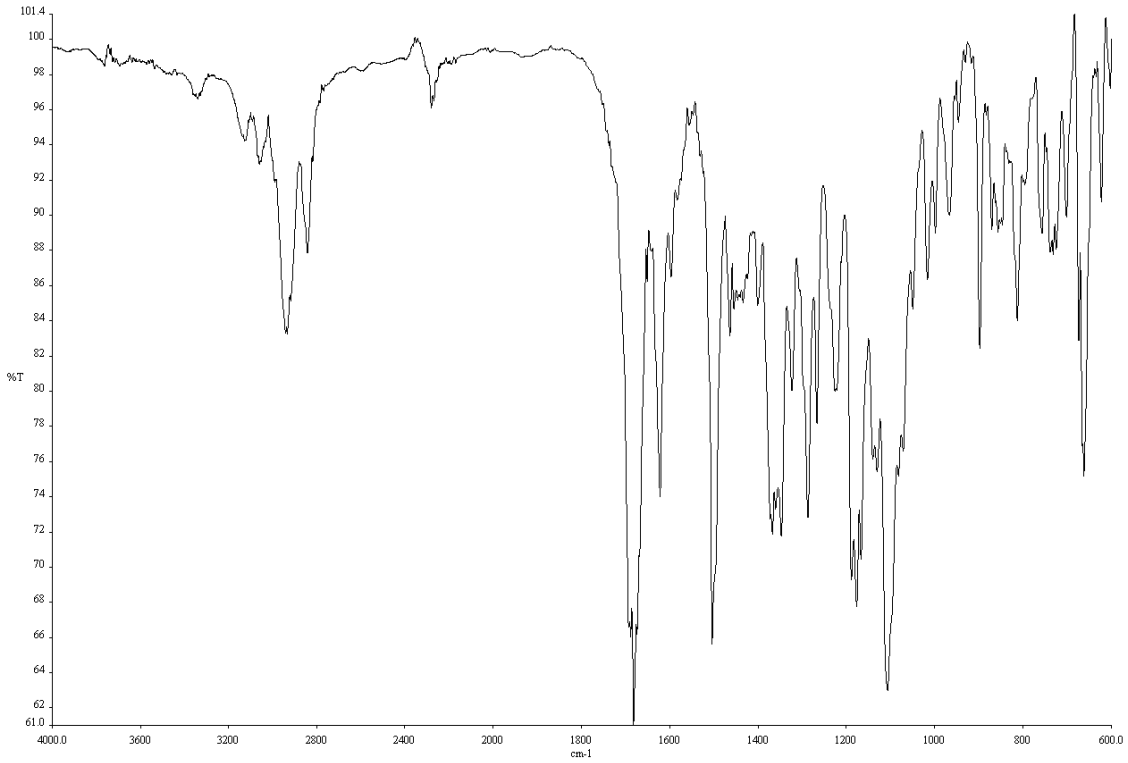


Figure A2.118 Infrared spectrum (Thin Film, NaCl) of compound **130**.

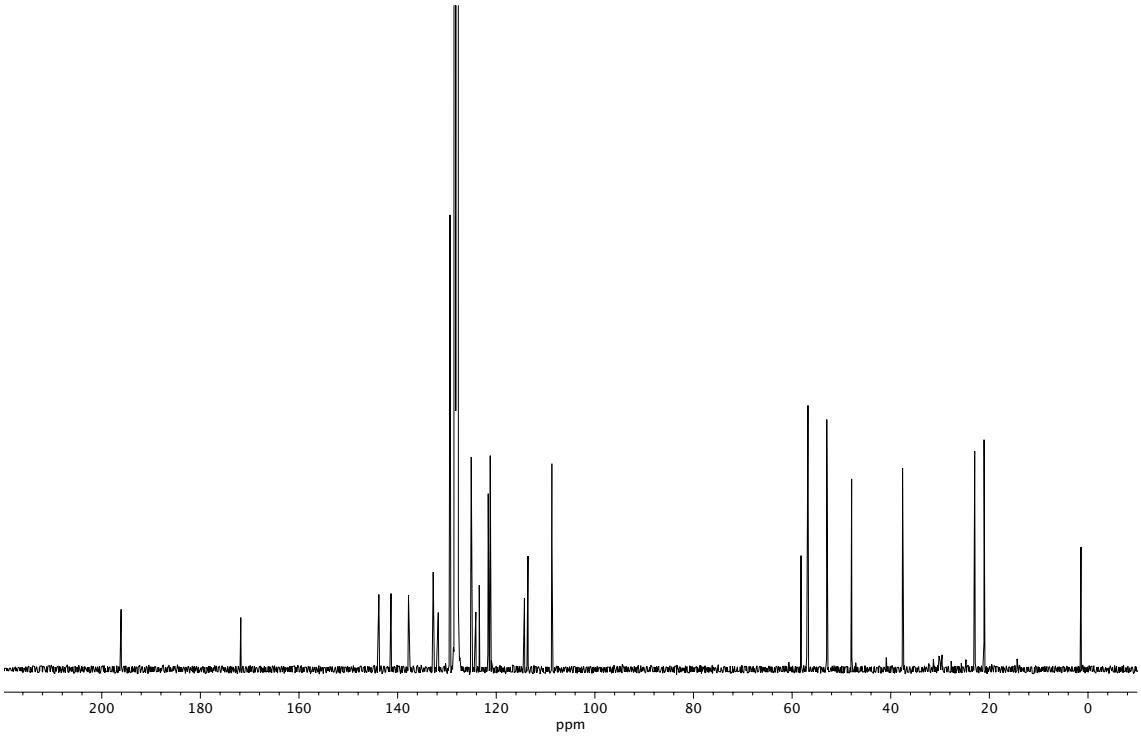


Figure A2.119 ^{13}C NMR (100 MHz, C_6D_6) of compound **130**.

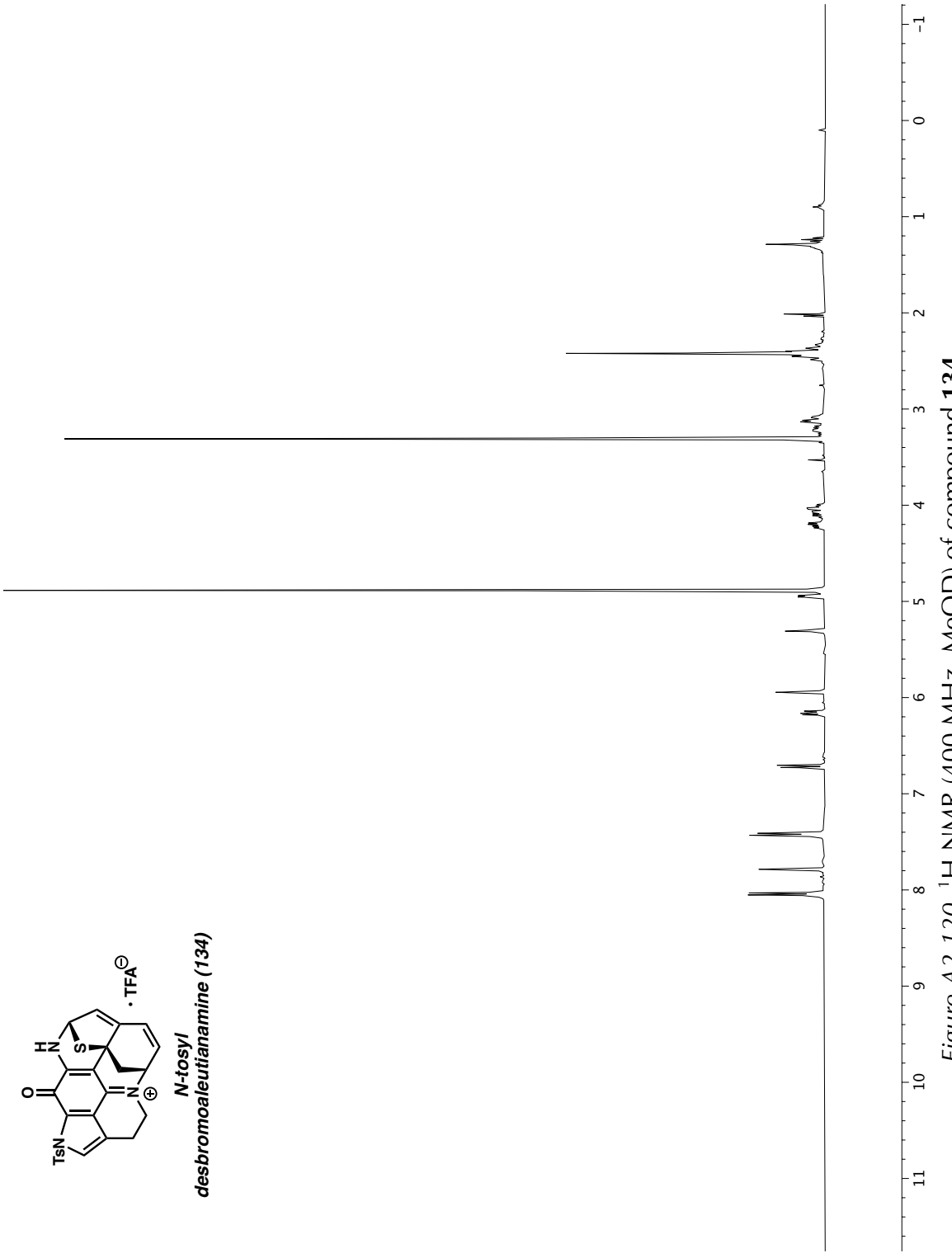


Figure A2.120. ^{1}H NMR (400 MHz, MeOD) of compound **134**.

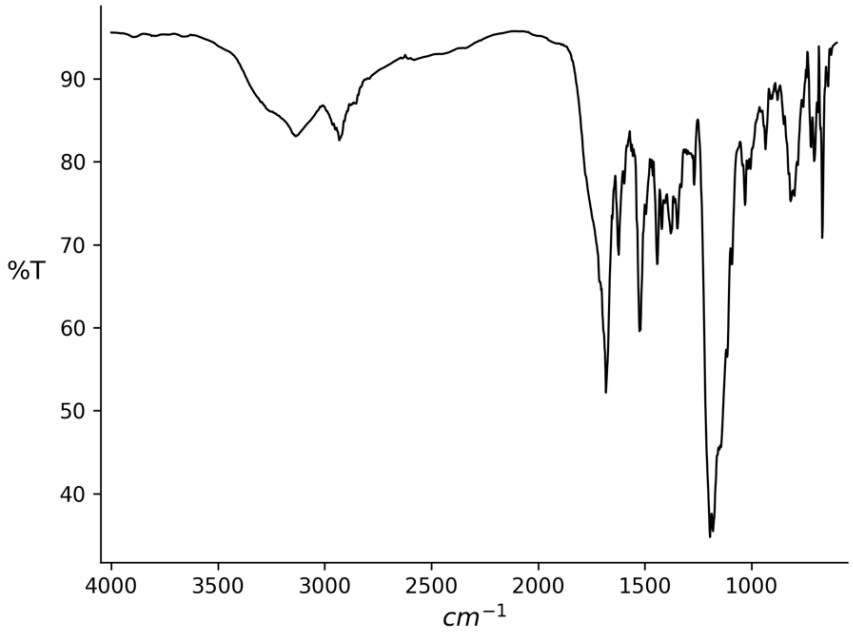


Figure A2.121 Infrared spectrum (Thin Film, NaCl) of compound **134**.

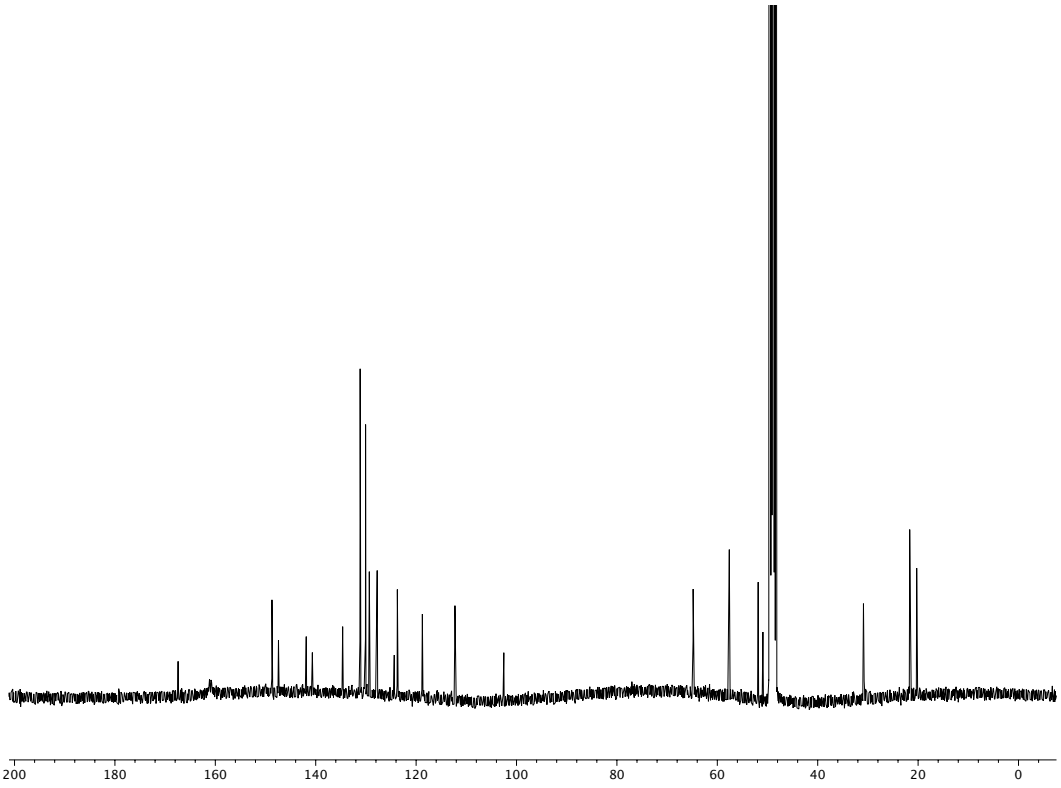


Figure A2.122 ^{13}C NMR (100 MHz, MeOD) of compound **134**.

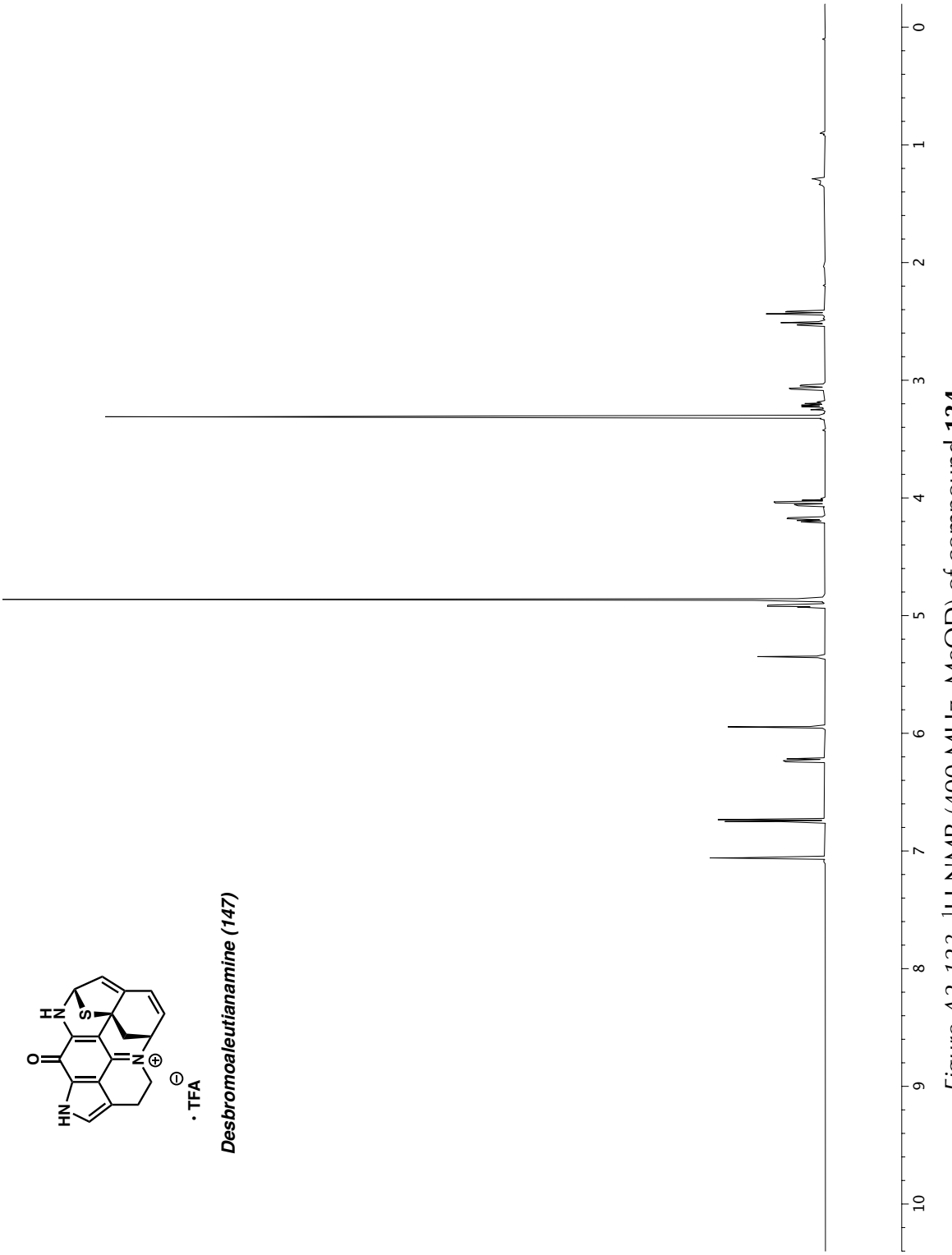


Figure A2.123. ^{1}H NMR (400 MHz, MeOD) of compound **134**.

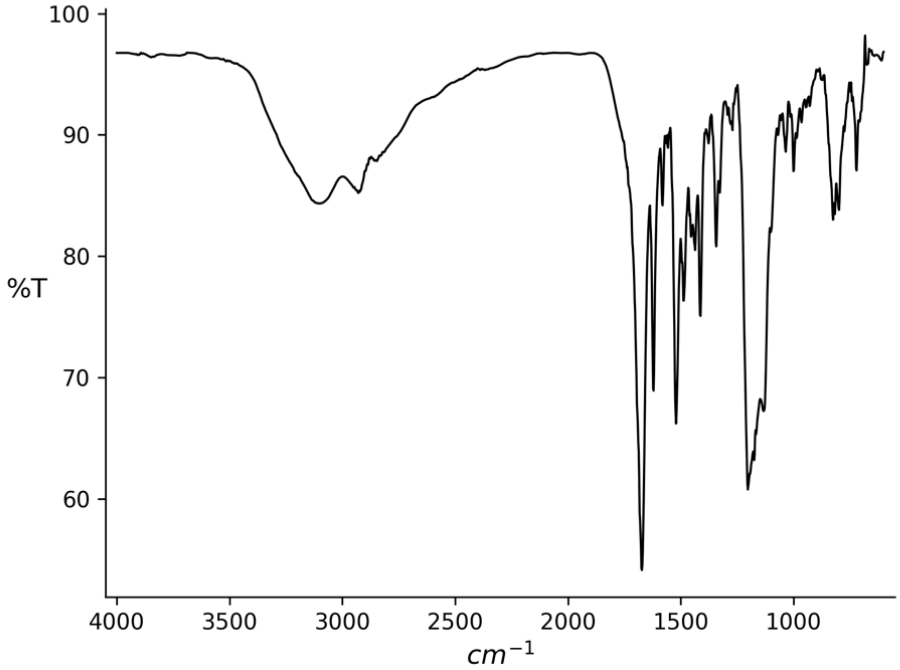


Figure A2.124 Infrared spectrum (Thin Film, NaCl) of compound **147**.

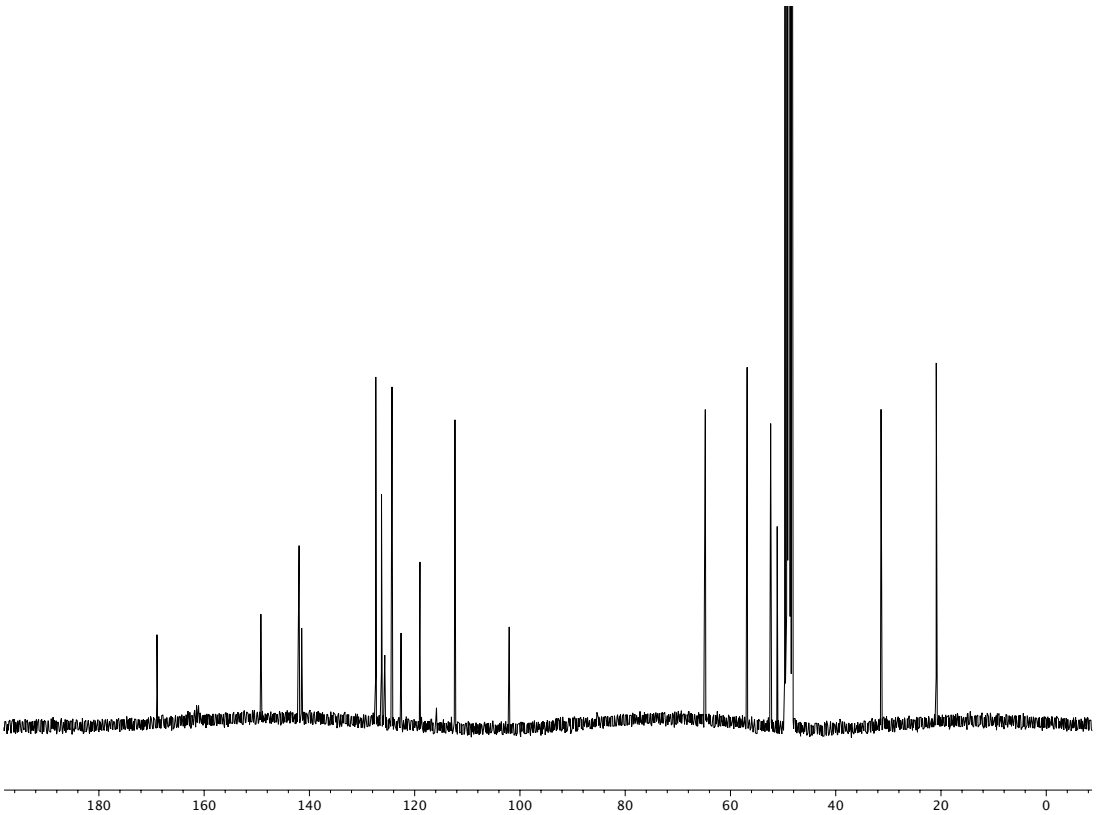


Figure A2.125 ^{13}C NMR (100 MHz, MeOD) of compound **147**.

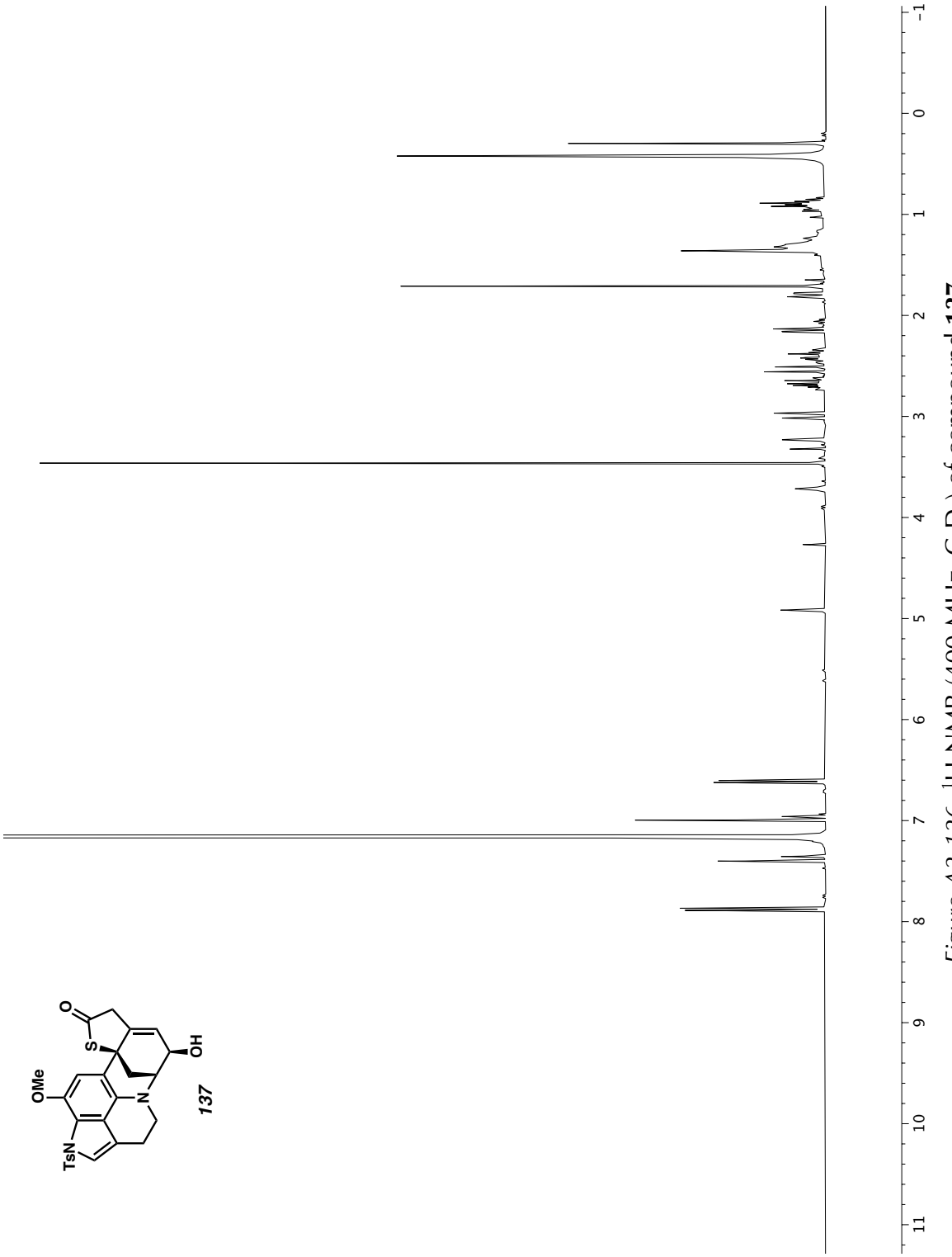


Figure A2.126. ^{1}H NMR (400 MHz, C_6D_6) of compound **137**.

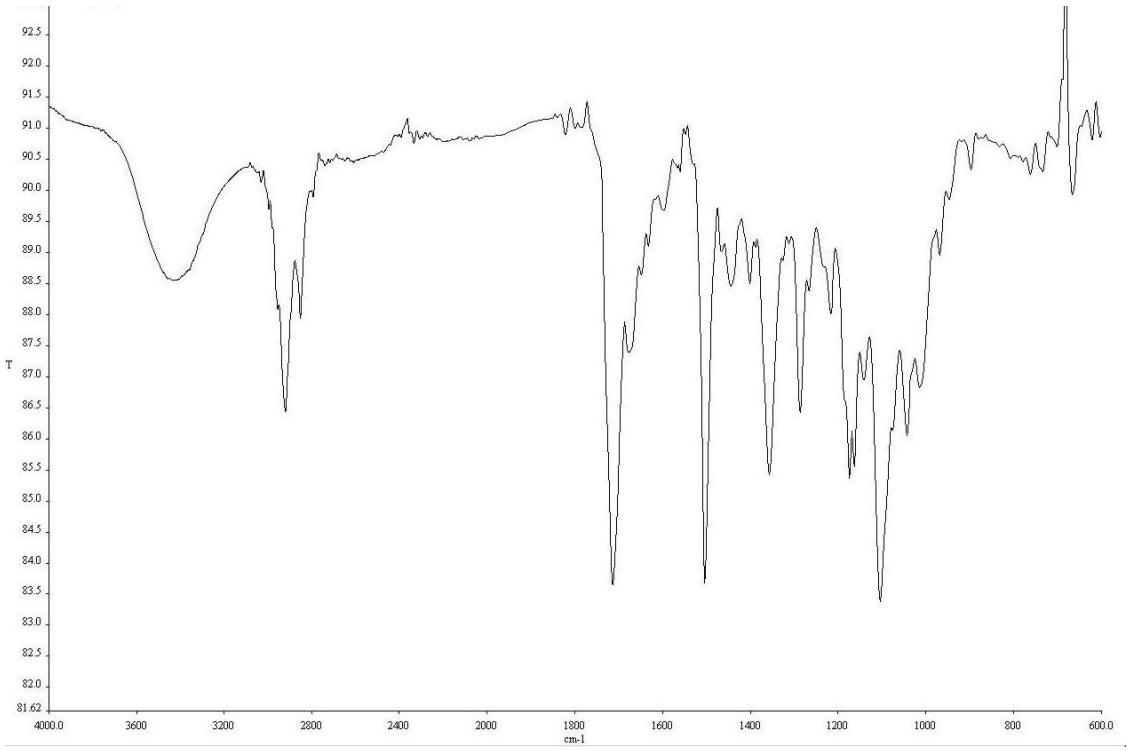


Figure A2.127 Infrared spectrum (Thin Film, NaCl) of compound **137**.

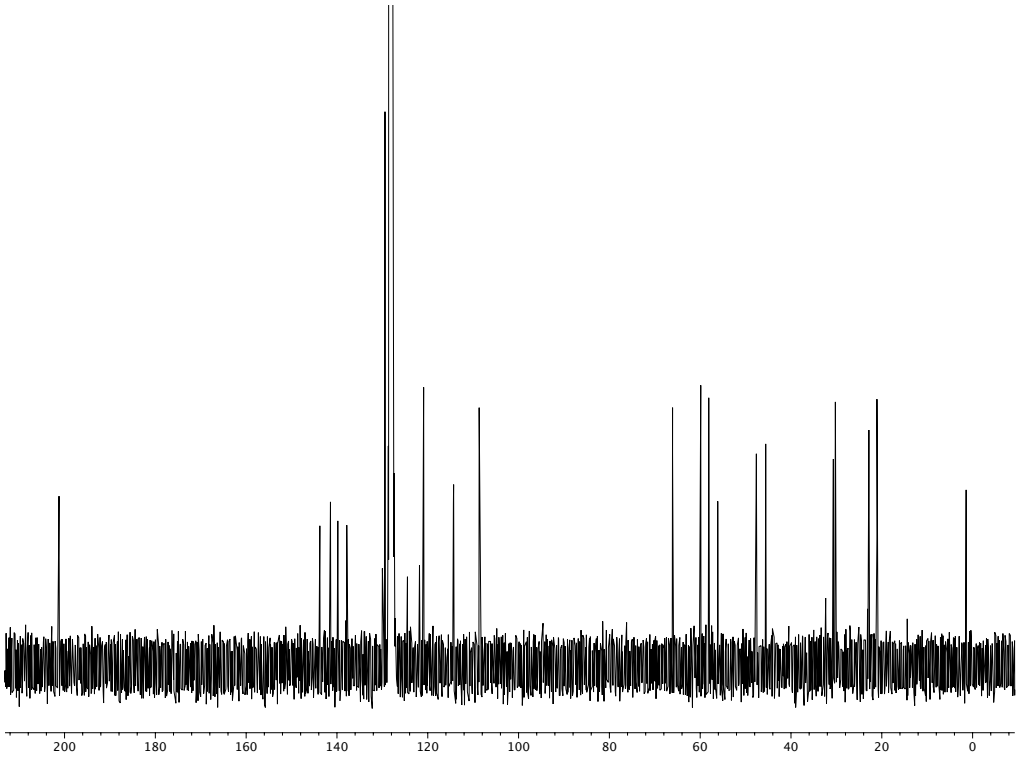


Figure A2.128 ^{13}C NMR (100 MHz, C_6D_6) of compound **137**.

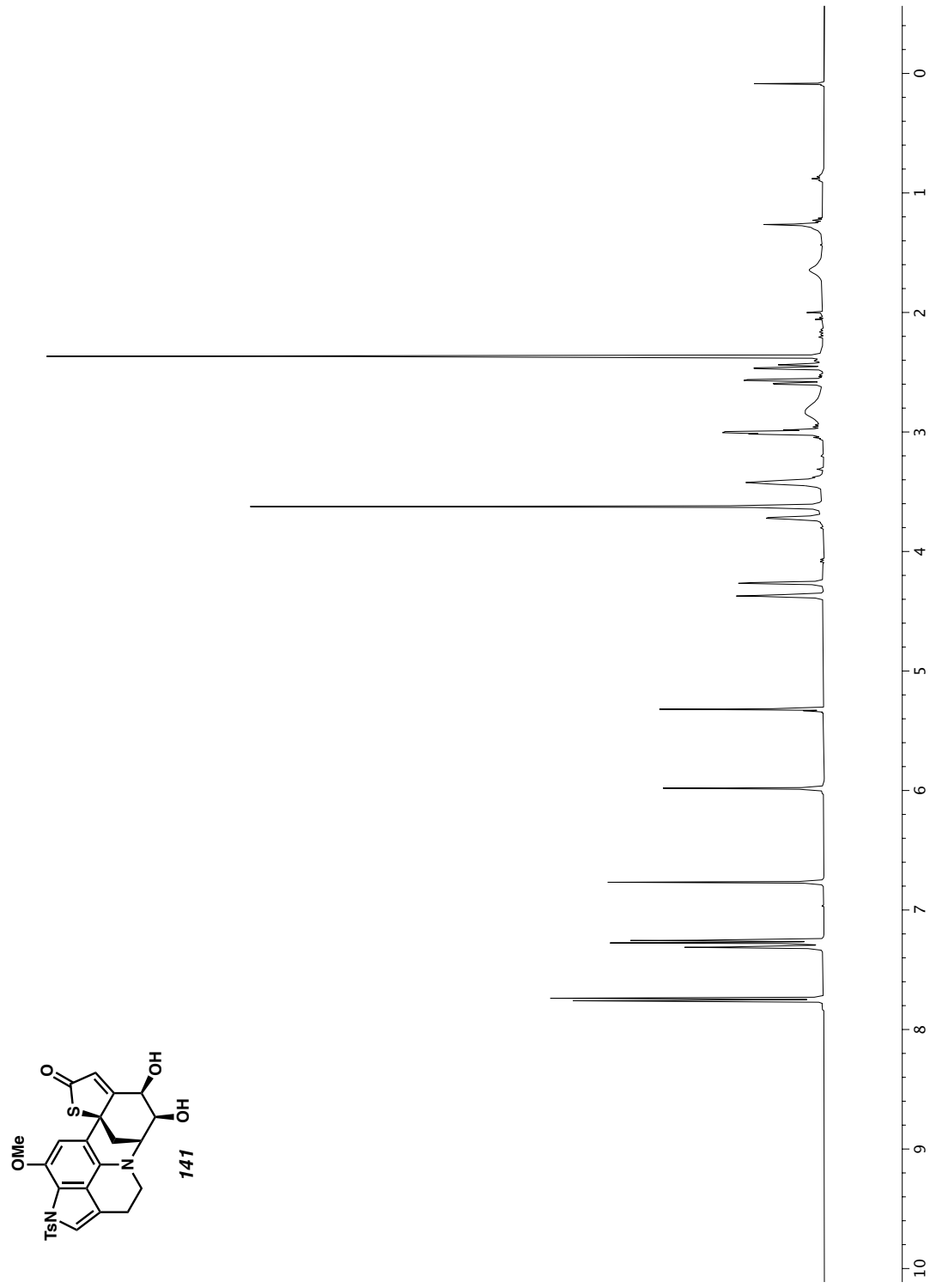


Figure A2.129. ^{1}H NMR (400 MHz, CD_2Cl_2) of compound **141**.

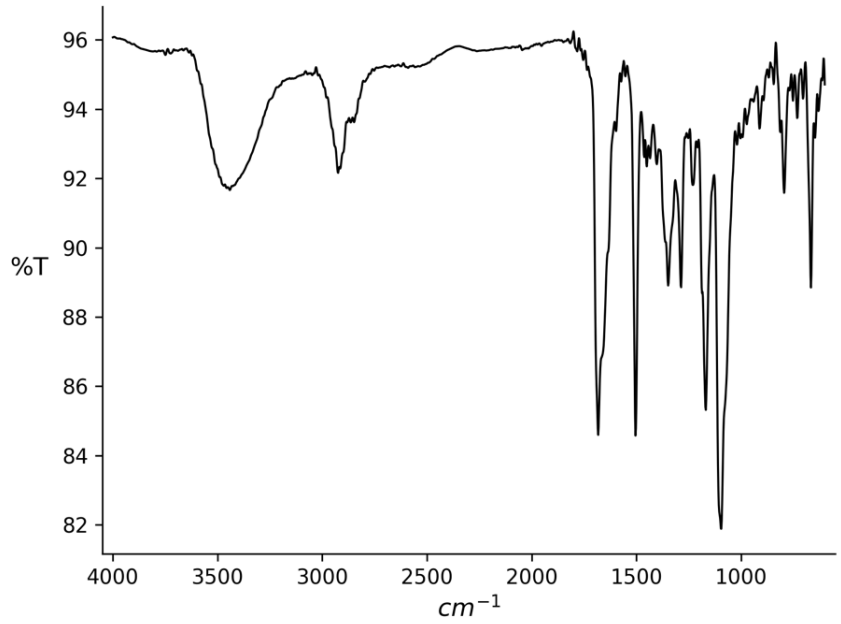


Figure A2.130 Infrared spectrum (Thin Film, NaCl) of compound **141**.

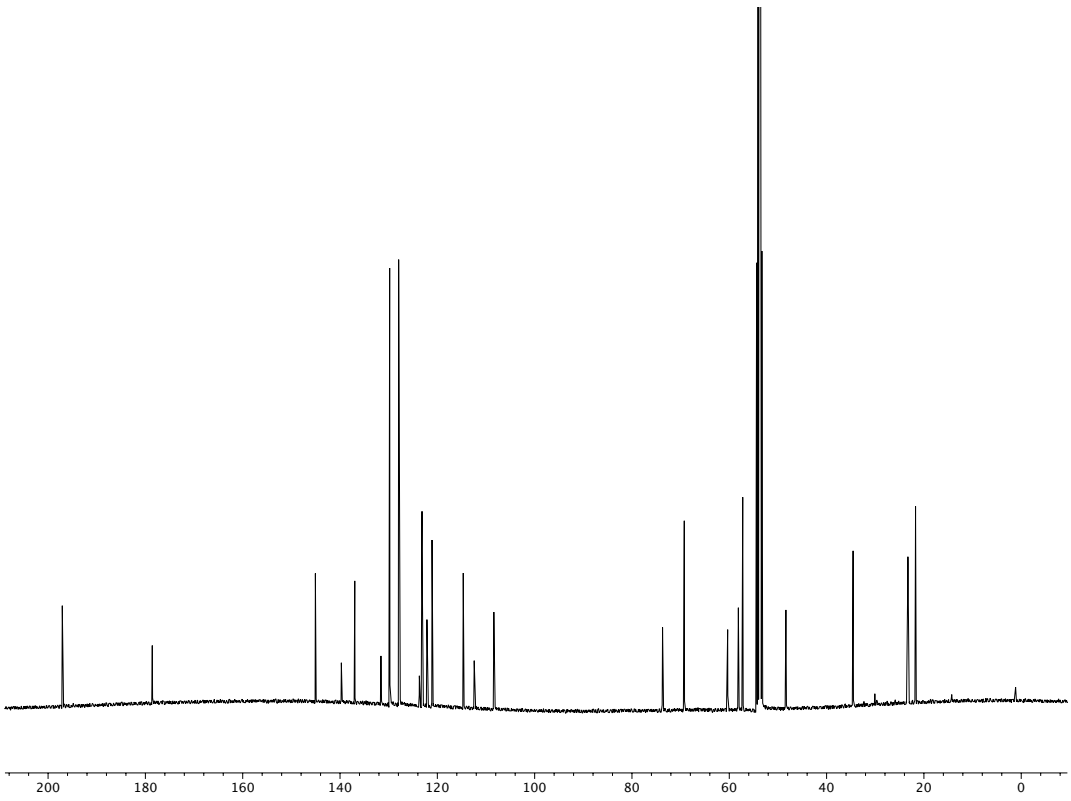


Figure A2.131 ^{13}C NMR (100 MHz, CD_2Cl_2) of compound **141**.

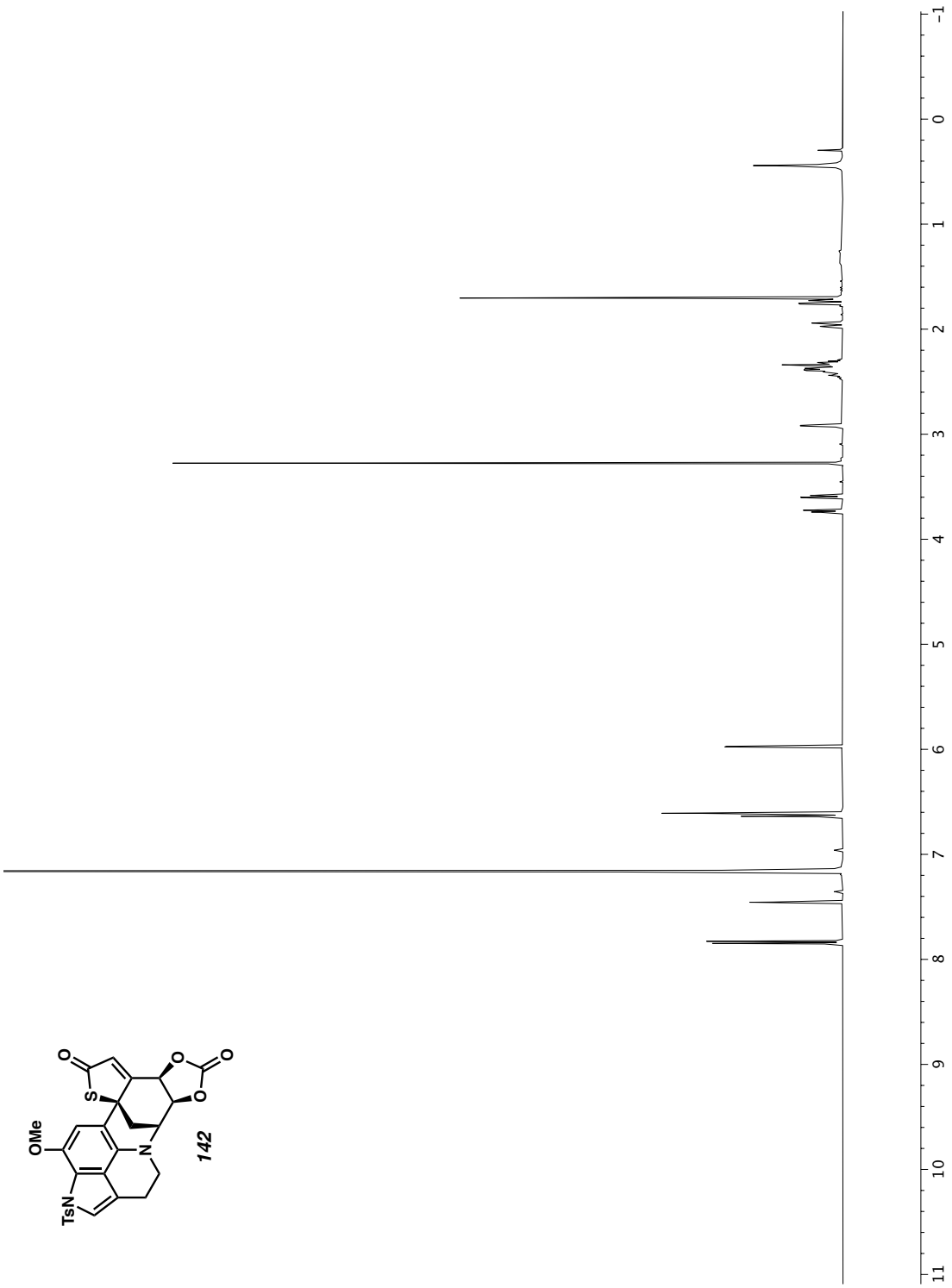


Figure A2.132. ^{1}H NMR (400 MHz, C_6D_6) of compound **142**.

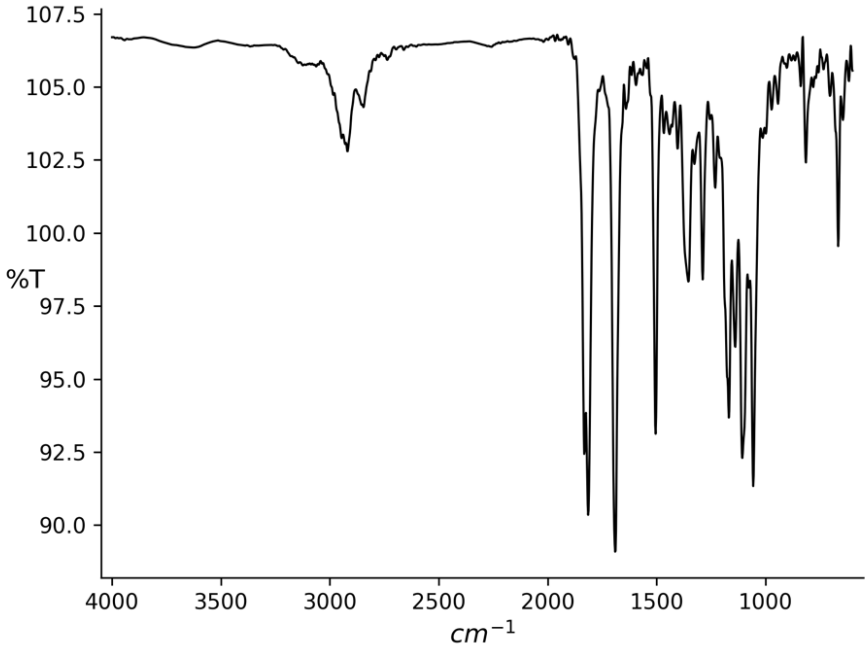


Figure A2.133 Infrared spectrum (Thin Film, NaCl) of compound **142**.

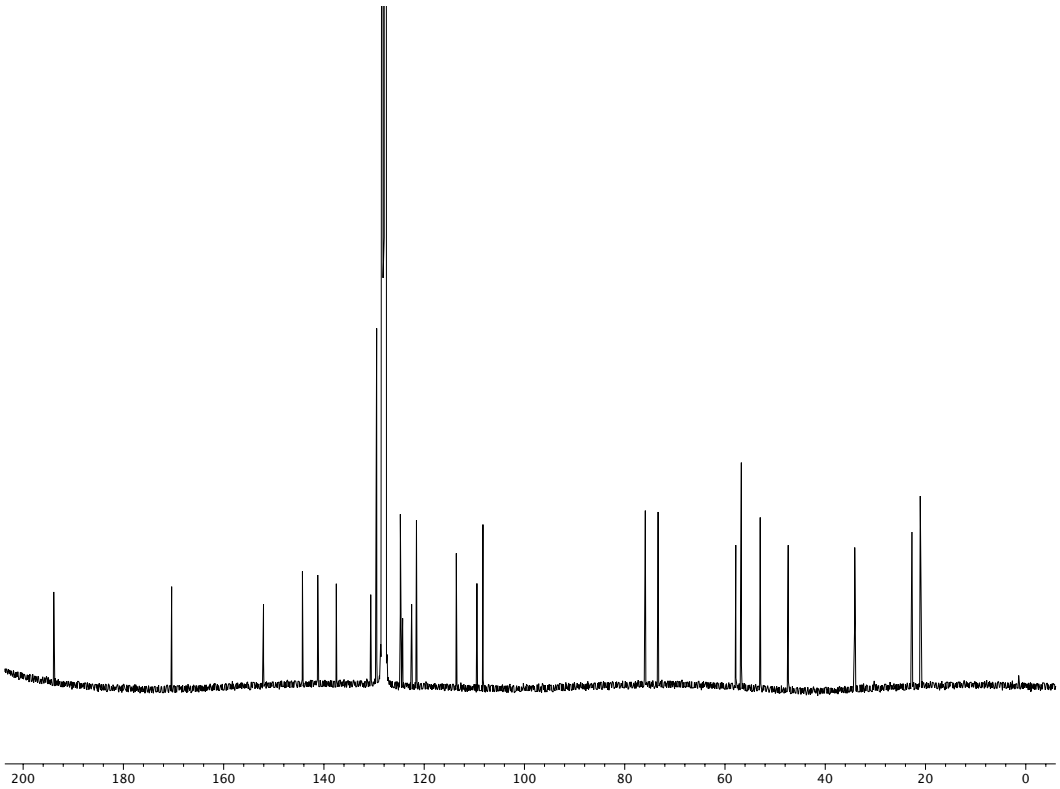


Figure A2.134 ^{13}C NMR (100 MHz, C_6D_6) of compound **142**.

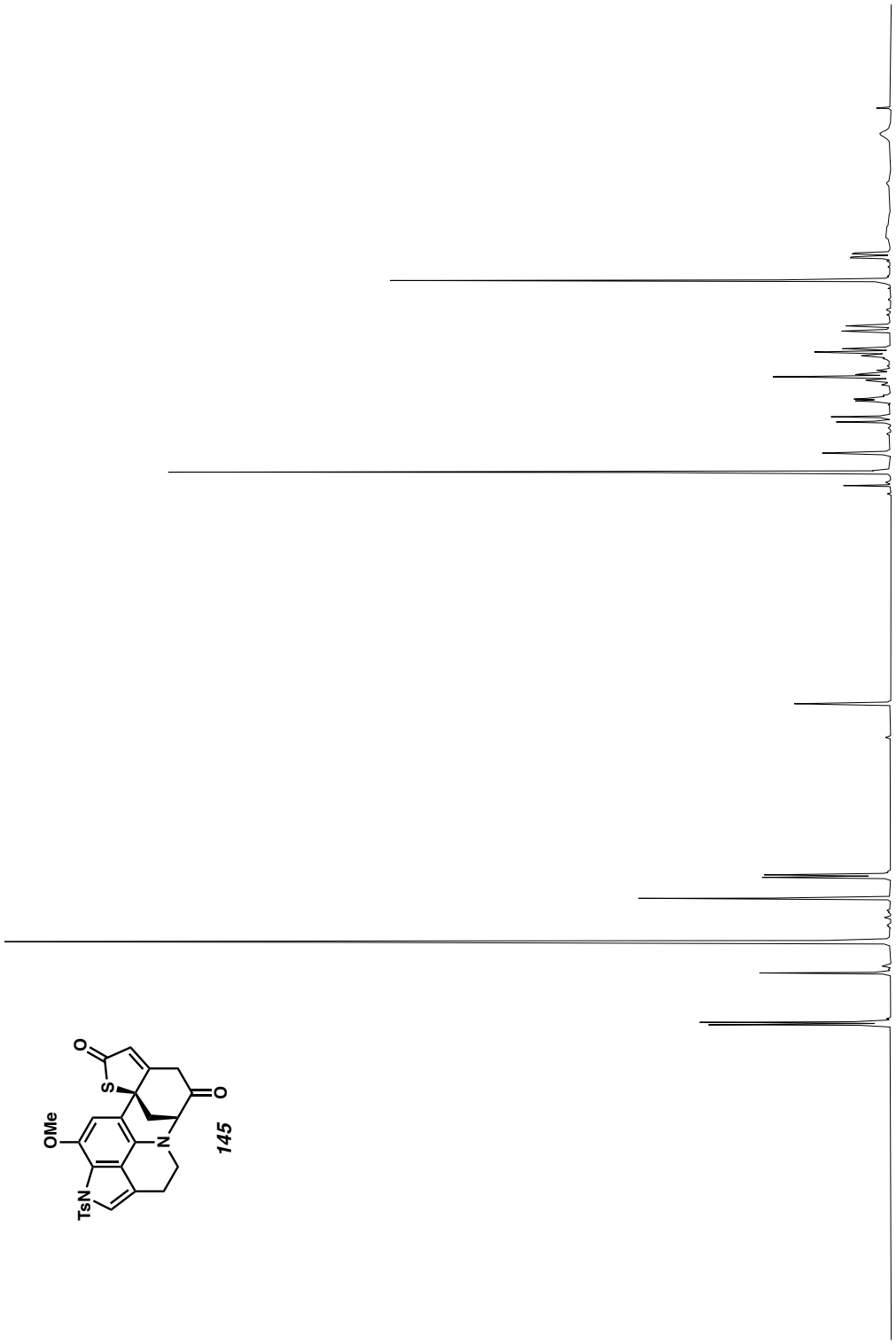


Figure A2.135. ^{1}H NMR (400 MHz, C_6D_6) of compound **145**.

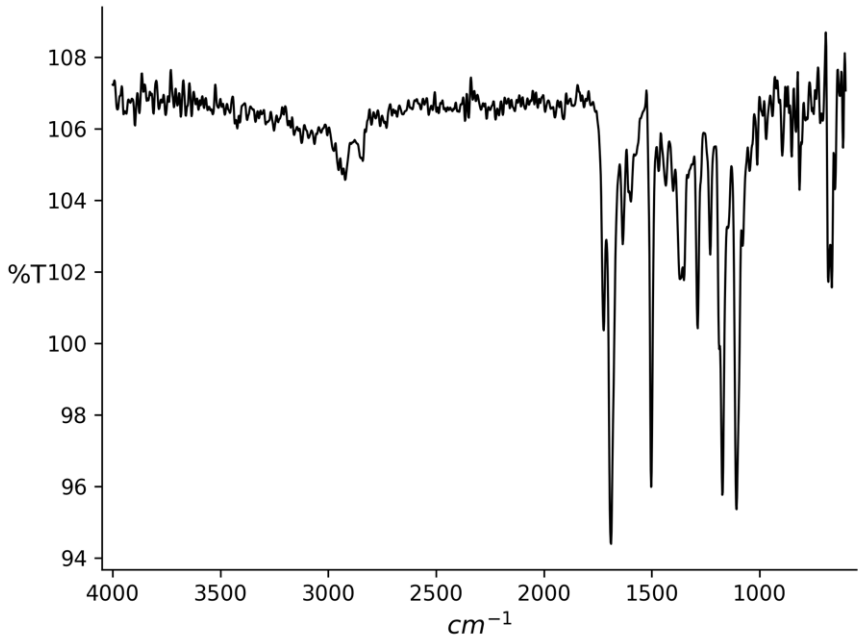


Figure A2.136 Infrared spectrum (Thin Film, NaCl) of compound **145**.

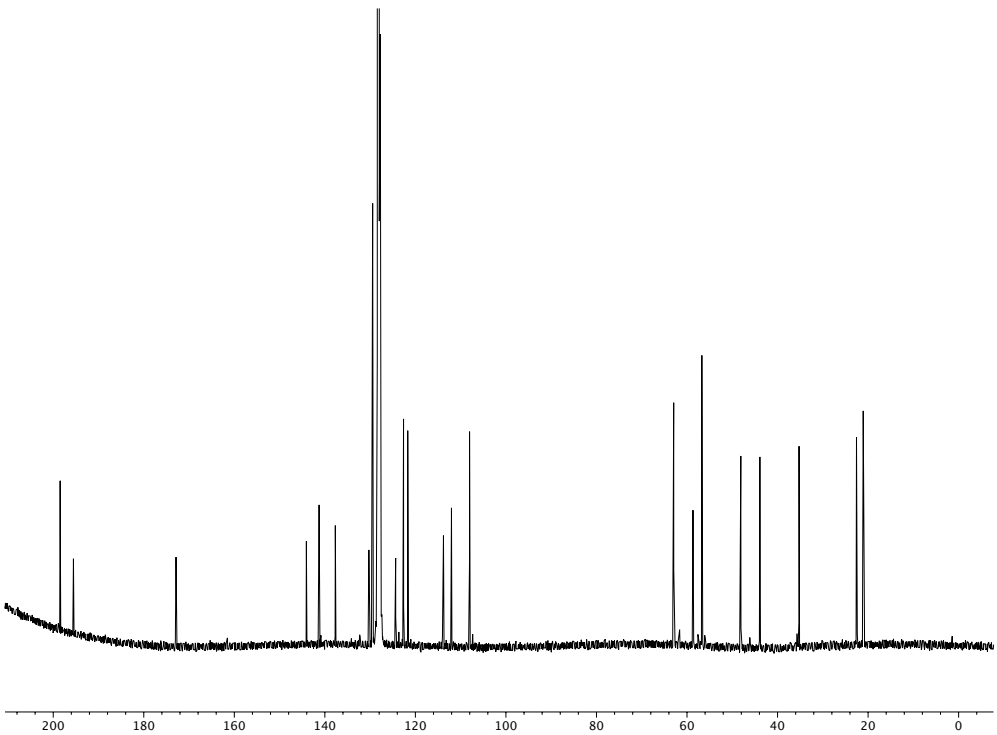


Figure A2.137 ^{13}C NMR (100 MHz, C_6D_6) of compound **145**.

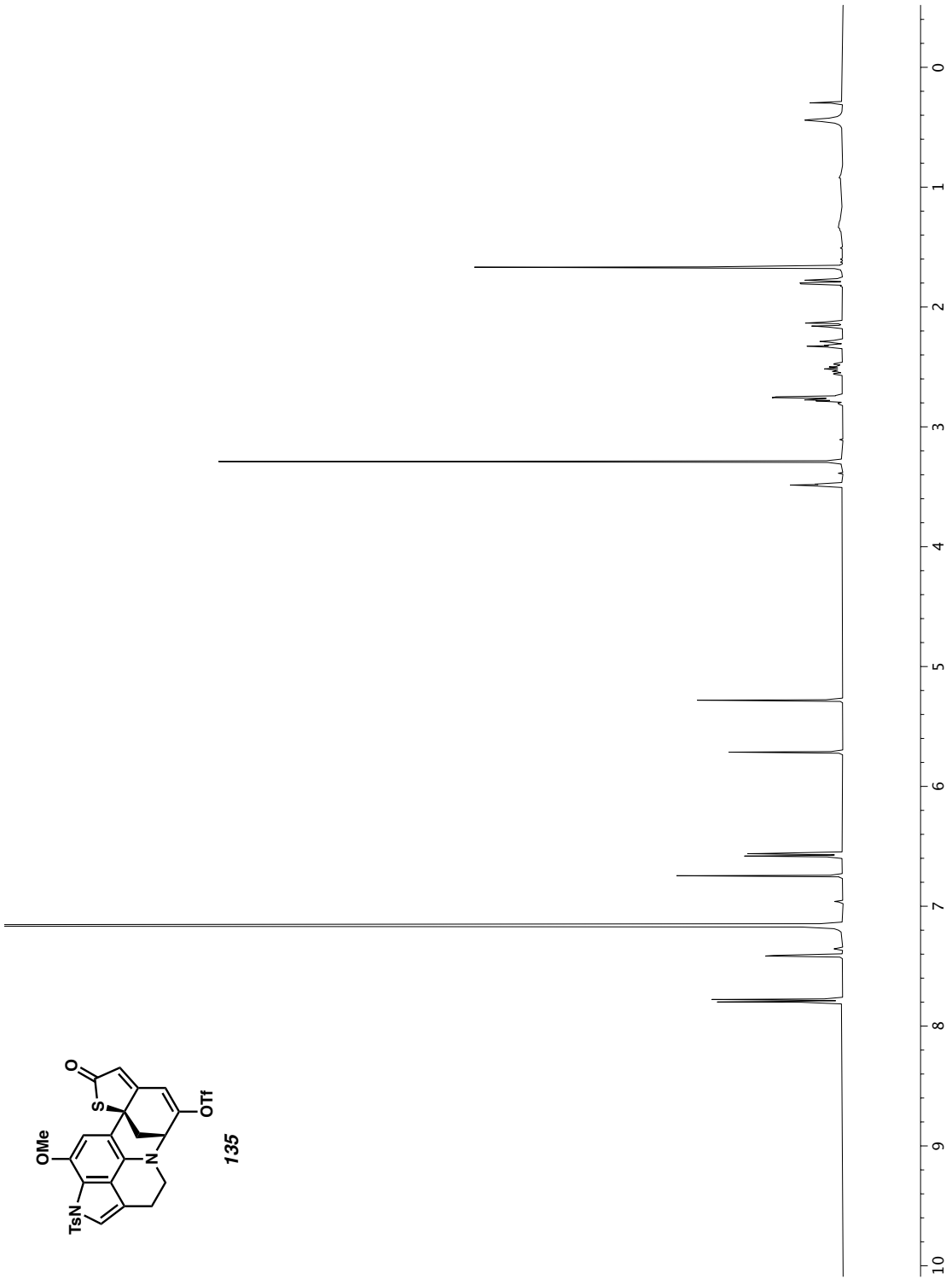


Figure A2.138. ^{1}H NMR (400 MHz, C_6D_6) of compound **135**.

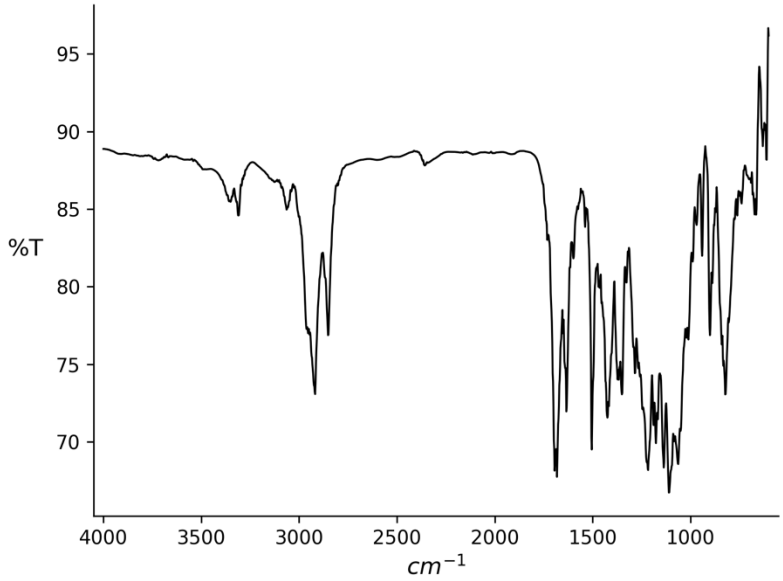


Figure A2.139 Infrared spectrum (Thin Film, NaCl) of compound **135**.

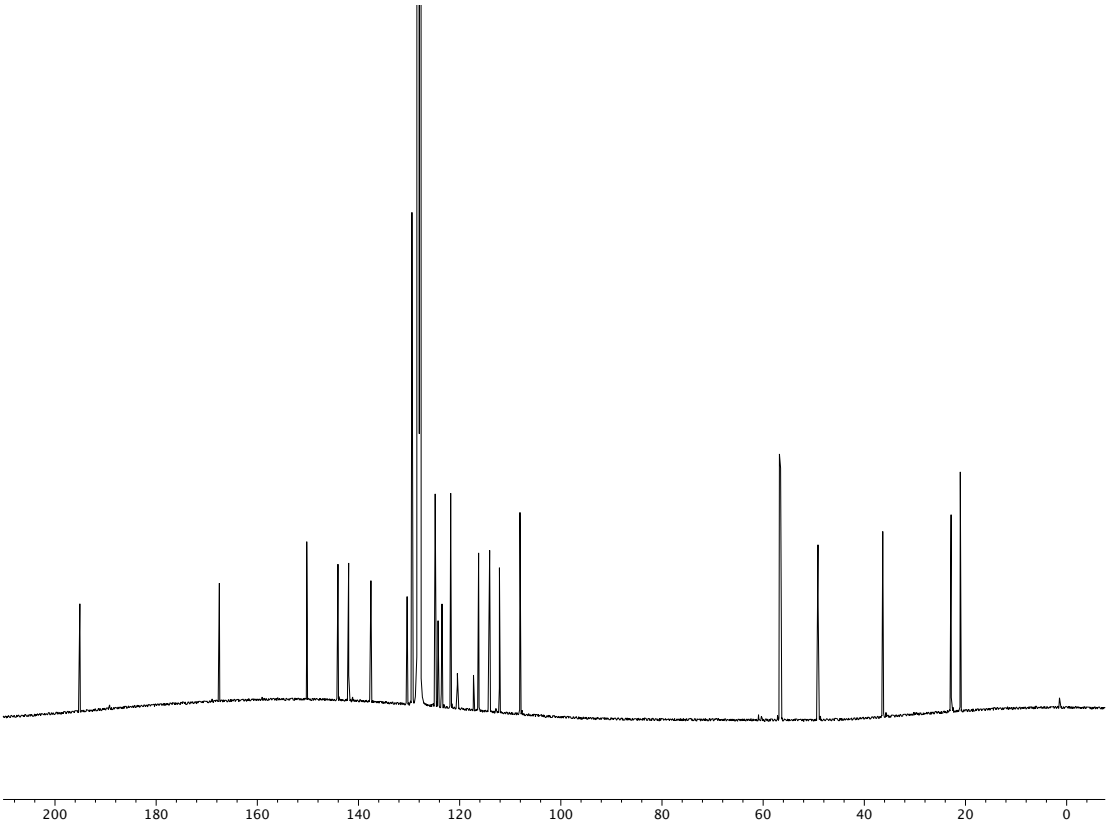


Figure A2.140 ^{13}C NMR (100 MHz, C_6D_6) of compound **135**.

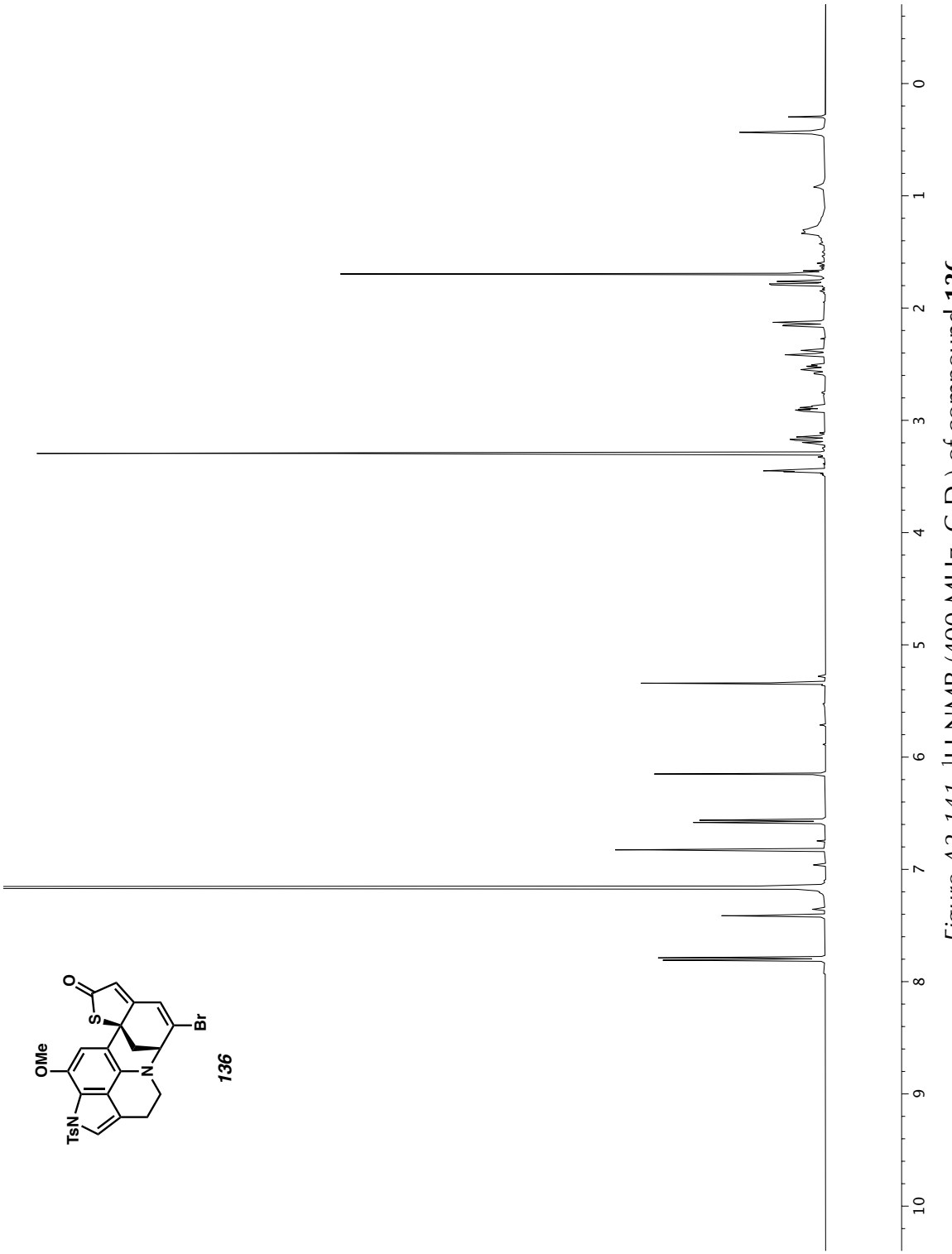


Figure A2.141. ^{1}H NMR (400 MHz, C_6D_6) of compound **136**.

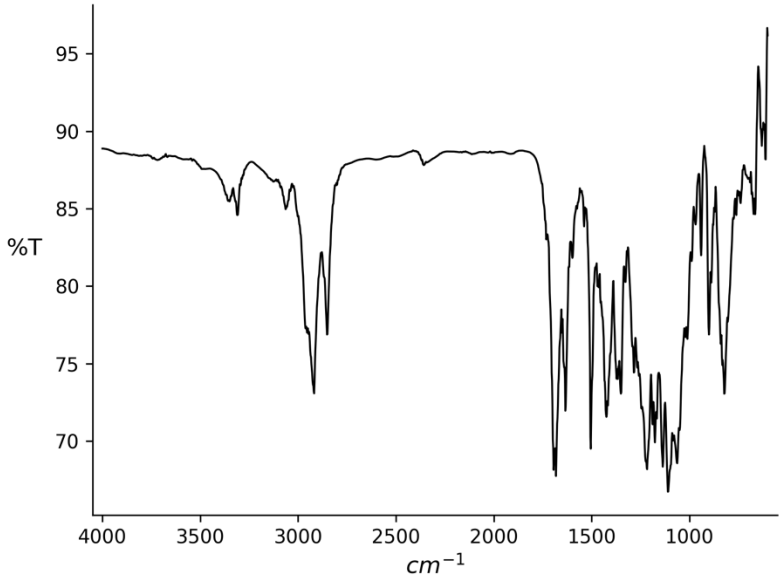


Figure A2.142 Infrared spectrum (Thin Film, NaCl) of compound **136**.

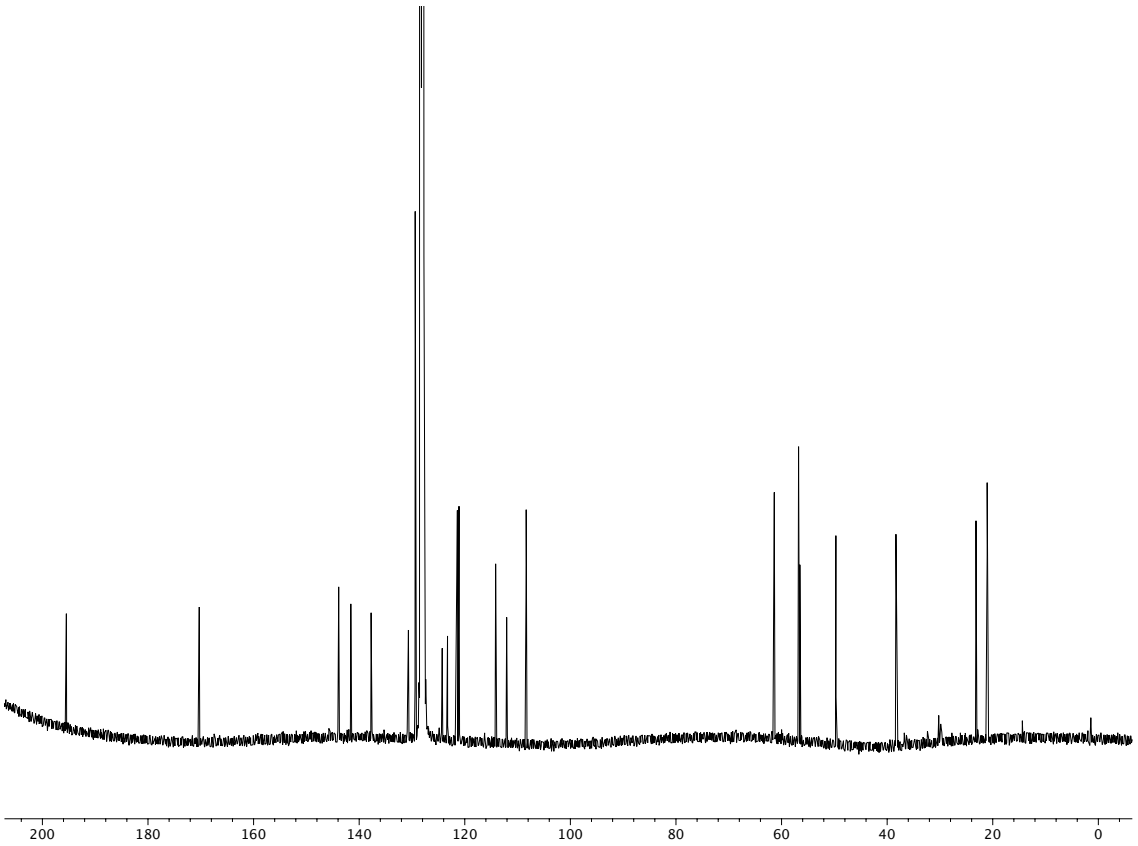


Figure A2.143 ^{13}C NMR (100 MHz, C_6D_6) of compound **136**.

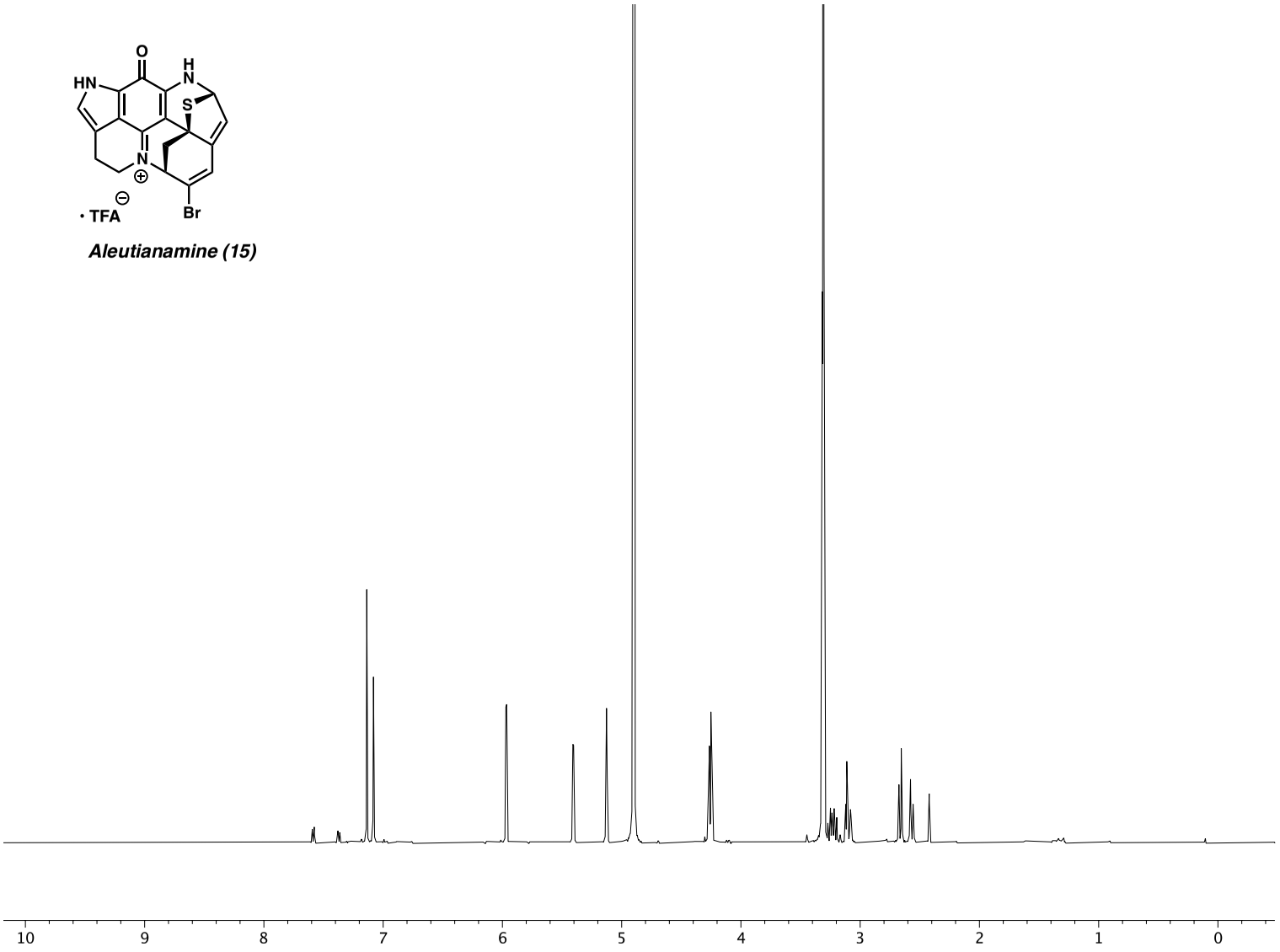


Figure A2.144. ^{1}H NMR (400 MHz, MeOD) of aleutianamine (**15**).

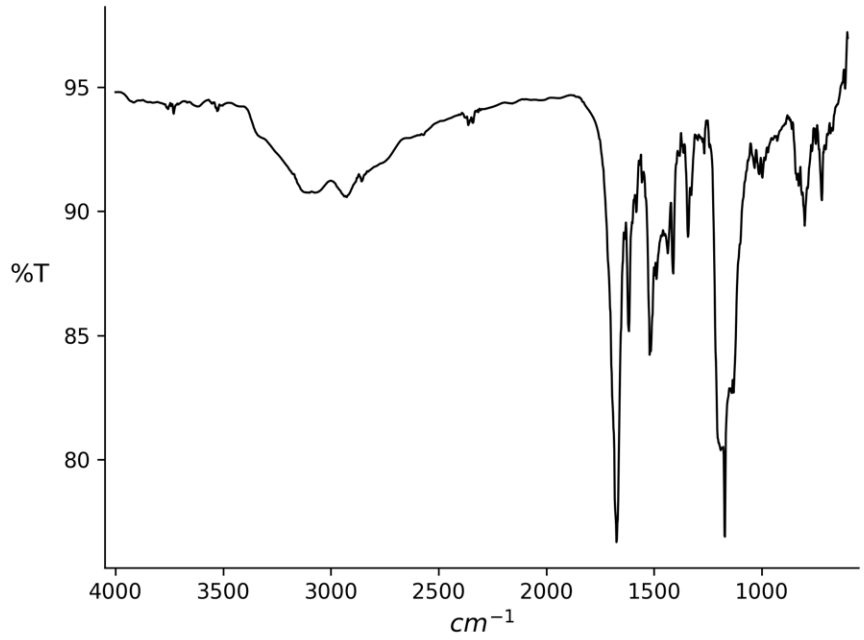


Figure A2.145 Infrared spectrum (Thin Film, NaCl) of aleutianamine (**15**).

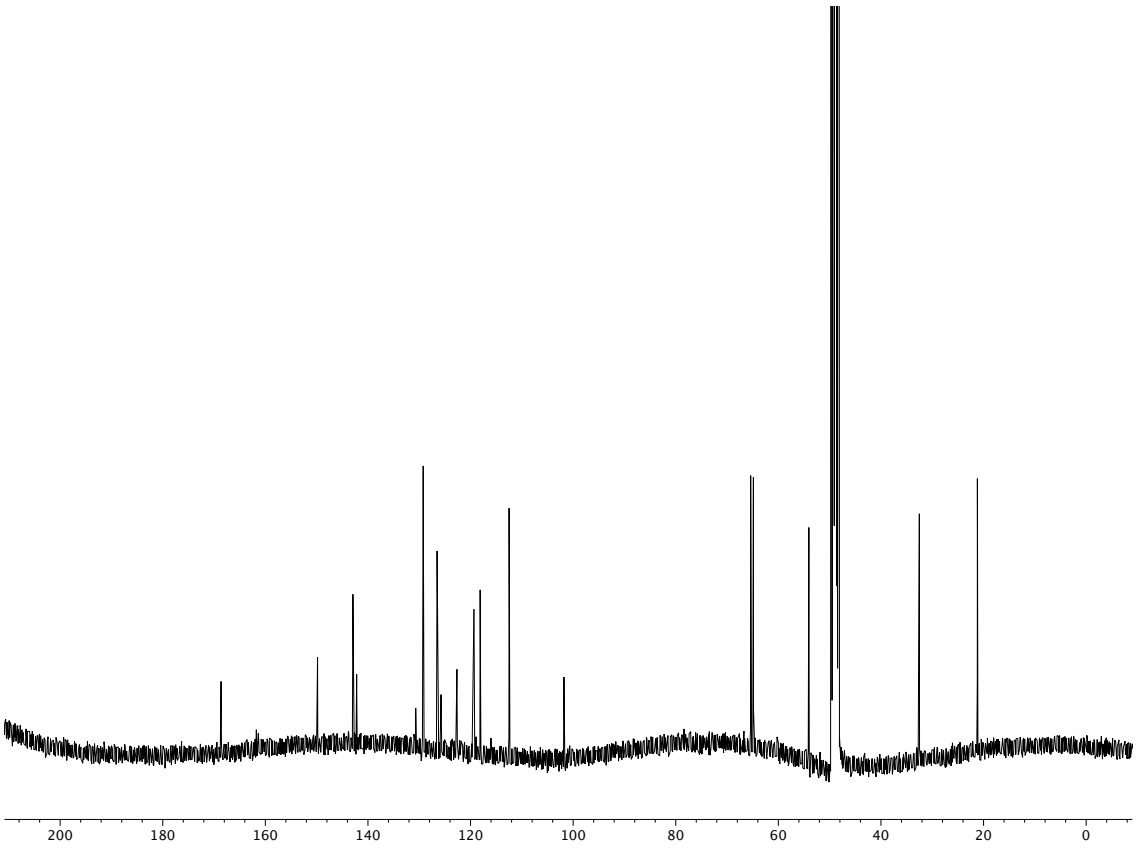


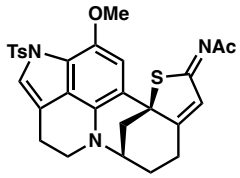
Figure A2.146 ^{13}C NMR (100 MHz, MeOD) of aleutianamine (**15**).

Appendix 3

X-Ray Crystallography Reports Relevant to Chapter 1:

Total Synthesis of Aleutianamine

A3.1 X-RAY CRYSTAL STRUCTURE ANALYSIS OF *N*-Ac THIOIMIDATE 74.



74

Contents

Table A3.1.1. Experimental Details

Table A3.1.2. Crystal Data

Table A3.1.3. Atomic Coordinates

Table A3.1.4. Full Bond Distances and Angles

Table A3.1.5. Anisotropic Displacement Parameters

Table A3.1.6. Hydrogen Atomic Coordinates

Table A3.1.7. Torsion Angles

Figure A3.1.1 *X-Ray Crystal Structure of N-Ac thioimidate* ***74***.

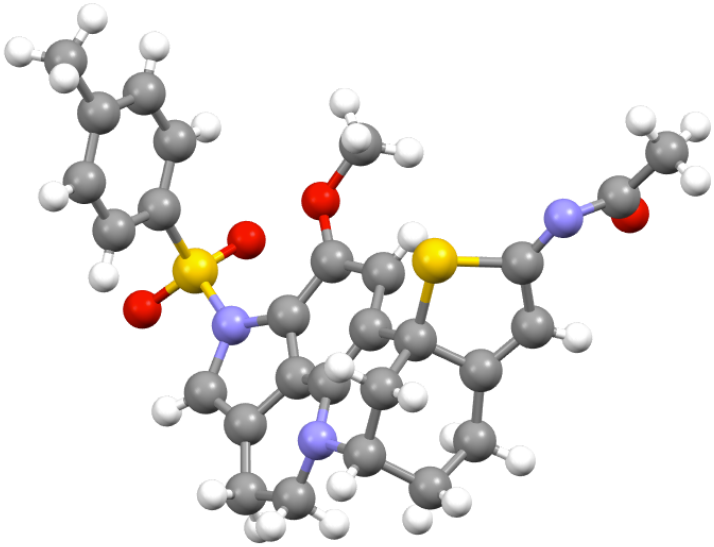


Table A3.1.1 *Experimental Details for X-Ray Structure Determination of N-Ac thioimidate* ***74***.

Low-temperature diffraction data (ϕ-and ω-scans) were collected on a Bruker AXS D8 VENTURE KAPPA diffractometer coupled to a PHOTON II CPAD detector with Cu K_α radiation (λ = 1.54178 Å) from an IμS micro-source for the structure of compound V22129. The structure was solved by direct methods using SHELXS and refined against F^2 on all data by full-matrix least squares with SHELXL-2017 using established refinement techniques. All non-hydrogen atoms were refined anisotropically. All hydrogen atoms were included into the model at geometrically calculated positions and refined using a riding model. The isotropic displacement parameters of all hydrogen atoms were fixed to 1.2 times the U value of the atoms they are linked to (1.5 times for methyl groups). All disordered atoms were refined with the help of similarity restraints on the 1,2- and 1,3-distances and displacement parameters as well as enhanced rigid bond restraints for anisotropic displacement parameters.

Compound **74** crystallizes in the triclinic space group P-1 with one molecule in the asymmetric unit along with 1.5 molecules of benzene.

Table A3.1.2 *Crystal Data and Structure Refinement for N-Ac thioimidate* ***74****.*

Identification code	V22129	
Empirical formula	C37 H36 N3 O4 S2	
Formula weight	650.81	
Temperature	100(2) K	
Wavelength	1.54178 Å	
Crystal system	Triclinic	
Space group	P-1	
Unit cell dimensions	a = 10.1632(11) Å	a= 100.758(4)°.
	b = 12.1917(13) Å	b= 102.996(6)°.
	c = 13.5098(11) Å	g = 93.010(9)°.
Volume	1594.6(3) $Å^3$	
Z	2	
Density (calculated)	1.355 Mg/m^3	
Absorption coefficient	1.884 mm^{-1}	
F(000)	686	
Crystal size	0.300 x 0.200 x 0.100 mm^3	
Theta range for data collection	3.429 to 74.650°.	
Index ranges	-12<=h<=12, -15<=k<=15, -16<=l<=16	
Reflections collected	25359	
Independent reflections	6477 [R(int) = 0.0339]	
Completeness to theta = 67.679°	99.8 %	
Absorption correction	Semi-empirical from equivalents	
Max. and min. transmission	0.7538 and 0.6091	
Refinement method	Full-matrix least-squares on F^2	
Data / restraints / parameters	6477 / 718 / 527	
Goodness-of-fit on F^2	1.093	
Final R indices [I>2sigma(I)]	R1 = 0.0505, wR2 = 0.1211	
R indices (all data)	R1 = 0.0521, wR2 = 0.1221	
Extinction coefficient	n/a	
Largest diff. peak and hole	*0.759 and -0.549 e.$Å^{-3}$*	

Table A3.1.3 *Atomic coordinates (x 10^4) and equivalent isotropic displacement parameters ($Å^2$x 10^3)for thioimidate* ***74****. U(eq) is defined as one third of the trace of the orthogonalized U^{ij} tensor.*

	x	y	z	U(eq)
O(1)	5677(2)	8116(1)	4124(1)	29(1)
O(2)	5920(2)	6109(1)	4093(1)	26(1)
C(1)	3617(2)	6858(2)	4309(2)	22(1)
C(2)	2591(2)	7539(2)	4035(2)	26(1)
C(3)	1452(2)	7473(2)	4416(2)	28(1)
C(4)	1306(2)	6738(2)	5074(2)	27(1)
C(7)	54(3)	6676(2)	5491(2)	39(1)
C(5)	2345(3)	6069(2)	5334(2)	29(1)
C(6)	3503(2)	6120(2)	4953(2)	26(1)
S(1)	5092(1)	6974(1)	3842(1)	22(1)
N(1)	4497(2)	6754(1)	2562(1)	20(1)
C(8)	4539(2)	7626(2)	1996(2)	22(1)
C(9)	3995(2)	7196(2)	982(2)	24(1)
C(10)	3731(3)	7654(2)	9(2)	34(1)
C(11)	3567(4)	6701(2)	-927(2)	33(1)
N(2)	2698(3)	5707(2)	-931(2)	27(1)
C(12)	2982(3)	5269(2)	-34(2)	21(1)
C(13)	2635(3)	4177(2)	50(2)	19(1)
C(11A)	2795(16)	6848(11)	-914(10)	19(2)
N(2A)	1988(16)	5970(11)	-772(10)	31(2)
C(12A)	2500(20)	5452(14)	49(13)	21(4)
C(13A)	2060(20)	4390(13)	126(12)	27(3)
C(19)	2148(3)	4896(2)	-1916(2)	26(1)
C(20)	600(3)	4877(2)	-2242(2)	28(1)
C(21)	-70(4)	4448(3)	-1455(4)	26(1)
C(22)	447(3)	3363(2)	-1240(2)	22(1)
C(23)	-266(2)	2385(2)	-1322(2)	26(1)

C(19A)	1168(16)	5268(13)	-1762(11)	30(3)
C(20A)	2040(20)	4653(18)	-2414(17)	44(4)
C(21A)	2810(30)	3760(30)	-1920(30)	43(5)
C(22A)	1945(19)	3041(13)	-1483(16)	40(4)
C(23A)	1661(19)	1923(14)	-1561(15)	47(4)
C(24)	549(2)	1461(2)	-1151(2)	29(1)
S(2)	2280(1)	1893(1)	-883(1)	21(1)
C(25)	1968(2)	3348(2)	-956(2)	19(1)
C(26)	2534(4)	3711(3)	-1827(4)	24(1)
S(2A)	-52(8)	2653(5)	-550(5)	79(3)
C(25A)	1080(16)	3670(11)	-854(11)	26(3)
C(26A)	220(20)	4400(20)	-1510(20)	34(5)
N(3)	-25(2)	448(2)	-1239(2)	40(1)
C(27)	806(3)	-412(2)	-1145(2)	35(1)
O(3)	2049(2)	-282(1)	-916(1)	37(1)
C(28)	28(3)	-1548(2)	-1389(3)	50(1)
C(14)	2859(2)	3906(2)	1045(2)	24(1)
C(15)	3482(2)	4662(2)	1954(2)	20(1)
C(16)	3868(2)	5758(2)	1858(2)	19(1)
C(17)	3582(2)	6038(2)	891(2)	23(1)
O(4)	3744(2)	4429(1)	2926(1)	24(1)
C(18)	3226(3)	3357(2)	3022(2)	35(1)
C(11S)	6578(3)	9716(2)	8295(2)	40(1)
C(12S)	6752(3)	9733(2)	7318(2)	32(1)
C(13S)	5671(3)	9486(2)	6481(2)	38(1)
C(14S)	4401(3)	9215(2)	6595(3)	55(1)
C(15S)	4212(4)	9197(2)	7575(4)	70(1)
C(16S)	5317(4)	9453(2)	8431(3)	58(1)
C(21S)	8855(3)	9592(2)	4236(3)	50(1)
C(22S)	8919(3)	9463(2)	5223(3)	50(1)
C(23S)	10058(4)	9868(2)	5987(2)	54(1)

Table A3.1.4 *Bond lengths [Å] and angles [°] for thioimidate* ***74****.*

O(1)-S(1)	1.4324(15)
O(2)-S(1)	1.4256(15)
C(1)-C(6)	1.381(3)
C(1)-C(2)	1.395(3)
C(1)-S(1)	1.761(2)
C(2)-C(3)	1.373(3)
C(2)-H(2)	0.9500
C(3)-C(4)	1.399(3)
C(3)-H(3)	0.9500
C(4)-C(5)	1.391(3)
C(4)-C(7)	1.507(3)
C(7)-H(7A)	0.9800
C(7)-H(7B)	0.9800
C(7)-H(7C)	0.9800
C(5)-C(6)	1.390(3)
C(5)-H(5)	0.9500
C(6)-H(6)	0.9500
S(1)-N(1)	1.6643(17)
N(1)-C(16)	1.415(2)
N(1)-C(8)	1.424(2)
C(8)-C(9)	1.349(3)
C(8)-H(8)	0.9500
C(9)-C(17)	1.427(3)
C(9)-C(10)	1.497(3)
C(10)-C(11)	1.521(4)
C(10)-C(11A)	1.528(12)
C(10)-H(10A)	0.9900
C(10)-H(10B)	0.9900
C(10)-H(10C)	0.9900
C(10)-H(10D)	0.9900
C(11)-N(2)	1.460(3)
C(11)-H(11A)	0.9900
C(11)-H(11B)	0.9900

N(2)-C(12)	1.392(3)
N(2)-C(19)	1.476(3)
C(12)-C(13)	1.391(3)
C(12)-C(17)	1.404(4)
C(13)-C(14)	1.415(3)
C(13)-C(25)	1.527(3)
C(11A)-N(2A)	1.383(14)
C(11A)-H(11C)	0.9900
C(11A)-H(11D)	0.9900
N(2A)-C(12A)	1.391(15)
N(2A)-C(19A)	1.487(15)
C(12A)-C(13A)	1.377(15)
C(12A)-C(17)	1.438(17)
C(13A)-C(25A)	1.547(15)
C(13A)-C(14)	1.556(16)
C(19)-C(20)	1.534(4)
C(19)-C(26)	1.535(4)
C(19)-H(19)	1.0000
C(20)-C(21)	1.538(4)
C(20)-H(20A)	0.9900
C(20)-H(20B)	0.9900
C(21)-C(22)	1.502(4)
C(21)-H(21A)	0.9900
C(21)-H(21B)	0.9900
C(22)-C(23)	1.335(4)
C(22)-C(25)	1.509(3)
C(23)-C(24)	1.455(3)
C(23)-H(23)	0.9500
C(19A)-C(20A)	1.514(16)
C(19A)-C(26A)	1.526(17)
C(19A)-H(19A)	1.0000
C(20A)-C(21A)	1.535(19)
C(20A)-H(20C)	0.9900
C(20A)-H(20D)	0.9900
C(21A)-C(22A)	1.495(17)
C(21A)-H(21C)	0.9900

C(21A)-H(21D)	0.9900
C(22A)-C(23A)	1.358(16)
C(22A)-C(25A)	1.499(15)
C(23A)-C(24)	1.493(15)
C(23A)-H(23A)	0.9500
C(24)-N(3)	1.311(3)
C(24)-S(2A)	1.737(9)
C(24)-S(2)	1.746(2)
S(2)-C(25)	1.835(2)
C(25)-C(26)	1.543(4)
C(26)-H(26A)	0.9900
C(26)-H(26B)	0.9900
S(2A)-C(25A)	1.812(12)
C(25A)-C(26A)	1.540(17)
C(26A)-H(26C)	0.9900
C(26A)-H(26D)	0.9900
N(3)-C(27)	1.387(3)
C(27)-O(3)	1.225(3)
C(27)-C(28)	1.501(3)
C(28)-H(28A)	0.9800
C(28)-H(28B)	0.9800
C(28)-H(28C)	0.9800
C(14)-C(15)	1.388(3)
C(14)-H(14)	0.9500
C(15)-O(4)	1.366(2)
C(15)-C(16)	1.410(3)
C(16)-C(17)	1.384(3)
O(4)-C(18)	1.422(2)
C(18)-H(18A)	0.9800
C(18)-H(18B)	0.9800
C(18)-H(18C)	0.9800
C(11S)-C(16S)	1.364(5)
C(11S)-C(12S)	1.375(4)
C(11S)-H(11S)	0.9500
C(12S)-C(13S)	1.362(4)
C(12S)-H(12S)	0.9500

C(13S)-C(14S)	1.365(4)
C(13S)-H(13S)	0.9500
C(14S)-C(15S)	1.384(6)
C(14S)-H(14S)	0.9500
C(15S)-C(16S)	1.393(6)
C(15S)-H(15S)	0.9500
C(16S)-H(16S)	0.9500
C(21S)-C(22S)	1.360(5)
C(21S)-C(23S)#1	1.376(5)
C(21S)-H(21S)	0.9500
C(22S)-C(23S)	1.364(5)
C(22S)-H(22S)	0.9500
C(23S)-H(23S)	0.9500

C(6)-C(1)-C(2)	121.1(2)
C(6)-C(1)-S(1)	120.00(17)
C(2)-C(1)-S(1)	118.84(16)
C(3)-C(2)-C(1)	119.17(19)
C(3)-C(2)-H(2)	120.4
C(1)-C(2)-H(2)	120.4
C(2)-C(3)-C(4)	121.2(2)
C(2)-C(3)-H(3)	119.4
C(4)-C(3)-H(3)	119.4
C(5)-C(4)-C(3)	118.4(2)
C(5)-C(4)-C(7)	120.9(2)
C(3)-C(4)-C(7)	120.7(2)
C(4)-C(7)-H(7A)	109.5
C(4)-C(7)-H(7B)	109.5
H(7A)-C(7)-H(7B)	109.5
C(4)-C(7)-H(7C)	109.5
H(7A)-C(7)-H(7C)	109.5
H(7B)-C(7)-H(7C)	109.5
C(6)-C(5)-C(4)	121.3(2)
C(6)-C(5)-H(5)	119.3
C(4)-C(5)-H(5)	119.3
C(1)-C(6)-C(5)	118.8(2)

C(1)-C(6)-H(6)	120.6
C(5)-C(6)-H(6)	120.6
O(2)-S(1)-O(1)	119.27(10)
O(2)-S(1)-N(1)	109.30(9)
O(1)-S(1)-N(1)	104.24(9)
O(2)-S(1)-C(1)	109.72(10)
O(1)-S(1)-C(1)	109.57(10)
N(1)-S(1)-C(1)	103.48(9)
C(16)-N(1)-C(8)	108.46(16)
C(16)-N(1)-S(1)	129.34(14)
C(8)-N(1)-S(1)	122.19(14)
C(9)-C(8)-N(1)	108.67(17)
C(9)-C(8)-H(8)	125.7
N(1)-C(8)-H(8)	125.7
C(8)-C(9)-C(17)	107.20(18)
C(8)-C(9)-C(10)	135.3(2)
C(17)-C(9)-C(10)	117.52(19)
C(9)-C(10)-C(11)	109.7(2)
C(9)-C(10)-C(11A)	113.0(5)
C(9)-C(10)-H(10A)	109.7
C(11)-C(10)-H(10A)	109.7
C(9)-C(10)-H(10B)	109.7
C(11)-C(10)-H(10B)	109.7
H(10A)-C(10)-H(10B)	108.2
C(9)-C(10)-H(10C)	109.0
C(11A)-C(10)-H(10C)	109.0
C(9)-C(10)-H(10D)	109.0
C(11A)-C(10)-H(10D)	109.0
H(10C)-C(10)-H(10D)	107.8
N(2)-C(11)-C(10)	115.6(2)
N(2)-C(11)-H(11A)	108.4
C(10)-C(11)-H(11A)	108.4
N(2)-C(11)-H(11B)	108.4
C(10)-C(11)-H(11B)	108.4
H(11A)-C(11)-H(11B)	107.4
C(12)-N(2)-C(11)	116.1(2)

C(12)-N(2)-C(19)	116.5(2)
C(11)-N(2)-C(19)	119.2(2)
C(13)-C(12)-N(2)	126.8(3)
C(13)-C(12)-C(17)	117.0(2)
N(2)-C(12)-C(17)	116.0(2)
C(12)-C(13)-C(14)	119.4(2)
C(12)-C(13)-C(25)	116.8(2)
C(14)-C(13)-C(25)	123.8(2)
N(2A)-C(11A)-C(10)	121.1(10)
N(2A)-C(11A)-H(11C)	107.0
C(10)-C(11A)-H(11C)	107.0
N(2A)-C(11A)-H(11D)	107.0
C(10)-C(11A)-H(11D)	107.0
H(11C)-C(11A)-H(11D)	106.8
C(11A)-N(2A)-C(12A)	117.7(13)
C(11A)-N(2A)-C(19A)	113.2(11)
C(12A)-N(2A)-C(19A)	118.8(12)
C(13A)-C(12A)-N(2A)	125.1(14)
C(13A)-C(12A)-C(17)	115.7(11)
N(2A)-C(12A)-C(17)	119.2(11)
C(12A)-C(13A)-C(25A)	116.3(13)
C(12A)-C(13A)-C(14)	117.4(11)
C(25A)-C(13A)-C(14)	124.1(11)
N(2)-C(19)-C(20)	110.5(2)
N(2)-C(19)-C(26)	111.3(3)
C(20)-C(19)-C(26)	109.7(2)
N(2)-C(19)-H(19)	108.5
C(20)-C(19)-H(19)	108.5
C(26)-C(19)-H(19)	108.5
C(19)-C(20)-C(21)	110.9(2)
C(19)-C(20)-H(20A)	109.5
C(21)-C(20)-H(20A)	109.5
C(19)-C(20)-H(20B)	109.5
C(21)-C(20)-H(20B)	109.5
H(20A)-C(20)-H(20B)	108.0
C(22)-C(21)-C(20)	110.8(3)

C(22)-C(21)-H(21A)	109.5
C(20)-C(21)-H(21A)	109.5
C(22)-C(21)-H(21B)	109.5
C(20)-C(21)-H(21B)	109.5
H(21A)-C(21)-H(21B)	108.1
C(23)-C(22)-C(21)	128.4(3)
C(23)-C(22)-C(25)	115.2(2)
C(21)-C(22)-C(25)	116.3(2)
C(22)-C(23)-C(24)	114.7(2)
C(22)-C(23)-H(23)	122.7
C(24)-C(23)-H(23)	122.7
N(2A)-C(19A)-C(20A)	112.6(15)
N(2A)-C(19A)-C(26A)	108.4(15)
C(20A)-C(19A)-C(26A)	108.6(16)
N(2A)-C(19A)-H(19A)	109.1
C(20A)-C(19A)-H(19A)	109.1
C(26A)-C(19A)-H(19A)	109.1
C(19A)-C(20A)-C(21A)	113.6(17)
C(19A)-C(20A)-H(20C)	108.8
C(21A)-C(20A)-H(20C)	108.8
C(19A)-C(20A)-H(20D)	108.8
C(21A)-C(20A)-H(20D)	108.8
H(20C)-C(20A)-H(20D)	107.7
C(22A)-C(21A)-C(20A)	113.4(18)
C(22A)-C(21A)-H(21C)	108.9
C(20A)-C(21A)-H(21C)	108.9
C(22A)-C(21A)-H(21D)	108.9
C(20A)-C(21A)-H(21D)	108.9
H(21C)-C(21A)-H(21D)	107.7
C(23A)-C(22A)-C(21A)	136.2(18)
C(23A)-C(22A)-C(25A)	109.1(12)
C(21A)-C(22A)-C(25A)	114.5(16)
C(22A)-C(23A)-C(24)	122.3(13)
C(22A)-C(23A)-H(23A)	118.8
C(24)-C(23A)-H(23A)	118.8
N(3)-C(24)-C(23)	120.9(2)

N(3)-C(24)-C(23A)	133.8(7)
N(3)-C(24)-S(2A)	122.4(3)
C(23A)-C(24)-S(2A)	103.6(7)
N(3)-C(24)-S(2)	127.68(19)
C(23)-C(24)-S(2)	111.35(17)
C(24)-S(2)-C(25)	92.50(11)
C(22)-C(25)-C(13)	112.2(2)
C(22)-C(25)-C(26)	107.9(2)
C(13)-C(25)-C(26)	107.1(2)
C(22)-C(25)-S(2)	106.17(16)
C(13)-C(25)-S(2)	112.65(17)
C(26)-C(25)-S(2)	110.7(2)
C(19)-C(26)-C(25)	108.8(3)
C(19)-C(26)-H(26A)	109.9
C(25)-C(26)-H(26A)	109.9
C(19)-C(26)-H(26B)	109.9
C(25)-C(26)-H(26B)	109.9
H(26A)-C(26)-H(26B)	108.3
C(24)-S(2A)-C(25A)	96.8(6)
C(22A)-C(25A)-C(26A)	109.1(15)
C(22A)-C(25A)-C(13A)	106.8(14)
C(26A)-C(25A)-C(13A)	111.5(15)
C(22A)-C(25A)-S(2A)	108.0(9)
C(26A)-C(25A)-S(2A)	108.7(11)
C(13A)-C(25A)-S(2A)	112.7(10)
C(19A)-C(26A)-C(25A)	109.0(13)
C(19A)-C(26A)-H(26C)	109.9
C(25A)-C(26A)-H(26C)	109.9
C(19A)-C(26A)-H(26D)	109.9
C(25A)-C(26A)-H(26D)	109.9
H(26C)-C(26A)-H(26D)	108.3
C(24)-N(3)-C(27)	118.1(2)
O(3)-C(27)-N(3)	124.6(2)
O(3)-C(27)-C(28)	122.3(2)
N(3)-C(27)-C(28)	113.0(2)
C(27)-C(28)-H(28A)	109.5

C(27)-C(28)-H(28B)	109.5
H(28A)-C(28)-H(28B)	109.5
C(27)-C(28)-H(28C)	109.5
H(28A)-C(28)-H(28C)	109.5
H(28B)-C(28)-H(28C)	109.5
C(15)-C(14)-C(13)	123.34(19)
C(15)-C(14)-C(13A)	117.4(6)
C(15)-C(14)-H(14)	118.3
C(13)-C(14)-H(14)	118.3
O(4)-C(15)-C(14)	125.24(18)
O(4)-C(15)-C(16)	117.91(17)
C(14)-C(15)-C(16)	116.84(18)
C(17)-C(16)-C(15)	119.69(18)
C(17)-C(16)-N(1)	105.44(17)
C(15)-C(16)-N(1)	134.83(18)
C(16)-C(17)-C(12)	123.6(2)
C(16)-C(17)-C(9)	110.21(18)
C(12)-C(17)-C(9)	126.2(2)
C(16)-C(17)-C(12A)	122.5(6)
C(9)-C(17)-C(12A)	121.1(6)
C(15)-O(4)-C(18)	117.14(16)
O(4)-C(18)-H(18A)	109.5
O(4)-C(18)-H(18B)	109.5
H(18A)-C(18)-H(18B)	109.5
O(4)-C(18)-H(18C)	109.5
H(18A)-C(18)-H(18C)	109.5
H(18B)-C(18)-H(18C)	109.5
C(16S)-C(11S)-C(12S)	120.0(3)
C(16S)-C(11S)-H(11S)	120.0
C(12S)-C(11S)-H(11S)	120.0
C(13S)-C(12S)-C(11S)	120.3(3)
C(13S)-C(12S)-H(12S)	119.8
C(11S)-C(12S)-H(12S)	119.8
C(12S)-C(13S)-C(14S)	120.8(3)
C(12S)-C(13S)-H(13S)	119.6
C(14S)-C(13S)-H(13S)	119.6

C(13S)-C(14S)-C(15S)	119.4(3)
C(13S)-C(14S)-H(14S)	120.3
C(15S)-C(14S)-H(14S)	120.3
C(14S)-C(15S)-C(16S)	119.7(3)
C(14S)-C(15S)-H(15S)	120.1
C(16S)-C(15S)-H(15S)	120.1
C(11S)-C(16S)-C(15S)	119.7(3)
C(11S)-C(16S)-H(16S)	120.1
C(15S)-C(16S)-H(16S)	120.1
C(22S)-C(21S)-C(23S)#1	119.7(3)
C(22S)-C(21S)-H(21S)	120.2
C(23S)#1-C(21S)-H(21S)	120.2
C(21S)-C(22S)-C(23S)	120.0(3)
C(21S)-C(22S)-H(22S)	120.0
C(23S)-C(22S)-H(22S)	120.0
C(22S)-C(23S)-C(21S)#1	120.3(3)
C(22S)-C(23S)-H(23S)	119.8
C(21S)#1-C(23S)-H(23S)	119.8

Symmetry transformations used to generate equivalent atoms:
#1 -x+2,-y+2,-z+1

Table A3.1.5 *Anisotropic displacement parameters ($Å^2 x\ 10^3$) for thioimidate* ***74****. The anisotropic displacement factor exponent takes the form: $-2\pi^2[h^2 a^{*2} U^{11} + ... + 2 h k a^* b^* U^{12}]$*

	U^{11}	U^{22}	U^{33}	U^{23}	U^{13}	U^{12}
O(1)	38(1)	20(1)	26(1)	2(1)	4(1)	-6(1)
O(2)	26(1)	24(1)	26(1)	8(1)	2(1)	2(1)
C(1)	29(1)	18(1)	19(1)	2(1)	7(1)	0(1)
C(2)	34(1)	21(1)	25(1)	9(1)	8(1)	3(1)
C(3)	34(1)	22(1)	28(1)	6(1)	6(1)	5(1)
C(4)	35(1)	21(1)	25(1)	2(1)	10(1)	1(1)
C(7)	46(2)	33(1)	45(1)	10(1)	23(1)	5(1)
C(5)	42(1)	24(1)	25(1)	10(1)	11(1)	4(1)
C(6)	35(1)	20(1)	23(1)	7(1)	6(1)	3(1)
S(1)	26(1)	17(1)	20(1)	4(1)	3(1)	-1(1)
N(1)	27(1)	14(1)	19(1)	4(1)	5(1)	0(1)
C(8)	25(1)	16(1)	26(1)	9(1)	6(1)	1(1)
C(9)	24(1)	21(1)	28(1)	10(1)	5(1)	-2(1)
C(10)	41(1)	30(1)	30(1)	16(1)	-1(1)	-9(1)
C(11)	47(2)	29(1)	24(1)	11(1)	9(1)	-4(1)
N(2)	32(1)	28(1)	19(1)	11(1)	1(1)	-8(1)
C(12)	17(2)	25(1)	21(1)	9(1)	5(1)	0(1)
C(13)	15(1)	22(1)	20(1)	6(1)	3(1)	-1(1)
C(11A)	20(4)	25(4)	19(4)	15(3)	9(4)	6(4)
N(2A)	34(5)	32(4)	25(4)	12(3)	2(4)	-8(4)
C(12A)	24(9)	26(7)	15(6)	8(5)	6(6)	-7(6)
C(13A)	29(8)	28(7)	19(6)	5(5)	-2(6)	-10(6)
C(19)	32(1)	29(1)	18(1)	9(1)	7(1)	-2(1)
C(20)	29(1)	27(1)	22(1)	8(1)	-4(1)	-1(1)
C(21)	22(2)	29(2)	28(2)	9(1)	4(1)	5(1)
C(22)	17(1)	29(1)	17(1)	5(1)	1(1)	0(1)
C(23)	17(1)	33(1)	25(1)	7(1)	-1(1)	0(1)
C(19A)	26(7)	37(7)	25(6)	15(5)	-2(5)	-1(5)

C(20A)	44(10)	52(10)	37(9)	8(7)	14(8)	-2(8)
C(21A)	45(12)	68(10)	27(10)	13(8)	26(9)	15(8)
C(22A)	43(9)	49(7)	30(8)	6(6)	13(7)	8(6)
C(23A)	50(9)	50(7)	29(9)	-5(7)	-2(7)	0(7)
C(24)	31(1)	29(1)	24(1)	5(1)	0(1)	-2(1)
S(2)	19(1)	21(1)	21(1)	3(1)	3(1)	0(1)
C(25)	19(1)	22(1)	18(1)	5(1)	6(1)	0(1)
C(26)	23(2)	29(1)	21(2)	6(1)	8(1)	1(1)
S(2A)	113(6)	64(4)	37(4)	16(3)	-15(3)	-64(4)
C(25A)	31(7)	34(6)	15(6)	8(5)	6(5)	-8(5)
C(26A)	22(8)	40(9)	34(10)	5(8)	-3(7)	-3(6)
N(3)	35(1)	33(1)	48(1)	10(1)	2(1)	-5(1)
C(27)	43(2)	31(1)	27(1)	7(1)	-2(1)	-4(1)
O(3)	38(1)	32(1)	38(1)	7(1)	3(1)	3(1)
C(28)	51(2)	33(1)	56(2)	7(1)	-2(1)	-7(1)
C(14)	29(1)	20(1)	23(1)	7(1)	5(1)	-4(1)
C(15)	23(1)	20(1)	18(1)	7(1)	5(1)	1(1)
C(16)	20(1)	18(1)	19(1)	4(1)	5(1)	0(1)
C(17)	25(1)	22(1)	22(1)	9(1)	3(1)	-3(1)
O(4)	37(1)	17(1)	18(1)	7(1)	3(1)	-4(1)
C(18)	54(2)	25(1)	23(1)	11(1)	-1(1)	-14(1)
C(11S)	62(2)	25(1)	29(1)	6(1)	1(1)	7(1)
C(12S)	33(1)	26(1)	39(1)	6(1)	12(1)	6(1)
C(13S)	54(2)	31(1)	26(1)	1(1)	7(1)	18(1)
C(14S)	36(2)	32(1)	74(2)	-17(1)	-10(1)	8(1)
C(15S)	53(2)	25(1)	139(4)	-6(2)	58(2)	-8(1)
C(16S)	113(3)	24(1)	57(2)	10(1)	56(2)	4(2)
C(21S)	33(1)	38(1)	62(2)	-6(1)	-12(1)	12(1)
C(22S)	41(2)	29(1)	88(2)	4(1)	41(2)	3(1)
C(23S)	98(3)	38(2)	36(1)	14(1)	28(2)	29(2)

Table A3.1.6 *Hydrogen coordinates (x 10^4) and isotropic displacement parameters ($Å^2$x 10^3)for thioimidate* ***74***.

	x	y	z	U(eq)
H(2)	2680	8043	3591	31
H(3)	751	7934	4229	33
H(7A)	-748	6715	4943	58
H(7B)	126	7305	6076	58
H(7C)	-31	5967	5725	58
H(5)	2261	5567	5781	35
H(6)	4204	5656	5132	31
H(8)	4893	8383	2285	26
H(10A)	4497	8203	34	41
H(10B)	2896	8046	-50	41
H(10C)	4606	7820	-165	41
H(10D)	3316	8368	135	41
H(11A)	3191	6989	-1560	39
H(11B)	4477	6474	-967	39
H(11C)	2184	7308	-1307	23
H(11D)	3371	6519	-1371	23
H(19)	2541	5137	-2467	31
H(20A)	256	4384	-2935	33
H(20B)	354	5643	-2292	33
H(21A)	129	5017	-800	31
H(21B)	-1066	4334	-1731	31
H(23)	-1230	2299	-1479	31
H(19A)	611	5758	-2170	36
H(20C)	2703	5206	-2533	53
H(20D)	1451	4285	-3098	53
H(21C)	3169	3281	-2450	52
H(21D)	3586	4144	-1358	52
H(23A)	2188	1416	-1887	56

H(26A)	3533	3709	-1663	29
H(26B)	2149	3180	-2493	29
H(26C)	-339	3930	-2155	41
H(26D)	-392	4791	-1113	41
H(28A)	-268	-1808	-2143	74
H(28B)	-768	-1501	-1091	74
H(28C)	610	-2079	-1091	74
H(14)	2569	3168	1093	29
H(18A)	2247	3241	2712	53
H(18B)	3395	3320	3757	53
H(18C)	3677	2773	2662	53
H(11S)	7335	9887	8877	48
H(12S)	7630	9918	7226	38
H(13S)	5803	9503	5810	45
H(14S)	3653	9041	6007	66
H(15S)	3332	9010	7664	84
H(16S)	5194	9444	9106	70
H(21S)	8063	9311	3702	60
H(22S)	8170	9092	5381	60
H(23S)	10101	9776	6676	64

Table A3.1.7 *Torsion angles [°] for thioimidate* ***74***.

C(6)-C(1)-C(2)-C(3)	0.1(3)
S(1)-C(1)-C(2)-C(3)	-178.46(17)
C(1)-C(2)-C(3)-C(4)	0.2(3)
C(2)-C(3)-C(4)-C(5)	-0.2(3)
C(2)-C(3)-C(4)-C(7)	179.7(2)
C(3)-C(4)-C(5)-C(6)	-0.1(3)
C(7)-C(4)-C(5)-C(6)	180.0(2)
C(2)-C(1)-C(6)-C(5)	-0.4(3)
S(1)-C(1)-C(6)-C(5)	178.17(16)
C(4)-C(5)-C(6)-C(1)	0.4(3)
C(6)-C(1)-S(1)-O(2)	9.2(2)
C(2)-C(1)-S(1)-O(2)	-172.26(16)
C(6)-C(1)-S(1)-O(1)	-123.57(18)
C(2)-C(1)-S(1)-O(1)	55.01(19)
C(6)-C(1)-S(1)-N(1)	125.71(17)
C(2)-C(1)-S(1)-N(1)	-55.71(18)
O(2)-S(1)-N(1)-C(16)	48.3(2)
O(1)-S(1)-N(1)-C(16)	176.86(18)
C(1)-S(1)-N(1)-C(16)	-68.54(19)
O(2)-S(1)-N(1)-C(8)	-133.04(16)
O(1)-S(1)-N(1)-C(8)	-4.48(19)
C(1)-S(1)-N(1)-C(8)	110.12(17)
C(16)-N(1)-C(8)-C(9)	-1.4(2)
S(1)-N(1)-C(8)-C(9)	179.70(15)
N(1)-C(8)-C(9)-C(17)	0.6(2)
N(1)-C(8)-C(9)-C(10)	179.3(2)
C(8)-C(9)-C(10)-C(11)	159.6(3)
C(17)-C(9)-C(10)-C(11)	-21.8(3)
C(8)-C(9)-C(10)-C(11A)	-167.1(7)
C(17)-C(9)-C(10)-C(11A)	11.5(8)
C(9)-C(10)-C(11)-N(2)	45.5(3)
C(10)-C(11)-N(2)-C(12)	-50.7(4)
C(10)-C(11)-N(2)-C(19)	161.8(2)

C(11)-N(2)-C(12)-C(13)	-157.8(3)
C(19)-N(2)-C(12)-C(13)	-9.4(4)
C(11)-N(2)-C(12)-C(17)	27.9(4)
C(19)-N(2)-C(12)-C(17)	176.3(2)
N(2)-C(12)-C(13)-C(14)	-172.5(3)
C(17)-C(12)-C(13)-C(14)	1.8(4)
N(2)-C(12)-C(13)-C(25)	5.0(4)
C(17)-C(12)-C(13)-C(25)	179.3(2)
C(9)-C(10)-C(11A)-N(2A)	17.9(17)
C(10)-C(11A)-N(2A)-C(12A)	-34(2)
C(10)-C(11A)-N(2A)-C(19A)	-179.0(13)
C(11A)-N(2A)-C(12A)-C(13A)	-159(2)
C(19A)-N(2A)-C(12A)-C(13A)	-16(3)
C(11A)-N(2A)-C(12A)-C(17)	20(3)
C(19A)-N(2A)-C(12A)-C(17)	162.7(15)
N(2A)-C(12A)-C(13A)-C(25A)	10(3)
C(17)-C(12A)-C(13A)-C(25A)	-169.5(15)
N(2A)-C(12A)-C(13A)-C(14)	173.5(17)
C(17)-C(12A)-C(13A)-C(14)	-6(3)
C(12)-N(2)-C(19)-C(20)	98.6(3)
C(11)-N(2)-C(19)-C(20)	-114.1(3)
C(12)-N(2)-C(19)-C(26)	-23.5(3)
C(11)-N(2)-C(19)-C(26)	123.9(3)
N(2)-C(19)-C(20)-C(21)	-64.4(3)
C(26)-C(19)-C(20)-C(21)	58.5(4)
C(19)-C(20)-C(21)-C(22)	-50.6(4)
C(20)-C(21)-C(22)-C(23)	-125.2(3)
C(20)-C(21)-C(22)-C(25)	50.9(4)
C(21)-C(22)-C(23)-C(24)	174.4(3)
C(25)-C(22)-C(23)-C(24)	-1.7(3)
C(11A)-N(2A)-C(19A)-C(20A)	65.3(19)
C(12A)-N(2A)-C(19A)-C(20A)	-79(2)
C(11A)-N(2A)-C(19A)-C(26A)	-174.4(16)
C(12A)-N(2A)-C(19A)-C(26A)	41(2)
N(2A)-C(19A)-C(20A)-C(21A)	66(2)
C(26A)-C(19A)-C(20A)-C(21A)	-54(3)

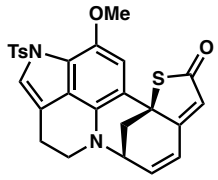
C(19A)-C(20A)-C(21A)-C(22A)	45(4)
C(20A)-C(21A)-C(22A)-C(23A)	129(3)
C(20A)-C(21A)-C(22A)-C(25A)	-45(4)
C(21A)-C(22A)-C(23A)-C(24)	-169(3)
C(25A)-C(22A)-C(23A)-C(24)	5(3)
C(22)-C(23)-C(24)-N(3)	-177.9(2)
C(22)-C(23)-C(24)-S(2)	-0.1(3)
C(22A)-C(23A)-C(24)-N(3)	170.0(14)
C(22A)-C(23A)-C(24)-S(2A)	-4(2)
N(3)-C(24)-S(2)-C(25)	179.0(2)
C(23)-C(24)-S(2)-C(25)	1.45(19)
C(23)-C(22)-C(25)-C(13)	-120.8(2)
C(21)-C(22)-C(25)-C(13)	62.6(3)
C(23)-C(22)-C(25)-C(26)	121.4(3)
C(21)-C(22)-C(25)-C(26)	-55.3(4)
C(23)-C(22)-C(25)-S(2)	2.6(3)
C(21)-C(22)-C(25)-S(2)	-174.0(2)
C(12)-C(13)-C(25)-C(22)	-87.6(3)
C(14)-C(13)-C(25)-C(22)	89.8(3)
C(12)-C(13)-C(25)-C(26)	30.7(3)
C(14)-C(13)-C(25)-C(26)	-151.9(3)
C(12)-C(13)-C(25)-S(2)	152.7(2)
C(14)-C(13)-C(25)-S(2)	-29.9(3)
C(24)-S(2)-C(25)-C(22)	-2.20(18)
C(24)-S(2)-C(25)-C(13)	120.95(18)
C(24)-S(2)-C(25)-C(26)	-119.1(2)
N(2)-C(19)-C(26)-C(25)	59.1(3)
C(20)-C(19)-C(26)-C(25)	-63.4(4)
C(22)-C(25)-C(26)-C(19)	59.6(4)
C(13)-C(25)-C(26)-C(19)	-61.4(3)
S(2)-C(25)-C(26)-C(19)	175.5(2)
N(3)-C(24)-S(2A)-C(25A)	-174.0(5)
C(23A)-C(24)-S(2A)-C(25A)	1.0(10)
C(23A)-C(22A)-C(25A)-C(26A)	-121.9(19)
C(21A)-C(22A)-C(25A)-C(26A)	54(3)
C(23A)-C(22A)-C(25A)-C(13A)	117.5(17)

C(21A)-C(22A)-C(25A)-C(13A)	-67(2)
C(23A)-C(22A)-C(25A)-S(2A)	-4(2)
C(21A)-C(22A)-C(25A)-S(2A)	172(2)
C(12A)-C(13A)-C(25A)-C(22A)	90(2)
C(14)-C(13A)-C(25A)-C(22A)	-72.9(18)
C(12A)-C(13A)-C(25A)-C(26A)	-29(2)
C(14)-C(13A)-C(25A)-C(26A)	168.0(16)
C(12A)-C(13A)-C(25A)-S(2A)	-151.8(16)
C(14)-C(13A)-C(25A)-S(2A)	45(2)
C(24)-S(2A)-C(25A)-C(22A)	1.6(12)
C(24)-S(2A)-C(25A)-C(26A)	119.9(15)
C(24)-S(2A)-C(25A)-C(13A)	-116.0(12)
N(2A)-C(19A)-C(26A)-C(25A)	-60(2)
C(20A)-C(19A)-C(26A)-C(25A)	63(2)
C(22A)-C(25A)-C(26A)-C(19A)	-63(2)
C(13A)-C(25A)-C(26A)-C(19A)	55(2)
S(2A)-C(25A)-C(26A)-C(19A)	179.8(16)
C(23)-C(24)-N(3)-C(27)	175.2(2)
C(23A)-C(24)-N(3)-C(27)	43.5(12)
S(2A)-C(24)-N(3)-C(27)	-143.2(3)
S(2)-C(24)-N(3)-C(27)	-2.2(4)
C(24)-N(3)-C(27)-O(3)	5.1(4)
C(24)-N(3)-C(27)-C(28)	-172.9(2)
C(12)-C(13)-C(14)-C(15)	-3.5(4)
C(25)-C(13)-C(14)-C(15)	179.2(2)
C(12A)-C(13A)-C(14)-C(15)	30(2)
C(25A)-C(13A)-C(14)-C(15)	-167.5(13)
C(13)-C(14)-C(15)-O(4)	-178.5(2)
C(13A)-C(14)-C(15)-O(4)	152.4(9)
C(13)-C(14)-C(15)-C(16)	1.6(3)
C(13A)-C(14)-C(15)-C(16)	-27.5(9)
O(4)-C(15)-C(16)-C(17)	-177.95(18)
C(14)-C(15)-C(16)-C(17)	2.0(3)
O(4)-C(15)-C(16)-N(1)	-0.6(3)
C(14)-C(15)-C(16)-N(1)	179.4(2)
C(8)-N(1)-C(16)-C(17)	1.6(2)

S(1)-N(1)-C(16)-C(17)	-179.63(16)
C(8)-N(1)-C(16)-C(15)	-176.1(2)
S(1)-N(1)-C(16)-C(15)	2.7(4)
C(15)-C(16)-C(17)-C(12)	-3.7(3)
N(1)-C(16)-C(17)-C(12)	178.2(2)
C(15)-C(16)-C(17)-C(9)	176.88(19)
N(1)-C(16)-C(17)-C(9)	-1.2(2)
C(15)-C(16)-C(17)-C(12A)	24.2(11)
N(1)-C(16)-C(17)-C(12A)	-153.9(10)
C(13)-C(12)-C(17)-C(16)	1.7(4)
N(2)-C(12)-C(17)-C(16)	176.6(2)
C(13)-C(12)-C(17)-C(9)	-179.0(2)
N(2)-C(12)-C(17)-C(9)	-4.1(4)
C(8)-C(9)-C(17)-C(16)	0.4(3)
C(10)-C(9)-C(17)-C(16)	-178.6(2)
C(8)-C(9)-C(17)-C(12)	-179.0(2)
C(10)-C(9)-C(17)-C(12)	2.0(4)
C(8)-C(9)-C(17)-C(12A)	153.5(10)
C(10)-C(9)-C(17)-C(12A)	-25.5(10)
C(13A)-C(12A)-C(17)-C(16)	-21(2)
N(2A)-C(12A)-C(17)-C(16)	159.8(13)
C(13A)-C(12A)-C(17)-C(9)	-170.8(14)
N(2A)-C(12A)-C(17)-C(9)	10(2)
C(14)-C(15)-O(4)-C(18)	-6.2(3)
C(16)-C(15)-O(4)-C(18)	173.8(2)
C(16S)-C(11S)-C(12S)-C(13S)	-0.2(4)
C(11S)-C(12S)-C(13S)-C(14S)	-0.2(4)
C(12S)-C(13S)-C(14S)-C(15S)	0.3(4)
C(13S)-C(14S)-C(15S)-C(16S)	-0.1(4)
C(12S)-C(11S)-C(16S)-C(15S)	0.3(4)
C(14S)-C(15S)-C(16S)-C(11S)	-0.2(4)
C(23S)#1-C(21S)-C(22S)-C(23S)	-0.1(5)
C(21S)-C(22S)-C(23S)-C(21S)#1	0.1(5)

Symmetry transformations used to generate equivalent atoms:
#1 -x+2,-y+2,-z+1

A3.2 X-RAY CRYSTAL STRUCTURE ANALYSIS OF DIENONE 130.



130

Contents

Table A3.2.1. Experimental Details

Table A3.2.2. Crystal Data

Table A3.2.3. Atomic Coordinates

Table A3.2.4. Full Bond Distances and Angles

Table A3.2.5. Anisotropic Displacement Parameters

Table A3.2.6. Hydrogen Atomic Coordinates

Table A3.2.7. Torsion Angles

Figure A3.2.1 *X-Ray Crystal Structure of dienone* ***130****.*

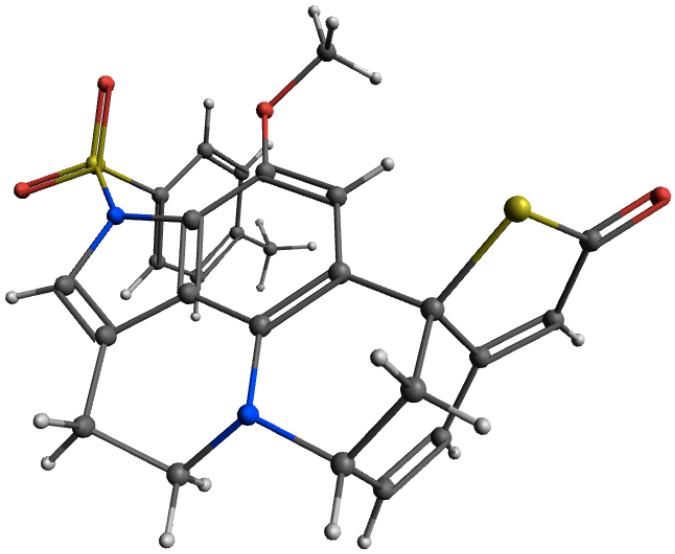


Table A3.2.1 *Experimental Details for X-Ray Structure Determination of dienone* ***130***.

Low-temperature diffraction data (ϕ-and ω-scans) were collected on a Bruker AXS D8 VENTURE KAPPA diffractometer coupled to a PHOTON II CPAD detector with Cu K_α radiation (λ = 1.54178 Å) from an IμS micro-source for the structure of compound V22129. The structure was solved by direct methods using SHELXS and refined against F^2 on all data by full-matrix least squares with SHELXL-2017 using established refinement techniques. All non-hydrogen atoms were refined anisotropically. All hydrogen atoms were included into the model at geometrically calculated positions and refined using a riding model. The isotropic displacement parameters of all hydrogen atoms were fixed to 1.2 times the U value of the atoms they are linked to (1.5 times for methyl groups). All disordered atoms were refined with the help of similarity restraints on the 1,2- and 1,3-distances and displacement parameters as well as enhanced rigid bond restraints for anisotropic displacement parameters.

Table A3.2.2 *Crystal Data and Structure Refinement for dienone* ***130***.

Identification code	V23030t5	
Empirical formula	C27.77 H25.55 Cl0.15 N2 O4.85 S2	
Formula weight	534.39	
Temperature	293(2) K	
Wavelength	1.54178 Å	
Crystal system	Monoclinic	
Space group	$P2_1/n$	
Unit cell dimensions	a = 12.9480(10) Å	a= 90°.
	b = 9.2322(7) Å	b= 105.963(5)°.
	c = 21.5405(16) Å	g = 90°.
Volume	2475.6(3) Å3	
Z	4	
Density (calculated)	1.434 Mg/m3	
Absorption coefficient	2.458 mm-1	
F(000)	1118	
Crystal size	0.100 x 0.100 x 0.100 mm3	
Theta range for data collection	3.604 to 74.640°.	
Index ranges -	16<=h<=15, 0<=k<=11, 0<=l<=26	
Reflections collected	9548	
Independent reflections	9548 [R(int) = ?]	
Completeness to theta = 67.679°	99.1 %	
Absorption correction	Semi-empirical from equivalents	

Max. and min. transmission 0.7538 and 0.6389

Refinement method Full-matrix least-squares on F2

Data / restraints / parameters 9548 / 9 / 349

Goodness-of-fit on F2 1.083

Final R indices [I>2sigma(I)] R1 = 0.0402, wR2 = 0.1294

R indices (all data) R1 = 0.0424, wR2 = 0.1341

Extinction coefficient n/a

Largest diff. peak and hole 0.438 and -0.469 e.Å-3

Table A3.2.3 *Atomic coordinates (x 104) and equivalent isotropic displacement parameters (Å2x 103) for dienone* ***130****. U(eq) is defined as one third of the trace of the orthogonalized Uij tensor.*

	x	y	z	U (eq)
S(1)	7235(1)	9050(1)	5511(1)	18(1)
C(1)	6129(2)	9442(3)	4822(1)	20(1)
O(1)	5869(2)	10669(2)	4641(1)	28(1)
C(2)	5658(2)	8090(3)	4520(1)	19(1)
C(3)	6144(2)	6889(3)	4807(1)	16(1)
C(4)	5978(2)	5407(3)	4570(1)	19(1)
C(5)	6733(2)	4393(3)	4773(1)	20(1)
C(6)	7772(2)	4688(2)	5294(1)	16(1)
N(1)	7696(2)	4177(2)	5929(1)	15(1)
C(7)	7550(2)	2602(2)	5981(1)	17(1)
C(8)	7654(2)	2120(3)	6678(1)	19(1)
C(9)	6914(2)	3022(2)	6947(1)	15(1)
C(17)	6669(2)	4439(2)	6687(1)	14(1)
C(18)	7031(2)	5038(2)	6188(1)	14(1)
C(10)	6416(2)	2865(2)	7420(1)	17(1)
N(2)	5863(2)	4180(2)	7473(1)	16(1)
S(2)	4970(1)	4250(1)	7903(1)	17(1)

O(3)	5099(1)	5582(2)	8252(1)	23(1)
O(4)	5106(1)	2900(2)	8245(1)	23(1)
C(20)	3712(2)	4248(3)	7324(1)	17(1)
C(21)	3039(2)	5433(3)	7277(1)	24(1)
C(22)	2017(2)	5369(3)	6855(1)	26(1)
C(23)	1656(2)	4147(3)	6478(1)	23(1)
C(26)	538(2)	4090(4)	6034(2)	34(1)
C(24)	2361(2)	2986(3)	6522(1)	23(1)
C(25)	3387(2)	3021(3)	6946(1)	21(1)
C(11)	6013(2)	5158(2)	6998(1)	14(1)
C(12)	5662(2)	6572(3)	6804(1)	15(1)
O(2)	5001(1)	7251(2)	7109(1)	21(1)
C(19)	4898(3)	8784(3)	7036(2)	38(1)
C(13)	6016(2)	7173(2)	6307(1)	15(1)
C(14)	6695(2)	6438(2)	5997(1)	14(1)
C(15)	7032(2)	7103(2)	5430(1)	15(1)
C(16)	8032(2)	6303(2)	5354(1)	16(1)
O(1S)	4260(8)	2652(13)	9658(5)	104(3)
C(1S)	2782(8)	3909(9)	8865(5)	33(2)
C(2S)	3731(7)	3708(7)	9423(4)	21(2)
O(2S)	4378(5)	4986(7)	9660(3)	32(1)
C(3S)	5309(7)	4846(8)	10228(4)	25(2)
C(4S)	5903(6)	6276(7)	10425(3)	17(1)

C(1T)	3970(110)	5300(200)	8990(100)	400(190)
Cl(1T)	3079(11)	3857(13)	9023(7)	36(4)
Cl(2T)	4880(19)	4490(40)	9681(12)	107(8)

Table A3.2.4 *Bond lengths [Å] and angles [°] for dienone* ***130***.

S(1)-C(1)	1.793(2)
S(1)-C(15)	1.819(2)
C(1)-O(1)	1.215(3)
C(1)-C(2)	1.461(3)
C(2)-C(3)	1.339(3)
C(2)-H(2)	0.9300
C(3)-C(4)	1.455(3)
C(3)-C(15)	1.521(3)
C(4)-C(5)	1.338(4)
C(4)-H(4)	0.9300
C(5)-C(6)	1.521(3)
C(5)-H(5)	0.9300
C(6)-N(1)	1.476(3)
C(6)-C(16)	1.526(3)
C(6)-H(6)	0.9800
N(1)-C(18)	1.396(3)
N(1)-C(7)	1.475(3)
C(7)-C(8)	1.536(3)
C(7)-H(7A)	0.9700
C(7)-H(7B)	0.9700
C(8)-C(9)	1.500(3)

C(8)-H(8A) 0.9700

C(8)-H(8B) 0.9700

C(9)-C(10) 1.355(3)

C(9)-C(17) 1.423(3)

C(17)-C(11) 1.387(3)

C(17)-C(18) 1.400(3)

C(18)-C(14) 1.389(3)

C(10)-N(2) 1.431(3)

C(10)-H(10) 0.9300

N(2)-C(11) 1.417(3)

N(2)-S(2) 1.669(2)

S(2)-O(3) 1.4268(18)

S(2)-O(4) 1.4348(18)

S(2)-C(20) 1.758(2)

C(20)-C(21) 1.385(4)

C(20)-C(25) 1.392(3)

C(21)-C(22) 1.385(4)

C(21)-H(21) 0.9300

C(22)-C(23) 1.394(4)

C(22)-H(22) 0.9300

C(23)-C(24) 1.394(4)

C(23)-C(26) 1.500(4)

C(26)-H(26A) 0.9600

C(26)-H(26B) 0.9600

C(26)-H(26C) 0.9600

C(24)-C(25) 1.391(4)

C(24)-H(24) 0.9300

C(25)-H(25) 0.9300

C(11)-C(12) 1.408(3)

C(12)-O(2) 1.366(3)

C(12)-C(13) 1.390(3)

O(2)-C(19) 1.426(3)

C(19)-H(19A) 0.9600

C(19)-H(19B) 0.9600

C(19)-H(19C) 0.9600

C(13)-C(14) 1.416(3)

C(13)-H(13) 0.9300

C(14)-C(15) 1.534(3)

C(15)-C(16) 1.538(3)

C(16)-H(16A) 0.9700

C(16)-H(16B) 0.9700

O(1S)-C(2S) 1.218(13)

C(1S)-C(2S) 1.476(11)

C(1S)-H(1S1) 0.9600

C(1S)-H(1S2) 0.9600

C(1S)-H(1S3) 0.9600

C(2S)-O(2S) 1.455(9)

O(2S)-C(3S) 1.468(10)

C(3S)-C(4S) 1.528(9)

C(3S)-H(3S1) 0.9700

C(3S)-H(3S2) 0.9700

C(4S)-H(4S1) 0.9600

C(4S)-H(4S2) 0.9600

C(4S)-H(4S3) 0.9600

C(1T)-Cl(1T) 1.80(3)

C(1T)-Cl(2T) 1.80(3)

C(1T)-H(1T1) 0.9700

C(1T)-H(1T2) 0.9700

Cl(1T)-Cl(2T) 2.44(2)

C(1)-S(1)-C(15) 93.37(11)

O(1)-C(1)-C(2) 127.5(2)

O(1)-C(1)-S(1) 122.8(2)

C(2)-C(1)-S(1) 109.68(17)

C(3)-C(2)-C(1) 114.6(2)

C(3)-C(2)-H(2) 122.7

C(1)-C(2)-H(2) 122.7

C(2)-C(3)-C(4) 127.7(2)

C(2)-C(3)-C(15) 116.4(2)

C(4)-C(3)-C(15)	115.71(19)
C(5)-C(4)-C(3)	121.3(2)
C(5)-C(4)-H(4)	119.4
C(3)-C(4)-H(4)	119.4
C(4)-C(5)-C(6)	122.3(2)
C(4)-C(5)-H(5)	118.9
C(6)-C(5)-H(5)	118.9
N(1)-C(6)-C(5)	110.90(19)
N(1)-C(6)-C(16)	107.63(17)
C(5)-C(6)-C(16)	111.57(19)
N(1)-C(6)-H(6)	108.9
C(5)-C(6)-H(6)	108.9
C(16)-C(6)-H(6)	108.9
C(18)-N(1)-C(7)	115.17(19)
C(18)-N(1)-C(6)	113.17(18)
C(7)-N(1)-C(6)	115.35(18)
N(1)-C(7)-C(8)	112.43(18)
N(1)-C(7)-H(7A)	109.1
C(8)-C(7)-H(7A)	109.1
N(1)-C(7)-H(7B)	109.1
C(8)-C(7)-H(7B)	109.1
H(7A)-C(7)-H(7B)	107.9
C(9)-C(8)-C(7)	108.80(18)

C(9)-C(8)-H(8A)	109.9
C(7)-C(8)-H(8A)	109.9
C(9)-C(8)-H(8B)	109.9
C(7)-C(8)-H(8B)	109.9
H(8A)-C(8)-H(8B)	108.3
C(10)-C(9)-C(17)	107.0(2)
C(10)-C(9)-C(8)	135.8(2)
C(17)-C(9)-C(8)	117.2(2)
C(11)-C(17)-C(18)	124.1(2)
C(11)-C(17)-C(9)	110.5(2)
C(18)-C(17)-C(9)	125.4(2)
C(14)-C(18)-N(1)	126.1(2)
C(14)-C(18)-C(17)	116.9(2)
N(1)-C(18)-C(17)	117.1(2)
C(9)-C(10)-N(2)	108.79(19)
C(9)-C(10)-H(10)	125.6
N(2)-C(10)-H(10)	125.6
C(11)-N(2)-C(10)	108.16(18)
C(11)-N(2)-S(2)	128.92(16)
C(10)-N(2)-S(2)	121.11(15)
O(3)-S(2)-O(4)	119.85(10)
O(3)-S(2)-N(2)	109.11(10)
O(4)-S(2)-N(2)	104.22(10)

O(3)-S(2)-C(20)	109.01(11)
O(4)-S(2)-C(20)	108.81(11)
N(2)-S(2)-C(20)	104.78(10)
C(21)-C(20)-C(25)	121.1(2)
C(21)-C(20)-S(2)	119.54(19)
C(25)-C(20)-S(2)	119.21(19)
C(22)-C(21)-C(20)	118.9(2)
C(22)-C(21)-H(21)	120.5
C(20)-C(21)-H(21)	120.5
C(21)-C(22)-C(23)	121.6(2)
C(21)-C(22)-H(22)	119.2
C(23)-C(22)-H(22)	119.2
C(22)-C(23)-C(24)	118.3(2)
C(22)-C(23)-C(26)	120.7(2)
C(24)-C(23)-C(26)	121.0(2)
C(23)-C(26)-H(26A)	109.5
C(23)-C(26)-H(26B)	109.5
H(26A)-C(26)-H(26B)	109.5
C(23)-C(26)-H(26C)	109.5
H(26A)-C(26)-H(26C)	109.5
H(26B)-C(26)-H(26C)	109.5
C(25)-C(24)-C(23)	121.1(2)
C(25)-C(24)-H(24)	119.5

C(23)-C(24)-H(24) 119.5

C(24)-C(25)-C(20) 118.9(2)

C(24)-C(25)-H(25) 120.5

C(20)-C(25)-H(25) 120.5

C(17)-C(11)-C(12) 119.4(2)

C(17)-C(11)-N(2) 105.49(19)

C(12)-C(11)-N(2) 135.2(2)

O(2)-C(12)-C(13) 124.7(2)

O(2)-C(12)-C(11) 118.4(2)

C(13)-C(12)-C(11) 116.8(2)

C(12)-O(2)-C(19) 117.0(2)

O(2)-C(19)-H(19A) 109.5

O(2)-C(19)-H(19B) 109.5

H(19A)-C(19)-H(19B) 109.5

O(2)-C(19)-H(19C) 109.5

H(19A)-C(19)-H(19C) 109.5

H(19B)-C(19)-H(19C) 109.5

C(12)-C(13)-C(14) 123.5(2)

C(12)-C(13)-H(13) 118.3

C(14)-C(13)-H(13) 118.3

C(18)-C(14)-C(13) 119.4(2)

C(18)-C(14)-C(15) 118.3(2)

C(13)-C(14)-C(15) 122.3(2)

C(3)-C(15)-C(14)	109.85(18)
C(3)-C(15)-C(16)	107.38(18)
C(14)-C(15)-C(16)	108.91(18)
C(3)-C(15)-S(1)	105.50(15)
C(14)-C(15)-S(1)	112.64(15)
C(16)-C(15)-S(1)	112.38(16)
C(6)-C(16)-C(15)	107.76(18)
C(6)-C(16)-H(16A)	110.2
C(15)-C(16)-H(16A)	110.2
C(6)-C(16)-H(16B)	110.2
C(15)-C(16)-H(16B)	110.2
H(16A)-C(16)-H(16B)	108.5
C(2S)-C(1S)-H(1S1)	109.5
C(2S)-C(1S)-H(1S2)	109.5
H(1S1)-C(1S)-H(1S2)	109.5
C(2S)-C(1S)-H(1S3)	109.5
H(1S1)-C(1S)-H(1S3)	109.5
H(1S2)-C(1S)-H(1S3)	109.5
O(1S)-C(2S)-O(2S)	107.4(9)
O(1S)-C(2S)-C(1S)	133.3(9)
O(2S)-C(2S)-C(1S)	117.0(6)
C(2S)-O(2S)-C(3S)	118.8(5)
O(2S)-C(3S)-C(4S)	113.0(5)

O(2S)-C(3S)-H(3S1) 109.0

C(4S)-C(3S)-H(3S1) 109.0

O(2S)-C(3S)-H(3S2) 109.0

C(4S)-C(3S)-H(3S2) 109.0

H(3S1)-C(3S)-H(3S2) 107.8

C(3S)-C(4S)-H(4S1) 109.5

C(3S)-C(4S)-H(4S2) 109.5

H(4S1)-C(4S)-H(4S2) 109.5

C(3S)-C(4S)-H(4S3) 109.5

H(4S1)-C(4S)-H(4S3) 109.5

H(4S2)-C(4S)-H(4S3) 109.5

Cl(1T)-C(1T)-Cl(2T) 85.5(15)

Cl(1T)-C(1T)-H(1T1) 114.4

Cl(2T)-C(1T)-H(1T1) 114.4

Cl(1T)-C(1T)-H(1T2) 114.4

Cl(2T)-C(1T)-H(1T2) 114.4

H(1T1)-C(1T)-H(1T2) 111.5

C(1T)-Cl(1T)-Cl(2T) 47.3(10)

C(1T)-Cl(2T)-Cl(1T) 47.2(10)

Symmetry transformations used to generate equivalent atoms:

Table A3.2.5 *Anisotropic displacement parameters (Å2x 103) for dienone* ***130****. The anisotropic displacement factor exponent takes the form: -2p2[h2 a*2U11 + ... + 2 h k a* b* U12]*

	U11	U22	U33	U23	U13	U12
S(1)	23(1)	12(1)	17(1)	1(1)	3(1)	-2(1)
C(1)	24(1)	17(1)	19(1)	4(1)	6(1)	2(1)
O(1)	35(1)	18(1)	27(1)	6(1)	4(1)	4(1)
C(2)	20(1)	21(1)	15(1)	1(1)	1(1)	3(1)
C(3)	16(1)	18(1)	14(1)	0(1)	5(1)	-2(1)
C(4)	21(1)	19(1)	14(1)	-3(1)	0(1)	-3(1)
C(5)	28(1)	14(1)	15(1)	-4(1)	2(1)	-2(1)
C(6)	18(1)	16(1)	15(1)	-1(1)	5(1)	2(1)
N(1)	17(1)	12(1)	14(1)	1(1)	4(1)	1(1)
C(7)	21(1)	11(1)	19(1)	0(1)	4(1)	2(1)
C(8)	22(1)	14(1)	19(1)	2(1)	2(1)	3(1)
C(9)	15(1)	14(1)	15(1)	1(1)	-1(1)	1(1)
C(17)	15(1)	13(1)	13(1)	0(1)	-1(1)	-1(1)
C(18)	13(1)	13(1)	14(1)	-2(1)	1(1)	-1(1)
C(10)	17(1)	14(1)	17(1)	4(1)	0(1)	1(1)
N(2)	16(1)	15(1)	15(1)	3(1)	4(1)	1(1)
S(2)	17(1)	22(1)	13(1)	1(1)	4(1)	-3(1)

O(3)	25(1)	28(1)	17(1)	-5(1)	8(1)	-6(1)
O(4)	22(1)	28(1)	20(1)	9(1)	6(1)	-2(1)
C(20)	14(1)	21(1)	17(1)	2(1)	6(1)	-2(1)
C(21)	23(1)	23(1)	29(1)	-6(1)	10(1)	1(1)
C(22)	21(1)	26(1)	33(1)	0(1)	8(1)	7(1)
C(23)	18(1)	30(1)	21(1)	4(1)	5(1)	0(1)
C(26)	17(1)	45(2)	34(2)	2(1)	0(1)	3(1)
C(24)	23(1)	23(1)	22(1)	-2(1)	3(1)	-2(1)
C(25)	21(1)	19(1)	22(1)	1(1)	4(1)	2(1)
C(11)	13(1)	15(1)	12(1)	1(1)	0(1)	-2(1)
C(12)	14(1)	16(1)	14(1)	-2(1)	2(1)	2(1)
O(2)	23(1)	20(1)	21(1)	1(1)	10(1)	7(1)
C(19)	61(2)	27(2)	34(2)	8(1)	27(1)	24(1)
C(13)	17(1)	12(1)	15(1)	0(1)	1(1)	1(1)
C(14)	14(1)	14(1)	11(1)	-1(1)	0(1)	-2(1)
C(15)	18(1)	10(1)	15(1)	0(1)	3(1)	-1(1)
C(16)	*16(1)*	*16(1)*	*16(1)*	*0(1)*	*4(1)*	*-1(1)*

Table A3.2.6 *Hydrogen coordinates (x 104) and isotropic displacement parameters (Å2x 10 3)for dienone* ***130***.

	x	y	z	U(eq)
H(2)	5068	8066	4158	23
H(4)	5333	5160	4273	23
H(5)	6620	3475	4589	24
H(6)	8360	4176	5184	19
H(7A)	8083	2098	5822	21
H(7B)	6846	2331	5711	21
H(8A)	7465	1104	6685	23
H(8B)	8389	2242	6939	23
H(10)	6432	2037	7668	20
H(21)	3269	6257	7524	29
H(22)	1560	6160	6824	32
H(26A)		451	4838	5715 50
H(26B)		29	4232	6280 50
H(26C)		418	3163	5825 50
H(24)	2141	2174	6263	28
H(25)	3849	2236	6976	25
H(19A)		5599	9218	7149 56
H(19B)		4494	9152	7315 56

H(19C)	4533	9014	6596	56
H(13)	5795	8107	6172	18
H(16A)	8216	6643	4972	19
H(16B)	8638	6480	5727	19
H(1S1)	3008	4254	8502	50
H(1S2)	2307	4604	8972	50
H(1S3)	2415	3002	8757	50
H(3S1)	5804	4143	10136	30
H(3S2)	5069	4481	10587	30
H(4S1)	6128	6656	10069	26
H(4S2)	6520	6113	10785	26
H(4S3)	5432	6957	10547	26
H(1T1)	3705	6277	9084	475
H(1T2)	4215	5359	8609	475

Table A3.2.7 *Torsion angles [°] for dienone* ***130****.*

C(15)-S(1)-C(1)-O(1) 179.4(2)

C(15)-S(1)-C(1)-C(2) -3.11(18)

O(1)-C(1)-C(2)-C(3) 176.6(3)

S(1)-C(1)-C(2)-C(3) -0.7(3)

C(1)-C(2)-C(3)-C(4) -169.8(2)

C(1)-C(2)-C(3)-C(15) 5.4(3)

C(2)-C(3)-C(4)-C(5) 156.7(3)

C(15)-C(3)-C(4)-C(5) -18.5(3)

C(3)-C(4)-C(5)-C(6) 4.5(4)

C(4)-C(5)-C(6)-N(1) 97.8(3)

C(4)-C(5)-C(6)-C(16) -22.2(3)

C(5)-C(6)-N(1)-C(18) -72.3(2)

C(16)-C(6)-N(1)-C(18) 50.0(2)

C(5)-C(6)-N(1)-C(7) 63.3(3)

C(16)-C(6)-N(1)-C(7) -174.39(18)

C(18)-N(1)-C(7)-C(8) -54.2(3)

C(6)-N(1)-C(7)-C(8) 171.10(19)

N(1)-C(7)-C(8)-C(9) 52.5(3)

C(7)-C(8)-C(9)-C(10) 156.0(3)

C(7)-C(8)-C(9)-C(17) -27.5(3)

C(10)-C(9)-C(17)-C(11) -0.3(3)

C(8)-C(9)-C(17)-C(11)	-177.7(2)
C(10)-C(9)-C(17)-C(18)	179.8(2)
C(8)-C(9)-C(17)-C(18)	2.3(3)
C(7)-N(1)-C(18)-C(14)	-153.2(2)
C(6)-N(1)-C(18)-C(14)	-17.5(3)
C(7)-N(1)-C(18)-C(17)	26.9(3)
C(6)-N(1)-C(18)-C(17)	162.57(19)
C(11)-C(17)-C(18)-C(14)	-0.5(3)
C(9)-C(17)-C(18)-C(14)	179.4(2)
C(11)-C(17)-C(18)-N(1)	179.4(2)
C(9)-C(17)-C(18)-N(1)	-0.7(3)
C(17)-C(9)-C(10)-N(2)	-0.8(2)
C(8)-C(9)-C(10)-N(2)	176.0(2)
C(9)-C(10)-N(2)-C(11)	1.6(2)
C(9)-C(10)-N(2)-S(2)	167.59(16)
C(11)-N(2)-S(2)-O(3)	-57.6(2)
C(10)-N(2)-S(2)-O(3)	139.63(17)
C(11)-N(2)-S(2)-O(4)	173.28(19)
C(10)-N(2)-S(2)-O(4)	10.5(2)
C(11)-N(2)-S(2)-C(20)	59.0(2)
C(10)-N(2)-S(2)-C(20)	-103.76(18)
O(3)-S(2)-C(20)-C(21)	-0.4(2)
O(4)-S(2)-C(20)-C(21)	132.0(2)

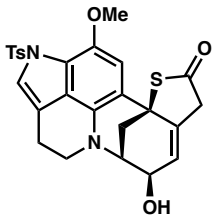
N(2)-S(2)-C(20)-C(21)	-117.0(2)
O(3)-S(2)-C(20)-C(25)	-176.84(18)
O(4)-S(2)-C(20)-C(25)	-44.5(2)
N(2)-S(2)-C(20)-C(25)	66.5(2)
C(25)-C(20)-C(21)-C(22)	1.5(4)
S(2)-C(20)-C(21)-C(22)	-174.9(2)
C(20)-C(21)-C(22)-C(23)	-0.3(4)
C(21)-C(22)-C(23)-C(24)	-1.4(4)
C(21)-C(22)-C(23)-C(26)	178.7(3)
C(22)-C(23)-C(24)-C(25)	2.0(4)
C(26)-C(23)-C(24)-C(25)	-178.1(2)
C(23)-C(24)-C(25)-C(20)	-0.8(4)
C(21)-C(20)-C(25)-C(24)	-1.0(4)
S(2)-C(20)-C(25)-C(24)	175.43(19)
C(18)-C(17)-C(11)-C(12)	1.1(3)
C(9)-C(17)-C(11)-C(12)	-178.92(19)
C(18)-C(17)-C(11)-N(2)	-178.8(2)
C(9)-C(17)-C(11)-N(2)	1.2(2)
C(10)-N(2)-C(11)-C(17)	-1.7(2)
S(2)-N(2)-C(11)-C(17)	-166.24(17)
C(10)-N(2)-C(11)-C(12)	178.5(2)
S(2)-N(2)-C(11)-C(12)	13.9(4)
C(17)-C(11)-C(12)-O(2)	178.8(2)

N(2)-C(11)-C(12)-O(2)	-1.4(4)
C(17)-C(11)-C(12)-C(13)	-0.8(3)
N(2)-C(11)-C(12)-C(13)	179.0(2)
C(13)-C(12)-O(2)-C(19)	-17.4(3)
C(11)-C(12)-O(2)-C(19)	163.1(2)
O(2)-C(12)-C(13)-C(14)	-179.5(2)
C(11)-C(12)-C(13)-C(14)	0.1(3)
N(1)-C(18)-C(14)-C(13)	179.9(2)
C(17)-C(18)-C(14)-C(13)	-0.2(3)
N(1)-C(18)-C(14)-C(15)	3.0(3)
C(17)-C(18)-C(14)-C(15)	-177.10(19)
C(12)-C(13)-C(14)-C(18)	0.4(3)
C(12)-C(13)-C(14)-C(15)	177.2(2)
C(2)-C(3)-C(15)-C(14)	114.3(2)
C(4)-C(3)-C(15)-C(14)	-69.8(3)
C(2)-C(3)-C(15)-C(16)	-127.4(2)
C(4)-C(3)-C(15)-C(16)	48.5(3)
C(2)-C(3)-C(15)-S(1)	-7.3(3)
C(4)-C(3)-C(15)-S(1)	168.52(17)
C(18)-C(14)-C(15)-C(3)	95.5(2)
C(13)-C(14)-C(15)-C(3)	-81.4(3)
C(18)-C(14)-C(15)-C(16)	-21.9(3)
C(13)-C(14)-C(15)-C(16)	161.3(2)

C(18)-C(14)-C(15)-S(1)	-147.26(17)
C(13)-C(14)-C(15)-S(1)	35.9(3)
C(1)-S(1)-C(15)-C(3)	5.52(17)
C(1)-S(1)-C(15)-C(14)	-114.32(17)
C(1)-S(1)-C(15)-C(16)	122.22(16)
N(1)-C(6)-C(16)-C(15)	-70.1(2)
C(5)-C(6)-C(16)-C(15)	51.8(2)
C(3)-C(15)-C(16)-C(6)	-64.7(2)
C(14)-C(15)-C(16)-C(6)	54.2(2)
S(1)-C(15)-C(16)-C(6)	179.75(14)
O(1S)-C(2S)-O(2S)-C(3S)	-17.0(9)
C(1S)-C(2S)-O(2S)-C(3S)	178.0(6)
C(2S)-O(2S)-C(3S)-C(4S)	-179.3(7)

Symmetry transformations used to generate equivalent atoms:

A3.3 X-RAY CRYSTAL STRUCTURE ANALYSIS OF ALLYLIC ALCOHOL 137.



137

Contents

Table A3.3.1. Experimental Details

Table A3.3.2. Crystal Data

Table A3.3.3. Atomic Coordinates

Table A3.3.4. Full Bond Distances and Angles

Table A3.3.5. Anisotropic Displacement Parameters

Table A3.3.6. Hydrogen Atomic Coordinates

Table A3.3.7. Torsion Angles

Table A3.3.8, Hydrogen Bond Distances and Angles

Figure A3.3.1 *X-Ray Crystal Structure of Allylic Alcohol* ***137****.*

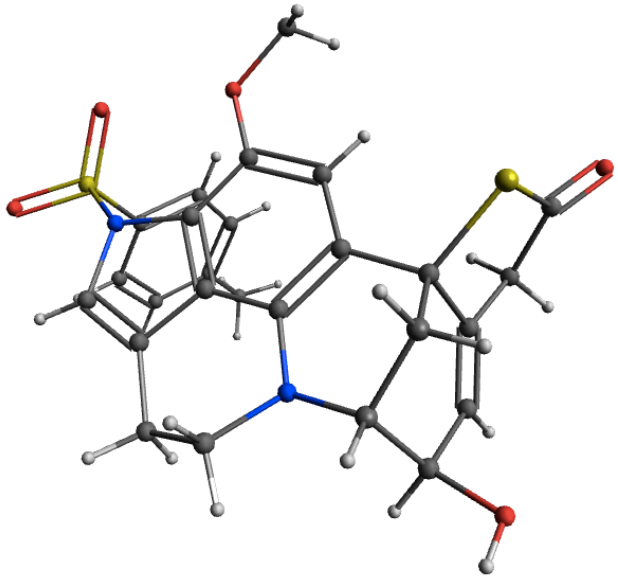


Table A3.3.1 *Experimental Details for X-Ray Structure Determination of Allylic Alcohol* ***137****.*

Low-temperature diffraction data (ϕ-and ω-scans) were collected on a Bruker AXS D8 VENTURE KAPPA diffractometer coupled to a PHOTON II CPAD detector with Cu K_α radiation (λ = 1.54178 Å) from an IμS micro-source for the structure of compound V22129. The structure was solved by direct methods using SHELXS and refined against F^2 on all data by full-matrix least squares with SHELXL-2017 using established refinement techniques. All non-hydrogen atoms were refined anisotropically. All hydrogen atoms were included into the model at geometrically calculated positions and refined using a riding model. The isotropic displacement parameters of all hydrogen atoms were fixed to 1.2 times the U value of the atoms they are linked to (1.5 times for methyl groups). All disordered atoms were refined with the help of similarity restraints on the 1,2- and 1,3-distances and displacement parameters as well as enhanced rigid bond restraints for anisotropic displacement parameters.

Compound **137** crystallizes in the triclinic space group P-1 with one molecule in the asymmetric unit along with one molecule of dicholoromethane. The highest residual density are located in the bonds between atoms. The coordinates for the hydrogen atoms bound to O2 were located in the difference Fourier synthesis and refined semi-freely with the help of a restraint on the O-H distance (0.84(4) Å).

Table A3.3.2 *Crystal Data and Structure Refinement for Allylic Alcohol* ***137****.*

Identification code	V23243	
Empirical formula	C27 H26 Cl2 N2 O5 S2	
Formula weight	593.52	
Temperature	100(2) K	
Wavelength	1.54178 Å	
Crystal system	Triclinic	
Space group	P-1	
Unit cell dimensions	a = 9.9341(11) Å	a= 68.752(6)°.
	b = 11.1021(10) Å	b= 79.513(6)°.
	c = 12.9734(11) Å	g = 81.600(8)°.
Volume	1306.3(2) $Å^3$	
Z	2	
Density (calculated)	1.509 Mg/m^3	
Absorption coefficient	4.093 mm^{-1}	
F(000)	616	
Crystal size	0.100 x 0.100 x 0.050 mm^3	
Theta range for data collection	3.692 to 74.612°.	
Index ranges	-12<=h<=12, -13<=k<=13, -16<=l<=16	
Reflections collected	39783	
Independent reflections	5328 [R(int) = 0.0583]	
Completeness to theta = 67.679°	99.9 %	
Absorption correction	Semi-empirical from equivalents	
Max. and min. transmission	0.7538 and 0.5834	
Refinement method	Full-matrix least-squares on F^2	
Data / restraints / parameters	5328 / 1 / 348	
Goodness-of-fit on F^2	1.027	
Final R indices [I>2sigma(I)]	R1 = 0.0411, wR2 = 0.1048	
R indices (all data)	R1 = 0.0480, wR2 = 0.1098	
Extinction coefficient	n/a	
Largest diff. peak and hole	0.455 and -0.444 $e.Å^{-3}$	

Table A3.3.3 *Atomic coordinates (x 10^4) and equivalent isotropic displacement parameters ($Å^2$x 10^3) for Allylic Alcohol* ***137****. U(eq) is defined as one third of the trace of the orthogonalized U^{ij} tensor.*

	x	y	z	U(eq)
S(1)	7922(1)	4539(1)	6722(1)	23(1)
C(1)	6124(2)	4537(2)	7229(2)	26(1)
O(1)	5678(2)	3996(2)	8190(1)	37(1)
C(2)	5301(2)	5258(2)	6296(2)	21(1)
C(3)	6226(2)	6161(2)	5370(2)	20(1)
C(4)	5886(2)	7375(2)	4750(2)	22(1)
C(5)	6901(2)	8273(2)	3936(2)	23(1)
O(2)	7099(2)	9158(2)	4456(1)	26(1)
C(6)	8269(2)	7527(2)	3686(2)	22(1)
N(1)	8121(2)	6857(2)	2926(1)	22(1)
C(7)	8781(2)	7422(2)	1760(2)	24(1)
C(8)	8283(2)	6921(2)	951(2)	24(1)
C(9)	8385(2)	5464(2)	1411(2)	19(1)
C(10)	8541(2)	4501(2)	987(2)	20(1)
N(2)	8515(2)	3278(2)	1874(1)	18(1)
C(11)	8269(2)	3522(2)	2905(2)	18(1)
C(12)	8128(2)	2759(2)	4046(2)	18(1)
O(3)	8242(2)	1436(1)	4369(1)	24(1)
C(19)	8383(3)	731(2)	5520(2)	28(1)
C(13)	7897(2)	3424(2)	4803(2)	19(1)
C(14)	7886(2)	4776(2)	4484(2)	20(1)
C(17)	8095(2)	5520(2)	3353(2)	19(1)
C(18)	8241(2)	4863(2)	2595(2)	18(1)
C(15)	7692(2)	5535(2)	5277(2)	20(1)
C(16)	8709(2)	6586(2)	4790(2)	22(1)
S(2)	8012(1)	2056(1)	1606(1)	18(1)
O(4)	8542(2)	2268(2)	459(1)	24(1)
O(5)	8426(2)	873(1)	2439(1)	23(1)

C(20)	6215(2)	2304(2)	1746(2)	19(1)
C(21)	5601(2)	3059(2)	807(2)	23(1)
C(22)	4178(2)	3258(2)	908(2)	24(1)
C(23)	3364(2)	2712(2)	1929(2)	22(1)
C(24)	4009(2)	1973(2)	2861(2)	22(1)
C(26)	1817(2)	2887(2)	2036(2)	28(1)
C(25)	5427(2)	1766(2)	2780(2)	21(1)
C(1S)	6900(3)	913(3)	9056(3)	44(1)
Cl(1S)	5618(1)	831(1)	8303(1)	66(1)
Cl(2S)	8520(1)	274(1)	8573(1)	47(1)

Table A3.3.4 *Bond lengths [Å] and angles [°] for allylic alcohol* ***137****.*

S(1)-C(1)	1.788(2)
S(1)-C(15)	1.836(2)
C(1)-O(1)	1.202(3)
C(1)-C(2)	1.497(3)
C(2)-C(3)	1.512(3)
C(2)-H(2A)	0.9900
C(2)-H(2B)	0.9900
C(3)-C(4)	1.326(3)
C(3)-C(15)	1.523(3)
C(4)-C(5)	1.506(3)
C(4)-H(4)	0.9500
C(5)-O(2)	1.430(3)
C(5)-C(6)	1.531(3)
C(5)-H(5)	1.0000
O(2)-H(2)	0.831(18)
C(6)-N(1)	1.472(3)
C(6)-C(16)	1.530(3)
C(6)-H(6)	1.0000
N(1)-C(17)	1.386(3)
N(1)-C(7)	1.477(3)
C(7)-C(8)	1.533(3)
C(7)-H(7A)	0.9900
C(7)-H(7B)	0.9900
C(8)-C(9)	1.502(3)
C(8)-H(8A)	0.9900
C(8)-H(8B)	0.9900
C(9)-C(10)	1.348(3)
C(9)-C(18)	1.425(3)
C(10)-N(2)	1.426(3)
C(10)-H(10)	0.9500
N(2)-C(11)	1.430(2)
N(2)-S(2)	1.6779(17)
C(11)-C(18)	1.391(3)

C(11)-C(12)	1.407(3)
C(12)-O(3)	1.367(2)
C(12)-C(13)	1.398(3)
O(3)-C(19)	1.435(2)
C(19)-H(19A)	0.9800
C(19)-H(19B)	0.9800
C(19)-H(19C)	0.9800
C(13)-C(14)	1.404(3)
C(13)-H(13)	0.9500
C(14)-C(17)	1.392(3)
C(14)-C(15)	1.521(3)
C(17)-C(18)	1.399(3)
C(15)-C(16)	1.536(3)
C(16)-H(16A)	0.9900
C(16)-H(16B)	0.9900
S(2)-O(5)	1.4274(15)
S(2)-O(4)	1.4305(15)
S(2)-C(20)	1.752(2)
C(20)-C(21)	1.393(3)
C(20)-C(25)	1.394(3)
C(21)-C(22)	1.388(3)
C(21)-H(21)	0.9500
C(22)-C(23)	1.395(3)
C(22)-H(22)	0.9500
C(23)-C(24)	1.398(3)
C(23)-C(26)	1.508(3)
C(24)-C(25)	1.385(3)
C(24)-H(24)	0.9500
C(26)-H(26A)	0.9800
C(26)-H(26B)	0.9800
C(26)-H(26C)	0.9800
C(25)-H(25)	0.9500
C(1S)-Cl(2S)	1.762(3)
C(1S)-Cl(1S)	1.771(3)
C(1S)-H(1S1)	0.9900
C(1S)-H(1S2)	0.9900

C(1)-S(1)-C(15)	94.70(10)
O(1)-C(1)-C(2)	126.5(2)
O(1)-C(1)-S(1)	122.89(19)
C(2)-C(1)-S(1)	110.57(15)
C(1)-C(2)-C(3)	107.52(17)
C(1)-C(2)-H(2A)	110.2
C(3)-C(2)-H(2A)	110.2
C(1)-C(2)-H(2B)	110.2
C(3)-C(2)-H(2B)	110.2
H(2A)-C(2)-H(2B)	108.5
C(4)-C(3)-C(2)	126.70(19)
C(4)-C(3)-C(15)	122.10(19)
C(2)-C(3)-C(15)	111.04(17)
C(3)-C(4)-C(5)	123.85(19)
C(3)-C(4)-H(4)	118.1
C(5)-C(4)-H(4)	118.1
O(2)-C(5)-C(4)	105.94(17)
O(2)-C(5)-C(6)	110.21(17)
C(4)-C(5)-C(6)	111.42(17)
O(2)-C(5)-H(5)	109.7
C(4)-C(5)-H(5)	109.7
C(6)-C(5)-H(5)	109.7
C(5)-O(2)-H(2)	109(2)
N(1)-C(6)-C(16)	112.28(17)
N(1)-C(6)-C(5)	109.53(17)
C(16)-C(6)-C(5)	108.85(17)
N(1)-C(6)-H(6)	108.7
C(16)-C(6)-H(6)	108.7
C(5)-C(6)-H(6)	108.7
C(17)-N(1)-C(6)	118.34(17)
C(17)-N(1)-C(7)	116.63(17)
C(6)-N(1)-C(7)	115.90(16)
N(1)-C(7)-C(8)	113.24(17)
N(1)-C(7)-H(7A)	108.9
C(8)-C(7)-H(7A)	108.9

N(1)-C(7)-H(7B)	108.9
C(8)-C(7)-H(7B)	108.9
H(7A)-C(7)-H(7B)	107.7
C(9)-C(8)-C(7)	109.09(17)
C(9)-C(8)-H(8A)	109.9
C(7)-C(8)-H(8A)	109.9
C(9)-C(8)-H(8B)	109.9
C(7)-C(8)-H(8B)	109.9
H(8A)-C(8)-H(8B)	108.3
C(10)-C(9)-C(18)	106.64(18)
C(10)-C(9)-C(8)	136.23(19)
C(18)-C(9)-C(8)	117.08(18)
C(9)-C(10)-N(2)	109.70(17)
C(9)-C(10)-H(10)	125.2
N(2)-C(10)-H(10)	125.2
C(10)-N(2)-C(11)	107.76(16)
C(10)-N(2)-S(2)	116.34(13)
C(11)-N(2)-S(2)	128.04(14)
C(18)-C(11)-C(12)	119.17(18)
C(18)-C(11)-N(2)	104.89(17)
C(12)-C(11)-N(2)	135.87(18)
O(3)-C(12)-C(13)	123.14(18)
O(3)-C(12)-C(11)	120.22(18)
C(13)-C(12)-C(11)	116.63(18)
C(12)-O(3)-C(19)	116.52(16)
O(3)-C(19)-H(19A)	109.5
O(3)-C(19)-H(19B)	109.5
H(19A)-C(19)-H(19B)	109.5
O(3)-C(19)-H(19C)	109.5
H(19A)-C(19)-H(19C)	109.5
H(19B)-C(19)-H(19C)	109.5
C(12)-C(13)-C(14)	123.78(18)
C(12)-C(13)-H(13)	118.1
C(14)-C(13)-H(13)	118.1
C(17)-C(14)-C(13)	119.17(19)
C(17)-C(14)-C(15)	115.17(18)

C(13)-C(14)-C(15)	125.64(18)
N(1)-C(17)-C(14)	125.07(19)
N(1)-C(17)-C(18)	117.91(18)
C(14)-C(17)-C(18)	116.99(19)
C(11)-C(18)-C(17)	124.06(18)
C(11)-C(18)-C(9)	110.89(18)
C(17)-C(18)-C(9)	125.05(19)
C(14)-C(15)-C(3)	110.45(16)
C(14)-C(15)-C(16)	107.04(17)
C(3)-C(15)-C(16)	110.01(17)
C(14)-C(15)-S(1)	114.32(14)
C(3)-C(15)-S(1)	104.17(14)
C(16)-C(15)-S(1)	110.85(14)
C(6)-C(16)-C(15)	107.42(16)
C(6)-C(16)-H(16A)	110.2
C(15)-C(16)-H(16A)	110.2
C(6)-C(16)-H(16B)	110.2
C(15)-C(16)-H(16B)	110.2
H(16A)-C(16)-H(16B)	108.5
O(5)-S(2)-O(4)	119.18(9)
O(5)-S(2)-N(2)	107.64(9)
O(4)-S(2)-N(2)	104.87(9)
O(5)-S(2)-C(20)	110.06(9)
O(4)-S(2)-C(20)	109.04(9)
N(2)-S(2)-C(20)	105.02(9)
C(21)-C(20)-C(25)	121.14(19)
C(21)-C(20)-S(2)	118.54(16)
C(25)-C(20)-S(2)	120.31(16)
C(22)-C(21)-C(20)	118.99(19)
C(22)-C(21)-H(21)	120.5
C(20)-C(21)-H(21)	120.5
C(21)-C(22)-C(23)	121.06(19)
C(21)-C(22)-H(22)	119.5
C(23)-C(22)-H(22)	119.5
C(22)-C(23)-C(24)	118.73(19)
C(22)-C(23)-C(26)	121.33(19)

C(24)-C(23)-C(26)	119.93(19)
C(25)-C(24)-C(23)	121.18(19)
C(25)-C(24)-H(24)	119.4
C(23)-C(24)-H(24)	119.4
C(23)-C(26)-H(26A)	109.5
C(23)-C(26)-H(26B)	109.5
H(26A)-C(26)-H(26B)	109.5
C(23)-C(26)-H(26C)	109.5
H(26A)-C(26)-H(26C)	109.5
H(26B)-C(26)-H(26C)	109.5
C(24)-C(25)-C(20)	118.88(19)
C(24)-C(25)-H(25)	120.6
C(20)-C(25)-H(25)	120.6
Cl(2S)-C(1S)-Cl(1S)	111.24(16)
Cl(2S)-C(1S)-H(1S1)	109.4
Cl(1S)-C(1S)-H(1S1)	109.4
Cl(2S)-C(1S)-H(1S2)	109.4
Cl(1S)-C(1S)-H(1S2)	109.4
H(1S1)-C(1S)-H(1S2)	108.0

Symmetry transformations used to generate equivalent atoms:

Table A3.3.5 *Anisotropic displacement parameters ($Å^2 x\ 10^3$) allylic alcohol* ***137****. The anisotropic displacement factor exponent takes the form: $-2\pi^2[h^2 a^{*2} U^{11} + ... + 2 h k a^* b^* U^{12}]$*

	U^{11}	U^{22}	U^{33}	U^{23}	U^{13}	U^{12}
S(1)	26(1)	25(1)	18(1)	-7(1)	-6(1)	-1(1)
C(1)	31(1)	26(1)	22(1)	-10(1)	0(1)	-4(1)
O(1)	42(1)	42(1)	20(1)	-5(1)	2(1)	-6(1)
C(2)	19(1)	28(1)	18(1)	-10(1)	3(1)	-6(1)
C(3)	19(1)	25(1)	19(1)	-10(1)	-2(1)	-5(1)
C(4)	17(1)	26(1)	24(1)	-9(1)	-4(1)	-2(1)
C(5)	26(1)	20(1)	22(1)	-6(1)	-5(1)	-2(1)
O(2)	35(1)	19(1)	24(1)	-7(1)	-2(1)	-6(1)
C(6)	22(1)	21(1)	21(1)	-6(1)	-1(1)	-6(1)
N(1)	27(1)	20(1)	18(1)	-6(1)	0(1)	-6(1)
C(7)	28(1)	23(1)	18(1)	-4(1)	0(1)	-8(1)
C(8)	28(1)	23(1)	17(1)	-4(1)	-1(1)	-5(1)
C(9)	15(1)	25(1)	16(1)	-5(1)	0(1)	-4(1)
C(10)	18(1)	25(1)	15(1)	-4(1)	0(1)	-6(1)
N(2)	18(1)	22(1)	14(1)	-6(1)	0(1)	-4(1)
C(11)	14(1)	23(1)	17(1)	-8(1)	-1(1)	-4(1)
C(12)	19(1)	20(1)	17(1)	-5(1)	-4(1)	-4(1)
O(3)	36(1)	19(1)	17(1)	-4(1)	-6(1)	-5(1)
C(19)	44(1)	21(1)	18(1)	-3(1)	-9(1)	-5(1)
C(13)	18(1)	23(1)	15(1)	-4(1)	-3(1)	-4(1)
C(14)	16(1)	24(1)	19(1)	-8(1)	-2(1)	-4(1)
C(17)	17(1)	22(1)	19(1)	-7(1)	-1(1)	-4(1)
C(18)	14(1)	22(1)	17(1)	-5(1)	0(1)	-4(1)
C(15)	20(1)	21(1)	18(1)	-5(1)	-4(1)	-2(1)
C(16)	18(1)	22(1)	24(1)	-7(1)	-3(1)	-5(1)
S(2)	18(1)	21(1)	17(1)	-8(1)	0(1)	-2(1)
O(4)	24(1)	30(1)	18(1)	-12(1)	2(1)	-4(1)
O(5)	24(1)	23(1)	22(1)	-9(1)	-2(1)	0(1)

C(20)	19(1)	21(1)	20(1)	-10(1)	-2(1)	-3(1)
C(21)	24(1)	27(1)	16(1)	-7(1)	-1(1)	-6(1)
C(22)	24(1)	26(1)	21(1)	-6(1)	-6(1)	-3(1)
C(23)	20(1)	25(1)	24(1)	-13(1)	-3(1)	-3(1)
C(24)	22(1)	27(1)	19(1)	-9(1)	1(1)	-7(1)
C(26)	20(1)	37(1)	30(1)	-15(1)	-3(1)	-3(1)
C(25)	22(1)	24(1)	17(1)	-6(1)	-3(1)	-3(1)
C(1S)	43(2)	52(2)	43(2)	-23(1)	-11(1)	3(1)
Cl(1S)	47(1)	102(1)	67(1)	-49(1)	-13(1)	-6(1)
Cl(2S)	41(1)	39(1)	61(1)	-19(1)	-2(1)	-4(1)

Table A3.3.6 *Hydrogen coordinates (x 10^4) and isotropic displacement parameters ($Å^2$x 10^3) for allylic alcohol* ***137***.

	x	y	z	U(eq)
H(2A)	4492	5761	6557	26
H(2B)	4974	4642	6023	26
H(4)	4947	7698	4824	26
H(5)	6509	8760	3226	27
H(2)	7520(30)	9770(20)	3980(20)	39
H(6)	8980	8160	3311	26
H(7A)	9788	7219	1733	28
H(7B)	8592	8377	1511	28
H(8A)	7318	7263	856	28
H(8B)	8855	7221	211	28
H(10)	8651	4619	215	24
H(19A)	9137	1042	5721	42
H(19B)	8583	-196	5634	42
H(19C)	7526	865	5991	42
H(13)	7739	2932	5577	23
H(16A)	8692	7052	5315	26
H(16B)	9655	6189	4659	26
H(21)	6147	3432	109	27
H(22)	3752	3774	272	28
H(24)	3464	1607	3562	26
H(26A)	1525	3763	1557	42
H(26B)	1432	2765	2815	42
H(26C)	1487	2246	1805	42
H(25)	5856	1266	3419	25
H(1S1)	6951	1828	8974	53
H(1S2)	6649	419	9860	53

Table A3.3.7 *Torsion angles [°] for allylic alcohol* ***137****.*

C(15)-S(1)-C(1)-O(1)	-179.4(2)
C(15)-S(1)-C(1)-C(2)	2.08(16)
O(1)-C(1)-C(2)-C(3)	159.8(2)
S(1)-C(1)-C(2)-C(3)	-21.8(2)
C(1)-C(2)-C(3)-C(4)	-138.7(2)
C(1)-C(2)-C(3)-C(15)	36.7(2)
C(2)-C(3)-C(4)-C(5)	172.32(19)
C(15)-C(3)-C(4)-C(5)	-2.6(3)
C(3)-C(4)-C(5)-O(2)	-104.9(2)
C(3)-C(4)-C(5)-C(6)	15.0(3)
O(2)-C(5)-C(6)-N(1)	-166.80(16)
C(4)-C(5)-C(6)-N(1)	75.9(2)
O(2)-C(5)-C(6)-C(16)	70.1(2)
C(4)-C(5)-C(6)-C(16)	-47.2(2)
C(16)-C(6)-N(1)-C(17)	13.4(3)
C(5)-C(6)-N(1)-C(17)	-107.6(2)
C(16)-C(6)-N(1)-C(7)	-132.47(19)
C(5)-C(6)-N(1)-C(7)	106.5(2)
C(17)-N(1)-C(7)-C(8)	48.8(3)
C(6)-N(1)-C(7)-C(8)	-164.74(18)
N(1)-C(7)-C(8)-C(9)	-50.8(2)
C(7)-C(8)-C(9)-C(10)	-153.7(2)
C(7)-C(8)-C(9)-C(18)	29.3(2)
C(18)-C(9)-C(10)-N(2)	-0.6(2)
C(8)-C(9)-C(10)-N(2)	-177.9(2)
C(9)-C(10)-N(2)-C(11)	2.6(2)
C(9)-C(10)-N(2)-S(2)	154.30(14)
C(10)-N(2)-C(11)-C(18)	-3.5(2)
S(2)-N(2)-C(11)-C(18)	-150.84(15)
C(10)-N(2)-C(11)-C(12)	179.9(2)
S(2)-N(2)-C(11)-C(12)	32.5(3)
C(18)-C(11)-C(12)-O(3)	-175.70(17)
N(2)-C(11)-C(12)-O(3)	0.6(3)

C(18)-C(11)-C(12)-C(13)	3.2(3)
N(2)-C(11)-C(12)-C(13)	179.5(2)
C(13)-C(12)-O(3)-C(19)	-11.8(3)
C(11)-C(12)-O(3)-C(19)	166.97(19)
O(3)-C(12)-C(13)-C(14)	174.76(18)
C(11)-C(12)-C(13)-C(14)	-4.1(3)
C(12)-C(13)-C(14)-C(17)	1.0(3)
C(12)-C(13)-C(14)-C(15)	-177.57(19)
C(6)-N(1)-C(17)-C(14)	15.4(3)
C(7)-N(1)-C(17)-C(14)	161.03(19)
C(6)-N(1)-C(17)-C(18)	-166.98(18)
C(7)-N(1)-C(17)-C(18)	-21.3(3)
C(13)-C(14)-C(17)-N(1)	-179.40(19)
C(15)-C(14)-C(17)-N(1)	-0.7(3)
C(13)-C(14)-C(17)-C(18)	2.9(3)
C(15)-C(14)-C(17)-C(18)	-178.37(17)
C(12)-C(11)-C(18)-C(17)	0.7(3)
N(2)-C(11)-C(18)-C(17)	-176.63(18)
C(12)-C(11)-C(18)-C(9)	-179.45(17)
N(2)-C(11)-C(18)-C(9)	3.2(2)
N(1)-C(17)-C(18)-C(11)	178.31(18)
C(14)-C(17)-C(18)-C(11)	-3.8(3)
N(1)-C(17)-C(18)-C(9)	-1.5(3)
C(14)-C(17)-C(18)-C(9)	176.34(18)
C(10)-C(9)-C(18)-C(11)	-1.7(2)
C(8)-C(9)-C(18)-C(11)	176.17(17)
C(10)-C(9)-C(18)-C(17)	178.13(19)
C(8)-C(9)-C(18)-C(17)	-4.0(3)
C(17)-C(14)-C(15)-C(3)	79.9(2)
C(13)-C(14)-C(15)-C(3)	-101.5(2)
C(17)-C(14)-C(15)-C(16)	-39.9(2)
C(13)-C(14)-C(15)-C(16)	138.7(2)
C(17)-C(14)-C(15)-S(1)	-163.02(15)
C(13)-C(14)-C(15)-S(1)	15.6(3)
C(4)-C(3)-C(15)-C(14)	-95.1(2)
C(2)-C(3)-C(15)-C(14)	89.2(2)

C(4)-C(3)-C(15)-C(16)	22.8(3)
C(2)-C(3)-C(15)-C(16)	-152.83(17)
C(4)-C(3)-C(15)-S(1)	141.69(18)
C(2)-C(3)-C(15)-S(1)	-33.97(19)
C(1)-S(1)-C(15)-C(14)	-102.83(15)
C(1)-S(1)-C(15)-C(3)	17.81(15)
C(1)-S(1)-C(15)-C(16)	136.09(15)
N(1)-C(6)-C(16)-C(15)	-53.1(2)
C(5)-C(6)-C(16)-C(15)	68.3(2)
C(14)-C(15)-C(16)-C(6)	65.7(2)
C(3)-C(15)-C(16)-C(6)	-54.4(2)
S(1)-C(15)-C(16)-C(6)	-169.05(14)
C(10)-N(2)-S(2)-O(5)	163.49(14)
C(11)-N(2)-S(2)-O(5)	-51.47(18)
C(10)-N(2)-S(2)-O(4)	35.63(16)
C(11)-N(2)-S(2)-O(4)	-179.33(16)
C(10)-N(2)-S(2)-C(20)	-79.25(16)
C(11)-N(2)-S(2)-C(20)	65.79(18)
O(5)-S(2)-C(20)-C(21)	-154.32(16)
O(4)-S(2)-C(20)-C(21)	-21.85(19)
N(2)-S(2)-C(20)-C(21)	90.09(17)
O(5)-S(2)-C(20)-C(25)	26.4(2)
O(4)-S(2)-C(20)-C(25)	158.91(16)
N(2)-S(2)-C(20)-C(25)	-89.15(18)
C(25)-C(20)-C(21)-C(22)	-1.0(3)
S(2)-C(20)-C(21)-C(22)	179.81(16)
C(20)-C(21)-C(22)-C(23)	-0.2(3)
C(21)-C(22)-C(23)-C(24)	1.1(3)
C(21)-C(22)-C(23)-C(26)	-177.9(2)
C(22)-C(23)-C(24)-C(25)	-0.8(3)
C(26)-C(23)-C(24)-C(25)	178.2(2)
C(23)-C(24)-C(25)-C(20)	-0.3(3)
C(21)-C(20)-C(25)-C(24)	1.2(3)
S(2)-C(20)-C(25)-C(24)	-179.59(16)

Symmetry transformations used to generate equivalent atoms:

Table A3.3.8 *Hydrogen bonds for allylic alcohol* ***137*** *[Å and °].*

D-H...A	d(D-H)	d(H...A)	d(D...A)	<(DHA)
O(2)-H(2)...O(3)#1	0.831(18)	2.32(3)	2.878(2)	125(3)
O(2)-H(2)...O(5)#1	0.831(18)	2.06(2)	2.842(2)	158(3)
C(8)-H(8B)...O(4)#2	0.99	2.65	3.411(3)	134.0
C(16)-H(16B)...S(1)#3	0.99	2.93	3.843(2)	154.2
C(21)-H(21)...O(1)#4	0.95	2.45	3.160(3)	131.2
C(25)-H(25)...O(2)#5	0.95	2.51	3.348(3)	147.6
C(1S)-H(1S1)...O(1)	0.99	2.50	3.308(4)	139.1

Symmetry transformations used to generate equivalent atoms:

#1 x,y+1,z #2 -x+2,-y+1,-z #3 -x+2,-y+1,-z+1
#4 x,y,z-1 #5 x,y-1,z

Appendix 4

Additional Strategies Toward the Total Synthesis of Aleutianamine

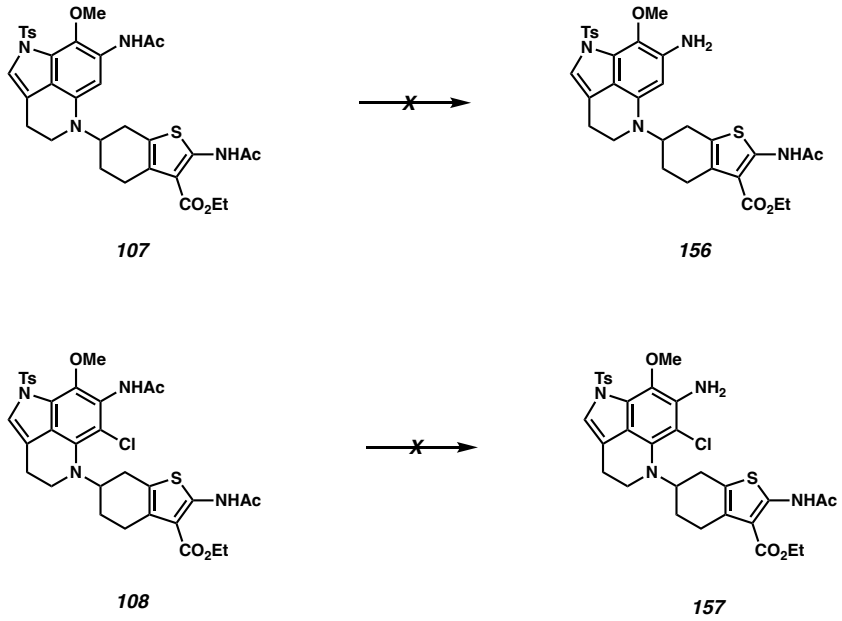
A4.1 INTRODUCTION

Throughout our studies toward aleutianamine (**15**), many other synthetic strategies were pursued that were ultimately unsuccessful in accessing the natural product. However, many of these failed strategies were invaluable sources of information, which helped inform decision making and synthetic planning that eventually culminated in the successful total synthesis of aleutianamine (**15**). Some of these failed approaches will be described briefly.

A4.2 ALTERNATIVE PROTECTING GROUPS ON THE AMINO TRICYCLE SYSTEM

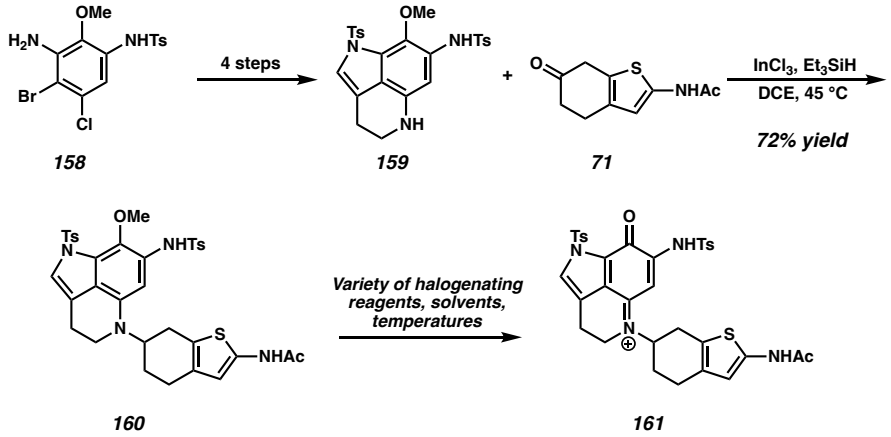
Given the undesired benzoxazole formation when attempting the dearomative thiophene arylation on the amino tricycle system (see section 1.5), we were interested in exploring alternative nitrogen protecting groups to avoid undesired reactivity. This was first explored by attempting to selectively deprotect the Ac group of the aniline nitrogen on substrates **107** and **108** (Scheme A4.2.1). Unfortunately, under acidic, basic, or transition metal-mediated conditions, the desired primary aniline products **156** and **157** were not observed.

Scheme A4.2.1 *Failed deprotection of NAc on* ***107*** *and* ***108****.*



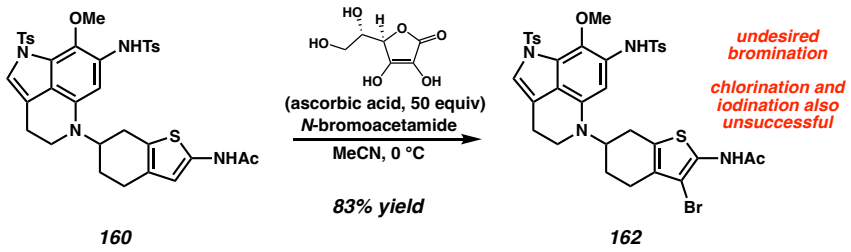
Instead, *N*-Ts aniline **158** was prepared in six steps and was successfully employed in the Larock/Buchwald–Hartwig annulation/cyclization and subsequent protecting group manipulation sequence to yield *N*-Ts aminotricycle **159** (Scheme A4.2.2). Gratifyingly, the reductive amination between **159** and ketothiophene **71** proceeded smoothly to provide arene **160**. At this stage, we were interested if the *N*-Ts group would influence the regioselectivity of halogenation such that selective halogenation of the arene could be achieved. We were hopeful, as in simple *N*-Ts aniline systems, we had observed much faster rates of halogenation compared with *N*-Ac systems, indicating the *N*-Ts group exerts greater directing effects compared to the *N*-Ac group. However, when subjecting **160** to a variety of halogenation conditions, oxidized iminoquinone **161** was typically observed via LC/MS. This was interesting, as oxidized products had been observed in the *N*-Ac system, albeit usually as minor components of the reaction profile.

Scheme A4.2.2 *Failed halogenation of arene* ***160*** *under standard conditions.*



Given that oxidation was in issue in this system, presumably through single electron pathways, we hypothesized that adding an antioxidant could mitigate this undesired reactivity. After a small investigation of antioxidants, it was discovered that the addition of a large excess of ascorbic acid in the presence of *N*-bromoacetamide led to clean monobromination of **160** (Scheme A4.2.3). However, ^{1}H NMR data indicated that bromination once again occurred at the undesired C3 position of the thiophene, leading to clean formation of **162**. Chlorination and iodination of **160** also failed. Given the difficulties of accessing the requisite dearomative thiophene arylation substrate on the amino tricycle system, it was at this point we decided all efforts should be dedicated toward advancing *N*-Ac thioimidate **74**.

Scheme A4.2.3 *Undesired bromination of arene* ***160***.

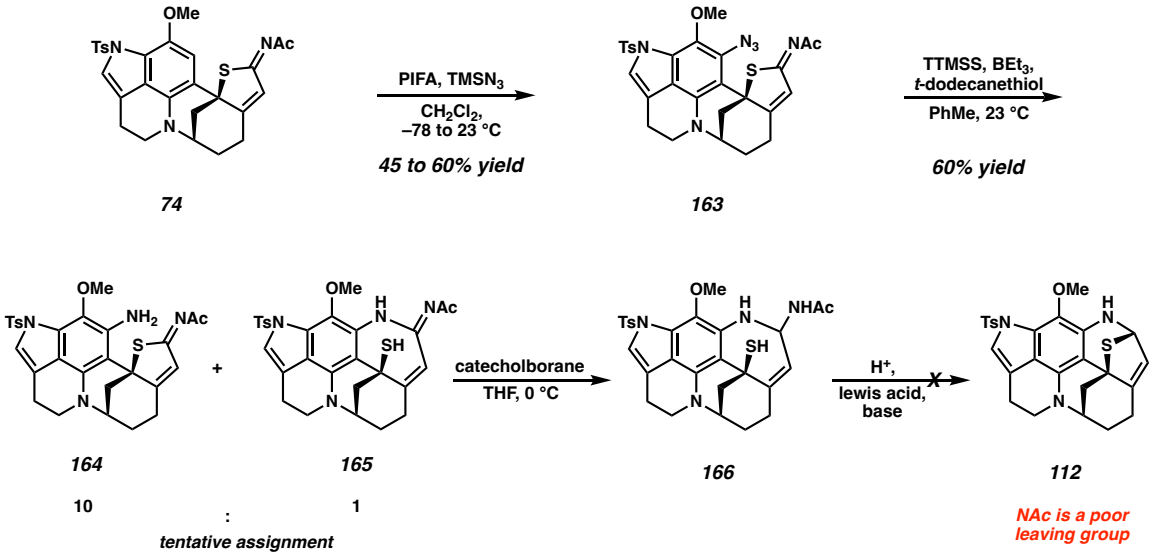


A4.3 FAILED ADVANCEMENT OF *N*-AC THIOIMIDATE 74.

Given that thioimidate **74** possesses the full carbon skeleton of aleutianamine (**15**), significant efforts were made to advance this intermediate. The remaining challenges were to install the C10 nitrogen, reduce the thioimidate and form the thioaminal, and install the alkenyl bromide. At this stage, we were particularly concerned with the formation of the thioaminal, as this bond forming event creates significant ring strain; thus, our efforts were focused on thioaminal formation.

Excitingly, we found that azidation of the arene could be achieved employing Kita's conditions[1], which provided aryl azide **163** (Scheme A4.3.1). Reduction of the azide proved challenging, but eventually using the conditions reported by Zanardi[2] yielded a 10:1 mixture of aniline **164** and cyclic amidine **165.**

Scheme A4.3.1 *Failed thioaminal formation from thioimidate* ***74***.



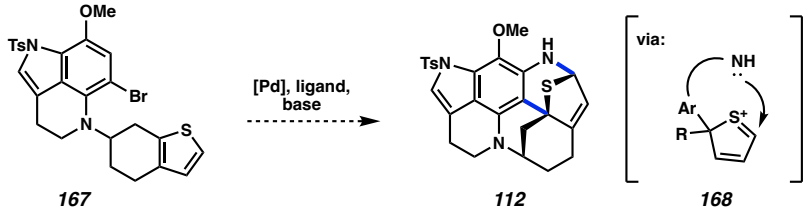
Despite extensive investigation, 1,2 reduction of thioimidate **164** proved unsuccessful— in most cases, undesired reduction of the *N*-Ac group was observed. Excitingly, 1,2 reduction of amidine **165** was achieved with catecholborane which provided

cyclic aminal **166**, containing the correct oxidation state of the desired thioaminal. However, thioaminal formation and extrusion of NH_2Ac was never achieved despite extensive investigation; under a variety of forcing acidic or basic conditions, *N*-Ac cleavage was typically observed. The failed thioaminal formation was largely attributed to the poor leaving group ability of NH_2Ac, which is perhaps exacerbated given that aminal **112** contains significant ring strain, requiring a significant thermodynamic driving force for its formation. This result is what elected us to pursue alternative protecting groups on the thioimidate nitrogen.

A4.4 ATTEMPTED DEVELOPMENT OF AN INTRAMOLECULAR DEAROMATIVE 2,5-DIFUNCTIONALIZATION OF THIOPHENE

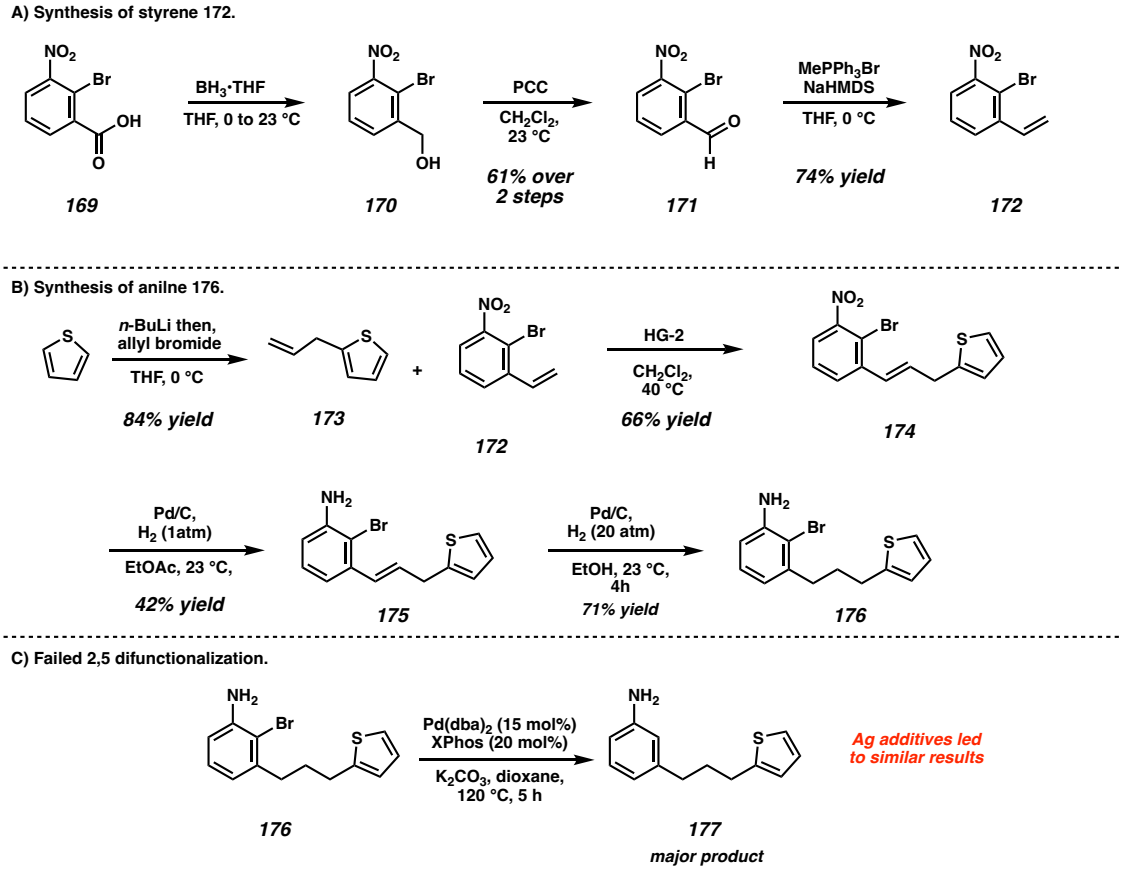
Given the difficulties in redox manipulation of thioimidate **74**, we were interested if the desired thioaminal oxidation state could be brought in on the thiophene fragment. To achieve this, we hypothesized that an intramolecular dearomative 2,5-difunctionalization of a thiophene fragment could directly form the thioaminal linkage, and preclude the need for redox manipulations (Figure A4.4.1). We hypothesized that potentially thiophene mediated nucleophilic ligand substitution and subsequent reductive elimination could provide sulefnium **168**, which could then undergo nucleophilic attack from the pendant aniline nitrogen to directly form the thioaminal (see section 1.3 for mechanistic details).

Figure A4.4.1 *Ideal intramolecular dearomative 2,5-difunctionalization to directly form thioaminal* ***112***.



We elected to first pursue a model system to investigate this strategy. Commercially available nitro arene **169** was elaborated to aldehyde **171** through a reduction/oxidation sequence, and was subsequently converted to styrene **172** via Wittig olefination (Scheme A4.4.1A). Thiophene was alkylated and then underwent cross-metathesis with **172** to provide alkene **174** Scheme A4.4.1B).

Scheme A4.4.1 *Failed dearomative 2,5-difunctionalization.*



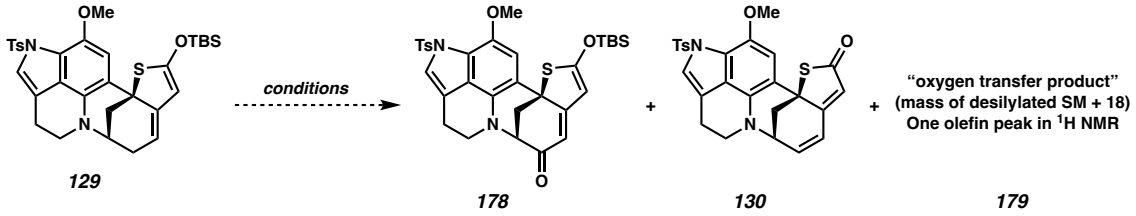
A two-step hydrogenation sequence then yielded the desired substrate **176**. Unfortunately, under the same reaction conditions employed in the dearomative thiophene arylation, only protodebromination of **176** was observed Scheme A4.4.1C). To try and access cationic palladium intermediates to help facility nucleophilic mediated ligand substitution, a series

of silver additives were investigated, but led to similar results in which **177** was primarily observed. Further reaction investigation was not pursued.

A4.5 FAILED LATE-STAGE VINYL BROMIDE INSTALLATION STRATEGIES

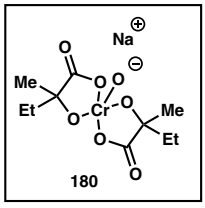
Significant efforts were focused on the functionalization of late-stage intermediates in order to install the vinyl bromide found in aleutianamine (**15**). The first strategy targeted an allylic oxidation of silyl enol ether **129**in order to install a ketone at this position, which would later serve as a functional handle to install the vinyl bromide.

Table A4.5.1 *Failed allylic oxidation of* ***129****.*



129 ***178*** ***130*** ***179***

Entry	Conditions	Result
1	$Pd(OH)_2/C$, TBHP, Cs_2CO_3, CH_2Cl_2, 0 °C	complex mixture, including 130
2	PIDA, TBHP, $Mg(OAc)_2 \cdot 4H_2O$, *n*-BuOC(O)*n*-Pr, 0 °C	complex mixture, few olefin peaks by ^{1}H NMR
3	$Mn(OAc)_3 \cdot 2H_2O$, TBHP, 4 Å mol. sieves, O_2, EtOAc, 23°C	complex mixture by ^{1}H NMR, trace mass of 178 by LC/MS
4	$Rh_2(esp)_2$, TBHP, EtOAc, 23 °C	SM + 2-3 new products. Major new product is 179.
5	$Rh_2(cap)_4$, TBHP, K_2CO_3, CH_2Cl_2, 40 °C	complex mixture; no clear olefinic peaks in ^{1}H NMR
6	180 (10 equiv), MnO_2 (20 equiv), 15-crown-5, DCE, 80 °C, 2 d	decomp to baseline
7	180 (5 equiv), MnO_2 (10 equiv), 15-crown-5, DCE, 80 °C, 4.5 h	decomp to baseline
8	PDC, 4 Å mol. sieves, CH_2Cl_2, 60 °C	SM + many oxidized products



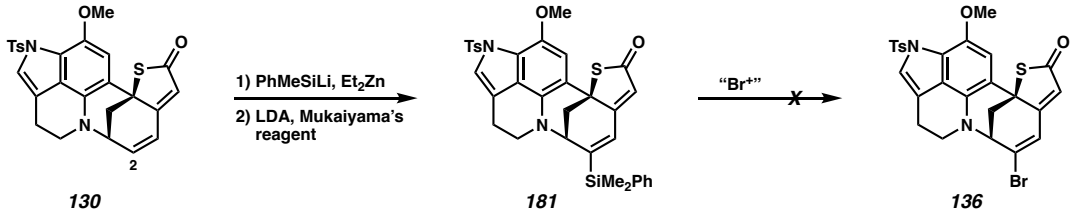
180

Unfortunately, under a variety of conditions that were investigated, desired ketone **178** was only observed in trace quantities (Table A4.5.1). Most experiments led to hydrolysis affording dienone **130**, an oxygen transfer product that was unassigned (**179**),

or decomposition consisting of unidentified oxidation products. These results highlight the sensitivity of our late-stage intermediates to oxidative conditions.

The next strategy targeted installation of a silyl group at C2 in order to activate this position for electrophilic bromination, or to serve as a functional handle for ketone installation (i.e. Tamao-Fleming oxidation). Excitingly, 1,6-conjugate addition of $PhMe_2Si$ zinc species followed by desaturation afforded the desired C2 silyl compound **181** (Scheme A4.5.1). Unfortunately, attempts at affecting the desired bromination of **181** with a variety of electrophilic bromine sources did not result in formation of desired alkenyl bromide **136**. Additionally, limited attempts at affecting a Tamao-Fleming oxidation failed to yield the desired diketone.

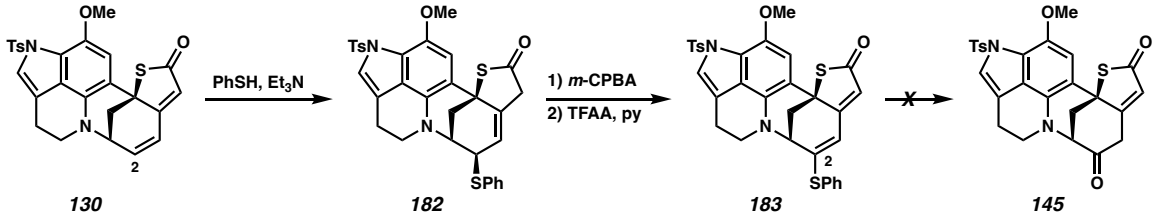
Scheme A4.5.1 *Failed bromination of* ***181***.



130 ***181*** ***136***

Given our success with the 1,6-conjugate addition, we hypothesized that addition of a thiol nucleophile could be followed by a Pummerer rearrangement to install the desired oxidation at C2. Treatment of dienone **130** with thiophenol resulted in clean formation of thioether **182** (Scheme A4.5.2).

Scheme A4.5.2 *Failed hydrolysis of* ***183*** *to* ***145***.



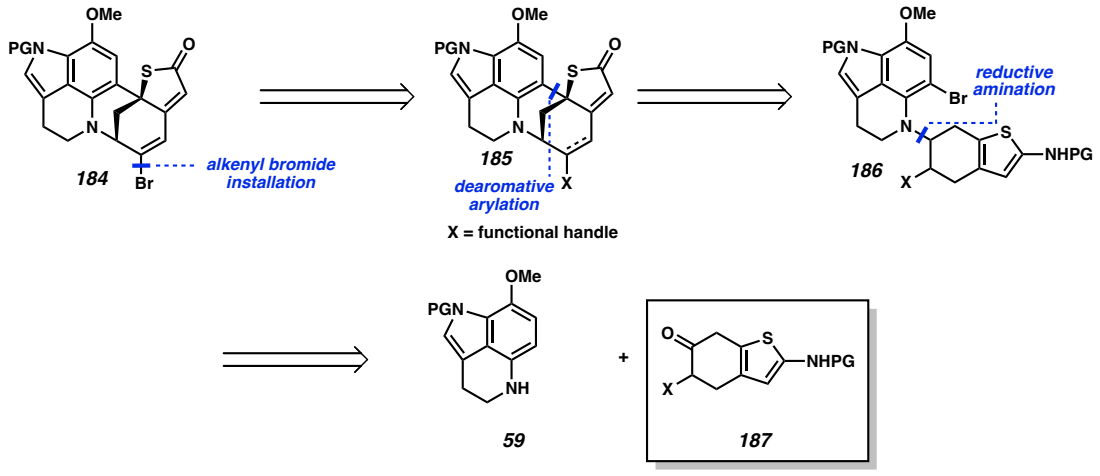
130 ***182*** ***183*** ***145***

Excitingly, the two step Pummerer rearrangement was successful in providing alkenyl sulfide **183**, which importantly contains the correct oxidation state at C2. However, attempts to hydrolyze **183** under either acidic or basic conditions failed to deliver the requisite diketone **145**.

A4.6 ATTEMPTED SYNTHESIS OF A THIOPHENE FRAGMENT CONTAINING A PRE-INSTALLED FUNCTIONAL HANDLE FOR ALKENYL BROMIDE INSTALLATION

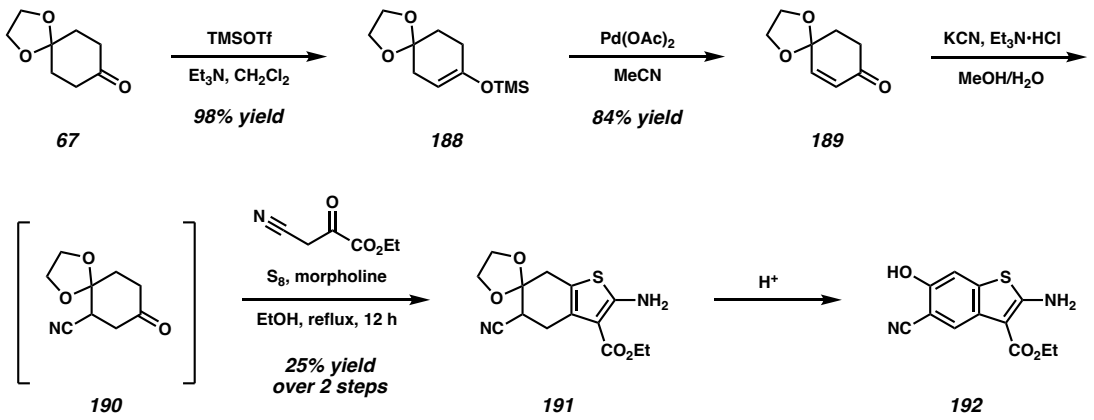
Perhaps the most challenging task of our synthetic endeavors was the installation of the alkenyl bromide found in aleutianamine (**15**). This is highlighted by the failed strategies to install this functionality on late-stage intermediates (see appendix A4.5). Thus, we envisaged that a pre-installed functional handle on advanced intermediates (i.e. **185**) might enable facile alkenyl bromide formation (Scheme A4.6.1). This functional handle was thought to arise from thiophene coupling fragment **187**, and substrates of this nature became the target of our investigations.

Scheme A4.6.1 *Strategy for pre-installed functional handle for alkenyl bromide installation.*



We first targeted the installation of a carboxylate moiety, as we envisaged a desaturation and decarboxylative halogenation sequence could access the alkenyl bromide. The requisite thiophene fragment was synthesized starting from **67**, which was converted to silyl enol ether **188**, followed by Saegusa-Ito oxidation which provided enone **189** (Scheme A4.6.2). Treatment of **189** with KCN affected a 1,4 addition and the intermediate cyano ketone **190** was subjected to Gewald conditions, affording thiophene **191** as a single isomer. Unfortunately, attempts to affect hydrolysis of the ethyl ester resulted in decomposition. Planning on decarboxylating the C3 ester later in the sequence, we attempted to hydrolyze the ketal **191** under acidic conditions (to afford the necessary ketone for reductive amination), but unfortunately this occurred with concomitant aerobic oxidation of the intermediate ketone, yielding phenol **192** as the sole product.

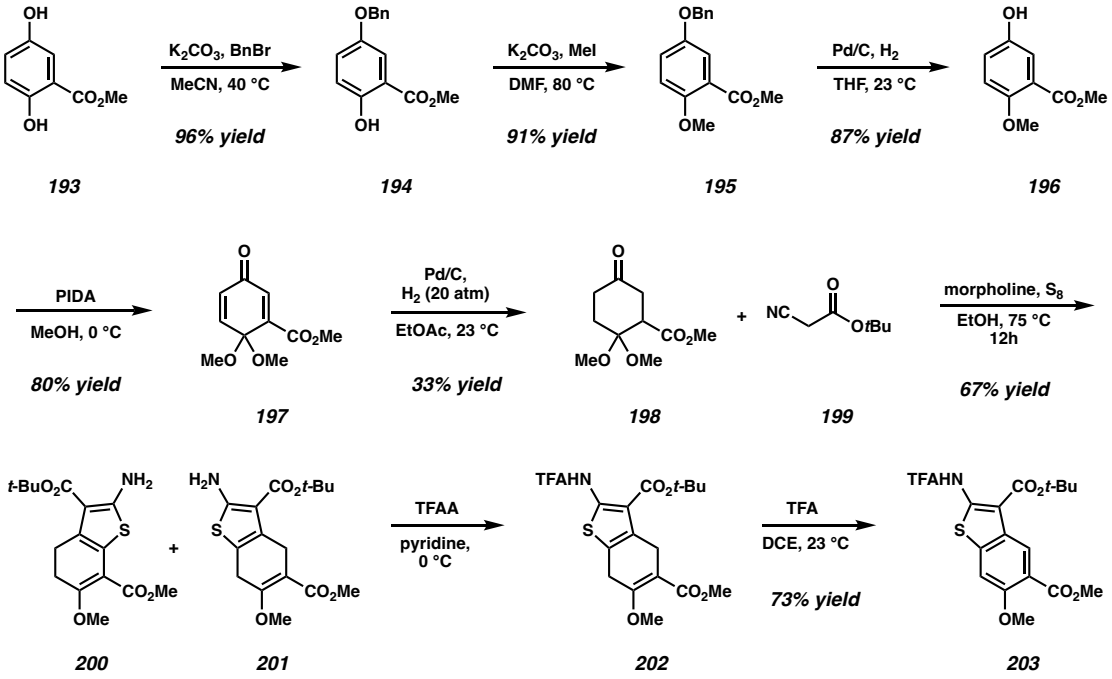
Scheme A4.6.2 *Failed synthesis of a thiophene fragment containing a nitrile as the functional handle.*



To circumvent the problematic hydrolysis of the ethyl ester, and acidic hydrolysis of the ketal, we targeted a thiophene substrate with instead a *tert*-butyl ester to allow for facile decarboxylation, and a dimethoxy acetal which we hoped could be removed under mild conditions. This commenced from commercially available hydroquinone **193** that was

elaborated to phenol **196** over three steps (Scheme A4.6.3). Oxidation of phenol **196** was achieved using PIDA, and the resulting dienone was reduced to ketone **198**. With this substrate, the Gewald thiophene synthesis was nonselective, providing a 1:1 mixture of thiophene constitutional isomers **200** and **201**. The desired thiophene **201** was carried forward by first protection of the nitrogen to afford **202**. Attempted *tert*-butyl ester

Scheme A4.6.3 *Failed synthesis of a thiophene fragment containing a methyl ester as the functional handle.*



deprotection under acidic conditions was met with failure, as oxidized anisole **203** was solely observed. It appears that with this extra degree of oxidation on the thiophene, aerobic oxidation to the aromatic system is a major challenge. Attempts to bring in alternative functional groups such as silylated alcohols, methyl ethers, or protected aldehydes similarly resulted in undesired oxidation of the thiophene prior to fragment coupling. Additionally, attempts to functionalize the thiophene after reductive amination, but before dearomative

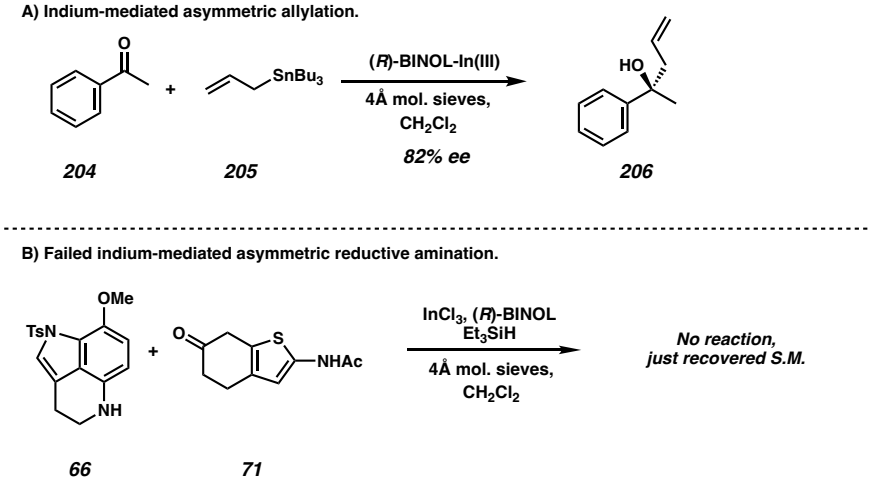
arylation, proved unsuccessful. These results highlight the oxidative sensitivity of these particular substituted thiophene systems.

A4.7 PRELIMINARY EFFORTS TOWARD AN ASYMMETRIC SYNTHESIS OF ALEUTIANAMINE

One major drawback of the synthetic route we developed to access aleutianamine (**15**) was that it was a racemic synthesis. Given the reductive amination between the tricyclic fragment **66** and ketothiophene **116** sets the first stereocenter, we performed a preliminary investigation to render this transformation asymmetric.

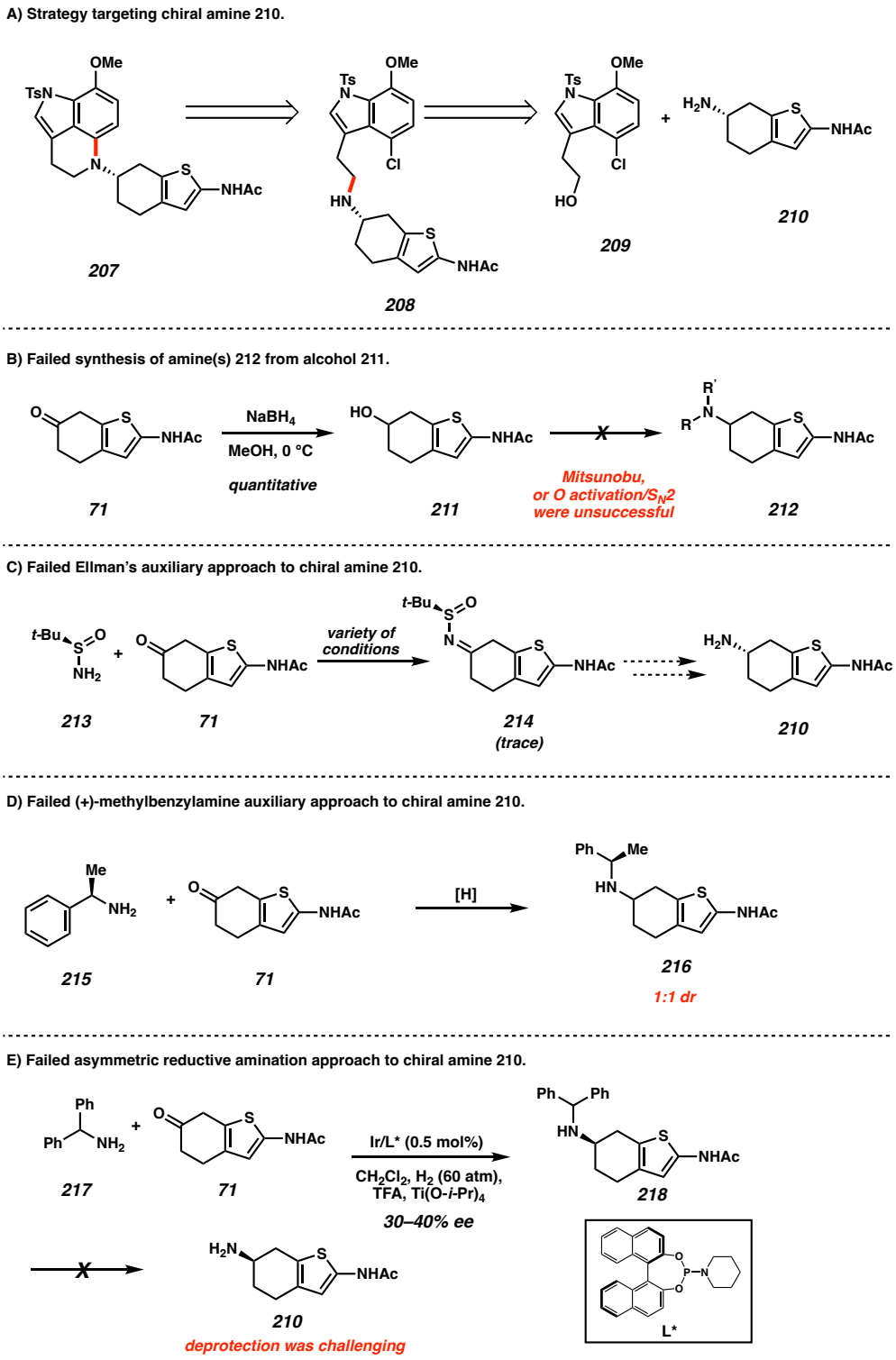
The first strategy we pursued was an indium-mediated asymmetric reductive amination, as the indium system was uniquely effective for the reductive amination of secondary aniline **66**. We were inspired from a report by Loh and coworkers[3] wherein they demonstrated a chiral indium(III) complex with a (*R*)-BINOL ligand scaffold could promote asymmetric allylations of ketones (Scheme A4.7.1A). Unfortunately, attempting to use the same catalyst they described led to no reaction between tricycle **66** and ketone **71**.

Scheme A4.7.1 *Failed indium-mediated asymmetric reductive amination.*



The next strategy we investigated aimed to access enantioenriched substrate **207** through a Buchwald–Hartwig amination of chiral secondary amine **208** (Scheme A4.7.2A).

Scheme A4.7.2 *Failed attempts at the preparation of chiral amine* ***210***.



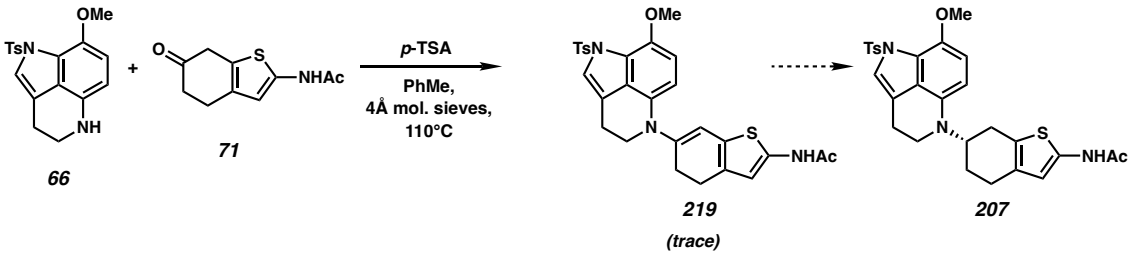
In turn, we envisaged accessing **208** through a substitution of tryptophol **209** and chiral amine **210**. We first attempted to prepare **210** (or a derivate thereof i.e. **212**) via a Mitsunobu or related substitution reaction of alcohol **211**, which was prepared from ketothiophene **71** (Scheme A4.7.2B). We hypothesized that enantioenriched alcohol **211** could be accessed using asymmetric ketone reduction strategies (i.e. CBS reduction), but wanted to first demonstrate the substitution reaction was feasible. Unfortunately, initial attempts to convert alcohol to some amine (i.e. **212**) were unsuccessful.

We were next interested in attempting to apply a chiral auxiliary strategy to access **210**. However, when trying to employ Ellman's auxiliary, the desired sulfinamide (**214**) was only formed in trace amounts (Scheme A4.7.2C). When utilizing more forcing reaction conditions (i.e. higher temperatures), oxidation of **71** to the phenol was observed. Using the same auxiliary logic, reductive amination between (+)-methylbenzylamine (**215**) and ketothiophene **71** proceeded smoothly to provide **216**, albeit with a 1:1 d.r (Scheme A4.7.2D). Moreover, the diastereomers could not be not be separated via conventional silica gel chromatography.

Finally, we attempted to employ asymmetric reductive amination conditions that have been established for dibenzylamine (**217**) that utilize an iridium-phosphoramidite catalyst system.[4] Employing these reaction conditions with ketohiophene **71** provided the desired adduct **218** in good yield, but only modest enantioselectivity was observed (30-40% ee, Scheme A4.7.2E). The original report employed benzylic ketones, whereas ketothiophene **71** contains an extra methylene group adjacent to the aromatic system, likely making the differentiation of the two neighboring methylene groups flanking the intermediate iminium ion by the chiral catalyst more challenging.

Our final attempt at inducing asymmetry in our synthesis was through an asymmetric enamine hydrogenation strategy (Scheme A4.7.3).[5]

Scheme A4.7.3 *Failed attempts at the preparation of enamine* ***219***.



However, limited attempts to prepare enamine **219** from tricycle **66** were unfruitful. Once again, aerobic oxidation of ketothiophene **71** proved to be a challenge and more forcing reaction conditions were not tolerated.

A4.8 REFERENCES AND NOTES

(1) Kita, Y.; Tohma, H.; Hatanaka, K.; Takada, T.; Fujita, S.; Mitoh, S.; Sakurai, H.; Oka, S. Hypervalent Iodine-Induced Nucleophilic Substitution of *para*-Substituted Phenol Ethers. Generation of Cation Radicals as Reactive Intermediates. *J. Am. Chem. Soc*. **1994**, *116*, 3684–3691.

(2) Benati, L.; Bencivenni, G.; Leardini, R.; Minozzi, M.; Nanni, D.; Scialpi, R.; Spagnolo, P.; Zanardi, G. Radical Reduction of Aromatic Azides to Amines with Triethylsilane. *J. Org. Chem.* **2006**, *71*, 5822–5825.

(3) Teo, Y-C.; Goh, J-D.; Loh, T-P. Catalytic Enantioselective Allylation of Ketones via a Chiral Indium(III) Complex. *Org. Lett.* **2005**, *7*, 2743–2745.

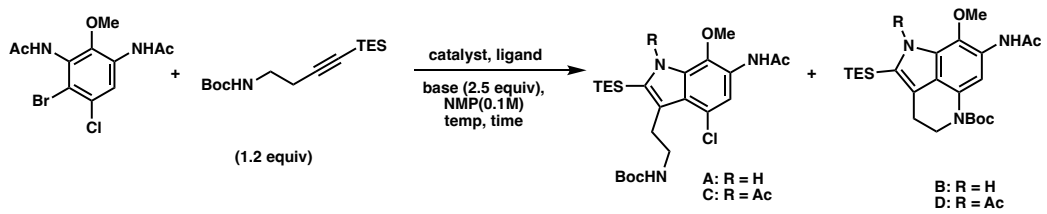
(4) Huang, H.; Wu, Z.; Gao, G.; Zhou, L.; Chang, M. Iridium-catalyzed direct asymmetric reductive amination of aromatic ketones. *Org. Chem. Front.* **2017**, *4*, 1976.

(5) Hou, G-H.; Xie, J-H, Yan, P-C.; Zhou, Q-L. Iridium Catalyzed Asymmetric Hydrogenation of Cyclic Enamines. *J. Am. Chem. Soc.* **2009**, *131*, 1366-1367.

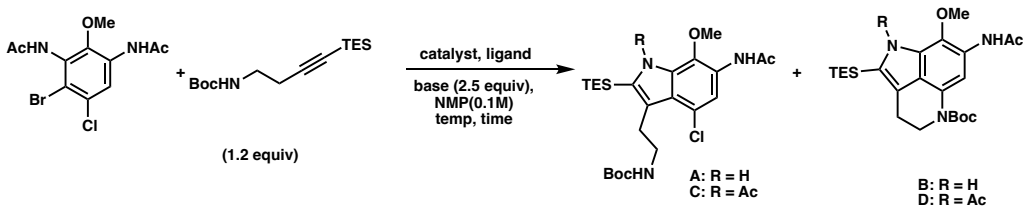
Appendix 5

Full Investigation of the Larock/Buchwald–Hartwig

Annulation/Cyclization



Entry	Catalyst	Ligand	Base	Temp	Time	Yield
1	$Pd(OAc)_2$ (7 mol%)	D^tBPF (10 mol%)	K_2CO_3	110 °C	24h	15% B
2 (3 equiv of alkyne)	$Pd(OAc)_2$ (5 mol%)	D^tBPF (8 mol%)	K_2CO_3	110 °C	24h	19% B
3	$Pd(OAc)_2$ (11 mol%)	D^tBPF (12 mol%)	Cs_2CO_3	110 °C	24h	0% just SM
4	$Pd(OAc)_2$ (8 mol%)	XPhos (7 mol%)	K_2CO_3	110 °C	24h	11% B
5	$Pd(OAc)_2$ (7 mol%)	D^tBPF (10 mol%)	K_2CO_3	110 °C	24h	25% A
6	XPhos Pd G3 (10 mol%)	-	K_2CO_3	110 °C	24h	22% A + 8% B
7	$Pd(OAc)_2$ (10 mol%)	D^tBPF (25 mol%)	K_2CO_3	110 °C	24h	7% A + 18% B
8	$Pd(OAc)_2$ (10 mol%)	xanthphos (17 mol%)	K_2CO_3	110 °C	24h	0%, just SM
9	$Pd(OAc)_2$ (15 mol%)	D^tBPF (30 mol%)	K_2CO_3 (5 equiv)	110 °C	48h	19% B
10	$Pd(OAc)_2$ (10 mol%)	D^tBPF (20 mol%)	K_2CO_3 + LiCl (1equiv)	110 °C	48h	31% A w/ impurity
11 (toluene instead of NMP)	$Pd(OAc)_2$ (10 mol%)	D^tBPF (23 mol%)	K_2CO_3 (5 equiv)	110 °C	48h	0%, mostly proto-debromination
12 (DMA instead of NMP)	$Pd(OAc)_2$ (8 mol%)	D^tBPF (19 mol%)	K_2CO_3 (5 equiv)	110 °C	48h	3% A
13 -freshly dried K_2CO_3	$Pd(OAc)_2$ (9 mol%)	D^tBPF (18 mol%)	K_2CO_3	110 °C	48h	19% A + 19% B
14 -freshly dried K_2CO_3	*t*-BuXPhos Pd G3 (8 mol%)	-	K_2CO_3	110 °C	48h	11% A
15 -freshly dried K_2CO_3 -5 equiv alkyne	$Pd(OAc)_2$ (15 mol%)	D^tBPF (30 mol%)	K_2CO_3 (5 equiv)	110 °C	48h	32% B
16 -freshly dried K_2CO_3 -9 equiv alkyne	$Pd(OAc)_2$ (15 mol%)	D^tBPF (30 mol%)	K_2CO_3 (5 equiv)	110 °C	48h	15% B



Entry	Catalyst	Ligand	Base	Temp	Time	Yield
17 -freshly dried K_2CO_3 -5 equiv alkyne -4 Å mol sieves	$Pd(OAc)_2$ (15 mol%)	D^tBPF (30 mol%)	K_2CO_3 (5 equiv)	110 °C	48h	41% B
18 -freshly dried K_2CO_3 -5 equiv alkyne -4 Åmol sieves 20 mg scale	$Pd(OAc)_2$ (15 mol%)	D^tBPF (30 mol%)	K_2CO_3 (5 equiv)	110 °C	48h	26% B
19 -freshly dried K_2CO_3 -2 equiv alkyne -AuCl (20 mol%)	$Pd(OAc)_2$ (15 mol%)	XPhos (30 mol%)	K_2CO_3 (5 equiv)	110 °C	48h	23% B
20 -freshly dried K_2CO_3 -2.5 equiv alkyne -CuI (10 mol%)	$Pd(OAc)_2$ (15 mol%)	XPhos (30 mol%)	K_2CO_3 (5 equiv)	110 °C	48h	trace B
21 (dioxane instead of NMP)	$Pd(P(t\text{-}Bu)_3)_2$ (10 mol%)	-	Cy_2NMe (2.5 equiv)	80 °C	6d	trace A
22	$Pd(OAc)_2$ (16 mol%)	D^tBPF (22 mol%)	K_2CO_3 (3.5 equiv)	130 °C	30h	trace B
23	$Pd(OAc)_2$ (10 mol%)	pheynyl urea (40 mol%)	K_2CO_3 (3 equiv)	130 °C	30h	SM + decomp
24 (dioxane instead of NMP)	$Pd(P(t\text{-}Bu)_3)_2$ (5 mol%)	-	Cy_2NMe (2.5 equiv)	130 °C	30h	proto-debromination
25 (DMF instead of NMP)	$Pd_2(DBA)_3$ (10 mol%)	D^tBPF (20 mol%)	TEA (2.5 equiv)	130 °C	30h	proto-debromination + trace C
26 (DMF instead of NMP)	$Pd(OAc)_2$ (10 mol%)	D^tBPF (20 mol%)	TEA (2.5 equiv)	130 °C	30h	proto-debromination + trace C
27	$Pd(OAc)_2$ (15 mol%)	D^tBPF (20 mol%)	K_3PO_4 (2.5 equiv)	130 °C	30h	trace A
28	$Pd(OAc)_2$ (16 mol%)	D^tBPF (26 mol%)	K_2CO_3 (2.5 equiv)	110 °C	5h	8% A 2% B
29	$Pd(OAc)_2$ (6 mol%)	D^tBPF (7 mol%)	Cy_2NMe (2.5 equiv)	110 °C	24h	sm + proto-debromination
30 (DMF instead of NMP)	$Pd(OAc)_2$ (5 mol%)	D^tBPF (7 mol%)	K_2CO_3 (2.5 equiv)	110 °C	24h	trace A
31	$Pd(P(t\text{-}Bu)_3)_2$ (5 mol%)	-	K_2CO_3 (2.5 equiv)	110 °C	24h	trace B

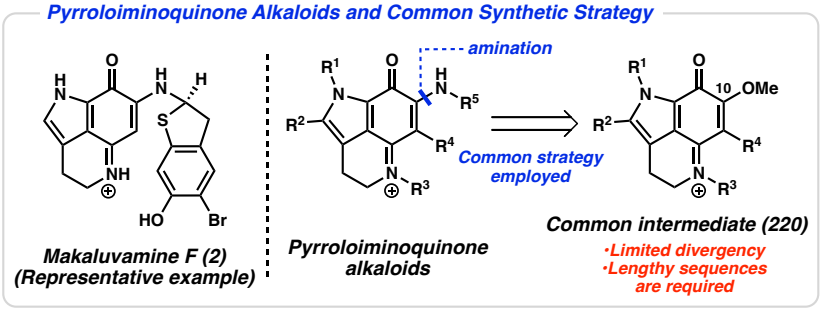
CHAPTER 2

Divergent Total Syntheses of Pyrroloiminoquinone Alkaloids Enabled by the Development of a Larock/ Buchwald–Hartwig Annulation/Cyclization[†]

2.1 INTRODUCTION

As previously discussed (*vide supra,* Chapter 1.1), the complex and unique structures of pyrroloiminoquinone natural products have inspired synthetic efforts for decades and several successful total syntheses of these alkaloids have been reported.[1,2] Strategies typically utilize a common late-stage C10-oxygenated pyrroloiminoquinone intermediate **220**, with amination serving to introduce the final nitrogen atom (Figure 2.1.1). While this approach has proved successful, there is limited divergency from

Figure 2.1.1 *Common synthetic strategy to pyrroloiminoquinone alkaloids.*

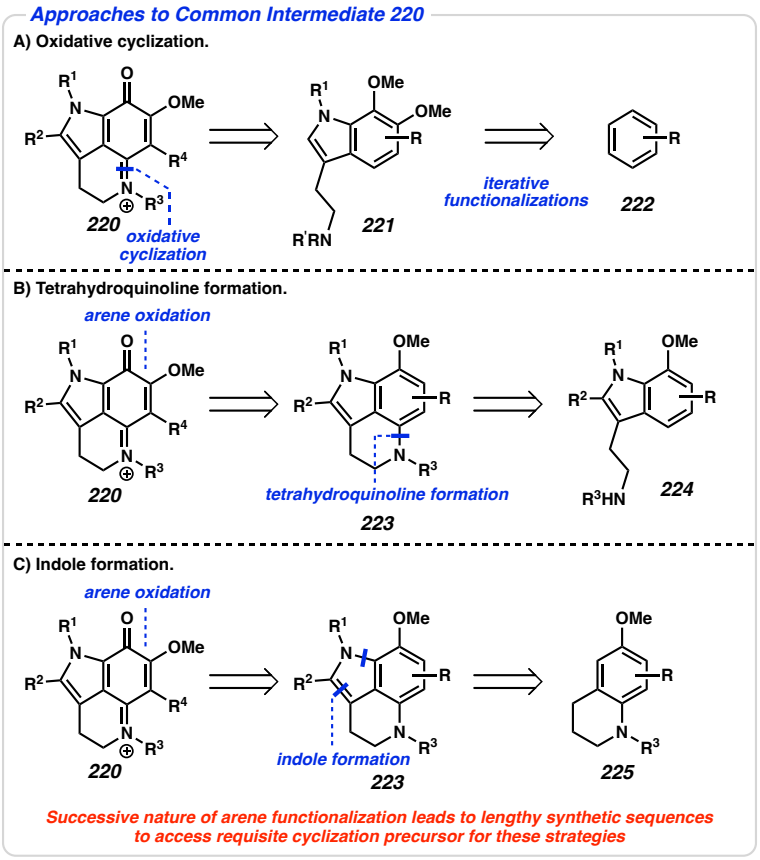


[†]This research was performed in collaboration with Jonathan Farhi, Hao Yu, and Zachary Sercel. Portions of this chapter are reproduced with permission from Stoltz, et al. *Chem. Sci.* **2024**, *15*, 12284–12290; and from NSF grant # 2247315.

common iminoquinone intermediate **220**, and other functionality appended to the central core (i.e., R^1– R^4) must be introduced earlier in the synthesis. This lack of divergency could explain the paucity of structure–activity relationship (SAR) studies of pyrroloiminoquinone alkaloids.[3] Additionally, access to the common intermediate **220** typically necessitates lengthy synthetic sequences due to the linear nature of arene functionalization steps.

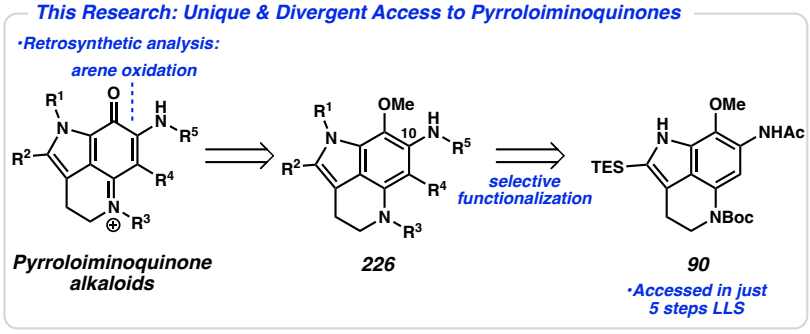
Given that most syntheses of pyrroloiminoquinones proceed through the common iminoquinone intermediate **200**, much of the research in the field has focused on its construction which has resulted in three major strategies. The first utilizes an oxidative cyclization strategy, wherein the iminoquinone is constructed from a tryptamine (**221**) through a sequential arene oxidation and nitrogen cyclization (Scheme 2.1.1A). This tryptamine in turn is accessed through iterative arene functionalizations from a simple arene starting material (**222**). The second is a tetrahydroquinoline formation approach, in which the iminoquinone oxidation state is first adjusted back to an anisole derivative (**223**, Scheme 2.1.1B). The tetrahydroquinoline C–N bond is then forged through a cyclization event, once again tracing back to a tryptamine derivative (**224**). The third approach focuses on an indole formation, where again arene oxidation state adjustment leads back to an anisole type intermediate (**223**, Scheme 2.1.1C). The indole is then disconnected tracing back to a tetrahydroquinoline derivative (**225**) which is accessed through iterative functionalizations from a simple arene starting material. Although these approaches have proved successful in numerous syntheses, the successive nature of arene functionalization leads to lengthy synthetic sequences in order to access the requisite cyclization precursor.[4]

Scheme 2.1.1 *Approaches to common intermediate* ***220****.*



We devised an alternative approach in order to address the issues of divergence and step count, envisioning a direct arene oxidation state adjustment leading back to an aminoindole (**226**) that already contains the C10 nitrogen atom— an uncommon disconnection that avoids the use of the common intermediate **220** (Scheme 2.1.2).[5] We hypothesized that with judicious choice of nitrogen protecting groups, selective functionalization of all five possible positions of the pyrroloiminoquinone scaffold (R^1–R^5) could be achieved. We identified that amino tricycle **90**, accessed through the development of the Larock/Buchwald–Hartwig annulation/cyclization during our synthetic studies toward aleutianamine (**90**), possessed the appropriate orthogonal protecting groups to realize this selective functionalization approach.

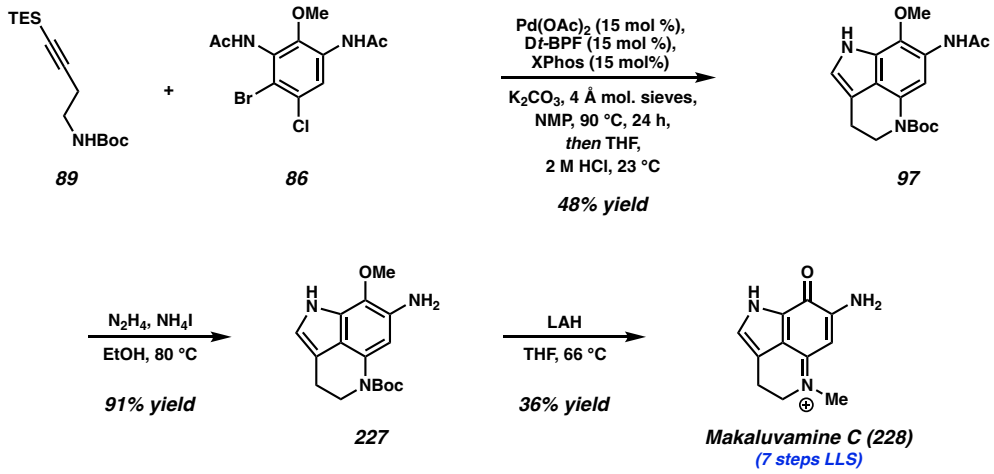
Scheme 2.1.2 *Our divergent strategy to access pyrroloiminoquinones.*



2.2 TOTAL SYNTHESIS OF MAKALUVAMINE C

Our studies commenced by targeting the selective functionalization of the secondary aniline nitrogen of amino tricycle **90** (R^3). To this end, the Larock/Buchwald-Hartwig annulation/cyclization could be followed by an acidic workup to provide desilylated tricycle **97** (Scheme 2.2.1). Employing modified conditions from Ohshima and coworkers,[6] the acetamide could be selectively removed in the presence of the carbamate, yielding aniline **227**. Finally, lithium aluminum hydride (LAH) reduction of the carbamate to the *N*-Me moiety was accompanied by spontaneous aerobic oxidation to yield makaluvamine C (**228**) in just seven steps (LLS).

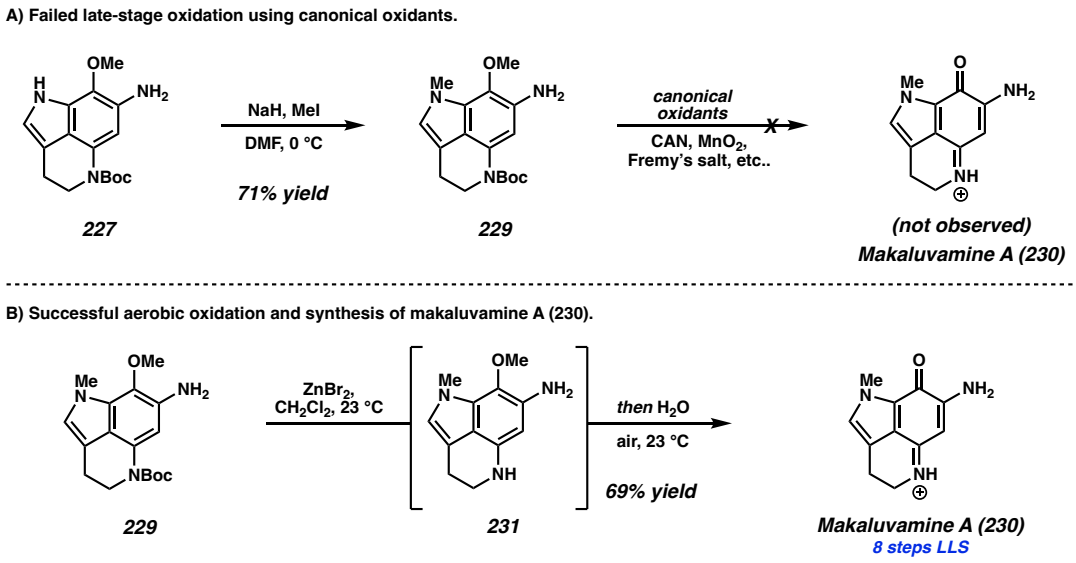
Scheme 2.2.1 *Total synthesis of makaluvamine C (**228**).*



2.3 TOTAL SYNTHESIS OF MAKALUVAMINE A

We next investigated the selective functionalization of the indole nitrogen (Scheme 2.3.1A). Starting with aniline **227**, selective *N*-methylation of the indole nitrogen was achieved under basic conditions to give tricycle **229**. We attempted canonical arene oxidation conditions to pyrroloiminoquinones such as CAN, Fremy's salt, or MnO_2, but unfortunately non-specific decomposition of tricycle **229** was observed under these conditions. Excitingly, when the Boc group was first removed using $ZnBr_2$,[7] the resulting highly electron-rich aniline intermediate **231** underwent spontaneous aerobic oxidation, providing makaluvamine A (**230**) in eight steps (LLS, Scheme 2.3.1B).

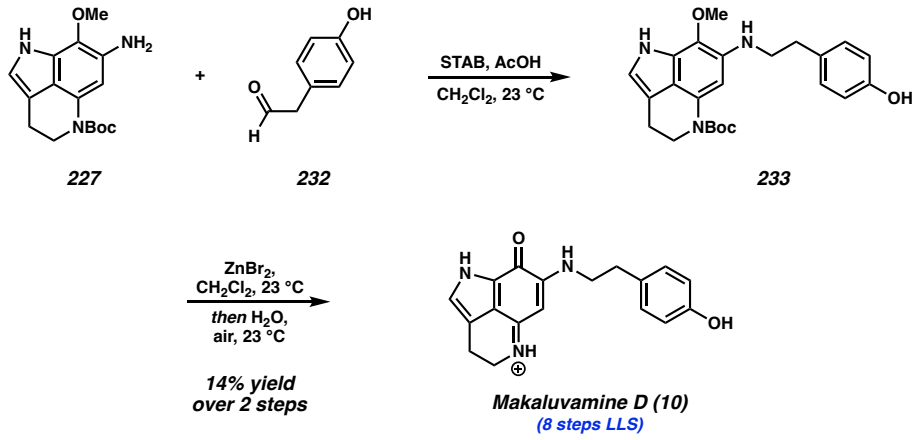
Scheme 2.3.1 *Total synthesis of makaluvamine A (**230**).*



2.4 TOTAL SYNTHESIS OF MAKALUVAMINE D

Next, we targeted the selective functionalization of the 1° aniline nitrogen (Scheme 2.4.1). This was achieved using a reductive amination between aniline **227** and aldehyde **232**, to yield *N*-alkylated aniline **233**. Then, our mild arene oxidation protocol was employed to yield makaluvamine D (**10**) in eight steps (LLS).

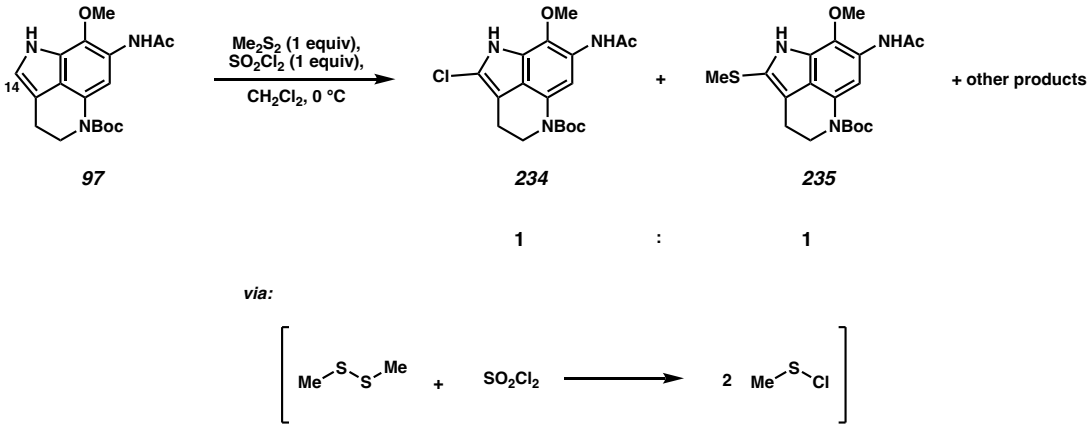
Scheme 2.4.1 *Total synthesis of makaluvamine D (**10**).*



2.5 TOTAL SYNTHESIS OF ISOBATZELLINE B

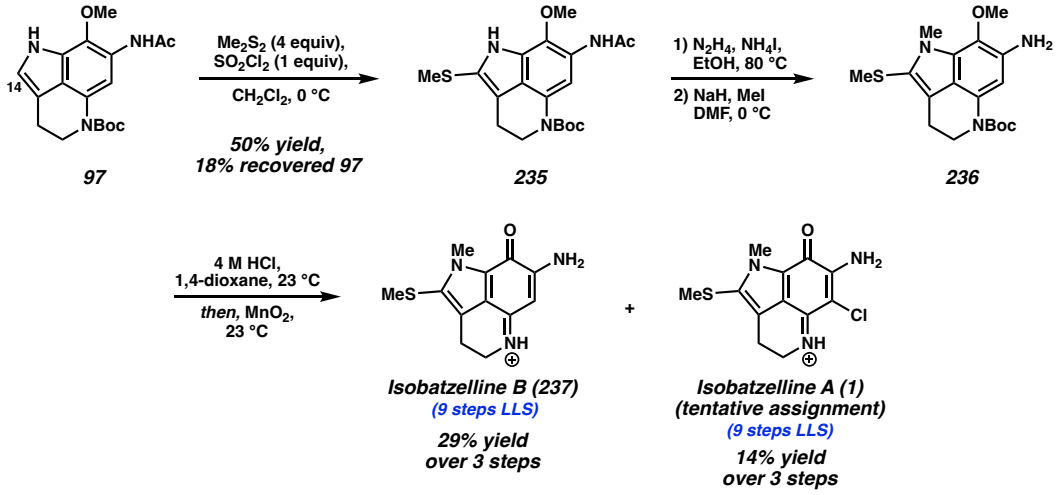
We then turned our attention to functionalizing the indole C14 position (Scheme 2.5.1). Using thiomethylation conditions reported by Joule and coworkers,[1i] which employ a 1:1 stoichiometry of Me_2S_2 and SO_2Cl_2 to generate the active thiomethylating reagent MeSCl prior to substrate addition, a mixture of chlorinated product **234** and desired thiomethylated product **235** was obtained, along with other oxidized/decomposition products. We hypothesized that unconsumed SO_2Cl_2 was promoting the undesired reaction pathways.

Scheme 2.5.1 *Non-selective thiomethylation of tricycle **97**.*



To circumvent this, an excess of Me_2S_2 was employed to ensure complete consumption of SO_2Cl_2 prior to substrate addition (Scheme 2.5.2). This modified protocol led to clean formation of the desired thiomethylated product **235**, and only trace amounts of undesired chlorinated arene **234** were observed. From thiomethylated arene **235**, acetamide cleavage followed by indole *N*-methylation provided tricycle **236**. Unfortunately, this substrate performed poorly in the $ZnBr_2/O_2$ deprotection/oxidation step. Instead, we found that the Boc deprotection could be achieved using anhydrous HCl in dioxane, and the resulting intermediate (not shown) could undergo arene oxidation with MnO_2 in the same flask to provide isobatzelline B (**237**) in 9 steps (LLS). Interestingly, we also isolated

Scheme 2.5.2 *Total synthesis of isobatzelline B (**237**).*

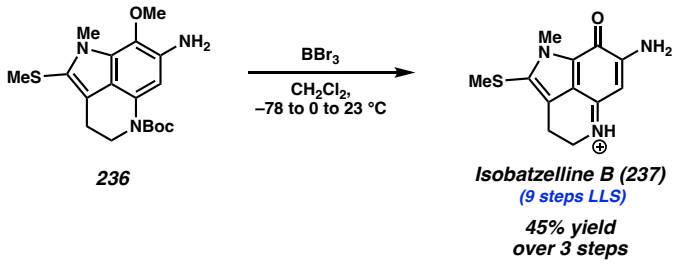


isobatzelline A (**1**) from the reaction mixture, representing a 9 step synthesis (LLS) of this natural product. We report this as a tentative assignment as decomposition was observed during the ^{13}C NMR experiment, although the ^{1}H NMR spectra was in good agreement with those previously reported.[1n] We hypothesize that isobatzelline A (**1**) forms from isobatzelline B (**237**) under the reaction conditions through an oxidative nucleophilic substitution of hydrogen (ONSH) type transformation, wherein Cl^- addition into

isobatzelline B (**237**) is followed by oxidation. Alternatively, Cl_2 could be generated from HCl and MnO_2, which then chlorinates the pyrroloiminoquinone double bond in isobatzelline B (**237**), followed by elimination to provide isobatzelline A (**1**).[8]

To improve the selectivity for the formation of isobatzelline B (**237**), an alternative protocol was developed: treatment of tricycle **236** with BBr_3 affected a deprotection of the Boc group and demethylation of the anisole (Scheme 2.5.3). The resulting aminophenol (not shown) then underwent spontaneous aerobic oxidation to yield isobatzelline B (**237**). Notably, this reaction sequence led to much cleaner reaction profiles, simplified the purification process, and formed isobatzelline B (**237**) in a greater 45% yield. Additionally, this BBr_3 deprotection/aerobic oxidation protocol could be extended to other substrates (i.e. tricycle **229** and **233)**, and typically performed superior to the $ZnBr_2$ deprotection/aerobic oxidation protocol on larger scales.

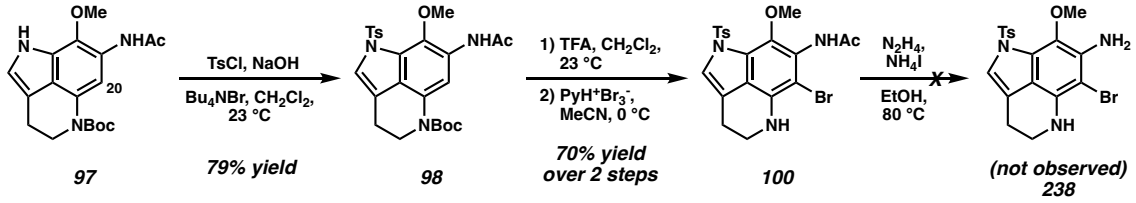
Scheme 2.5.3 *Alternative reaction conditions to access isobatzelline B (**237**).*



2.6 TOTAL SYNTHESIS OF MAKALUVAMINE N

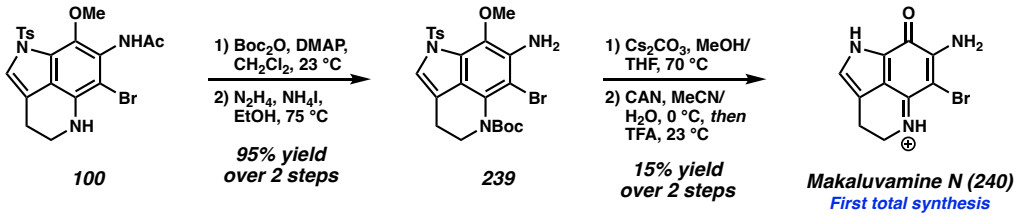
Finally, we set out to selectively functionalize the C20 position of tricycle **97** (Scheme 2.6.1). The indole nitrogen was first protected as a sulfonamide to yield tricycle **98**, which then underwent Boc removal and selective C20 bromination to provide bromo-tricycle **100**. Unfortunately, direct acetamide cleavage of this compound proved unsuccessful. Instead, the 2° aniline nitrogen of bromo-tricycle **100** was reprotected as the

Scheme 2.6.1 *Failed synthesis of bromoarene* ***238***.



carbamate, which was followed by acetamide removal to yield bromoaniline **239** (Scheme 2.6.2). The tosyl group was then removed under basic conditions, and arene oxidation using CAN followed by Boc deprotection yielded makaluvamine N (**240**) in twelve steps (LLS), representing the first total synthesis of this natural product to date.

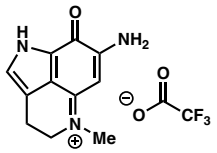
Scheme 2.6.2 *Total synthesis of makaluvamine N (****240****).*



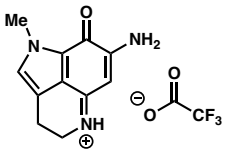
2.7 PRELIMINARY INVESTIGATION OF BIOLOGICAL ACTIVITIES

With the several synthetic intermediates and natural products in hand, we collaborated with the Chou lab at Caltech to investigate the preliminary biological activity of these compounds against five different human cancer cell lines (Figure 2.7.1). Makaluvamines C, A, and D (**228, 230,** and **10**) were moderately active against all five cells lines with IC_{50} values in the single digit μM range. Interestingly, makaluvamines C and D (**228** and **10**) were much less active against the human prostate cancer cell line LNCaP compared to makaluvamine A (**230**), which retained respectable activity. The two halogenated pyrroloiminoquinones makaluvamine N (**240**) and isobatzelline A (**1**) displayed significantly higher levels of toxicity across all cell lines, with particular potency to the human prostate cancer cell line DU145 (IC_{50} = 9 and 8 nM, respectively). This is in

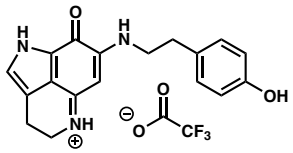
Figure 2.7.1 *Preliminary biological activities of simpler pyrroloiminoquinones.*



Makaluvamine C (228)

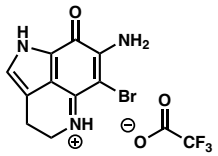


Makaluvamine A (230)

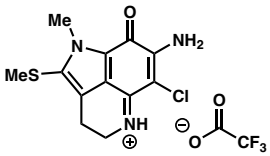


Makaluvamine D (10)

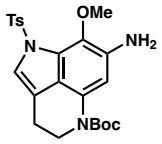
Cell line:	IC50 (μM):	IC50 (μM):	IC50 (μM):
HCT116	7	2	12
PANC1	7	3	26
MCF7	10	1.7	5.2
LNCaP	>55	6	>55
PC3	3.5	1.7	4.9
DU145	55	6	>55



Makaluvamine N (240)



Isobatzelline A (1)



amino tricycle 241

Cell line:	IC50 (μM):	IC50 (μM):	IC50 (μM):
HCT116	0.1	0.3	25
PANC1	0.21	0.74	33
MCF7	0.09	0.2	24
LNCaP	0.31	0.84	>55
PC3	0.24	0.55	23
DU145	0.009	0.008	30

line with aforementioned observations in the aleutianamine series (see Chapter 1.8), wherein aleutianamine (**15**) was significantly more active than *des*-bromoaleutianamine **(147**), potentially highlighting the importance of halogenation in order to render these scaffolds highly toxic toward cancer cells. Also in line with the aforementioned observations (see Chapter 1.8), oxidation of the central arene is required for significant levels of activity; reduced amino tricycle **241** was less active across the series compared to the oxidized natural products.

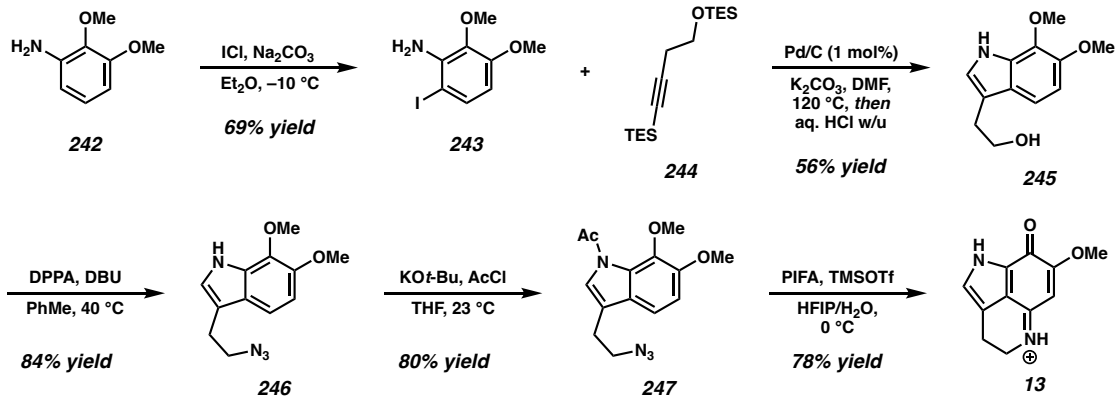
2.8 CONCLUSION

In summary, we devised a unique approach to five pyrroloiminoquinone alkaloids, which could likely be applied to additional natural products and analogs. Our strategy was

enabled by the development of a novel Larock/Buchwald–Hartwig annulation/cyclization to rapidly access the core of these natural products. By judicious choice of nitrogen protecting groups, the key tricyclic intermediate was selectively functionalized in five different positions to provide the shortest total syntheses at the time of makaluvamines A (**230**), C (**228**), and D (**10**) and isobatzelline B (**237**), and the first total synthesis of makaluvamine N (**240**). We believe that this strategy will facilitate analog synthesis and the advancement of pyrroloiminoquinones as therapeutic candidates, which has historically been a challenge due to the lack of divergent synthetic routes.

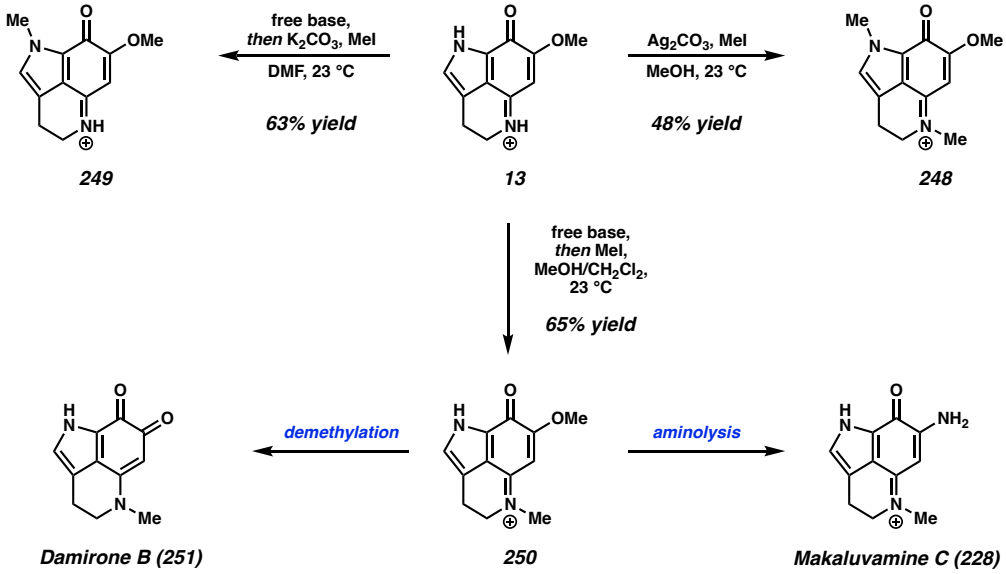
It should be noted that after our studies were disclosed, Vanderwal and coworkers reported the synthesis of several members in the class using common intermediate **13** as a point of divergence.[9] They demonstrated an improved route to Kita's previously prepared common intermediate **13**[1j], which hinged upon a Larock indolization to access tryptophol **245** (Scheme 2.8.1). Indole **245** was then elaborated to azide **247** over two steps, at which point they used modified conditions reported by Kita[1j] to affect an oxidative cyclization that provided common intermediate **13**.

Scheme 2.8.1 *Vanderwal's improved sequence to common intermediate* ***13***.



From **13**, they showcased that selective methylation could be achieved based upon the reaction conditions (i.e. base and solvent), and were able to access methylated products **248**, **249**, and **250** (Scheme 2.8.2). From each of these products, they demonstrated that either aminolysis (i.e. **250** to **228**) or demethylation (i.e. **250** to **251**) could be accomplished, which yielded several different pyrroloiminoquinone alkaloids. Additionally, they highlighted that the C20 position on the scaffold could be halogenated. However, no examples of C14 functionalization were described.

Scheme 2.8.2 *Vanderwal's divergent synthesis of pyrroloiminoquinones from common intermediate* ***13***.



2.9 EXPERIMENTAL SECTION

2.9.1 METHODS AND MATERIALS

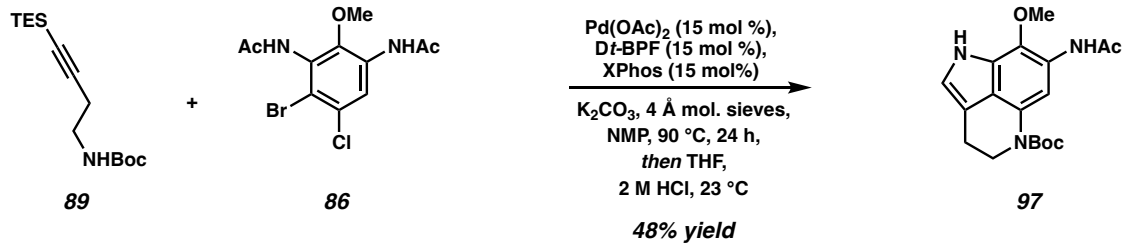
Unless otherwise stated, reactions were performed in flame-dried glassware under a nitrogen atmosphere using dry, deoxygenated solvents. Solvents were dried by passage through an activated alumina column under Ar. Reagents were purchased from commercial sources and used as received. K_2CO_3 was freshly flame-dried under vacuum prior to use.

4Å molecular sieves were activated via microwave heating (1100 W, full power, 45 s X 4), cooled under N_2, and stored in a N_2 filled glovebox. Reaction temperatures were controlled by an IKAmag temperature modulator. Thin-layer chromatography (TLC) was performed using E. Merck silica gel 60 F254 pre-coated plates (250 μm) and visualized by UV fluorescence quenching, potassium permanganate staining, or *p*-anisaldehyde staining. Silicycle SiliaFlash P60 Academic Silica gel (particle size 40–63 μm) was used for flash chromatography. Preparative HPLC was performed on an Agilent 1100 Series HPLC system using a 9.4 x 250 mm Agilent Eclipse XDB-C18 column, or on an Agilent 1200 Series HPLC system using a 9.4 x 250 mm Agilent Zorbax Rx-SIL column. ^{1}H and ^{13}C NMR spectra were recorded on Varian Inova 500 (500 and 125 MHz, respectively), Varian Inova 600 (600 and 150 MHz, respectively), and Bruker 400 (400 and 100 MHz, respectively) spectrometers and are reported in terms of chemical shift relative to $CHCl_3$ (δ 7.26 and 77.16 ppm, respectively), DMSO (δ 2.50 and 39.52 ppm, respectively), or CH_3OH (δ 3.31 and 49.01 ppm, respectively). Data for ^{1}H NMR are reported as follows: chemical shift (δ ppm) (multiplicity, coupling constant, integration). Abbreviations are used as follows: br s = broad singlet, s = singlet, d = doublet, t = triplet, q = quartet, m = multiplet. IR spectra were obtained from thin films deposited on NaCl plates using a Perkin Elmer Spectrum BXII spectrometer and are reported in frequency of absorption (cm^{-1}). High resolution mass spectra (HRMS) were obtained from the Caltech Mass Spectral Facility using a JEOL JMS-600H High Resolution Mass Spectrometer in fast atom bombardment (FAB+), GC field ionization (GCFI+), or electron ionization (EI+) mode, or using an Agilent 6200 Series TOF with an Agilent G1978A Multimode source in

electrospray ionization (ESI+), atmospheric pressure chemical ionization (APCI+), or mixed ionization mode (MM: ESI-APCI+).

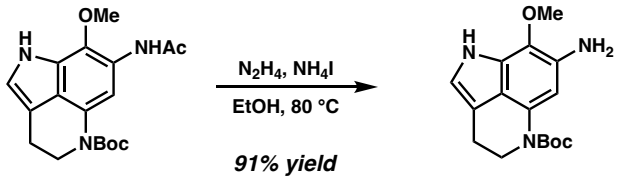
2.9.2 EXPERIMENTAL PROCEDURES

For experimental procedures for compounds **86, 89**, **98**, and **100** see chapter 1.10.2.



One-step Larock/Buchwald-Hartwig/silyl deprotection procedure.

Prepared according to general procedure A (see chapter 1.10.2) using 100 mg of bromo arene **86** (0.298 mmol). After 24 h of stirring at 90 °C, LC/MS analysis indicated consumption of the starting material and formation of direct Larock/Buchwald-Hartwig product **90** (not shown). The reaction mixture was cooled to 23 °C and THF (3.0 mL, 0.1 M) and aq. 2 M HCl (3.0 mL, 0.1 M) were added. The reaction mixture was stirred at 23 °C for 5 h, at which point LC/MS analysis indicated complete formation of the desilylated product. The reaction mixture was transferred to a separatory funnel with EtOAc, and further diluted with saturated aq. $NaHCO_3$ (20 mL), 1 M aq. LiCl (30 mL) and EtOAc (30 mL). The product was extracted with EtOAc (5 x 30 mL). The combined organic layers were washed with 1 M aq. LiCl (x 3), dried over Na_2SO_4, filtered, and concentrated under reduced pressure. The crude product was purified by column chromatography (SiO_2, 60-70%-80%-90% EtOAc/Hexanes) to afford the title compound (**97**, 49.1 mg, 48% yield) as a brown solid.



97 ***227***

Deprotected amino tricycle 227: Prepared using a modified procedure.[6] Under an ambient atmosphere, a flame dried 4 mL vial was charged with indole **97** (66.3 mg, 0.19 mmol, 1.0 equiv). EtOH (1.9 mL, 0.1M), N_2H_4•H_2O (0.288 mL, 5.76 mmol, 30.0 equiv), and NH_4I (275.5 mg, 1.9 mmol, 10.0 equiv) were then added. The solution was degassed with argon for 1 minute and sealed with a PTFE cap. The reaction mixture was heated at 80 °C for 24 h, at which point LC/MS analysis indicated complete consumption of the starting material. The reaction mixture was concentrated under reduced pressure to near dryness. Ethyl acetate (10 mL) was used to transfer the mixture to a separatory funnel. Water (10 mL) was then added and the product was extracted with EtOAc (3 x 10 mL). The combined organic layers were washed with brine, dried over Na_2SO_4, filtered, and concentrated under reduced pressure. The crude product was purified by column chromatography (SiO_2, 60% EtOAc/Hexanes) to afford the title compound (52.7 mg, 91% yield) as a brown solid.

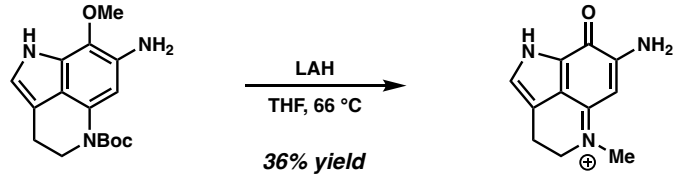
^{1}H NMR (600 MHz, CD_3OD): δ 6.93 (s, 1H), 6.67 (s, 1H), 3.96 – 3.91 (m, 2H), 3.88 (s, 3H), 2.90 – 2.85 (m, 2H), 1.56 (s, 9H);

^{13}C NMR (100 MHz, CD_3OD): δ 155.4, 134.3, 130.7, 129.6, 128.8, 118.3, 116.8, 111.1, 103.8, 82.1, 60.1, 46.9, 28.7, 23.9.

IR (Neat film, NaCl): 3345, 2916, 2849, 1684, 1635, 1524, 1443, 1589, 1364, 1241, 1217, 1160, 1127, 963, 835 cm^1.

HRMS (ESI+): *m/z* calc'd for $C_{16}H_{22}N_3O_3$ $[M+H]^+$: 304.1656, found 304.1652.

Note: This compound is stable under ambient conditions (i.e., air atmosphere) frozen in benzene at –20 °C for up to 1 month. However, this compound is indefinitely stable when stored at room temperature in a nitrogen filled glovebox.



227 ***Makaluvamine C (228)***

Makaluvamine C (228): Under an ambient atmosphere, a flame dried 4 mL vial was charged lithium aluminum hydride (LAH, 406 mg, 10.7 mmol, 30.0 equiv) and THF (3.57 mL, 0.1M). This solution was cooled to 0 °C and stirred for 1 minute. Amino indole **227** (108.2 mg, 0.357 mmol, 1.0 equiv) in THF (0.8 mL) was then added dropwise. This solution was stirred at 0 °C for 5 minutes. The vial was sealed with a PTFE cap and heated to 66 °C for 36 h, at which point LC/MS analysis indicated complete consumption of the starting material. The reaction mixture was then cooled to 0 °C and Rochelle's salt (6 mL) was added dropwise. This mixture was stirred for 5 minutes at 0 °C and then transferred to a separatory funnel with ethyl acetate (20 mL). Water (20 mL) was then added and the product was extracted with EtOAc (8 x 20 mL). The combined organic layers were directly dried over Na_2SO_4, filtered, and concentrated under reduced pressure. The crude product was purified by column chromatography (SiO_2, 10% MeOH/CH_2Cl_2, 1% TFA) to afford Makaluvamine C as a brown solid. This solid was dissolved in MeOH (1 mL) and TFA (5 drops) was added. The resulting purple solution was concentrated under reduced pressure to yield the TFA salt of Makaluvamine C (**228**, 70.0 mg, 62% yield) as a purple solid.

^{1}H NMR (600 MHz, DMSO-*d*6): δ 13.09 (s, 1H), 9.42 (s, 1H), 8.65 (s, 1H), 7.28 (s, 1H), 5.71 (s, 1H), 3.89 (t, J = 7.6 Hz, 2H), 3.31 (s, 3H), 2.91 (t, J = 7.6 Hz, 2H).

^{13}C NMR (100 MHz, DMSO-*d*6): δ 167.5, 156.6, 155.8, 126.7, 123.4, 123.3, 118.1, 85.4, 52.7, 18.9. *Note: The carbon signal at 39.0 was obscured by the DMSO peak.*

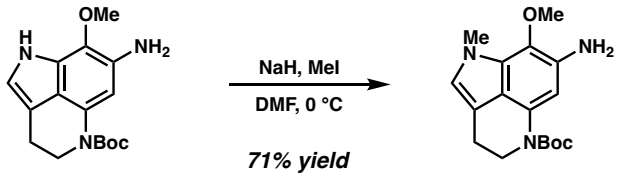
^{1}H NMR (600 MHz, MeOD): δ 7.11 (s, 1H), 5.71 (s, 1H), 3.94 (t, J = 7.6 Hz, 2H), 3.38 (s, 3H), 3.00 (t, J = 7.6 Hz, 2H).

^{13}C NMR (100 MHz, MeOD): δ 167.1, 157.1, 156.8, 125.5, 123.6, 123.4, 118.1, 85.3, 52.9, 38.2, 18.9.

IR (Neat film, NaCl): 3742, 3136, 3045, 2921, 2852, 2364, 1610, 1435, 1409, 1401, 1036, 730.

HRMS (ESI+): *m/z* calc'd for $C_{11}H_{12}N_3O$ $[M]^+$: 202.0975, found 202.0975.

These characterization data are in good agreement with those previously reported.[5,10]



227 ***229***

***N*-methylated tricycle 229:** A flame dried 4 mL vial was charged with NaH (12.0 mg, 0.3 mmol, 1.5 equiv), DMF (0.5 mL, 2.5 M), and brought to 0 °C. Aniline **227** (60.8 mg, 0.2 mmol, 1.0 equiv) in DMF (4.0 mL, 0.05M) was then added dropwise. The solution was stirred at 0 °C for 30 min, at which point MeI (0.0125 mL, 0.2 mmol, 1.0 equiv) was added. The solution was stirred for 30 min at 0 °C, at which point LC/MS analysis indicated complete consumption of the starting material. Saturated aq. NH_4Cl (2 mL), water (20 mL) and EtOAc (20 mL) were added, and the product was extracted with EtOAc (3 x 30 mL). The combined organic layers were washed with 1M aq. LiCl (x2), dried over Na_2SO_4, filtered, and concentrated under reduced pressure. The crude product was purified by

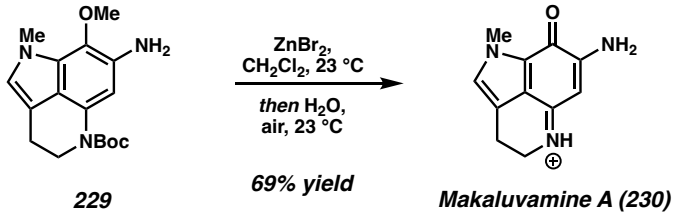
column chromatography (SiO_2, 40%-50% EtOAc/Hexanes) to afford the title compound (44.8 mg, 71% yield) as a brown foam.

^{1}H NMR (400 MHz, CD_3OD): δ 6.91 (s, 1H), 6.50 (s, 1H), 3.93 – 3.88 (m, 2H), 3.87 (s, 3H), 3.81 (s, 3H), 2.86 – 2.81 (m, 2H), 1.56 (s, 9H).

^{13}C NMR (100 MHz, CD_3OD): δ 155.4, 135.8, 131.2, 130.1, 129.5, 122.1, 118.6, 110.6, 103.9, 82.2, 61.8, 46.7, 34.6, 28.7, 23.8.

IR (Neat film, NaCl): 3356, 2929, 2500, 2218, 2068, 1693, 1623, 1518, 1454, 1389, 1375, 1268, 1255, 1215, 1160, 1123, 1017, 960, 847, 765 cm^1.

HRMS (ESI+): *m/z* calc'd for $C_{17}H_{24}N_3O_3$ $[M+H]^+$: 318.1812, found 318.1817.



229 ***69% yield*** ***Makaluvamine A (230)***

Makaluvamine A (230): To a flame dried 20 mL scintillation vial in a nitrogen filled glove box were added amino indole **24** (44.8 mg, 0.14 mmol, 1.0 equiv), anhydrous $ZnBr_2$ (252.2 mg, 1.12 mmol, 8.0 equiv), and CH_2Cl_2 (1.4 mL, 0.1M). The vial was sealed with a red septum, removed from the glovebox, and stirred under N_2 at 23 °C for 2 h. Water (4.0 mL, 0.035 M) was then added, and the mixture was stirred at 23 °C for 10 min. The red septum was removed and a gas dispersion tube connected to a compressed air line was fitted onto the vial and lowered into the solution. The mixture was further stirred at 23 °C with air bubbling into the solution for 20 min, at which point LC/MS analysis indicated consumption of most of the starting material and formation of the product. The reaction mixture was diluted with saturated aq. $NaHCO_3$ (20 mL) and a 4:1 CH_3Cl:MeOH mixture (20 mL). The product was extracted with a 4:1 CH_3Cl:MeOH mixture (20 mL x 15). The

combined organic layers were dried over Na_2SO_4, filtered, and concentrated under reduced pressure. The crude product was purified by column chromatography (SiO_2, 10% MeOH/DCM + 1% TFA). The combined product fractions were concentrated under reduced pressure, were redissolved in MeOH (2 mL) and TFA (0.1 mL), and concentrated under reduced pressure to afford the TFA salt of makaluvamine A (**230**, 30.4 mg, 69% yield) as a brown/purple solid.

^{1}H NMR (400 MHz, DMSO-*d6*): δ 10.64 (s, 1H), 9.15 (s, 1H), 8.35 (s, 1H), 7.30 (s, 1H), 5.64 (s, 1H), 3.88 (s, 3H), 3.74 (td, J = 7.7, 2.8 Hz, 2H), 2.82 (t, J = 7.6 Hz, 2H).

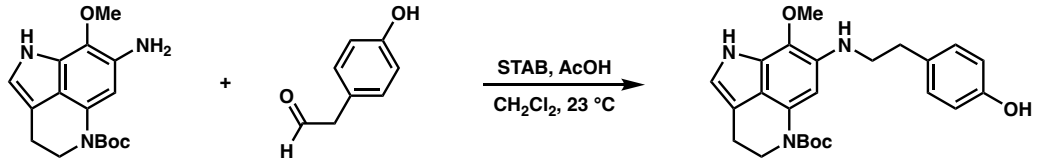
^{1}H NMR (600 MHz, MeOD): δ 7.11 (s, 1H), 5.62 (s, 1H), 3.96 (s, 3H), 3.82 (t, J = 7.6 Hz, 2H), 2.92 (t, J = 7.6 Hz, 2H).

^{13}C NMR (100 MHz, DMSO-*d6*): δ 168.4, 156.8, 156.0, 131.1, 123.1, 122.4, 117.9, 86.6, 42.1, 35.9, 18.0.

IR (Neat film, NaCl): 2914, 1667, 1601, 1527, 1430, 1392, 1320, 1251, 1169, 801, 708 cm^1.

HRMS (ESI+): *m/z* calc'd for $C_{11}H_{12}N_3O$ $[M]^+$: 202.0975, found 202.0976.

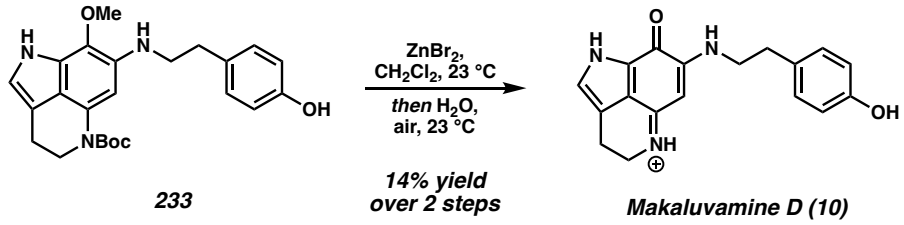
The characterization data are in good agreement with those previously reported.[1o,10]



227 ***232*** ***233***

***N*-alkylated tricycle 233:** A flame dried 4 mL vial was charged with aniline **227** (41.8 mg, 0.138 mmol, 1.0 equiv), and CH_2Cl_2 (1.4 mL, 0.1M). Aldehyde **232**[11] (18.76 mg, 0.138 mmol, 1.0 equiv) in CH_2Cl_2 (0.5 mL), sodium triacetoxyborohydride (STAB, 58.5 mg, 0.276 mmol, 2.0 equiv), and AcOH (0.004 mL, 0.276 mmol, 2.0 equiv) were then added.

The reaction mixture was stirred at 23 °C for 30 min, at which point LC/MS analysis indicated consumption of the starting material. The reaction mixture was transferred to a separatory funnel with EtOAc, and further diluted with EtOAc (10 mL) and saturated aq. $NaHCO_3$ (10 mL). The product was extracted with EtOAc (10 mL x 3). The combined organic layers were dried over Na_2SO_4, filtered, and concentrated under reduced pressure. The resulting crude brown solid (48.1 mg, 82% yield) was taken directly to the next step without further purification.



233 ***14% yield over 2 steps*** ***Makaluvamine D (10)***

Makaluvamine D (10): To a flame dried 20 mL scintillation vial in a nitrogen filled glove box was added amino indole **28** (32.0 mg, 0.076 mmol, 1.0 equiv), anhydrous $ZnBr_2$ (136.0 mg, 0.6 mmol, 8.0 equiv), and CH_2Cl_2 (1.5 mL, 0.05M). The vial was sealed with a red septum, removed from the glovebox, and stirred under N_2 at 23 °C for 2 h. Water (7.6 mL, 0.01 M) was then added, and the mixture was stirred at 23 °C for 10 min. The red septum was removed and a gas dispersion tube connected to a compressed air line was fitted onto the vial and lowered into the solution. The mixture was further stirred at 23 °C with air bubbling into the solution for 1 h, at which point LC/MS analysis indicated consumption of most of the starting material and formation of the product. The reaction mixture was diluted with saturated aq. $NaHCO_3$ (20 mL) and a 4:1 CH_3Cl:*i*-PrOH mixture (20 mL). The product was extracted with a 4:1 CH_3Cl: *i*-PrOH mixture (20 mL x 10). The combined organic layers were dried over Na_2SO_4, filtered, and concentrated under reduced pressure. The crude product was purified by column chromatography (SiO_2, 10% MeOH/DCM +

1% TFA). The combined product fractions were concentrated under reduced pressure, were redissolved in MeOH (2 mL) and TFA (0.1 mL), and concentrated under reduced pressure to afford the TFA salt of makaluvamine D (**10**, 4.0 mg, 17% yield) as a brown/purple solid.

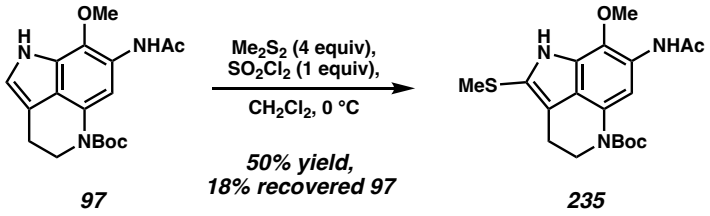
^{1}H NMR (600 MHz, CD_3OD): δ 7.15 (s, 1H), 7.07 (d, J = 8.4 Hz, 2H), 6.72 (d, J = 8.5 Hz, 2H), 5.38 (s, 1H), 3.84 (t, J = 7.6 Hz, 2H), 3.55 (t, J = 7.3 Hz, 2H), 2.95 (t, J = 7.5 Hz, 2H), 2.88 (t, J = 7.3 Hz, 2H).

^{13}C NMR (100 MHz, CD_3OD): δ 168.5, 159.7, 157.4, 155.1, 130.9, 130.0, 127.2, 125.5, 124.0, 120.2, 116.5, 85.2, 46.5, 44.2, 34.4, 19.5.

IR (Neat film, NaCl): 3442, 2921, 2368, 1688, 1440, 1211, 1143, 1025, 835, 737, 727, 629 cm[1].

HRMS (ESI+): *m/z* calc'd for $C_{18}H_{18}N_3O_2$ $[M]^+$: 308.1394, found 308.1391.

The characterization data are in good agreement with those previously reported.[12]



97 ***235***

Thiomethylated tricycle 235: Prepared using a modified procedure.[1i] To a flame dried 4 mL vial was added CH_2Cl_2 (1 mL, 0.56 M) and Me_2S_2 (0.15 mL, 1.72 mmol, 4.0 equiv). The solution was cooled to 0 °C and SO_2Cl_2 (0.035 mL, 0.43 mmol, 1.0 equiv) was added. The reaction mixture was stirred at 0 °C for 1 h to provide a 0.86 M solution of MeSCl in CH_2Cl_2.

To a separate flame dried 4 mL vial was added indole **97** (43.0 mg, 0.125 mmol, 1.0 equiv) and CH_2Cl_2 (2.5 mL, 0.05 M). The solution was cooled to –78 °C, and freshly prepared 0.86 M MeSCl solution in CH_2Cl_2 (0.145 mL, 0.125 mmol, 1.0 equiv) was added

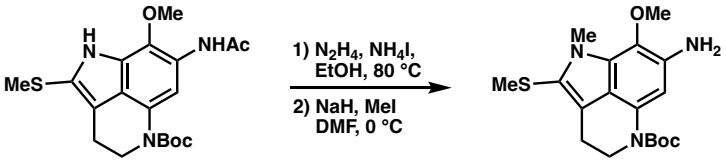
dropwise over 2 min. The reaction mixture was stirred for 5 min at –78 °C, at which point LC/MS analysis indicated near complete consumption of the starting material. Saturated aq. $Na_2S_2O_3$ solution (1 mL) was added at –78 °C, and the reaction mixture was warmed to 23 °C. The reaction mixture was transferred to a separatory funnel with EtOAc, and further diluted with EtOAc (30 mL) and H_2O (30 mL). The product was extracted with EtOAc (3 x 30 mL), the combined organic layers were washed with brine, dried over Na_2SO_4, filtered, and concentrated under reduced pressure. The product was purified via preparative TLC (2 plates, SiO_2, 80% EtOAc/hexanes) to afford the title compound (24.6 mg, 50% yield) as a yellow foam. 7.9 mg of indole **97** was re-isolated (18% recovered SM).

^{1}H NMR (600 MHz, CD_3OD): δ 7.58 (s, 1H), 3.98 (t, J = 5.6 Hz, 2H), 3.90 (s, 3H), 2.91 (t, J = 5.7 Hz, 2H), 2.41 (s, 3H), 2.18 (s, 3H), 1.56 (s, 9H).

^{13}C NMR (100 MHz, CD_3OD): δ 172.3, 155.3, 128.7, 128.6, 125.3, 125.0, 122.5, 115.9, 110.6, 109.7, 82.5, 61.1, 46.4, 28.7, 23.6, 23.3, 19.6.

IR (Neat film, NaCl): 3280, 2977, 2926, 1674, 1537, 1385, 1317, 1265, 1248, 1157, 1131, 1084, 1046, 1026, 958, 853, 737 cm^1.

HRMS (ESI+): *m/z* calc'd for $C_{19}H_{25}N_3O_4SNa$ $[M+Na]^+$: 414.1458, found 414.1464.



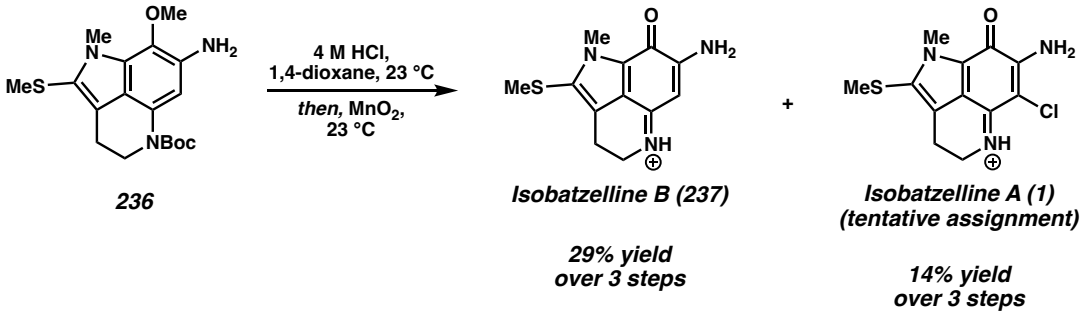
235 ***236***

Deprotected *N*-methylated thiomethylether tricycle 236: Under an ambient atmosphere, a flame dried 8 mL vial was charged with indole **235** (51.0 mg, 0.13 mmol, 1.0 equiv). EtOH (1.3 mL, 0.1M), N_2H_4•H_2O (0.122 mL, 3.9 mmol, 30.0 equiv), and NH_4I (188.5 mg, 0.1.3 mmol, 10.0 equiv) were then added. The solution was degassed with argon for 1

minute and sealed with a PTFE cap. The reaction mixture was heated at 80 °C for 16 h, at which point TLC analysis indicated complete consumption of the starting material. The reaction mixture was concentrated under reduced pressure to near dryness. Ethyl acetate (10 mL) was used to transfer the mixture to a separatory funnel. Water (10 mL) was then added and the mixture was extracted with EtOAc (3 x 20 mL). The combined organic layers were washed with brine, dried over Na_2SO_4, filtered, and concentrated under reduced pressure to afford an intermediate primary aniline (not shown, 45.1 mg, crude) as a brown solid which was used directly in the next step without further purification.

Note: This compound (intermediate primary aniline, not shown) was found to be unstable upon standing in air for >1 h, and was thus carried immediately forward after its preparation.

A flame dried 4 mL vial was charged with NaH (2.2 mg, 0.055 mmol, 1.5 equiv), DMF (0.074 mL, 0.5 M), and brought to 0 °C. The intermediate primary aniline (not shown, 12.9 mg, 0.037 mmol, 1.0 equiv) in DMF (0.74 mL, 0.05M) was then added dropwise. The solution was stirred at 0 °C for 30 min, at which point MeI (0.0023 mL, 0.037 mmol, 1.0 equiv) was added. The solution was stirred for 30 min at 0 °C, at which point TLC analysis indicated complete consumption of the starting material. Saturated aq. NH_4Cl (2 mL), water (2 mL) and EtOAc (2 mL) were added, and the product was extracted with EtOAc (3 x 3 mL). The combined organic layers were washed with 1M aq. LiCl (x2), dried over Na_2SO_4, filtered, and concentrated under reduced pressure to afford the title compound (9.2 mg, crude) as a brown solid which was used directly in the next step without further purification. *Note: This compound was found to be unstable upon standing in air for >1 h, and was thus carried immediately forward after its preparation*



236

Isobatzelline B (237)

29% yield over 3 steps

Isobatzelline A (1) (tentative assignment)

14% yield over 3 steps

Isobatzelline B (237) and Isobatzelline A (1): A flame dried 8 mL vial was charged with sulfide **236** (15.0 mg, 0.041 mmol, 1.0 equiv) and 4M HCl in dioxane (2.5 mL, 0.0165M). The reaction was stirred at 23 °C for 2 hours, at which point MnO_2 (35.7 mg, 0.41 mmol, 10.0 equiv) was added in one portion. The reaction was further stirred for 5 minutes, at which point saturated aq. $NaHCO_3$ (3 mL) was added. The reaction mixture was transferred to a separatory funnel and saturated aq. $NaHCO_3$ was added until the pH of the mixture was 7. The products were extracted with 4:1 $CHCl_3$:iso-propanol (10 mL X 10). The combined organic layers were dried over Na_2SO_4, filtered, and concentrated under reduced pressure. The crude brown solid was purified by preparatory TLC (4 plates, 9:1 DCM:MeOH) to afford isobatzelline B (**237**, 4.4 mg, 29% yield over three steps) as a red/brown solid and isobatzelline A (**1**, 2.3 mg, 14% yield over three steps) as a red solid.

Isobatzelline B (237):

^{1}H NMR (600 MHz, 1:1 CD_3OD:$CDCl_3$): δ 5.71 (s, 1H), 3.98 (s, 3H), 3.89 (t, J = 7.7 Hz, 2H), 2.87 (t, J = 7.7 Hz, 2H), 2.34 (s, 3H).

^{1}H NMR (600 MHz, CD_3OD, TFA salt): δ 5.65 (s, 1H), 4.01 (s, 3H), 3.86 (t, J = 7.6 Hz, 2H), 2.98 (t, J = 7.6 Hz, 2H), 2.40 (s, 3H).

^{13}C NMR (100 MHz, CD_3OD, TFA salt): δ 169.1, 159.2, 158.0, 136.5, 126.3, 124.5, 123.0, 87.7, 43.8, 33.7, 19.8, 18.4.

IR (Neat film, NaCl): 3214, 2921, 2853, 1665, 1616, 1463, 1265, 1122, 736 cm^1.

HRMS (ESI+): *m/z* calc'd for $C_{12}H_{14}N_3OS$ $[M+H]^+$: 248.0852, found 248.0855.

The characterization data are in good agreement with those previously reported.[13]

Isobatzelline A (1):

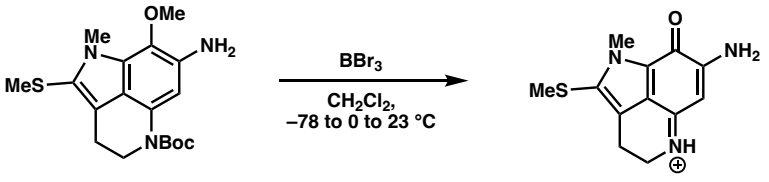
^{1}H NMR (600 MHz, 1:1 CD_3OD:$CDCl_3$): δ 4.05 (t, J = 7.8 Hz, 2H), 3.95 (s, 3H), 2.75 (d, J = 7.7 Hz, 2H), 2.31 (s, 3H). This data is in good agreement with those previously reported.[13]

Note: Decomposition of isobatzelline A was observed when acquiring the ^{13}C NMR, and thus we have reported this as a tentative assignment.

^{13}C NMR (100 MHz, 1:1 CD_3OD:$CDCl_3$): δ 169.5, 153.2, 142.5, 133.4, 131.7, 129.3, 127.4, 123.5, 121.9, 113.2, 68.8, 39.4, 32.9, 30.2, 23.2, 19.0.

IR (Neat film, NaCl): 3332, 3222, 2921, 2358, 1666, 1591, 1525, 1425, 1401, 1266, 1233, 1000, 721 cm^1.

HRMS (ESI+): *m/z* calc'd for $C_{12}H_{13}ClN_3OS$ $[M+H]^+$: 282.0462, found 282.0463.



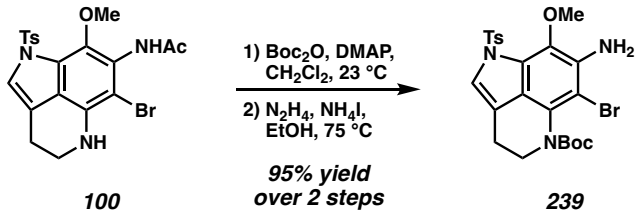
236 ***Isobatzelline B (237)***

45% yield over 3 steps

Alternative procedure for the preparation of isobatzelline B (237): A flame dried 1 dram vial was charged with aniline **236** (10.0 mg, 0.027 mmol, 1.0 equiv) and CH_2Cl_2 (0.4 mL, 0.07M). The resulting homogenous solution was cooled to –78 °C, at which point BBr_3 (0.081 mmol, 3.0 equiv) was added dropwise as a freshly prepared solution in CH_2Cl_2 (0.1 mL, 0.81 M). The reaction mixture was stirred at –78 °C for 1 h. Then, the reaction mixture was warmed to 0 °C and stirred at this temperature for 2 hours. The reaction mixture was then warmed to 23 °C and stirred at this temperature for 16 hours, at which point LC/MS

analysis indicated complete consumption of the starting material. The reaction was quenched with a saturated aqueous solution of $NaHCO_3$ (1 mL). The mixture was diluted with EtOAc (2 mL) and the product was extracted with EtOAc (3 x 1 mL). The combined organic layers were dried over Na_2SO_4, filtered, and concentrated under reduced pressure to afford a crude brown solid. Purification as previously described afforded isobatzelline B (**247**, 4.5 mg, 45% yield over three steps) as a red/brown solid.

*Note: The reaction profile was much cleaner by LC/MS compared to the previously described procedure, with the major product being isobatzelline B (**247**). No isobatzelline A (**1**) was observed when using this protocol.*



Bromoarene 239: A flame-dried 1 dram vial was charged with bromoindole **100** (19.3 mg, 0.0403 mmol, 1.0 equiv), DMAP (0.5 mg, 0.00403 mmol, 0.1 equiv), Boc_2O (26.4 mg, 0.121 mmol, 3.0 equiv), and CH_2Cl_2 (4 mL, 0.1M). The resulting mixture was stirred at 23 °C, and after 1 h the mixture was concentrated under reduced pressure to afford crude *N*-Boc bromoaniline (not shown), which was used directly without further purification.

A flame-dried ½ dram vial was charged with the intermediate *N*-Boc bromoaniline (not shown, *ca*. 0.0403 mmol, 1.0 equiv), NH_4I (175 mg, 1.21 mmol, 30 equiv), EtOH (0.4 mL, 0.1M) and $N_2H_4{\cdot}H_2O$ (0.26 mL, 4.03 mmol, 100 equiv). The resulting mixture was stirred at 75 °C for 2 days, at which point LC/MS analysis showed full consumption of the starting material. The reaction mixture was diluted with H_2O (2 mL) and extracted with CH_2Cl_2 (4x4 mL). The combined organic extracts were dried over Na_2SO_4 and

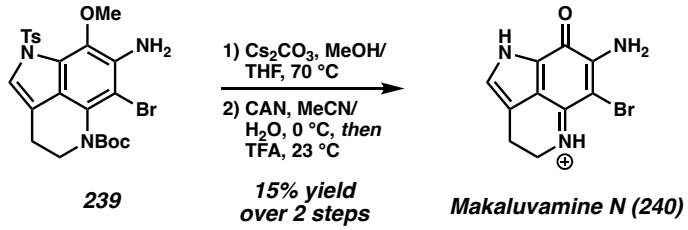
concentrated under reduced pressure. The resulting residue was purified by preparatory TLC (65% EtOAc/Hex) to the title compound (20.4 mg, 0.0382 mmol, 95% over 2 steps) as a brown solid.

^{1}H NMR (400 MHz, C_6D_6): δ 7.92 (d, J = 8.4 Hz, 2H), 7.30 (s, 1H), 6.69 (d, J = 7.9 Hz, 2H), 5.69 (s, 1H), 3.89 (s, 3H), 3.82, (s, 1H), 2.53 (t, J = 5.9 Hz, 2H), 2.24 (t, J = 6.0, 2H), 1.70 (s, 3H), 1.43 (s, 9H).

^{13}C NMR (100 MHz, C_6D_6): δ 154.0, 144.2, 137.7, 137.0, 135.9, 129.7 (2C), 126.1, 121.5, 120.9, 115.2, 101.3, 79.6, 61.9, 42.0, 28.4, 22.2, 21.1. (*Note: an additional ^{13}C resonance associated with the tosyl group is likely obscured by the solvent signal).*

IR (Neat film, NaCl): 2921, 1722, 1688, 1633, 1501, 1350, 1286, 1228, 1171, 1106, 850, 813, 664, 611.

HRMS (FD+): *m/z* calc'd for $C_{23}H_{27}BrN_3O_5S$ $[M+H]^+$: 536.0855, found 536.0852.



239 ***15% yield over 2 steps*** ***Makaluvamine N (240)***

Makaluvamine N (240): A flame-dried 1 dram vial was charged with bromoaniline **239** (19.1 mg, 0.0356 mmol, 1.0 equiv), Cs_2CO_3 (116 mg, 0.356 mmol, 10 equiv), MeOH (0.3 mL, 0.1M), and THF (0.6 mL, 0.05M), and the resulting mixture was stirred at 70 °C for 1.5 h. The reaction mixture was diluted with H_2O (5 mL), and extracted with CH_2Cl_2 (3x3 mL). The combined organic extracts were dried over Na_2SO_4 and concentrated under reduced pressure to afford the intermediate deprotected indole (not shown) as a brown solid which was used immediately in the next reaction without purification.

To a 20 mL vial containing deprotected indole (*ca.* 0.0356 mmol, 1.0 equiv) under nitrogen was added MeCN (2.0 mL). The resulting solution was cooled to 0 °C, then added CAN (25.4 mg, 0.0463 mmol, 1.3 equiv) in H_2O (1 mL). The reaction mixture was stirred at 0 °C for 5 min at which point LC/MS analysis showed full consumption of starting material. The reaction was diluted with H_2O (5 mL), extracted with DCM (3x5 mL). The combined organic phases were dried over Na_2SO_4, concentrated under reduced pressure, and the resulting residue was dissolved in TFA (1.8 mL). The mixture was allowed to stand at 23 °C for 10 min before being concentrated *in vacuo* to afford crude makaluvamine N (**240**). The crude product was purified by preparative reverse-phase HPLC (Eclipse XDB-C18, 5 μm, 9.4 x 250 mm, MeCN-H_2O (0.1% TFA) = 0:100 to 100:0, linear gradient for 6 min, flow rate = 5 mL/min) to afford makaluvamine N (**240**) as the TFA salt (2 mg, 0.00526 mmol, 15% over 2 steps).

^{1}H NMR (400 MHz, MeOD): δ 7.17 (s, 1H), 3.94 (t, *J* = 7.6 Hz, 2H), 2.99 (t, *J* = 7.6 Hz, 2H).

^{13}C NMR (100 MHz, MeOD): δ 166.4, 157.1, 155.5, 127.5, 125.1, 123.7, 120.9, 82.1, 45.0, 19.5.

IR (Neat film, NaCl): 3386, 3111, 1681, 1612, 1409, 1206, 721.

HRMS (FD+): *m/z* calc'd for $C_{10}H_9BrN_3O$ $[M+H]^+$: 265.9929, found 265.9930.

The characterization data are in good agreement with those previously reported.[14]

2.9.3 COMPARISON OF SYNTHETIC MAKALUVAMINE N TO PUBLISHED DATA

Table 2.9.3.1 *^{1}H NMR comparison table for makaluvamine N (**240**)*

Natural[14] (δ)	**Synthetic** (δ)
2.98 (2H, t, *J* = 7.5 Hz)	2.99 (t, *J* = 7.6 Hz, 2H).
3.93 (2H, t, *J* = 7.5 Hz)	3.94 (t, *J* = 7.6 Hz, 2H),
7.15 (1H, s,)	7.17 (s, 1H),

*Spectra acquired in MeOD.

Table 2.9.3.2 *^{13}C NMR comparison table for makaluvamine N (**240**)*

Natural[14] (δ)	**Synthetic** (δ)
19.5	19.5
45.1	45.0
82.3	82.1
121.0	120.9
123.7	123.7
125.1	125.1
127.6	127.5
155.4	155.5
157.2	157.1
166.3	166.4

*Spectra acquired in MeOD.

2.10 REFERENCES AND NOTES

(1) For representative syntheses of simpler pyrroloiminoquinones see: (a) X. L. Tao, S. Nishiyama and S. Yamamura, Total Syntheses of Batzelline C and Isobatzelline C, the Novel Pyrroloquinoline Alkaloids Isolated from the Marine Sponge *Batzella* Sp. *Chem. Lett*., **1991**, *20*, 1785–1786; (b) J. D. White, K. M. Yager and T. Yakura, Synthetic Studies of the Pyrroloquinoline Nucleus of the Makaluvamine Alkaloids. Synthesis of the Topoisomerase II Inhibitor Makaluvamine D. *J. Am. Chem. Soc.*, **1994**, *116*, 1831–1838; (c) T. Izawa, S. Nishiyama and S. Yamamura, Total syntheses of makaluvamines A, B, C, D and E, cytotoxic pyrroloiminoquinone alkaloids isolated from marine sponge bearing inhibitory activities against topoisomerase II. *Tetrahedron*, **1994**, *50*, 13593–13600; (d) D. Roberts, L. Venemalm, M. Alvarez and J. A. Joule, Synthesis of damirones A and B from a quinoline. *Tetrahedron Lett*., **1994**, *35*, 7857–7860; (e) E. V. Sadanandan, S. K. Pillai, M. V. Lakshmikantham, A. D. Billimoria, J. S. Culpepper and M. P. Cava, Efficient Syntheses of the Marine Alkaloids Makaluvamine D and Discorhabdin C: The 4,6,7-Trimethoxyindole Approach. *J. Org. Chem.*, **1995**, *60*, 1800–1805; (f) A. J. Peat and S. L. Buchwald, Novel Syntheses of Tetrahydropyrroloquinolines: Applications to Alkaloid Synthesis. *J. Am. Chem. Soc.*, **1996**, *118*, 1028–1030; (g) D. Roberts, J. A. Joule, M. A. Bros and M. Alvarez, Synthesis of Pyrrolo[4,3,2-de]quinolines from 6,7-Dimethoxy-4-methylquinoline. Formal Total Syntheses of Damirones A and B, Batzelline C, Isobatzelline C, Discorhabdin C, and Makaluvamines A−D. *J. Org. Chem.*, **1997**, *62*, 568–577; (h) M. Iwao, O. Motoi,

T. Fukuda and F. Ishibashi, New synthetic approach to pyrroloiminoquinone marine alkaloids. Total synthesis of makaluvamines A, D, I, and K. *Tetrahedron*, **1998**, *54*, 8999–9010; (i) M. Alvarez, M. A. Bros, G. Gras, W. Ajana and J. A. Joule, Syntheses of Batzelline A, Batzeline B, Isobatzelline A, and Isobatzelline B. *Eur. J. Org Chem.*, **1999**, 1173–1183; (j) Y. Kita, M. Egi and H. Tohma, Total synthesis of sulfur-containing pyrroloiminoquinone marine product, (±)-makaluvamine F using hypervalent iodine(III)-induced reactions. *Chem. Commun*., **1999**, 143–144; (k) T. Oshiyama, T. Satoh, K. Okano and H. Tokuyama, Total synthesis of batzelline C and isobatzelline C. *RSC Adv*., **2012**, *2*, 5147–5149; (l) T. Oshiyama, T. Satoh, K. Okano and H. Tokuyama, Total synthesis of makaluvamine A/D, damirone B, batzelline C, makaluvone, and isobatzelline C featuring one-pot benzyne-mediated cyclization- functionalization. *Tetrahedron*, **2012**, *68*, 9376–9383; (m) J. Backenköhler, S. Spindler and P. Spiteller, Total Synthesis of Damirone C, Makaluvamine O, Makaluvone, Batzelline C and Batzelline D. *ChemistrySelect*, **2017**, *2*, 2589–2592; (n) Y. Yamashita, L. Poignant, J. Sakata and H. Tokuyama, Divergent Total Syntheses of Isobatzellines A/B and Batzelline A. *Org. Lett*., **2020**, *22*, 6239–6243; (o) J. An, R. K. Jackson III, J. P. Tuccinardi and J. L. Wood, Pyrroloiminoquinone Alkaloids: Total Synthesis of Makaluvamines A and K. *Org. Lett.*, **2023**, *25*, 1868–1871; and references therein.

(2) For representative syntheses of complex pyrroloiminoquinones see: (a) S. Nishiyama, J.-F. Cheng, X. L. Tao and S. Yamamura, Synthetic studies on novel sulfur-containing alkaloids, prianosins and discorhabdins: total synthesis of

discorhabdin C. *Tetrahedron Lett*., **1991**, *32*, 4151–4154; (b) Y. Kita, H. Tohma, M. Inagaki, K. Hatanaka and T. Yakura, Total synthesis of discorhabdin C: a general aza spiro dienone formation from O-silylated phenol derivatives using a hypervalent iodine reagent. *J. Am. Chem. Soc*., **1992**, *114*, 2175–2180; (c) X. L. Tao, J.-F. Cheng, S. Nishiyama and S. Yamamura, Synthetic studies on tetrahydropyrroloquinoline-containing natural products: Syntheses of discorhabdin C, batzelline C and isobatzelline C. *Tetrahedron*, **1994**, *50*, 2017–2028; (d) K. M. Aubart and C. H. Heathcock, A Biomimetic Approach to the Discorhabdin Alkaloids: Total Syntheses of Discorhabdins C and E and Dethiadiscorhabdin D. *J. Org. Chem.*, **1999**, *64*, 16–22; (e) H. Tohma, Y. Harayama, M. Hashizume, M. Iwata, M. Egi and Y. Kita, Synthetic Studies on the Sulfur-Cross-Linked Core of Antitumor Marine Alkaloid, Discorhabdins: Total Synthesis of Discorhabdin A. *Angew. Chem., Int. Ed*., **2002**, *41*, 348–350; (f) H. Tohma, Y. Harayama, M. Hashizume, M. Iwata, Y. Kiyono, M. Egi and Y. Kita, The first total synthesis of discorhabdin A. *J. Am. Chem. Soc.*, **2003**, *125*, 11235–11240; (g) M. W. Smith, I. D. Falk, H. Ikemoto and N. Z. Burns, A Convenient C-H Functionalization Platform for Pyrroloiminoquinone Alkaloid Synthesis. *Tetrahedron*, **2019**, *75*, 3366–3370; (h) T. Noro, J. Sakata and H. Tokuyama, Synthetic studies on discorhabdin V: Construction of the A–F hexacyclic framework. *Tetrahedron Lett*., **2021**, *81*, 153333; (i) B. C. Derstine, A. J. Cook, J. D. Collings, J. Gair, J. Saurí, E. E. Kwan and N. Z. Burns, Total Synthesis of (+)-Discorhabdin V. *Angew. Chem., Int. Ed*., **2024**, *63*, e202315284; and references therein.

(3) Limited SAR studies have been reported focusing on diversification of R^5. See: (a) B. A. Shinkre, K. P. Raisch, L. Fan and S. E. Velu, *Bioorg. Med. Chem. Lett.*, **2007**, *17*, 2890–2893; (b) D. Passarella, F. Belinghieri, M. Scarpellini, G. Pratesi, F. Zunino, O. M. Gia, L. D. Via, G. Santoro and B. Danieli, *Bioorg. Med. Chem*., **2008**, *16*, 2431–2438; (c) Y. Wada, K. Otani, N. Endo, Y. Harayama, D. Kamimura, M. Yoshida, H. Fujioka and Y. Kita, *Org. Lett.*, **2009**, *11*, 4048–4050; (d) Y. Wada, Y. Harayama, D. Kamimura, M. Yoshida, T. Shibata, K. Fujiwara, K. Morimoto, H. Fujioka and Y. Kita, *Org. Biomol. Chem.*, **2011**, *9*, 4959– 4976; (e) B. Nijampatnam, D. H. Nadkarni, H. Wu and S. E. Velu, *Microorganisms*, **2014**, *2*, 128–139; (f) Z. Aburjania, J. D. Whitt, S. Jang, D. H. Nadkarni, H. Chen, J. B. Rose, S. E. Velu and R. Jaskula-Sztul, *Molecules*, **2020**, *25*, 4940.

(4) Refer to references 1 and 2 for examples of these strategies.

(5) For a synthesis of pyrroloiminoquinones that does not use the common intermediate see: G. A. Kraus and N. Selvakumar, *J. Org. Chem*., **1998**, *63*, 9846–9849.

(6) Y. Shimizu, M. Noshita, Y. Mukai, H. Morimoto and T. Ohshima, Cleavage of unactivated amide bonds by ammonium salt-accelerated hydrazinolysis *Chem. Commun.*, **2014**, *50*, 12623–12625.

(7) S. C. Nigam, A. Mann, M. Taddei and C. G. Wermutha, Selective Removal of the Tert-Butoxycarbonyl Group from Secondary Amines: $ZnBr_2$ as the Deprotecting Reagent. *Synth. Commun*., **1989**, *19*, 3139–3142. Canonical acidic Boc deprotection conditions did not yield any desired product employing the deprotection/aerobic oxidation protocol.

(8) For an example of ONSH with chloride nucleophiles see: F. Frank, L. M. Alice, P. Mauker, A. A. Alsimaree, P. G. Waddell, M. R. Probert, T. J. Penfold, J. G. Knight and M. J. Hall, Synthesis of 3,5-dichloro-4,4-difluoro-4-bora-3a,4a-diaza-*s*-indacenes (BODIPYs) via $Cu(OTf)_2$ mediated oxidative nucleophilic substitution of hydrogen by chloride. *Tetrahedron*, **2020**, *76*, 131113.

(9) Barnes, G. L.; Magann, N. L.; Perrotta, D.; Hörmann, F. M.; Fernandez, S.; Vydyam, P.; Choi, J.-Y.; Prudhomme, J.; Neal, A.; Le Roch, K. G.; Ben Mamoun, C.; Vanderwal, C. D. A Divergent Synthesis of Numerous Pyrroloiminoquinone Alkaloids Identifies Promising Antiprotozoal Agents. *J. Am. Chem. Soc.* **2024**, *146*, 29883− 29894.

(10) D. C. Radisky, E. S. Radisky, L. R. Barrows, B. R. Copp, R. A. Kramer, C. M. Ireland, *J. Am. Chem. Soc.* **1993**, *115*, 1632–1638.

(11) V. Vece, G. Vuocolo, *Tetrahedron*, **2015**, *71*, 8781–8785.

(12) E. V. Sadanandan, S. K. Pillai, M. V. Lakshmikantham, A. D. Billimoria, J. S. Culpepper, M. P. Cava, *J. Org. Chem.* **1995**, *60*, 1800–1805.

(13) a) H. H. Sun, S. Sakemi, N. Burres, P. McCarthy, *J. Org. Chem.* **1990**, *55*, 4964–4966. b) M. Alvarez, A. Bros, G. Gras, W. Ajana, J. A. Joule, *Eur. J. Org. Chem.* **1999**, *1173–1183*. c) Yamashita, L. Poignant, J. Sakata, H. Tokuyama, *Org. Lett.* **2020**, *22*, 6239–6234.

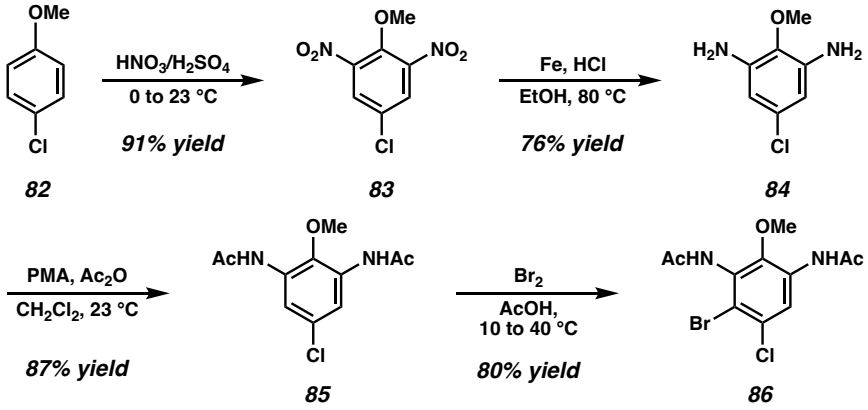
(14) D. A. Venables, G. P. Concepción, S. S. Matsumoto, L. R. Barrows, C. M. Ireland, *J. Nat. Prod.* **1997**, *60*, 408–410.

APPENDIX 6

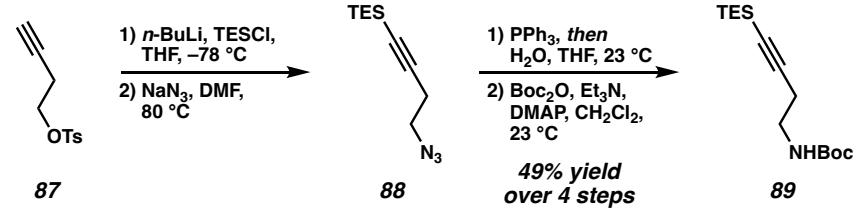
Synthetic Summary for Chapter 2:

Divergent Total Syntheses of Pyrroloiminoquinone Alkaloids Enabled by the Development of a Larock/ Buchwald–Hartwig Annulation/Cyclization

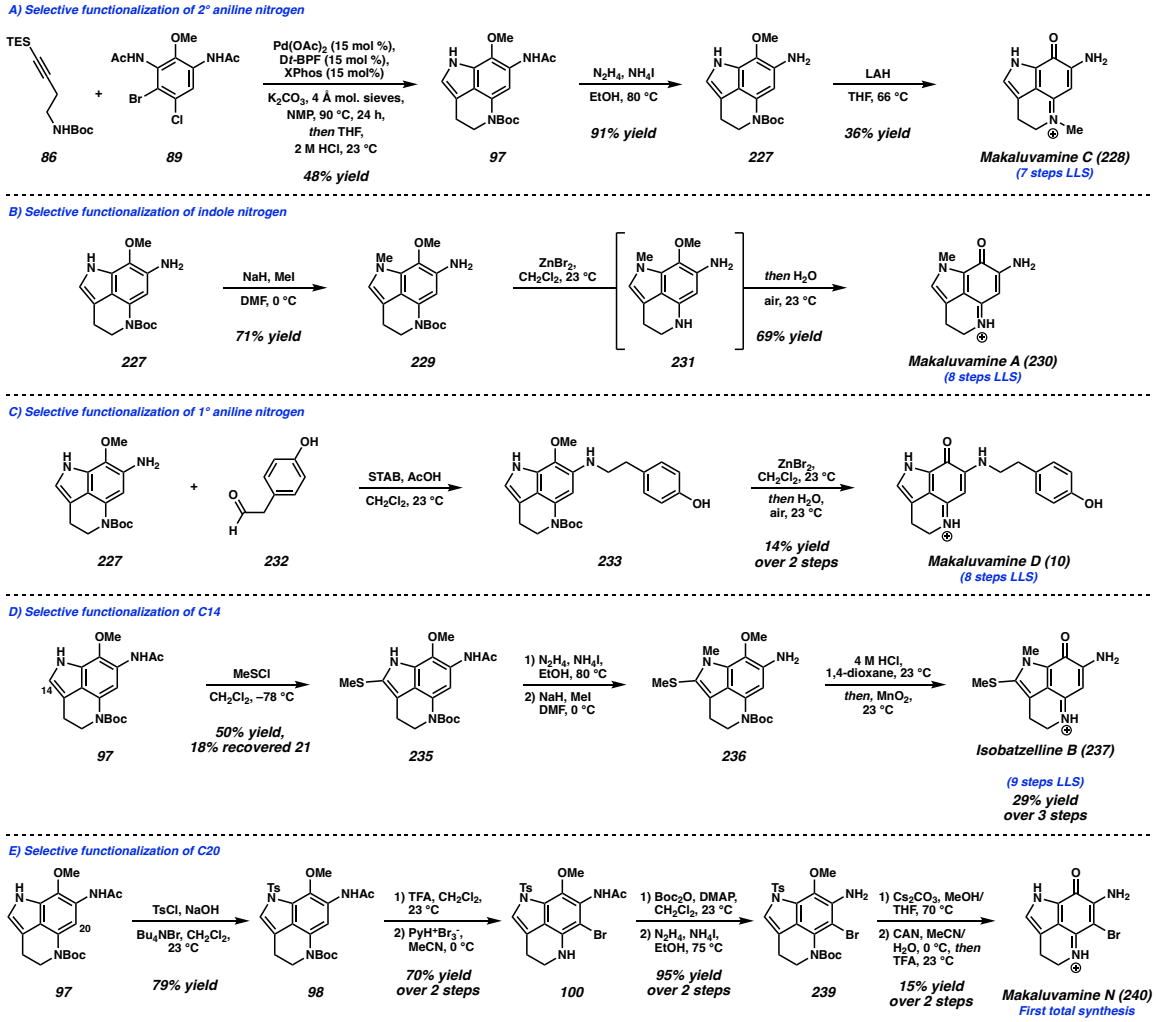
Scheme A6.1 *Synthesis of bromoarene* ***86***.



Scheme A6.2 *Synthesis of alkyne* ***89***.



Scheme A6.3 *Divergent synthesis of pyrroloiminoquinone alkaloids.*



Appendix 7

Spectra Relevant to Chapter 2:

Divergent Total Syntheses of Pyrroloiminoquinone Alkaloids Enabled by the Development of a Larock/ Buchwald–Hartwig Annulation/Cyclization

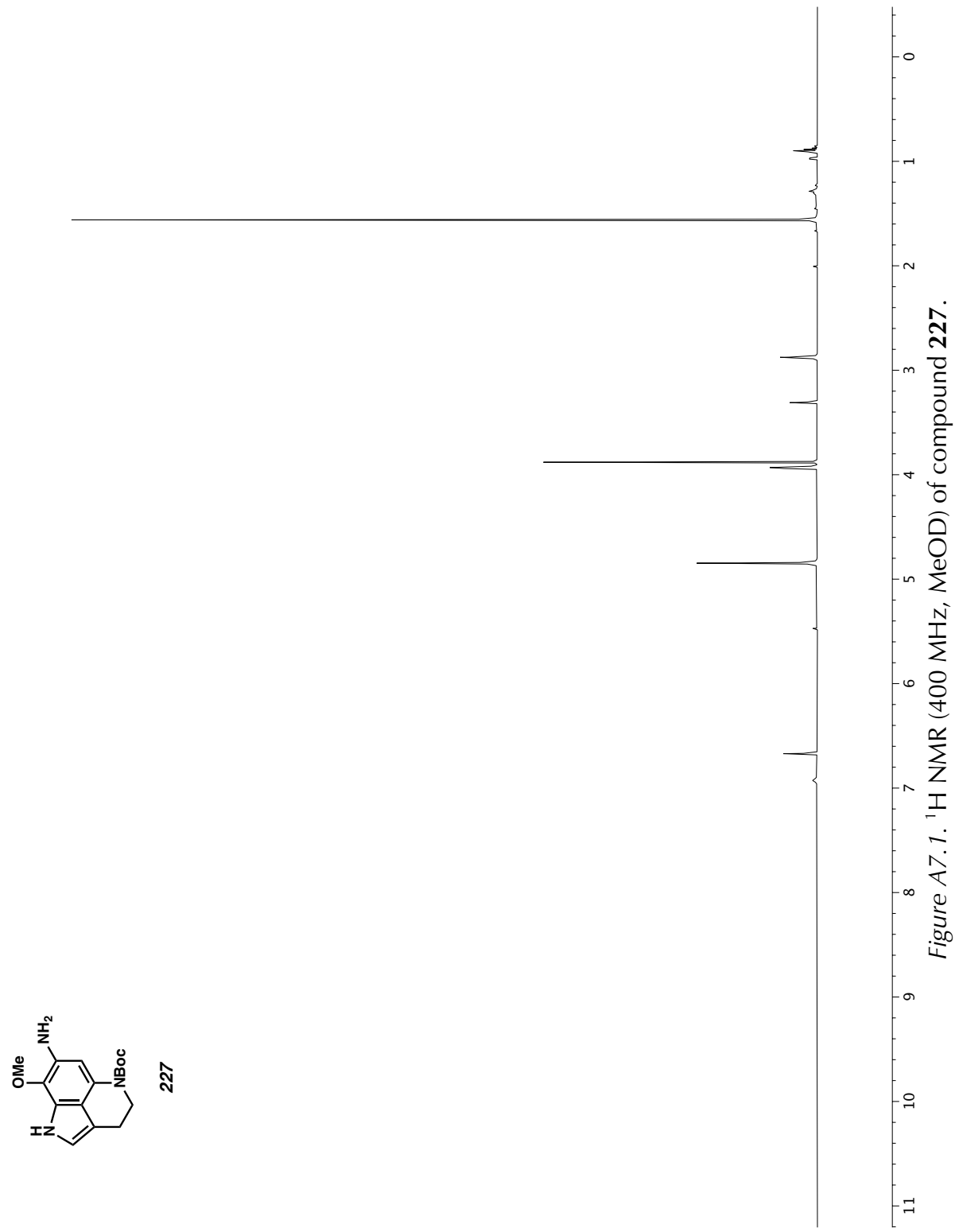


Figure A7.1. ^{1}H NMR (400 MHz, MeOD) of compound **227**.

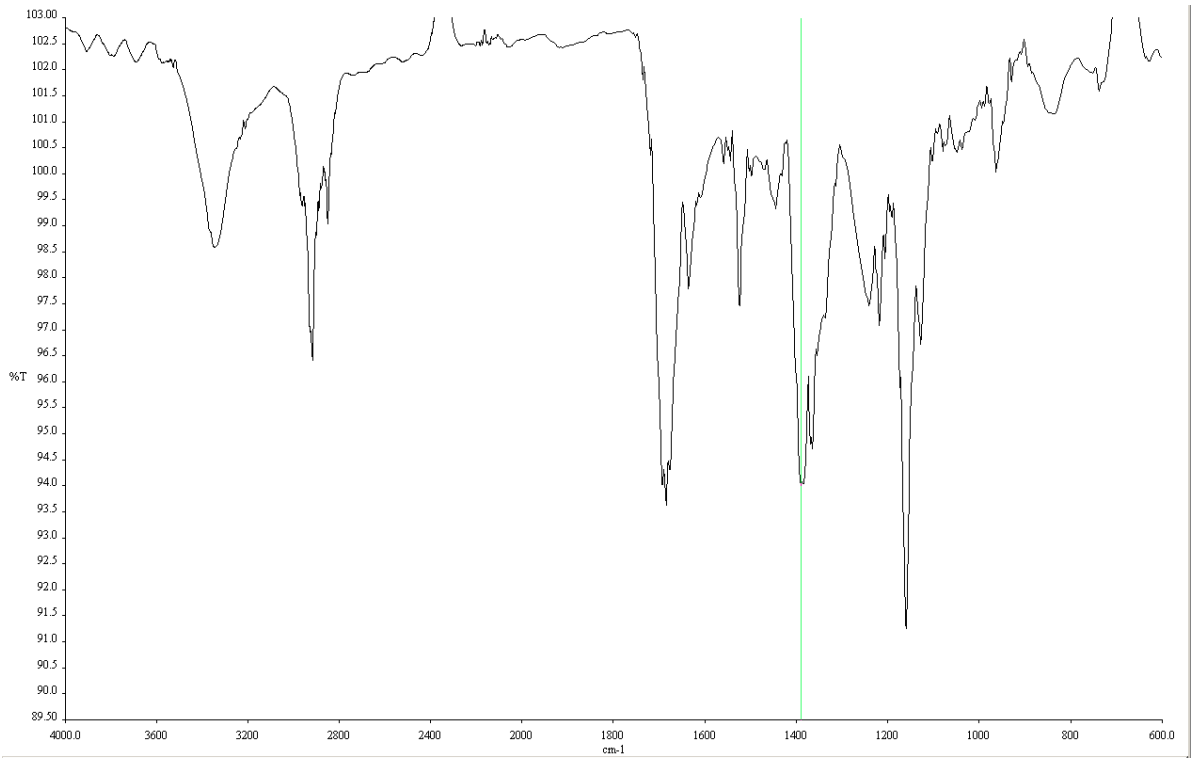


Figure A7.2. Infrared spectrum (Thin Film, NaCl) of compound **227**.

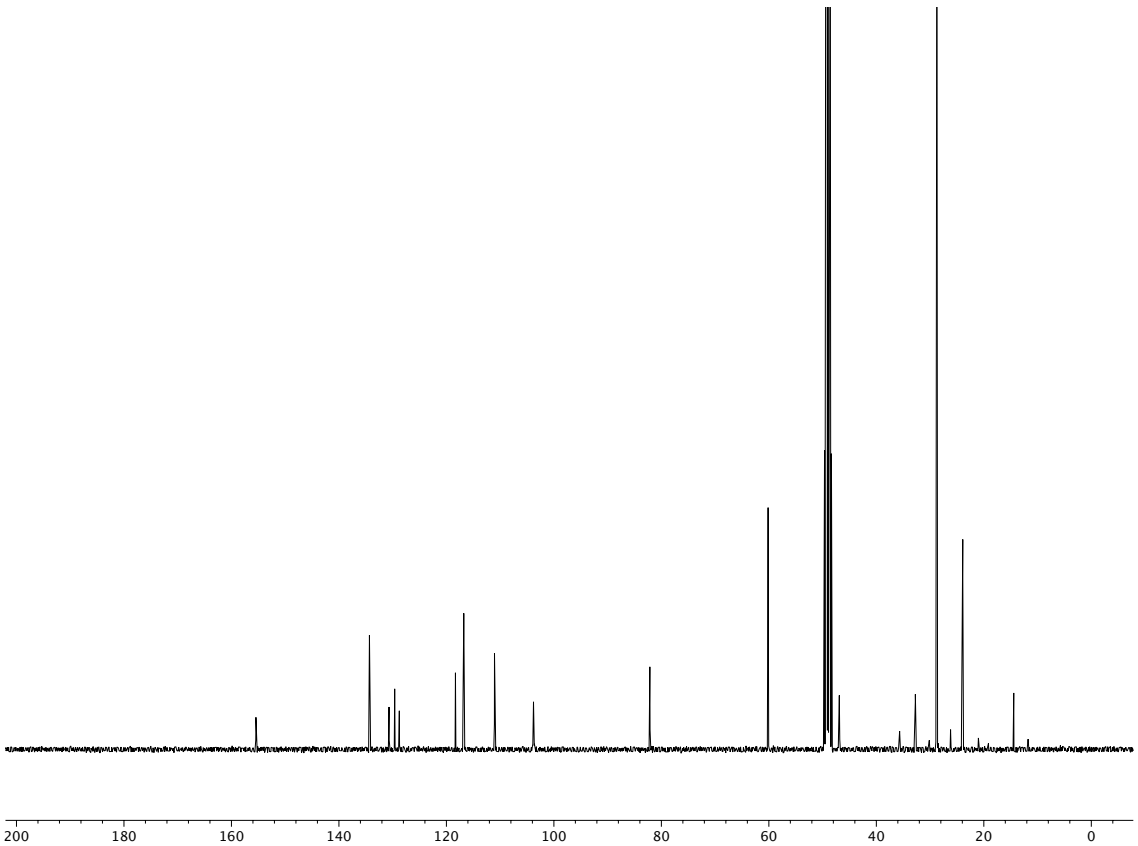


Figure A7.3. ^{13}C NMR (100 MHz, MeOD) of compound **227**.

Figure A7.4. ^{1}H NMR (400 MHz, DMSO-d6) of makaluvamine C (**228**).

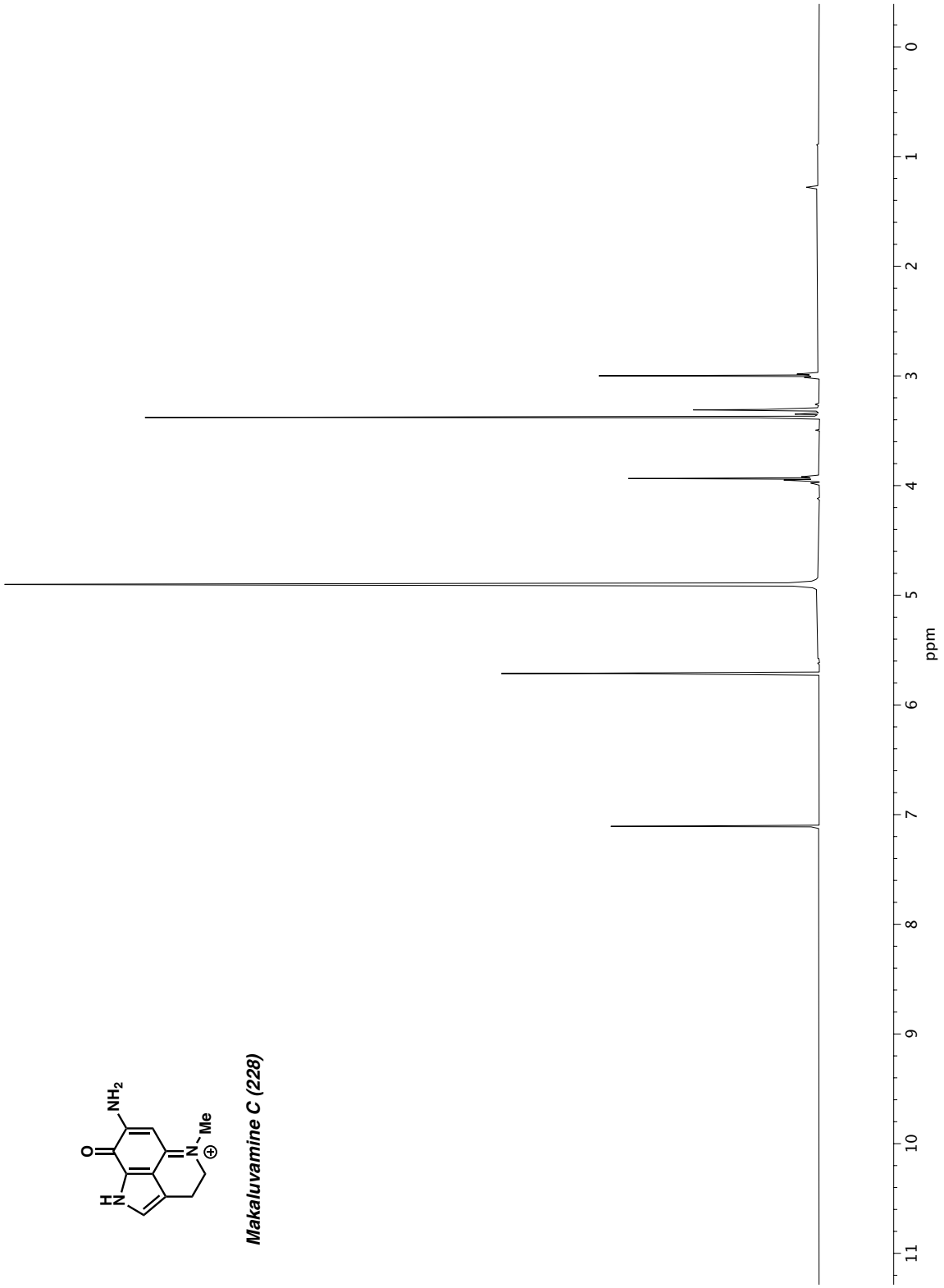


Figure A7.5. ^{1}H NMR (400 MHz, MeOD) of makaluvamine C (**228**).

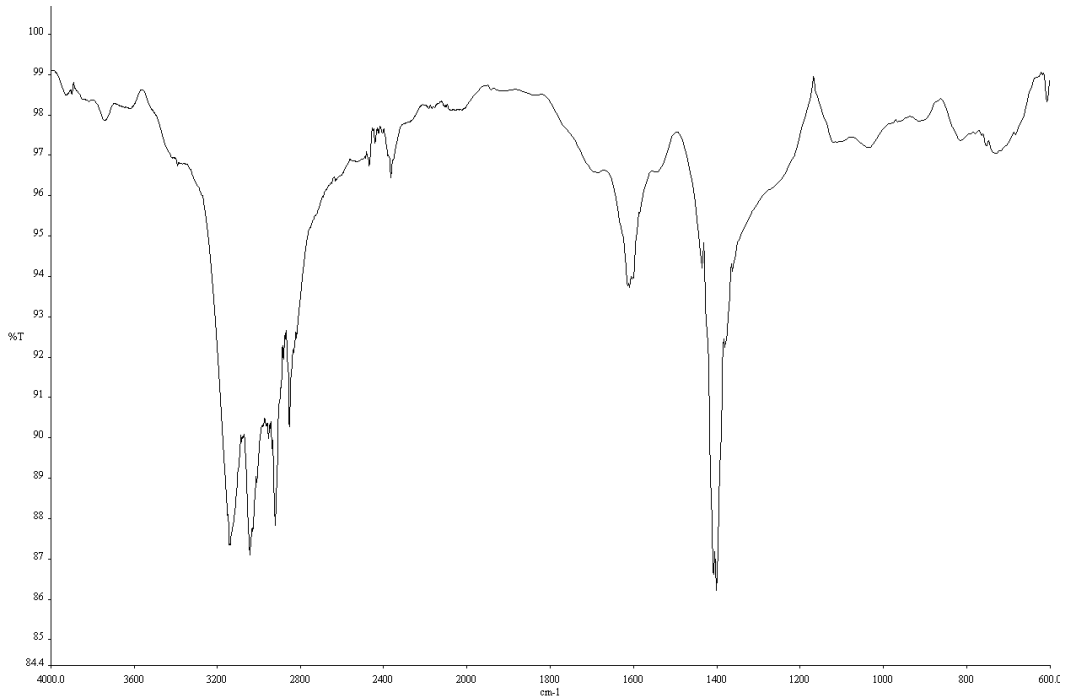


Figure A7.6. Infrared spectrum (Thin Film, NaCl) of makaluvamine C (**228**).

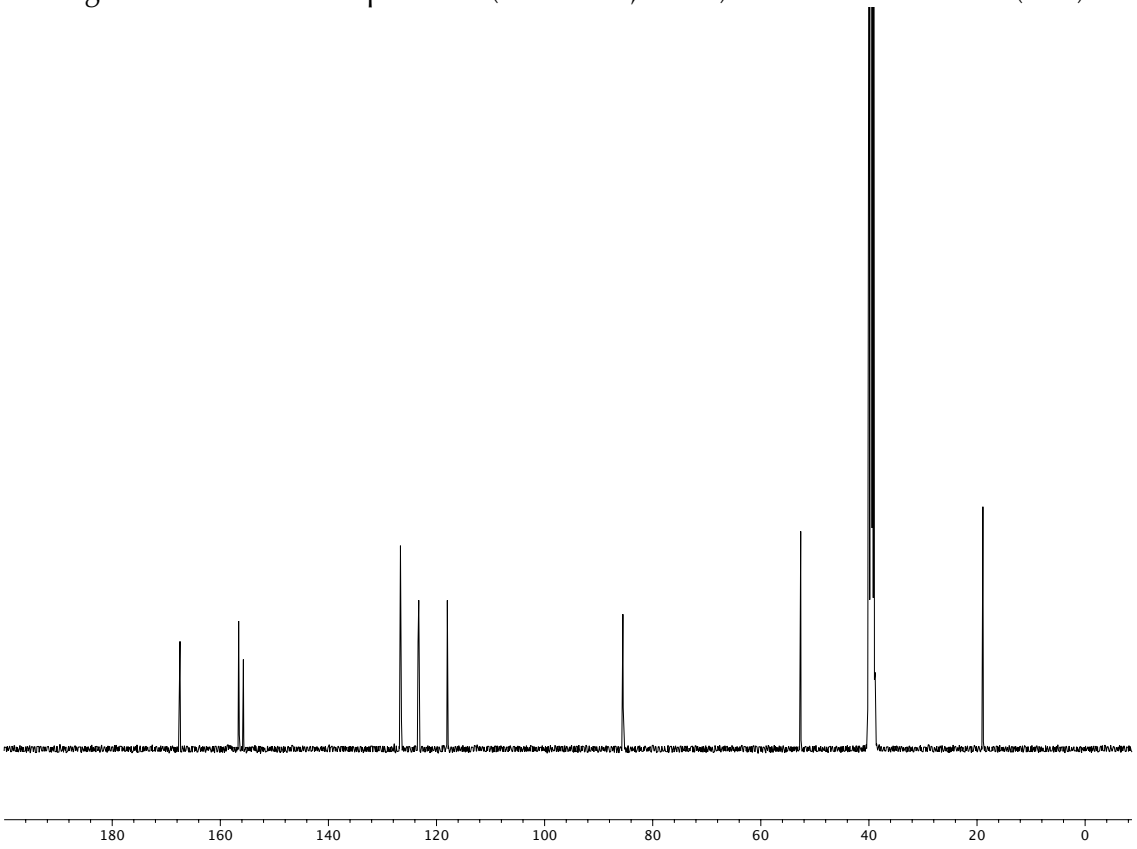


Figure A7.7. ^{13}C NMR (100 MHz, DMSO-d6) of makaluvamine C (**228**).

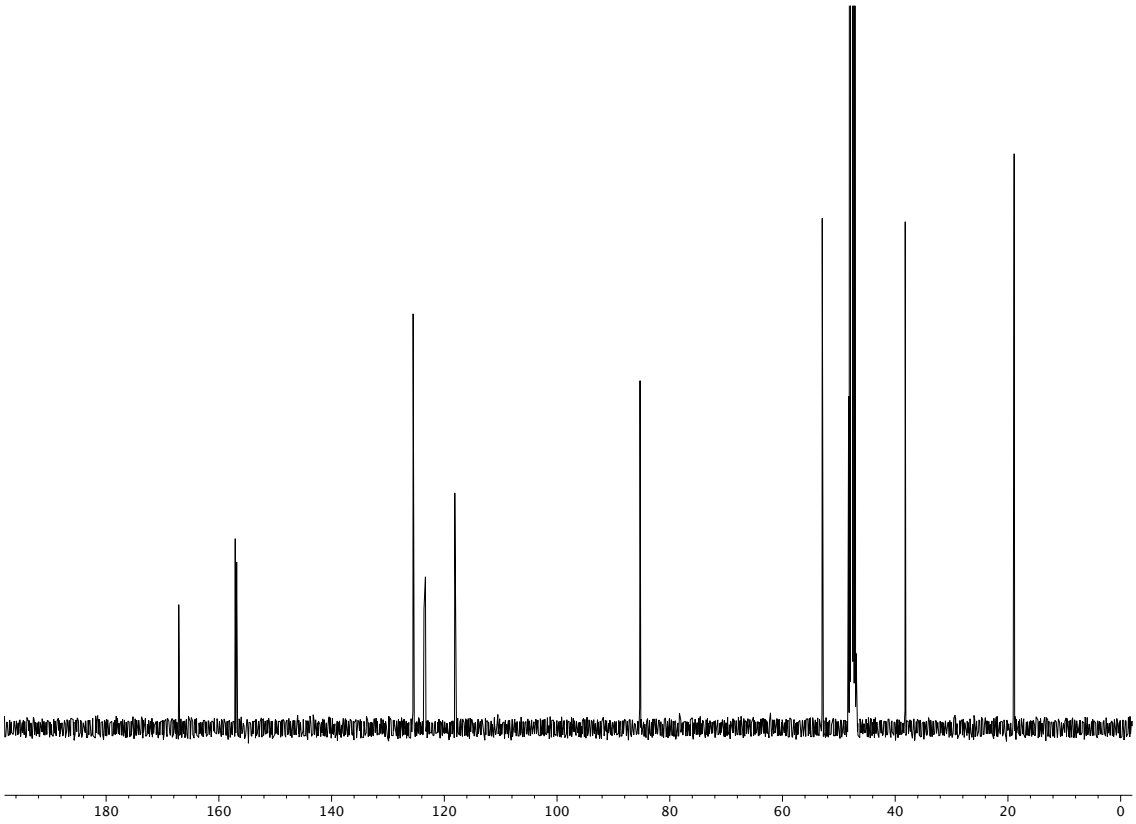


Figure A7.8. ^{13}C NMR (100 MHz, MeOD) of makaluvamine C (**228**).

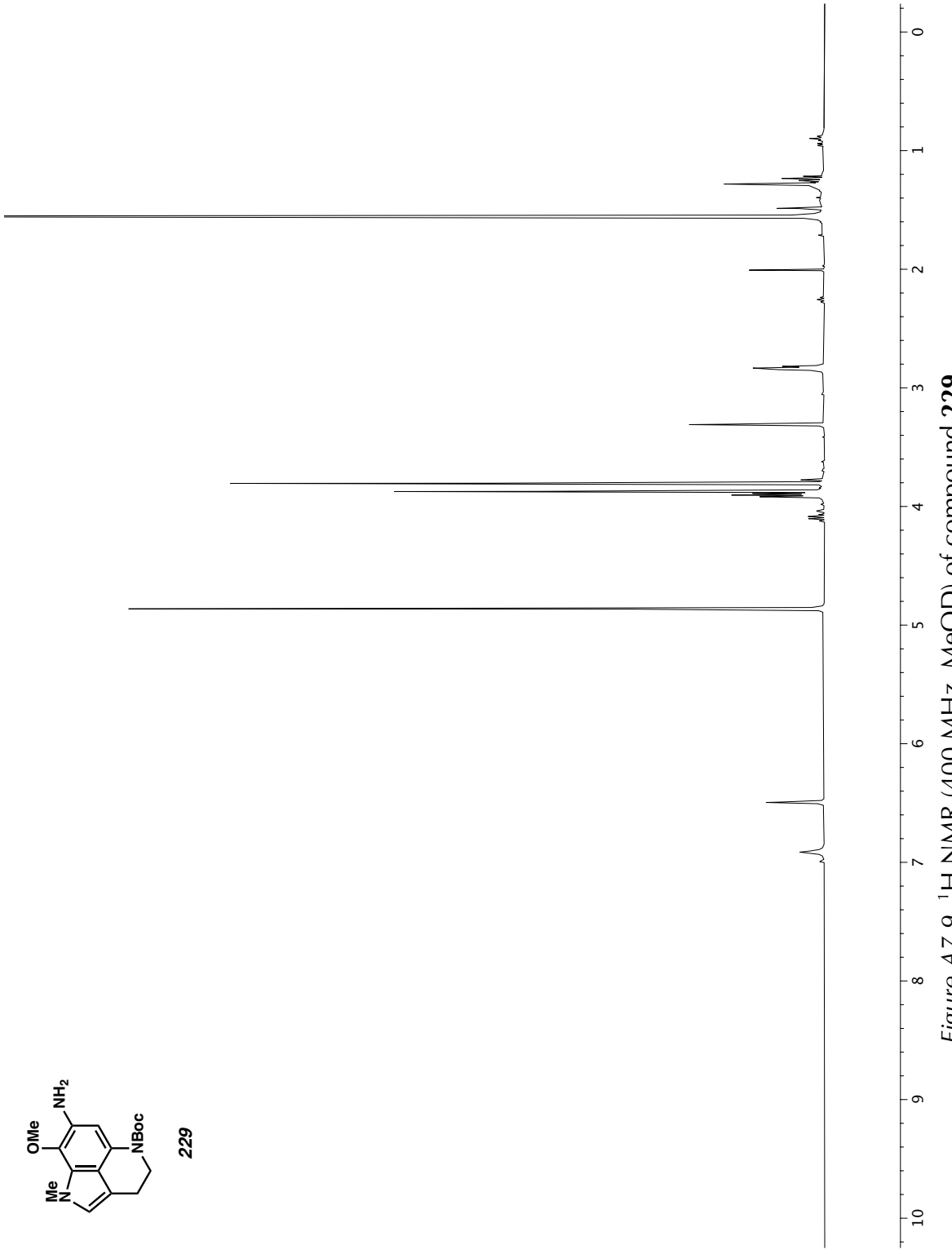


Figure A7.9. ^{1}H NMR (400 MHz, MeOD) of compound **229**.

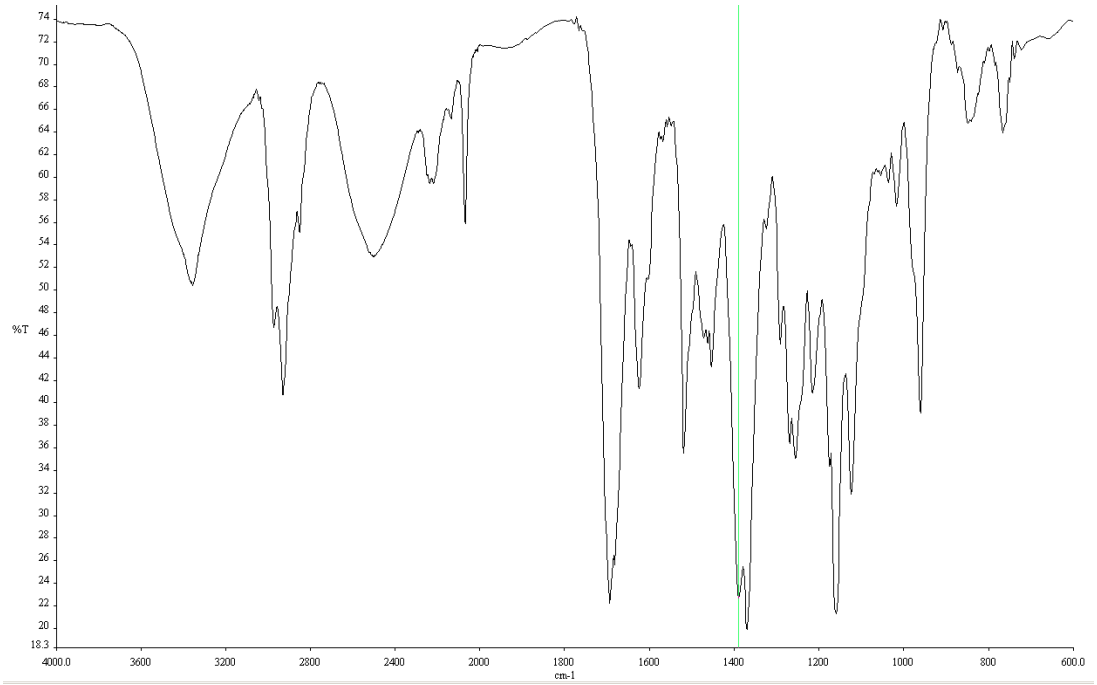


Figure A7.10. Infrared spectrum (Thin Film, NaCl) of compound **229**.

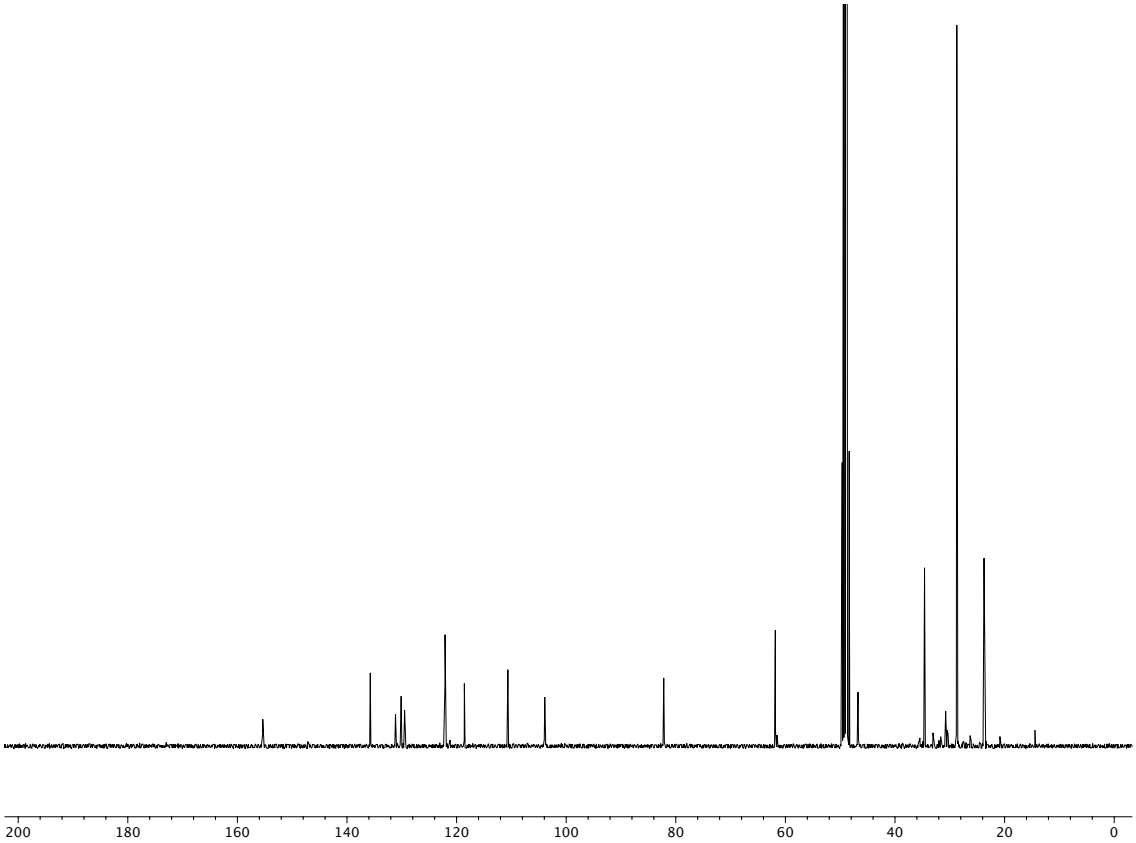


Figure A7.11. ^{13}C NMR (100 MHz, MeOD) of compound **229**.

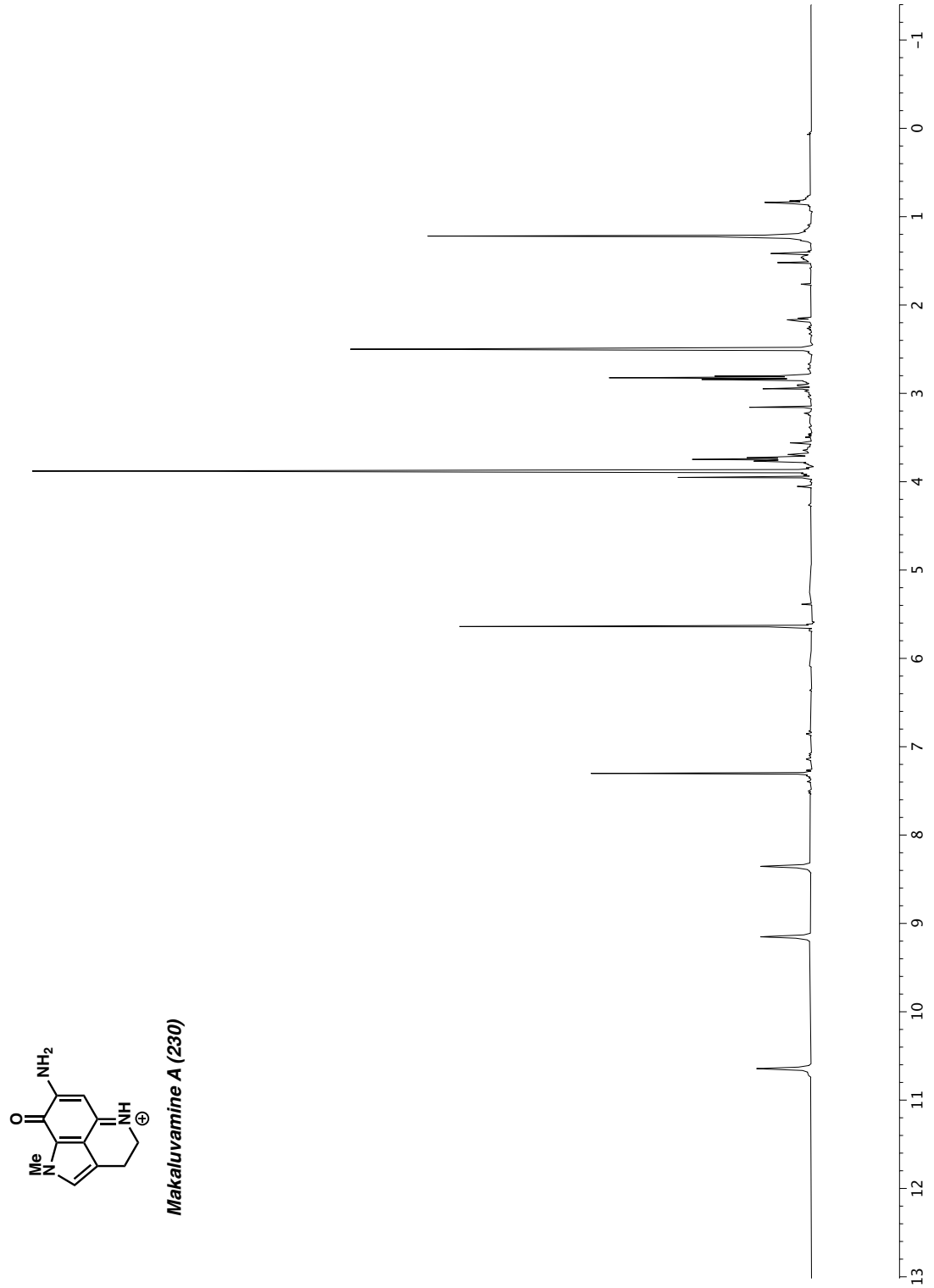


Figure A7.12. ^{1}H NMR (400 MHz, DMSO-d6) of makaluvamine A (**230**).

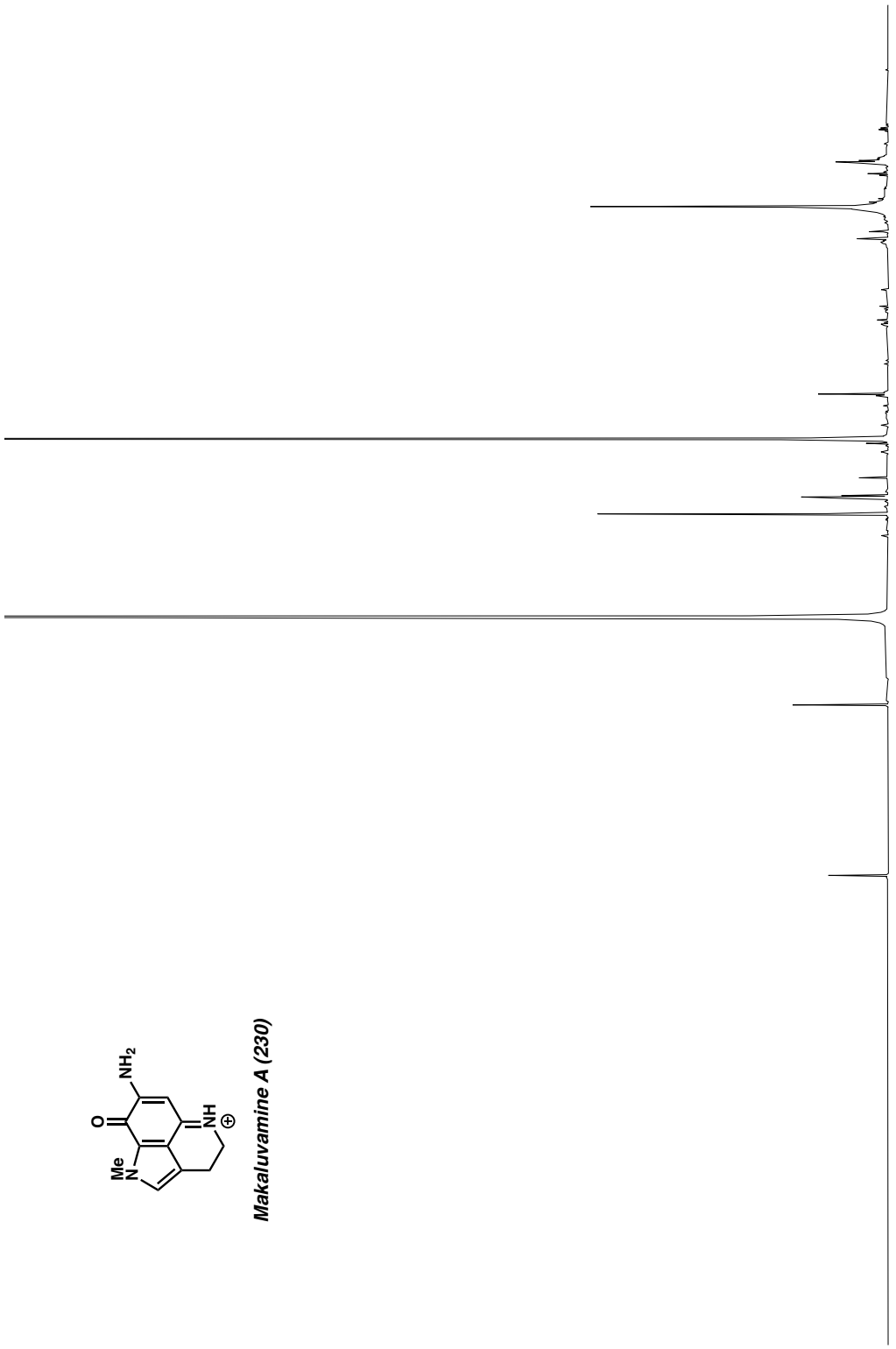


Figure A7.13. ^{1}H NMR (400 MHz, MeOD) of makaluvamine A (**230**).

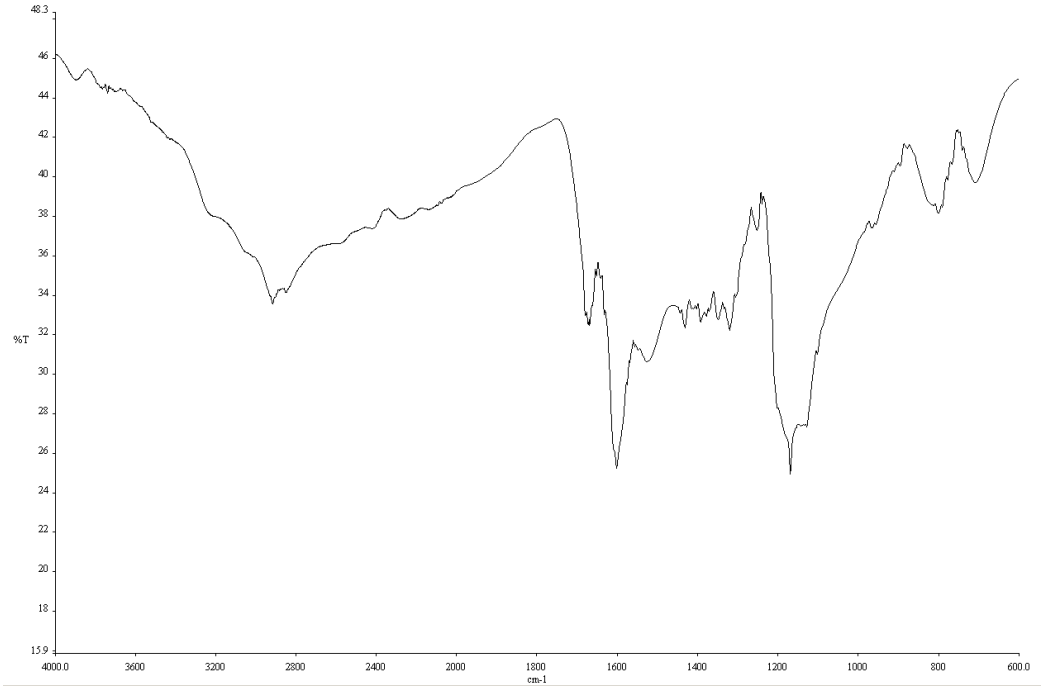


Figure A7.14. Infrared spectrum (Thin Film, NaCl) of makaluvamine A (**230**).

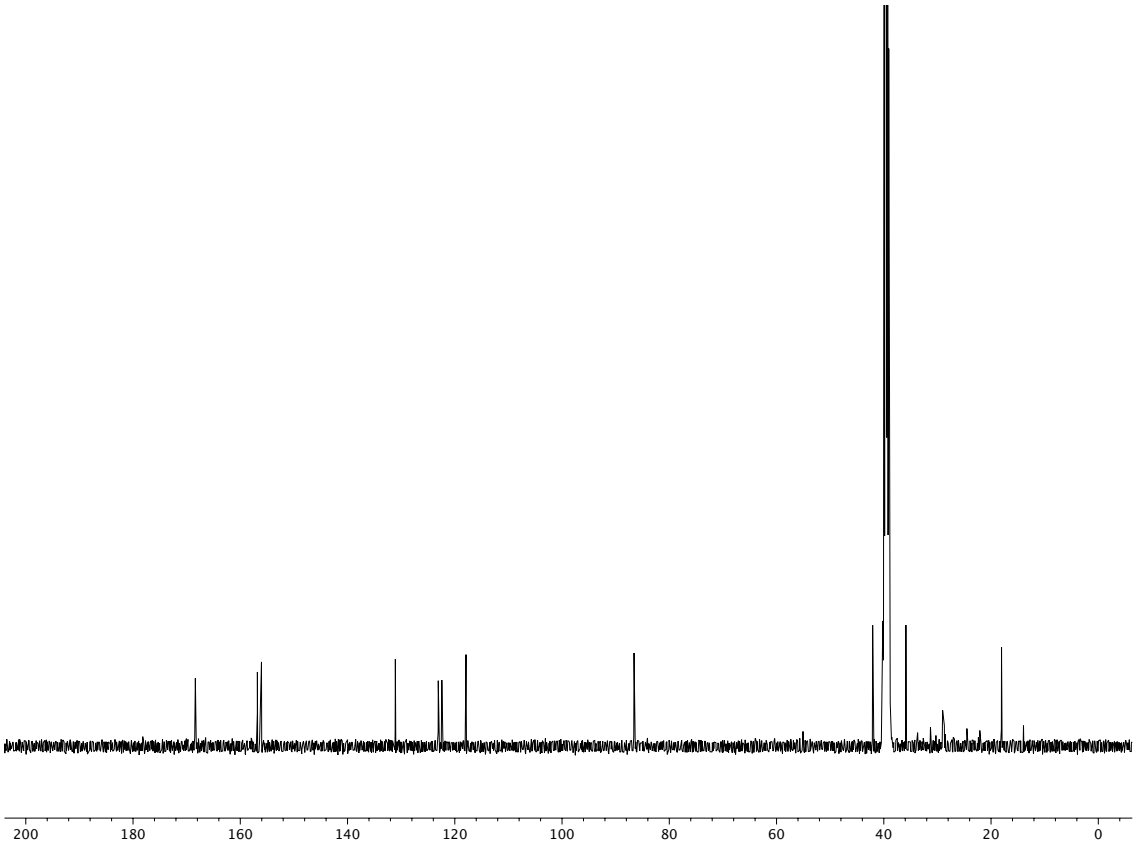


Figure A7.15. ^{13}C NMR (100 MHz, DMSO-d6) of makaluvamine A (**230**).

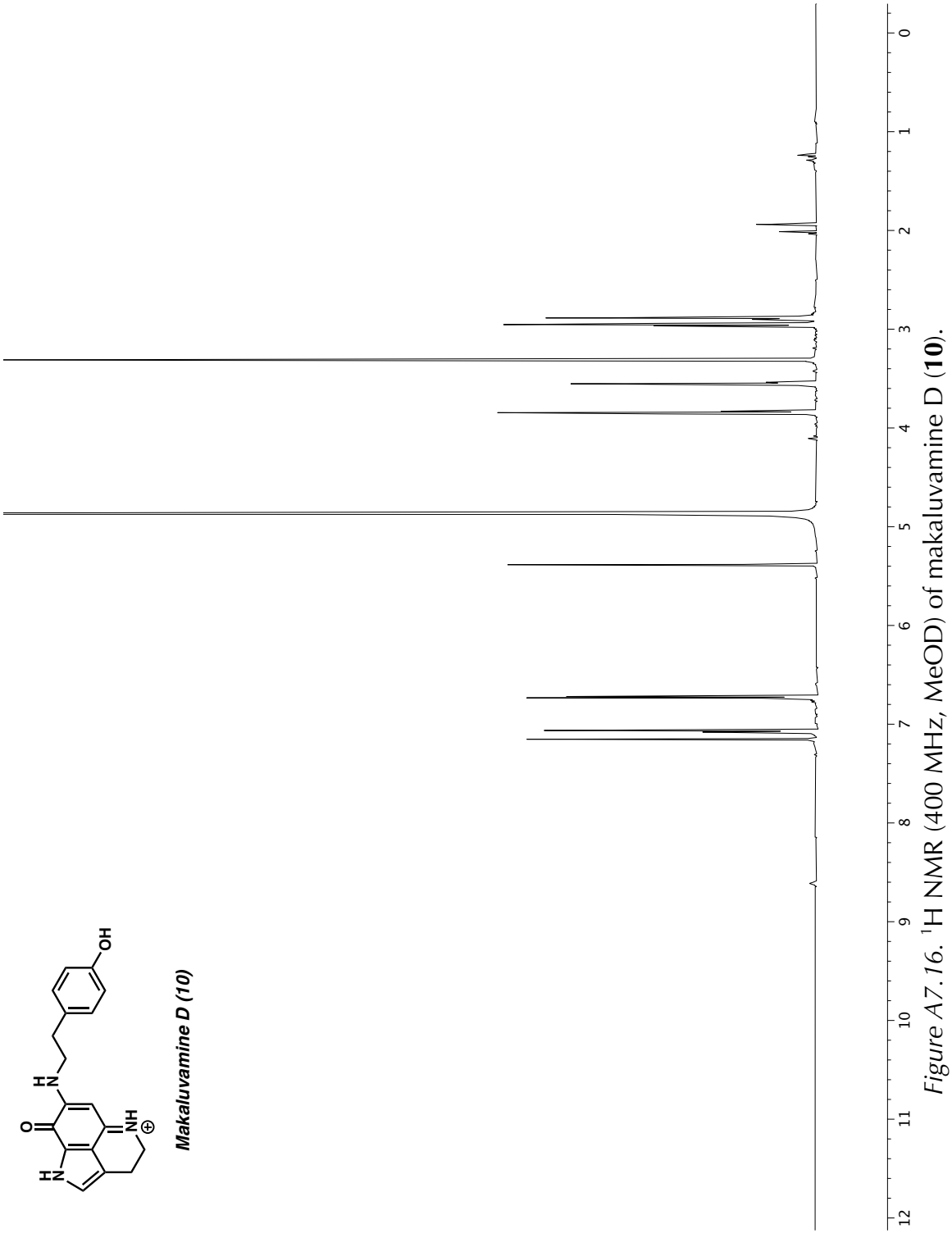


Figure A7.16. ^{1}H NMR (400 MHz, MeOD) of makaluvamine D (**10**).

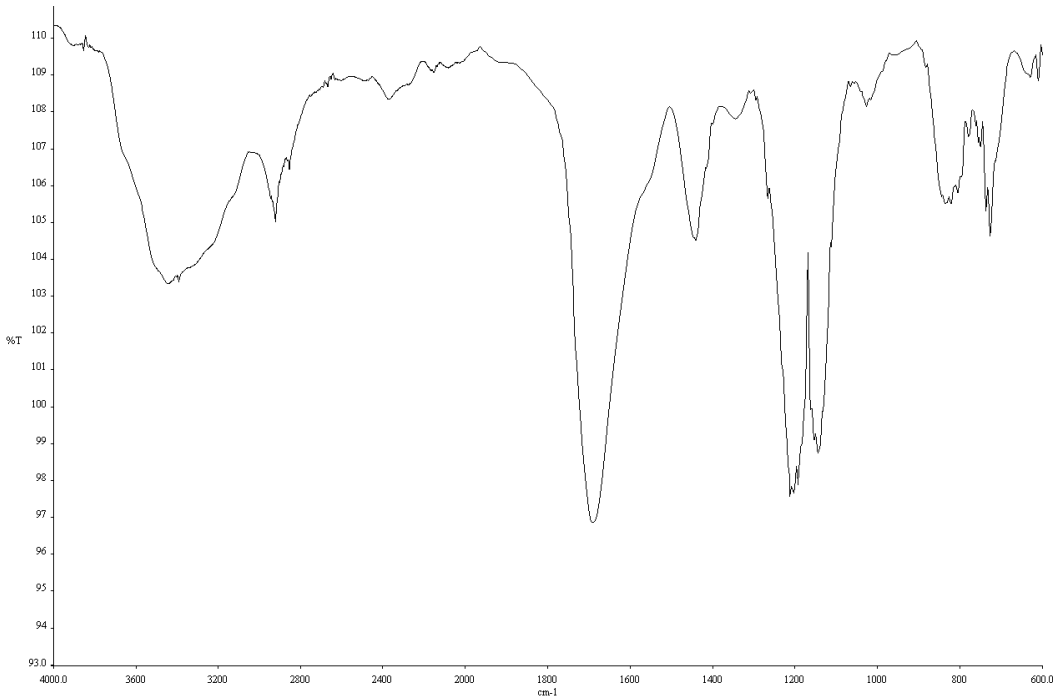


Figure A7.17. Infrared spectrum (Thin Film, NaCl) of makaluvamine D (**10**).

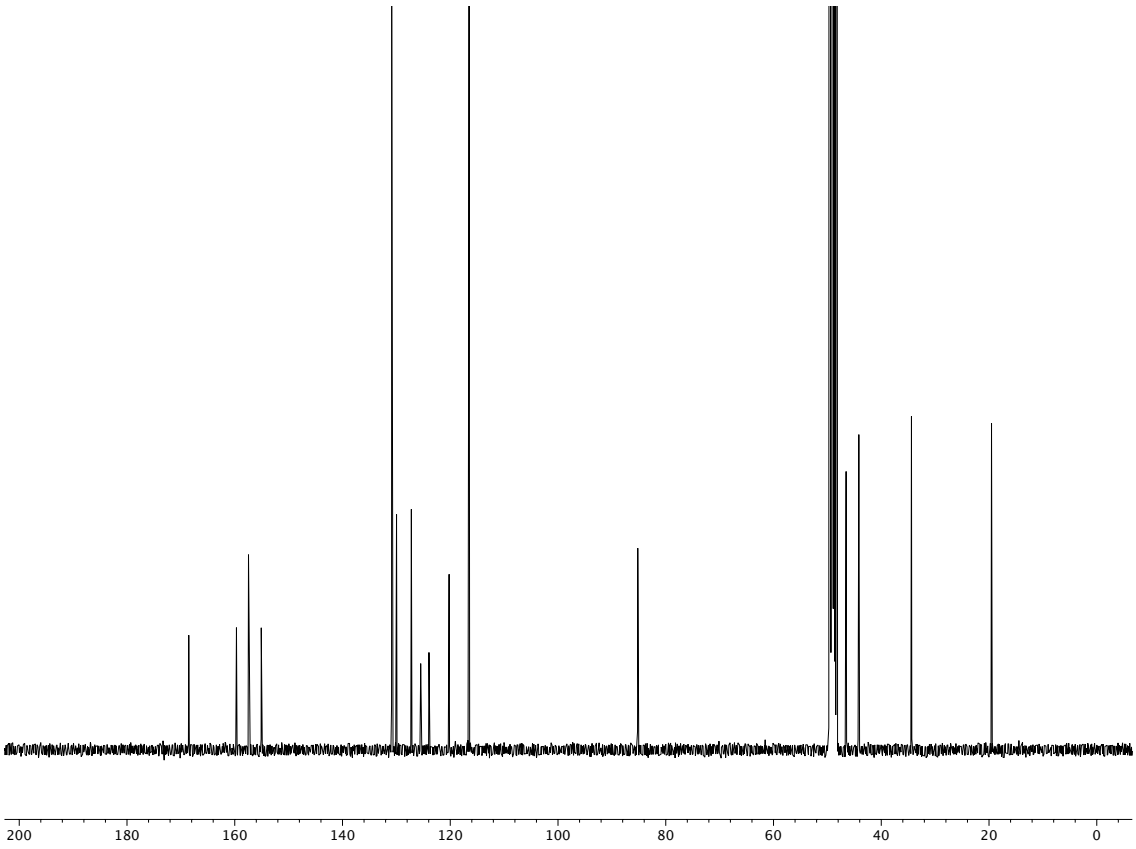


Figure A7.18. ^{13}C NMR (100 MHz, MeOD) of makaluvamine D (**10**).

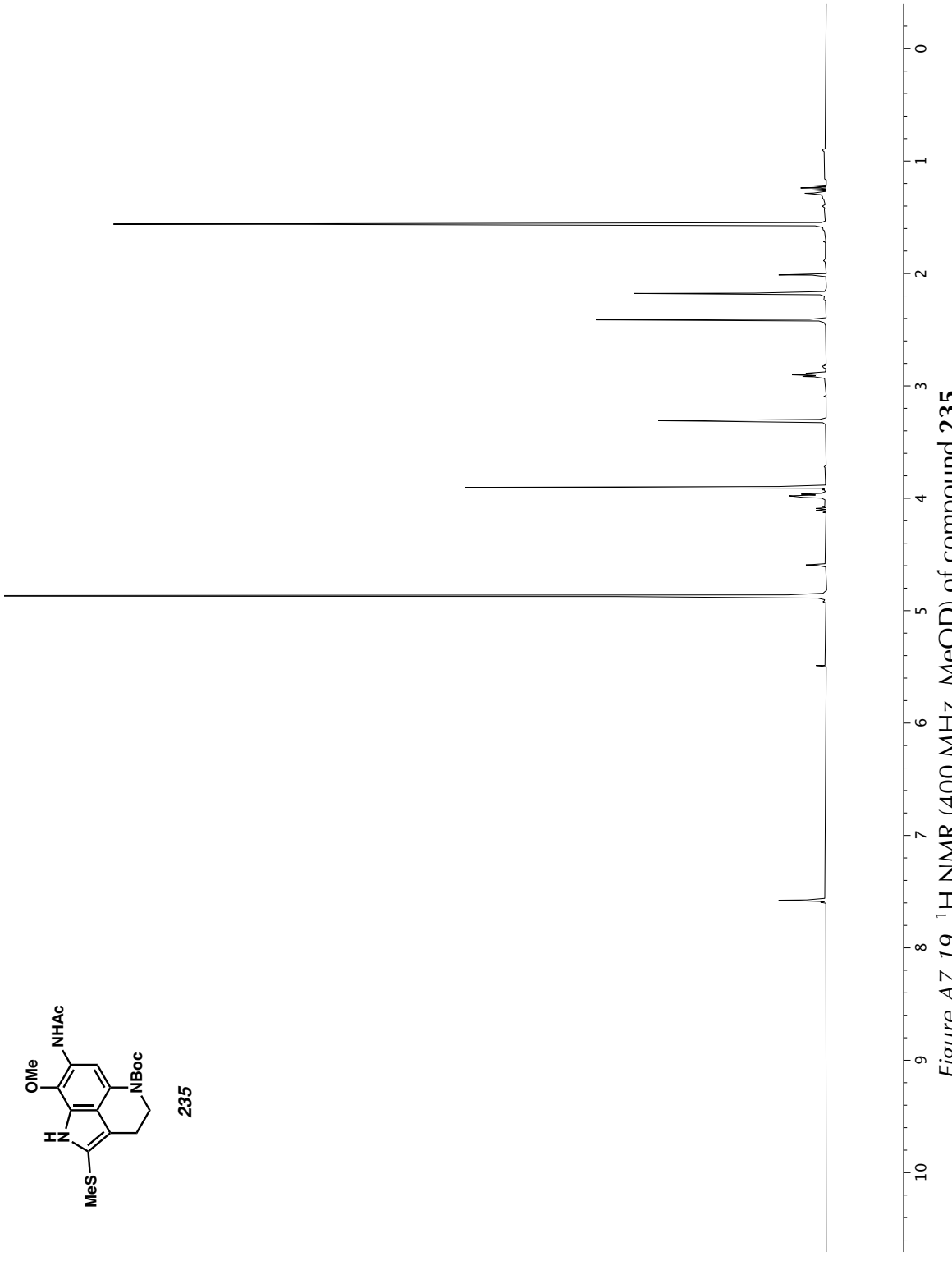


Figure A7.19. ^{1}H NMR (400 MHz, MeOD) of compound **235**.

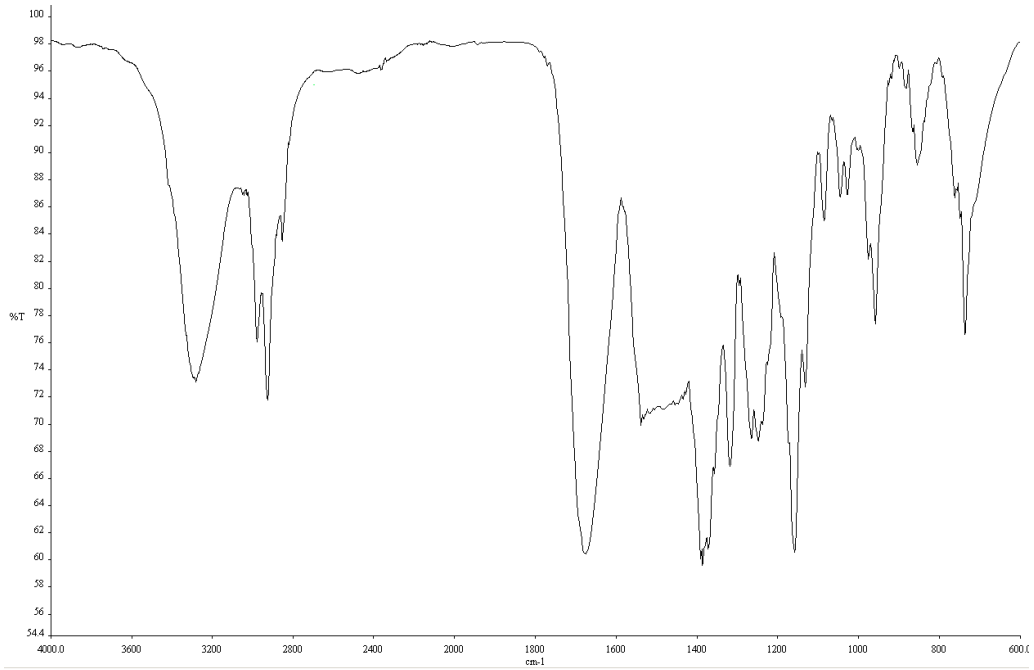


Figure A7.20. Infrared spectrum (Thin Film, NaCl) of compound **235**.

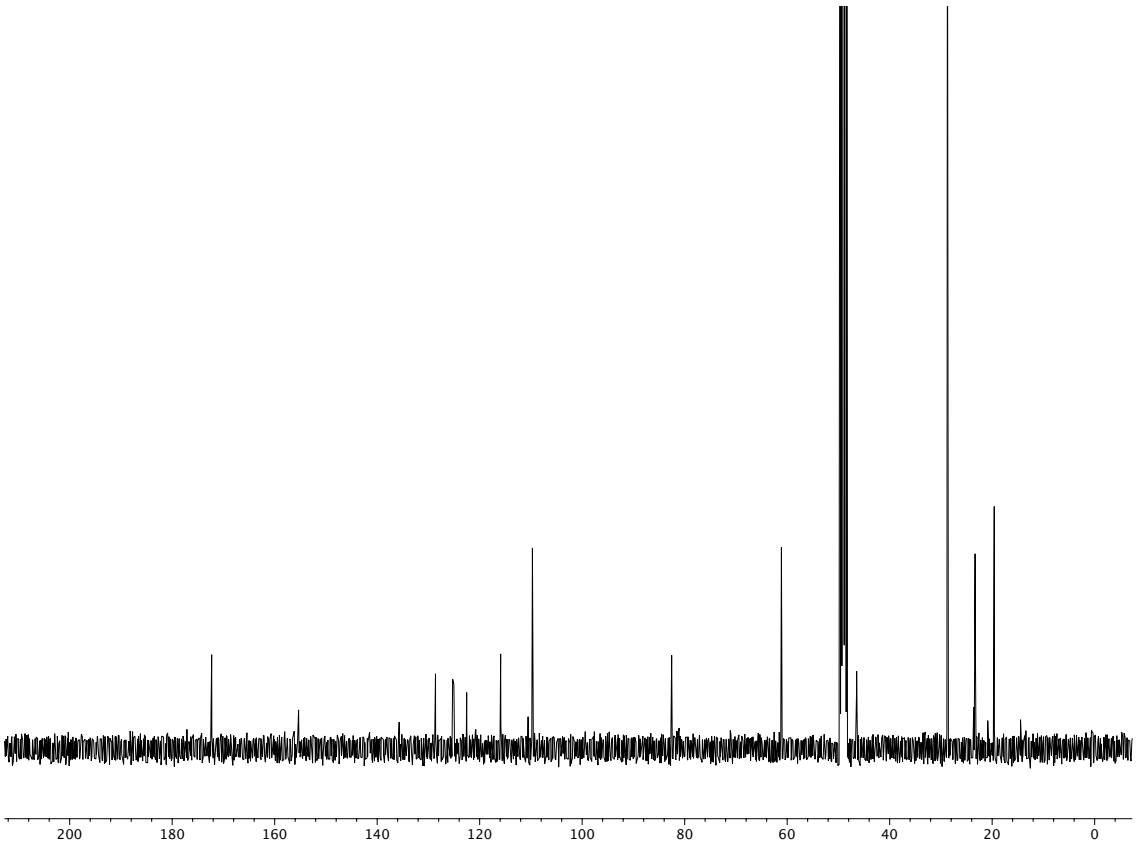


Figure A7.21. ^{13}C NMR (100 MHz, MeOD) of compound **235**.

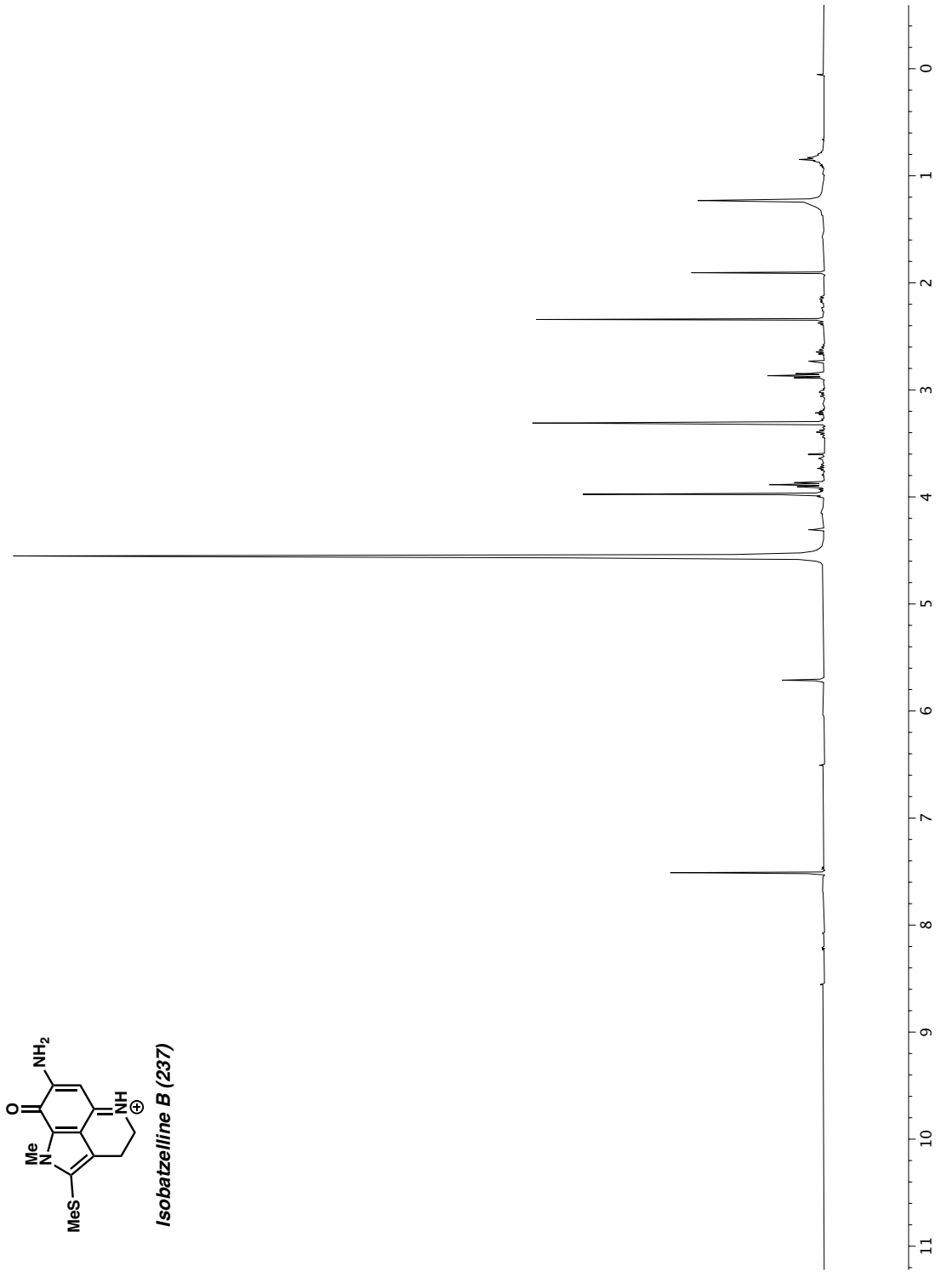


Figure A7.22. ^{1}H NMR (400 MHz, 1:1 MeOD:$CDCl_3$) of isobatzelline B (**237**).

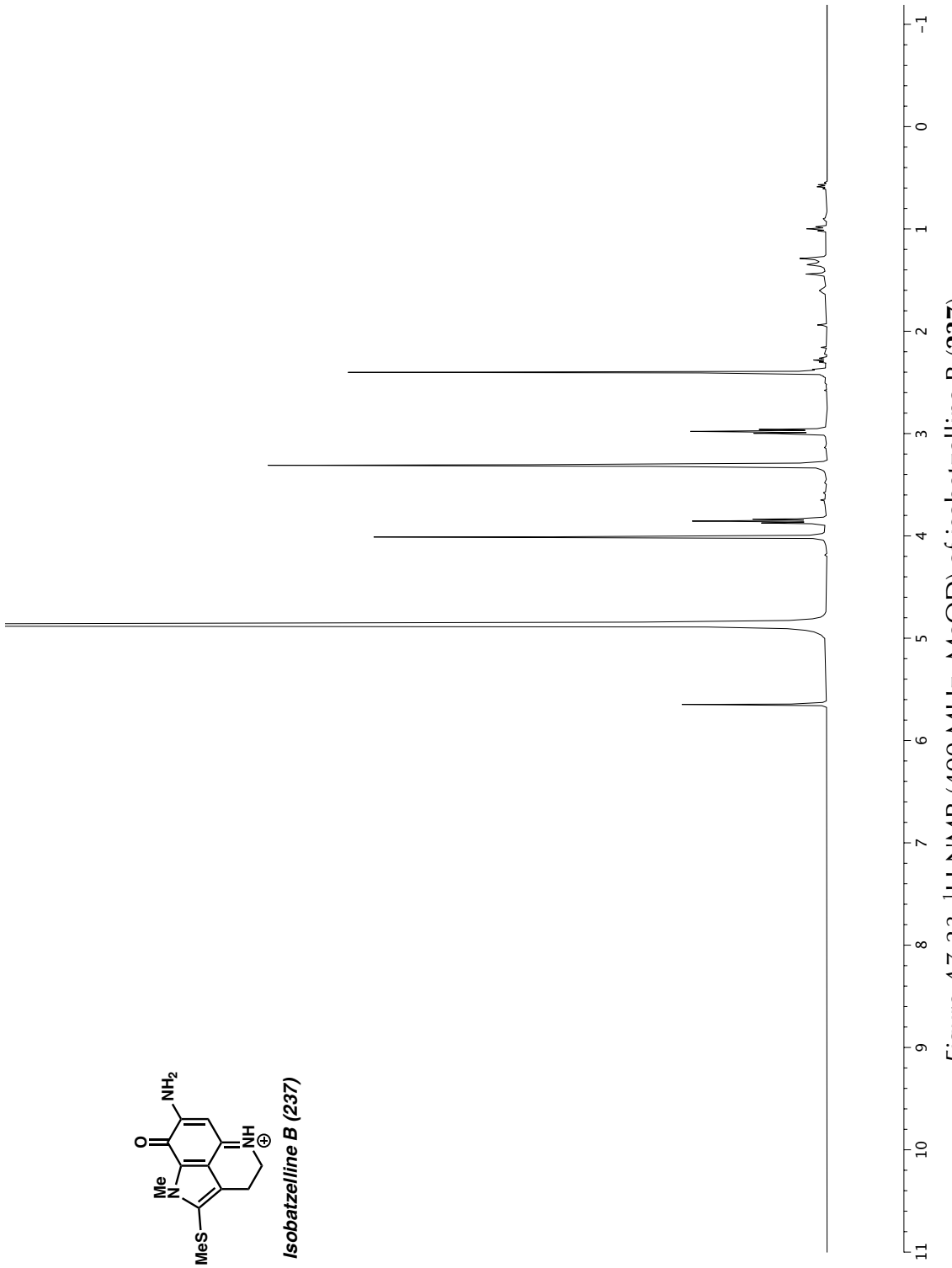


Figure A7.23. ^{1}H NMR (400 MHz, MeOD) of isobatzelline B (**237**).

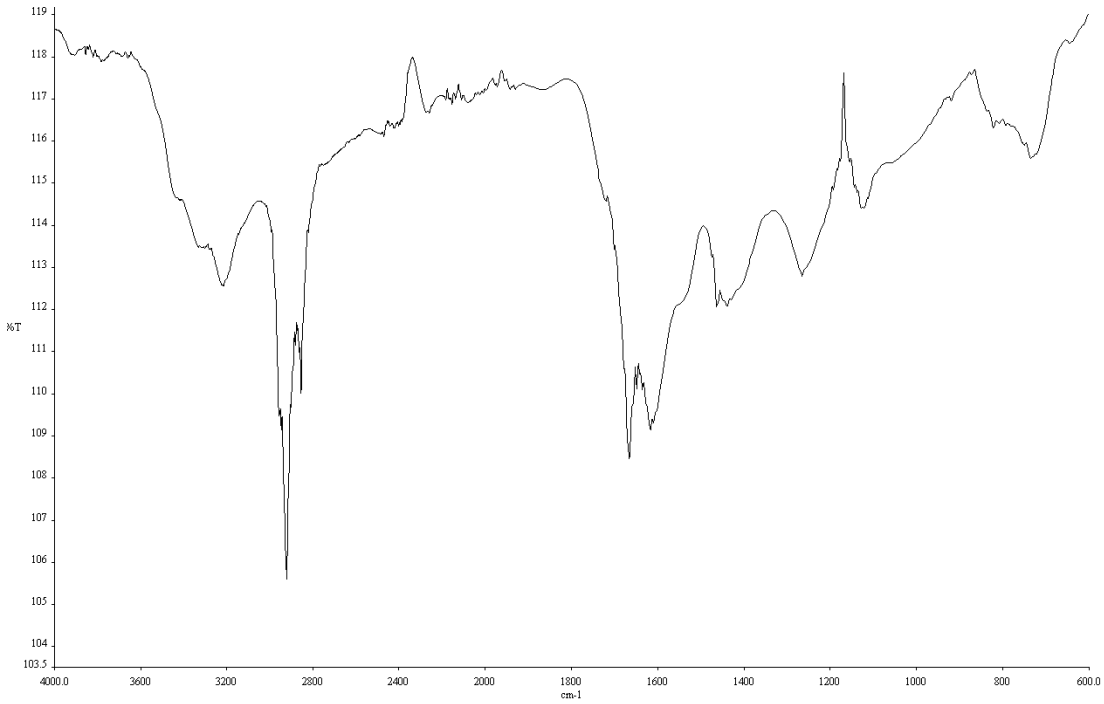


Figure A7.24. Infrared spectrum (Thin Film, NaCl) of isobatzelline B (**237**).

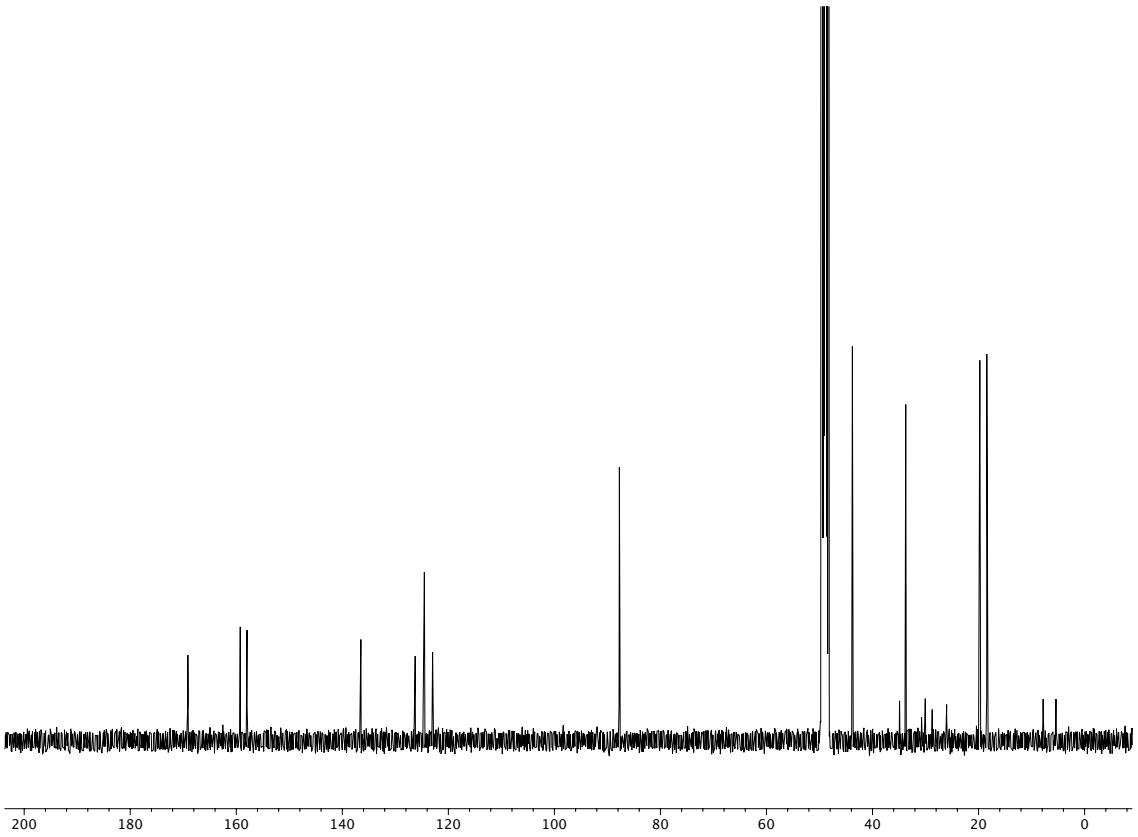


Figure A7.25. ^{13}C NMR (100 MHz, MeOD) of isobatzelline B (**237**).

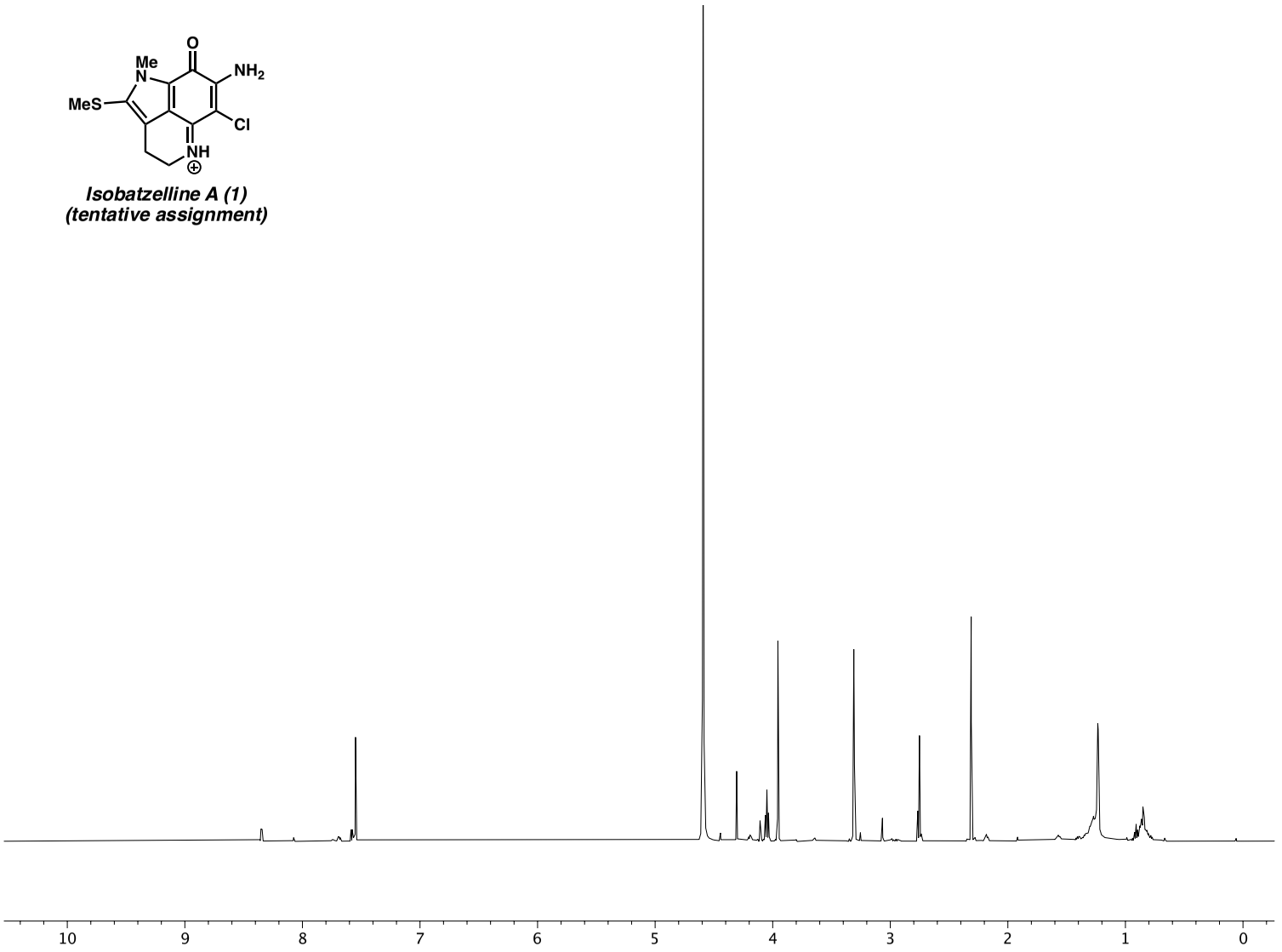


Figure A7.26. ^{1}H NMR (400 MHz, 1:1 MeOD:$CDCl_3$) of isobatzelline A (**1**).

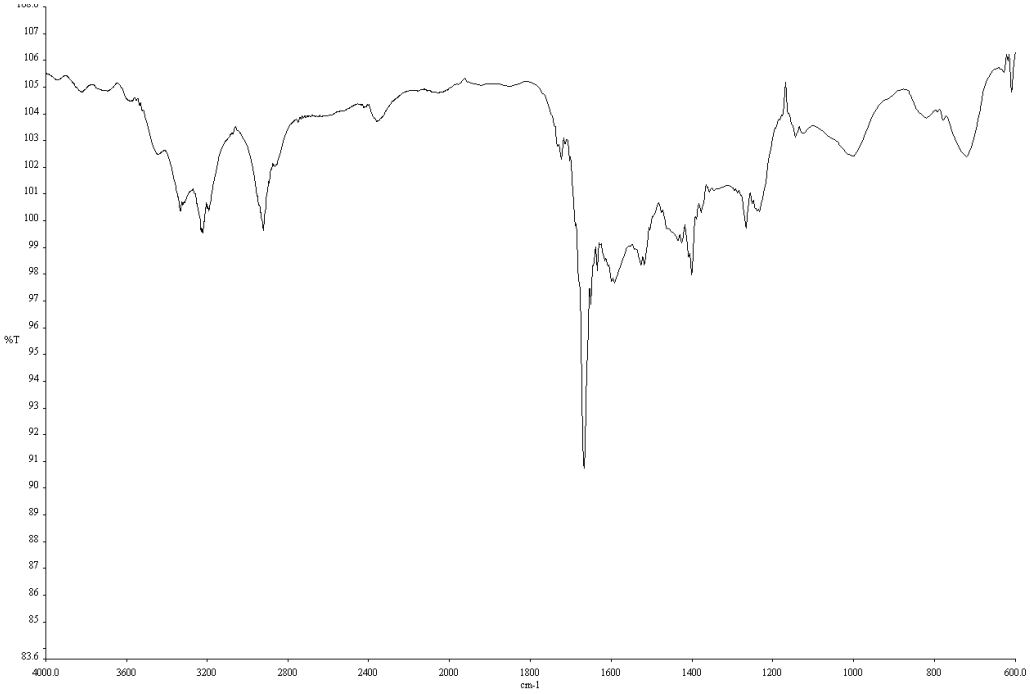


Figure A7.27. Infrared spectrum (Thin Film, NaCl) of isobatzelline A (**1**).

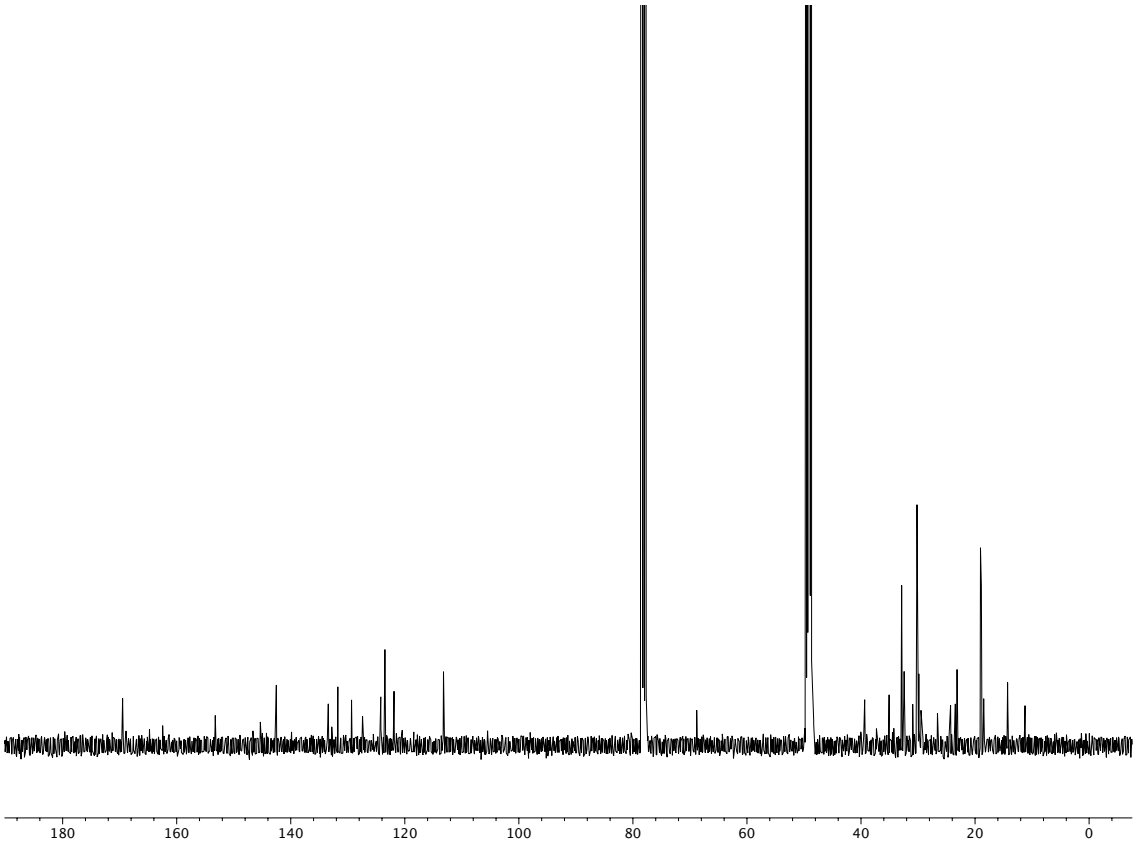


Figure A7.28. ^{13}C NMR (100 MHz, 1:1 MeOD:$CDCl_3$) of isobatzelline A (**1**).

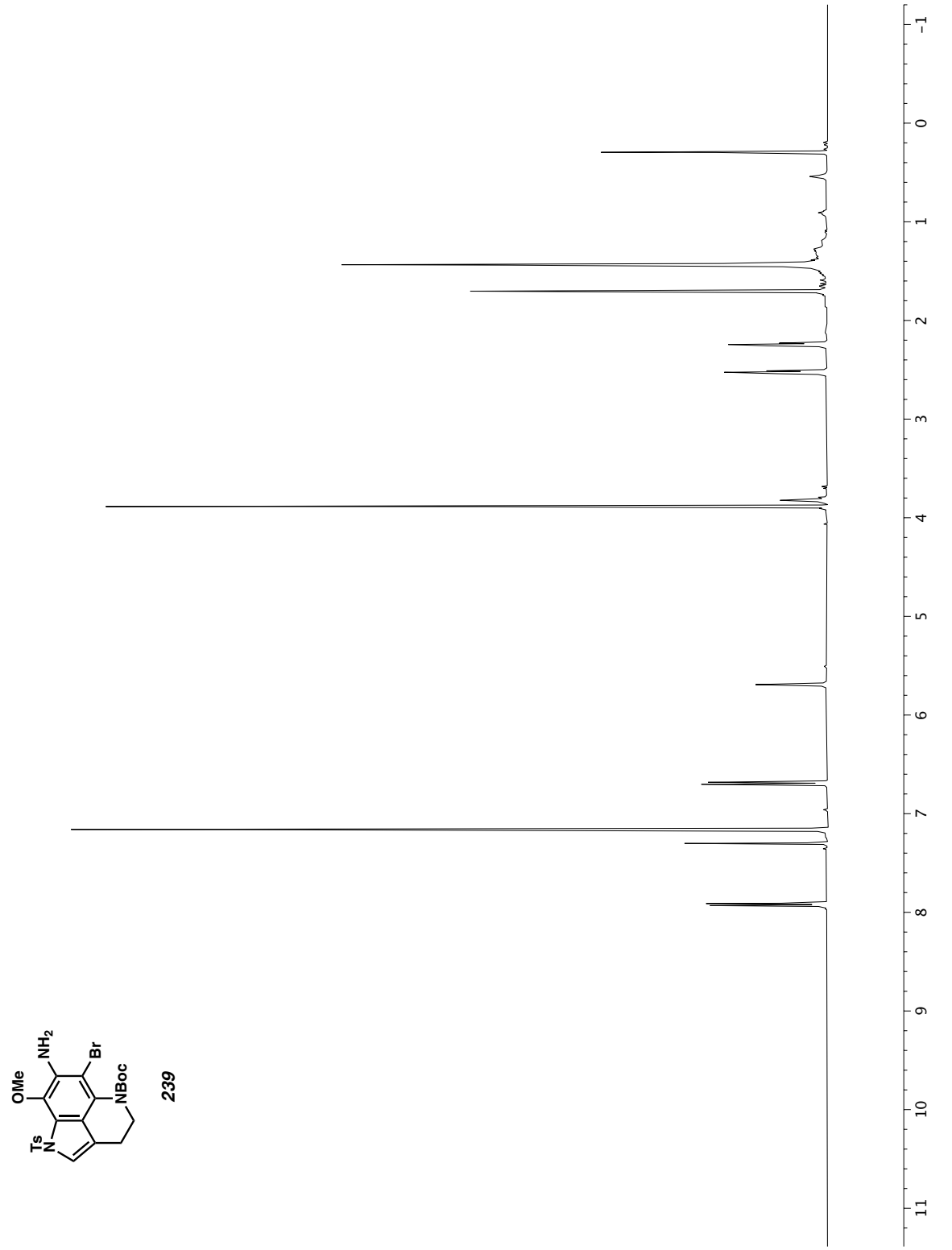


Figure A7.29. ^{1}H NMR (400 MHz, C_6D_6) of compound **239**.

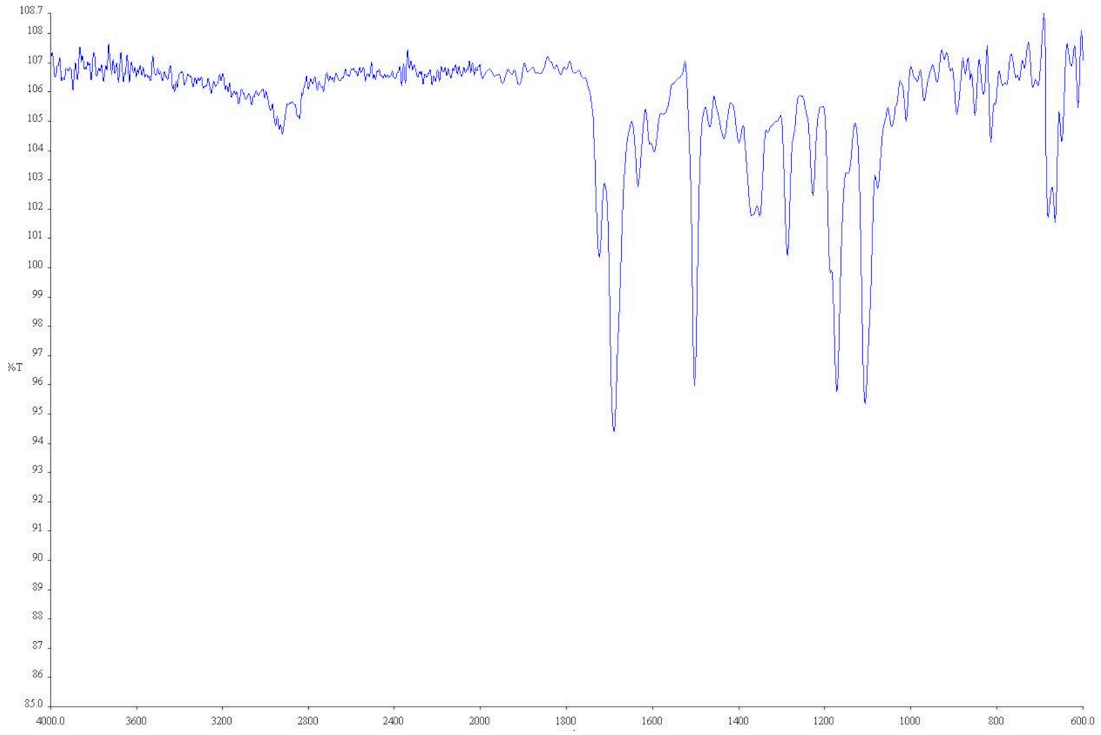


Figure A7.30. Infrared spectrum (Thin Film, NaCl) of compound **239**.

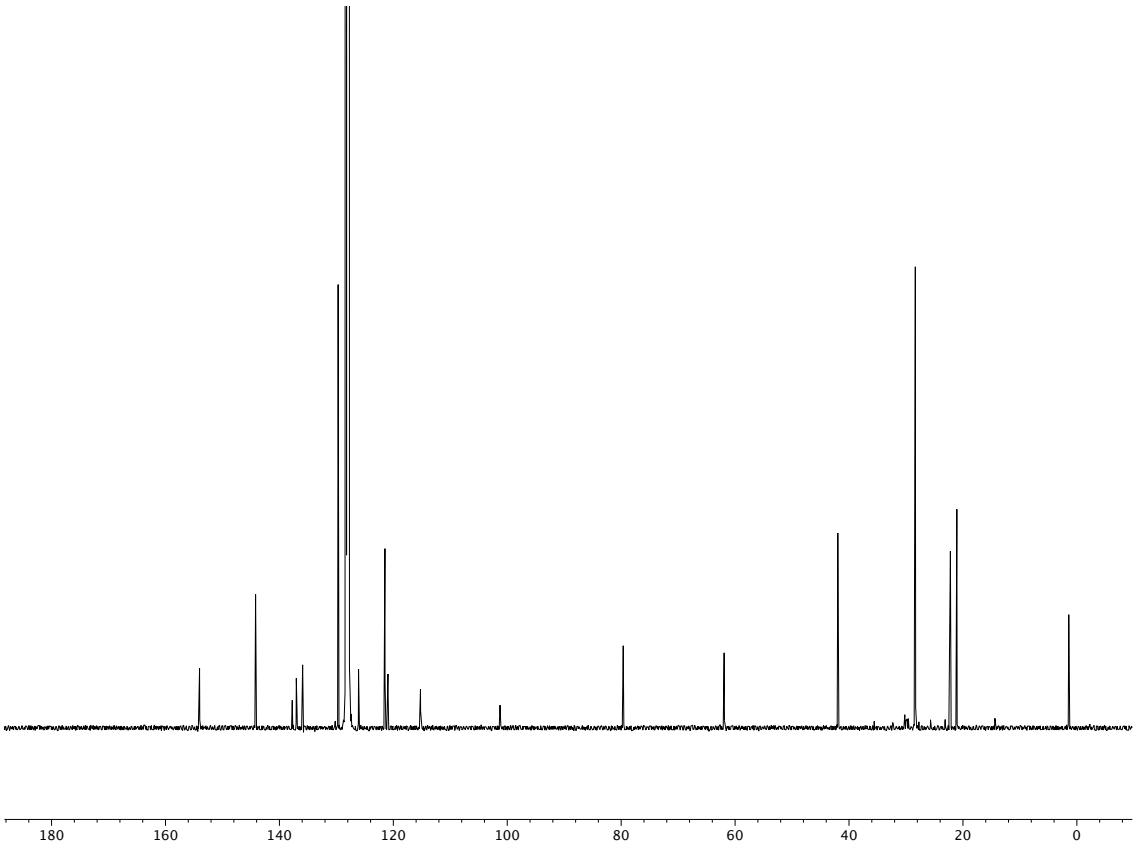


Figure A7.31. ^{13}C NMR (100 MHz, C_6D_6) of compound **239**.

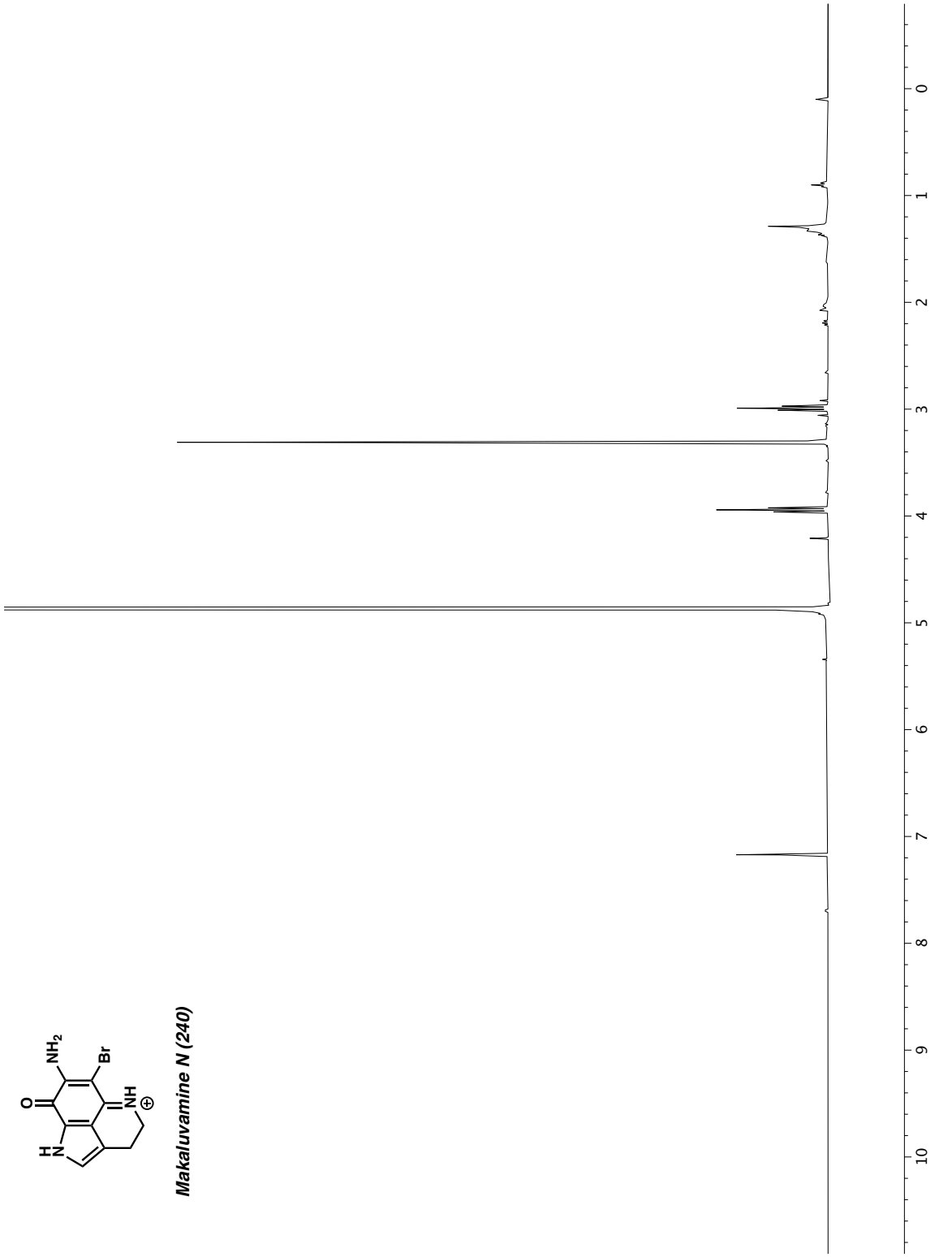


Figure A7.32. ^{1}H NMR (400 MHz, MeOD) of makaluvamine N (**240**).

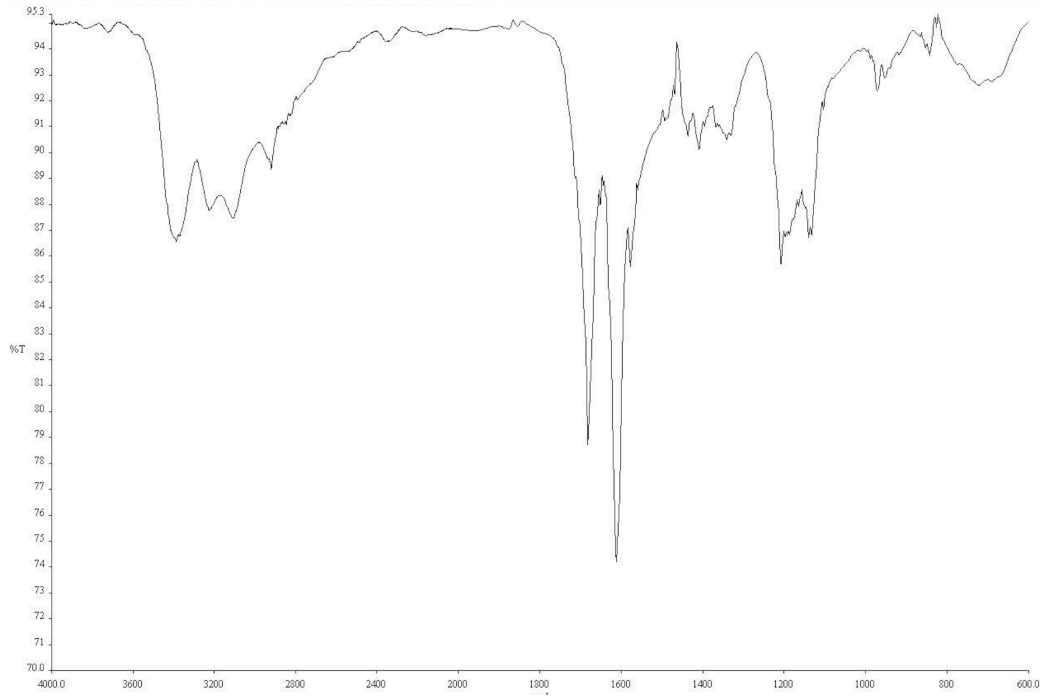


Figure A7.33. Infrared spectrum (Thin Film, NaCl) of makaluvamine N (**240**).

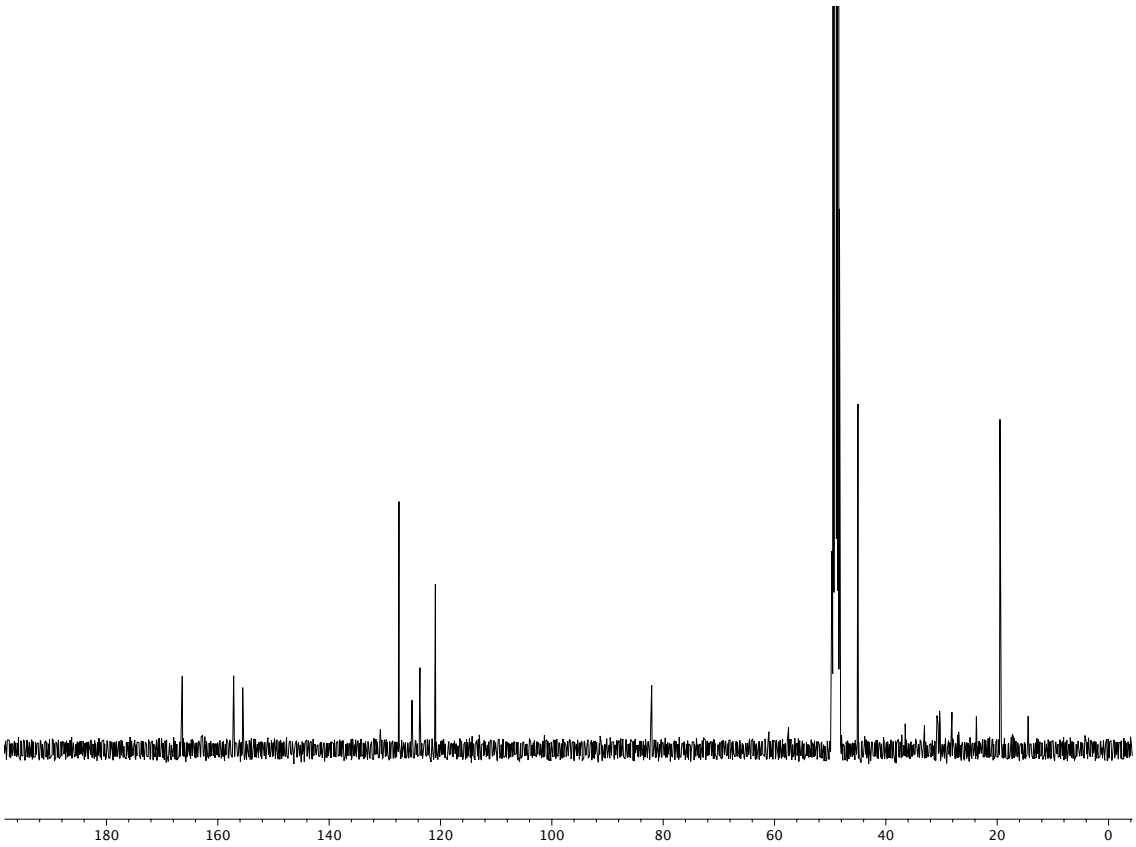


Figure A7.34. ^{13}C NMR (100 MHz, MeOD) of makaluvamine N (**240**).

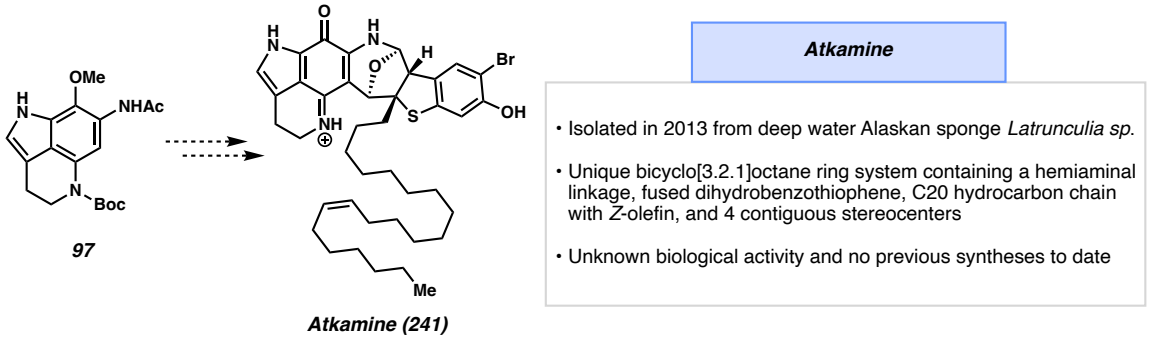
CHAPTER 3

Progress Toward the Total Synthesis of Atkamine†

3.1 INTRODUCTION

Having successfully employed aminotricycle **97** toward the synthesis of several simple pyrroloiminoquinone alkaloids, we were interested in attempting to leverage this same intermediate to access more complex members of the family: atkamine (**241**) represented a fantastic target for this endeavor (Figure 3.1.1). Atkamine (**241**) was isolated

Figure 3.1.1 *Atkamine (**241**).*



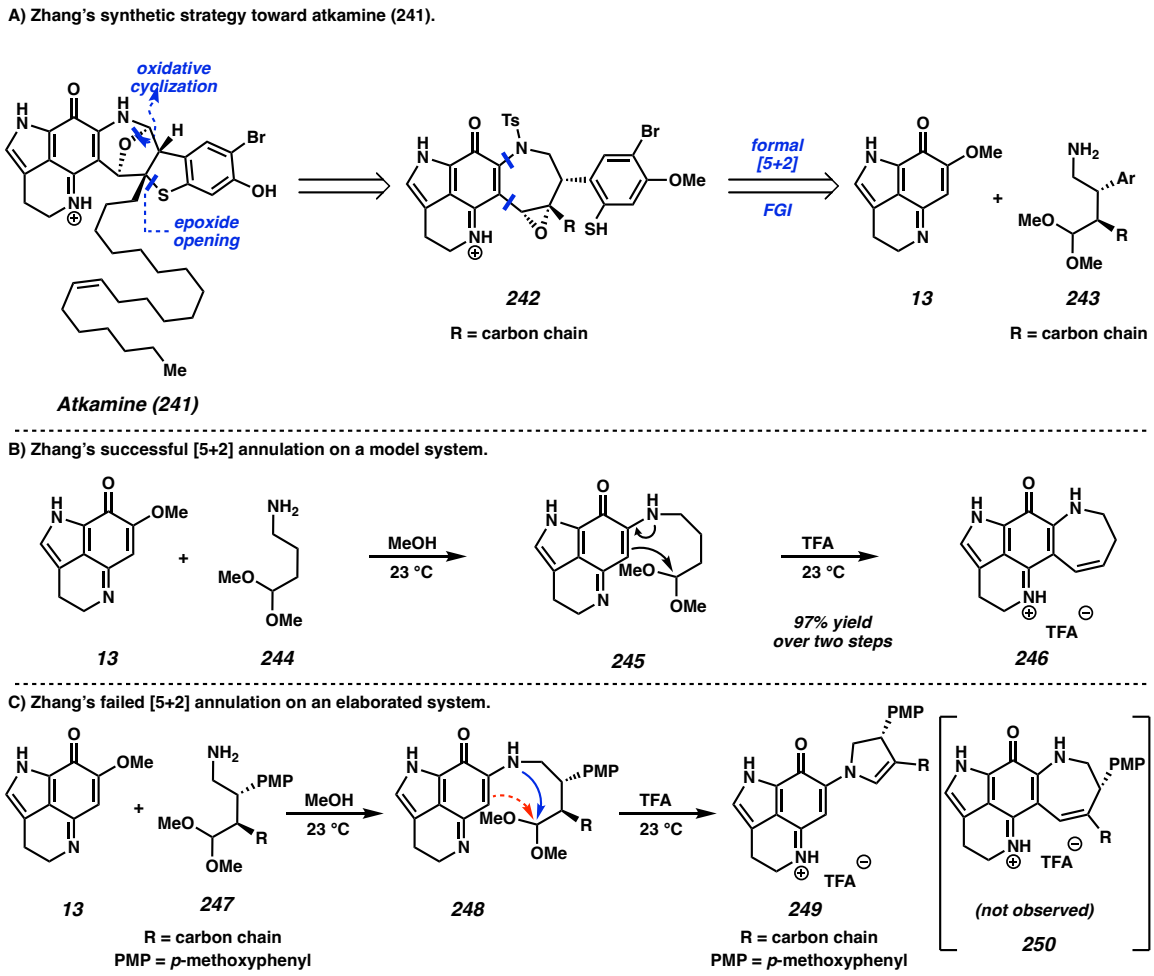
in 2013 by Hamann and coworkers from the cold-water Alaska sponge *Latrunculia* sp., and was named after a major Aleutian Island- Atka Island.[1] Its structure was elucidated by the orchestration of chemical degradation studies, NMR and ECD spectroscopy, and computational tools. Atkamine (**241**) possesses an unprecedented bicyclo[3.2.1]octane ring system appended to the conserved pyrroloiminoquinone core; this ring system contains a hemiaminal linkage, a protruding C20 fatty acid-derived carbon chain with a *Z*-olefin, is

†*Portions of this research were performed in collaboration with Eric Lee, a visiting scholar from Korea Advanced Institute of Science & Technology (KAIST).*

fused to a substituted dihydrobenzothiophene, and contains four contiguous stereocenters, all of which make atkamine (**241**) a formidable synthetic challenge.

The isolation chemists did not report any investigatios into atkamine's (**241**) biological activity, and no subsequent biological studies of atkamine (**241**) have been disclosed. To date, there have been no reported total syntheses of atkamine (**241**). In 2021, Zhang and coworkers disclosed their synthetic studies toward atkamine (**241**).[2] They envisaged that atkamine (**241**) could arise via epoxide opening of a pendent thiophenol to construct the dihydrothiophene motif and a subsequent oxidative cyclization to access the [3.2.1] bicycle (Scheme 3.1.1A). In a key step, they hypothesized that azepine **242** could

Scheme 3.1.1 *Zhang's progress toward the total synthesis of atkamine (**241**).*



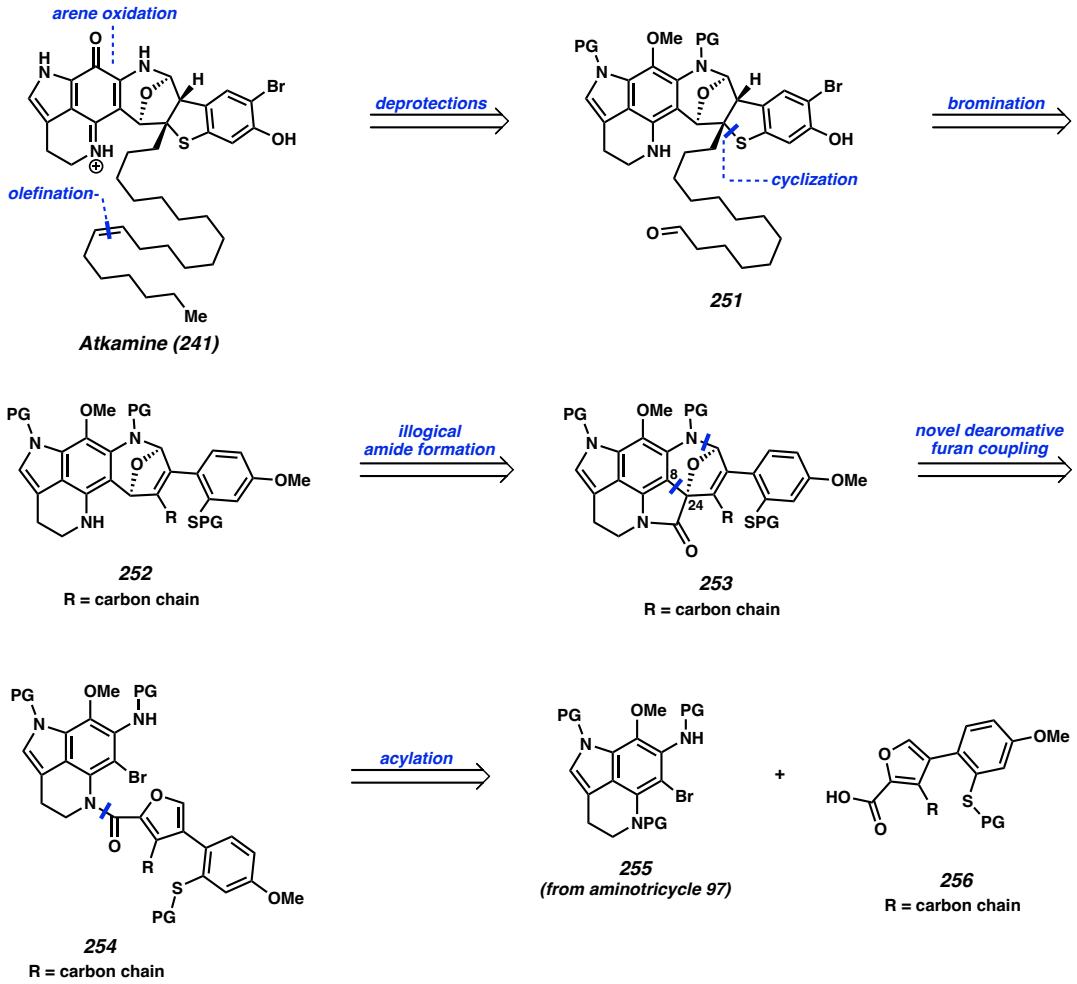
be formed via a formal [5+2] annulation of common intermediate **13** and amino acetal **243**. This key transformation was validated on a model system as treatment of pyrroloiminoquinone **13** with simplified amino acetal **244** first affected an aminolysis, and upon treatment with TFA, aminated pyrroloiminoquinone **245** underwent the desired cyclization to yield azepine **246** (Scheme 3.1.1B). However, when attempting the same sequence with elaborated amino acetal **247**, no desired azepine (**250**) was obtained and instead dihydropyrrole **249** was isolated (Scheme 3.1.1C). They attributed the lack of 7-membered ring formation to steric interactions, highlighting the difficulty of accessing the highly substituted azepine ring system found in atkamine (**241**).

Given its complex and unique structure, lack of successful total syntheses, and unknown biological activities, we viewed atkamine (**241**) as an excellent target to further leverage aminotricycle **97**.

3.2 1st GENERATION RETROSYNTHETIC ANALYSIS

Our retrosynthetic analysis began with adjustment of the arene oxidation state, as again we were interested in carrying intermediates in the anisole oxidation state through the synthesis (Scheme 3.2.1). This was followed by cleavage of the *Z*-olefin, tracing back to aldehyde **251**: in the forward direction we envisaged employing a *Z*-selective olefination to install the remainder of the fatty acid chain.[3] This disconnection was largely motivated by the lack of readily available fatty acid chain precursors that contain the correct number of carbons, olefin position, and olefin geometry. Next, the aryl bromide was disconnected as well as the C–S bond, cleaving the dihydrobenzothiophene unit, yielding pentacycle **252**. We hypothesized that an intramolecular addition of a thiyl radical onto the tetrasubstituted olefin of **252**, known as the thiol-ene "click" reaction, could form the desired five

Scheme 3.2.1 *1st generation retrosynthesis of atkamine (**241**).*

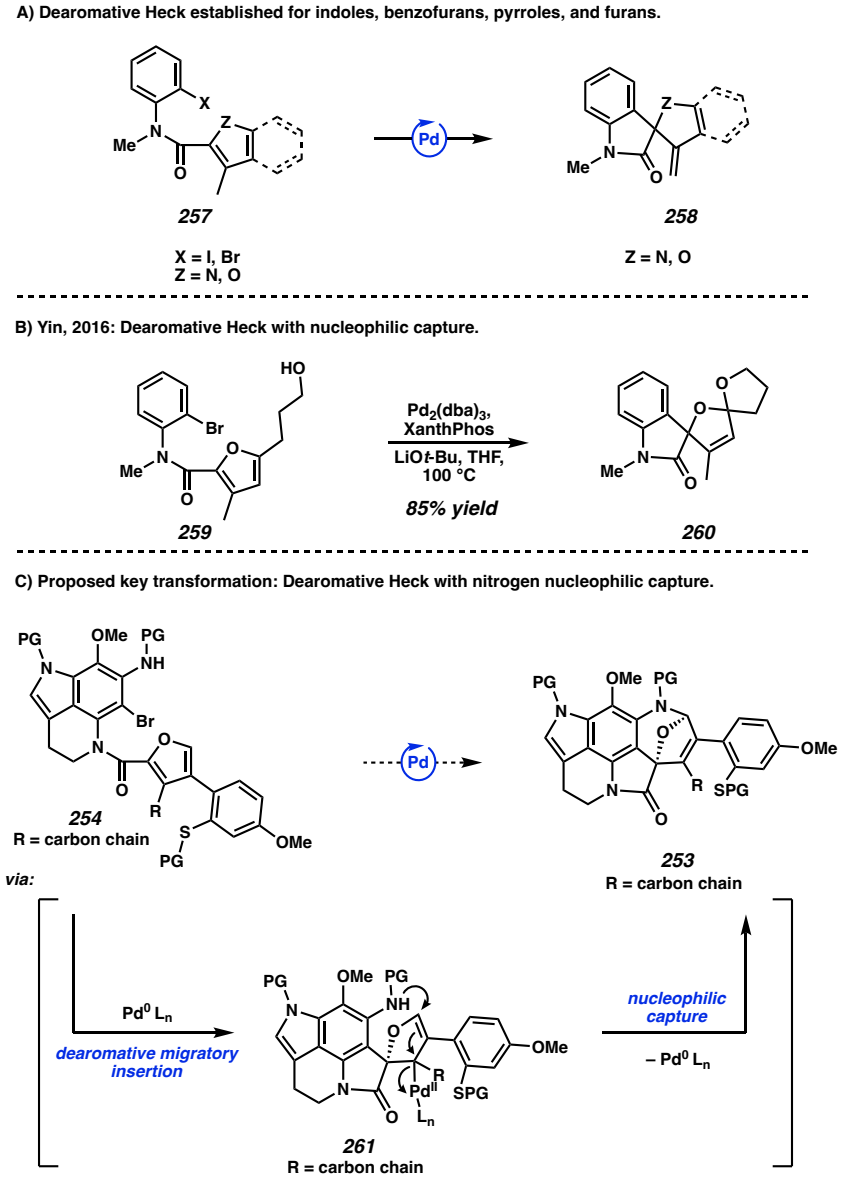


membered ring as it is well documented that the *5-endo* cyclization is typically favored over the *4-exo* pathway.[4] Although at this point, the diastereoselectivity of this proposed cyclization was unclear. From **252**, an illogical disconnection was performed in which an amide bond was formed in the retrosynthetic direction, leading back to aryl lactam **253**. The key disconnection of our synthetic strategy was simultaneous cleavage of the thioaminal linkage and C8–C24 bond. This was viewed as an ideal bond disconnection as it simplifies the complex bicyclo[3.2.1]octane ring system back to fully planarized intermediate **254**. As in Chapters 1 and 2, we were again motivated to develop novel reaction methodology to enable a critical bond disconnection: in particular we envisaged

developing a novel dearomative furan coupling to achieve these bond formations in a single step. It was anticipated that an intermolecular dearomative furan coupling would be difficult to achieve, thus the illogical amide bond formation disconnection was conducted to allow for an intramolecular variant. From planarized amide **254**, disconnection of the amide bond revealed aryl bromide **255** and furan **256**, which could be coupled in a convergent fashion. Notably, **255** could be quickly accessed from aminotricycle **97**.

The proposed key dearomative furan coupling was partially inspired by previous studies in this area. For example, dearomative Heck cyclizations have been well established for a variety of π-excessive heterocycles, and although less explored, furan substrates have proved feasible in this transformation (Scheme 3.2.2A).[5] In 2016, Yin and coworkers described a dearomative Heck arylation of furans with nucleophilic capture (Scheme 3.2.2B).[6] However, this report was limited to oxygen nucleophiles and no examples of bridged bicycle formation was demonstrated. Our proposed dearomative cyclization aims to advance the field of dearomative furan arylations by extending the scope to nitrogen nucleophilic capture and to form bridged bicyclic products, both of which have yet to be achieved (Scheme 3.2.2C). We hypothesize this would occur first through dearomative migratory insertion, followed by intramolecular nucleophilic capture of the intermediate Pd^{II} π-allyl species **261**.[7]

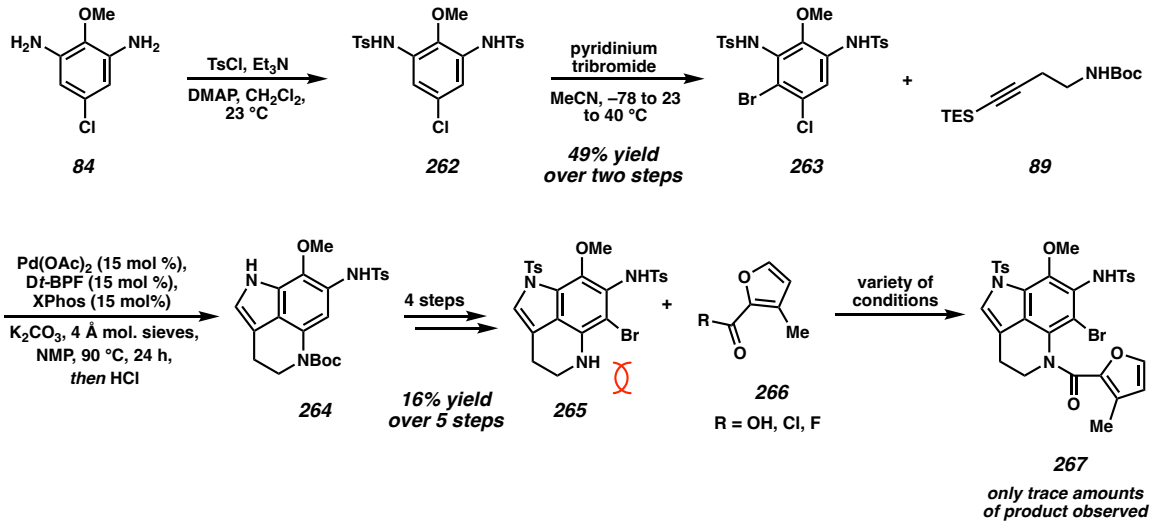
Scheme 3.2.2 *Previous studies on dearomative furan arylations.*



3.3 FAILED SYNTHESIS OF THE DEAROMATIVE CYCLIZATION SUBSTRATE

Our studies commenced by targeting the requisite dearomative cyclization substrate. At this point, we elected to modify the primary aniline nitrogen protecting group on aminotricycle **97** from Ac to Ts, as it was previously discovered the Ac group proved problematic under palladium catalysis (*vide supra*, Chapter 1.5).[8] To this end, previously prepared dianiline **84** was ditosylated followed by bromination with pyridinium

Scheme 3.3.1 *Failed synthesis of dearomative substrate* ***267****.*

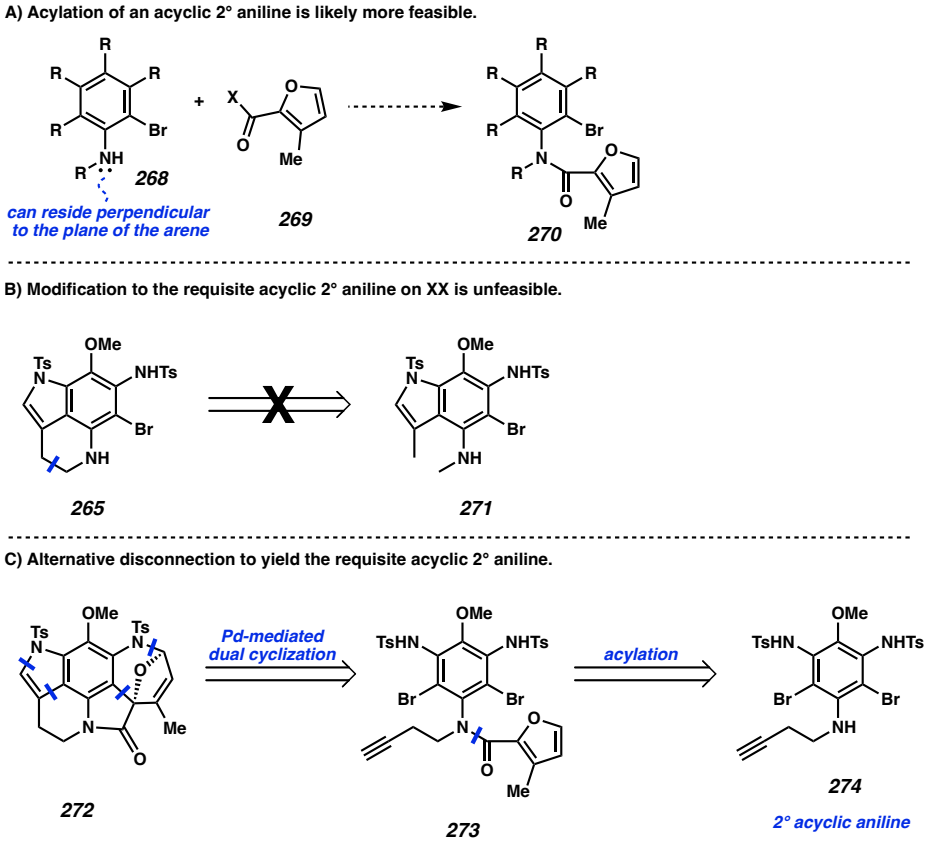


tribromide to yield bromoarene **263** (Scheme 3.3.1). This substrate proved competent in the Larock/Buchwald–Hartwig annulation/cyclization to afford *N*-tosyl aminotricycle **264**. This product was then elaborated through a three-step protecting group manipulation sequence to provide aryl bromide **265**. A simplified furan substrate was pursued to initiate the dearomative furan coupling. Importantly, a substrate containing alkyl substitution at the three position was necessary to mimic the real system.[9] Unfortunately, despite extensive investigation, acylation of tricycle **265** under a variety of reaction conditions proved unsuccessful, and only trace amounts of the desired coupled product **267** was observed via LC/MS. Because the secondary aniline is constrained to the same plane as the aromatic system, it is likely that a sterically congested environment exists because of the *o*-bromide substituent, preventing engagement with the activated acid electrophile **266**.[10]

3.4 DESIGN OF THE MODIFIED DEAROMATIVE CYCLIZATION SUBSTRATE

To circumvent this challenge, we targeted an acyclic secondary aniline. It was hypothesized that the lone pair of an acyclic secondary aniline (i.e. **268**) could reside perpendicular to the plane of the highly substituted arene, avoiding unfavorable steric

Scheme 3.4.1 *Design of the modified dearomatization substrate* ***273****.*



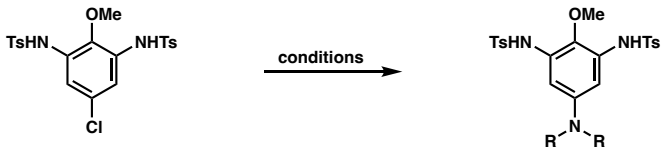
interactions with the *o*-bromide substituent, which could potentially allow for the challenging acylation to be achieved (Scheme 3.4.1A). Modification of aminotricycle **265** to the requisite acyclic secondary aniline would require cleavage of the tetrahydroquinoline ring (Scheme 3.4.1B). However, this C–C bond formation would likely be unfeasible to achieve in the forward direction. Instead, desired dearomative cyclization product **272** was examined and subsequently disconnected to reveal pseudo symmetric bromo arene **273** (Scheme 3.4.1C). In the forward direction, we envisaged developing a palladium-mediated dual cyclization— specifically a tandem Larock indolization/dearomative furan coupling sequence to construct the full ring system of atkamine (**241**) in a single synthetic step. From arene **273**, the amide bond was cleaved to reveal a fully substituted acyclic secondary

aniline (**274**), which again we believed could be successfully acylated. Additionally, the symmetry of arene **274** would greatly simplify its synthesis.

3.5 SYNTHESIS OF THE MODIFIED DEAROMATIVE CYCLIZATION SUBSTRATE AND FAILED DEAROMATIVE CYCLIZATION

The synthesis of the modified dearomative cyclization substrate began from previously accessed aryl chloride **262**, as a scalable route was already established for this intermediate. Unfortunately, attempting to install the third nitrogen atom of the arene utilizing a Buchwald–Hartwig amination proved to be challenging (Table 3.5.1).

Table 3.5.1 *Investigation of the Buchwald–Hartwig amination of aryl chloride* ***262***.

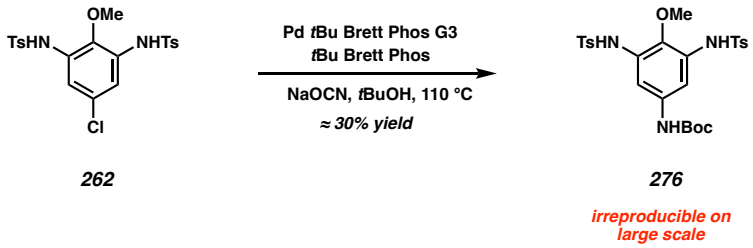


262 ***275***

[Pd]	ligand	nucleophile	base	solvent	temp	result
$Pd(OAc)_2$	XPhos	NH_2Boc	Cs_2CO_3	dioxane	100 °C	no rxn
$Pd(OAc)_2$	XPhos	NH_2Boc -variety of equiv.	K_2CO_3	NMP	90 °C	no rxn
$Pd(OAc)_2$	XPhos	NH_2Boc -variety of equiv.	K_2CO_3	NMP	110 °C	detosylation
Pd XPhos G3	XPhos	NH_2Boc	K_2CO_3	NMP	90 °C	no rxn
$Pd(P(o\text{-tol})_3)_2$	Josiphos	$(NH_4)_2SO_4$	NaO*t*Bu	dioxane	100 °C	sm consumed, unknown pdt
$[Pd(cinanmyl)Cl]_2$	BippyPhos	NH_3 in THF	NaO*t*Bu	dioxane	110 °C	detosylation
$[Pd(cinanmyl)Cl]_2$	BippyPhos	$(NH_4)_2SO_4$	NaO*t*Bu	dioxane	110 °C	no rxn
XPhos Pd G3	XPhos	LiHMDS	-	THF	65 °C	detosylation
$Pd(P(t\text{Bu})_3)_2$	-	LiHMDS	-	PhMe	65 °C	detosylation

We hypothesize that upon deprotonation of either Ts group, the resulting electron rich aryl chloride is reluctant to undergo oxidative addition. After extensive experimentation, it was eventually discovered that the desired C–N bond could be forged utilizing Buchwald's conditions for the synthesis of *N*-aryl carbamates (Scheme 3.5.1).[11] By employing sodium

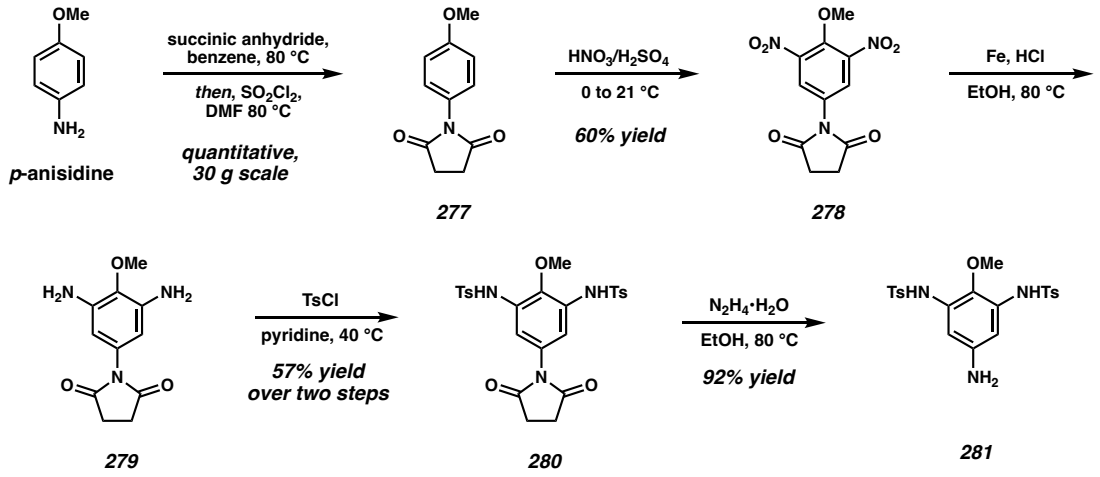
Scheme 3.5.1 *Synthesis of carbamate* ***276***.



cyanate as the coupling partner in the presence of *t*-BuOH, *N*-Boc trianiline **276** could be obtained. Unfortunately, this transformation gave unsatisfactory yields and was irreproducible on large scale, so an alternative strategy to synthesize the requisite dearomative cyclization substrate was developed.

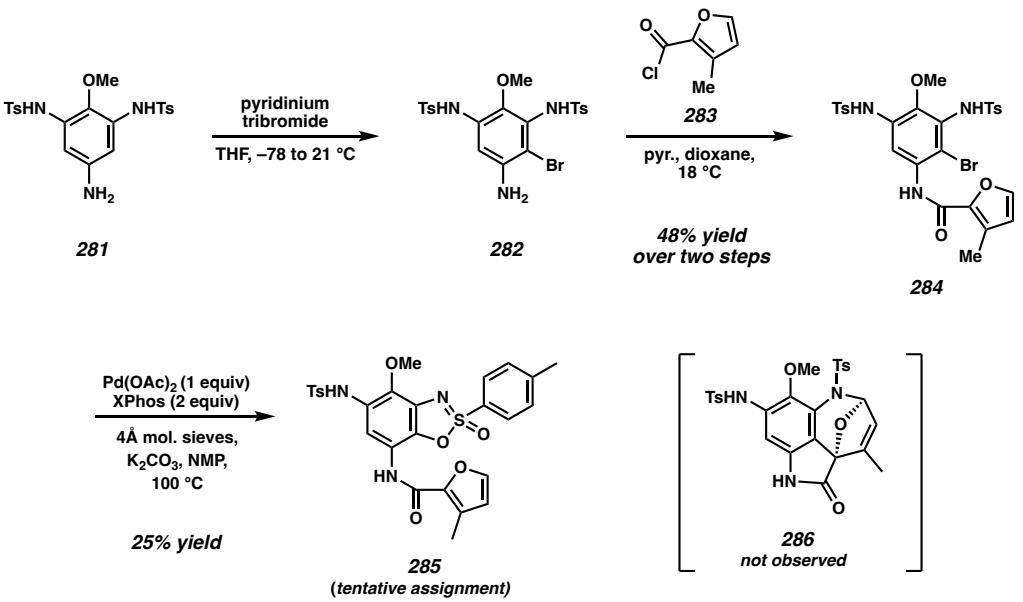
The second-generation approach commenced from *p*-anisidine, in which the third nitrogen atom was preinstalled. Utilizing modified conditions reported from Kraus and coworkers[12], protection of the aniline nitrogen to yield succinimide **277** could be achieved in quantitative yield on 30 g scale (Scheme 3.5.2). Dinitration proceeded smoothly and was followed by reduction of the nitro groups to provide dianiline **279**. The aniline nitrogens were then tosylated and succinimide deprotection was conducted under standard to conditions to yield the desired trianiline **281**. This improved sequence required no column chromatography and proved scalable as multigram quantities of **281** could be prepared in a single pass.

Scheme 3.5.2 *Synthesis of trianiline* ***281***.



Before attempting the palladium-mediated dual cyclization, we turned our attention toward investigating the dearomative furan coupling component (Scheme 3.5.3). After extensive experimentation, it was discovered that pyridinium tribromide was unique at affecting the desired monobromination of aniline **281**. Other brominating reagents (i.e. NBS or Br_2) resulted in complex reaction profiles with much of the mass balance being various oxidized arene products. Subsequent acylation of bromoaniline **282** with acid chloride **283** yielded the requisite dearomative furan coupling substrate **284**. After investigating the dearomative furan coupling on similar model systems (see Appendix 9), $Pd(OAc)_2$ and XPhos proved to be the most promising reaction conditions. However, when subjecting bromide **284** to modified stoichiometric reaction conditions[13] the desired dearomative coupling product **286** was not observed. Instead, 2D NMR data suggested the formation of unusual tosyl insertion product **285**. Although the dearomative furan coupling failed under these reaction conditions, this could represent an attractive method to synthesize benxozathiazoles, which are pharmaceutically relevant motifs as they are chiral at sulfur. Future efforts will attempt to generalize this method. Additionally, future efforts will be focused on developing the desired dearomative furan coupling, with the ultimate

Scheme 3.5.3 *Failed dearomative furan arylation.*



goal of developing the palladium-mediated dual cyclization to access the full skeleton of atkamine (**241**) and subsequent completion of its total synthesis.

3.6 EXPERIMENTAL SECTION

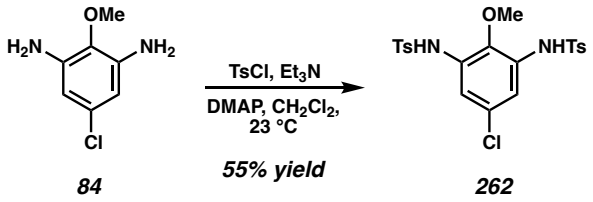
3.6.1 MATERIALS AND METHODS

Unless otherwise stated, reactions were performed in flame-dried glassware under an argon or nitrogen atmosphere using dry, deoxygenated solvents. Solvents were dried by passage through an activated alumina column under argon. K_2CO_3 was flame-dried under vacuum and stored in a nitrogen-filled glovebox prior to use. 4Å molecular sieves were activated via microwave heating (1100 W, full power, 45 s X 4), cooled under N_2, and stored in a N_2 filled glovebox. All other reagents were purchased from commercial sources and used as received unless otherwise indicated. Reaction temperatures were controlled by an IKAmag temperature modulator. Reaction progress was monitored by thin-layer chromatography (TLC) or Agilent 1290 UHPLC-MS. TLC was performed using E. Merck silica gel 60 F254 precoated glass plates (0.25 mm) and visualized by UV fluorescence

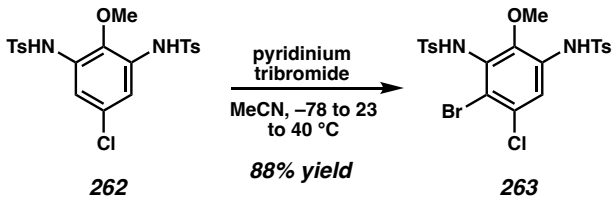
quenching, $KMnO_4$ staining, or *p*-anisaldehyde staining. Silicycle SiliaFlash® P60 Academic Silica gel (particle size 40–63 nm) was used for flash chromatography. Preparative HPLC was performed on an Agilent 1100 Series HPLC system using a 9.4 x 250 mm Agilent Eclipse XDB-C18 column, or on an Agilent 1200 Series HPLC system using a 9.4 x 250 mm Agilent Zorbax Rx-SIL column. ^{1}H NMR spectra were recorded on Varian Inova 500 MHz, Varian 600 MHz, and Bruker 400 MHz spectrometers and are reported relative to residual $CHCl_3$ (δ 7.26 ppm), C_6D_6 (δ 7.16 ppm), DMSO-d_6 (δ 2.50 ppm), CD_2Cl_2 (δ 5.32 ppm), or CD_3OD (δ 3.31 ppm). ^{13}C NMR spectra were recorded on a Bruker 400 MHz spectrometer (100 MHz) and are reported relative to $CHCl_3$ (δ 77.16 ppm), C_6D_6 (δ 128.06 ppm), DMSO-d_6 (δ 39.52 ppm), CD_2Cl_2 (δ 53.84 ppm), or CD_3OD (δ 49.00 ppm). Data for ^{1}H NMR are reported as follows: chemical shift (δ ppm) (multiplicity, coupling constant (Hz), integration). Multiplicities are reported as follows: s = singlet, d = doublet, t = triplet, q = quartet, p = pentet, sept = septuplet, m = multiplet, br s = broad singlet, br d = broad doublet. Data for ^{13}C NMR are reported in terms of chemical shifts (δ ppm). Some reported spectra include minor solvent impurities of water, ethyl acetate, diethyl ether, methylene chloride, acetone, grease, and/or silicon grease, which do not impact product assignments. IR spectra were obtained by use of a Perkin Elmer Spectrum BXII spectrometer using thin films deposited on NaCl plates and reported in frequency of absorption (cm^{-1}). High resolution mass spectra (HRMS) were obtained from an Agilent 6230 LC/TOF with an Agilent Jet Stream ion source in electrospray ionization (ESI+ or ESI–) mode, from the Caltech Mass Spectrometry Laboratory using a JEOL JMS-T2000GC AccuTOFTM GC-Alpha in field desorption (FD+) mode, or from a JEOL JMS-

600H High Resolution Mass Spectrometer in fast atom bombardment (FAB+), GC field ionization (GCFI+), or electron ionization (EI+) mode.

3.6.2 EXPERIMENTAL PROCEDURES



Ditosylated aniline 262: To a flame dried 250 mL round bottom flask was added dianline **84** (500.0 mg, 2.9 mmol, 1.0 equiv, TsCl (1.1 g, 5.8 mmol, 2.0 equiv), and CH_2Cl_2 (29 mL, 0.1 M). The resulting mixture was stirred for 30 seconds, at which point Et_3N (1.2 mL, 8.7 mmol, 3.0 equiv) and DMAP (35.4 mg, 0.29 mmol, 0.1 equiv) were added. The reaction mixture was stirred at 23 °C for 16 h, at which point TLC analysis indicated complete consumption of the starting material. Ethyl acetate (100 mL) and water (100 mL), and the product was extracted with EtOAc (3 x 50 mL). The combined organic layers were washed with brine, dried over Na_2SO_4, filtered, and concentrated under reduced pressure to afford the title compound (770 mg, 55% yield) as an off-white solid which was taken forward without further purification.



Bromoarene 263: To a flame dried 2 dram vial was added arene **262** (50.0 mg, 0.104 mmol, 1.0 equiv) and THF (1 mL, 0.1M). The resulting homogeneous solution was cooled to –78 °C, at which point pyridinium tribromide (39.9 mg, 0.125 mmol, 1.2 equiv) in THF (0.5

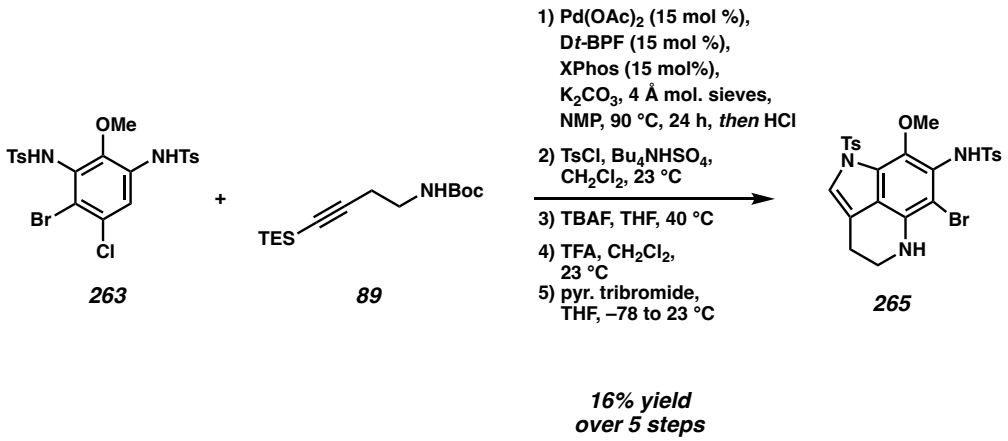
mL) was added dropwise. The reaction mixture was stirred at –78 °C for 10 min, then warmed to 23 °C and stirred for 2 hours, and finally heated to 40 °C for 16 h, at which point LC/MS analysis indicated complete consumption of the starting material. The reaction was quenched with saturated aq. $N_2S_2O_3$ (1 mL) and diluted with EtOAc (3 mL). The product was extracted with EtOAc (3 x 3 mL) and the combined organic layers were washed with brine, dried over Na_2SO_4, filtered, and concentrated under reduced pressure. The crude product was purified by column chromatography (SiO_2, 25% Acetone/Hexanes) to afford the title compound (51.3 mg, 88% yield) as a pink solid.

^{1}H NMR (400 MHz, $CDCl_3$): δ 7.92 (m, 4H), 7.42 – 7.31 (m, 4H), 6.29 (s, 1H), 3.70 (s, 3H), 2.48 (s, 6H).

^{13}C NMR (100 MHz, $CDCl_3$): δ 157.2, 145.5, 145.5, 144.4, 141.7, 136.5, 136.4, 129.7, 129.6, 129.5, 129.4, 127.6, 120.4, 111.9, 60.3, 21.9.

IR (Neat film, NaCl): 3464, 3383, 2949, 2332, 1616, 1595, 1490, 1429, 1374, 1237, 1167, 1085, 911, 813, 663 cm^{-1}.

HRMS (ESI+): *m/z* calc'd for $C_{21}H_{21}BrClN_2O_5S_2$ $[M+H]^+$: 558.9764, found 558.9754.



Bromotricycle 265: Step 1 was conducted according to general procedure A (see chapter 1.10) using bromoarene **263** (811.4 mg, 2.0 mmol) to afford a brown solid (430 mg, 41% yield) that was carried forward without additional purification.

^{1}H NMR (600 MHz, $CDCl_3$): δ 7.79 (s, 1H), 7.69 (d, J = 8.0 Hz, 2H), 7.57 (s, 1H), 7.19 (d, J = 8.1 Hz, 2H), 6.82 (s, 1H), 6.78 – 6.71 (m, 1H), 4.02 (t, J = 5.7 Hz, 2H), 3.53 (s, 3H), 2.93 (t, J = 5.7 Hz, 2H), 2.34 (s, 3H), 1.61 (s, 9H).

To a 25 mL round bottom flask was added the resulting Larock/Buchwald–Hartwig desilylated product (not shown, 180 mg, 0.39 mmol, 1.0 equiv) was added Ts Cl (297 mg, 1.56 mmol, 4.0 equiv), Bu_4NBr (12.5 mg, 0.039 mmol, 0.1 equiv), KOH (87.4 mg, 1.56 mmol, 4.0 equiv), and CH_2Cl_2 (3.9 mL, 0.1M). The reaction mixture was stirred vigorously at 23 °C for 2 h, at which point LC/MS analysis indicated complete consumption of the starting material. A small amount of SiO_2 was added directly to the reaction mixture and was concentrated to dryness under reduced pressure. The resulting free-flowing SiO_2 mixture was purified by column chromatography (SiO_2, 30 to 40 to 50 to 60% EtOAc/Hexanes) to afford an intermediate tritosylated tricycle (not shown, 257 mg, 86% yield) as a brown solid.

To a 2 dram vial was added the intermediate tritosylated tricycle (not shown, 257 mg, 0.34 mmol, 1.0 equiv) was added TBAF (0.68 mL, 0.68 mmol, 2.0 equiv) as a 1 M solution in THF, and THF (3.4 mL). The vial was sealed and heated to 40 °C for 16 h, at which point LC/MS analysis indicated incomplete consumption of the starting material. Another 1.0 equiv of TBAF was added, and the reaction mixture was stirred at 40 °C for an additional 8 h, at which point LC/MS analysis indicated complete consumption of the starting material. A small amount of SiO_2 was added directly to the reaction mixture and was concentrated to dryness under reduced pressure. The resulting free-flowing SiO_2 mixture was purified by column chromatography (SiO_2, 30 to 40% EtOAc/Hexanes) to afford an intermediate ditosylated tricycle (not shown– tosylated on the indole and aniline nitrogen, 119.2 mg, 57% yield) as a brown solid.

^{1}H NMR (600 MHz, $CDCl_3$): δ 7.82 (s, 1H), 7.76 (d, J = 8.1 Hz, 2H), 7.66 (d, J = 8.2 Hz, 2H), 7.25 – 7.18 (m, 3H), 7.16 (d, J = 8.1 Hz, 2H), 6.95 (s, 1H), 3.91 (t, J = 5.8 Hz, 2H), 3.49 (s, 3H), 2.82 (t, J = 5.7 Hz, 2H), 2.37 (s, 3H), 2.35 (s, 3H), 1.57 (s, 9H).

To a flame dried 10 mL round bottom flask was added the intermediate ditosylated tricycle (119.2 mg, 0.195 mmol, 1.0 equiv), TFA (0.67 mL, 8.77 mmol, 45.0 equiv), and CH_2Cl_2 (4 mL, 0.05 M). The reaction mixture was stirred at 23 °C at which point LC/MS analysis indicated complete consumption of the starting material. A small amount of SiO_2 was added directly to the reaction mixture and was concentrated to dryness under reduced pressure. The resulting free-flowing SiO_2 mixture was purified by column chromatography (SiO_2, 55 to 60% EtOAc/Hexanes) to afford the intermediate deprotected secondary aniline (79.1 mg, 79% yield) as a beige solid.

^{1}H NMR (600 MHz, $CDCl_3$): δ 7.71 (d, J = 8.3 Hz, 2H), 7.66 (d, J = 8.4 Hz, 2H), 7.24 – 7.18 (m, 2H), 7.15 – 7.07 (m, 3H), 7.02 (s, 1H), 6.75 (s, 1H), 3.42 (s, 3H), 3.31 (t, J = 6.0 Hz, 2H), 2.82 (td, J = 6.0, 1.4 Hz, 2H), 2.35 (s, 3H), 2.33 (s, 3H).

^{13}C NMR (100 MHz, $CDCl_3$): δ 144.5, 144.0, 137.7, 136.6, 135.2, 130.3, 129.8, 129.6, 129.4, 129.3, 127.6, 127.2, 126.2, 120.1, 119.0, 116.8, 98.8, 62.4, 42.4, 22.4, 21.7, 21.7.

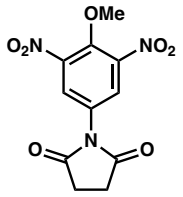
To a flame dried 2 dram vial was added the intermediate deprotected secondary aniline (not shown, 6.4 mg, 0.0125 mmol, 1.0 equiv), BHT (6.0 mg, 0.027 mmol, 2.1 equiv) and THF (2.0 mL, 0.005M). The mixture was cooled to –78 °C, at which point pyridinium tribromide (4.8 mg, 0.015 mmol, 1.2 equiv) was added as a solution in THF (0.5 mL). The reaction mixture was then warmed to 23 °C and stirred for 16 h, at which point LC/MS analysis indicated complete consumption of the starting material. The reaction was quenched with saturated aq. $N_2S_2O_3$ (1 mL) and diluted with EtOAc (3 mL). The product was extracted with EtOAc (3 x 3 mL) and the combined organic layers were washed with brine, dried over Na_2SO_4, filtered, and concentrated under reduced pressure. The crude product was purified by preparatory TLC (35% Acetone/Hexanes) to afford the titled compound (5.4 mg, 16% yield over 5 steps) as a white solid. This sample was pure by HPLC analysis. This pure material was used for all subsequent acylation experiments. However, when the sample was reprepared for characterization data, it was yielded as 1:1 inseparable mixture with the starting material. The characterization data for the mixture is reported.

^{1}H NMR (600 MHz, $CDCl_3$): δ 7.99 (d, J = 8.4 Hz, 1H), 7.88 – 7.59 (m, 8H), 7.41 – 7.28 (m, 4H), 7.23 – 7.04 (m, 4H), 7.04 – 6.78 (m, 2H), 6.38 (s, 1H), 3.48 – 3.31 (m, 6H), 3.29 (s, 3H), 2.86 (td, J = 6.0, 1.4 Hz, 4H), 2.48 (d, J = 7.9 Hz, 5H), 2.40 – 2.29 (m, 9H).

^{13}C NMR (100 MHz, $CDCl_3$): δ 171.3, 145.0, 144.8, 144.6, 144.0, 143.4, 138.7, 137.3, 136.7, 136.6, 135.5, 135.5, 135.2, 129.8, 129.6, 129.5, 129.3, 129.1, 128.0, 127.7, 127.6, 127.2, 126.6, 126.2, 125.9, 121.6, 120.9, 120.4, 116.5, 115.3, 98.8, 62.4, 62.3, 60.6, 60.5, 42.5, 22.3, 22.3, 21.9, 21.8, 21.7, 21.2.

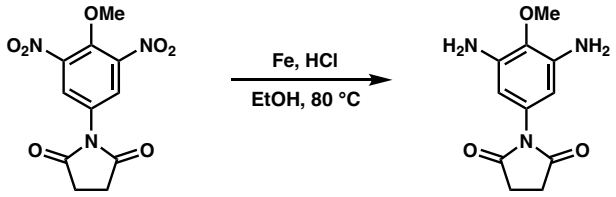
IR (Neat film, NaCl): 3391, 3061, 2925, 2850, 1622, 1596, 1505, 1454, 1360, 1167, 1092, 992, 944, 813, 737, 665 cm^{-1}.

HRMS (ESI+): *m/z* calc'd for $C_{25}H_{24}BrN_3O_5S_2Na$ $[M+Na]^+$: 612.0233, found 612.0233.



278

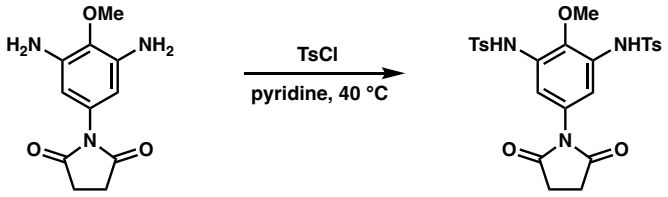
Dinitro arene 278: Prepared according to the procedure reported by Kraus.[12] All characterization data was in good accordance to those previously reported.



278 ***279***

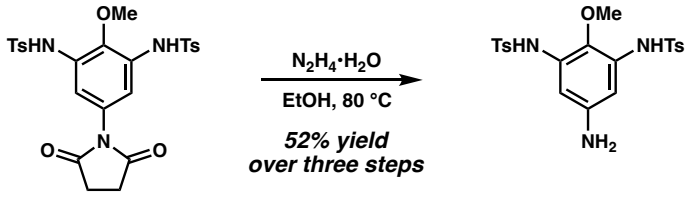
Dianiline 279: To a flame dried 50 mL round bottom flask equipped with a reflux condenser was added dinitro arene **278** (1.7 g, 5.7 mmol, 1.0 equiv), Fe powder (1.9 g, 34.2 mmol, 6.0 equiv), 1.5% aq. HCl solution (5.7 mL, 1M), and EtOH (16.3 mL, 0.35 M). The solution was heated to reflux (80 °C) for 1 h, at which point TLC analysis indicated complete consumption of the starting material. The reaction mixture was filtered through a thick pad of Celite. The filtrate was diluted with EtOAc (150 mL) and water (150 mL).

The product was extracted with EtOAc (3 x 100 mL) and the combined organic layers were washed with brine, dried over Na_2SO_4, filtered, and concentrated under reduced pressure to afford the titled compound (1.2 g, 90% yield) as a brown solid which was taken directly forward without further purification.



279 ***280***

Ditosylated arene 280: To a flame dried 250 mL round bottom flask was added aniline **279** (1.2 g, 5.12 mmol) and TsCl (1.99 g, 10.24 mmol, 2.0 equiv). This mixture was cooled to 0 °C and pyridine (51 mL, 0.1M) was added. Caution should be used as the mixture exotherms as the pyridine is added. The resulting mixture was then warmed to 23 °C, and then heated to 40 °C for 16 h, at which point TLC analysis indicated complete consumption of the starting material. The reaction mixture was diluted with EtOAc (200 mL), and the organic layer was washed with 10% aq. $CuSO_4$ (50 mL x 5). The organic layer was further washed with brine, dried over Na_2SO_4, filtered, and concentrated under reduced pressure to afford the titled compound (1.8g, 58% yield) as a brown solid which was taken directly forward without further purification.



280 ***281***

Trianilne 281: To a 2 dram vial was added arene **280** (283.7 mg, 0.52 mmol, 1.0 equiv), N_2H_4•H_2O (0.5 mL, 15.65 mmol, 30.0 equiv), and EtOH (5.2 mL, 0.1 M). The vial was

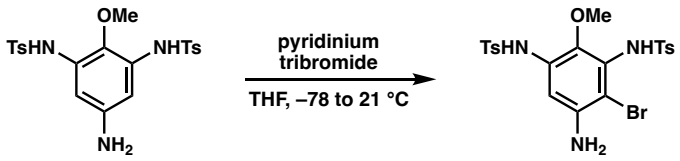
sealed and heated to 80 °C for 16 h, at which point LC/MS analysis indicated complete consumption of the starting material. The reaction mixture was concentrated under reduced pressure to near dryness. EtOAc (25 mL) was used to transfer the crude solid to a separatory funnel, and the mixture was further diluted with EtOAc (25 mL) and water (25 mL). the product was extracted with EtOAc (3 x 30 mL). The combined organic layers were washed with brine, dried over Na_2SO_4, filtered, and concentrated under reduced pressure to afford the titled compound (240 mg, quantitative, 52% yield over three steps) as a brown solid which was carried forward without further purification. A small sample was purified by column chromatography (SiO_2, 60% EtOAc/Hexanes) for characterization data.

^{1}H NMR (600 MHz, DMSO-d6): δ 9.28 (s, 2H), 7.66 (d, J = 8.3 Hz, 3H), 7.40 – 6.95 (m, 4H), 6.32 (s, 2H), 5.01 (s, 2H), 2.99 (s, 3H), 2.34 (s, 6H).

^{13}C NMR (100 MHz, DMSO-d6): δ 144.8, 137.6, 133.2, 130.9, 126.7, 102.9, 60.4, 21.0.

IR (Neat film, NaCl): 3476, 2284, 3254, 2923, 2357, 1595, 1514, 1391, 1315, 1160, 1089, 1041, 866, 809, 670 cm^{-1}.

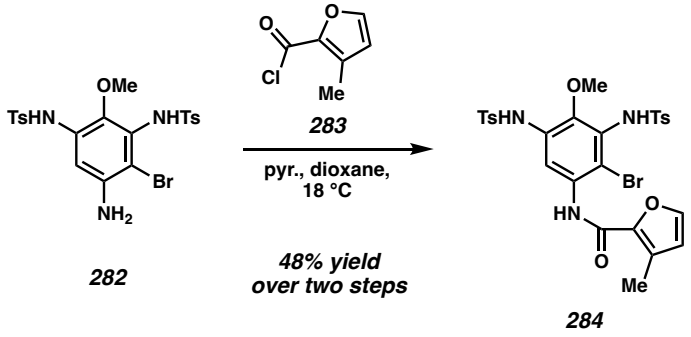
HRMS (ESI+): *m/z* calc'd for $C_{21}H_{24}N_3O_5S_2$ $[M+H]^+$: 462.1152, found 462.1158.



281 ***282***

Bromoaniline 282: To a flame dried 2 dram vial was added aniline **281** (108.3 mg, 0.235 mmol, 1.0 equiv) and THF (3.0 mL, 0.078 M). The solution was cooled to –78 °C, at which point pyridinium tribromide (187.8 mg, 0.587 mmol, 2.5 equiv) was added as a solution in THF (1 mL). The reaction mixture was stirred at –78 °C for 1 h, and was then warmed to 21 °C and stirred for an additional 16 h, at which point LC/MS analysis indicated complete

consumption of the starting material. The reaction was quenched with saturated aq. $N_2S_2O_3$ (2 mL) and diluted with EtOAc (2 mL). The product was extracted with EtOAc (3 x 4 mL) and the combined organic layers were washed with brine, dried over Na_2SO_4, filtered, and concentrated under reduced pressure to afford the titled compound (123.2 mg, 97% yield) as a brown solid which was taken forward without further purification.



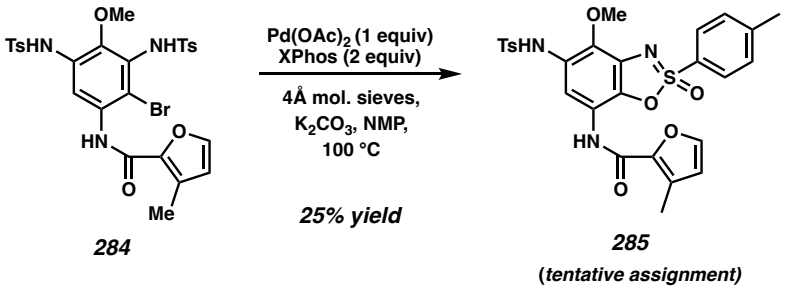
Amide 284: To a flame dried 2 dram vial was added bromoanilne **282** (92.1 mg, 0.17 mmol, 1.0 equiv), pyridine (0.041 mL, 0.51 mmol, 3.0 equiv) and dioxane (1.7 mL, 0.1 M). To this solution was added freshly prepared acid chloride **283** (0.51 mmol, 3.0 equiv) as a solution in dioxane (0.6 mL). The reaction mixture was stirred at 18 °C for 3 h, at which point LC/MS analysis indicated complete consumption of the starting material. A small amount of SiO_2 was added directly to the reaction mixture and was concentrated to dryness under reduced pressure. The resulting free-flowing SiO_2 mixture was purified by column chromatography (SiO_2, 45 to 50% EtOAc/Hexanes) to afford the title compound (53.2 mg, 48% yield over two steps) as a brown solid.

^{1}H NMR (400 MHz, $CDCl_3$): δ 8.65 (s, 1H), 8.34 (s, 1H), 7.89 (d, J = 8.4 Hz, 2H), 7.63 (d, J = 8.3 Hz, 2H), 7.38 (d, J = 1.7 Hz, 1H), 7.32 – 7.27 (m, 2H), 7.25 – 7.19 (m, 2H), 7.14 (s, 1H), 6.41 (d, J = 1.8 Hz, 1H), 6.36 (s, 1H), 3.30 (s, 3H), 2.47 (s, 3H), 2.42 (s, 3H), 2.38 (s, 3H).

^{13}C NMR (100 MHz, $CDCl_3$): δ 156.9, 144.5, 144.2, 143.2, 142.3, 141.8, 137.1, 135.9, 132.7, 131.2, 130.0, 129.9, 129.5, 128.5, 127.9, 127.8, 116.1, 110.8, 108.5, 60.4, 21.8, 21.7, 11.5.

IR (Neat film, NaCl): 3258, 2928, 2371, 1625, 1595, 1390, 1351, 1314, 1166, 1089, 1044, 860, 809, 767 cm^{-1}.

HRMS (ESI+): *m/z* calc'd for $C_{27}H_{27}BrN_3O_7S_2$ $[M+H]^+$: 648.0468, found 648.0462.



Arene 285: To a flame dried 1 dram vial in a nitrogen filled glovebox was added amide **284** (53.2 mg, 0.082 mmol, 1.0 equiv), $Pd(OAc)_2$ (18.4 mg, 0.082 mmol, 1.0 equiv), XPhos (78 mg, 0.164 mmol, 2.0 equiv), K_2CO_3 (28.3 mg, 0.205 mmol, 2.5 equiv), 4 Å mol. sieves (14 mg, 50 wt% with respect to K_2CO_3), and NMP (0.82 mL, 0.1M). The vial was sealed, removed from the glovebox, and ehated to 100 °C for 3 h, at which point LC/MS anlaysis indicated complete consumption of the starting material. The reaction mixture was diluted with EtOAc (2 mL) and 1M aq. LiCl (2 mL). The product was extracted with EtOAc (3 x 3 mL) and the combined organic layers were washed with brine, dried over Na_2SO_4, filtered, and concentrated under reduced pressure. The crude product was purified by column chromatography (SiO_2, 50% Acetone/Hexanes) to afford the title compound (11.2 mg, 25% yield) as a white solid. The NMR data suggests formation of product **285**, however, a crystal structure was not obtained so this is reported as a tentative assignment.

^{1}H NMR (400 MHz, $CDCl_3$): δ 8.45 (s, 1H), 8.43 (s, 1H), 7.98 (d, J = 8.4 Hz, 2H), 7.93 – 7.86 (m, 2H), 7.41 – 7.28 (m, 5H), 7.23 (s, 1H), 6.45 (d, J = 1.7 Hz, 1H), 3.68 (s, 3H), 2.54 (s, 3H), 2.39 (s, 3H), 2.36 (s, 3H).

^{13}C NMR (100 MHz, $CDCl_3$): δ 178.3, 157.2, 144.7, 143.2, 143.1, 142.1, 135.9, 135.1, 133.2, 131.8, 131.5, 130.8, 130.6, 130.1, 130.0, 128.9, 128.0, 127.7, 123.1, 116.3, 111.3, 109.2, 61.7, 21.9, 21.8, 11.5.

IR (Neat film, NaCl): 3244, 2926, 1679, 1601, 1520, 1448, 1397, 1324, 1173, 1162, 1076, 880 cm^{-1}.

HRMS (ESI+): *m/z* calc'd for $C_{27}H_{26}N_3O_7S_2$ $[M+H]^+$: 568.1207, found 568.1211.

3.7 REFERENCES AND NOTES

(1) Zou, Y.; Hamann, M. T. Atkamine: A New Pyrroloiminoquinone Scaffold from the Cold Water Aleutian Islands *Latrunculia* Sponge. *Org. Lett.* **2013**, *15*, 1516–1519.

(2) Zhang, F.; Niu, Y.; Hong, D.; Ye, Y.; Hua, Y.; Ding, S.; Zhang, Y. Synthetic studies towards atkamine. *Chinese Chemical Letters* **2021**, *32*, 668–671.

(3) Sakaine, G.; Leitis, Z.; Ločmele, Smits, G. Julia-Kocienski Olefination: A Tutorial Review. *Eur. J. Org. Chem.* **2023**, *26*, e202201217.

(4) Scanlan, E. M.; Corcé, Malone, A. Synthetic Applications of the Intramolecular Thiol-Ene "Click" Reactions. *Molecules,* **2014**, *19*, 19137–19151.

(5) a) Liu, J.; Peng, H.; Yang, Y.; Jiang, H.; Yin, B. Regioselective and Stereoselective Pd-Catalyzed Intramolecular Arylation of Furans: Access to Spirooxindoles and 5H‐Furo[2,3‐c]quinolin-4-ones. *J. Org. Chem.* **2016**, *81*, 9695–0706. b) Li, X.; Zhou, R-Z.; Yang, F-M.; Liang, R-X.; Liu, R-R.; Jia, Y-X. Palladium-Catalyzed Enantioselective Intramolecular Dearomative Heck Reaction. *J. Am. Chem. Soc.* **2018**, *140*, 13945–13951. c) Liang, R-X.; Jia, Y-X. Aromatic π-Components for Enantioselective Heck Reactions and Heck/Anion-Capture Domino Sequences. *Acc. Chem. Res.* **2022**, *55*, 734–745. And references therein.

(6) Liu, J.; Xu, X.; Li, J.; Liu, B.; Jiang, H.; Yin, B. Palladium-catalyzed dearomatizing 2,5-alkoxyarylation of furan rings: diastereospecific access to spirooxindoles. *Chem. Commun.* **2016**, *52*, 9550.

(7) Hyland, C. Cyclisations of allylic substrates via palladium catalysis. *Tetrahedron* **2005**, *61*, 3457–3471.

(8) When attempting the dearomative thiophene coupling, undesired benzoxazole formation resulted from oxygen insertion of the Ac group (*vide supra, Chapter 1.5*). We hypothesized this would likely occur when attempting the dearomative furan coupling.

(9) In the real system the furan contains an alkyl substituent at the three position. With the alkyl substituent present, undesired β-hydride elimination is possible after dearomative migratory insertion, so it was essential the reaction was optimized to suppress this undesired reaction pathway.

(10) Unreactivity was also observed when attempting a reductive amination with a similar *o*-bromo secondary aniline. See Chapter 1.5.

(11) Vinogradova, E. V.; Park, N. H.; Fors, B. P.; Buchwald, S. L. Palladium-Catalyzed Synthesis of *N*-Aryl Carbamates. *Org. Lett.* **2013**, *15*, 1394–1397.

(12) Kraus, G. A.; Selvakumar, N. Synthetic Routes to Pyrroloiminoquinone Alkaloids. A Direct Synthesis of Makaluvamine C. *J. Org. Chem.* **1998**, *63*, 9846–9849.

(13) Performing this reaction using catalytic amounts of $Pd(OAc)_2$ resulted in primarily protodebromination.

Appendix 8

Spectra Relevant to Chapter 3:

Progress Toward the Total Synthesis of Atkamine

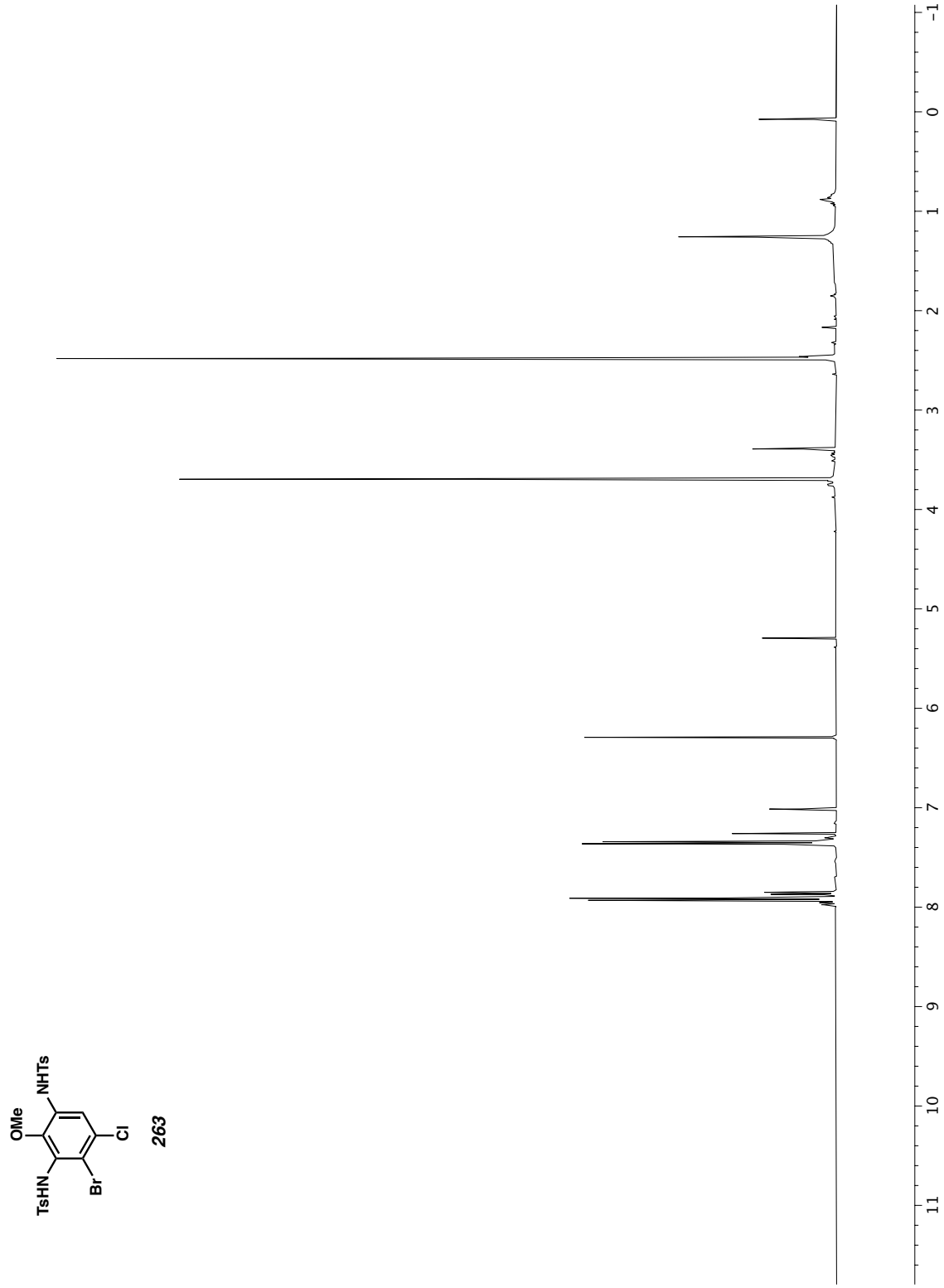


Figure A8.1. ^{1}H NMR (400 MHz, $CDCl_3$) of compound **263**.

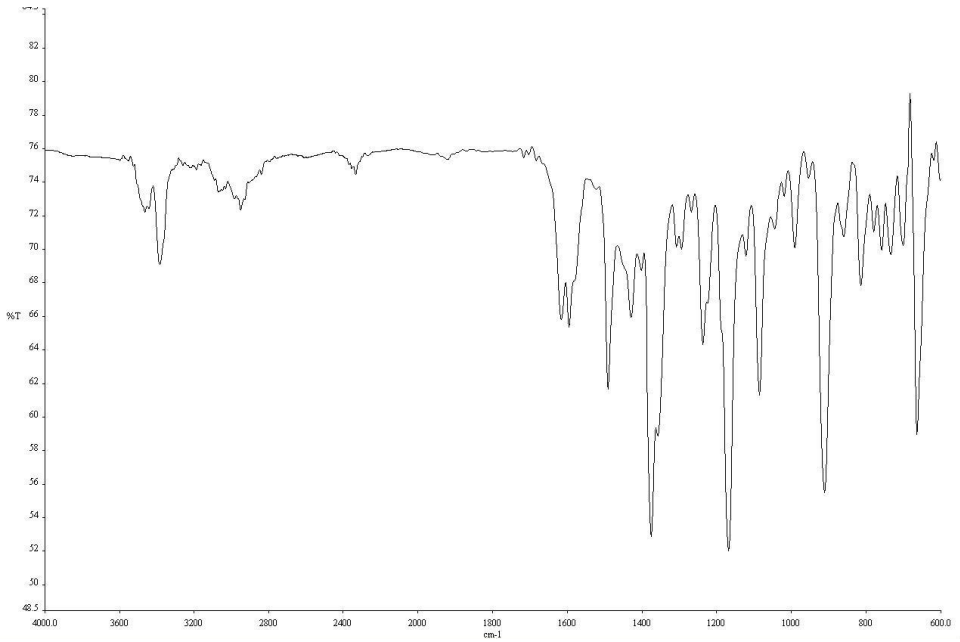


Figure A8.2. Infrared spectrum (Thin Film, NaCl) of compound **263**.

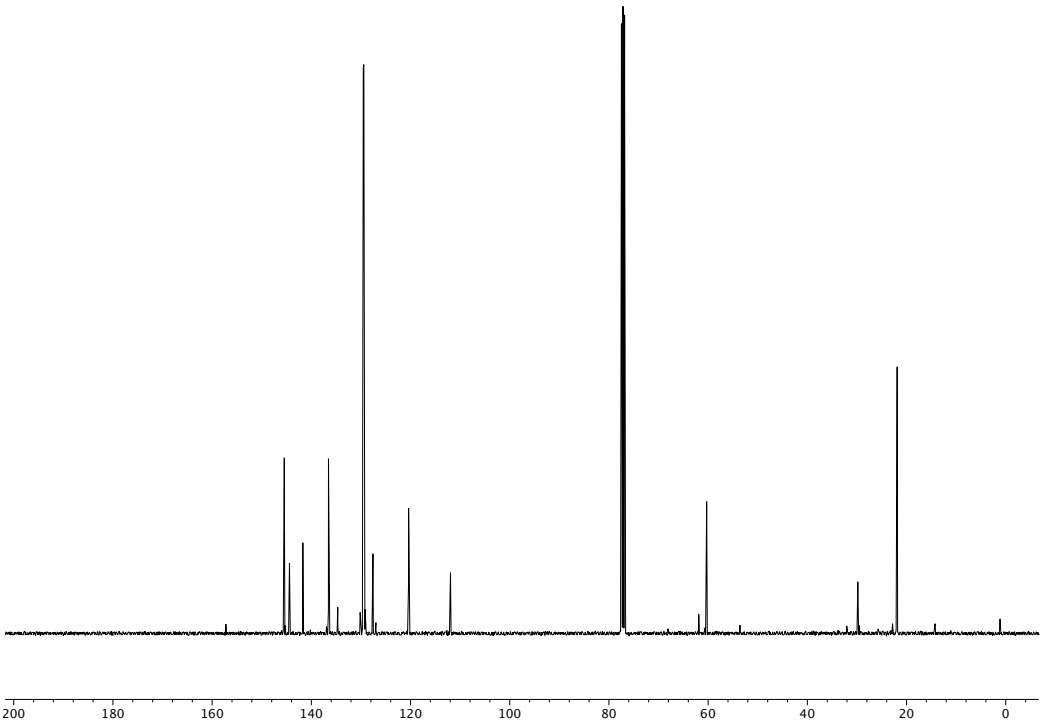


Figure A8.3. ^{13}C NMR (100 MHz, $CDCl_3$) of compound **263**.

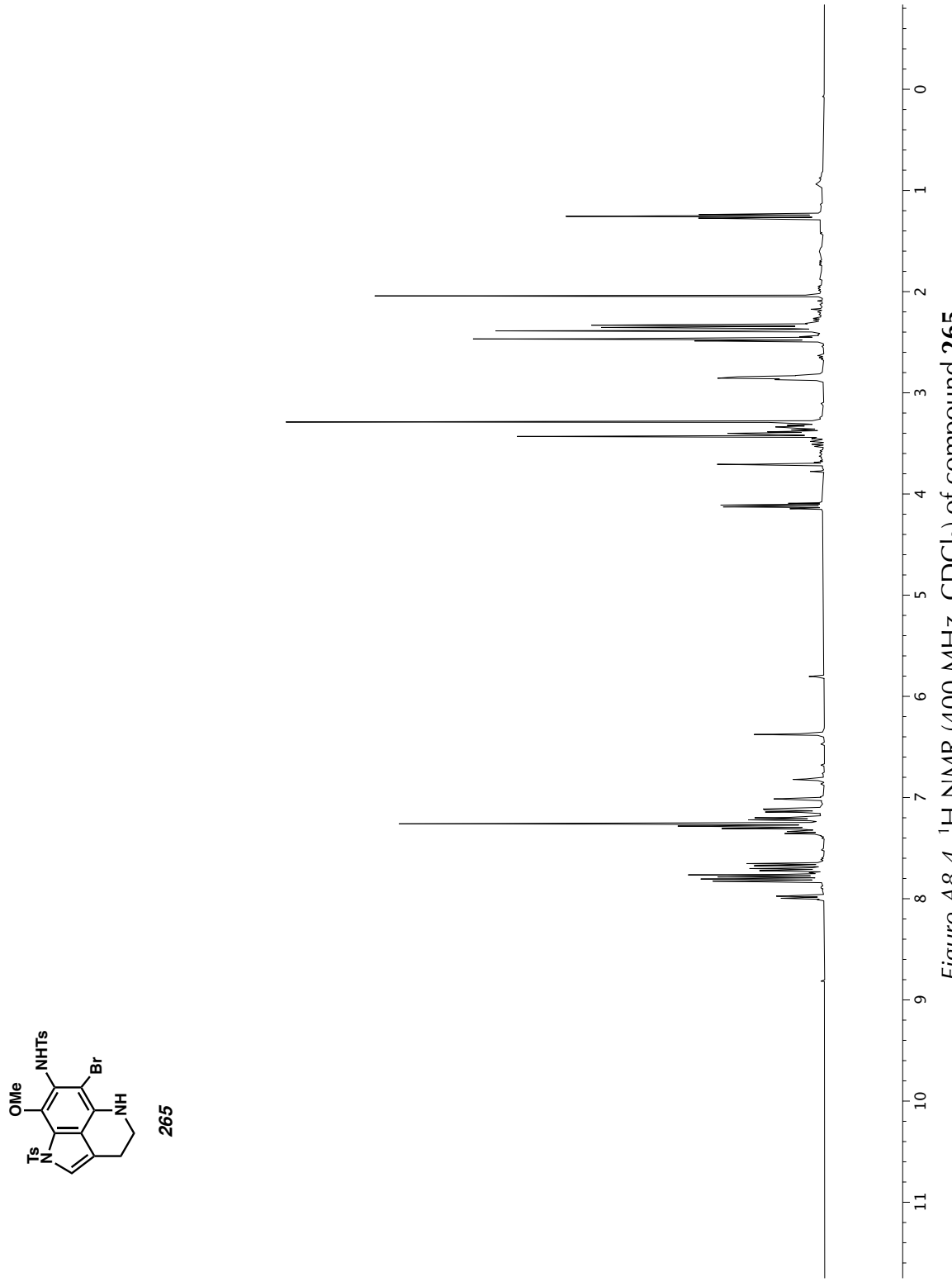


Figure A8.4. ^{1}H NMR (400 MHz, $CDCl_3$) of compound **265**.

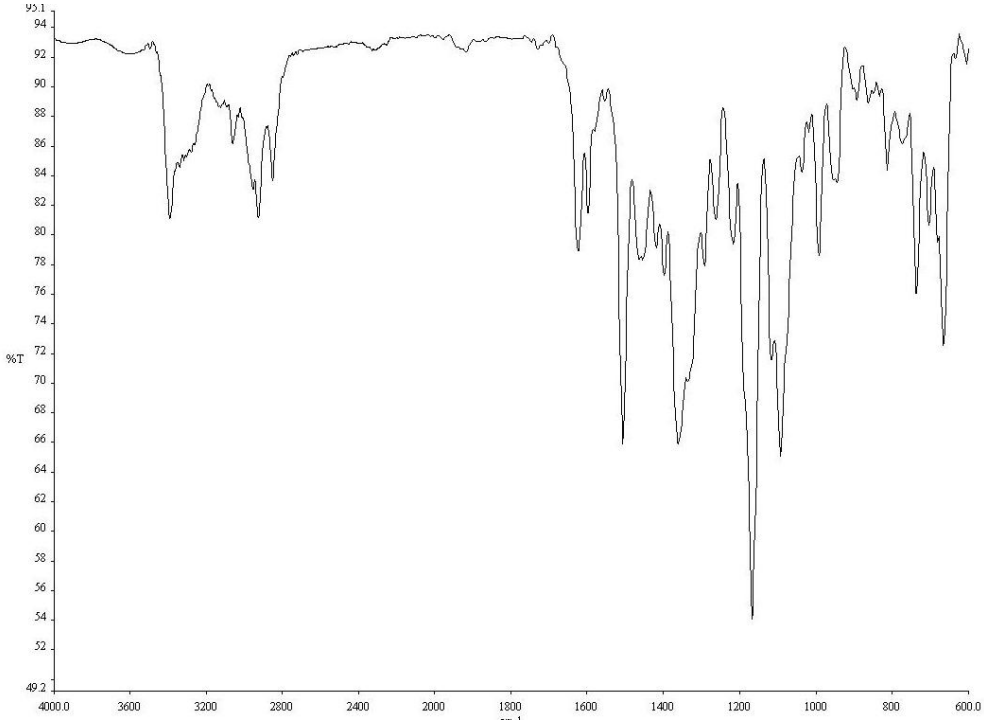


Figure A8.5. Infrared spectrum (Thin Film, NaCl) of compound **265**.

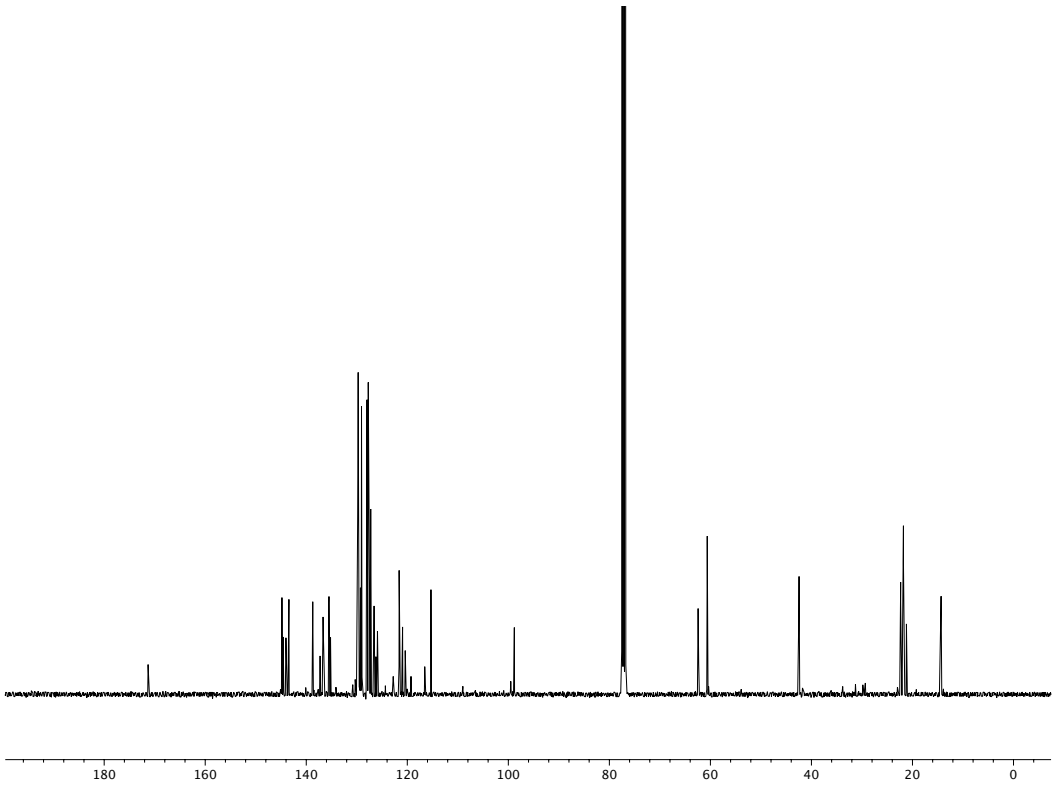


Figure A8.6. ^{13}C NMR (100 MHz, $CDCl_3$) of compound **265**.

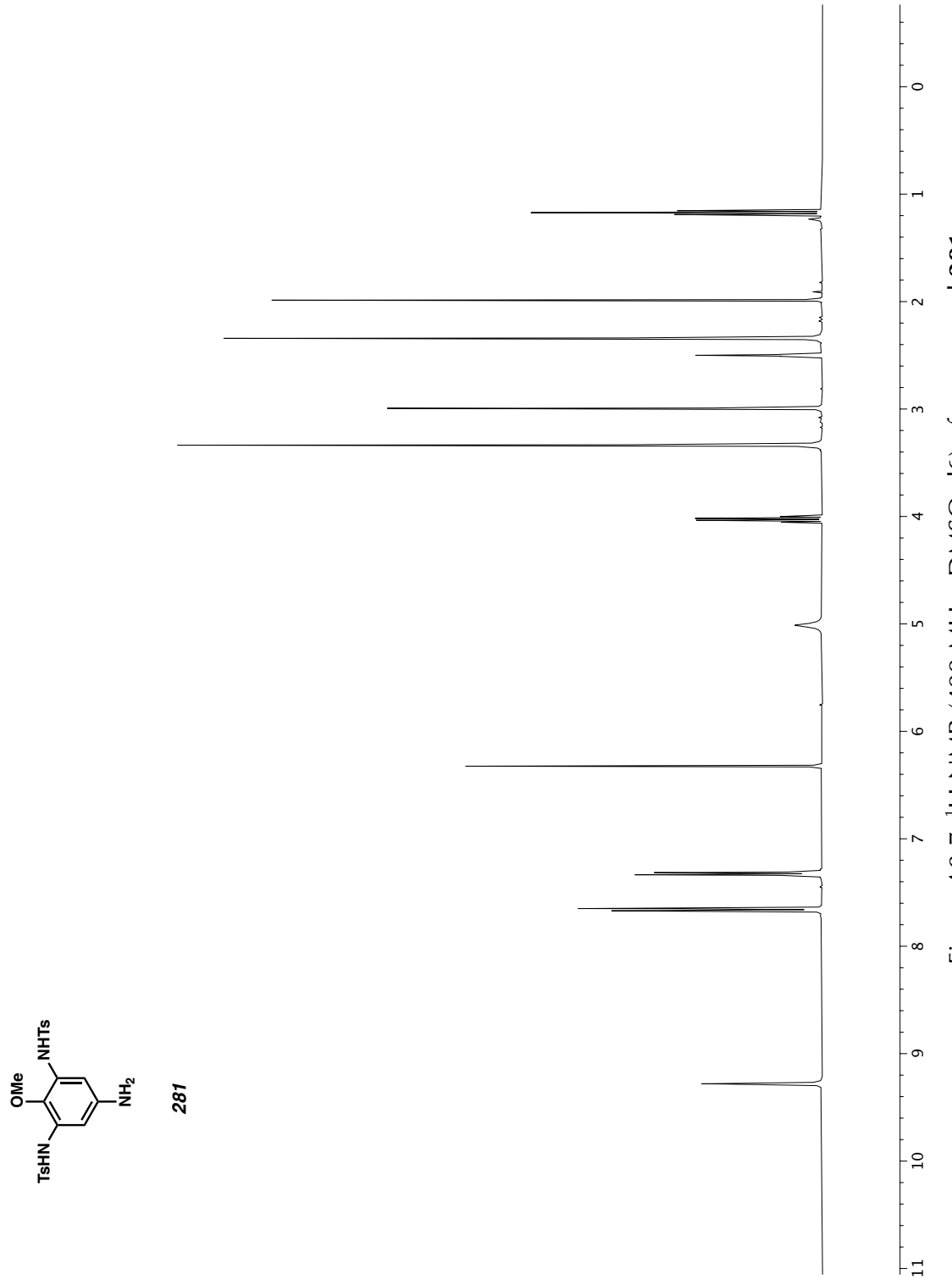


Figure A8.7. ^{1}H NMR (400 MHz, DMSO-d6) of compound **281**.

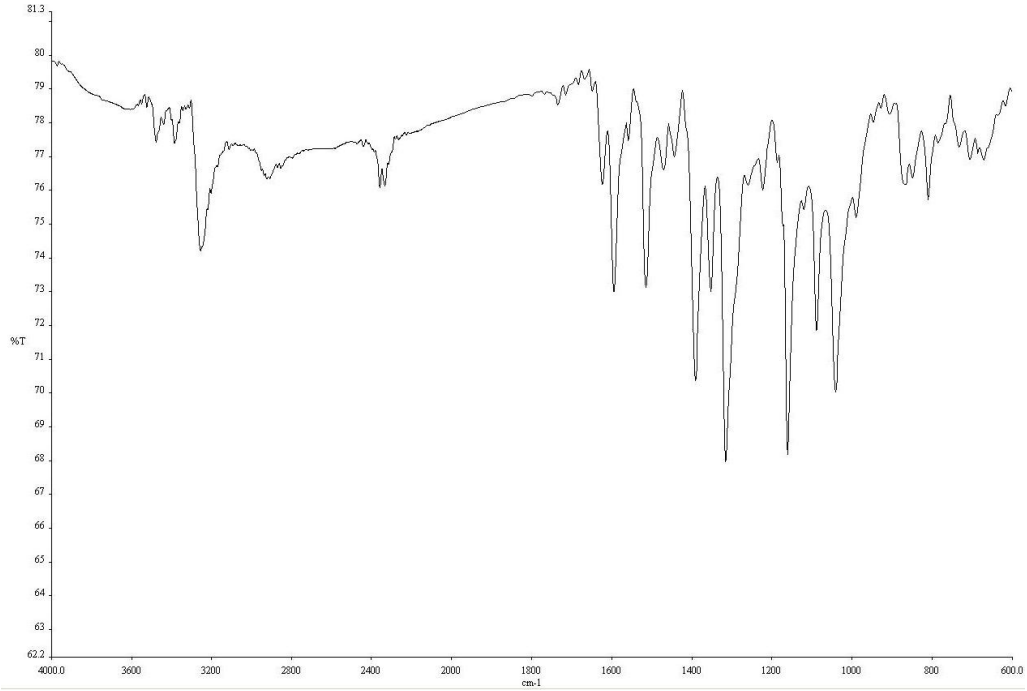


Figure A8.8. Infrared spectrum (Thin Film, NaCl) of compound **281**.

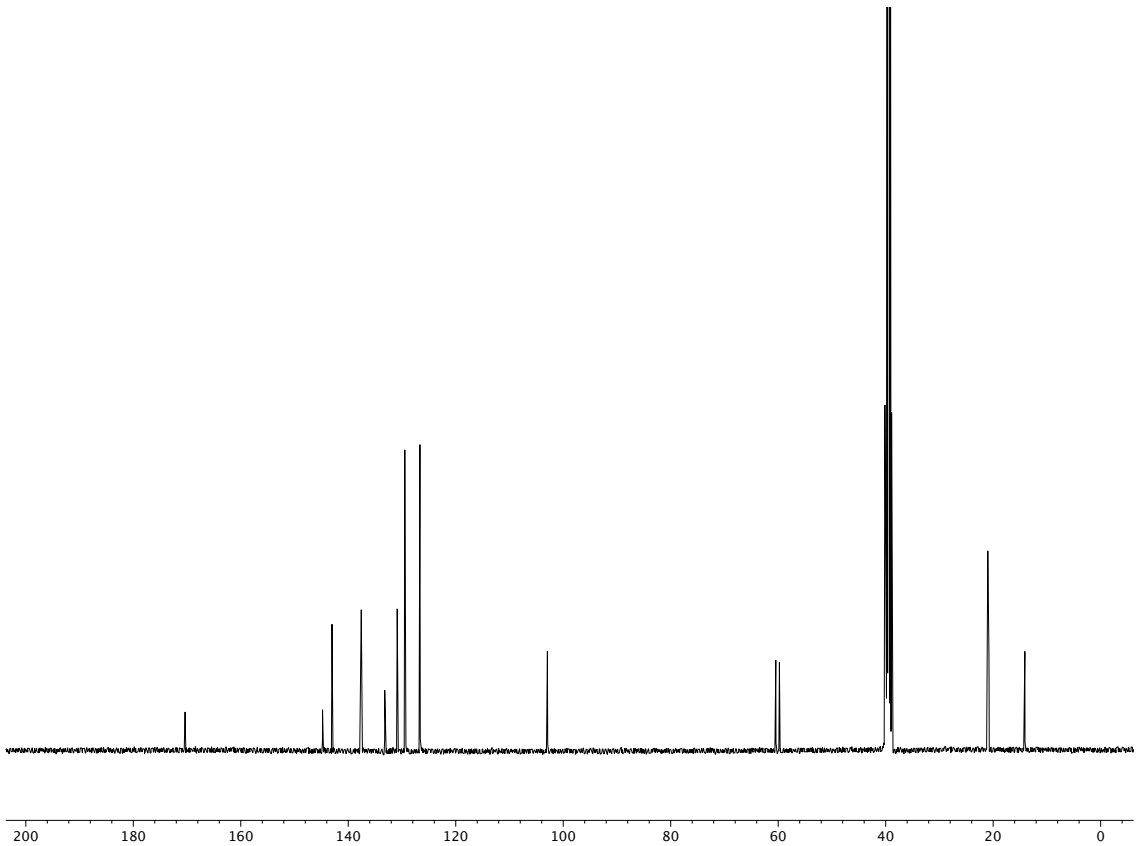


Figure A8.9. ^{13}C NMR (100 MHz, DMSO-d6) of compound **281**.

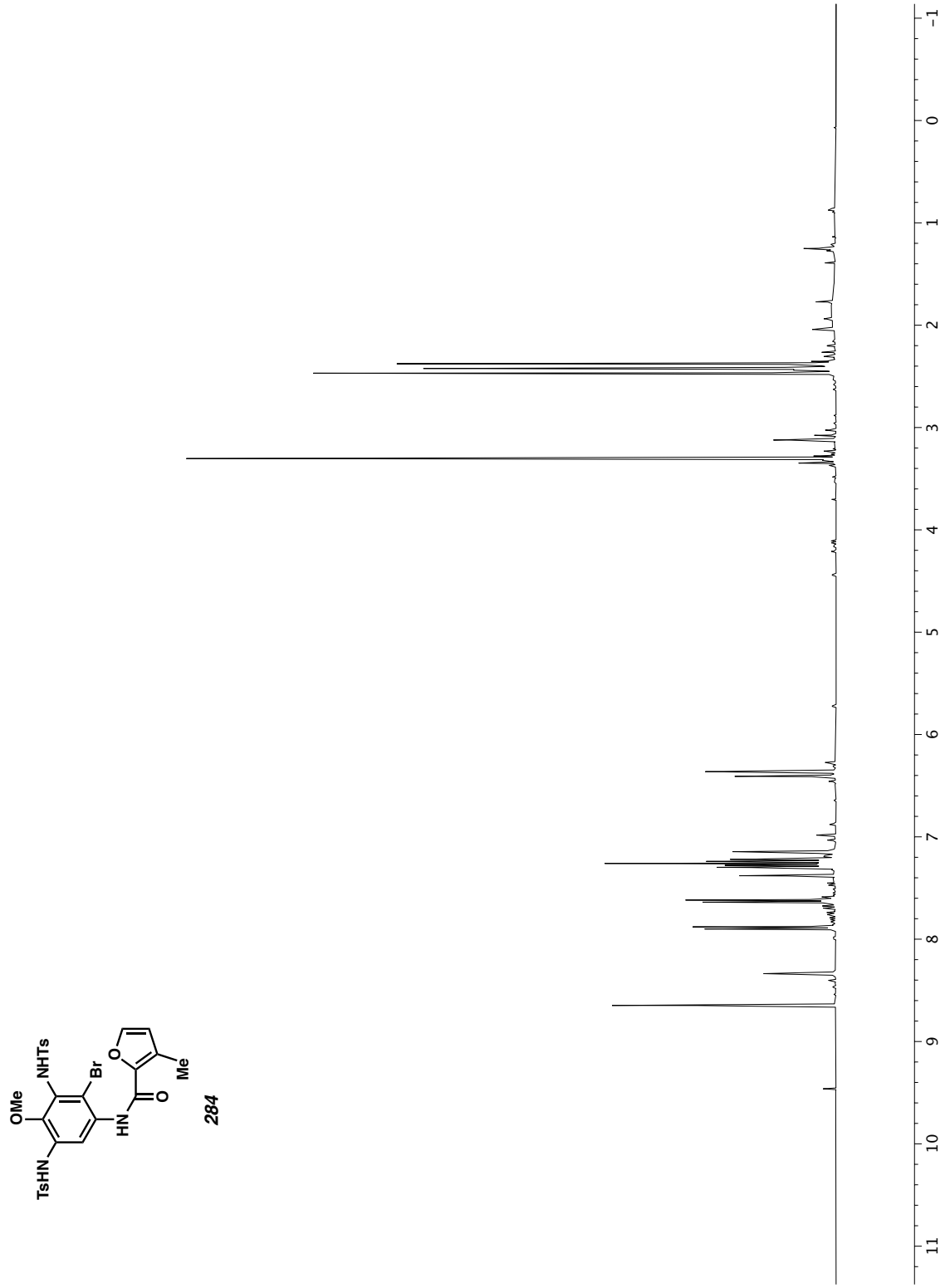


Figure A8.10. ^{1}H NMR (400 MHz, $CDCl_3$) of compound **284**.

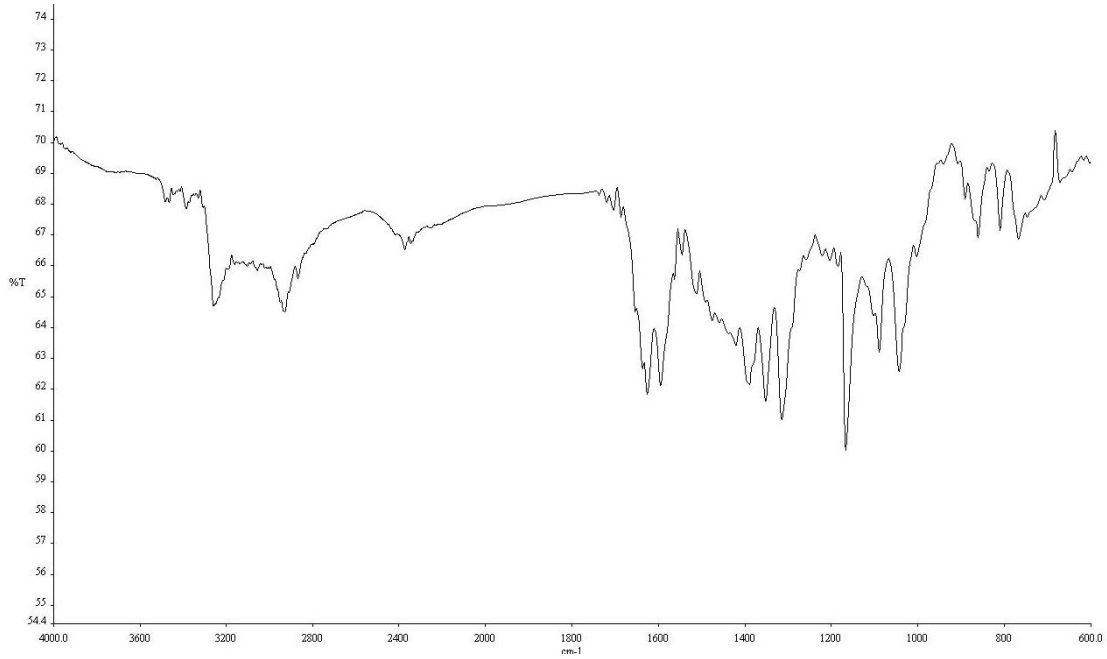


Figure A8.11. Infrared spectrum (Thin Film, NaCl) of compound **284**.

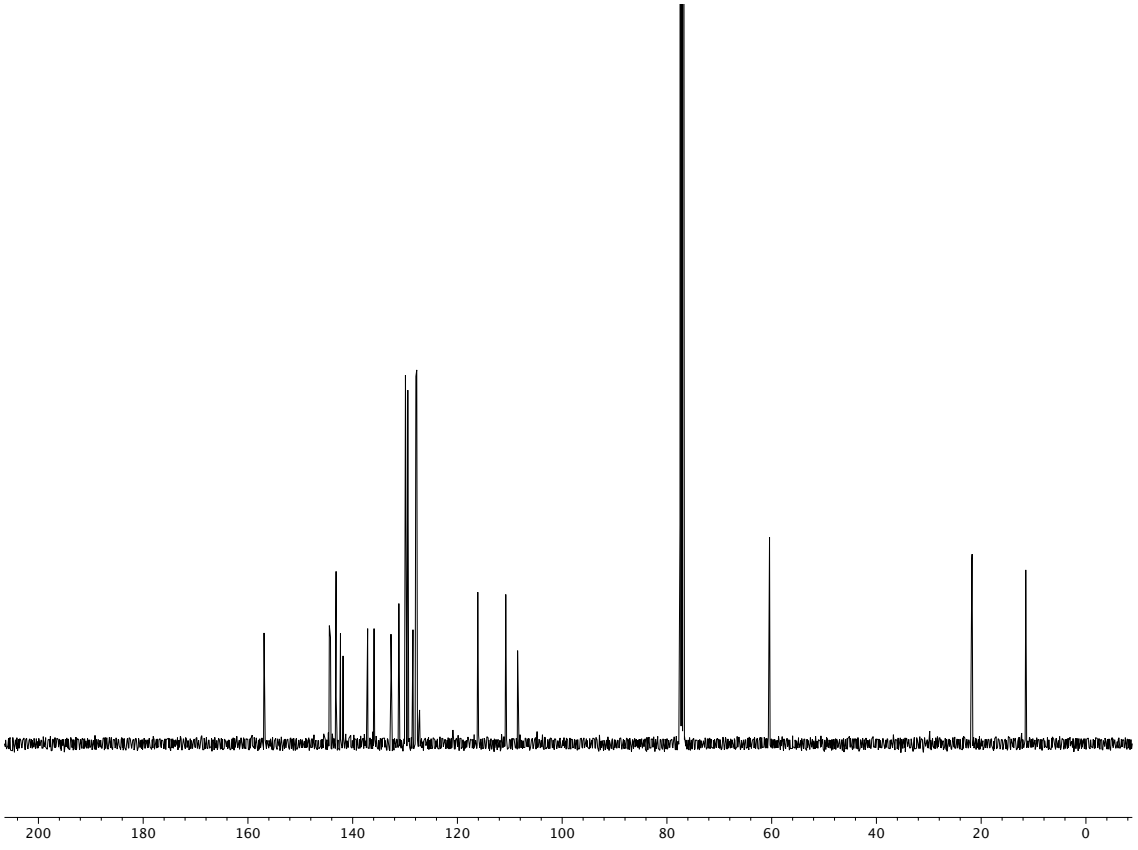


Figure A8.12. ^{13}C NMR (100 MHz, $CDCl_3$) of compound **284**.

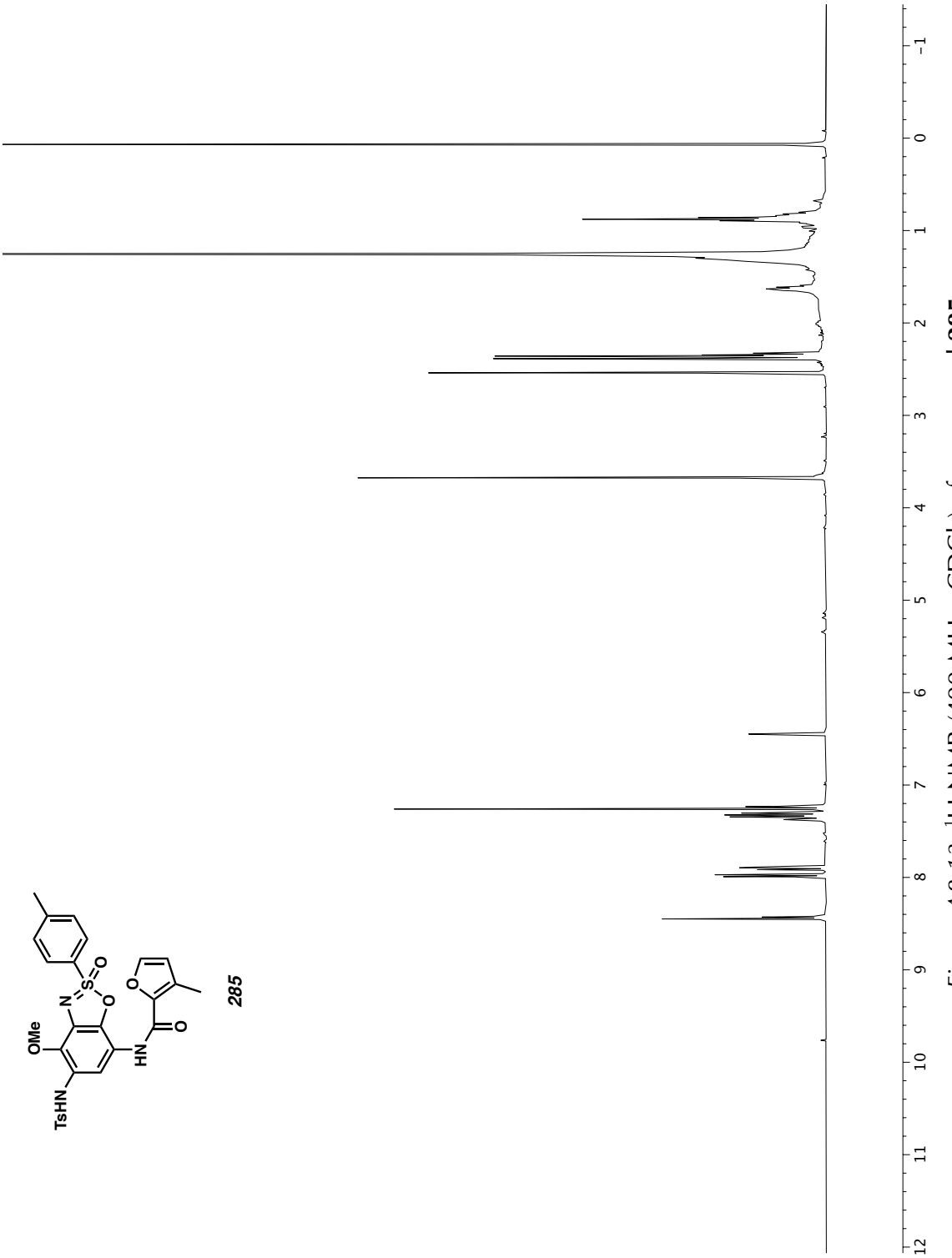


Figure A8.13. ^{1}H NMR (400 MHz, $CDCl_3$) of compound **285**.

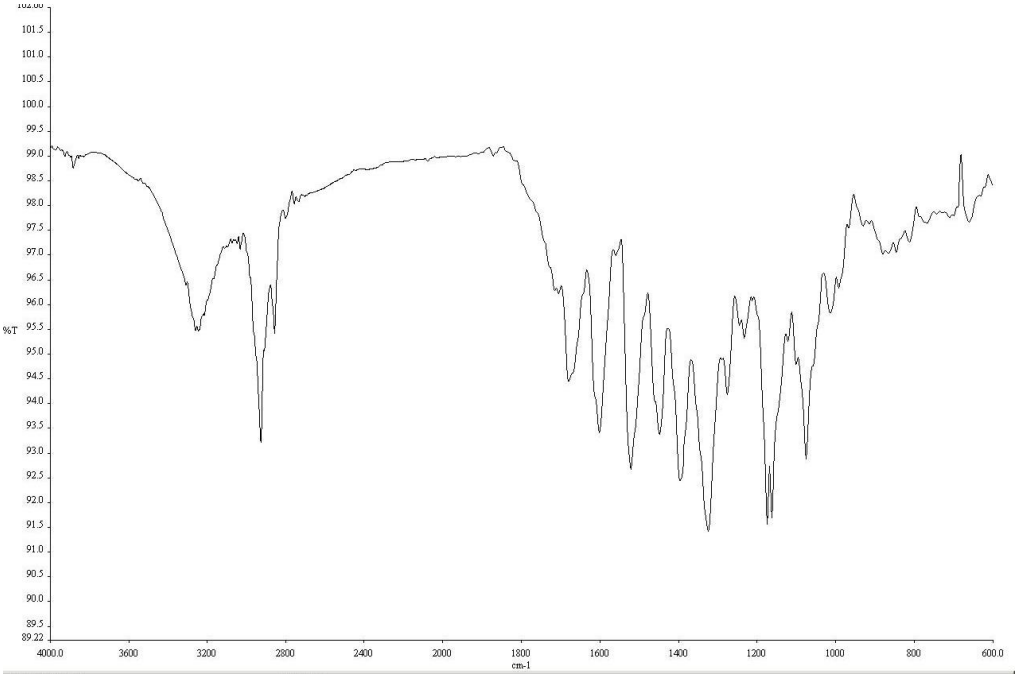


Figure A8.14. Infrared spectrum (Thin Film, NaCl) of compound **285**.

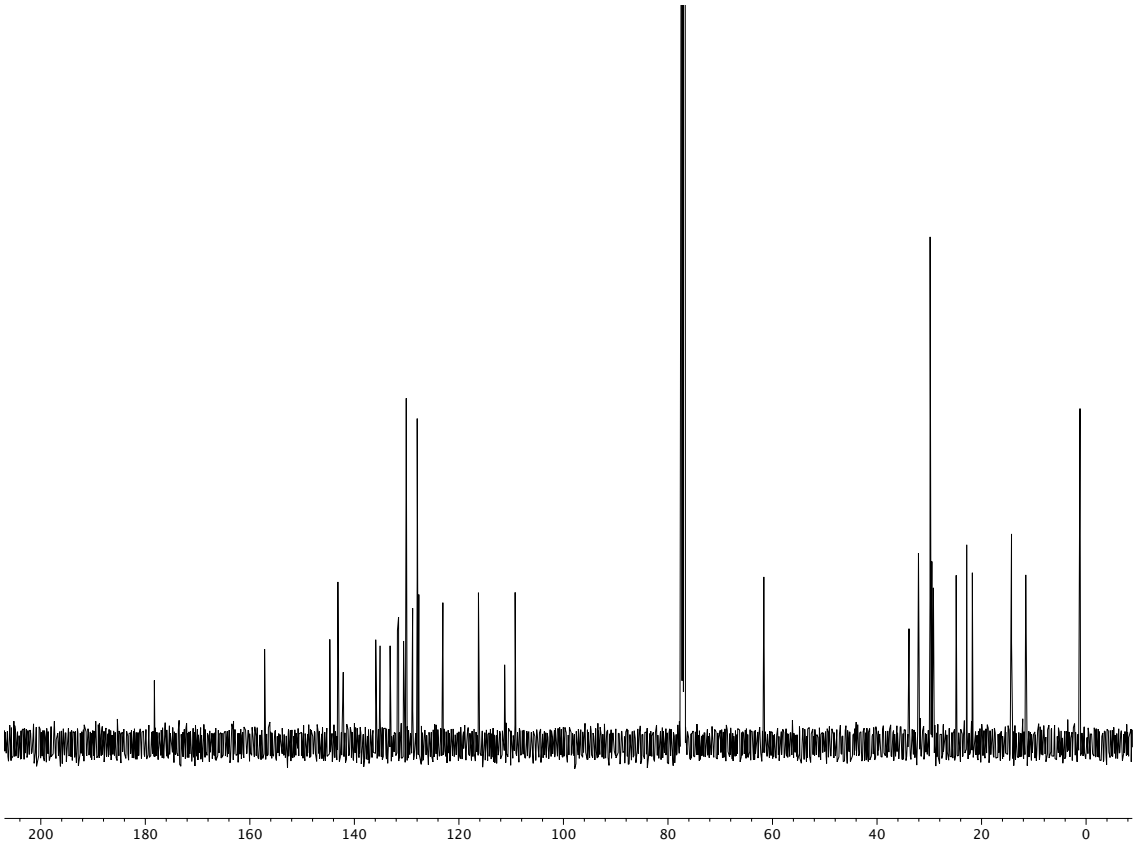


Figure A8.15. ^{13}C NMR (100 MHz, $CDCl_3$) of compound **285**.

Appendix 9

Additional Investigations Into the Dearomative Furan Coupling

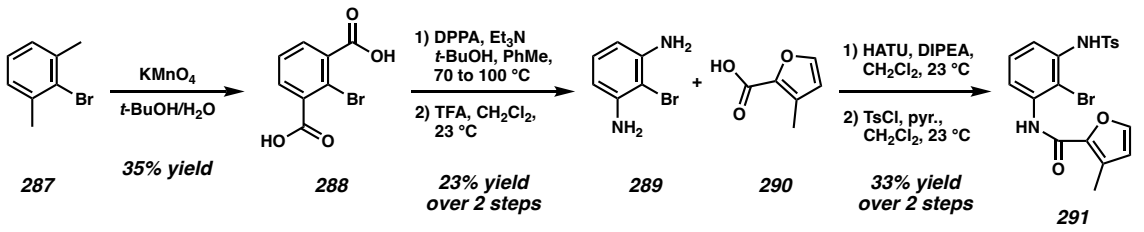
A9.1 INTRODUCTION

In parallel to our efforts toward the synthesis of dearomative furan substrate **284**, we began investigations into the desired dearomative furan coupling on simplified model systems in order to identify reaction conditions to initiate our investigation on the real system (i.e. **284)**.

A9.2 SYNTHESIS AND INVESTIGATION OF MODEL SYSTEM 291

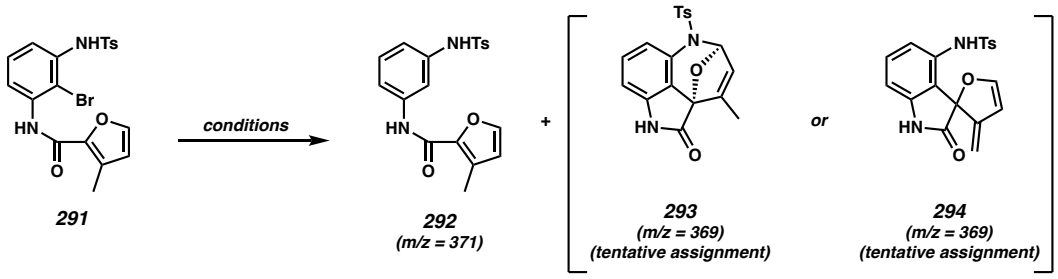
We began our investigations by synthesizing a model system that would be representative of the actual substrate for the desired intramolecular dearomative furan coupling to construct the full bicyclic ring system of atkamine (**241**)– a system which contains a sulfonamide nucleophile to intercept the Pd^{II} π-allyl species (see Chapter 3.2). These studies commenced from commercially available bromoarene **287** that was elaborated to the desired substrate **291** over five steps (Scheme A9.2.1). It should be noted that these *m*-dianilines with an *o*-halogen are not commercially available and are quite rare; this strategy of oxidation and bis-Curtius rearrangement might prove as a general strategy to access substrates of this type.

Scheme A9.2.1 *Synthesis of model substrate* ***291***.



Our reaction investigation began be evaluating the conditions reported by Yin and coworkers[1] wherein the reported intramolecular 2,5-difunctionalizations of furans– the most similar reported transformation for our desired system. Unfortunately, these reaction conditions led to just recovered starting material (**291,** TableA9.2.1, entry 1). In fact, most catalytic conditions led to no reaction. Thus, we investigated stoichiometric conditions. When employing Pd(0) precatalysts with BINAP or XPhos ligand systems, only protodebromination (**292**) was observed (entries 2-5). However, changing to Pd(II) precatalysts led to different reaction profiles and excitingly dearomative products **293** or **294** were observed by LC/MS analysis (entry 6,7). Unfortunately, we were unable to make a definitive structural assignment based on the 2D NMR data, and attempts to grow a crystal were unfruitful. Finally, using D*t*-BPF led to just protodebromination (entry 8). Although we were unable to make a definitive structural assignment, we felt that the Pd(II)-XPhos system was a good starting point to commence our investigations on the real system as it led to reactivity other than just protodebromination.

Table A9.2.1 *Investigation of the dearomative furan coupling on* ***291****.*



291

292
(m/z = 371)

293
(m/z = 369)
(tentative assignment)

294
(m/z = 369)
(tentative assignment)

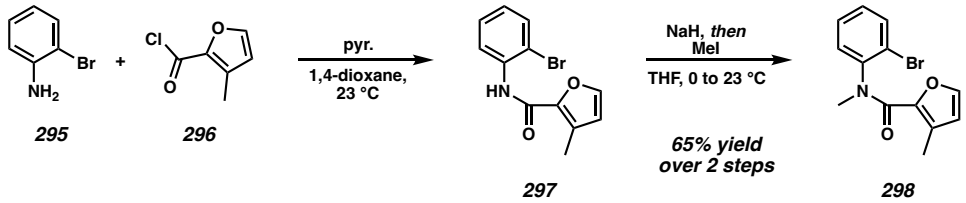
Entry	Catalyst	Ligand	Base	Solvent	Temp/Time	Result
1	$Pd_2(dba)_3$ (15 mol%)	Xanthphos (30 mol%)	LiO*t*-Bu	THF	100 °C, 16h	just sm
2	$Pd(OAc)_2$ (1 equiv)	BINAP (1.2 equiv)	Et_3N	MeOH	100 °C, 16h	292
3	$Pd(dba)_2$ (15 mol%)	XPhos (25 mol%)	K_2CO_3	1,4-dioxane	100 °C, 16h	292
4	$Pd(dba)_2$ (1 equiv)	XPhos (1.5 equiv)	K_2CO_3	1,4-dioxane	100 °C, 16h	292
5	$Pd(dba)_2$ (1 equiv)	XPhos (1.5 equiv)	K_2CO_3	NMP	100 °C, 16h	292
6	$Pd(OAc)_2$ (1 equiv)	XPhos (2 equiv)	K_2CO_3	1,4-dioxane	100 °C, 16h	1.3 : 1 292 : 293 *or* 294
7	$Pd(OAc)_2$ (1 equiv)	XPhos (2 equiv)	K_2CO_3	NMP	100 °C, 16h	1 : 2 292 : 293 *or* 294
8	$Pd(OAc)_2$ (1 equiv)	D*t*-BPF (2 equiv)	K_2CO_3	NMP	100 °C, 16h	292

Ratios were determined by from the absorbance at 254 nm on the LC/MS trace.

A9.3 SYNTHESIS AND INVESTIGATION OF MODEL SYSTEM 298

We were also interested in studying just the dearomative-Heck component of our desired difunctionalization reaction, as this importantly would still construct the central C–C bond, and we envisaged the C–N bond of the bicycle could be formed at a later stage. These studies commenced from commercially available *o*-bromoaniline (**295**) that was elaborated to the desired dearomative-Heck substrate over two steps. We decided to alkylate the amide nitrogen as all previous examples in the literature contained alkylated amides, and this would also mimic the real system for the desired tandem Larock/dearomative furan coupling reaction.

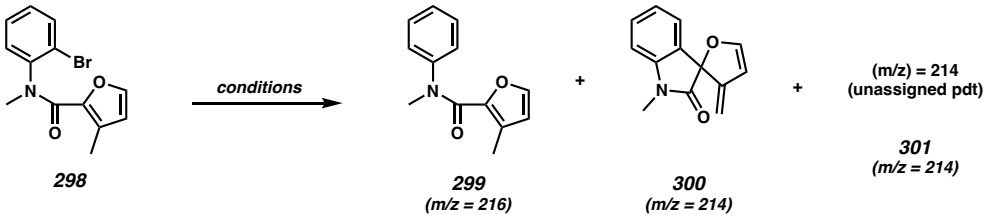
Scheme A9.3.1 *Synthesis of dearomative-Heck substrate* ***298****.*



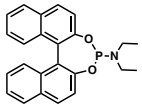
295 ***296*** ***297*** ***65% yield over 2 steps*** ***298***

We started our investigation by employing reaction conditions reported by Yin and coworkers[2] as they described a similar dearomative-Heck coupling of furans, albeit with 5-alkyl substituted furans (our system is 3-substituted). Unfortunately, these conditions led to recovered starting material and protodebromination (**299**, Table A9.3.1, entry 1). Employing Yin's 2,5-difunctionalization conditions[1] led only to recovered starting material (entry 2). Interestingly, switching to a Pd(II) precatalyst in combination with PPh_3 and $AgCO_3$ as the base yielded a new product (**301**) that possessed the same mass as the desired dearomative-Heck product **300** (entry 4). However, ^{1}H NMR data suggested **301** was not the desired product **300**, as there were no olefinic peaks in the spectrum. Unfortunately, we were unable to make a definitive structural assignment based on the NMR data, and attempts at growing a crystal of this product failed. Using Jia's conditions[3] wherein they achieved an enantioselective variant of our desired reaction (same substrate albiet with an *o*-iodoaniline) resulted in recovered starting material and protodebromination (**299**), highlighting the difference in reactivity of aryl bromides and aryl iodides (entry 6). Unassigned product **301** was observed as the sole product when employing a 1:1 mixture of XPhos:D*t*-BPF as the ligand source (entry 7). Unfortunately, employing alternative Pd precatalyts did not result in product formation (entry 9).

Table A9.3.1 *Investigation of the dearomative Heck reaction on* ***298****.*



Entry	Catalyst	Ligand	Base/Additive	Solvent	Temp/Time	Result
1	$Pd(OAc)_2$ (10 mol%)	PPh_3 (20 mol%)	K_2CO_3	DCE	80 °C, 16h	8 : 2 298 : 299
2	$Pd_2(dba)_3$ (10 mol%)	Xanthphos (20 mol%)	LiO*t*-Bu	THF	80 °C, 16h	298
3	$Pd(OAc)_2$ (10 mol%)	D*t*-BPF (20 mol%)	K_2CO_3	NMP	80 °C, 16h	7 : 3 298 : 299
4	$Pd(OAc)_2$ (10 mol%)	PPh_3 (20 mol%)	$AgCO_3$	1,4-dioxane	80 °C, 16h	1 : 1 299 : 301
5	$Pd(OAc)_2$ (10 mol%)	PPh_3 (20 mol%)	K_2CO_3 + $AgPF_6$	1,4-dioxane	100 °C, 16h	298
6	$Pd(OAc)_2$ (10 mol%)	L1 (20 mol%)	Cs_2CO_3	1,4-dioxane	100 °C, 16h	8 : 2 298 : 299
7	$Pd(OAc)_2$ (10 mol%)	XPhos (10 mol%) D*t*-BPF (10 mol%)	K_2CO_3	NMP	100 °C, 16h	301
8	$Pd(OAc)_2$ (10 mol%)	Xanthphos (20 mol%)	K_2CO_3	NMP	100 °C, 16h	8 : 2 298 : 299
9	$Pd(MeCN)_4$ (10 mol%)	PPh_3 (20 mol%)	K_2CO_3 + $AgBF_4$	1,4-dioxane	100 °C, 16h	1 : 1 298 : 299



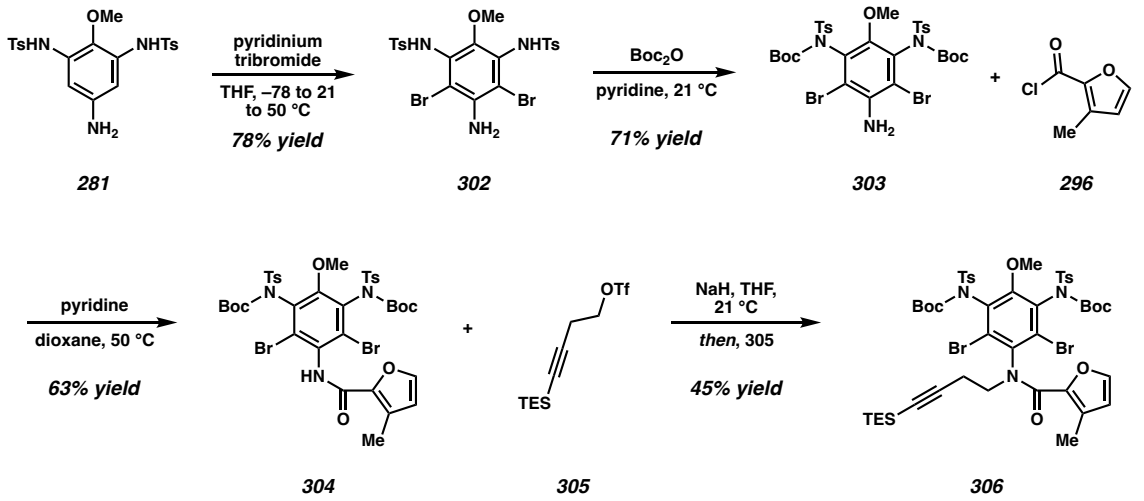
L1

Ratios were determined by from the absorbance at 254 nm on the LC/MS trace.

A9.4 PROGRESS TOWARD THE FULLY SUBSTITUTED LAROCK/DEAROMATIVE FURAN COUPLING SUBSTRATE

In parallel to our reaction investigations of the dearomative furan coupling, we focused on the synthesis of the desired tandem Larock/dearomative furan coupling substrate. Trianiline **281** could be dibrominated by using an increased reaction temperature of 50 °C, which yielded fully substituted arene **302**. At this point, regioselectivity issues

Scheme A9.4.1 *Synthesis of fully substituted arene* ***306***.



were observed when attempting to acylate/alkylate the primary aniline nitrogen–undesired acylation/alkylation of the sulfonamides was observed. Instead, the sulfonamides could be doubly protected in the presence of the primary aniline nitrogen. This surprising result can likely be explained by a steric argument as the primary aniline nitrogen is bis *o*-substituted. From double protected arene **303**, acylation of the primary aniline was achieved affording amide **304**. Alkylation of this amide proved difficult, however after extensive investigation, alkylation with triflate **305** was achieved to yield arene **306**. Interestingly, alkyl triflate **305** proved to be the only competent electrophile as employing the analogous alkyl bromide or iodide led to no reaction. From **306**, a Boc deprotection of the sulfonamides would then yield the desired Larock/dearomative furan coupling substrate.

A9.5 REFERENCES AND NOTES

(1) Liu, J.; Xu, X.; Li, J.; Liu, B.; Jiang, H.; Yin, B. Palladium-catalyzed dearomatizing 2,5-alkoxyarylation of furan rings: diastereospecific access to spirooxindoles. *Chem. Commun.* **2016**, *52*, 9550.

(2) Liu, J.; Peng, H.; Yang, Y.; Jiang, H.; Yin. B. Regioselective and Stereoselective Pd-Catalyzed Intramolecular Arylation of Furans: Access to Spirooxindoles and 5H‐Furo[2,3‐c]quinolin-4-ones. *J. Org. Chem.* **2016**, *81*, 9695–9706.

(3) Li, X.; Zhou, B.; Yang, R-Z.; Yang, F-M.; Liang, R.X.; Liu, R-R.; Jia, Y.X. Palladium-Catalyzed Enantioselective Intramolecular Dearomative Heck Reaction. *J. Am. Chem. Soc.* **2018**, *140*, 13945–13951.

Appendix 10

Additional Strategies and Tactics Toward the Total Synthesis of Atkamine

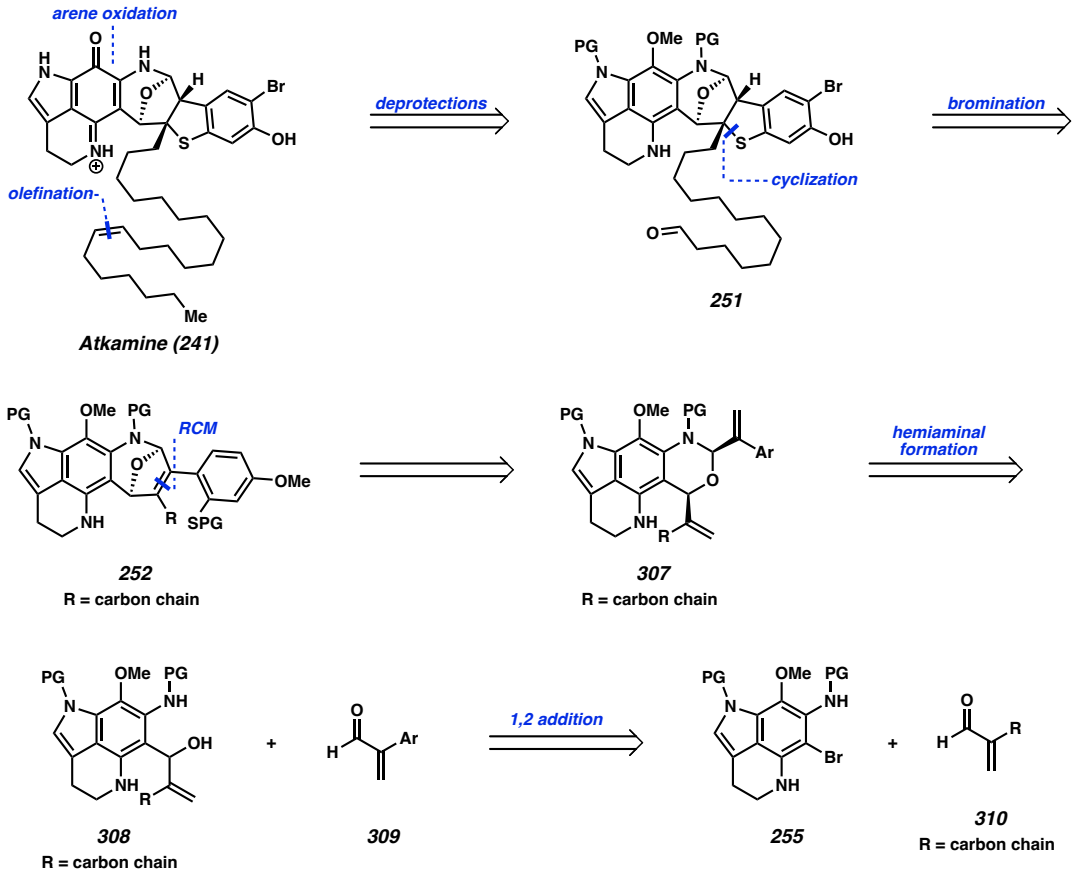
A10.1 INTRODUCTION

Given our failures at developing the dearomative furan coupling to access atkamine (**241**), we briefly explored alternative strategies toward its total synthesis. These preliminary efforts focused on model systems for the construction of the bicyclo[3.2.1]octane ring system found in atkamine (**241**) as this represented the greatest synthetic challenge.

A10.2 RING-CLOSING METATHESIS STRATEGY

One of the alternative strategies that was considered to access atkamine (**241**) commenced from previously identified intermediate **252** (see Chapter 3.2), at which point the olefin of the tetrahydrofuran was cleaved to reveal hemiaminal **307** (Scheme A10.2.1). In the forward direction, we envisaged performing a ring-closing metathesis to form the bicyclo[3.2.1]octane ring. Although ring-closing metathesis to form tetrasubstituted olefins is notoriously challenging, we hypothesized it could be feasible given a five-membered ring would be formed (i.e. low entropic cost). From hemiaminal **307**, the aminal linkage was disconnected, which afforded benzyl alcohol **308**. In turn, simple condensation of **308**

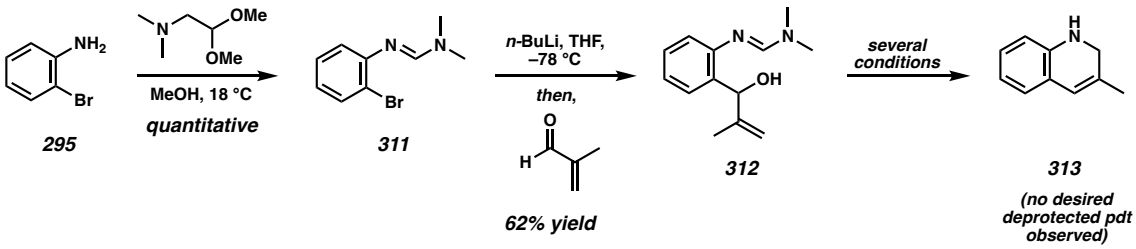
Scheme A10.2.1 *Ring-closing metathesis strategy.*



and acrolein **309** could form the hemiaminal. Finally, **308** was traced back to bromoarene **255**, once again intercepting an aminotricycle accessible through the Larock/Buchwald–Hartwig route. The C–C bond could be formed via 1,2 addition of metalated **255** and acrolein **310**.

Our studies commenced from **295**, which was converted to amidine **311** as this was shown to be a competent protecting group for the metalation of *o*-anilines and subsequent 1,2 addition.[1] Lithium-halogen exchange and subsequent 1,2 addition into methacrolein (a model acrolein chosen for this system) proceeded smoothly and delivered benzyl alcohol **312**. Unfortunately, all attempts to deprotect the amidine at this stage failed, and typically

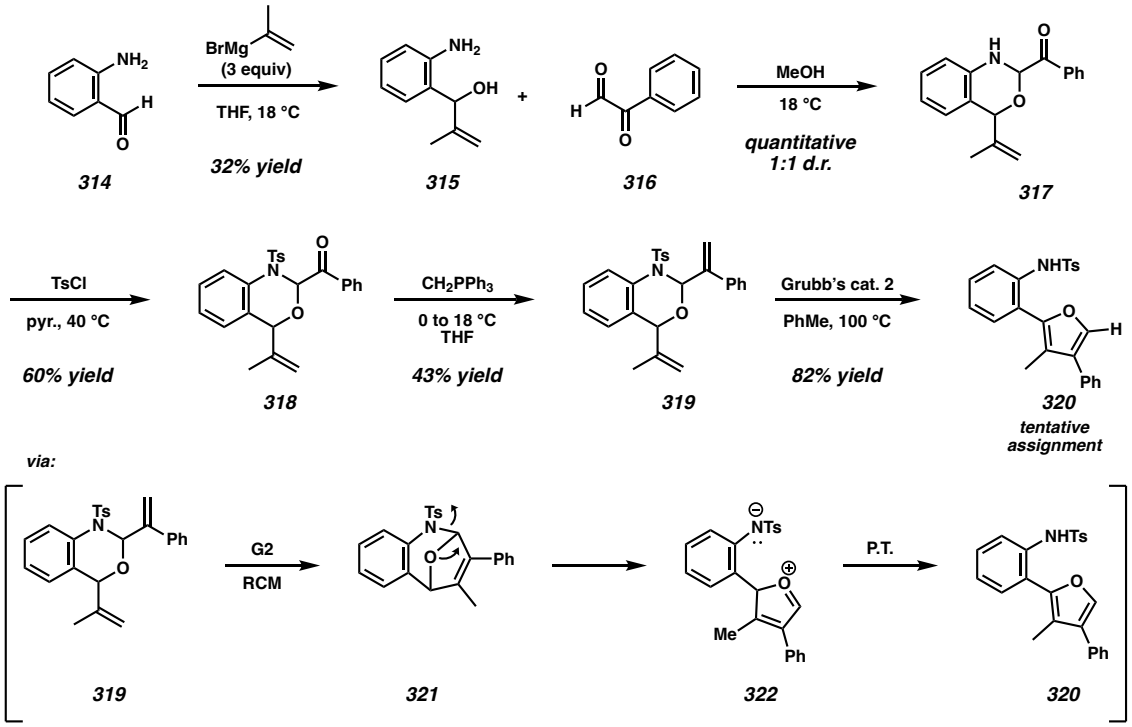
Scheme A10.2.2 *Failed deprotection of amidine* ***312***.



dihydroquinoline **313** was observed. Additionally, alternative aniline protecting groups (or no protecting group) resulted in poor 1,2 addition.

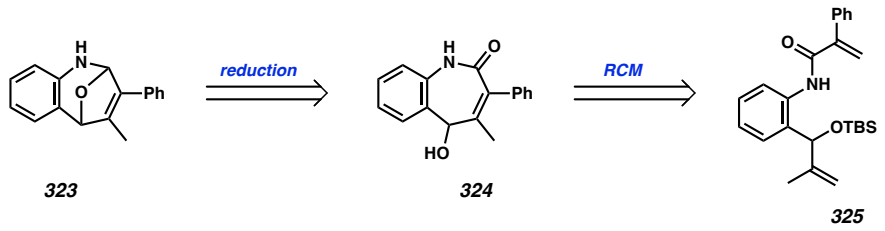
To circumvent this challenge, we decided to switch the electrophile and nucleophile components. Starting from commercially available benzaldehyde **314**, 1,2 addition of isopropyl magnesium bromide provided the desired benzylic alcohol **315**, albeit in low yield (Scheme A10.2.3). At this point, attempted hemiaminal formation with acrolein derivatives resulted in complicated reaction mixtures, likely due to undesired 1,4 addition/oligomerization. Ketoaldehyde **316** was employed instead, which resulted in quantitative formation of hemiaminal **317**. Attempting to perform an olefination on **317** under a variety of standard conditions proved unsuccessful. However, first protecting the nitrogen as the sulfonamide proved necessary, as Wittig olefination of sulfonamide **318** occurred readily to provide the requisite ring-closing metathesis substrate **319**. Exposing **319** to Grubb's catalyst 2nd generation (G2) at elevated temperatures resulted in clean formation of tentatively assigned furan **320**. We hypothesize that after ring-closing metathesis, intermediate dihydrofuran **321** is unstable under the reaction conditions and funnels to the thermodynamically favored aromatic furan **320** via the intermediacy of **322**. Given the observation of an aromatized product, we thought the formation of this thermodynamically favored product would likely be a significant challenge to overcome.

Scheme A10.2.3 *Failed ring-closing metathesis of hemiaminal* ***318****.*



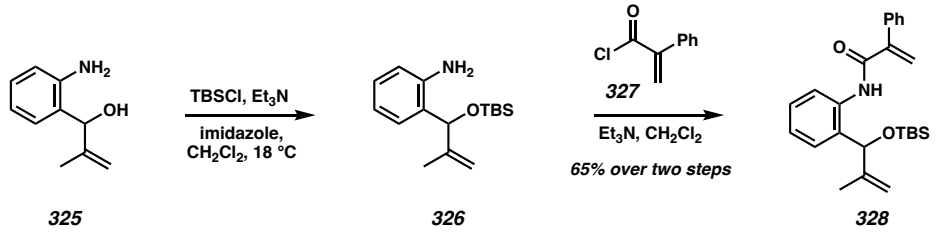
To address this issue of aromatization, the strategy was altered. From desired dihydrofuran **323**, oxidation of the hemiaminal linkage revealed azepine **324**: in the forward direction we hypothesized that amide reduction could allow for transannular cyclization to form the bridging tetrahydrofuran (Scheme A10.2.4). Importantly, we envisaged this transformation could occur under ambient conditions, which would hopefully mitigate funneling to the aromatic furan product. From azepine **324**, cleavage of the olefin yields acrylamide **325**.

Scheme A10.2.4 *Altered ring-closing metathesis strategy.*



This altered strategy commenced from previously accessed amino alcohol **325**, which was first protected as the silyl enol ether (**326**, Scheme A10.2.5). Acylation with acid chloride **327** then provide acrylamide **328**— the requisite ring-closing metathesis substrate.

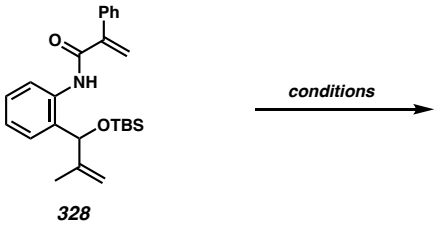
Scheme A10.2.5 *Synthesis of acrylamide* ***328****.*



325 ***326*** ***328***

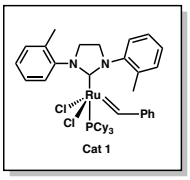
With **328** in hand, we began our preliminary investigation of the ring-closing metathesis. Treatment of **328** with G2, even at elevated temperatures and prolonged reaction time, resulted in no reaction (Table A10.2.1, entry 1). Using specialized catalysts for the formation of tetrasubstituted olefins[2] similarly resulted in no reaction, even upon heating at 140 °C (entries 2-6). This is perhaps unsurprising as examples to form seven-membered rings containing tetrasubstituted olefins using ring-closing metathesis are rare, and to the best of our knowledge, there are no examples in which the terminal olefin substituents are not methyl groups. Given these difficulties, we opted to pursue alternative strategies for the formation of the bicyclo[3.2.1]octane ring system in atkamine (**241**).

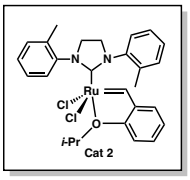
Table A10.2.1 *Preliminary investigation into the ring-closing metathesis of* ***328****.*



328

Entry	Catalyst	Solvent	Temp	Time	Result
1	G2	PhMe	100 °C	4 d	no rxn
2	Cat 1	PhMe	60 °C	16 h	no rxn
3	Cat 2	PhMe	60 °C	32 h	no rxn
4	Cat 1	PhMe	60 to 80 to 105 °C	2 d	no rxn
5	Cat 2	PhMe	60 to 80 to 105 °C	2 d	no rxn
6	Cat 1	*o*-xylene	140 °C	1 d	no rxn

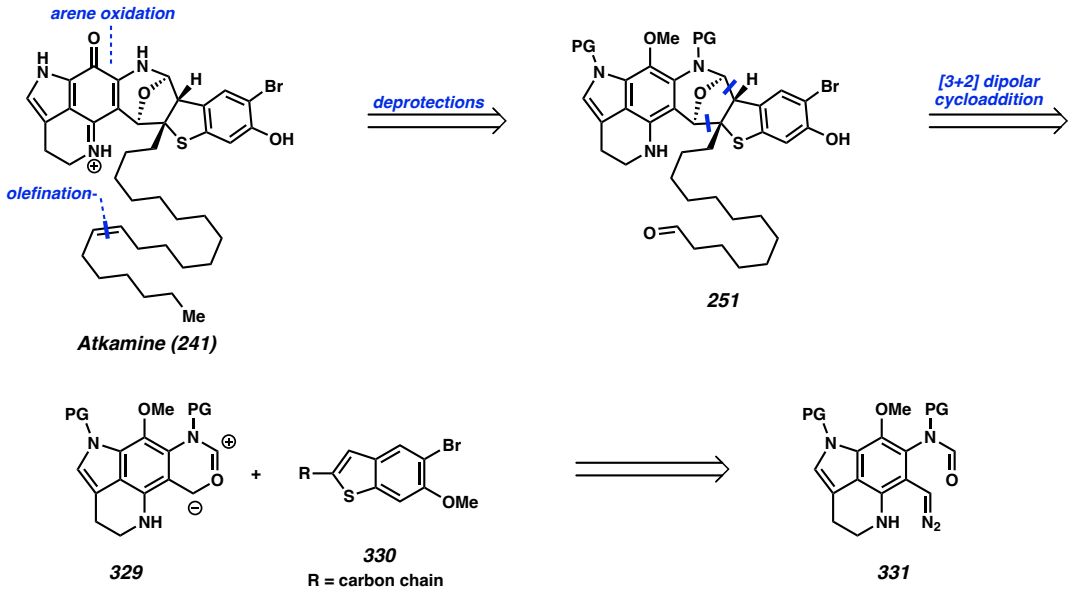




A10.3 [3+2] DIPOLAR CYCLOADDITION STRATEGY

The next strategy we pursued hinged upon a [3+2] dipolar cycloaddition. Specifically, the bicyclic ring system of **251** was cleaved to reveal synthon **329** and benzothiophene **330** (Scheme A10.3.1). We envisaged developing a [3+2] dipolar cycloaddition of carbonyl ylide **329** and benzothiophene **330** to construct the bicyclo[3.2.1]octane ring system in atkamine (**241**). This is perhaps the most ideal bond disconnection of this ring system, as it is convergent and would form the tertiary centers in a single step. Carbonyl ylide **329** in turn was thought to arise from nonstabilized diazo compound **331**. We elected to pursue a nonstabilized diazo compound is this would limit subsequent functional group interconversions that would be necessary to remove a stabilizing group (i.e. ester).

Scheme A10.3.1 *[3+2] dipolar cycloaddition strategy.*

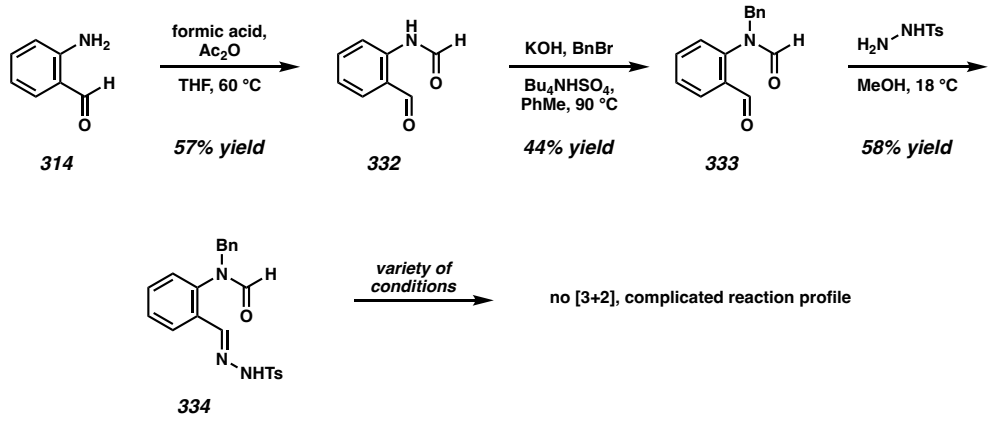


Although carbonyl ylide [3+2] dipolar cycloadditions are well documented[3], examples of nonstabilized carbonyl ylides are rare (i.e. no electron withdrawing group α to the diazo). Additionally, there have been no reports of a benzothiophene used as a dipolarophile in a [3+2] cycloaddition— only activated benzothiophene (i.e. containing electron withdrawing groups) substrates have been reported.[4] Additionally, these reports only utilized azomethine ylide 1,3 dipoles.

This [3+2] carbonyl ylide dipolar cycloaddition strategy has been examined in the context of atkamine (**241**). Higuchi and coworkers attempted to apply this strategy to access the bicyclo[3.2.1]octane ring system in atkamine (**241**)[5], however in their report they utilized stabilized carbonyl ylides (which would require removal of the stabilizing group following cycloaddition), and no benzothiophene-based dipolarophiles were reported. Additionally, the substrates showcased in their report could not be readily advanced to the requisite ring system of atkamine (**241**).

We were excited to build upon this existing precedent, and our preliminary studies began once again targeting a model system. Benzaldehyde **314** was converted to formamide **332** (Scheme A10.3.2); it was envisaged that the formamide oxygen would insert into the adjacent carbene to form the carbonyl ylide (*vide infra*).[6] This moiety was chosen as it would afford a bicycle containing hemiaminal linkage with the correct oxidation state, which would limit subsequent functional group manipulations. At this point the aniline nitrogen needed to be doubly protected to allow for carbonyl ylide formation. Benzylation proceeded smoothly to provide **333**, but surprisingly attempts to install alternative protecting groups (i.e. Ts or formamide) proved unsuccessful. **333** was carried forward and condensed with tosyl hydrazine to afford the carbonyl ylide precursor **334**. These motifs are known to form diazo compounds *in situ* upon treatment with base and metal source (typically rhodium).[7] However, employing various conditions (i.e. base, metal source, dipolarophile) resulted in complicated reaction profiles and no [3+2] adducts were observed.

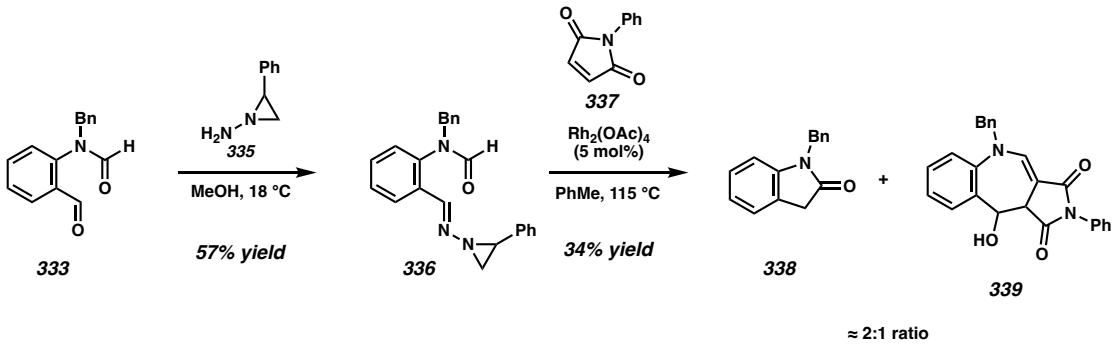
Scheme A10.3.2 *Failed [3+2] cycloaddition of tosyl hydrazone* ***334****.*



We therefore elected to pursue an alternative diazo precursor, and identified *N*-aziridinylimines as an attractive candidate.[8] Aldehyde **333** was condensed with hydrazine

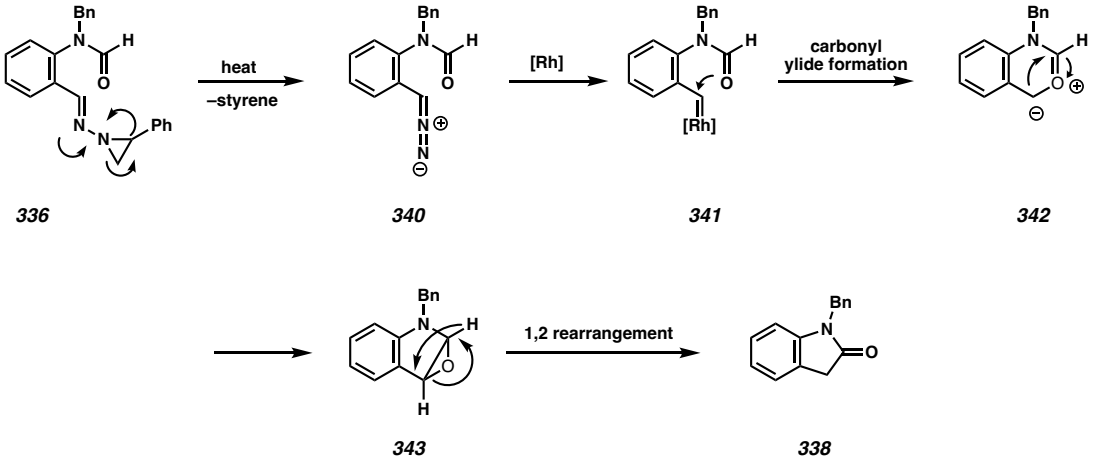
335 to afford the desired *N*-aziridinylimine **336**. Excitingly, heating **336** with *N*-phenylmaleimide (**337**, a common dipolarophile for carbonyl ylides) in the presence of $Rh_2(OAc)_4$ resulted in a 2:1 ratio of oxindole **338** and rearranged [3+2] adduct **339**. Although **339** was not the major product, we were encouraged that this nonstabilized system could in fact participate in a [3+2] dipolar cycloaddition.

Scheme A10.3.3 *Successful [3+2] cycloaddition employing hydrazone* ***336****.*



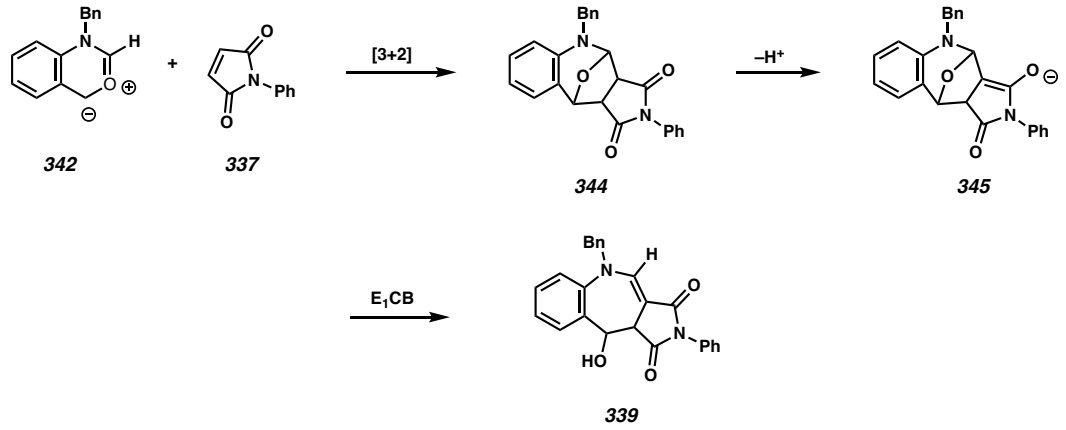
We hypothesize that oxindole **338** forms from carbonyl ylide **342** via nucleophilic attack, followed by 1,2 rearrangement, although a direct C-H insertion mechanism cannot be ruled out (Scheme A10.3.4).

Scheme A10.3.4 *Proposed mechanism of oxindole* ***338*** *formation.*



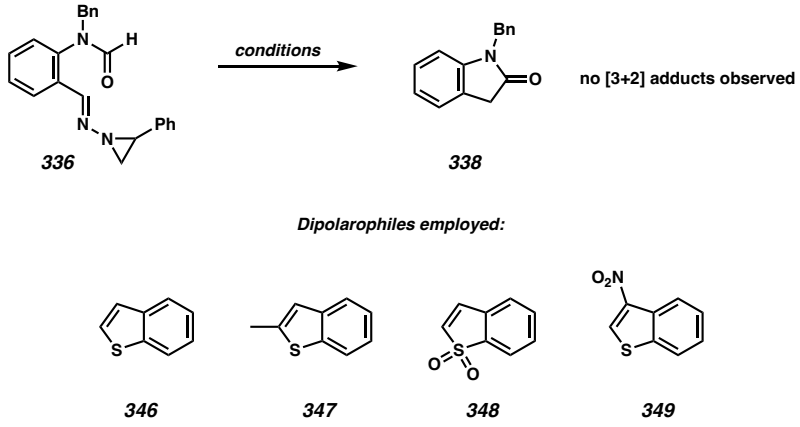
We hypothesize that adduct **339** forms via first [3+2] cycloaddition between **342** and **337**, followed by deprotonation/elimination (or conversely direct elimination from **344**, Scheme A10.3.5).

Scheme A10.3.5 *Proposed mechanism for the formation of adduct **339**.*



Nevertheless, we were encouraged by this result and wanted to apply it to a benzothiophene-based dipolarophile. Unfortunately, despite investigating a variety of conditions (i.e. catalyst, temperature, solvent), no desired cycloaddition with any of the benzothiophene substrates (**346-349)** was observed (Scheme A10.3.6). Efforts in this area are on going.

Scheme A10.3.6 *Failed [3+2] cycloaddition with benzothiophene-based dipolarophiles.*



A10.4 REFERENCES AND NOTES

(1) Varchi, G.; Jensen, A. E.; Dohle, W.; Ricci, A.; Cahiez, G.; Knochel, P. Preparation of Functionalized Magnesiated Aniline Derivatives. *Synlett* **2001**, *4*, 477–480.

(2) a) Paek, S-M. Synthesis of Tetrasubstituted Alkenes via Metathesis. *Molecules* **2012**, *17*, 3348–3358. b) Heinrich, C. F.; Durand, D.; Starck, J.; Michelet, V. Ruthenium Metathesis: A Key Step To Access a New Cyclic Tetrasubstituted Olefin Platform.

(3) a) Padwa, A. Generation and Utilization of Carbonyl Ylides via the Tandem Cyclization-Cycloaddition method. *Acc. Chem. Res.* **1991**, *24*, 22–28. b) Padwa, A.; Zhang, Z. J.; Zhi, L. Cyclization-Cycloaddition Cascade of Rhodium Carbenoids Using Different Carbonyl Groups. Highlighting the Position of Interaction. *J. Org. Chem.* **2000**, *65*, 5223–5232.

(4) a) Harada, M.; Kato, S.; Haraguchi, R.; Fukuzawa, S-I. Metal Complex-Controlled Regio-,Diastero- and Enantioselective 1,3-Dipolar Cycloaddition of Azomethine Ylides with Benzo[b]thiophene Sulfones. *Chem. Eur. J.* **2018**, *24*, 2580–2583. b) Wang, K-K.; Xie, Y-X.; Li, Y-L.; Chen, R.; Wang, Z-Y. Dearomative [3+2] cycloaddition reaction of nitrobenzothiophenes with nonstabilized azomethine ylides. *RSC Adv.* **2020**, *10*, 28720.

(5) Higuchi, K.; Matsubayashi, Y.; Sakurai, T.; Ito, M.; Sugiyama, S. Synthesis of 8-OXA-2-AZABICYCLO[3.2.1]OCTANE USING A 1,3-DIPOLAR CYCLOADDITION REACTION. *Heterocycles* **2019**, *98*, 1055–1073.

(6) Carbonyl ylide dipolar cycloadditions employing formamides are rare. Typically, carbamates are employed, but this would yield a bicycle containing an undesired amide oxidation state and would necessitate further functional group manipulation.

(7) Fulton, J. R.; Aggarwal, V. K.; Vicente, J. The Use of Tosylhydrazone Salts as Safe Alternative for Handling Diazo Compounds and Their Applications in Organic Synthesis. *Eur. J. Org. Chem* **2005**, 1479–1492.

(8) Kirmse, W. Reactive Intermediates from *N*-Aziridinylimines. *Eur. J. Org. Chem.* **1998**, 201–212.

CHAPTER 4

Synthesis of Authentic Standards To Enable Investigations of Pinene Secondary Organic Aerosols[†]

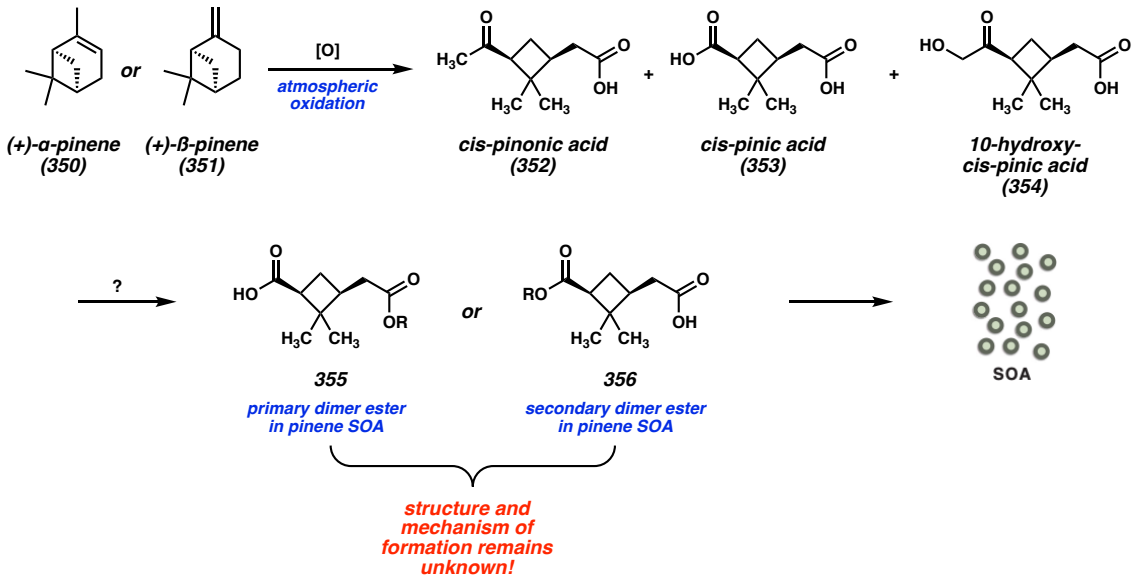
4.1 INTRODUCTION

Secondary organic aerosol (SOA) contributes substantially (15 to 80% by mass) to the global burden of atmospheric fine particulate matter ($PM_{2.5}$),[1] which exerts large but uncertain effects on climate[2] as well as adverse impacts on air quality and human health.[3,4] The oxidation of monoterpenes ($C_{10}H_{16}$), emitted in appreciable quantities from forested regions (~150 Tg $year^{-1}$)[5], represents a dominant source of SOA.[6,7,8] For more than two decades, high-molecular weight dimeric compounds, notably those proposed to contain ester linkages, have been identified using advanced mass spectrometric techniques as important components of both laboratory-derived and ambient monoterpene SOA and have been implicated as key players in particle formation and growth, volatility, viscosity, and cloud condensation nuclei (CCN) activity.[9] Particle-phase reactions of closed-shell monomers (e.g., esterification and peroxyhemiacetal or diacyl peroxide decomposition) and gas-phase reactions involving early-stage oxidation products and/or reactive intermediates [e.g., stabilized Criegee intermediates (SCIs), carboxylic acids, and organic peroxy radicals (RO_2)] have been advanced as possible dimer ester formation pathways. Owing to a lack of authentic standards,[10] however, the structures of the dimer esters are not

[†]This research was performed in collaboration with Christopher M. Kenseth, Nicholas J. Hafeman, Jing Chen, Yuanlong Huang, Nathan F. Dalleska, and Henrik G. Kjaergaard. Portions of this chapter have been reproduced with permission from Kenseth et. al. *Science*, **2023**, *382*, 787–792.

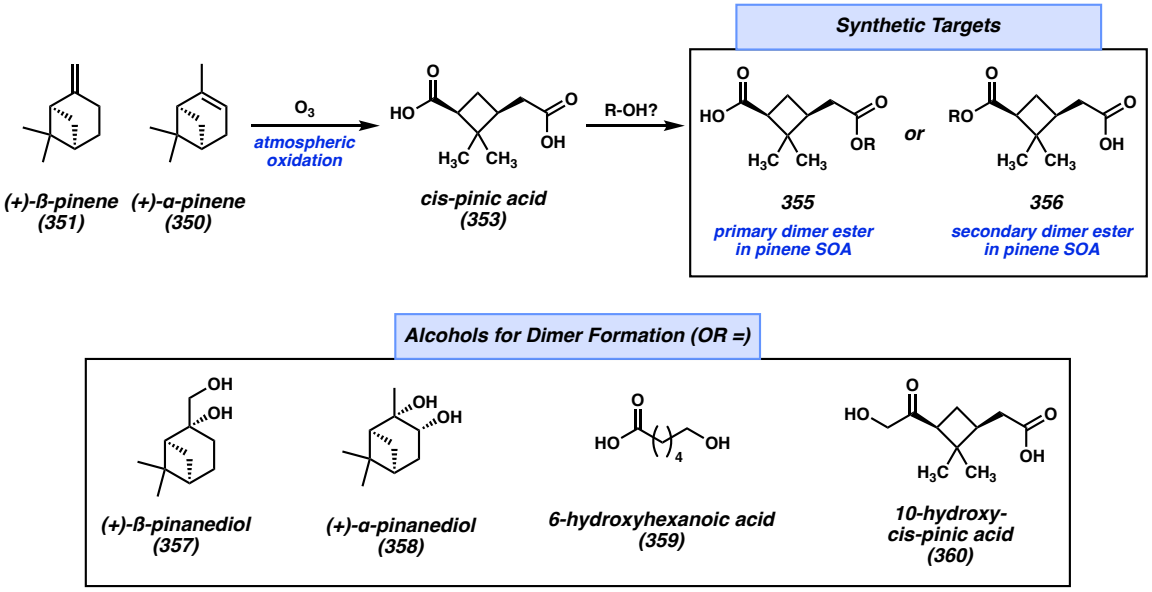
known but only inferred from accurate mass and fragmentation data (Figure 4.1.1). As a result, mechanistic understanding of dimer ester formation (i.e. **355** and **356**), in particular the relevance of gas- versus particle-phase chemistry, remains unconstrained.

Figure 4.1.1 *Structure's of secondary dimer esters in pinene SOA remain unknown.*



Guided by our previous work on dimers formed from synergistic O_3 + OH oxidation,[9b] and further experiments in the Caltech dual 24-m^3 Teflon environmental chambers (CTEC)[11], the structures of the major dimers identified in SOA from α- and β-pinene (**350** and **351**) ozonolysis were proposed to consist of an ester of *cis*-pinic acid (**353**), the most abundant carboxylic acid measured in pinene SOA[9c] and a commonly reported dimer subunit,[12] and a sufficiently low volatile alcohol. Because *cis*-pinic acid (**353**) is an asymmetric dicarboxylic acid, however, structures containing either a primary or secondary ester are possible for each dimer ester and cannot be definitively resolved by MS/MS analysis. To address this ambiguity, primary and secondary esters of *cis*-pinic acid (**353**) and the identified alcohol subunits of dimer esters formed in the CTEC experiments (**357-360**) were targeted for authentic standard synthesis (Figure 4.1.2).We hypothesized

Figure 4.1.2 *Synthetic targets for this study.*

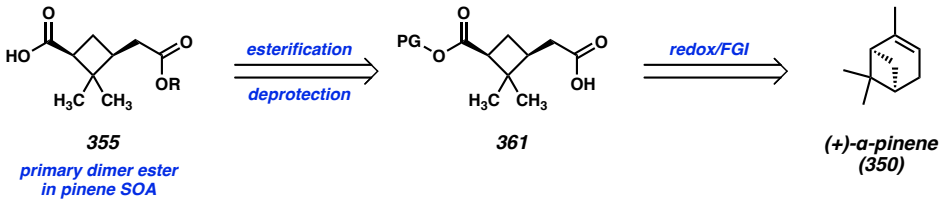


that with the series of authentic dimer ester products in hand, the structures and mechanism of formation of major dimer esters in secondary organic aerosols from ozonolysis of α-pinene (**350**) and β-pinene (**351**) could be elucidated, which has been a longstanding challenge in the field.

4.2 SYNTHESIS OF PRIMARY DIMER ESTERS

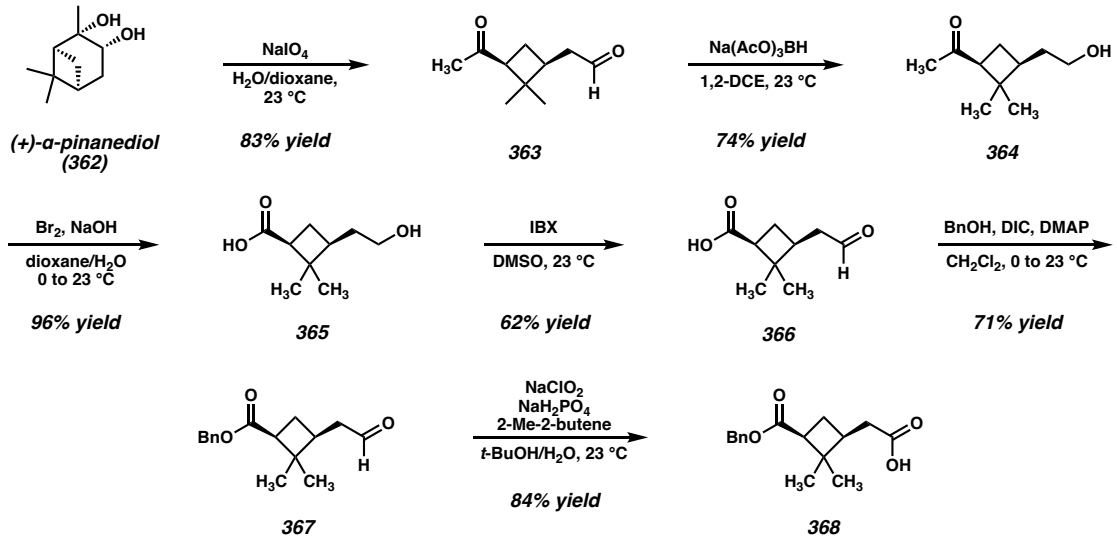
The strategy to access primary dimer esters (**355**) hinged upon divergency to maximize synthetic efficiency: late-stage installation of the requisite alcohols would greatly simplify the synthetic task (Scheme 4.2.1). However, in order to selectively form the desired primary esters, the other carboxylate group needed to be protected. These requirements revealed ester/acid **361** as a key intermediate. In turn, **361** could arise from α-pinene (**350**) through a series of redox manipulations and functional group interconversions. By employing this cheap chiral pool feedstock (**350**), the final targets could be accessed with high levels of enantiopurity, which would greatly simplify the subsequent atmospheric chamber oxidation experiments.

Scheme 4.2.1 *Retrosynthetic analysis for primary ester dimer target* ***355***.



Our synthetic efforts commenced from commercially available α-pinanediol (**362**) which underwent oxidative cleavage using a modified procedure[13] to yield keto aldehyde **363** (Scheme 4.2.2). Selective reduction of the aldehyde was achieved using $Na(AcO)_3BH$ to provide keto alcohol **364**, and a subsequent haloform reaction afforded acid **365**. The alcohol was then oxidized under standard conditions and at this point the acid moiety was protected as the benzyl ester to provide ester aldehyde **367**. Finally, a Pinnick oxidation provided the requisite divergent acid **368**.

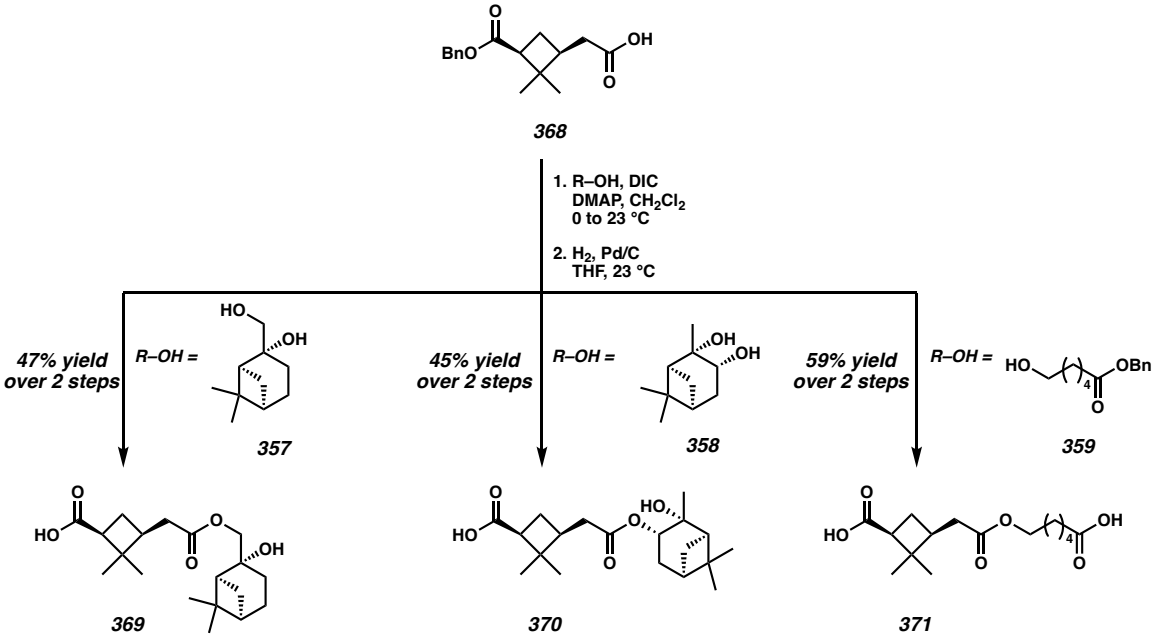
Scheme 4.2.2 *Synthesis of divergent acid* ***368***.



With divergent acid **368**, the primary dimer esters were accessed through a Steglich Esterification with the requisite alcohol, which was then followed by benzyl ether

hydrogenolysis under standard conditions (Scheme 4.2.3). This approach proceeded smoothly to provide sufficient quantities of primary dimer esters **369**-**371**.

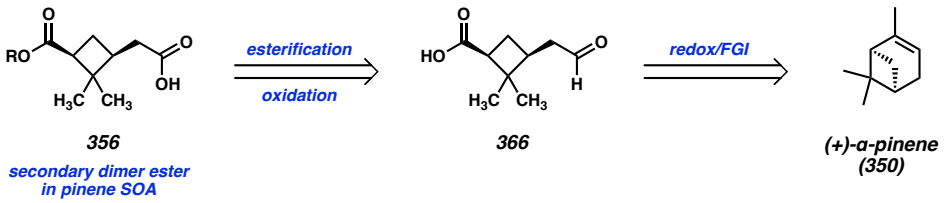
Scheme 4.2.3 *Synthesis of primary dimer esters* ***369***-***371***.



4.3 SYNTHESIS OF SECONDARY DIMER ESTERS

The strategy for the synthesis of secondary dimer esters was similarly centered around divergency. In this case, it was hypothesized that previously accessed acid aldehyde **366** could serve as the key divergent intermediate wherein an esterification and subsequent Pinnick oxidation could afford the desired products (Scheme 4.3.1).

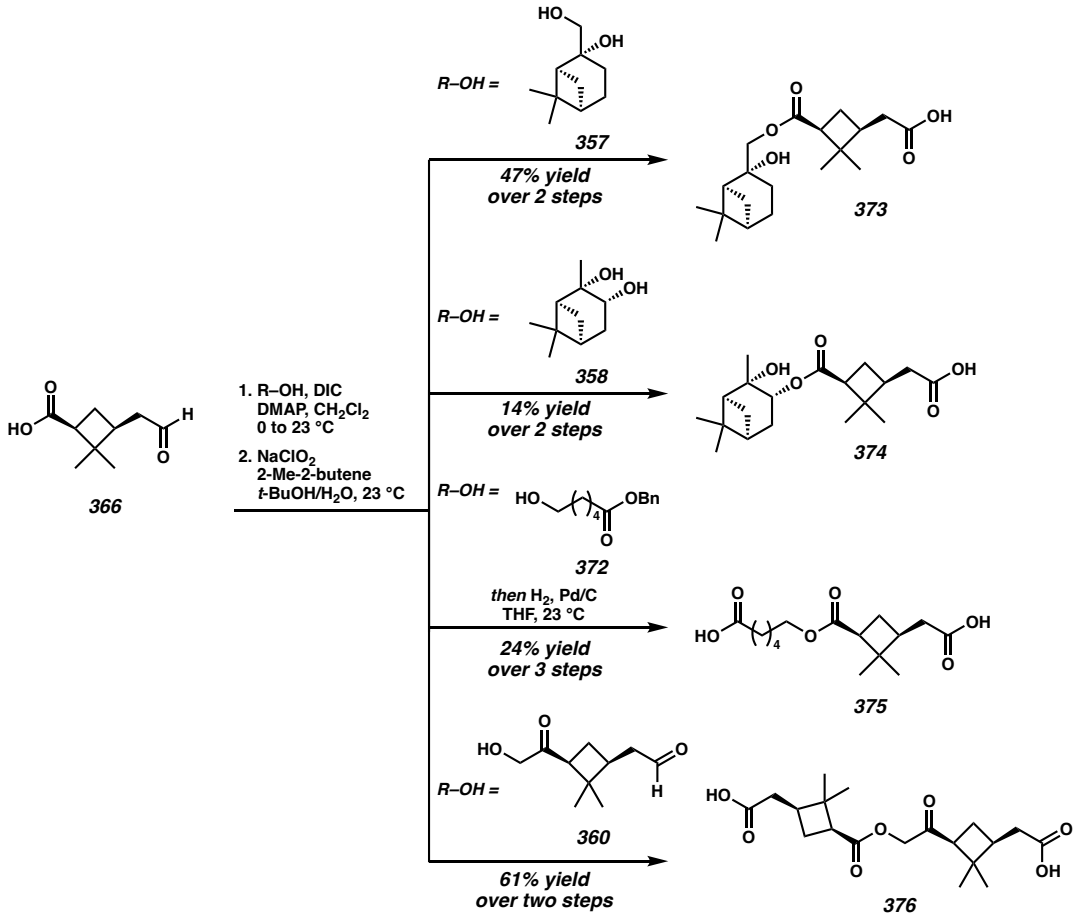
Scheme 4.3.1 *Retrosynthetic analysis of secondary dimer ester* ***356***.



Steglich Esterification with alcohols **357** and **358** proceeded smoothly and was followed by Pinnick oxidation to provide secondary dimer esters **372** and **373** (Scheme

4.3.2). When employing alcohol **372**, an additional benzyl ether hydrogenolysis was necessary to yield desired diacid **375**. Finally, using alcohol **360** (accessed in six steps from α-pinene (**350**)) necessitated a double Pinnick oxidation as the last step of the sequence, which proceeded smoothly to afford the final secondary dimer ester **376**.

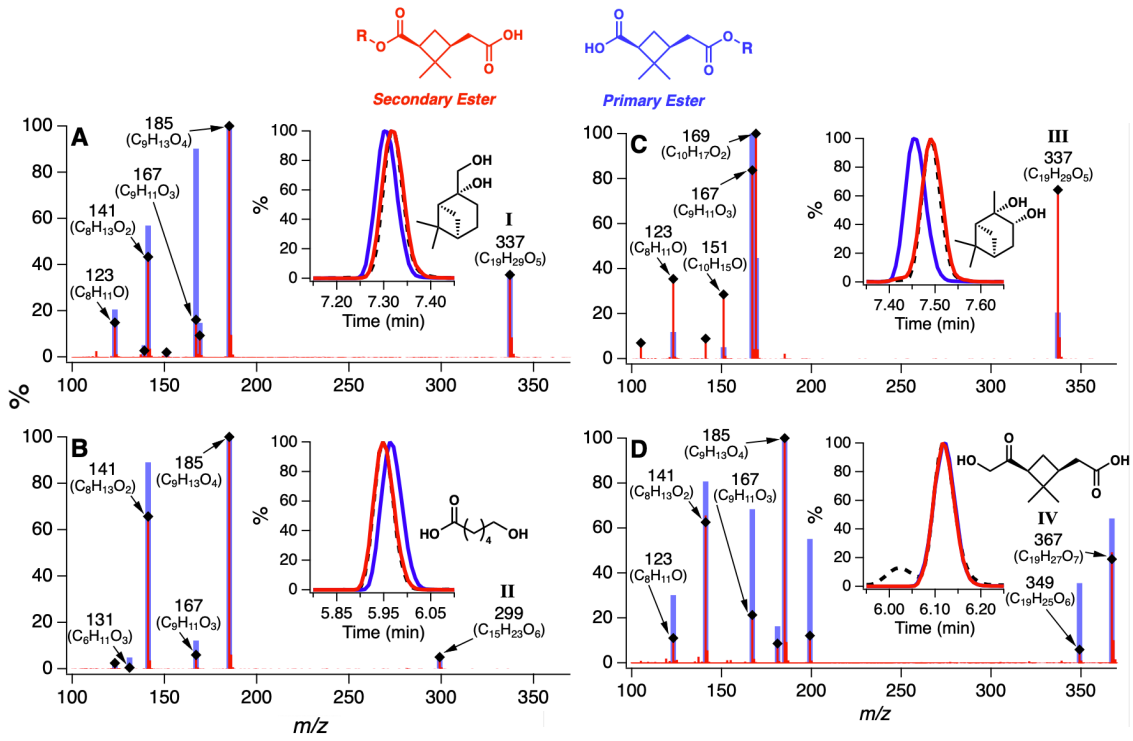
Scheme 4.3.2 *Synthesis of secondary dimer esters **373**-**376**.*



4.4 DETERMINATION OF DIMER ESTER STRUCTURES IN PINENE SECONDARY ORGANIC AEROSOL

Comparison of the LC retention times and MS/MS fragmentation patterns of dimer esters from the CTEC experiments (α- and β-pinene (**350** and **351**) oxidation experiments) with those of the synthesized primary and secondary esters (**369**-**376**) reveals that dimer

Figure 4.4.1 *(**A** to **D**) Extracted ion chromatograms (EICs) and MS/MS spectra of synthesized secondary (red) and primary (blue) dimer esters of (+)-cis-pinic acid (**353**) and (+)-β-Pdiol (**357**) (A), 6- hydroxyhexanoic acid (**359**) (B), (+)-α-Pdiol (**358**) (C), and (+)-OH- pinonic acid (**360**) (D) as well as of dimer esters identified in SOA (black diamonds and dashed lines)*



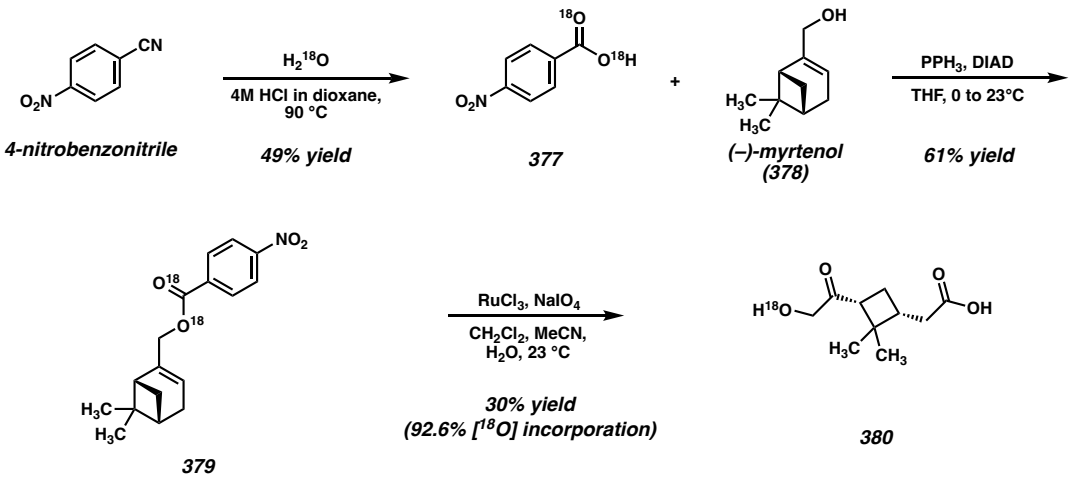
ester production from the *cis*-pinic acid derivative is regioselective and forms the more sterically hindered secondary ester in each case. To our knowledge, this represents the first synthesis of authentic standards of dimer esters identified in SOA from ozonolysis of α-pinene and β-pinene (**350** and **351**), including the extensively studied dimer ester **376**.

4.5 FORMATION MECHANISM OF DIMER ESTERS

As a means of elucidating a central feature of the dimerization reaction– namely which monomeric species contributes the O atom in the ester linkage–β-pinene (**351**)

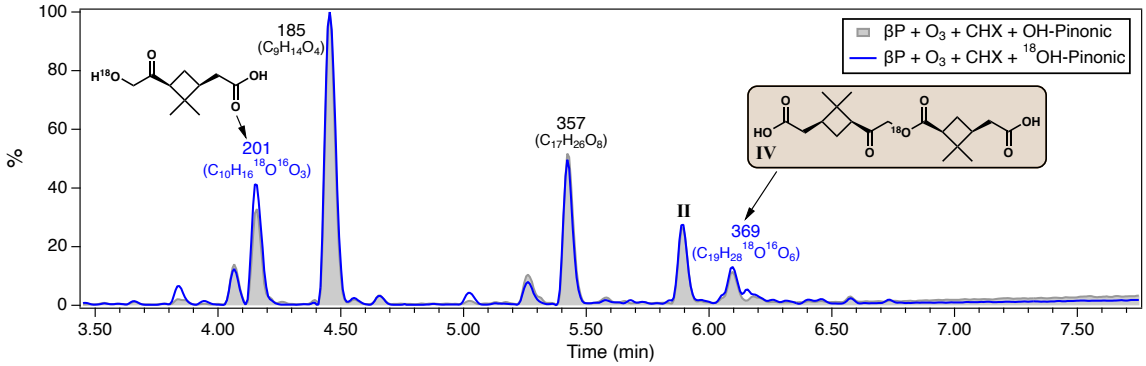
ozonolysis with cyclohexene was carried out in the presence of synthesized ^{18}OH-pinonic acid (**380**), labeled at the hydroxy group. Briefly, 4-nitrobenzonitrile was hydrolyzed to the corresponding acid using $H_2{}^{18}O$ under acidic conditions (Scheme 4.5.1).[14] A Mitsonobu reaction was then utilized to install the ^{18}O label on (–)-myrtenol (**378**) to yield labeled adduct **379**. Finally, a one pot dihydroxylation/oxidative cleavage/acid hydrolysis sequence was achieved to provide ^{18}OH-pinonic acid (**380**).

Scheme 4.5.1 *Synthesis of ^{18}O labeled OH-pinonic acid (**380**)*



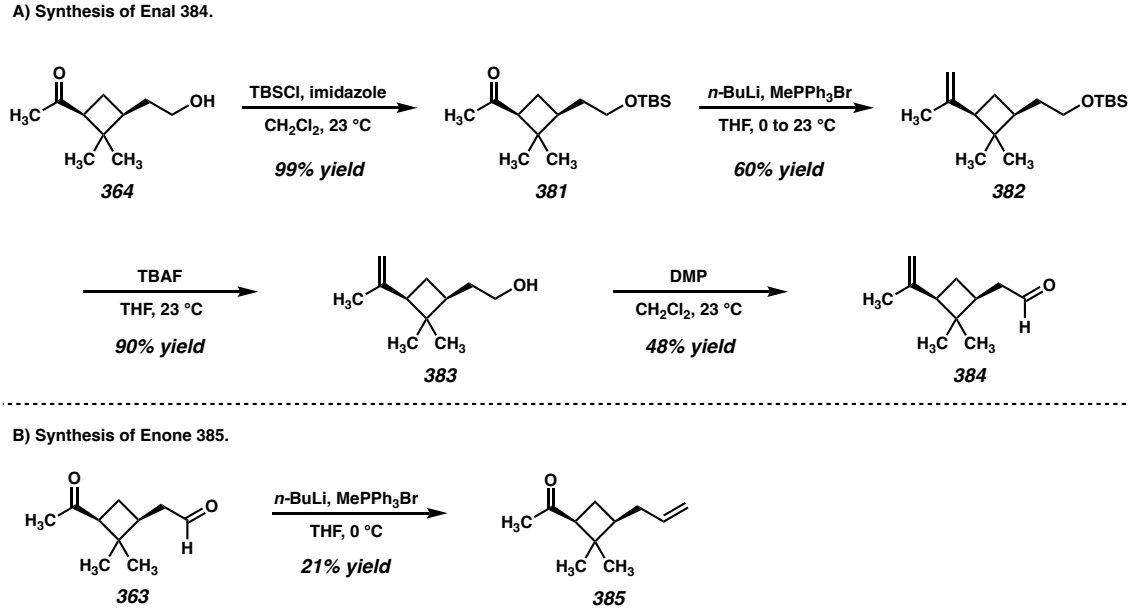
Formation of ^{18}O-labeled dimer ester **IV** at the same retention time as its ^{16}O isotopologue establishes that the ester O atom in dimer ester **276**, and by extension dimer esters **369** to **376**, originates from the alcohol and suggests that the particle-phase accretion reaction proceeds through nucleophilic addition of the semivolatile or low-volatility alcohol to the reactive *cis*-pinic acid derivative (Figure 4.5.1).

Figure 4.5.1 *Formation of ^{18}O dimer ester **IV**.*



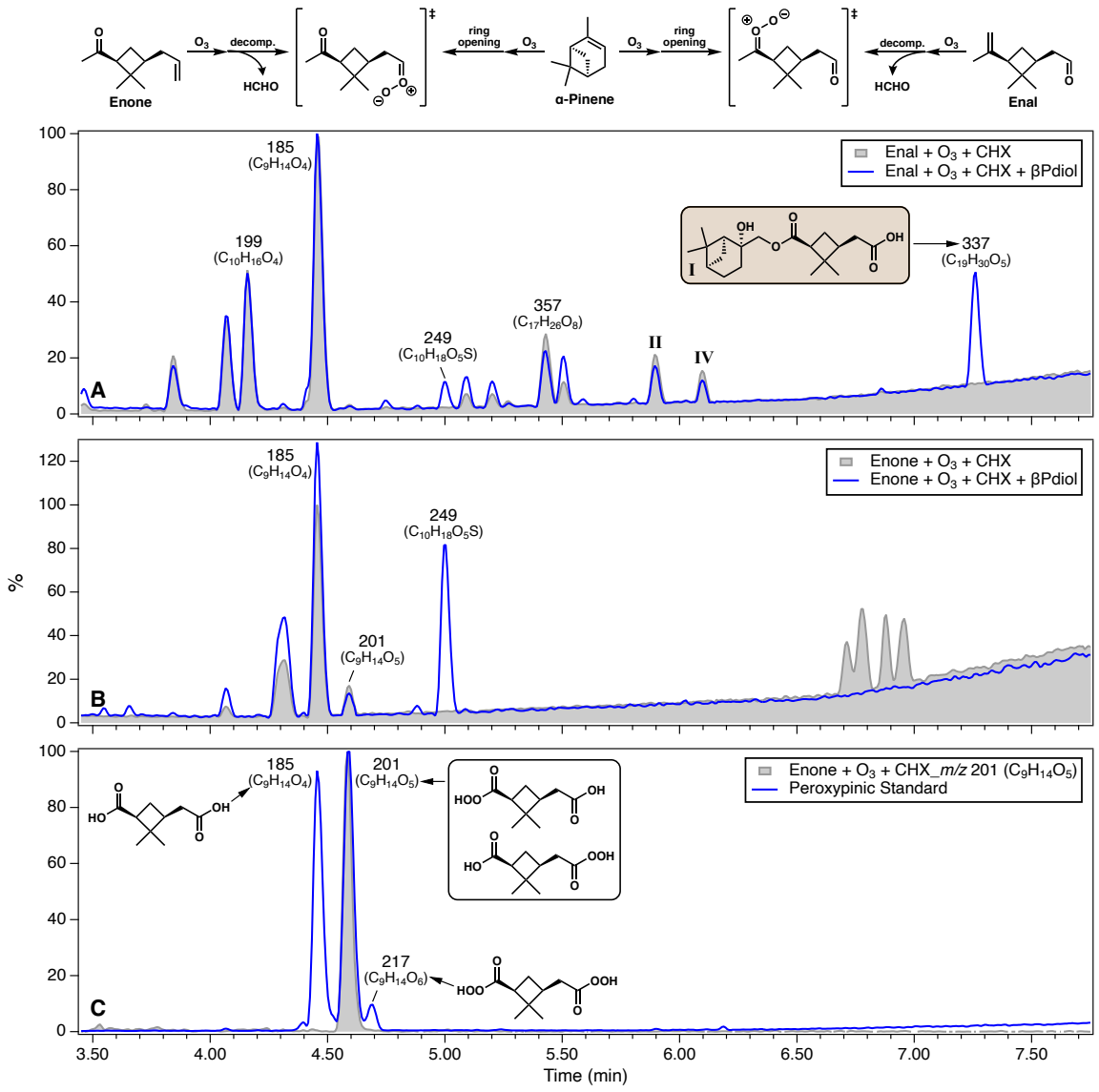
Additional mechanistic evidence is provided by ozonolysis experiments with cyclohexene and β-pinanediol (**357**) featuring one of two synthesized unsaturated carbonyl isomers ($C_{11}H_{18}O$), an enone (**385**) or enal (**384**). The synthesis of enal **385** began with protection of keto alcohol **364** as the silyl ether (**381**, Scheme 4.5.2A). Wittig olefination of silyl ether **381** then yielded olefin **382**, which underwent subsequent deprotection and alcohol oxidation to provide the desired enal **384**. Enone **385** was prepared directly in one step from keto aldehyde **363** via Wittig olefination (Scheme 4.5.2B). Although low yielding, this reaction provided sufficient material for subsequent experiments.

Scheme 4.5.2 *Synthesis of enal* ***384*** *and enone* ***385***.



Enone **385** and enal **384** produce only one of the two Criegee intermediates (CIs) on ozonolysis that form concurrently from ozonolysis of α-pinene (Figure 4.5.2). As anticipated, dimer esters **373**, **375**, and **376**, as well as the major $C_{17}H_{26}O_8$ dimer, were observed to form only from ozonolysis of enal **384**, given that only the CI arising from enal **384** is understood to yield the acyl peroxy radical common to α-pinene (**250**) and β-pinene (**251**) ozonolysis from which the *cis*-pinic acid derivative is hypothesized to stem.

Figure 4.5.2 *Enone* ***285*** *and enal* ***284*** *ozonolysis experiments.*



4.6 CONCLUSION

The formation of dimer esters **369** to **376**–shown through synthesis of authentic standards to be secondary esters of *cis*-pinic acid–through particle-phase accretion of alcohols with an acylperoxyhemiacetal resolves a long-standing puzzle in atmospheric aerosol chemistry and rationalizes a number of experimental and ambient observations from past studies. This chemistry likely represents a general pathway to dimeric

compounds in ambient SOA, which exerts large but uncertain effects on climate as well as adverse impacts on air quality and human health.

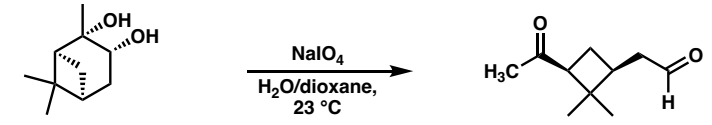
4.7 EXPERIMENTAL SECTION

4.7.1 MATERIALS AND METHODS

Unless otherwise stated, reactions were performed in flame-dried glassware under ambient conditions using dry, deoxygenated solvents. Solvents were dried by passage through an activated alumina column under Ar. Reagents were purchased from commercial sources and used as received. Reaction temperatures were controlled by an IKAmag temperature modulator. Thin-layer chromatography (TLC) was performed using E. Merck silica gel 60 F254 pre-coated plates (250 μm) and visualized by UV fluorescence quenching, potassium permanganate staining, or *p*-anisaldehyde staining. Silicycle Silia*Flash* P60 Academic Silica gel (particle size 40–63 μm) was used for flash chromatography. ^{1}H and ^{13}C NMR spectra were recorded on Varian Inova 500 (500 and 125 MHz, respectively), Varian Inova 600 (600 and 150 MHz, respectively), and Bruker 400 (400 and 100 MHz, respectively) spectrometers and are reported in terms of chemical shift relative to $CHCl_3$ (δ 7.26 and 77.16 ppm, respectively) or CH_3OH (δ 3.31 and 49.01 ppm, respectively). Data for ^{1}H NMR are reported as follows: chemical shift (δ ppm) (multiplicity, coupling constant, integration). Abbreviations are used as follows: s = singlet, d = doublet, t = triplet, q = quartet, m = multiplet. IR spectra were obtained from thin films deposited on NaCl plates using a Perkin Elmer Spectrum BXII spectrometer and are reported in frequency of absorption (cm^{-1}). Optical rotations were measured with a Jasco P-2000 polarimeter operating on the sodium D-line (589 nm) using a 100 mm path-length cell. High-resolution mass spectra (HRMS) were acquired using a Waters ACQUITY UPLC I-Class system

coupled to a Xevo G2-S ESI-Q-TOF-MS, an Agilent 6200 Series TOF-MS with an Agilent G1978A multimode ESI-atmospheric pressure chemical ionization (MM:ESI-APCI) source, or a JEOL JMS-T2000GC AccuTOF GC-Alpha equipped with a field ionization (FI) source.

4.7.2 EXPERIMENTAL PROCEDURES

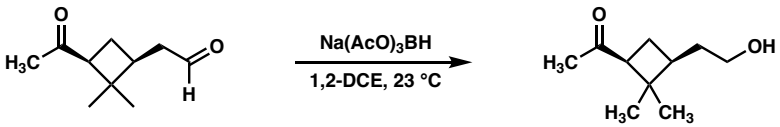


(+)-α-pinanediol (362) ***83% yield*** ***363***

Ketoaldehyde 363: Ketoaldehyde **363** was prepared according to a modified literature procedure[15] from commercial (+)-α-pinanediol (**362**, 99%, 99% ee, Sigma-Aldrich). To a stirred solution of (+)-α-pinanediol (**362**, 4.05 g, 23.8 mmol, 1.0 equiv) in H_2O/dioxane (1:2, 80 mL) at 23 °C was added $NaIO_4$ (12.2 g, 57.1 mmol, 2.4 equiv) in one portion. The mixture was stirred for 6 h at 23 °C, at which point TLC indicated complete consumption of the starting material. The solution was diluted with Et_2O (200 mL) and H_2O (200 mL). The layers were separated and the aqueous layer was extracted with Et_2O (3 × 200 mL). The combined organic phases were washed with brine, dried over $MgSO_4$, and concentrated to afford the title compound as a colorless oil (3.31 g, 19.7 mmol, 83% yield) in sufficient purity by NMR for use in the subsequent reaction.

^{1}H NMR (400 MHz, $CDCl_3$): δ 9.74 (t, *J* = 1.5 Hz, 1H), 2.92 (dd, *J* = 10.0, 7.7 Hz, 1H), 2.55 – 2.35 (m, 3H), 2.04 (s, 3H), 2.02 – 1.90 (m, 2H), 1.34 (s, 3H), 0.84 (s, 3H).

^{13}C NMR (100 MHz, $CDCl_3$): δ 207.5, 201.6, 54.5, 45.3, 43.4, 35.9, 30.5, 30.3, 22.9, 17.8. Spectral data are in good accordance with previously reported values.[15]



363 ***74% yield*** ***364***

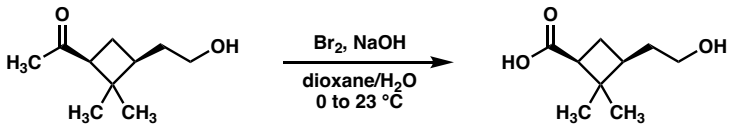
Ketoalcohol 364: To a stirred solution of **363** (2.50 g, 14.9 mmol, 1.0 equiv) in 1,2-DCE (25 mL) at 23 °C was added $Na(OAc)_3BH$ (7.25 g, 34.2 mmol, 2.3 equiv) in one portion. The resulting suspension was stirred for 24 h at 23 °C, at which point TLC indicated complete consumption of **363**. The mixture was quenched by addition of H_2O (25 mL) and diluted with Et_2O (100 mL) and H_2O (100 mL). The layers were separated and the aqueous layer was extracted with Et_2O (3 × 100 mL). The combined organic phases were washed with brine, dried over $MgSO_4$, and concentrated. The crude product was purified by flash chromatography (30–60% EtOAc/hexanes) to afford the title compound as a colorless oil (1.88 g, 11.0 mmol, 74% yield). $[\alpha]_D^{25}$ +65.5° (*c* 1.0, $CHCl_3$).

^{1}H NMR (600 MHz, $CDCl_3$): δ 3.61 – 3.45 (m, 2H), 2.80 (dd, *J* = 10.2, 7.5 Hz, 1H), 2.02 – 1.97 (m, 4H), 1.92 – 1.78 (m, 2H), 1.58 (dq, *J* = 13.5, 6.8 Hz, 1H), 1.46 – 1.38 (m, 1H), 1.26 (s, 3H), 0.83 (s, 3H).

^{13}C NMR (150 MHz, $CDCl_3$): δ 208.3, 61.2, 54.5, 43.4, 38.7, 33.2, 30.5, 30.2, 23.1, 17.3.

IR (thin film, NaCl): 3413, 2948, 2872, 1702, 1461, 1384, 1367, 1357, 1224, 1181, 1157, 1181, 1053 cm^{-1}.

HRMS (MM:ESI-APCI+) *m/z* calc'd for $[M+Na]^+$ $C_{10}H_{18}O_2Na$ = 193.1204, found 193.1205.



364 ***365***

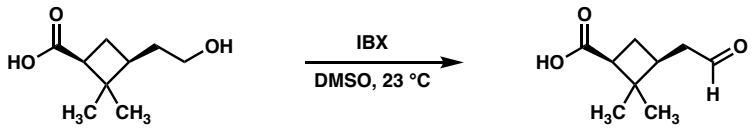
Alcohol 365: To a stirred solution of alcohol **364** (750 mg, 4.40 mmol, 1.0 equiv) in H_2O/dioxane (1:5, 65 mL) at 0 °C was added dropwise an aqueous solution of NaOBr, prepared via addition of Br_2 (745 µL, 14.5 mmol, 3.3 equiv) to a solution of NaOH (2.29 g, 57.2 mmol, 13.0 equiv) in H_2O (22 mL) at 0 °C. The mixture was stirred for 2 h and gradually allowed to warm to 23 °C, at which point TLC indicated complete consumption of **364**. The mixture was diluted with H_2O (100 mL) and washed with Et_2O (2 × 100 mL). The aqueous phase was acidified to pH 2 with concentrated HCl and extracted with EtOAc (3 × 100 mL). The combined organic phases were washed with brine, dried over $MgSO_4$, and concentrated to afford the title compound as a colorless oil (729 mg, 4.23 mmol, 96% yield) in sufficient purity by NMR for use in the subsequent reaction. $[\alpha]_D^{25} = -9.4°$ (*c* 1.0, $CHCl_3$).

^{1}H NMR (400 MHz, $CDCl_3$): δ 3.62 – 3.51 (m, 2H), 2.72 (dd, *J* = 10.2, 7.3 Hz, 1H), 2.08 – 1.95 (m, 2H), 1.93 – 1.78 (m, 1H), 1.64 (dq, *J* = 13.4, 6.9 Hz, 1H), 1.55 – 1.44 (m, 1H), 1.20 (s, 3H), 0.98 (s, 3H).

^{13}C NMR (100 MHz, $CDCl_3$): δ 178.5, 61.2, 46.2, 43.0, 39.0, 33.3, 30.3, 24.5, 17.6.

IR (thin film, NaCl): 3373, 2952, 2885, 2730, 1699, 1460, 1417, 1369, 1332, 1244, 1203, 1050, 1029 cm^{-1}.

HRMS (MM:ESI-APCI–): *m/z* calc'd for $[M–H]^-$ $C_9H_{15}O_3$ = 171.1021, found 171.1021.



365 ***62% yield*** ***366***

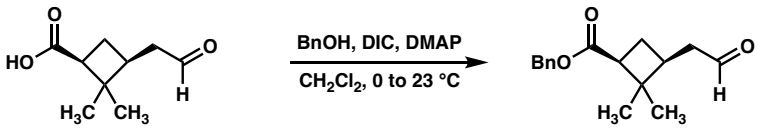
Aldehyde 366: To a stirred solution of acid **365** (729 mg, 4.23 mmol, 1.0 equiv) in DMSO (42 mL) at 23 °C was added IBX (7.25 g, 6.35 mmol, 1.5 equiv) in one portion. The mixture was stirred for 16 h at 23 °C, at which point TLC indicated complete consumption of **365**. The solution was diluted with EtOAc (100 mL) and H_2O (100 mL). The layers were separated and the aqueous layer was extracted with EtOAc (3 × 100 mL). The combined organic phases were washed with brine, dried over $MgSO_4$, and concentrated. The crude product was purified by flash chromatography (20–50% EtOAc/hexanes) to afford the title compound as a colorless oil (443 mg, 2.60 mmol, 62% yield). $[\alpha]_D^{25} = -0.80°$ (*c* 1.0, $CHCl_3$).

^{1}H NMR (600 MHz, $CDCl_3$): δ 9.72 (t, *J* = 1.5 Hz, 1H), 2.81 (dd, *J* = 10.2, 7.9 Hz, 1H), 2.56 – 2.49 (m, 1H), 2.48 – 2.40 (m, 2H), 2.13 (dt, *J* = 11.4, 7.8 Hz, 1H), 1.92 (dt, *J* = 11.3, 10.0 Hz, 1H), 1.25 (s, 3H), 0.97 (s, 3H).

^{13}C NMR (100 MHz, $CDCl_3$): δ 201.6, 179.0, 46.4, 45.4, 43.1, 36.1, 30.2, 24.2, 18.0.

IR (thin film, NaCl): 2960, 1873, 1733, 1705, 1698, 1650, 1425, 1247, 1216, 1161, 935 cm^{-1}.

HRMS (ESI-TOF): *m/z* calc'd for $[M-H]^-$ $C_9H_{13}O_3$ = 169.0865, found 169.0864.



366 ***71% yield*** ***367***

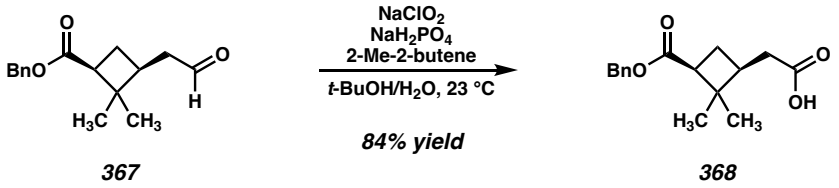
Benzyl ester 366: To a stirred solution of aldehyde **367** (200 mg, 1.18 mmol, 1.0 equiv), benzyl alcohol (245 µL, 2.36 mmol, 2.0 equiv), and DMAP (7.2 mg, 0.0590 mmol, 0.05 equiv) in CH_2Cl_2 (12 mL) at 0 °C was added DIC (370 µL, 2.36 mmol, 2.0 equiv) dropwise. The mixture was stirred for 2 h and gradually allowed to warm to 23 °C, at which point TLC indicated complete consumption of **367**. The solution was diluted with Et_2O (50 mL) and H_2O (50 mL). The layers were separated and the aqueous layer was extracted with Et_2O (3 × 50 mL). The combined organic phases were washed with brine, dried over $MgSO_4$, and concentrated. The crude product was purified by flash chromatography (10–20% EtOAc/hexanes) to afford the title compound as a colorless oil (219 mg, 0.841 mmol, 71% yield). $[\alpha]_D^{25} = -5.1°$ (*c* 0.83, $CHCl_3$).

^{1}H NMR (400 MHz, $CDCl_3$): δ 9.68 (t, *J* = 1.7 Hz, 1H), 7.38 – 7.21 (m, 5H), 5.13 – 5.02 (m, 2H), 2.79 (dd, *J* = 10.2, 7.9 Hz, 1H), 2.53 – 2.33 (m, 3H), 2.14 – 2.06 (m, 1H), 2.02 – 1.88 (m, 1H), 1.20 (s, 3H), 0.83 (s, 3H).

^{13}C NMR (100 MHz, $CDCl_3$): δ 201.4, 172.6, 136.2, 128.6, 128.3, 128.2, 66.0, 46.4, 45.4, 42.9, 36.1, 30.2, 24.4, 18.0.

IR (thin film, NaCl): 2954, 2880, 2718, 1726, 1455, 1383, 1336, 1231, 1173, 1130, 1023, 749, 735, 696 cm^{-1}.

HRMS (ESI-TOF): *m/z* calc'd for $[M+Na]^+$ $C_{16}H_{20}O_3Na$ = 283.1310, found 283.1307.



367 ***368***

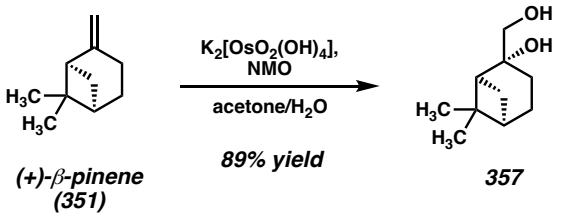
Acid 368: To a stirred solution of benzyl ester **368** (397 mg, 1.52 mmol, 1.0 equiv), NaH_2PO_4 (1.09 g, 9.12 mmol, 6.0 equiv), and 2-Me-2-butene (12.9 mL, 122 mmol, 80.0 equiv) in *t*-BuOH/H_2O (5:1, 180 mL) at 23 °C was added $NaClO_2$ (413 mg, 4.56 mmol, 3.0 equiv) in one portion. The mixture was stirred for 2 h at 23 °C, at which point TLC indicated complete consumption of **368**. The *t*-BuOH was removed by rotary evaporation, and the remaining solution was diluted with EtOAc (50 mL) and H_2O (50 mL). The layers were separated and the aqueous layer was extracted with EtOAc (3 × 50 mL). The combined organic phases were washed with brine, dried over $MgSO_4$, and concentrated. The crude product was purified by flash chromatography (50–60% EtOAc/hexanes) to afford the title compound as a colorless oil (353 mg, 1.28 mmol, 84% yield). $[\alpha]_D^{25} = -9.4°$ (*c* 1.0, $CHCl_3$).

^{1}H NMR (400 MHz, $CDCl_3$): δ 7.38 – 7.29 (m, 5H), 5.17 – 5.05 (m, 2H), 2.80 (dd, *J* = 10.3, 7.8 Hz, 1H), 2.46 – 2.28 (m, 2H), 2.20 – 2.07 (m, 1H), 2.06 – 1.92 (m, 1H), 1.30 – 1.15 (m, 4H), 0.90 (s, 3H).

^{13}C NMR (100 MHz, $CDCl_3$): δ 179.0, 172.7, 136.3, 128.6, 128.4, 128.3, 66.1, 46.3, 43.0, 38.2, 35.2, 30.1, 24.6, 17.8.

IR (thin film, NaCl): 3064, 3032, 2956, 1731, 1705, 1455, 1385, 1234, 1170, 747, 697 cm^{-1}.

HRMS (MM:ESI-APCI–): *m/z* calc'd for $[M-H]^-$ $C_{16}H_{19}O_4$ = 275.1283, found 275.1290.

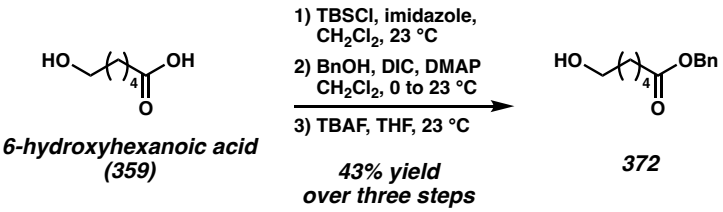


(+)-β-pinene (351) *357*

(+)-β-Pinanediol 357: (+)-β-Pinanediol (**357**) was prepared from commercial (+)-β-pinene (**351**, ≥98%, 97% ee, Sigma-Aldrich). To a stirred solution of (+)-β-pinene (**351**, 1.00 mL, 6.36 mmol, 1.0 equiv) and NMO (1.12 g, 9.54 mmol, 1.5 equiv) in acetone/H_2O (4:1, 15 mL) at 23 °C was added $K_2[OsO_2(OH)_4]$ (117 mg, 0.318 mmol, 0.05 equiv) in one portion. The mixture was stirred for 24 h at 23 °C, at which point TLC indicated complete consumption of the starting material. The mixture was quenched by addition of saturated aqueous $NaHSO_3$ (25 mL), stirred for an additional 30 min, then diluted with EtOAc (30 mL) and H_2O (30 mL). The layers were separated and the aqueous layer was extracted with EtOAc (3 × 30 mL). The combined organic phases were washed with brine, dried over $MgSO_4$, and concentrated. The crude product was purified by flash chromatography (65% EtOAc/hexanes) to afford to afford the title compound as a white solid (962 mg, 5.65 mmol, 89% yield).

^{1}H NMR (400 MHz, $CDCl_3$): δ 3.52 – 3.46 (m, 2H), 2.25 – 2.17 (m, 1H), 2.05 (t, *J* = 4.9 Hz, 1H), 1.98 – 1.88 (m, 2H), 1.83 – 1.66 (m, 3H), 1.46 (d, *J* = 10.2 Hz, 1H), 1.24 (s, 3H), 0.92 (s, 3H).

^{13}C NMR (100 MHz, $CDCl_3$): δ 77.2, 69.9, 48.5, 41.2, 38.3, 27.6, 27.4, 27.0, 24.8, 23.5. Spectral data are in good accordance with previously reported values.[16]



Alcohol 372: To a stirred solution of 6-hydroxyhexanoic acid (**359**, 150 mg, 1.14 mmol, 1.0 equiv) and imidazole (310 mg, 4.56 mmol, 4.0 equiv) in CH_2Cl_2 (12 mL) at 23 °C was added TBSCl (344 mg, 2.28 mmol, 2.0 equiv) in one portion. The mixture was stirred for 16 h at 23 °C, at which point TLC indicated complete consumption of the starting material. The solution was diluted with Et_2O (30 mL) and H_2O (30 mL). The layers were separated and the aqueous layer was extracted with Et_2O (3 × 30 mL). The combined organic phases were washed with brine, dried over $MgSO_4$, and concentrated. The crude product was purified by flash chromatography (30% Et_2O/hexanes) to afford an intermediate silyl ether a colorless oil (163 mg, 0.661 mmol, 58% yield).

^{1}H NMR (500 MHz, $CDCl_3$): δ 3.61 (t, *J* = 6.4 Hz, 2H), 2.37 (t, *J* = 7.5 Hz, 2H), 1.70 – 1.64 (m, 2H), 1.57 1.52 (m, 2H), 1.44 – 1.37 (m, 2H), 0.90 (s, 9H), 0.05 (s, 6H).

^{13}C NMR (125 MHz, $CDCl_3$): δ 180.3, 63.0, 34.2, 32.5, 26.1, 25.5, 24.6, 18.5, -5.2. Spectral data are in good accordance with previously reported values.[17]

To a stirred solution of the intermediate silyl ether (not shown, 150 mg, 0.609 mmol, 1.0 equiv), benzyl alcohol (127 μL, 1.22 mmol, 2.0 equiv), and DMAP (3.7 mg, 0.0305 mmol, 0.05 equiv) in CH_2Cl_2 (6.1 mL) at 0 °C was added DIC (191 μL, 1.22 mmol, 2.0 equiv) dropwise. The mixture was stirred for 16 h and gradually allowed to warm to 23 °C, at which point TLC indicated complete consumption of the starting material. The solution was diluted with Et_2O (30 mL) and H_2O (30 mL). The layers were separated and the aqueous layer was extracted with Et_2O (3 × 30 mL). The combined organic phases were

washed with brine, dried over $MgSO_4$, and concentrated. The crude product was purified by flash chromatography (10% Et_2O/hexanes) to afford the title compound as a colorless oil (181 mg, 0.538 mmol, 88% yield).

^{1}H NMR (400 MHz, $CDCl_3$): δ 7.39 – 7.31 (m, 5H), 5.11 (s, 2H), 3.59 (t, *J* = 6.5 Hz, 2H), 2.37 (t, *J* = 7.6 Hz, 2H), 1.67 (p, *J* = 7.6 Hz, 2H), 1.60 – 1.47 (m, 2H), 1.42 – 1.30 (m, 2H), 0.89 (s, 9H), 0.04 (s, 6H).

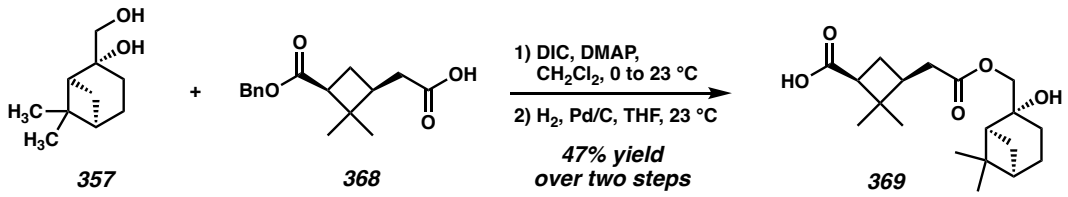
^{13}C NMR (100 MHz, $CDCl_3$): δ 173.7, 136.3, 128.7, 128.6, 128.3, 66.2, 63.1, 34.5, 32.6, 26.1, 25.6, 24.9, 18.5, -5.1.

Spectral data are in good accordance with previously reported values.[17]

To a stirred solution of the intermediate benzyl ester (not shown, 175 mg, 0.520 mmol, 1.0 equiv) in THF (5.2 mL) at 23 °C was added TBAF (1.0 M in THF, 1.56 mL, 1.56 mmol, 3.0 equiv) in one portion. The mixture was stirred for 3 h at 23 °C, at which point TLC indicated complete consumption of the starting material. The solution was diluted with Et_2O (30 mL) and H_2O (30 mL). The layers were separated and the aqueous layer was extracted with Et_2O (3 × 30 mL). The combined organic phases were washed with brine, dried over $MgSO_4$, and concentrated. The crude product was purified by flash chromatography (60% Et_2O/hexanes) to afford the title compound as a colorless oil (98.3 mg, 0.442 mmol, 85% yield, 43% yield over three steps).

^{1}H NMR (400 MHz, $CDCl_3$): δ 7.41 – 7.29 (m, 5H), 5.11 (s, 2H), 3.62 (t, *J* = 6.5 Hz, 2H), 2.37 (t, *J* = 7.5 Hz, 2H), 1.74 – 1.62 (m, 2H), 1.60-1.53 (m, 2H), 1.44 – 1.34 (m, 2H).

^{13}C NMR (100 MHz, $CDCl_3$): δ 173.7, 136.1, 128.7, 128.3 (2C), 66.3, 62.7, 34.3, 32.4, 25.3, 24.7. Spectral data are in good accordance with previously reported values.[17]



Primary dimer ester 369: To a stirred solution of acid **368** (40.0 mg, 0.145 mmol, 1.0 equiv), **357** (24.7 mg, 0.145 mmol, 1.0 equiv), and DMAP (0.9 mg, 0.00725 mmol, 0.05 equiv) in CH_2Cl_2 (1.5 mL) at 0 °C was added DIC (23 μL, 0.145 mmol, 1.0 equiv) dropwise. The mixture was stirred for 16 h and gradually allowed to warm to 23 °C, at which point TLC indicated complete consumption of **368**. The solution was diluted with EtOAc (10 mL) and H_2O (10 mL). The layers were separated and the aqueous layer was extracted with Et_2O (3 X 10 mL). The combined organic phases were washed with brine, dried over $MgSO_4$, and concentrated. The crude product was purified by flash chromatography (20–40% EtOAc/hexanes) to afford an intermediate diester as a colorless oil (30.4 mg, 0.0709 mmol, 49% yield).

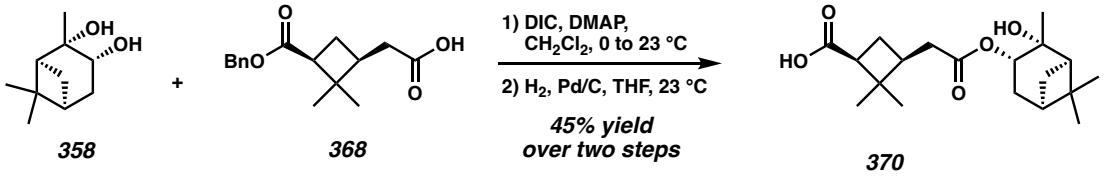
In a 2-necked round bottom flask equipped with a 3-way valve at 23 °C, the intermediate diester (30.4 mg, 0.0709 mmol, 1.0 equiv) was dissolved in THF (3.5 mL) and to this solution was added Pd/C (10% w/w, 15 mg). The flask was evacuated and backfilled with N_2 (3X), then purged and backfilled with H_2 (3X). The suspension was stirred for 3 h at 23 °C under H_2 (1 atm, balloon), at which point TLC indicated complete consumption of the diester. The flask was evacuated and backfilled with N_2 (3X), then the suspension was diluted with EtOAc (10 mL), filtered through celite, and concentrated. The crude product was purified by flash chromatography (50–60% EtOAc/hexanes) to afford the title compound as a colorless oil (23.0 mg, 0.0680 mmol, 96% yield, 47% yield over two steps). $[\alpha]_D^{25}$ = +6.2° (c 1.0, $CHCl_3$).

^{1}H NMR (400 MHz, $CDCl_3$): δ 4.11 (d, J = 11.3 Hz, 1H), 4.04 (d, J = 11.3 Hz, 1H), 2.79 (dd, J = 10.3, 7.8 Hz, 1H), 2.46 – 2.30 (m, 3H), 2.26 – 2.19 (m, 1H), 2.17 – 2.09 (m, 1H), 2.01 – 1.90 (m, 4H), 1.86 – 1.72 (m, 3H), 1.54 (d, J = 10.3 Hz, 1H), 1.25 (s, 3H), 1.24 (s, 3H), 1.01 (s, 3H), 0.94 (s, 3H).

^{13}C NMR (100 MHz, $CDCl_3$): δ 178.0, 173.0, 75.7, 71.4, 49.0, 46.1, 43.0, 41.0, 38.5, 38.4, 35.4, 30.1, 27.6, 27.4, 26.9, 24.7, 24.6, 23.3, 17.8.

IR (thin film, NaCl): 2922, 2872, 1711, 1233, 1204, 757 cm^{-1}.

HRMS (ESI-TOF) m/z calc'd for $[M+H]^+$ $C_{19}H_{29}O_5$ = 337.2015, found 337.2013.



358 *368* *370*

Primary dimer ester 370: Dimer ester **370** was prepared from commercial (+)-α-pinanediol (**358**, 99%, 99% ee, Sigma-Aldrich). To a stirred solution of acid **368** (40.0 mg, 0.145 mmol, 1.0 equiv), (+)-α-pinanediol (**358**, 24.7 mg, 0.145 mmol, 1.0 equiv), and DMAP (0.9 mg, 0.00725 mmol, 0.05 equiv) in CH_2Cl_2 (1.5 mL) at 0 °C was added DIC (23 μL, 0.145 mmol, 1.0 equiv) dropwise. The mixture was stirred for 16 h and gradually allowed to warm to 23 °C, at which point TLC indicated complete consumption of **368**. The solution was diluted with EtOAc (10 mL) and H_2O (10 mL). The layers were separated and the aqueous layer was extracted with Et_2O (3 × 10 mL). The combined organic phases were washed with brine, dried over $MgSO_4$, and concentrated. The crude product was purified by flash chromatography (50–60% EtOAc/hexanes) to afford an intermediate diester as a colorless oil (44.1 mg, 0.103 mmol, 71% yield).

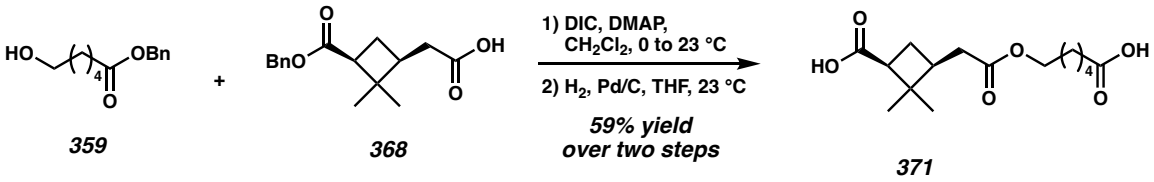
In a 2-necked round bottom flask equipped with a 3-way valve at 23 °C, the intermediate diester (22.0 mg, 0.0513 mmol, 1.0 equiv) was dissolved in THF (2.6 mL) and to this solution was added Pd/C (10% w/w, 11 mg). The flask was evacuated and backfilled with N_2 (3×), then purged and backfilled with H_2 (3×). The suspension was stirred for 3 h at 23 °C under H_2 (1 atm, balloon), at which point TLC indicated complete consumption of the diester. The flask was evacuated and backfilled with N_2 (3×), then the suspension was diluted with EtOAc (10 mL), filtered through celite, and concentrated. The crude product was purified by flash chromatography (50–60% EtOAc/hexanes) to afford the title compound as a colorless oil (11.0 mg, 0.0325 mmol, 63% yield, 45% yield over two steps). $[\alpha]_D^{25} = -2.6°$ (*c* 1.0, $CHCl_3$).

^{1}H NMR (400 MHz, $CDCl_3$): δ 5.12 (dd, *J* = 9.6, 5.4 Hz, 1H), 2.80 (dd, *J* = 10.2, 7.9 Hz, 1H), 2.54 – 2.34 (m, 4H), 2.24 (dtd, *J* = 10.6, 6.1, 2.5 Hz, 1H), 2.19 – 2.11 (m, 1H), 2.04 – 1.89 (m, 3H), 1.62 (ddd, *J* = 14.1, 5.5, 2.5 Hz, 1H), 1.46 (d, *J* = 10.5 Hz, 1H), 1.30 (s, 3H), 1.28 (s, 3H), 1.27 (s, 3H), 1.02 (s, 3H), 0.99 (s, 3H).

^{13}C NMR (100 MHz, $CDCl_3$): δ 177.7, 172.1, 74.0, 72.0, 54.3, 46.1, 43.0, 40.5, 38.8, 38.6, 35.7, 34.9, 30.1, 30.0, 28.4, 28.0, 24.5, 24.3, 17.9.

IR (thin film, NaCl): 3794, 2953, 2924, 2873, 1726, 1705, 1234, 1217, 1187, 1157, 1010, 931, 828, 758 cm^{-1}.

HRMS (ESI-TOF): *m/z* calc'd for $[M-H]^-$ $C_{19}H_{29}O_5$ = 337.2015, found 337.2016.



Primary dimer ester 371: To a stirred solution of acid **368** (25.0 mg, 0.0905 mmol, 1.0 equiv), alcohol **359** (20.1 mg, 0.0905 mmol, 1.0 equiv), and DMAP (0.6 mg, 0.00453 mmol, 0.05 equiv) in CH_2Cl_2 (1.0 mL) at 0 °C was added DIC (14 μL, 0.0905 mmol, 1.0 equiv) dropwise. The mixture was stirred for 16 h and gradually allowed to warm to 23 °C, at which point TLC indicated complete consumption of **368**. The solution was diluted with EtOAc (10 mL) and H_2O (10 mL). The layers were separated and the aqueous layer was extracted with Et_2O (3 × 10 mL). The combined organic phases were washed with brine, dried over $MgSO_4$, and concentrated. The crude product was purified by flash chromatography (40–50% EtOAc/hexanes) to afford an intermediate triester as a colorless oil (29.0 mg, 0.0603 mmol, 67% yield).

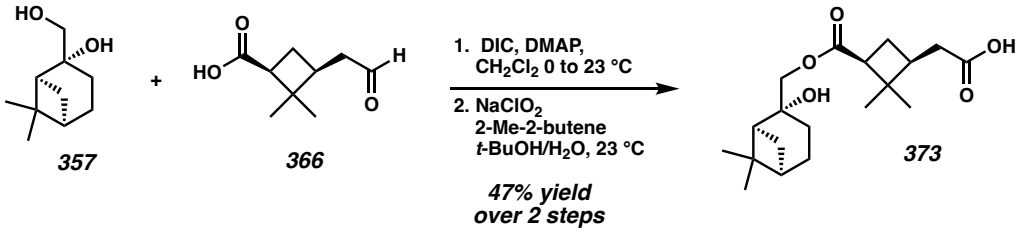
In a 2-necked round bottom flask equipped with a 3-way valve at 23 °C, the intermediate triester (20.0 mg, 0.0416 mmol, 1.0 equiv) was dissolved in THF (2.1 mL) and to this solution was added Pd/C (10% w/w, 10 mg). The flask was evacuated and backfilled with N_2 (3×), then purged and backfilled with H_2 (3×). The suspension was stirred for 3 h at 23 °C under H_2 (1 atm, balloon), at which point TLC indicated complete consumption of the triester. The flask was evacuated and backfilled with N_2 (3×), then the suspension was diluted with EtOAc (10 mL), filtered through celite, and concentrated. The crude product was purified by flash chromatography (50–80% EtOAc/hexanes) to afford the title compound as a colorless oil (11.0 mg, 0.0366 mmol, 88% yield, 59% yield over two steps). $[\alpha]_D^{25} = -1.3°$ (*c* 1.0, $CHCl_3$).

^{1}H NMR (400 MHz, $CDCl_3$): δ 4.07 (t, *J* = 6.4 Hz, 2H), 2.79 (dd, *J* = 10.2, 7.8 Hz, 1H), 2.44 – 2.22 (m, 5H), 2.16 – 2.04 (m, 1H), 1.97 – 1.87 (m, 1H), 1.73 – 1.58 (m, 4H), 1.47 – 1.38 (m, 2H), 1.24 (s, 3H), 1.00 (s, 3H).

^{13}C NMR (100 MHz, $CDCl_3$): δ 179.4, 178.4, 172.9, 64.3, 46.2, 43.1, 38.5, 35.6, 33.9, 30.0, 28.4, 25.7, 24.5, 24.4, 17.7.

IR (thin film, NaCl): 3801, 2352, 1725, 1704, 1416, 1255, 1234, 1219, 1204, 1187, 817, 682 cm^{-1}.

HRMS (ESI-TOF): *m/z* calc'd for $[M–H]^-$ $C_{15}H_{23}O_6$ = 299.1495, found 299.1493.



Secondary dimer ester 373: To a stirred solution of aldehyde **366** (50.0 mg, 0.294 mmol, 1.0 equiv), (+)-β-pinanediol (**357**) (50.0 mg, 0.294 mmol, 1.0 equiv), and DMAP (2.0 mg, 0.0147 mmol, 0.05 equiv) in CH_2Cl_2 (3.0 mL) at 0 °C was added DIC (46 μL, 0.294 mmol, 1.0 equiv) dropwise. The mixture was stirred for 16 h and gradually allowed to warm to 23 °C, at which point TLC indicated complete consumption of **366**. The solution was diluted with EtOAc (10 mL) and H_2O (10 mL). The layers were separated and the aqueous layer was extracted with Et_2O (3 × 10 mL). The combined organic phases were washed with brine, dried over $MgSO_4$, and concentrated. The crude product was purified by flash chromatography (30–50% EtOAc/hexanes) to afford an intermediate ester as a colorless oil (80.6 mg, 0.250 mmol, 85% yield).

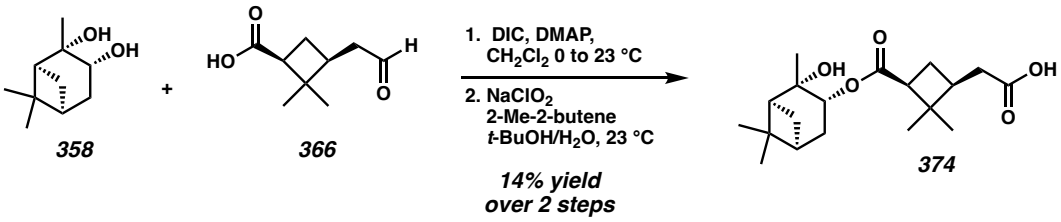
To a stirred solution of the intermediate ester (30.0 mg, 0.0930 mmol, 1.0 equiv), NaH_2PO_4 (66.7 mg, 0.558 mmol, 6.0 equiv), and 2-Me-2-butene (789 μL, 7.44 mmol, 80.0 equiv) in *t*-BuOH/H_2O (5:1, 11 mL) at 23 °C was added $NaClO_2$ (25.3 mg, 0.279 mmol, 3.0 equiv) in one portion. The mixture was stirred for 2 h at 23 °C, at which point TLC indicated complete consumption of the ester. The *t*-BuOH was removed by rotary evaporation, and the remaining solution was diluted with EtOAc (10 mL) and H_2O (10 mL). The layers were separated and the aqueous layer was extracted with EtOAc (3 × 10 mL). The combined organic phases were washed with brine, dried over $MgSO_4$, and concentrated. The crude product was purified by flash chromatography (20–50% EtOAc/hexanes) to afford the title compound as a colorless oil (17.3 mg, 0.0511 mmol, 55% yield, 47% yield over two steps). $[\alpha]_D^{25} = +11.2°$ (*c* 1.0, $CHCl_3$).

^{1}H NMR (400 MHz, $CDCl_3$): δ 4.11 (d, *J* = 11.2 Hz, 1H), 4.02 (d, *J* = 11.2 Hz, 1H), 2.79 (dd, *J* = 10.3, 7.8 Hz, 1H), 2.45 – 2.29 (m, 3H), 2.26 – 2.18 (m, 1H), 2.18 – 2.10 (m, 1H), 2.03 – 1.90 (m, 4H), 1.86 – 1.72 (m, 3H), 1.54 (d, *J* = 10.1 Hz, 1H), 1.24 (s, 6H), 0.96 (s, 3H), 0.95 (s, 3H).

^{13}C NMR (100 MHz, $CDCl_3$): δ 178.3, 173.0, 75.7, 71.4, 49.1, 46.4, 43.0, 41.0, 38.4, 38.2, 35.2, 30.2, 27.6, 27.5, 26.9, 24.7, 24.7, 23.4, 18.1.

IR (thin film, NaCl): 3793, 2953, 2923, 2869, 1725, 1710, 1386, 1233, 1219, 1187, 1175, 918, 828, 759 cm^{-1}.

HRMS (ESI-TOF): *m/z* calc'd for $[M–H]^-$ $C_{19}H_{29}O_5$ = 337.2015, found 337.2018.



Secondary dimer ester 374: To a stirred solution of aldehyde **366** (50.0 mg, 0.294 mmol, 1.0 equiv), (+)-α-pinanediol (**358**, 50.0 mg, 0.294 mmol, 1.0 equiv), and DMAP (2.0 mg, 0.0147 mmol, 0.05 equiv) in CH_2Cl_2 (3.0 mL) at 0 °C was added DIC (46 μL, 0.294 mmol, 1.0 equiv) dropwise. The mixture was stirred for 16 h and gradually allowed to warm to 23 °C, at which point TLC indicated complete consumption of **366**. The solution was diluted with EtOAc (10 mL) and H_2O (10 mL). The layers were separated and the aqueous layer was extracted with Et_2O (3 × 10 mL). The combined organic phases were washed with brine, dried over $MgSO_4$, and concentrated. The crude product was purified by flash chromatography (20–40% EtOAc/hexanes) to afford an intermediate ester as a colorless oil (43.8 mg, 0.136 mmol, 46% yield).

To a stirred solution of the intermediate ester (20.0 mg, 0.0620 mmol, 1.0 equiv), NaH_2PO_4 (44.6 mg, 0.372 mmol, 6.0 equiv), and 2-Me-2-butene (526 μL, 4.96 mmol, 80.0 equiv) in *t*-BuOH/H_2O (5:1, 7.5 mL) at 23 °C was added $NaClO_2$ (16.9 mg, 0.186 mmol, 3.0 equiv) in one portion. The mixture was stirred for 2 h at 23 °C, at which point TLC indicated complete consumption of the ester. The *t*-BuOH was removed by rotary evaporation, and the remaining solution was diluted with EtOAc (10 mL) and H_2O (10 mL). The layers were separated and the aqueous layer was extracted with EtOAc (3 × 10 mL). The combined organic phases were washed with brine, dried over $MgSO_4$, and concentrated. The crude product was purified by flash chromatography (20–50%

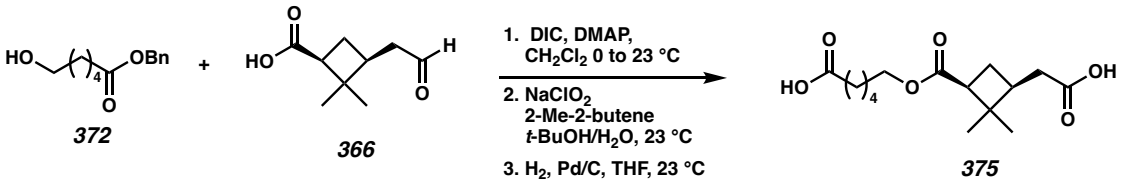
EtOAc/hexanes) to afford the title compound as a colorless oil (6.0 mg, 0.0177 mmol, 29% yield, 14% yield over two steps). $[\alpha]_D^{25} = -0.68°$ (*c* 0.83, $CHCl_3$).

^{1}H NMR (400 MHz, $CDCl_3$): δ 5.14 (dd, *J* = 9.6, 5.5 Hz, 1H), 2.83 (dd, *J* = 10.2, 7.8 Hz, 1H), 2.56 – 2.30 (m, 4H), 2.28 – 2.21 (m, 1H), 2.20 – 2.11 (m, 1H), 2.04 – 1.91 (m, 3H), 1.63 (ddd, *J* = 14.1, 5.5, 2.5 Hz, 1H), 1.47 (d, *J* = 10.5 Hz, 1H), 1.30 (s, 3H), 1.29 (s, 3H), 1.27 (s, 3H), 0.99 (s, 3H), 0.98 (s, 3H).

^{13}C NMR (100 MHz, $CDCl_3$): δ 177.8, 172.1, 74.0, 71.8, 54.2, 46.3, 43.0, 40.5, 38.8, 38.3, 35.3, 35.0, 30.3, 29.9, 28.5, 28.0, 24.7, 24.4, 17.9.

IR (thin film, NaCl): 3812, 2952, 2352, 2339, 1712, 1254, 1238, 1219, 1187, 829, 668 cm^{-1}.

HRMS (ESI-TOF): *m/z* calc'd for $[M–H]^-$ $C_{19}H_{29}O_5$ = 337.2015, found 337.2016.



24% yield over 3 steps

Secondary dimer ester 375: To a stirred solution of aldehyde **366**(28.0 mg, 0.165 mmol, 1.0 equiv), alcohol **372** (36.6 mg, 0.165 mmol, 1.0 equiv), and DMAP (1.0 mg, 0.00825 mmol, 0.05 equiv) in CH_2Cl_2 (1.7 mL) at 0 °C was added DIC (26 μL, 0.165 mmol, 1.0 equiv) dropwise. The mixture was stirred for 16 h and gradually allowed to warm to 23 °C, at which point TLC indicated complete consumption of **366**. The solution was diluted with EtOAc (10 mL) and H_2O (10 mL). The layers were separated and the aqueous layer was extracted with Et_2O (3 × 10 mL). The combined organic phases were washed with brine, dried over $MgSO_4$, and concentrated. The crude product was purified by flash

chromatography (20–50% EtOAc/hexanes) to afford an intermediate diester as a colorless oil (31.6 mg, 0.0844 mmol, 51% yield).

To a stirred solution of the intermediate diester (16.0 mg, 0.0427 mmol, 1.0 equiv), NaH_2PO_4 (30.7 mg, 0.256 mmol, 6.0 equiv), and 2-Me-2-butene (363 μL, 3.42 mmol, 80.0 equiv) in *t*-BuOH/H_2O (5:1, 5.2 mL) at 23 °C was added $NaClO_2$ (11.6 mg, 0.128 mmol, 3.0 equiv) in one portion. The mixture was stirred for 2 h at 23 °C, at which point TLC indicated complete consumption of the diester. The *t*-BuOH was removed by rotary evaporation, and the remaining solution was diluted with EtOAc (10 mL) and H_2O (10 mL). The layers were separated and the aqueous layer was extracted with EtOAc (3 × 10 mL). The combined organic phases were washed with brine, dried over $MgSO_4$, and concentrated. The crude product was purified by flash chromatography (30–60% EtOAc/hexanes) to afford an intermediate diester acid as a colorless oil (8.0 mg, 0.0204 mmol, 48% yield).

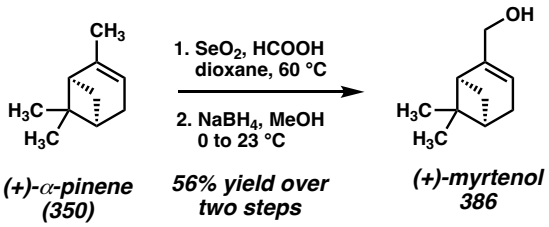
In a 2-necked round bottom flask equipped with a 3-way valve at 23 °C, the intermediate diester acid (8.0 mg, 0.0204 mmol, 1.0 equiv) was dissolved in THF (1.0 mL) and to this solution was added Pd/C (10% w/w, 10 mg). The flask was evacuated and backfilled with N_2 (3×), then purged and backfilled with H_2 (3×). The suspension was stirred for 3 h at 23 °C under H_2 (1 atm, balloon), at which point TLC indicated complete consumption of the diester acid. The flask was evacuated and backfilled with N_2 (3×), then the suspension was diluted with EtOAc (10 mL), filtered through celite, and concentrated. The crude product was purified by flash chromatography (50–80% EtOAc/hexanes) to afford the title compound as a colorless oil (5.9 mg, 0.0197 mmol, 97% yield, 24% yield over three steps). $[\alpha]_D^{25} = +6.1°$ (*c* 0.50, $CHCl_3$).

^{1}H NMR (400 MHz, $CDCl_3$): δ 4.08 (qt, *J* = 11.0, 6.2 Hz, 2H), 2.74 (dd, *J* = 10.3, 7.8 Hz, 1H), 2.45 – 2.28 (m, 5H), 2.17 – 2.06 (m, 1H), 2.01 – 1.91 (m, 1H), 1.71 – 1.61 (m, 4H), 1.49 – 1.40 (m, 2H), 1.23 (s, 3H), 0.94 (s, 3H).

^{13}C NMR (100 MHz, $CDCl_3$): δ 179.5, 178.7, 173.0, 64.0, 46.4, 42.9, 38.2, 35.2, 33.9, 30.1, 28.5, 25.7, 24.5, 24.4, 17.8.

IR (thin film, NaCl): 3550, 3278, 2957, 2925, 1729, 1707, 1687, 1638, 1233, 1179 cm^{-1}.

HRMS (ESI-TOF): *m/z* calc'd for $[M–H]^-$ $C_{15}H_{23}O_6$ = 299.1495, found 299.1495.



(+)-myrtenol 386: To a stirred solution of (+)-α-pinene (**350**, 5.83 mL, 36.7 mmol, 1.0 equiv) and HCOOH (2.08 mL, 55.1 mmol, 1.5 equiv) in dioxane (93 mL) at 23 °C was added SeO2 (4.07 g, 36.7 mmol, 1.0 equiv) in one portion. The mixture was heated to 60 °C and stirred for 24 h, at which point TLC indicated complete consumption of the starting material. The solution was diluted with saturated aqueous $NaHCO_3$ (200 mL) and EtOAc (200 mL). The layers were separated and the aqueous layer was extracted with EtOAc (3 × 150 mL). The combined organic phases were washed with brine, dried over $MgSO_4$, and concentrated to afford an intermediate aldehyde as an orange oil (3.86 g, 25.7 mmol, 70% yield) that was used in the next step without further purification.

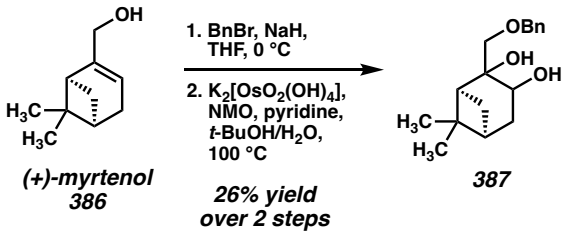
To a stirred solution of the intermediate aldehyde (3.86 g, 25.7 mmol, 1.0 equiv) in MeOH (205 mL) at 0 °C was added $NaBH_4$ (1.95 g, 51.4 mmol, 1.4 equiv) in one portion. The mixture was stirred for 1 h and gradually allowed to warm to 23 °C, at which point TLC indicated complete consumption of the aldehyde. The mixture was quenched by

addition of H_2O (100 mL) and diluted with EtOAc (150 mL) and H_2O (100 mL). The layers were separated and the aqueous layer was extracted with EtOAc (3 × 150 mL). The combined organic phases were washed with brine, dried over $MgSO_4$, and concentrated. The crude product was purified by flash chromatography (40% EtOAc/hexanes) to afford the title compound as a colorless oil (3.16 g, 20.8 mmol, 81% yield, 57% yield over two steps).

^{1}H NMR (600 MHz, $CDCl_3$): δ 5.47 (m, 1H), 3.99 (m, 2H), 2.45 – 2.38 (m, 1H), 2.35 – 2.21 (m, 2H), 2.17 – 2.08 (m, 2H), 1.30 (s, 3H), 1.18 (dd, *J* = 8.6, 1.2 Hz, 1H), 0.84 (s, 3H).

^{13}C NMR (100 MHz, $CDCl_3$): δ 147.9, 118.1, 66.2, 43.5, 41.1, 38.1, 31.8, 31.3, 26.3, 21.3.

Spectral data are in good accordance with previously reported values.[18]



Diol 387: To a stirred solution of NaH (60% w/w dispersion in mineral oil, 1.66 g, 41.6 mmol, 2.0 equiv) in THF (60 mL) at 0 °C was added (+)-myrtenol (**386**) (3.17 g, 20.8 mmol, 1.0 equiv) in one portion and the mixture was stirred for 1 h. Benzyl bromide (4.94 mL, 41.6 mmol, 2.0 equiv) was added dropwise and the mixture was stirred for an additional 2 h at 0 °C, at which point TLC indicated complete consumption of **386**. The mixture was quenched by addition of saturated aqueous NH_4Cl (50 mL) and diluted with EtOAc (150 mL) and H_2O (150 mL). The layers were separated and the aqueous layer was extracted with EtOAc (3 × 150 mL). The combined organic phases were washed with brine, dried over $MgSO_4$, and concentrated to afford an intermediate benzyl ether as a yellow oil (4.99 g, 20.6 mmol, 99% yield) that was used in the next step without further purification.

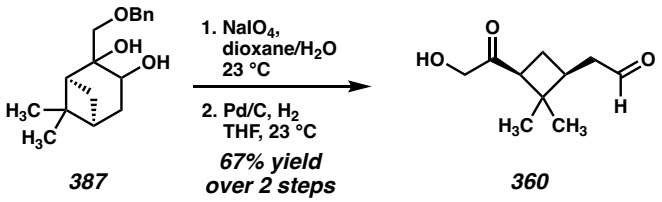
To a stirred solution of the intermediate benzyl ether (4.99 g, 20.6 mmol, 1.0 equiv), NMO (2.53 g, 21.6 mmol, 1.05 equiv), and pyridine (1.66 mL, 20.6 mmol, 1.0 equiv) in *t*-BuOH/H_2O (5:1, 18 mL) at 23 °C was added $K_2[OsO_2(OH)_4]$ (19.0 mg, 0.0515 mmol, 0.0025 equiv) in one portion. A reflux condenser was attached, the mixture was heated to 100 °C, and the mixture was stirred for 24 h at 100 °C, at which point TLC indicated complete consumption of the benzyl ether. The solution was cooled to 23 °C and diluted with saturated aqueous $NaHSO_3$ (30 mL) and EtOAc (30 mL). The layers were separated and the aqueous layer was extracted with EtOAc (3 × 50 mL). The combined organic phases were washed with brine, dried over $MgSO_4$, and concentrated. The crude product was purified by flash chromatography (35% EtOAc/hexanes) to afford the title compound as a white solid (1.51 g, 5.46 mmol, 27% yield, 26% yield over two steps). $[\alpha]_D^{25} = +2.9°$ (*c* 1.0, $CHCl_3$).

^{1}H NMR (400 MHz, $CDCl_3$): δ 7.38 – 7.27 (m, 5H), 4.63 – 4.51 (m, 2H), 4.16 (ddd, *J* = 9.4, 6.1, 0.9 Hz, 1H), 3.50 (dd, *J* = 9.2, 0.8 Hz, 1H), 3.37 (dd, *J* = 9.2, 0.8 Hz, 1H), 2.48 – 2.36 (m, 1H), 2.26 – 2.15 (m, 1H), 2.07 (t, *J* = 5.9 Hz, 1H), 1.91 (m, 1H), 1.66 (ddd, *J* = 13.9, 6.1, 2.3 Hz, 1H), 1.50 (d, *J* = 10.3 Hz, 1H), 1.23 (s, 3H), 0.83 (s, 3H).

^{13}C NMR (100 MHz, $CDCl_3$): δ 138.0, 128.7, 128.0, 127.9, 77.6, 75.3, 73.7, 66.4, 49.4, 40.8, 38.9, 36.9, 28.1, 28.1, 24.3.

IR (thin film, NaCl): 3798, 3435, 2904, 2366, 1454, 1085 cm^{-1}.

HRMS (FI): *m/z* calc'd for $[M]^{\bullet+}$ $C_{17}H_{24}O_3$ = 276.1725, found 276.1724.



387 *360*

Alcohol 360: To a stirred solution of diol **387** (1.50 g, 5.43 mmol, 1.0 equiv) in dioxane/H_2O (3:1, 28 mL) at 23 °C was added $NaIO_4$ (4.65 g, 21.7 mmol, 4.0 equiv) in one portion. The mixture was stirred for 24 h at 23 °C, at which point TLC indicated complete consumption of **387**. The solution was diluted with Et_2O (100 mL) and H_2O (100 mL). The layers were separated and the aqueous layer was extracted with Et_2O (3 × 100 mL). The combined organic phases were washed with brine, dried over $MgSO_4$, and concentrated to afford an intermediate benzyl ether aldehyde as a colorless oil (1.25 g, 4.56 mmol, 84% yield) that was used in the next step without further purification.

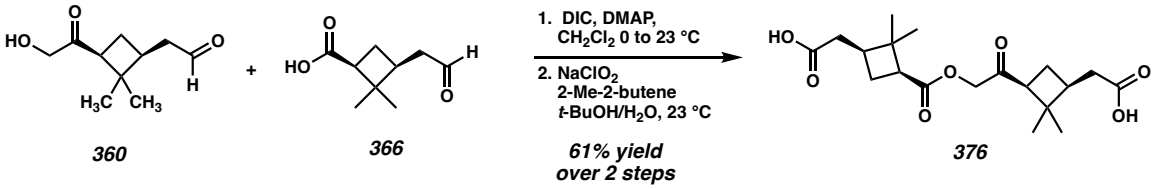
In a 2-necked round bottom flask equipped with a 3-way valve at 23 °C, the intermediate benzyl ether aldehyde (1.25 g, 4.56 mmol, 1.0 equiv) was dissolved in THF (46 mL) and to this solution was added Pd/C (10% w/w, 483 mg). The flask was evacuated and backfilled with N_2 (3×), then purged and backfilled with H_2 (3×). The suspension was stirred for 20 h at 23 °C under H_2 (1 atm, balloon), at which point TLC indicated complete consumption of the benzyl ether. The flask was evacuated and backfilled with N_2 (3×), then the suspension was diluted with EtOAc (40 mL), filtered through celite, and concentrated. The crude product was purified by flash chromatography (50–60% EtOAc/hexanes) to afford the title compound as a colorless oil (670 mg, 3.64 mmol, 80% yield, 67% yield over two steps). $[\alpha]_D^{25} = +7.9°$ (*c* 1.0, $CHCl_3$).

^{1}H NMR (400 MHz, $CDCl_3$): δ 9.74 (t, *J* = 1.2 Hz, 1H), 4.12 (q, *J* = 18.9 Hz, 2H), 3.21 – 3.08 (m, 1H), 2.91 (dd, *J* = 10.0, 7.6 Hz, 1H), 2.59 – 2.40 (m, 3H), 2.15 – 1.96 (m, 2H), 1.29 (s, 3H), 0.83 (s, 3H).

^{13}C NMR (100 MHz, $CDCl_3$): δ 207.9, 201.2, 68.8, 49.9, 45.2, 44.0, 36.2, 30.7, 22.4, 17.9.

IR (thin film, NaCl): 3439, 2952, 1713, 1367, 1274, 1226, 1078 cm^{-1}.

HRMS (FI): *m/z* calc'd for $[M]^{\bullet+}$ $C_{10}H_{16}O_3$ = 184.1099, found 184.1104.



Secondary dimer ester 376: To a stirred solution of aldehyde **366** (277 mg, 1.63 mmol, 1.0 equiv), alcohol **360** (300 mg, 1.63 mmol, 1.0 equiv), and DMAP (10.0 mg, 0.0815 mmol, 0.05 equiv) in CH_2Cl_2 (32.6 mL) at 0 °C was added DIC (255 μL, 1.63 mmol, 1.0 equiv) dropwise. The mixture was stirred for 16 h and gradually allowed to warm to 23 °C, at which point TLC indicated complete consumption of **366**. The solution was diluted with EtOAc (50 mL) and H_2O (50 mL). The layers were separated and the aqueous layer was extracted with Et_2O (3 × 50 mL). The combined organic phases were washed with brine, dried over $MgSO_4$, and concentrated. The crude product was purified by flash chromatography (30–40% EtOAc/hexanes) to afford an intermediate ester as a colorless oil (454 mg, 1.35 mmol, 83% yield).

To a stirred solution of the intermediate ester (454 mg, 1.35 mmol, 1.0 equiv), NaH_2PO_4 (1.94 g, 16.2 mmol, 12.0 equiv), and 2-Me-2-butene (11.5 mL, 108 mmol, 80.0 equiv) in *t*-BuOH/H_2O (5:1, 170 mL) at 23 °C was added $NaClO_2$ (733 mg, 8.10 mmol, 6.0 equiv) in one portion. The mixture was stirred for 3 h at 23 °C, at which point TLC

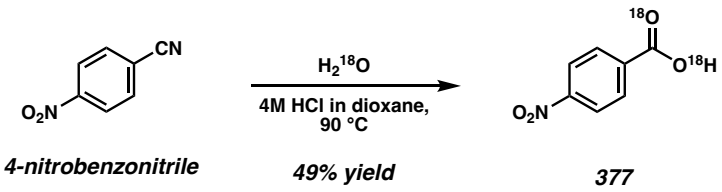
indicated complete consumption of the ester. The *t*-BuOH was removed by rotary evaporation, and the remaining solution was diluted with EtOAc (50 mL) and H_2O (50 mL). The layers were separated and the aqueous layer was extracted with EtOAc (3 × 50 mL). The combined organic phases were washed with brine, dried over $MgSO_4$, and concentrated. The crude product was purified by flash chromatography (30–40% EtOAc/hexanes; 1% AcOH). Residual AcOH was removed by rotary evaporation with added toluene to afford the title compound as a white solid (363 mg, 0.0985 mmol, 73% yield, 61% yield over two steps). $[\alpha]_D^{25} = -38.7°$ (*c* 0.08, $CHCl_3$).

^{1}H NMR (400 MHz, $CDCl_3$): δ 4.64 – 4.47 (m, 2H), 2.97 – 2.82 (m, 2H), 2.46 – 2.29 (m, 6H), 2.21 – 1.91 (m, 4H), 1.32 (s, 3H), 1.27 (s, 3H), 1.03 (s, 3H), 0.91 (s, 3H).

^{13}C NMR (100 MHz, $CDCl_3$): δ 202.0, 179.4, 179.3, 172.0, 68.2, 50.0, 46.0, 43.9, 43.2, 38.2, 38.0, 35.2, 35.0, 30.5, 30.1, 24.6, 22.4, 17.8, 17.5.

IR (thin film, NaCl): 2915, 1708, 1457, 1416, 1168 cm^{-1}.

HRMS (ESI-TOF): *m/z* calc'd for $[M–H]^-$ $C_{19}H_{27}O_7$ = 367.1757, found 367.1753.

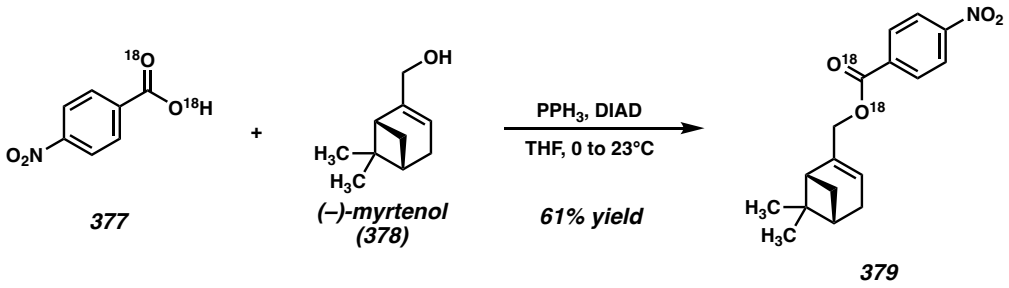


Acid 377: Prepared according to a modified literature procedure[14] from commercial 4-nitrobenzonitrile (98%, Fisher Scientific), $H_2{}^{18}O$ (98 atom % ^{18}O, Sercon Limited), and 4 M HCl in dioxane (Fisher Scientific). In a round bottom flask equipped with a rotary evaporator bump trap containing P_2O_5 (5.0 g), 4-nitrobenzonitrile (3.74 g, 25.2 mmol, 1.0 equiv) was heated to 50 °C for 18 h under vacuum. The dried 4-nitrobenzonitrile was transferred to a 20 mL Biotage® microwave vial, which was first flame dried under vacuum

and allowed to cool to 23 °C under Ar. The vial was evacuated and backfilled with Ar (4×), and 4 M HCl in dioxane (10.1 mL, 40.4 mmol, 1.6 equiv) followed by $H_2{}^{18}O$ (1.00 mL, 55.5 mmol, 2.2 equiv) were added. The mixture was heated to 90 °C and stirred for 20 h, at which point TLC indicated complete consumption of the starting material. The solution was cooled to 23 ° C, $CHCl_3$ (15 mL) was added, and the precipitate was collected by vacuum filtration. The filter cake was washed with $CHCl_3$ (15 mL) and dried under vacuum to afford the title compound as a white solid (2.10 g, 12.3 mmol, 49% yield).

^{1}H NMR (400 MHz, CD_3OD): δ 8.33 (d, *J* = 8.9 Hz, 2H), 8.24 (d, *J* = 8.9 Hz, 2H).

^{13}C NMR (100 MHz, CD_3OD): δ 167.5, 152.0, 137.6, 131.9, 124.5. Spectral data are in good accordance with previously reported values.[14]

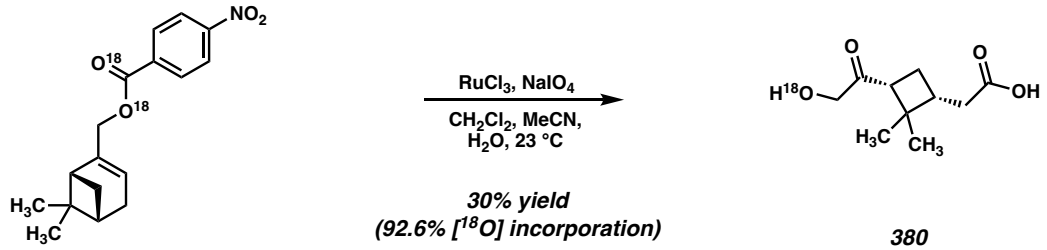


Ester 379: To a stirred solution of 4-nitrobenzoic-$^{18}O_2$ acid (**377**) (2.10 g, 12.3 mmol, 1.0 equiv), (–)-myrtenol (1.87 g, 12.3 mmol, 1.0 equiv), and PPh_3 (3.88 g, 14.8 mmol, 1.2 equiv) in THF (50 mL) at 0 °C was added DIAD (2.90 mL, 14.8 mmol, 1.2 equiv) dropwise. The mixture was stirred for 3 h and gradually allowed to warm to 23 °C, at which point TLC indicated complete consumption of **377**. The solution was diluted with saturated aqueous $NaHCO_3$ (100 mL) and EtOAc (100 mL). The layers were separated and the aqueous layer was extracted with EtOAc (3 × 100 mL). The combined organic phases were washed with brine, dried over $MgSO_4$, and concentrated. The crude product was purified

by flash chromatography (5–15% EtOAc/hexanes) to afford to afford the title compound as a white solid (2.26 g, 7.40 mmol, 60% yield).

^{1}H NMR (500 MHz, $CDCl_3$): δ 8.32 – 8.26 (m, 2H), 8.22 – 8.16 (m, 2H), 5.69 (tt, *J* = 3.0, 1.5 Hz, 1H), 4.78 – 4.71 (m, 2H), 2.45 (dt, *J* = 8.7, 5.6 Hz, 1H), 2.40 – 2.27 (m, 2H), 2.22 (td, *J* = 5.6, 1.4 Hz, 1H), 2.18 – 2.12 (m, 1H), 1.31 (s, 3H), 1.24 (d, *J* = 8.7 Hz, 1H), 0.87 (s, 3H).

^{13}C NMR (100 MHz, $CDCl_3$): δ 164.7, 150.6, 142.5, 136.0, 130.8, 123.7, 122.9, 68.6, 43.9, 40.8, 38.3, 31.7, 31.5, 26.3, 21.3. Spectral data are in good accordance with previously reported values.[14]



379 *380*

Acid 380: To a stirred solution of (–)-myrtenyl 4-nitrobenzoate-$^{18}O_2$ (**379**) (2.20 g, 7.20 mmol, 1.0 equiv) in CH_2Cl_2/MeCN/H_2O (2:2:3, 63 mL) at 23 °C was added $NaIO_4$ (6.16 g, 28.8 mmol, 4.0 equiv) followed by catalytic $RuCl_3$ hydrate (55 mg). After 48 h, TLC indicated complete conversion of **379** and the mixture was diluted with Et_2O (50 mL). The layers were separated and the aqueous layer was extracted with Et_2O (3 × 40 mL). The combined organic phases were filtered through celite and concentrated. The crude residue was dissolved in Et_2O (25 mL) and extracted with 10% aqueous Na_2CO_3 (3 × 40 mL). The aqueous phases were combined, acidified to pH 1 with concentrated H_2SO_4, and extracted with Et_2O (3 × 40 mL). The combined organic phases were washed with brine, dried over $MgSO_4$, and concentrated. The crude product was purified by flash chromatography (40–

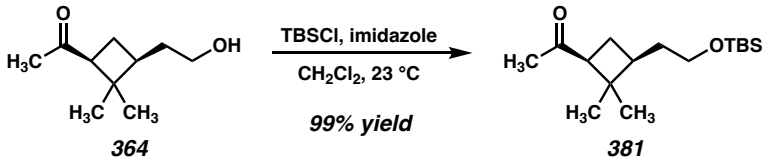
70% EtOAc/hexanes; 1% AcOH). Residual AcOH was removed by rotary evaporation with added toluene to afford the title compound as a white solid (436 mg, 2.16 mmol, 30% yield). $[\alpha]_D^{25} = -47.5°$ (*c* 0.50, $CHCl_3$).

^{1}H NMR (400 MHz, $CDCl_3$): δ 4.21 – 4.04 (m, 2H), 2.89 (dd, *J* = 10.1, 7.6 Hz, 1H), 2.49 – 2.30 (m, 3H), 2.17 – 1.98 (m, 2H), 1.29 (s, 3H), 0.87 (s, 3H).

^{13}C NMR (100 MHz, $CDCl_3$): δ 207.9, 177.9, 68.8, 49.8, 44.0, 38.1, 34.8, 30.5, 22.5, 17.6.

IR (thin film, NaCl): 2954, 2366, 1706, 1399, 1218, 1025 cm^{-1}.

HRMS (ESI-TOF): *m/z* calc'd for $[M-H]^-$ $C_{10}H_{15}{}^{18}O^{16}O_3$ = 201.1013, found 201.1012, 92.6% ^{18}O incorporation.



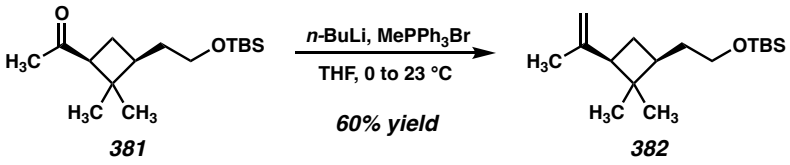
Silyl ether 381: To a stirred solution of alcohol **364** (1.50 g, 8.80 mmol, 1.0 equiv) and imidazole (2.40 g, 35.2 mmol, 4.0 equiv) in CH_2Cl_2 (88 mL) at 23 °C was added TBSCl (2.65 g, 17.6 mmol, 2.0 equiv) in one portion. The mixture was stirred for 16 h at 23 °C, at which point TLC indicated complete consumption of **364**. The solution was diluted with Et_2O (100 mL) and H_2O (100 mL). The layers were separated and the aqueous layer was extracted with Et_2O (3 × 100 mL). The combined organic phases were washed with brine, dried over $MgSO_4$, and concentrated. The crude product was purified by flash chromatography (15% Et_2O/hexanes) to afford the title compound as a colorless oil (2.48 g, 8.72 mmol, 99% yield). $[\alpha]_D^{25} = +21.5°$ (*c* 0.80, $CHCl_3$).

^{1}H NMR (400 MHz, $CDCl_3$): δ 3.58 – 3.47 (m, 2H), 2.81 (dd, *J* = 9.9, 7.5 Hz, 1H), 2.03 (s, 3H), 2.00 – 1.93 (m, 1H), 1.92 – 1.80 (m, 2H), 1.59 – 1.51 (m, 1H), 1.45 – 1.34 (m, 1H), 1.27 (s, 3H), 0.88 (s, 9H), 0.85 (s, 3H), 0.03 (s, 6H).

^{13}C NMR (100 MHz, $CDCl_3$): δ 208.3, 61.7, 54.6, 43.5, 39.0, 33.4, 30.6, 30.3, 26.1, 23.3, 18.5, 17.5, –5.2.

IR (thin film, NaCl): 2952, 2928, 2858, 1707, 1461, 1362, 1254, 1179, 1103 cm^{-1}.

HRMS (FI): *m/z* calc'd for $[M]^{\bullet+}$ $C_{16}H_{32}O_2Si$ = 284.2172, found 284.2171.



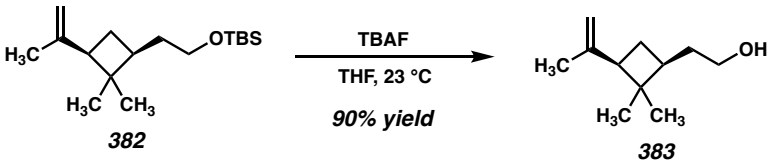
Alkene 382: To a round bottom flask charged with $MePPh_3Br$ (2.51 g, 7.03 mmol, 2.0 equiv) and evacuated and backfilled with N_2 (3×) at 23 °C was added THF (35 mL). The solution was cooled to 0 °C, *n*-BuLi (2.5 M in THF, 2.81 mL, 7.03 mmol, 2.0 equiv) was added dropwise, and the solution was stirred for 10 min at 0 °C. Silyl ether **381** (1.00 g, 3.51 mmol, 1.0 equiv) in THF (5.0 mL) was then added dropwise at 0 °C. The mixture was stirred for 12 h and gradually allowed to warm to 23 °C, at which point TLC indicated complete consumption of **381**. The solution was diluted with Et_2O (50 mL) and H_2O (50 mL). The layers were separated and the aqueous layer was extracted with Et_2O (3 × 50 mL). The combined organic phases were washed with brine, dried over $MgSO_4$, and concentrated. The crude product was purified by flash chromatography (0–7% Et_2O/hexanes) to afford the title compound as a colorless oil (710 mg, 2.51 mmol, 71% yield). $[\alpha]_D^{25} = -18.3°$ (*c* 1.0, $CHCl_3$).

^{1}H NMR (600 MHz, $CDCl_3$): δ 4.78 (d, *J* = 2.0 Hz, 1H), 4.55 (d, *J* = 2.1 Hz, 1H), 3.54 (td, *J* = 6.9, 1.2 Hz, 2H), 2.33 (dd, *J* = 10.6, 7.0 Hz, 1H), 1.94 – 1.82 (m, 2H), 1.65 (s, 3H), 1.60 – 1.49 (m, 2H), 1.45 – 1.35 (m, 1H), 1.14 (s, 3H), 0.90 (s, 9H), 0.76 (s, 3H), 0.05 (s, 6H).

^{13}C NMR (100 MHz, $CDCl_3$): δ 145.9, 109.1, 62.1, 49.6, 41.6, 38.8, 33.7, 30.9, 26.5, 26.2, 23.2, 18.5, 16.5, –5.1.

IR (thin film, NaCl): 2959, 1749, 1722, 1415, 1372, 1269, 1230, 1170, 1151, 1051 cm^{-1}.

HRMS (FI): *m/z* calc'd for $[M]^{\bullet+}$ $C_{17}H_{34}OSi$ = 282.2379, found 282.2388.



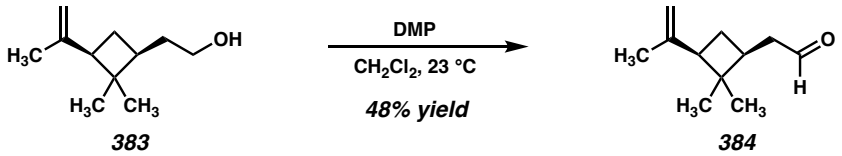
Alcohol 383: To a stirred solution of silyl ether **382** (300 mg, 1.06 mmol, 1.0 equiv) in THF (11 mL) at 23 °C was added TBAF (1.0 M in THF, 1.59 mL, 1.59 mmol, 1.5 equiv) in one portion. The mixture was stirred for 16 h at 23 °C, at which point TLC indicated complete consumption of **382**. The solution was diluted with Et_2O (30 mL) and H_2O (30 mL). The layers were separated and the aqueous layer was extracted with Et_2O (3 × 30 mL). The combined organic phases were washed with brine, dried over $MgSO_4$, and concentrated. The crude product was purified by flash chromatography (30% Et_2O/hexanes) to afford the title compound as a colorless oil (161 mg, 0.957 mmol, 90% yield). $[\alpha]_D^{25}$ = –22.6° (*c* 0.80, $CHCl_3$).

^{1}H NMR (400 MHz, $CDCl_3$): δ 4.78 (dt, *J* = 2.1, 1.4 Hz, 1H), 4.67 – 4.53 (m, 1H), 3.59 (td, *J* = 6.8, 1.0 Hz, 2H), 2.42 – 2.31 (m, 1H), 1.99 – 1.85 (m, 2H), 1.65 (dt, *J* = 1.5, 0.8 Hz, 3H), 1.63 – 1.52 (m, 2H), 1.49 – 1.39 (m, 1H), 1.15 (s, 3H), 0.77 (s, 3H).

^{13}C NMR (100 MHz, $CDCl_3$): δ 145.7, 109.3, 61.9, 49.6, 41.7, 38.7, 33.5, 30.8, 26.4, 23.2, 16.5.

IR (thin film, NaCl): 3311, 3079, 2953, 2881, 1646, 1457, 1437, 1366, 1052 cm^{-1}.

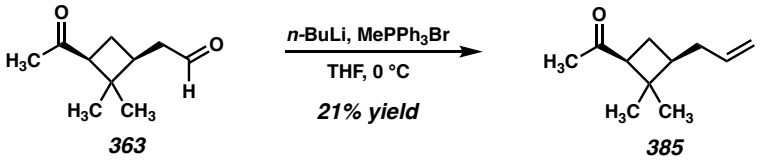
HRMS (FI): *m/z* calc'd for $[M]^{\bullet+}$ $C_{11}H_{20}O$ = 168.1514, found 168.1510.



Enal 384: To a stirred solution of alcohol **383** (420 mg, 2.50 mmol, 1.0 equiv) in CH_2Cl_2 (50 mL) at 23 °C was added DMP (2.12 g, 5.00 mmol, 2.0 equiv) in one portion. The mixture was stirred for 16 h at 23 °C, at which point TLC indicated complete consumption of **383**. The solution was diluted with saturated aqueous $Na_2S_2O_3$ (25 mL), Et_2O (100 mL), and H_2O (60 mL). The layers were separated and the aqueous layer was extracted with Et_2O (3 × 50 mL). The combined organic phases were washed with brine, dried over $MgSO_4$, and concentrated. The crude product was purified by flash chromatography (10% Et_2O/hexanes) to afford the title compound as a colorless oil (200 mg, 1.20 mmol, 48% yield).

^{1}H NMR (500 MHz, $CDCl_3$): δ 9.73 (t, *J* = 2.0 Hz, 1H), 4.81 (dt, *J* = 2.0, 1.4 Hz, 1H), 4.56 (td, *J* = 1.9, 0.9 Hz, 1H), 2.49 – 2.42 (m, 2H), 2.39 – 2.28 (m, 2H), 2.08 – 1.98 (m, 1H), 1.66 (d, *J* = 0.7 Hz, 3H), 1.63 (d, *J* = 10.4 Hz, 1H), 1.19 (s, 3H), 0.78 (s, 3H).

^{13}C NMR (100 MHz, $CDCl_3$): δ 202.1, 145.0, 109.5, 49.6, 45.2, 41.9, 35.8, 30.5, 26.3, 22.9, 16.7. Spectral data are in good accordance with previously reported values.[15]



Enone 385: To a round bottom flask charged with $MePPh_3Br$ (2.33 g, 6.53 mmol, 1.1 equiv) and evacuated and backfilled with N_2 (3×) at 23 °C was added THF (60 mL). The solution was cooled to 0 °C, *n*-BuLi (2.5 M in THF, 2.38 mL, 5.94 mmol, 1.0 equiv) was added dropwise, and the solution was stirred for 10 min at 0 °C. (+)-*cis*-Pinonaldehyde (**363**) (1.00 g, 5.94 mmol, 1.0 equiv) in THF (25 mL) was then added dropwise at 0 °C. After 1 min, TLC indicated complete consumption of **363**. The solution was diluted with Et_2O (100 mL) and H_2O (100 mL). The layers were separated and the aqueous layer was extracted with Et_2O (3 × 100 mL). The combined organic phases were washed with brine, dried over $MgSO_4$, and concentrated. The crude product was purified by flash chromatography (10% Et_2O/hexanes) to afford the title compound as a colorless oil (228 mg, 1.37 mmol, 23% yield).

^{1}H NMR (500 MHz, $CDCl_3$): δ 5.76 – 5.63 (m, 1H), 5.04 – 4.90 (m, 2H), 2.82 (dd, *J* = 9.9, 7.4 Hz, 1H), 2.12 – 2.06 (m, 1H), 2.03 (s, 3H), 2.01 – 1.80 (m, 4H), 1.29 (s, 3H), 0.87 (s, 3H).

^{13}C NMR (100 MHz, $CDCl_3$): δ 208.2, 136.9, 115.4, 54.4, 43.6, 41.6, 34.8, 30.7, 30.3, 23.2, 17.3. Spectral data are in good accordance with previously reported values.[15]

4.8 REFERENCES AND NOTES

(1) Jimenez, J. L. *et. al.*, Evolution of Organic Aerosols in the Atmosphere. *Science,* **2009**, *326*, 1525–1529.

(2) Intergovernmental Panel on Climate Change, Climate Change 2013: The Physical Science Basis. Contribution of Working Group I to the Fifth Assessment Report of the Intergovernmental Panel on Climate Change, T. F. Stocker et al., Eds. (Cambridge Univ. Press, 2013).

(3) Cohen, A. J. *et. al.* Estimates and 25-year trends of the global burden of disease attributable to ambient air pollution: an analysis of data from the Global Burden of Diseases Study 2015. *Lancet* **2017**, *389*, 1907–1918.

(4) R. Burnett et al., *Proc. Natl. Acad. Sci. U.S.A.* **2018** *115*, 9592–9597.

(5) Guenther, A. B.; Jiang, X.; Heald, C. L.; Sakulyanontvittaya, T.; Duhl, T.; Emmons, L. K.; Wang, X. The Model of Emissions of Gases and Aerosols from Nature version 2.1 (MEGAN2.1): an extended and updated framework for modeling biogenic emissions. *Geosci. Model Dev.* **2012**, *5*, 1471–1492.

(6) M. Hallquist et al., *Atmos. Chem. Phys*. **2009** *9*, 5155–5236.

(7) C. L. Heald et al., *J. Geophys. Res*. **2008**, *113*, D05211.

(8) H. Zhang et al., *Proc. Natl. Acad. Sci. U.S.A*. **2018** *115*, 2038–2043.

(9) a) T. Hoffmann, R. Bandur, U. Marggraf, M. Linscheid, Molecular composition of organic aerosols formed in the α-pinene/O_3 reaction: Implications for new particle formation processes. *J. Geophys. Res.* **1998**, *103*, 25569–25578. b) C. M. Kenseth et al., Synergistic O_3 + OH oxidation pathway to extremely low-volatility dimers

revealed in the β-pinene secondary organic aerosol. *Proc. Natl. Acad. Sci. U.S.A.* **2018**, *115*, 8301–8306. c) C. M. Kenseth et al., Synthesis of Carboxylic Acid and Dimer Ester Surrogates to Constrain the Abundance and Distribution of Molecular Products in α-Pinene and β-Pinene Secondary Organic Aerosol. *Environ. Sci. Technol.* **2020**, *54*, 12829–12839. d) R. Zhao, C. M. Kenseth, Y. Huang, N. F. Dalleska, J. H. Seinfeld. Iodometry-Assisted Liquid Chromatography Electrospray Ionization Mass Spectrometry for Analysis of Organic Peroxides: An Application to Atmospheric Secondary Organic Aerosol. *Environ. Sci. Technol.* **2018**, *52*, 2108–2117. e) Y. Huang, C. M. Kenseth, N. F. Dalleska, J. H. Seinfeld. Coupling Filter-Based Thermal Desorption Chemical Ionization Mass Spectrometry with Liquid Chromatography/Electrospray Ionization Mass Spectrometry for Molecular Analysis of Secondary Organic Aerosol. *Environ. Sci. Technol.* **2020**, *54*, 13238–13248. f) O. Peräkylä et al., Large Gas-Phase Source of Esters and Other Accretion Products in the Atmosphere. *J. Am. Chem. Soc.* **2023**, *145*, 7780–7790. And references therein.

(10) M. A. Upshur et al., Organic synthesis in the study of terpene-derived oxidation products in the atmosphere. *Nat. Prod. Rep.* **2023**, *40*, 890–921.

(11) Kenseth et. al. Particle-phase accretion forms dimer esters in pinene secondary organic aerosol. *Science*, **2023**, *382*, 787–792

(12) a) F. Yasmeen et al., Terpenylic acid and related compounds: precursors for dimers in secondary organic aerosol from the ozonolysis of α- and β-pinene. *Atmos. Chem. Phys*. **2010**, *10*, 9383–9392. b) F. Yasmeen et al., Characterisation of tracers for

aging of α-pinene secondary organic aerosol using liquid chromatography/negative ion electrospray ionisation mass spectrometry. *Environ. Chem.* **2012**, *9*, 236–246. c) K. Kristensen et al., High-molecular weight dimer esters are major products in aerosols from α-pinene ozonolysis and the boreal forest. *Environ. Sci. Technol. Lett.* **2016**, *3*, 280–285. d) X. Zhang et al., Formation and evolution of molecular products in α-pinene secondary organic aerosol. *Proc. Natl. Acad. Sci. U.S.A.* **2015**, *112*, 14168–14173.

(13) K. S. Docherty, W. Wu, Y. B. Lim, P. J. Ziemann, Contributions of organic peroxides to secondary aerosol formed from reactions of monoterpenes with O_3. *Environ. Sci. Technol.* **2005**, *39*, 4049–4059.

(14) R. H. Beddoe, D. C. Edwards, L. Goodman, H. F. Sneddon, R. M. Denton, Synthesis of ^{18}O-labelled alcohols from unlabelled alcohols. *Chem. Commun*. **2020**, *56*, 6480–6483.

(15) Z. Zhao, W. Zhang, T. Alexander, X. Zhang, D. B. C. Martin, H. Zhang, Isolating α-Pinene Ozonolysis Pathways Reveals New Insights into Peroxy Radical Chemistry and Secondary Organic Aerosol Formation. *Environ. Sci. Technol.* **55**, 6700–6709 (2021).

(16) M. Gomes, O. A. C. Antunes, Upjohn catalytic osmium tetroxide oxidation process: Diastereoselective dihydroxylation of monoterpenes. *Catalysis Communications*. **2**, 225–227 (2001).

(17) C. Samorì, H. Ali-Boucetta, R. Sainz, C. Guo, F. M. Toma, C. Fabbro, T. da Ros, M. Prato, K. Kostarelos, A. Bianco, Enhanced anticancer activity of multi-walled carbon nanotube–methotrexate conjugates using cleavable linkers. *Chem. Commun.* **46**, 1494–1496 (2010).

(18) H.-X. Liu, H.-B. Tan, M.-T. He, L. Li, Y.-H. Wang, C.-L. Long, Isolation and synthesis of two hydroxychavicol heterodimers from Piper nudibaccatum. *Tetrahedron*. **71**, 2369–2375 (2015).

Appendix 11

Spectra Relevant to Chapter 4:

Synthesis of Authentic Standards to Enable Investigations of Pinene Secondary Organic Aerosols

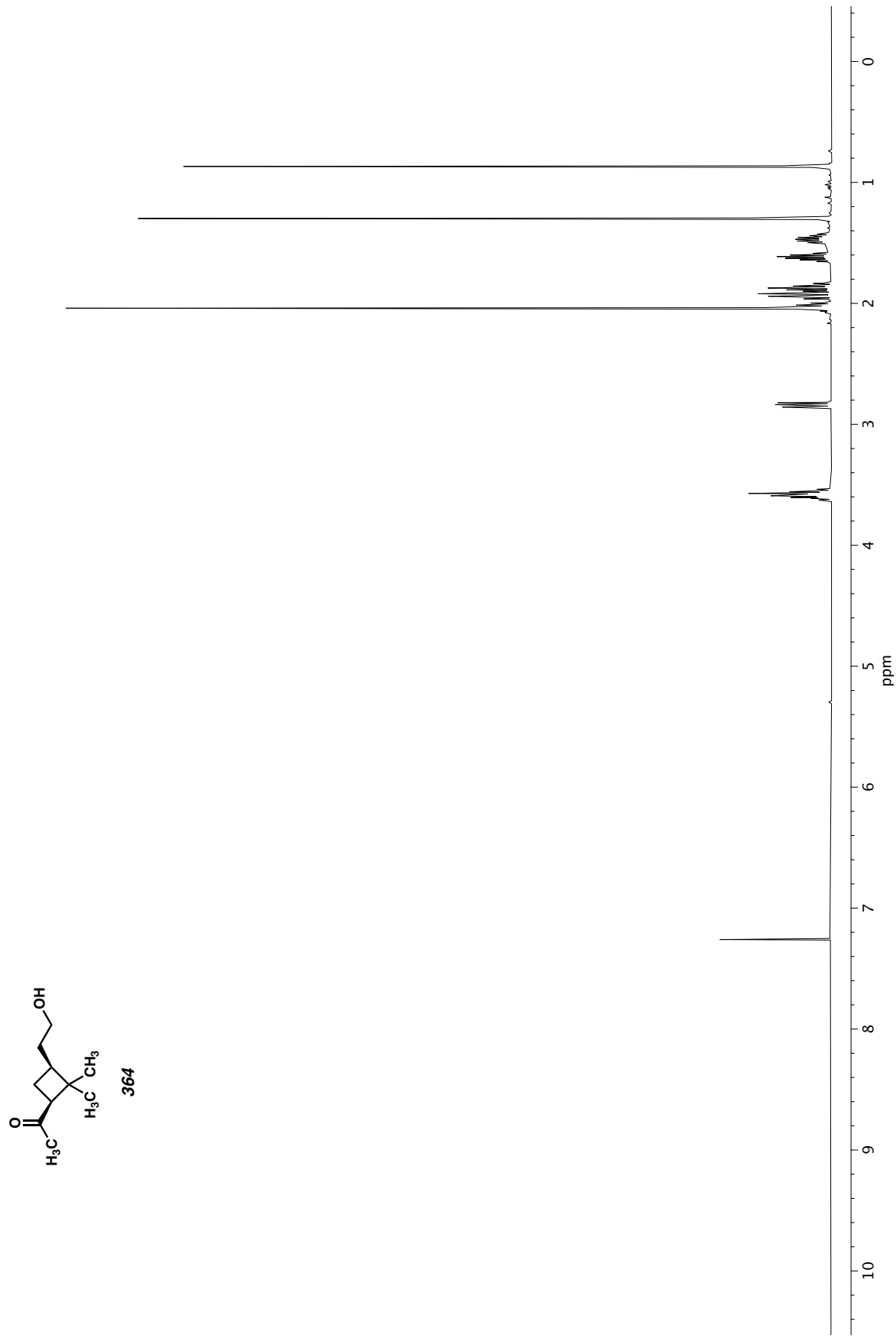


Figure A11.1. ^{1}H NMR (400 MHz, $CDCl_3$) of compound **364**.

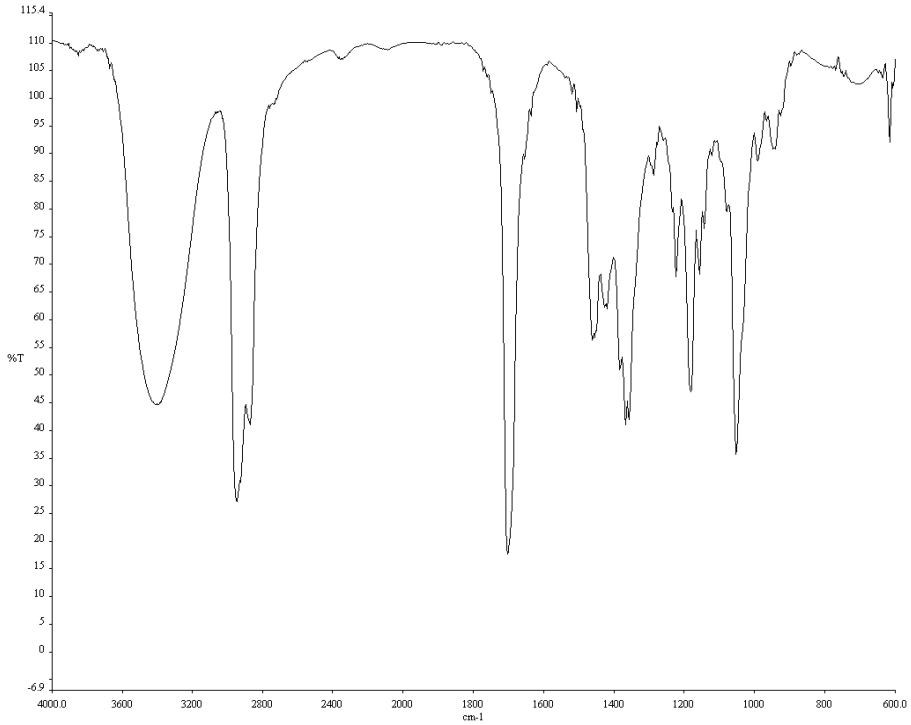


Figure A11.2. Infrared spectrum (Thin Film, NaCl) of compound **364**.

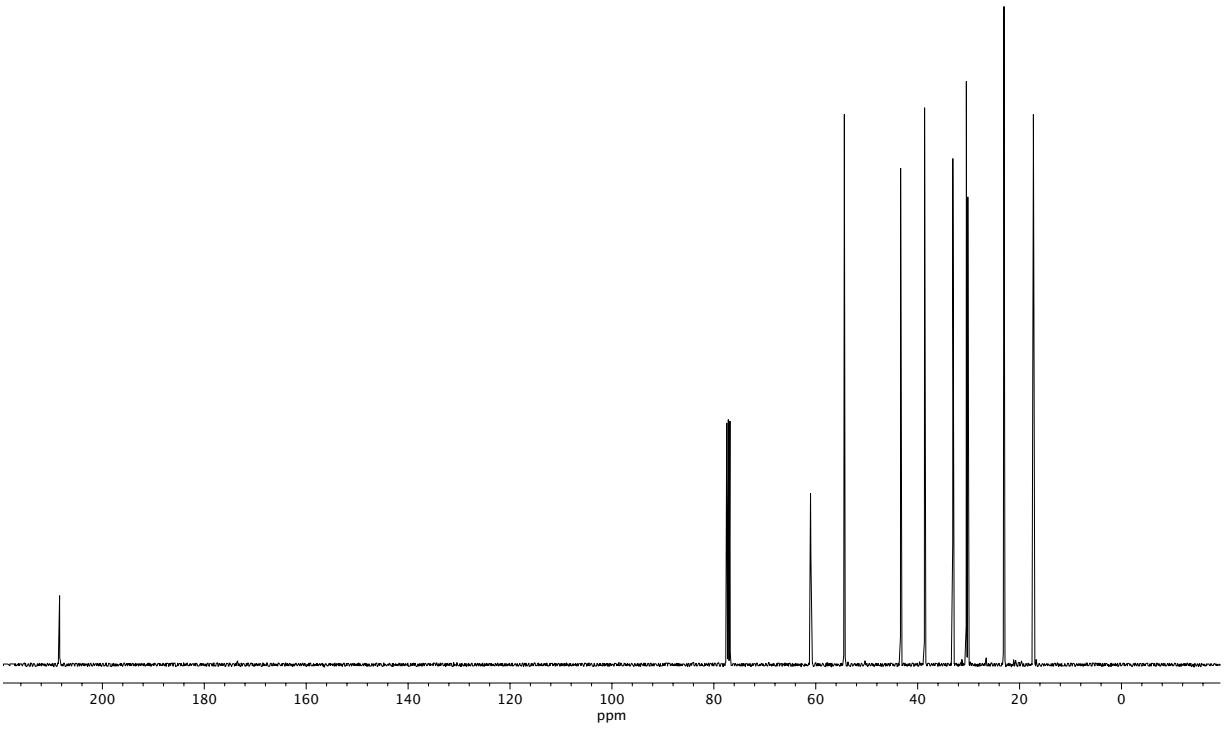


Figure A11.3. ^{13}C NMR (100 MHz, $CDCl_3$) of compound **364**.

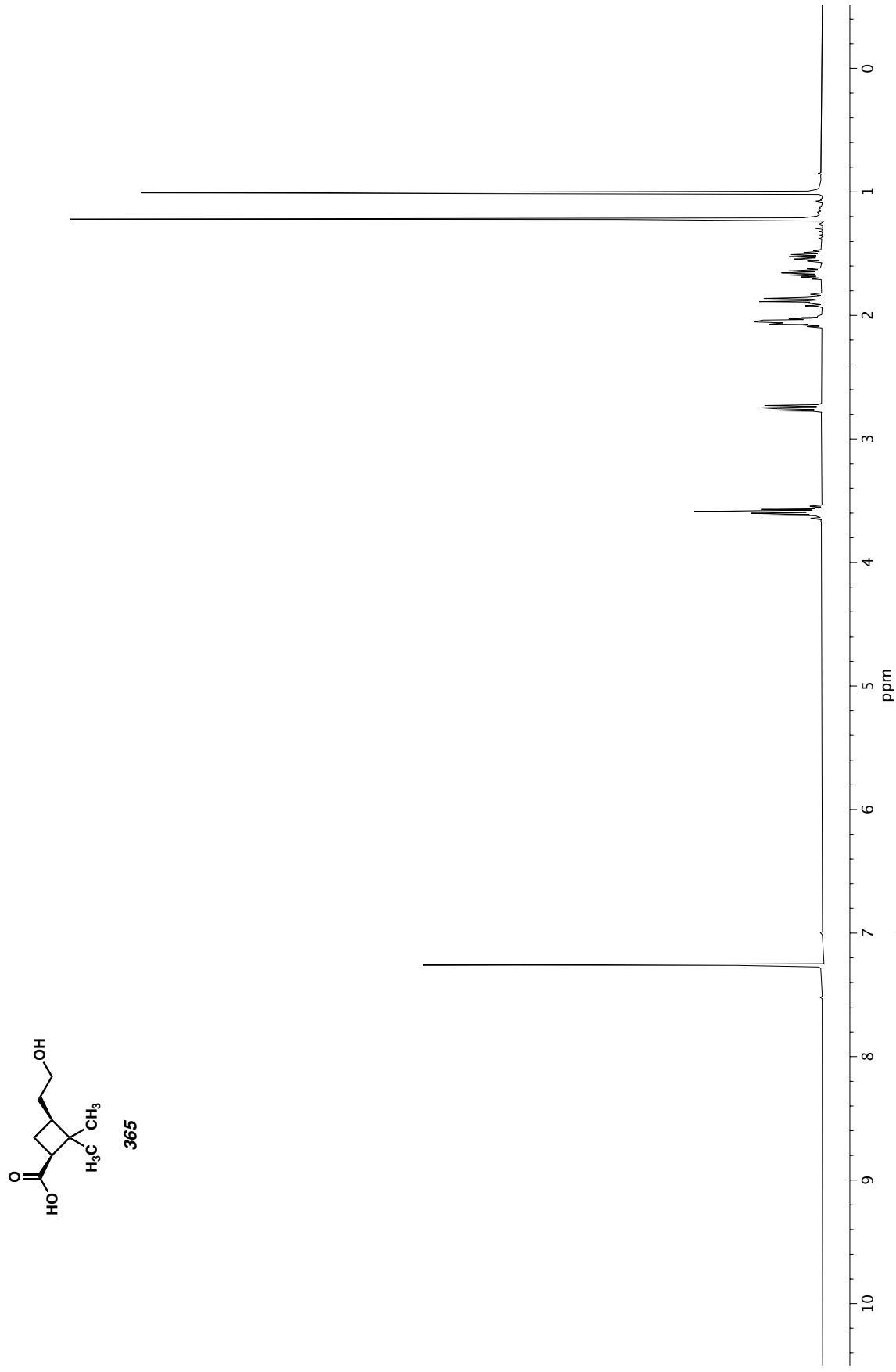


Figure A11.4. ^{1}H NMR (400 MHz, $CDCl_3$) of compound **365**.

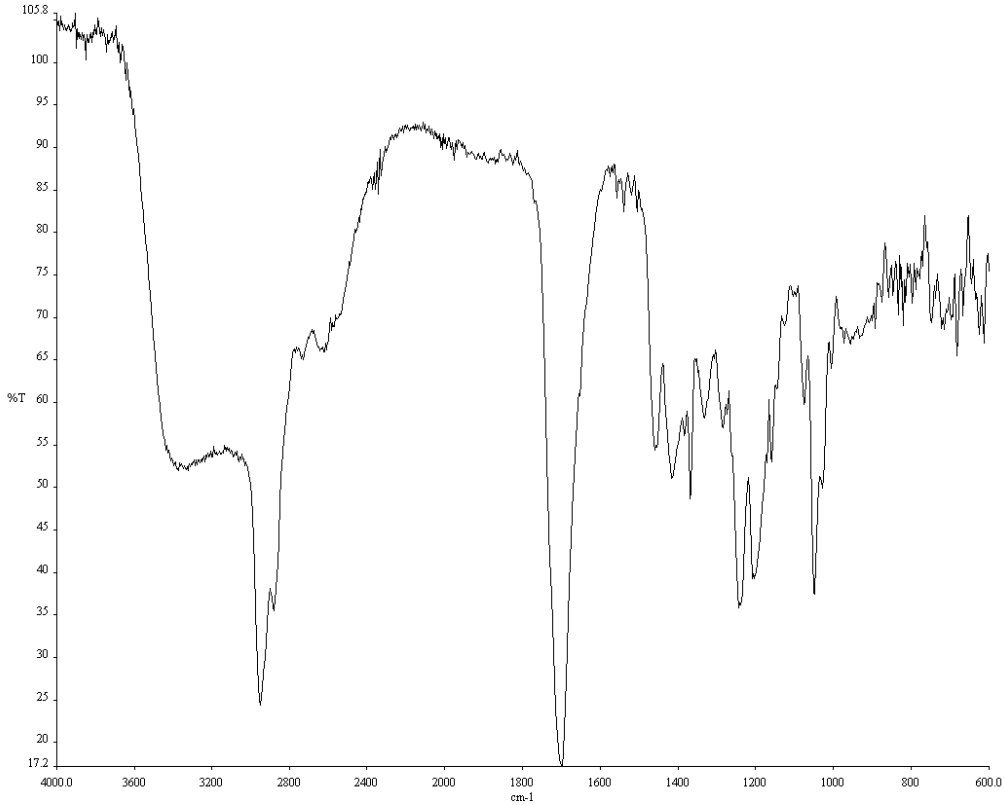


Figure A11.5. Infrared spectrum (Thin Film, NaCl) of compound **365**.

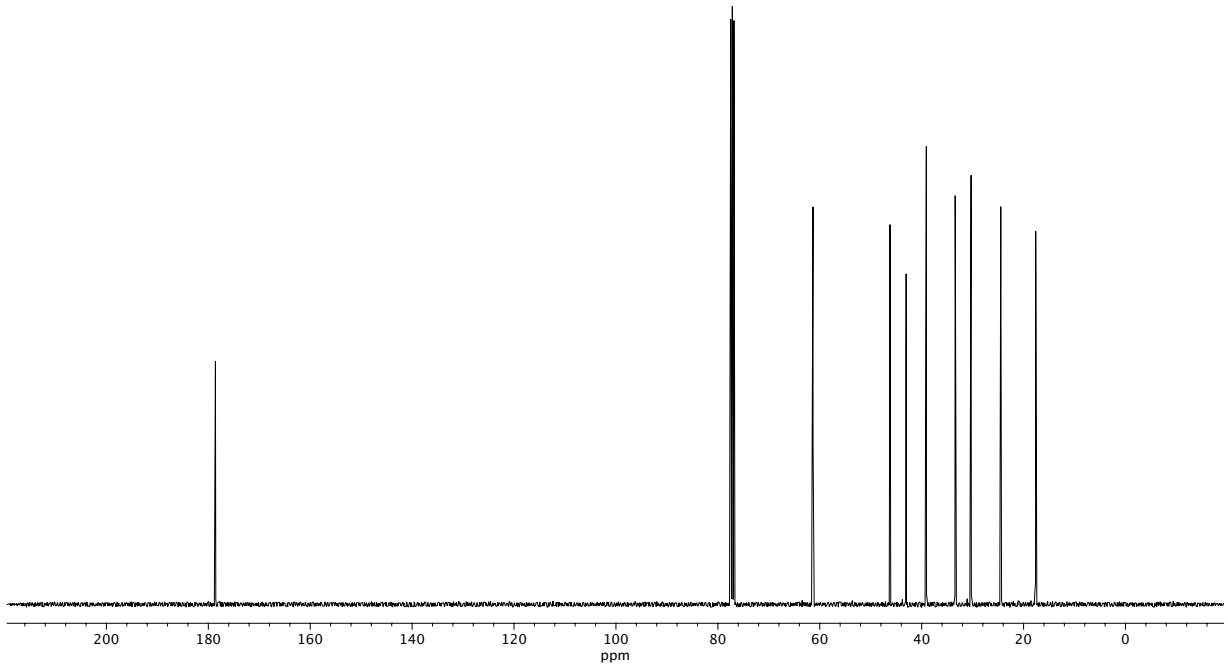


Figure A11.6. ^{13}C NMR (100 MHz, $CDCl_3$) of compound **365**.

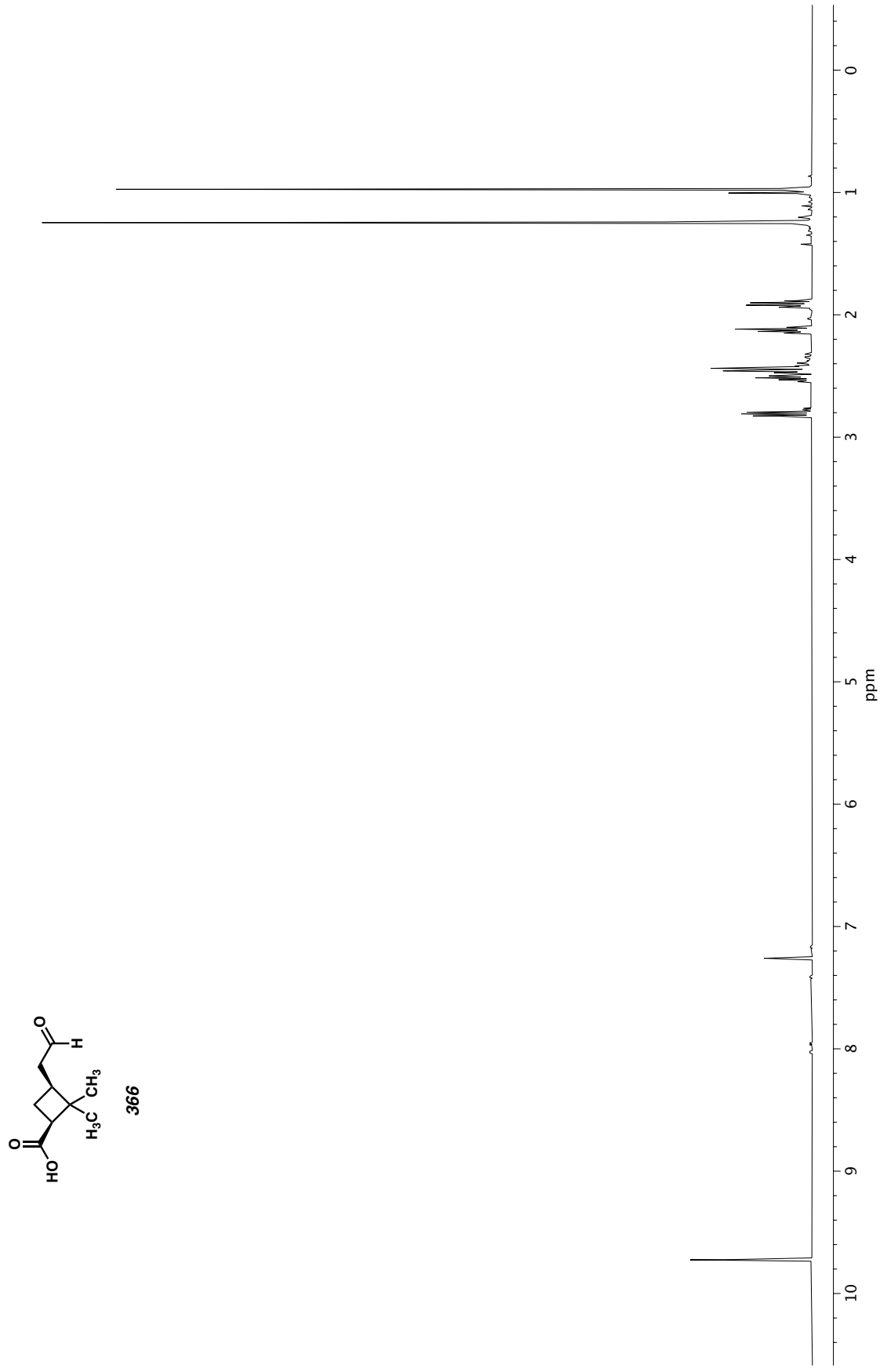


Figure A11.7. ^{1}H NMR (400 MHz, $CDCl_3$) of compound **366**.

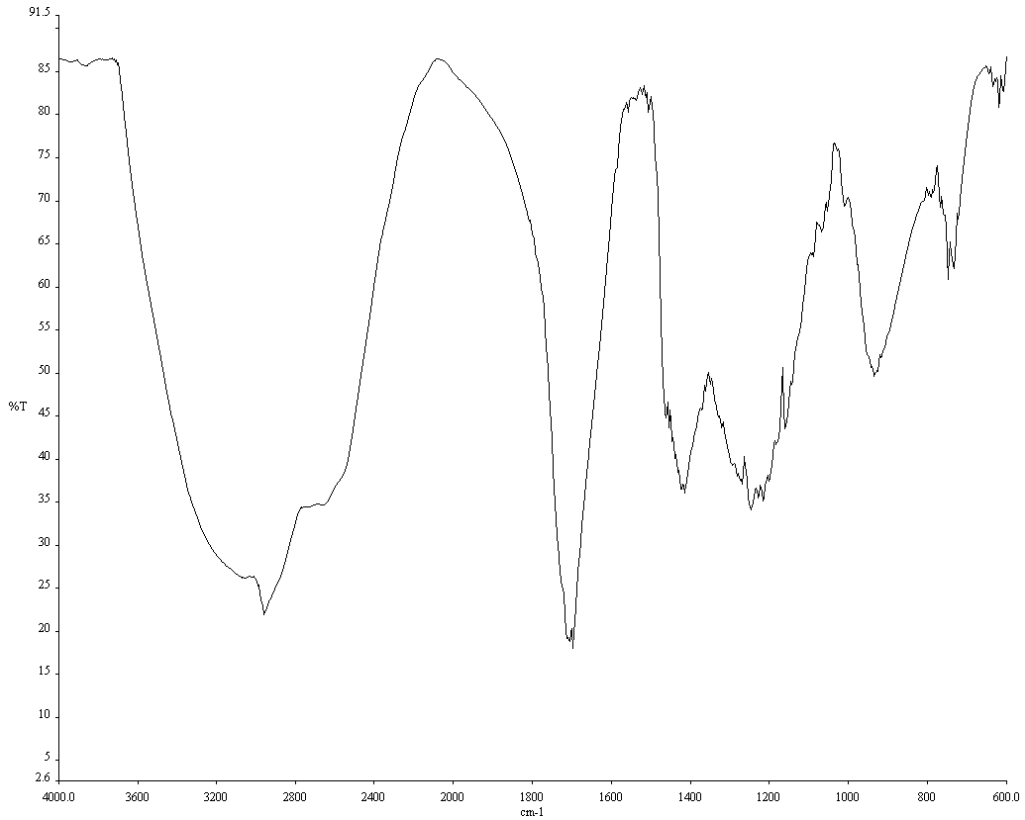


Figure A11.8. Infrared spectrum (Thin Film, NaCl) of compound **366**.

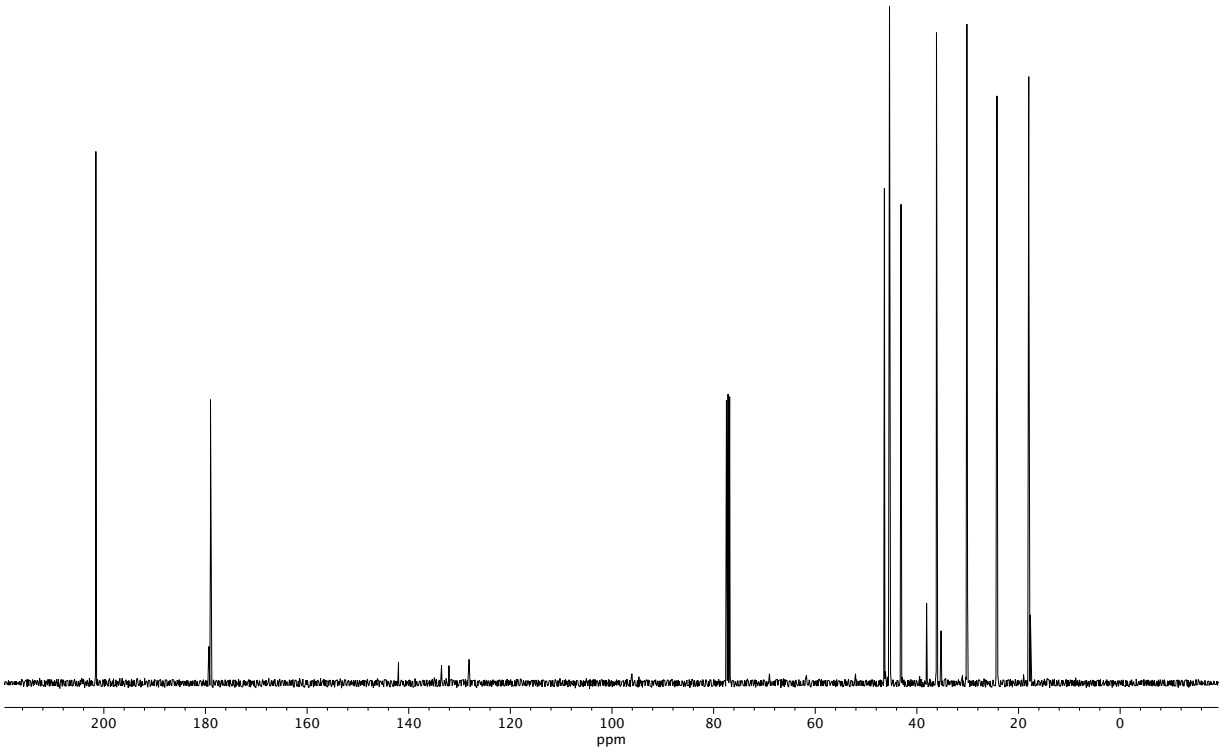


Figure A11.9. ^{13}C NMR (100 MHz, $CDCl_3$) of compound **366**.

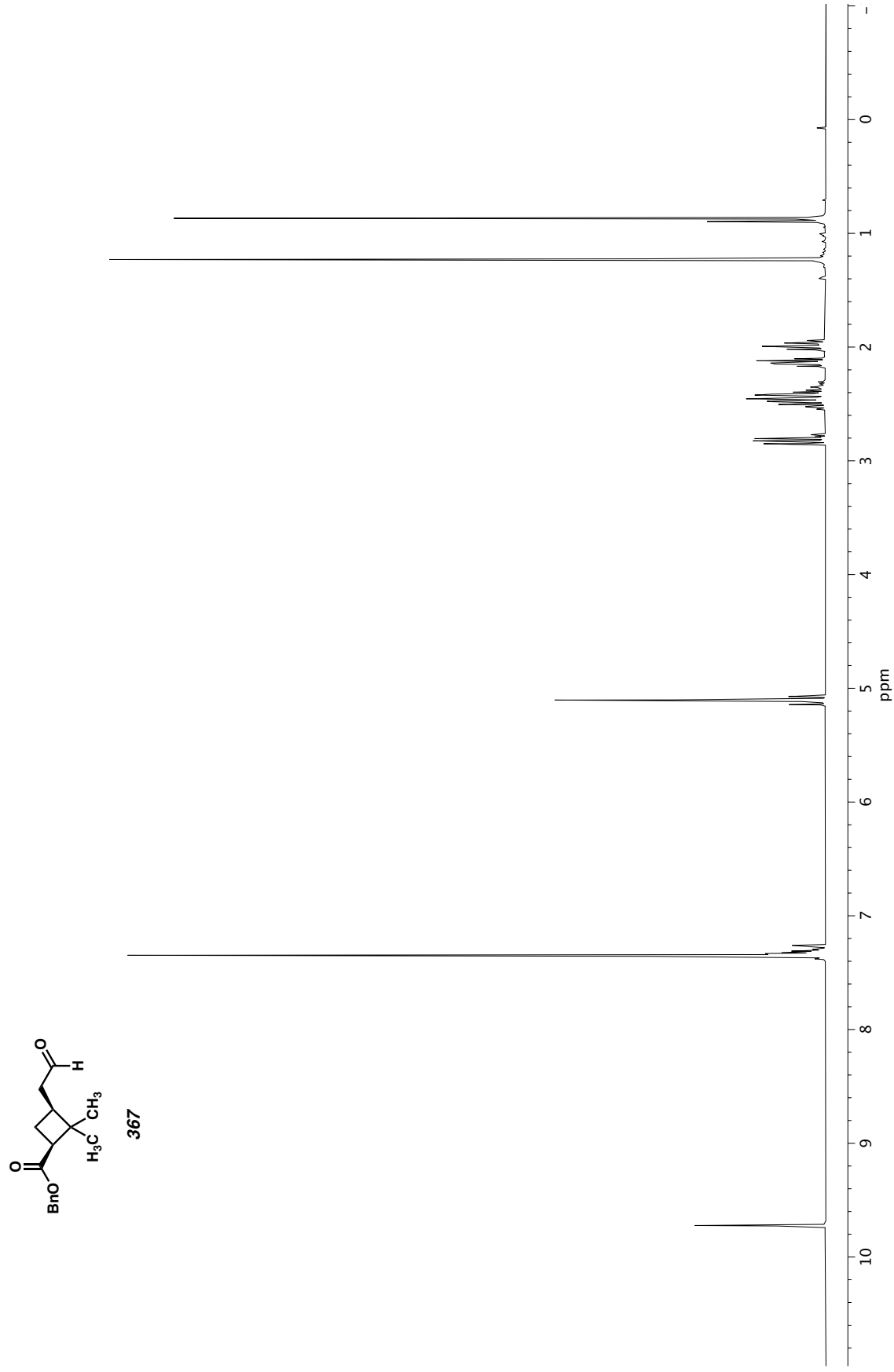


Figure A11.10. ^{1}H NMR (400 MHz, $CDCl_3$) of compound **367**.

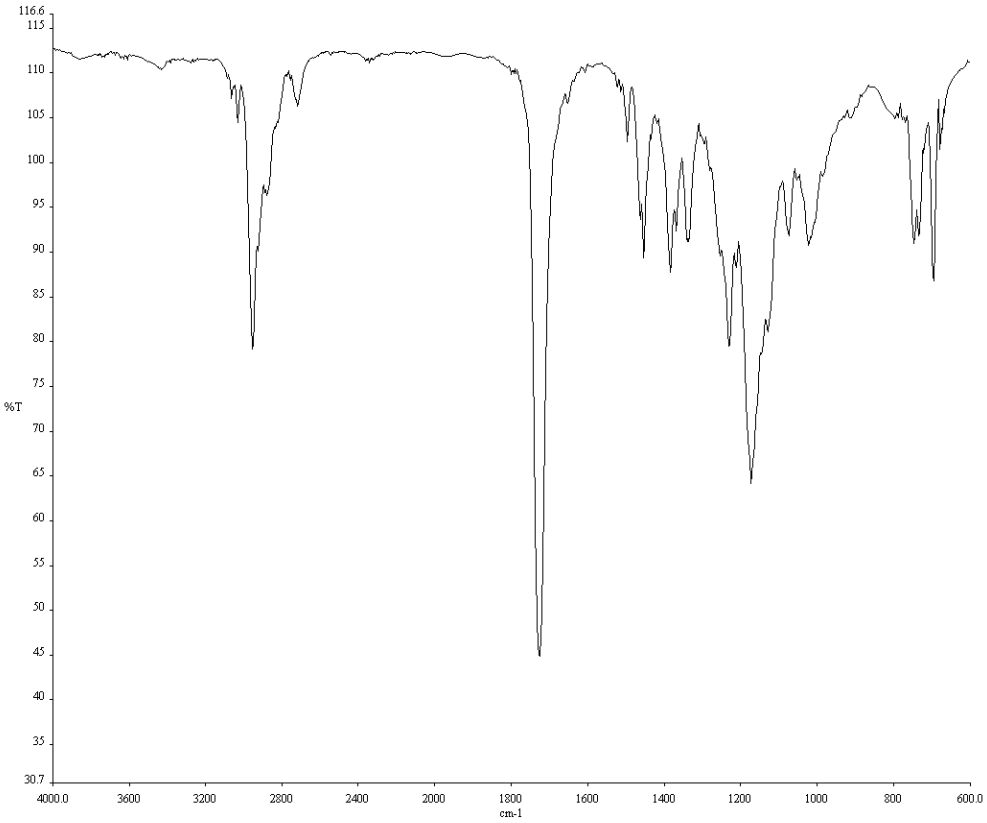


Figure A11.11. Infrared spectrum (Thin Film, NaCl) of compound **367**.

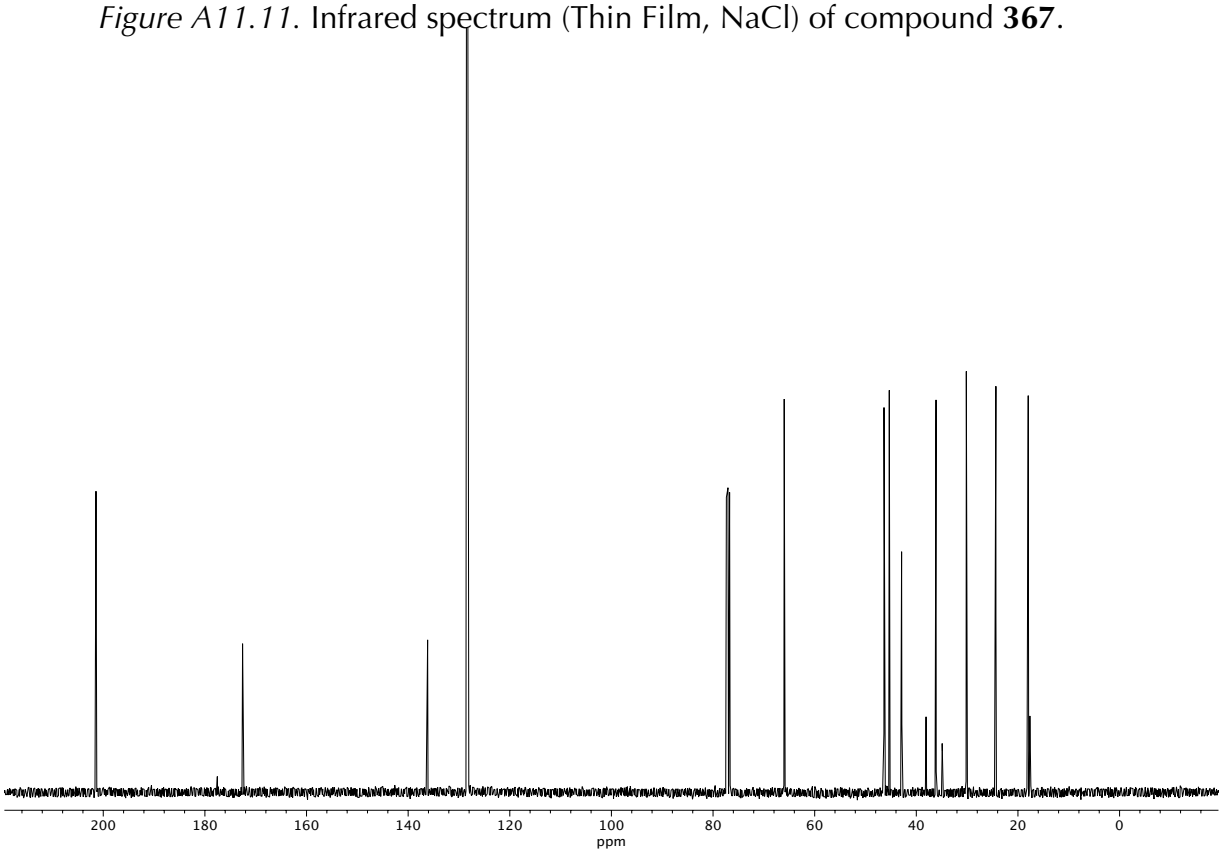


Figure A11.12. ^{13}C NMR (100 MHz, $CDCl_3$) of compound **367**.

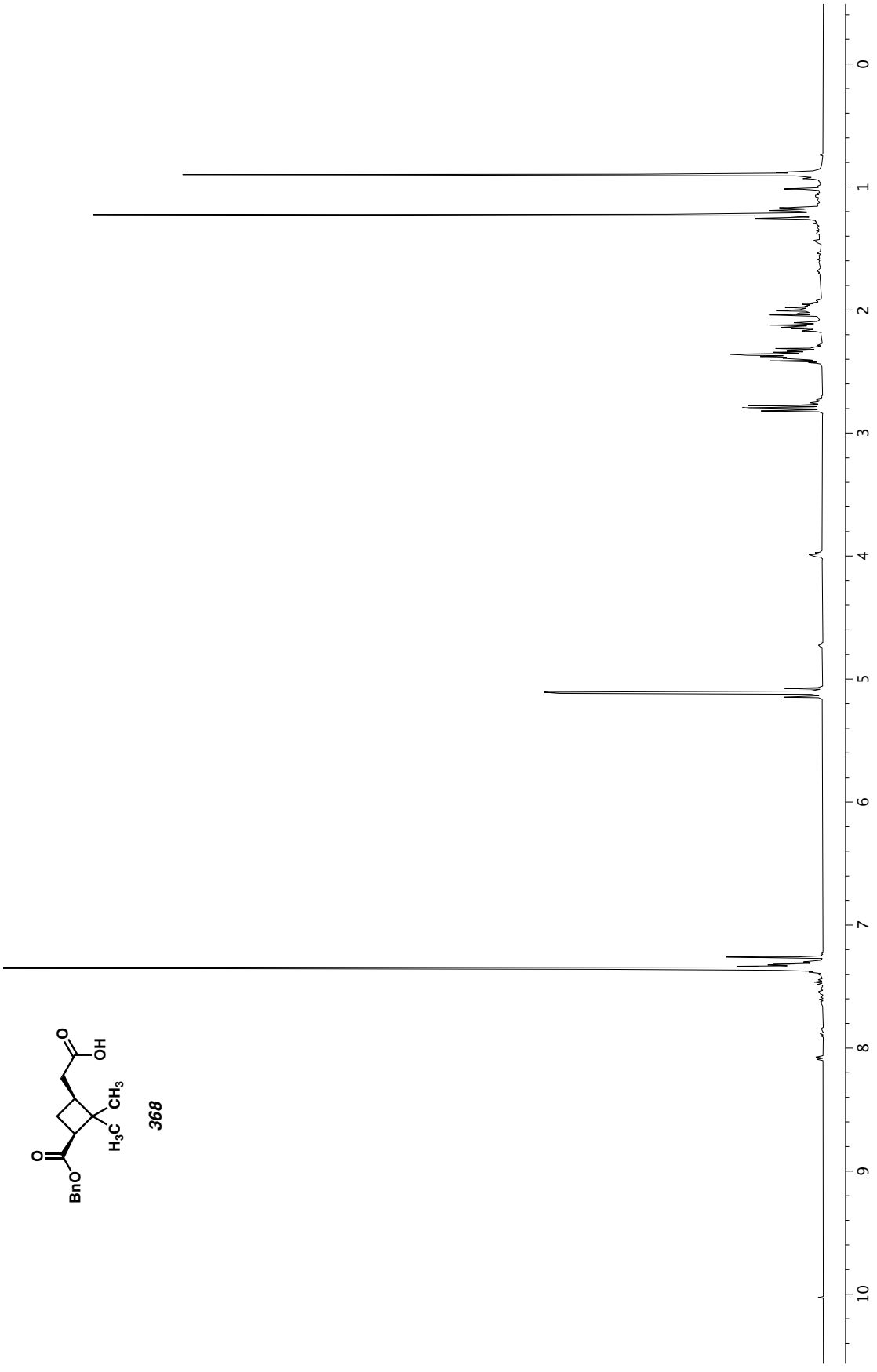


Figure A11.13. ^{1}H NMR (400 MHz, $CDCl_3$) of compound **368**.

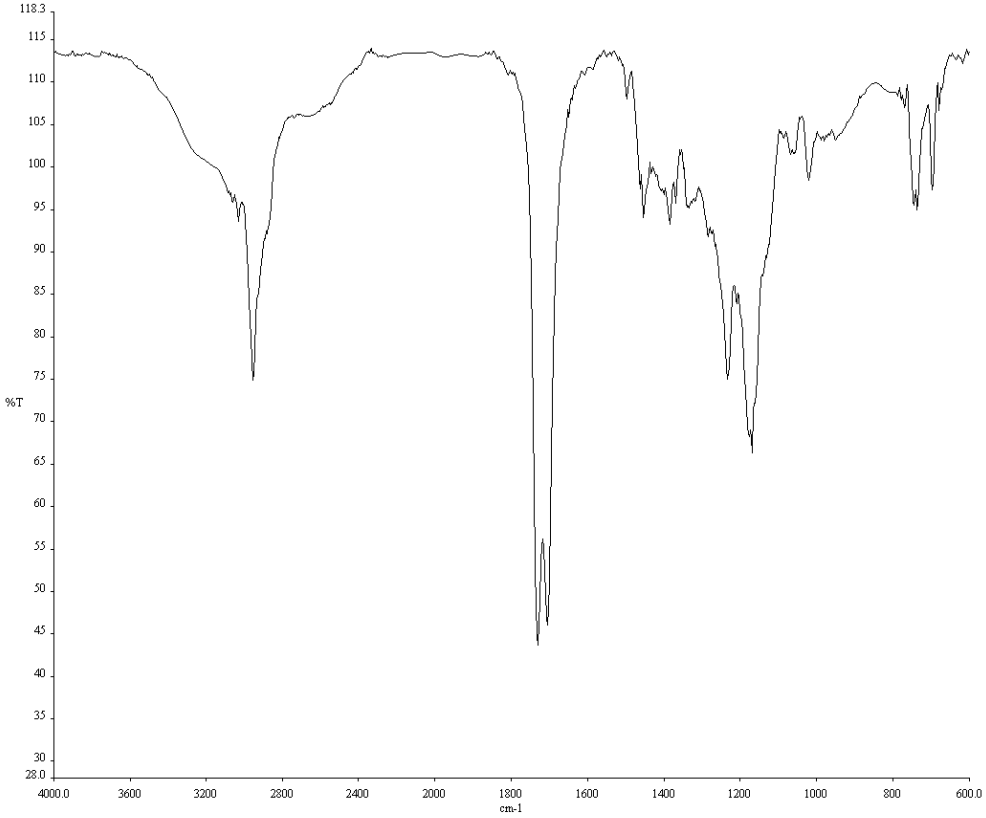


Figure A11.14. Infrared spectrum (Thin Film, NaCl) of compound **368**.

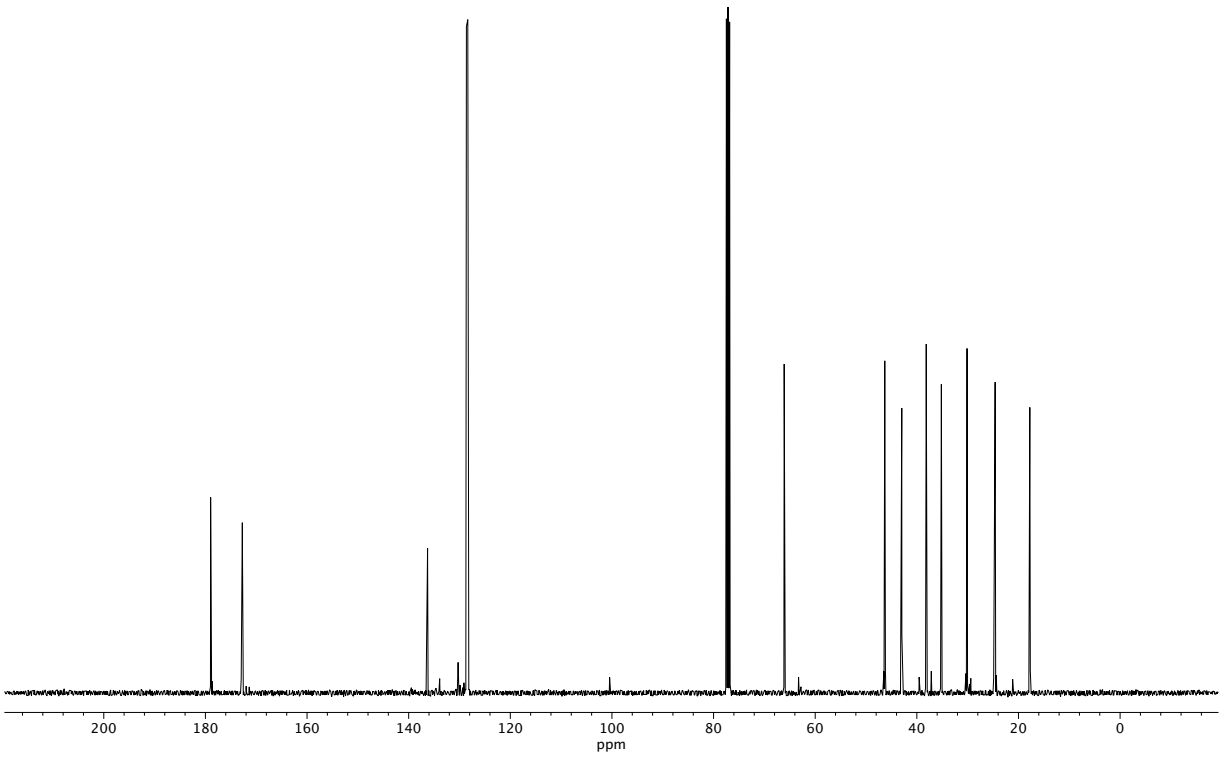


Figure A11.15. ^{13}C NMR (100 MHz, $CDCl_3$) of compound **368**.

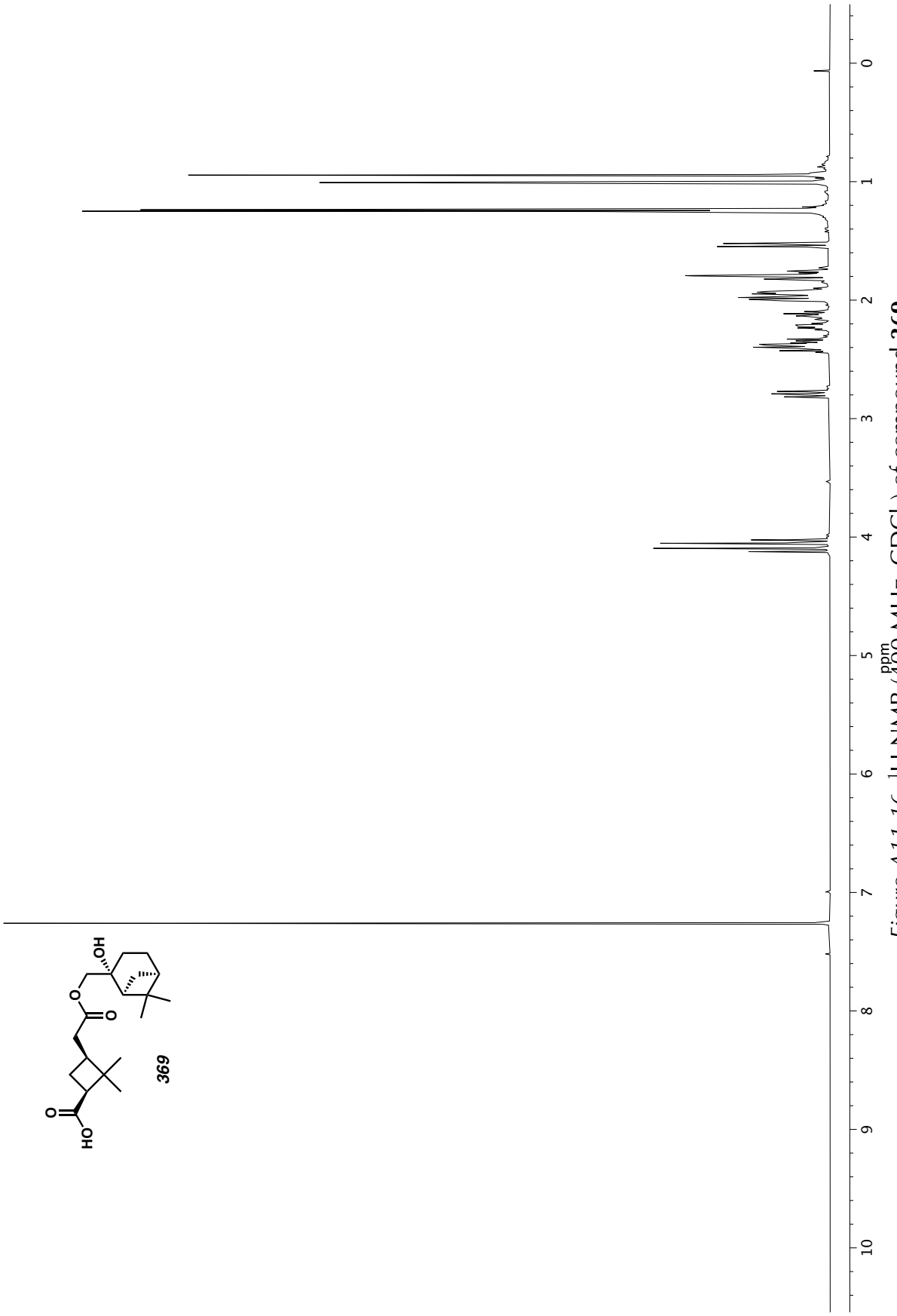


Figure A11.16. ^{1}H NMR (400 MHz, $CDCl_3$) of compound **369**.

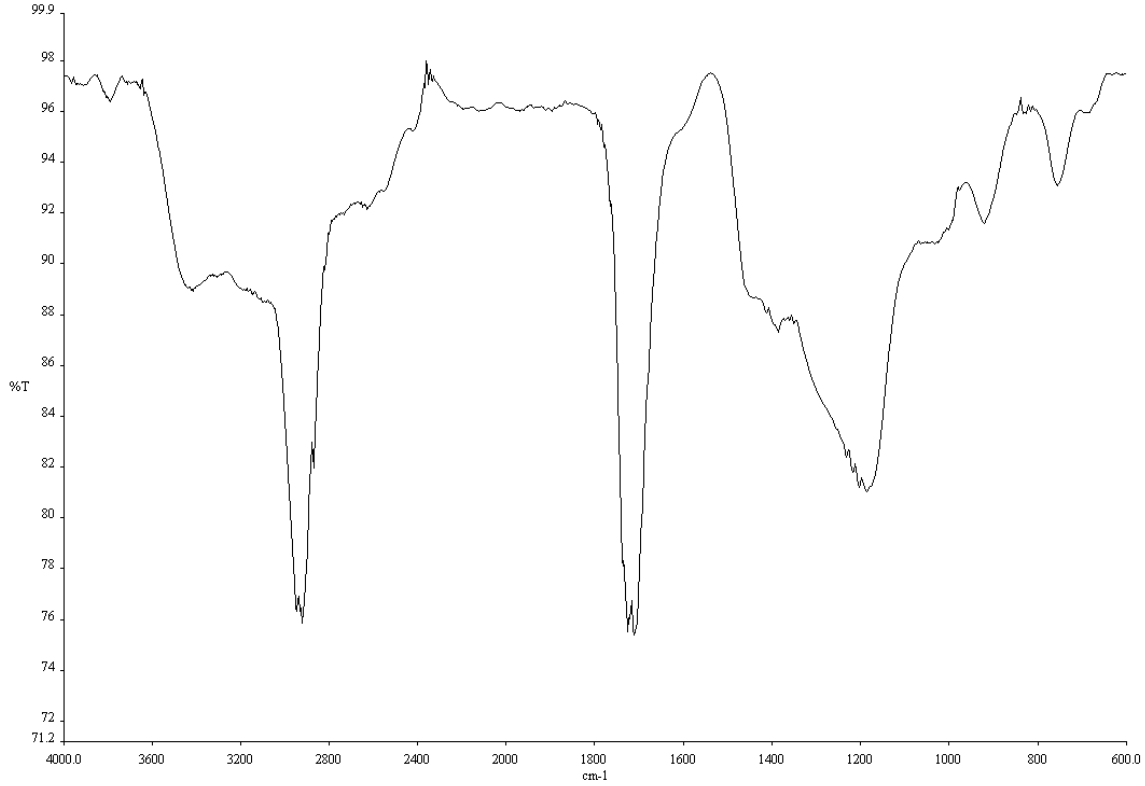


Figure A11.17. Infrared spectrum (Thin Film, NaCl) of compound **369**.

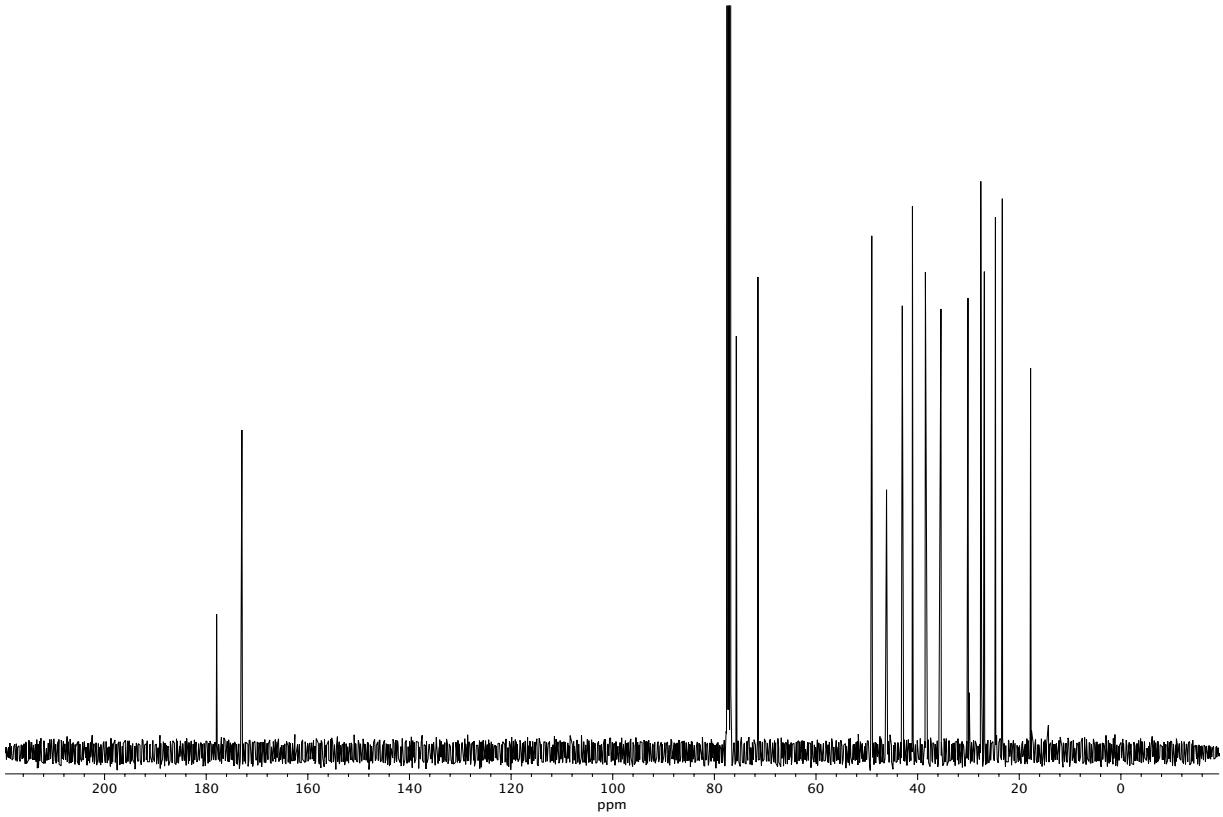


Figure A11.18. ^{13}C NMR (100 MHz, $CDCl_3$) of compound **369**.

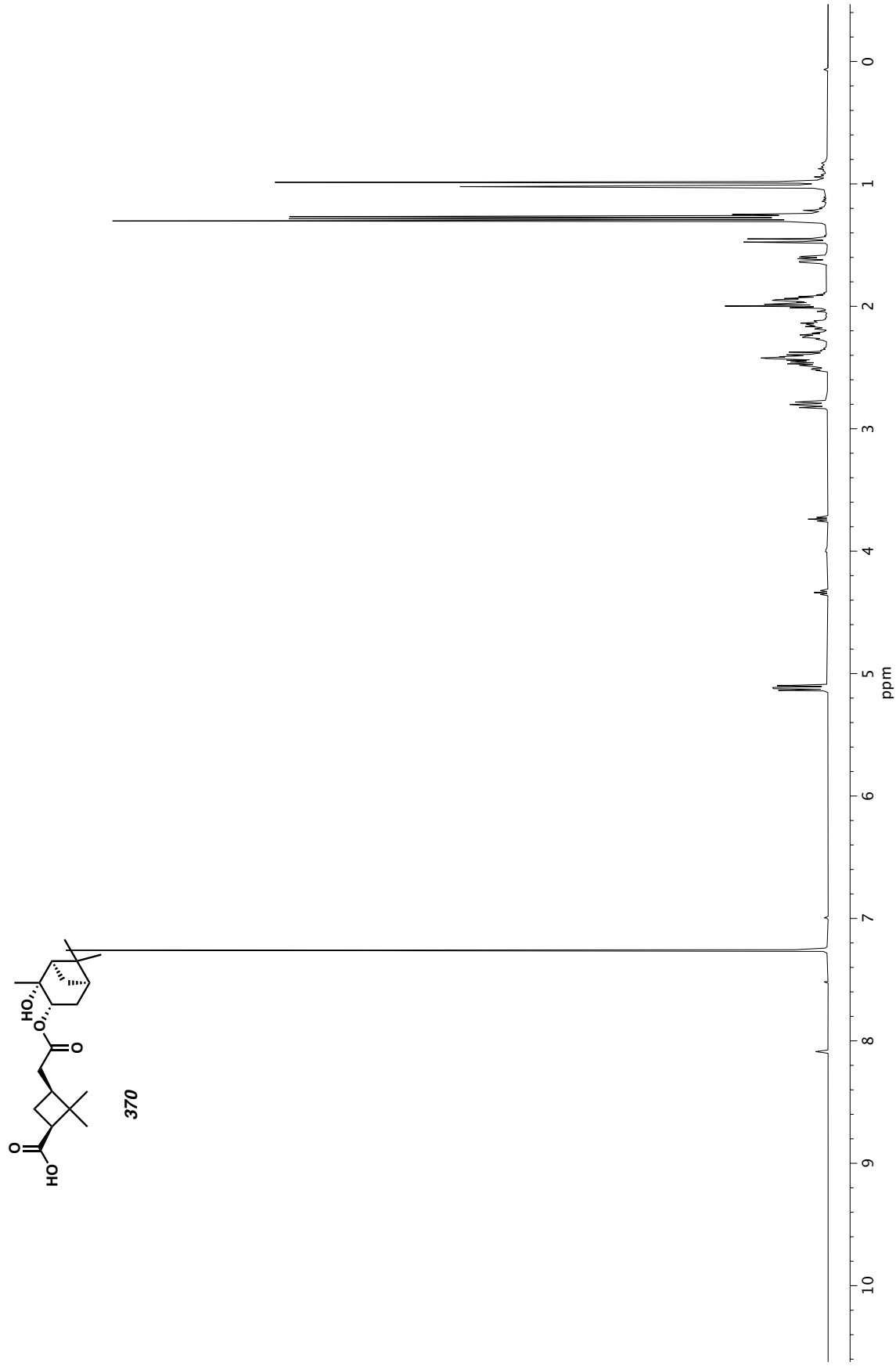


Figure A11.19. ^{1}H NMR (400 MHz, $CDCl_3$) of compound **370**.

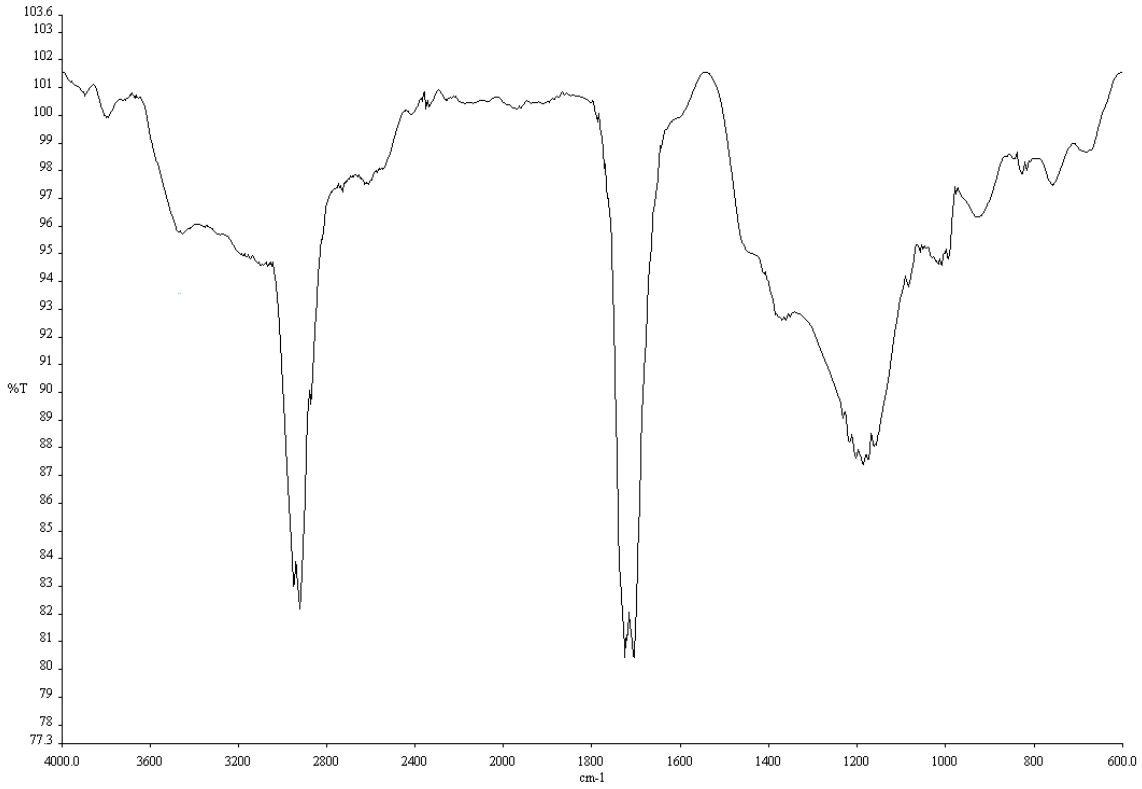


Figure A11.20. Infrared spectrum (Thin Film, NaCl) of compound **370**.

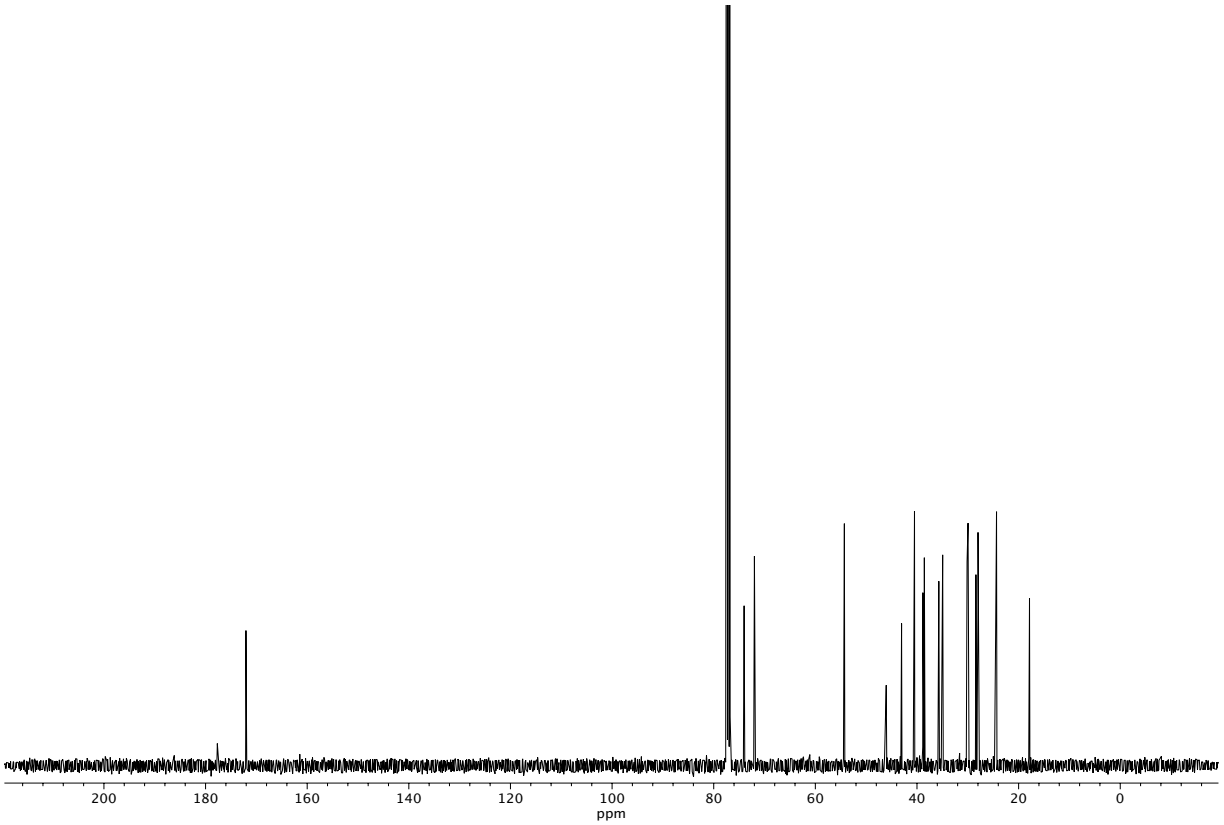


Figure A11.21. ^{13}C NMR (100 MHz, $CDCl_3$) of compound **370**.

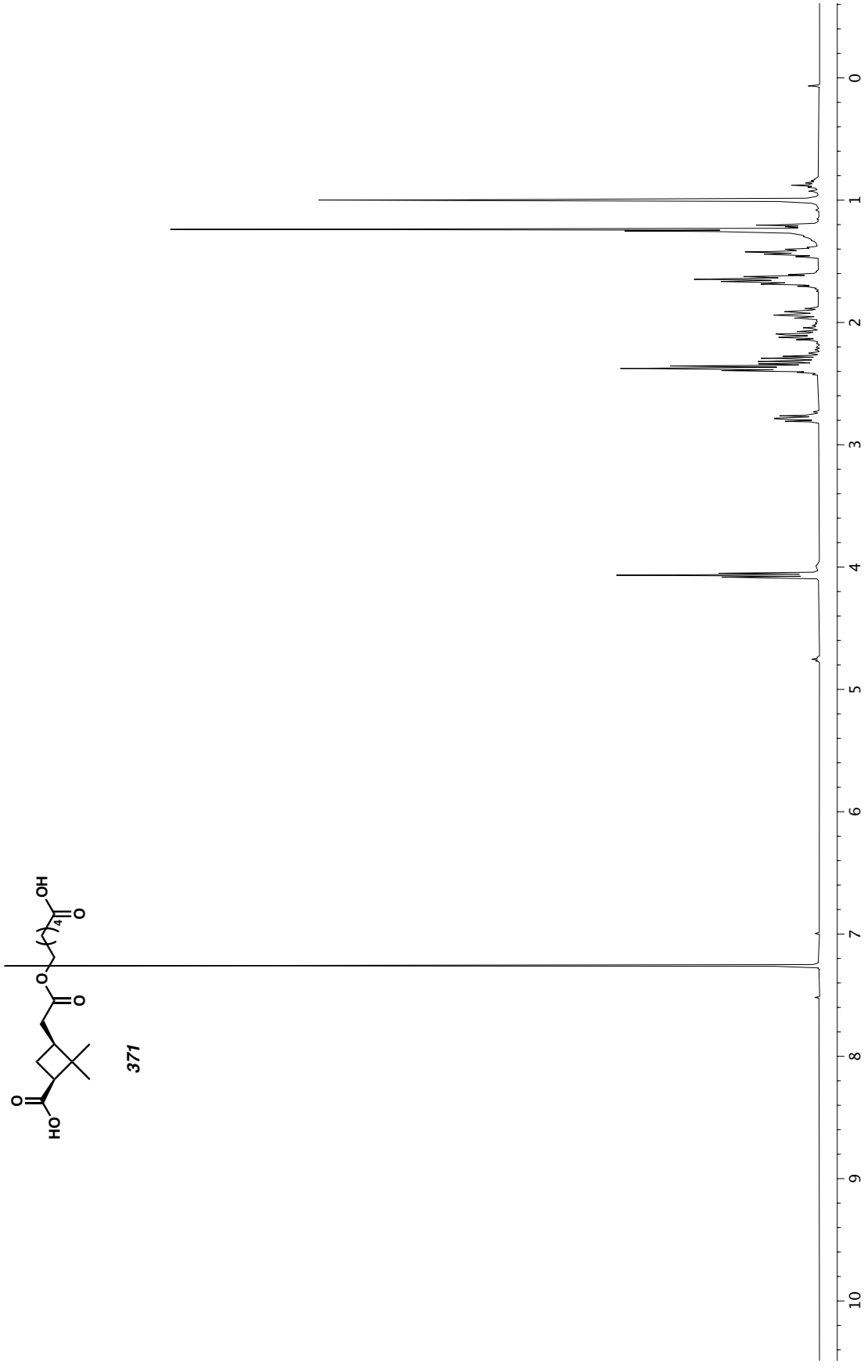


Figure A11.22. ^{1}H NMR (400 MHz, $CDCl_3$) of compound **371**.

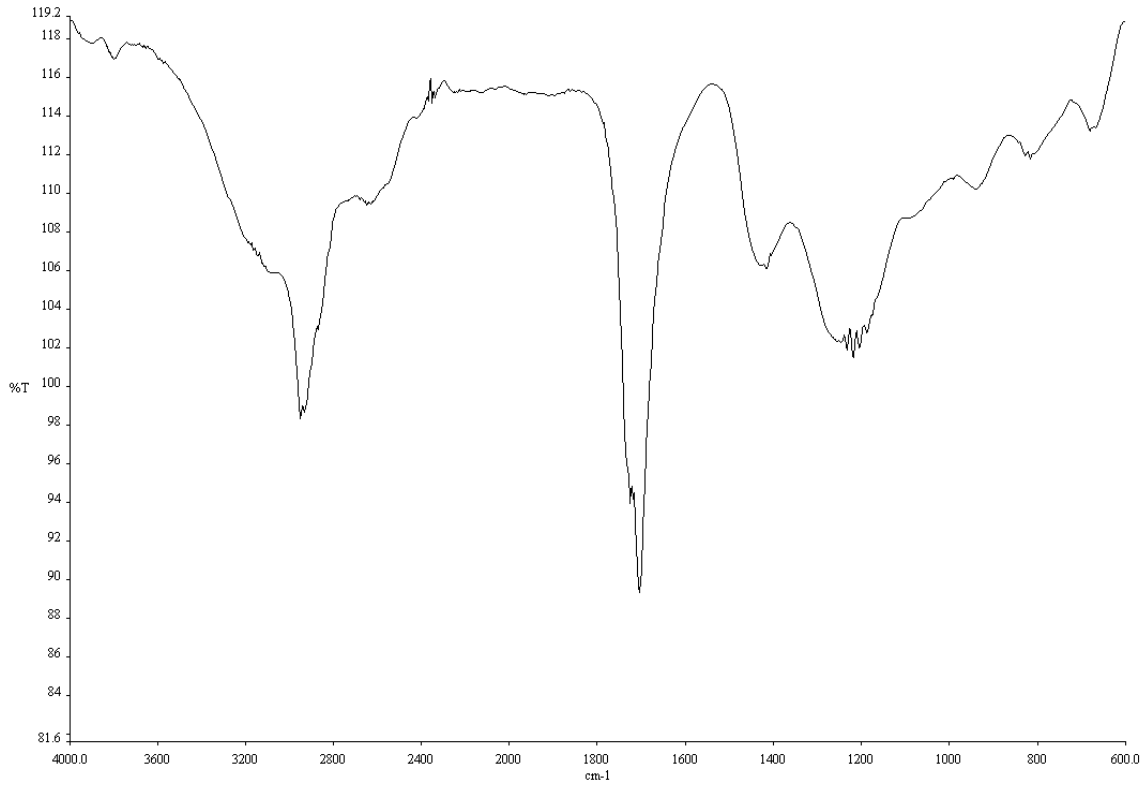


Figure A11.23. Infrared spectrum (Thin Film, NaCl) of compound **371**.

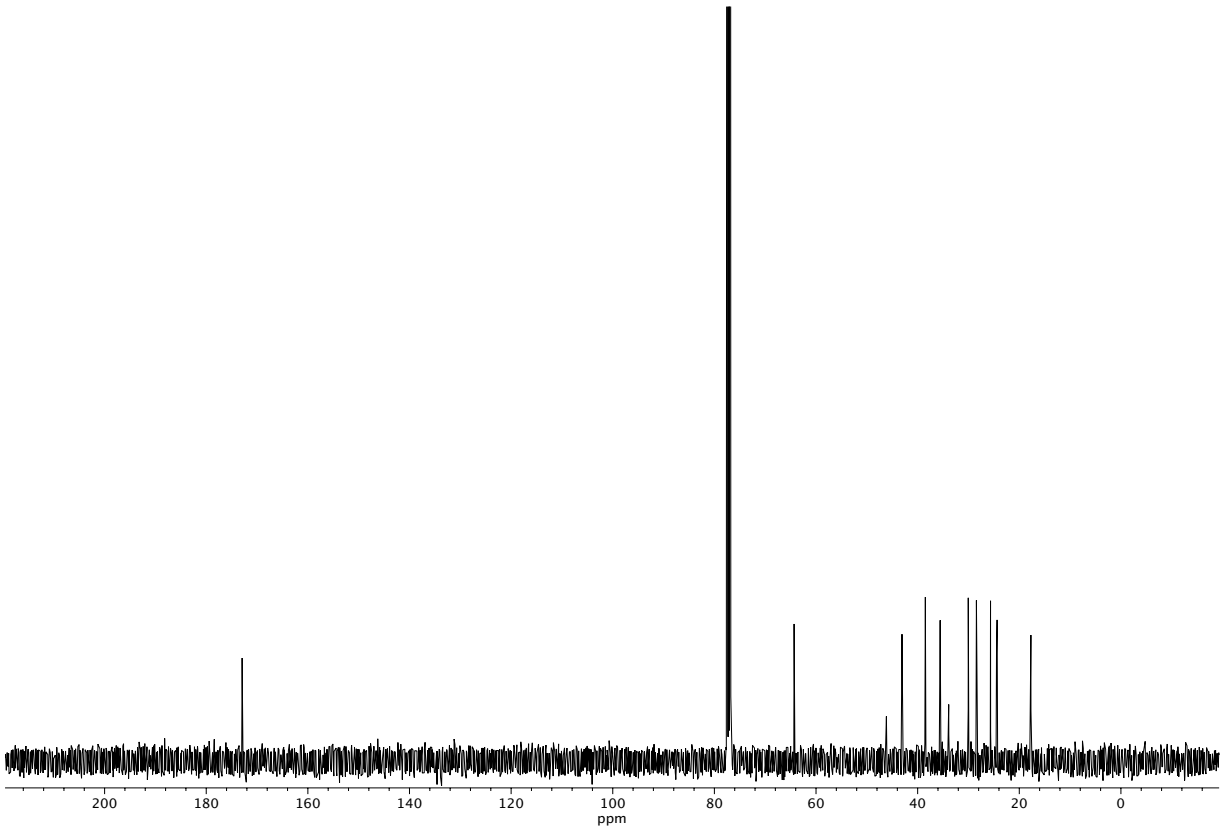


Figure A11.24. ^{13}C NMR (100 MHz, $CDCl_3$) of compound **371**.

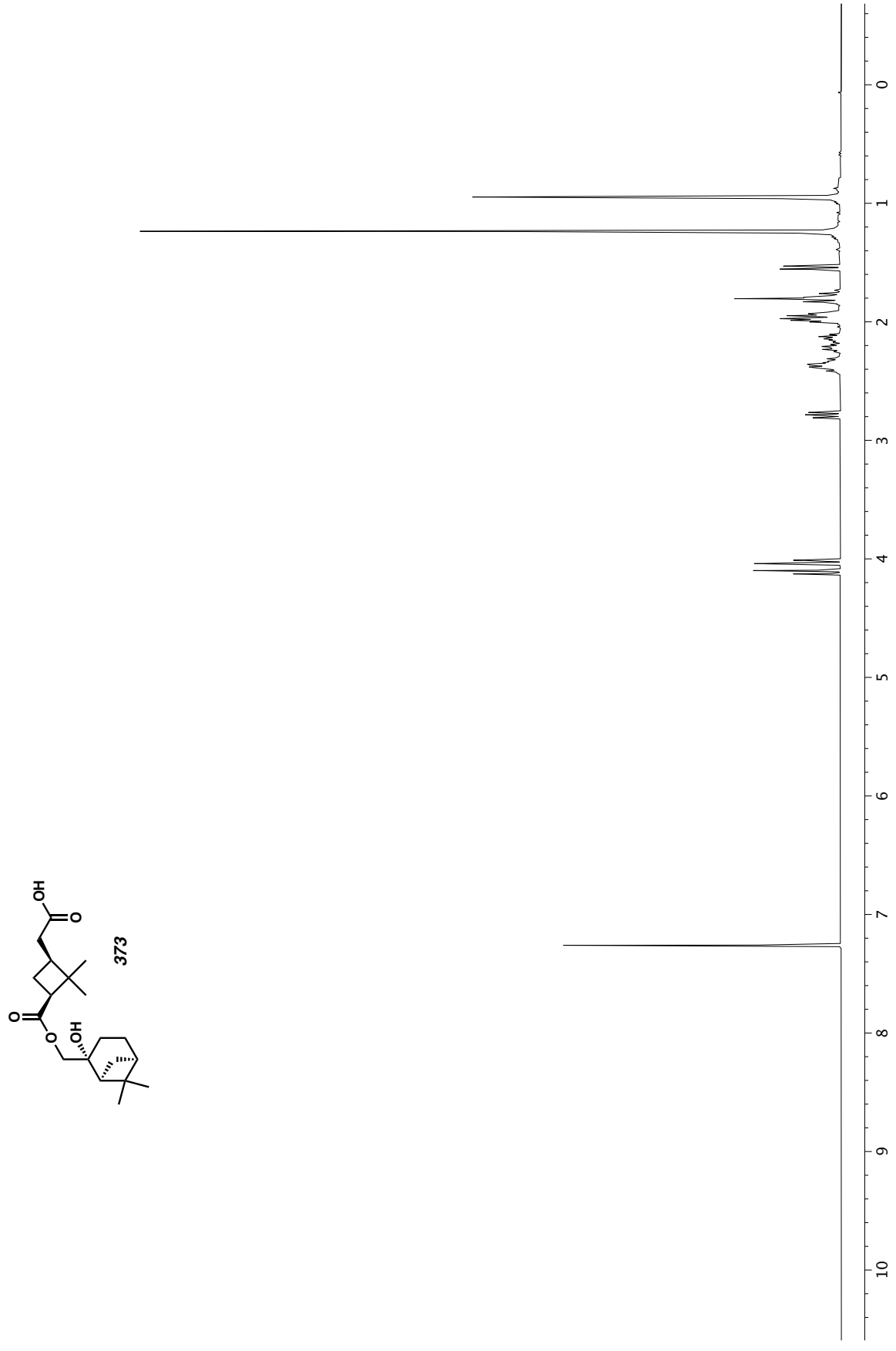


Figure A11.25. ^{1}H NMR (400 MHz, $CDCl_3$) of compound **373**.

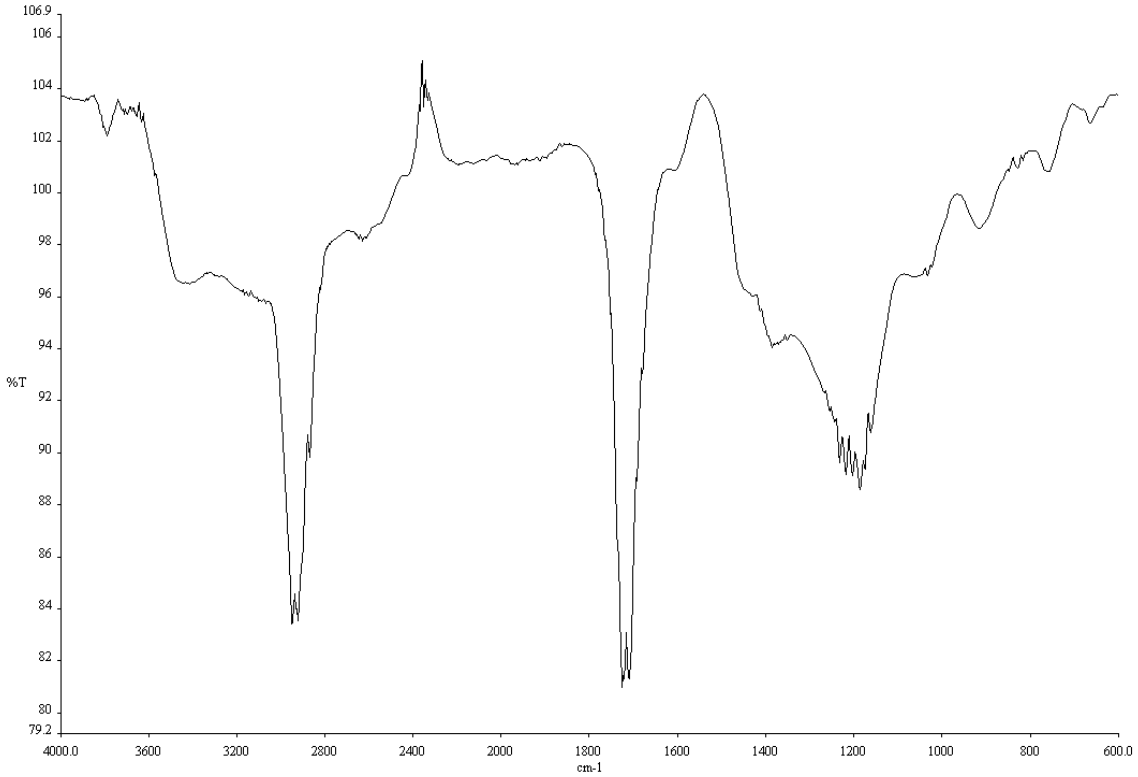


Figure A11.26. Infrared spectrum (Thin Film, NaCl) of compound **373**.

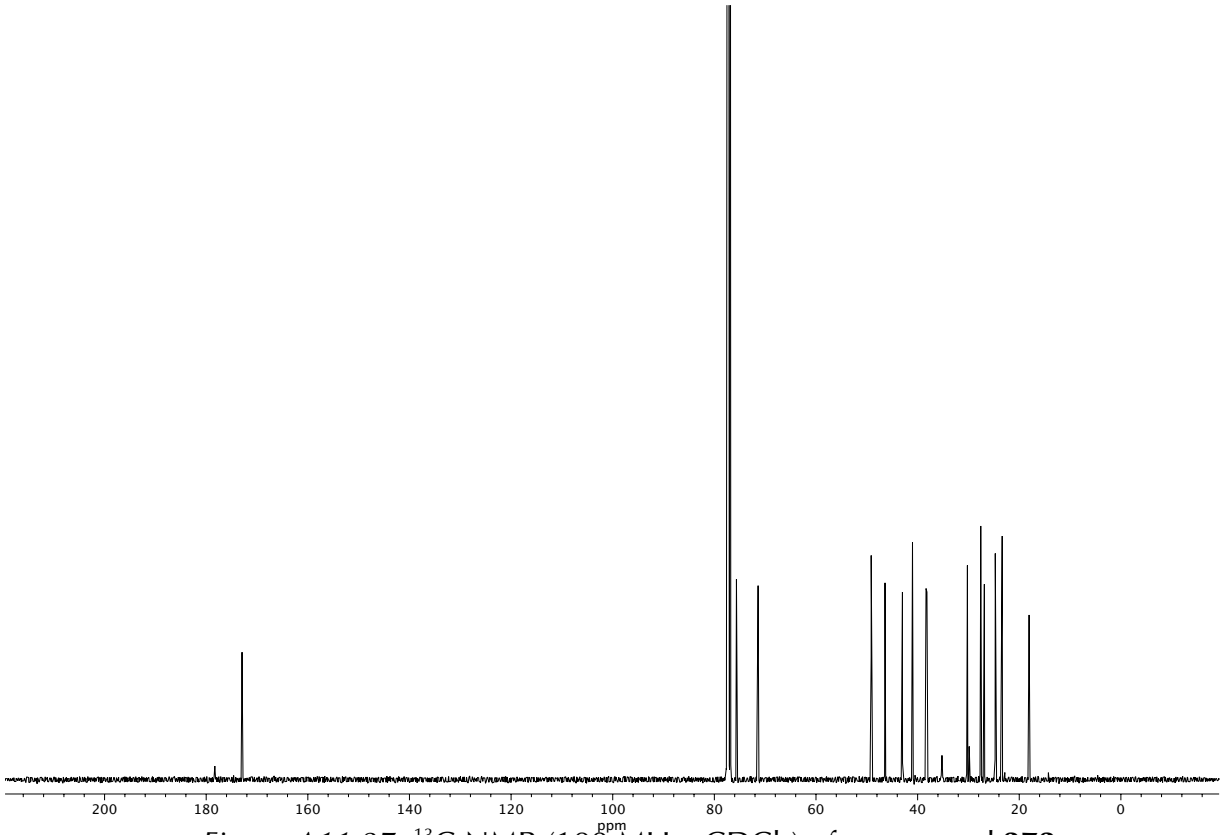


Figure A11.27. ^{13}C NMR (100 MHz, $CDCl_3$) of compound **373**.

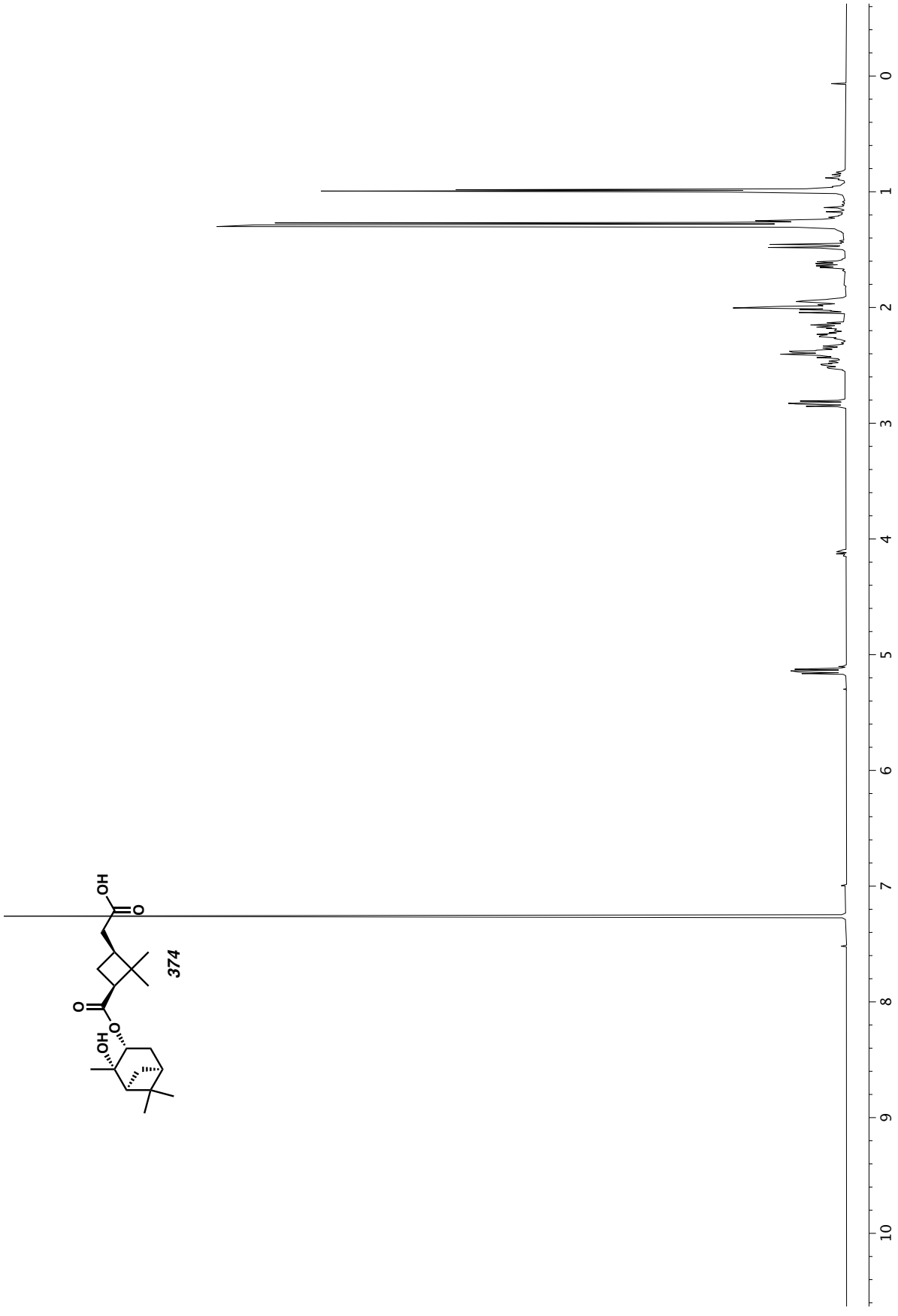


Figure A11.28. ^{1}H NMR (400 MHz, $CDCl_3$) of compound **374**.

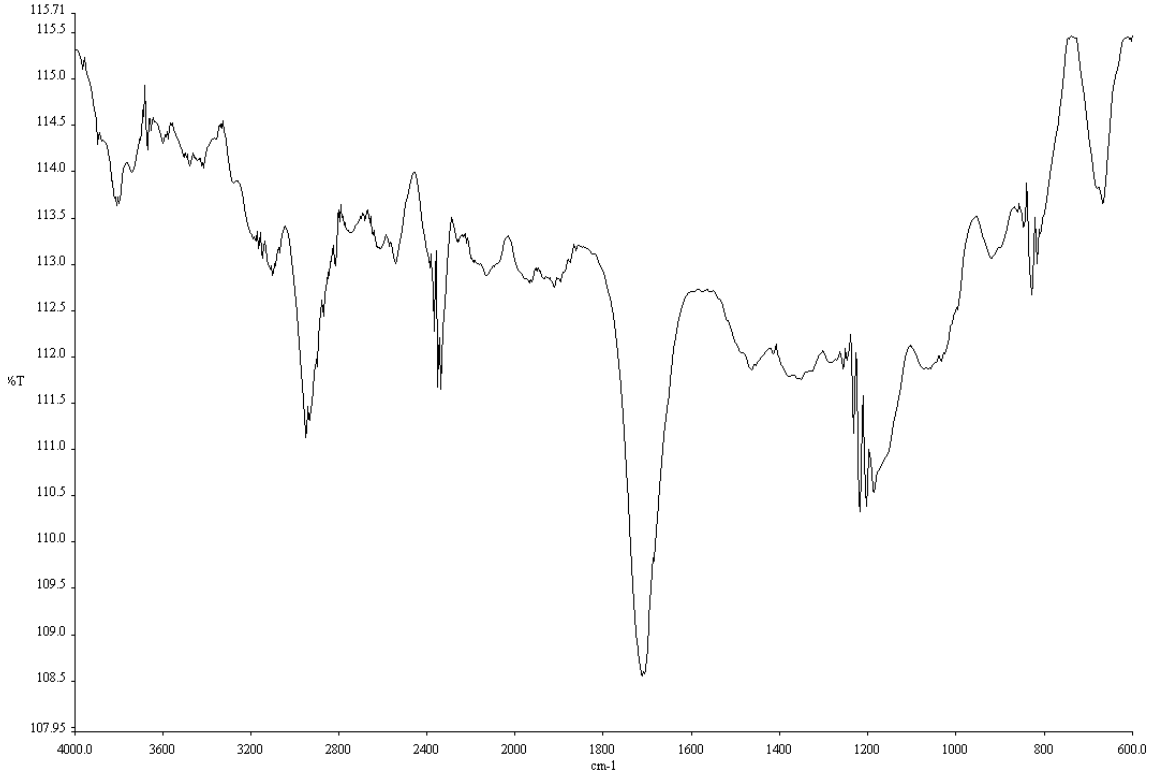


Figure A11.29. Infrared spectrum (Thin Film, NaCl) of compound **374**.

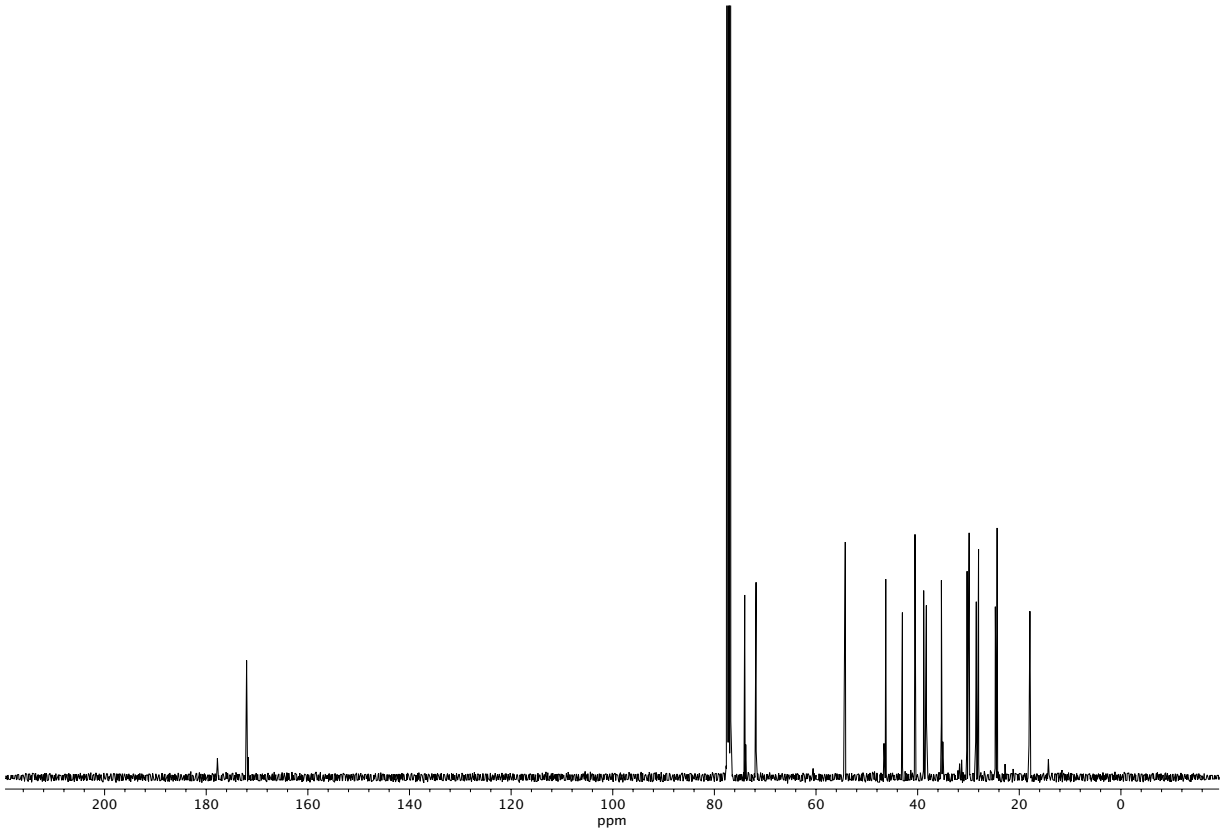


Figure A11.30. ^{13}C NMR (100 MHz, $CDCl_3$) of compound **374**.

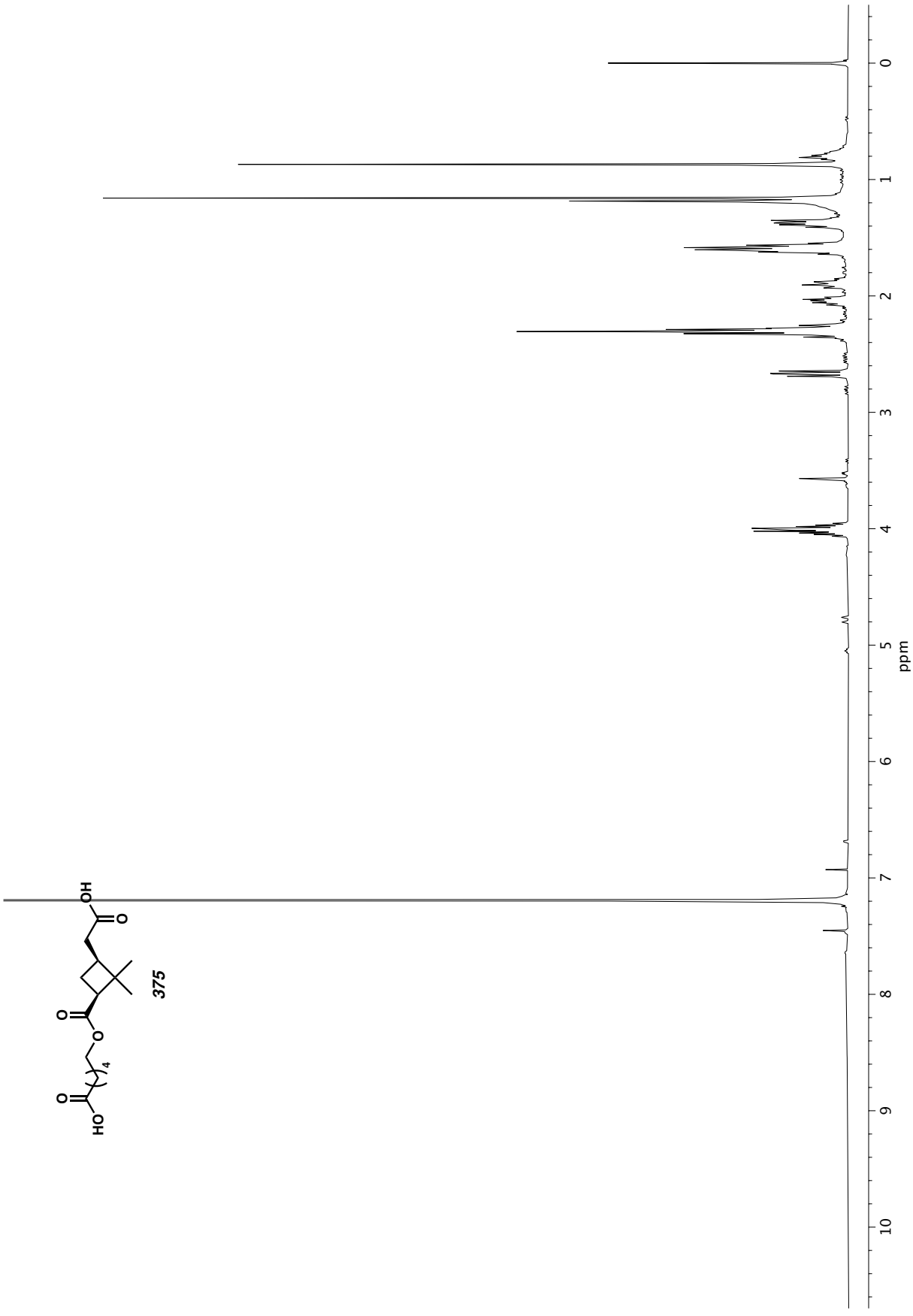


Figure A11.31. ^{1}H NMR (400 MHz, $CDCl_3$) of compound **375**.

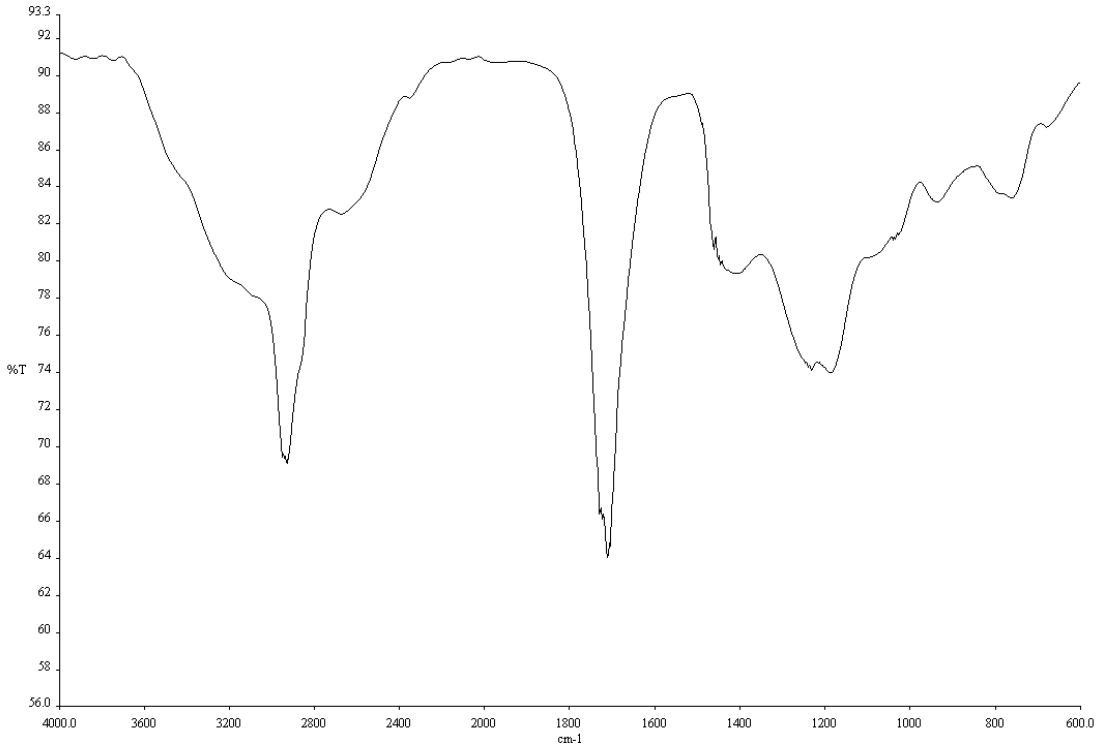


Figure A11.32. Infrared spectrum (Thin Film, NaCl) of compound **375**.

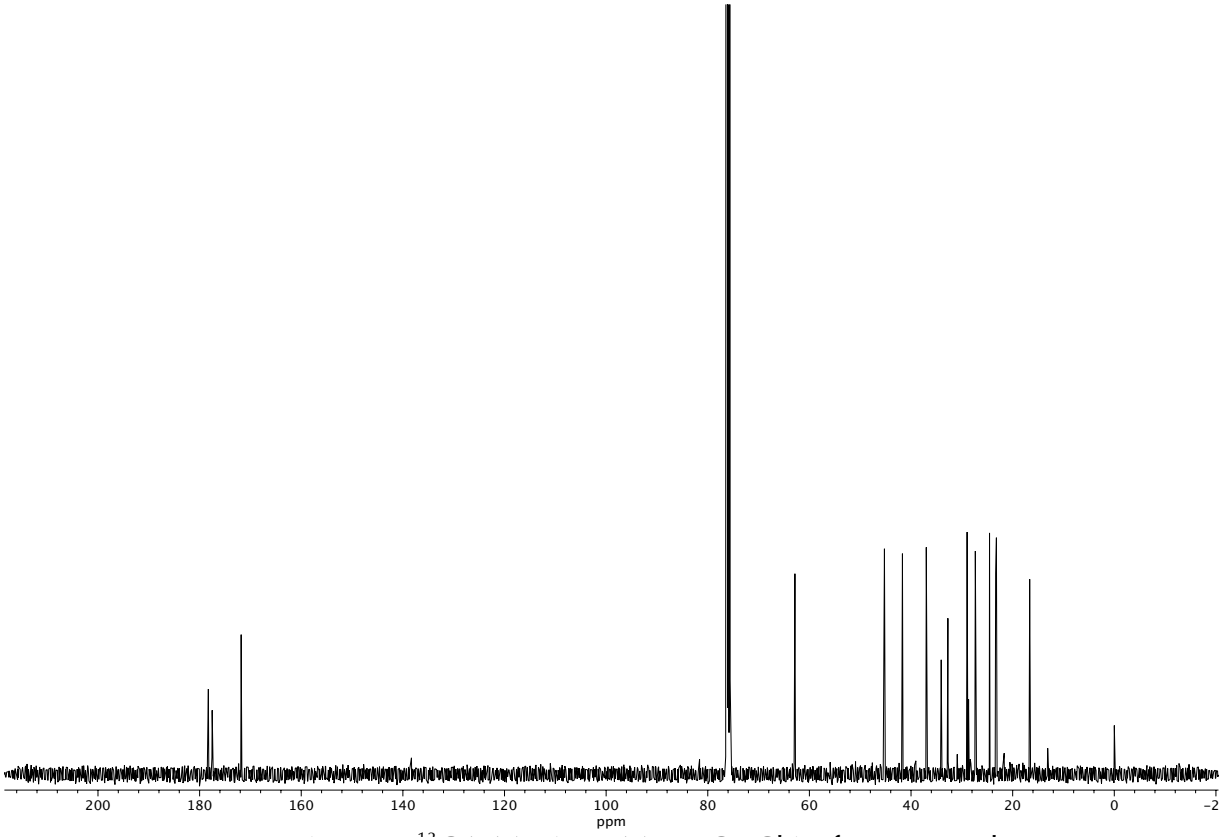


Figure A11.33. ^{13}C NMR (100 MHz, $CDCl_3$) of compound **375**.

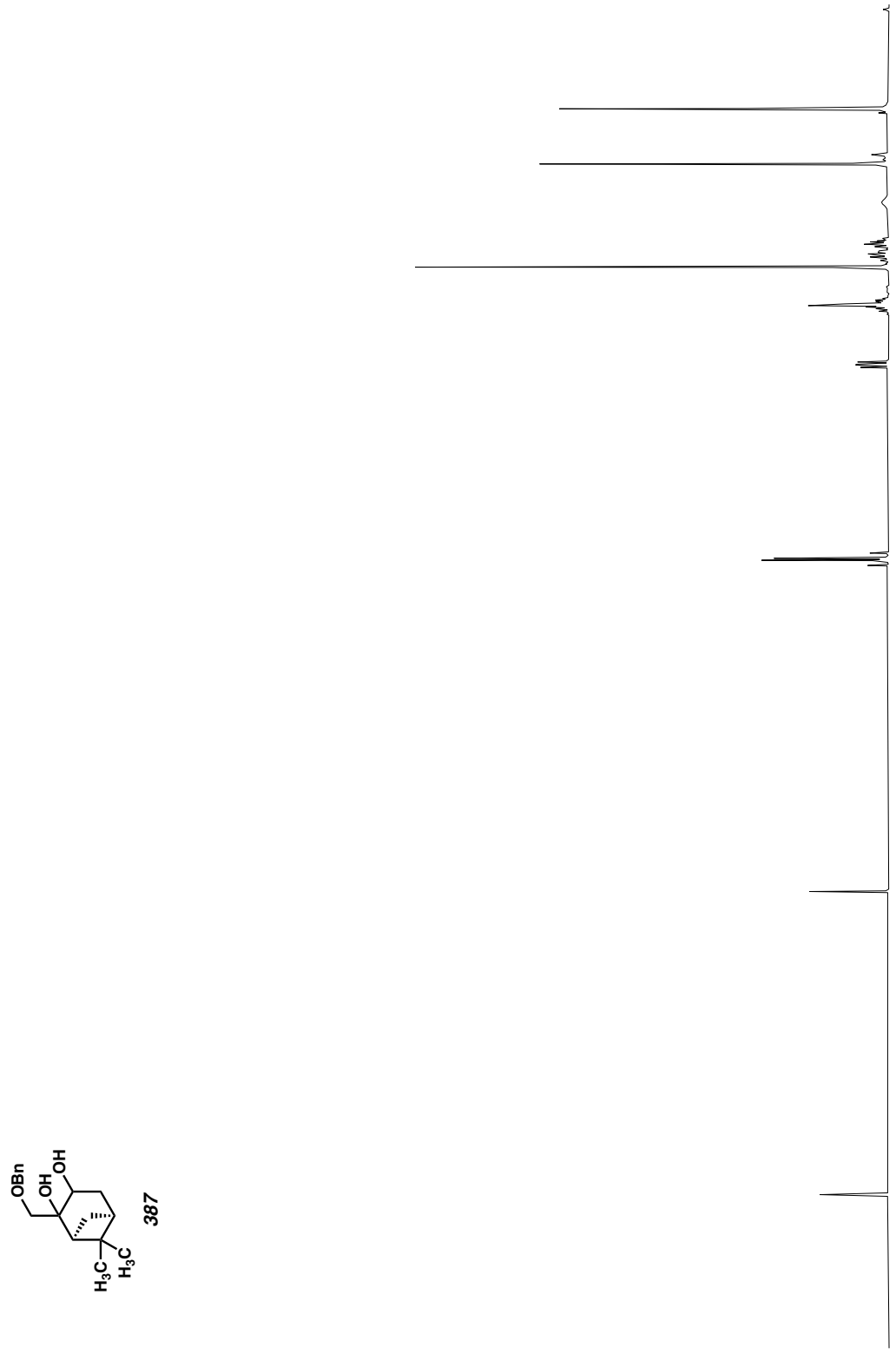


Figure A11.34. ^{1}H NMR (400 MHz, $CDCl_3$) of compound **387**.

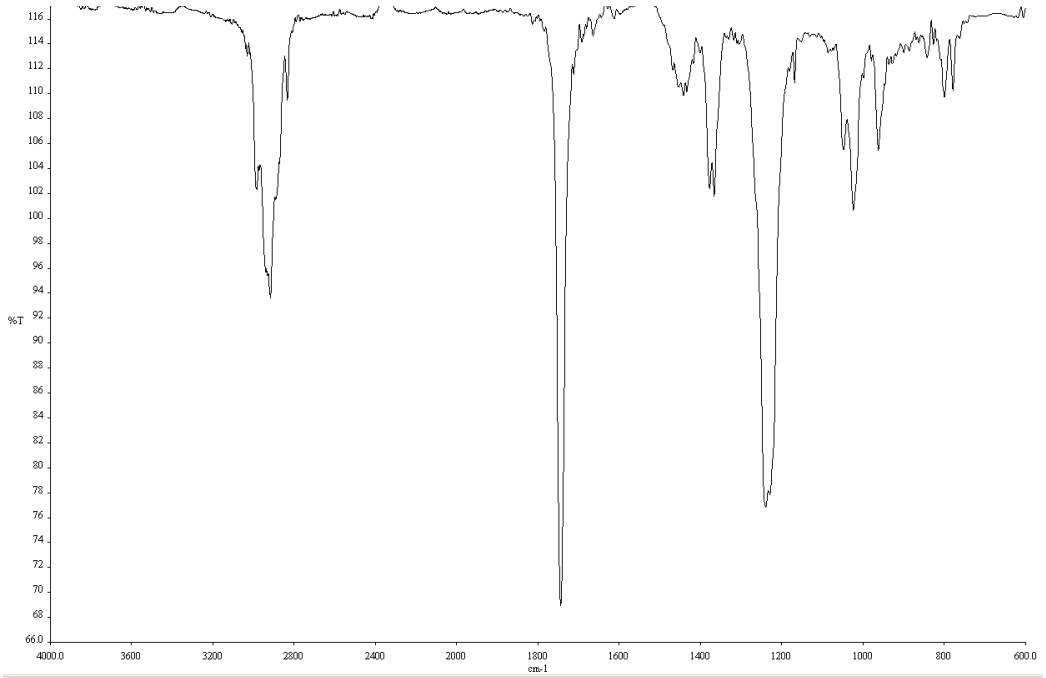


Figure A11.35. Infrared spectrum (Thin Film, NaCl) of compound **387**.

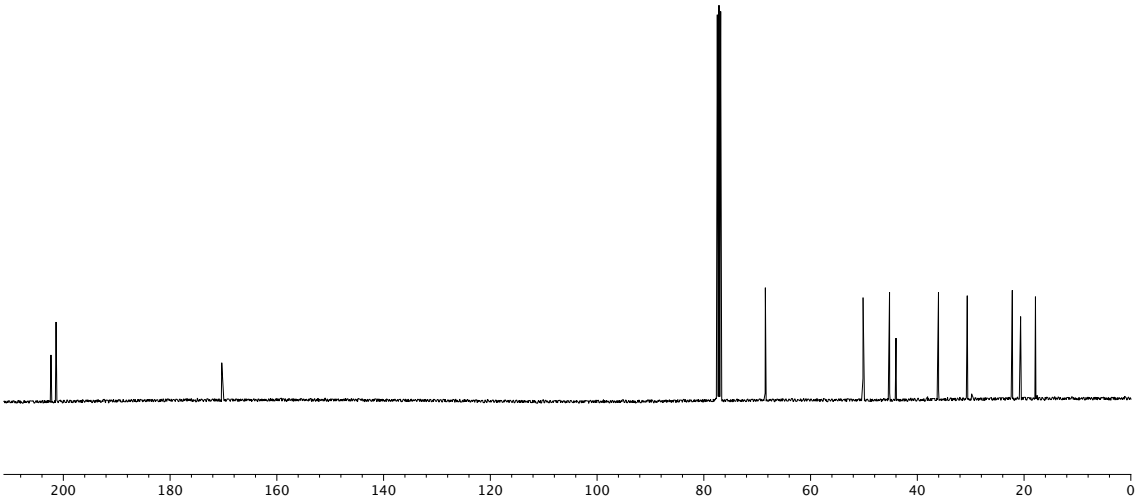


Figure A11.36. ^{13}C NMR (100 MHz, $CDCl_3$) of compound **387**.

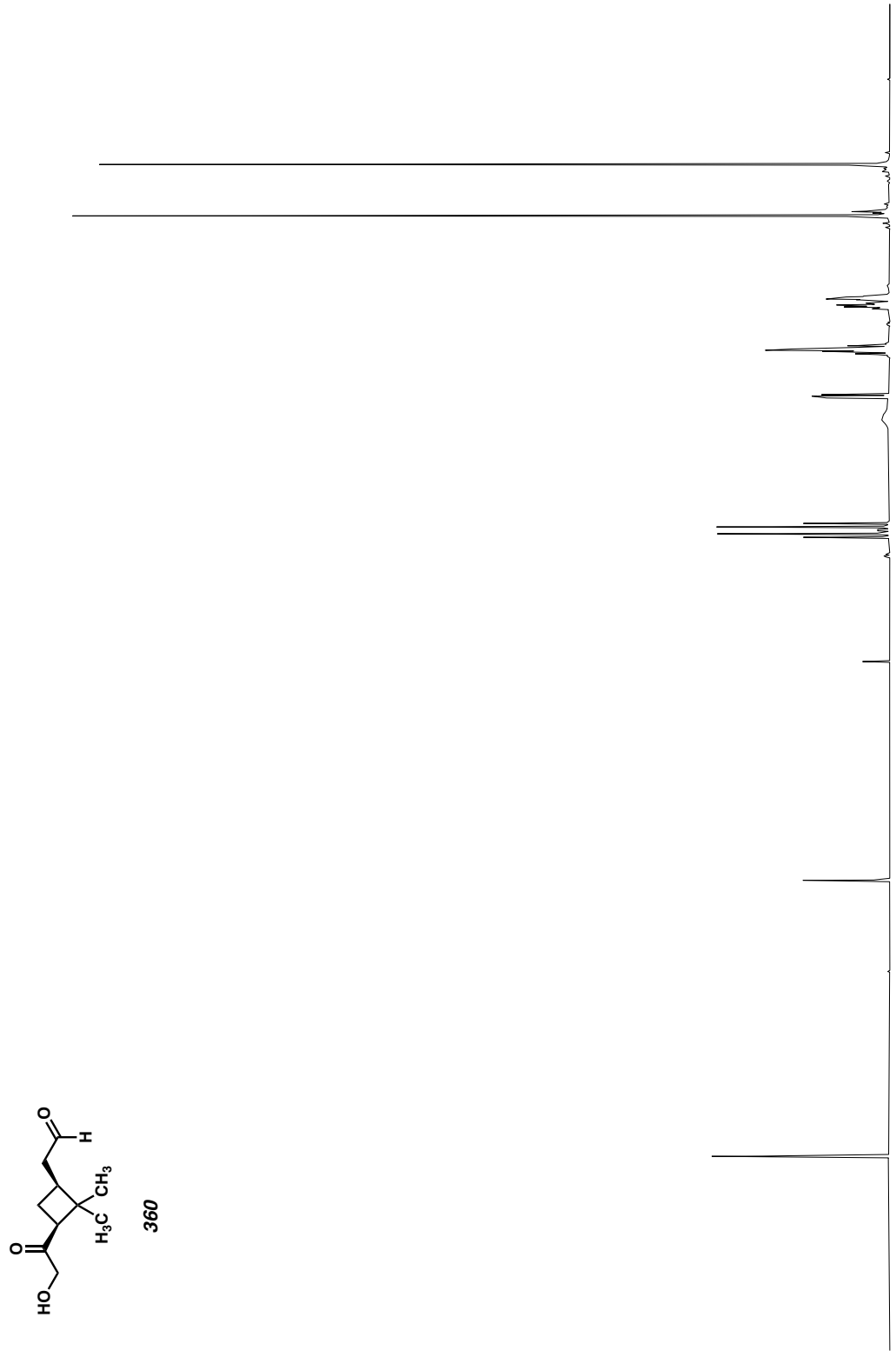


Figure A11.37. ^{1}H NMR (400 MHz, $CDCl_3$) of compound **360**.

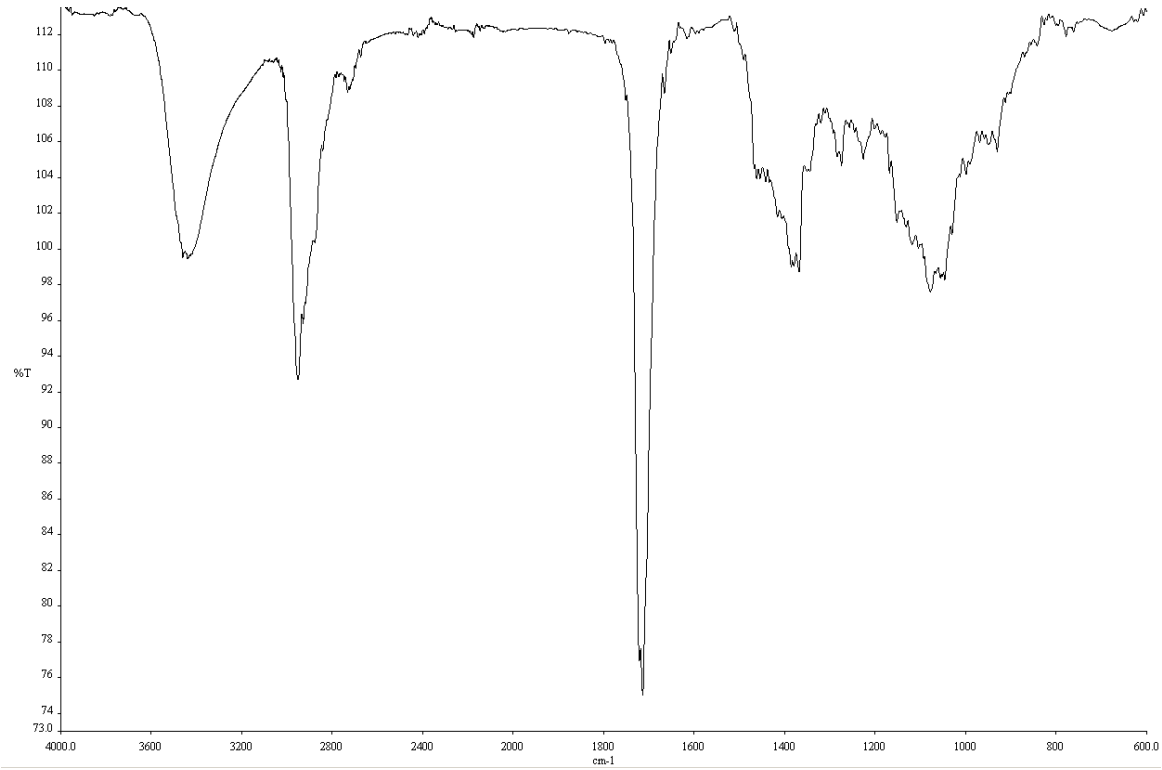


Figure A11.38. Infrared spectrum (Thin Film, NaCl) of compound **360**.

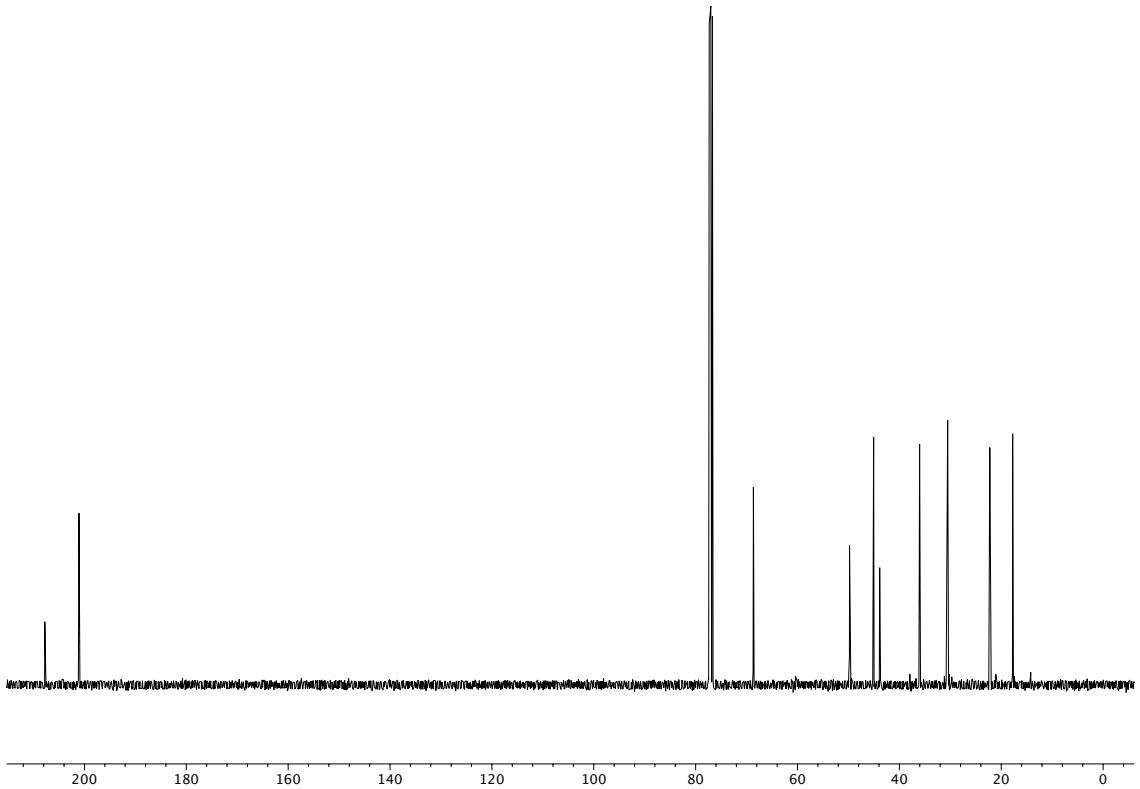


Figure A11.39. ^{13}C NMR (100 MHz, $CDCl_3$) of compound **360**.

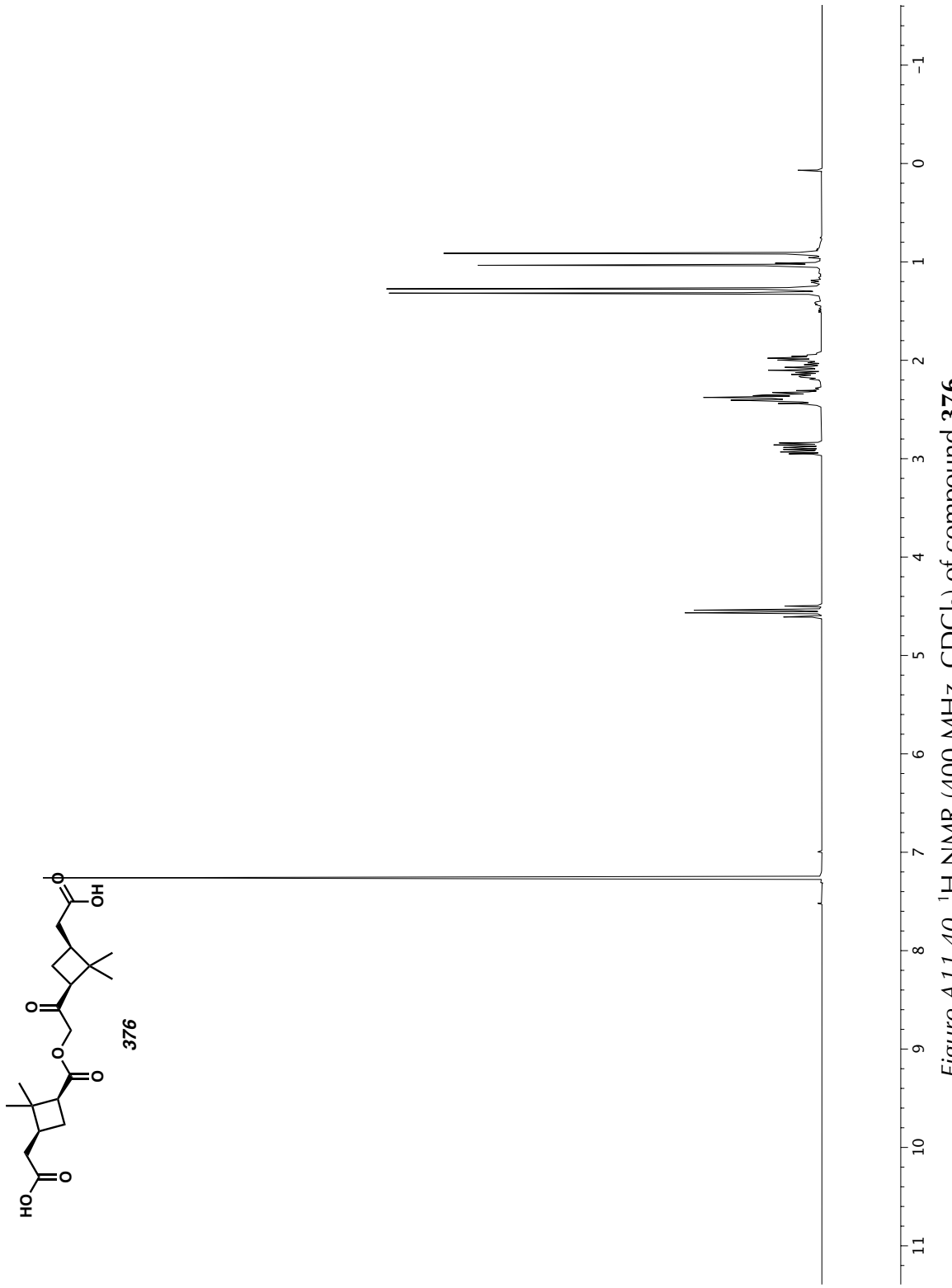


Figure A11.40. ^{1}H NMR (400 MHz, $CDCl_3$) of compound **376**.

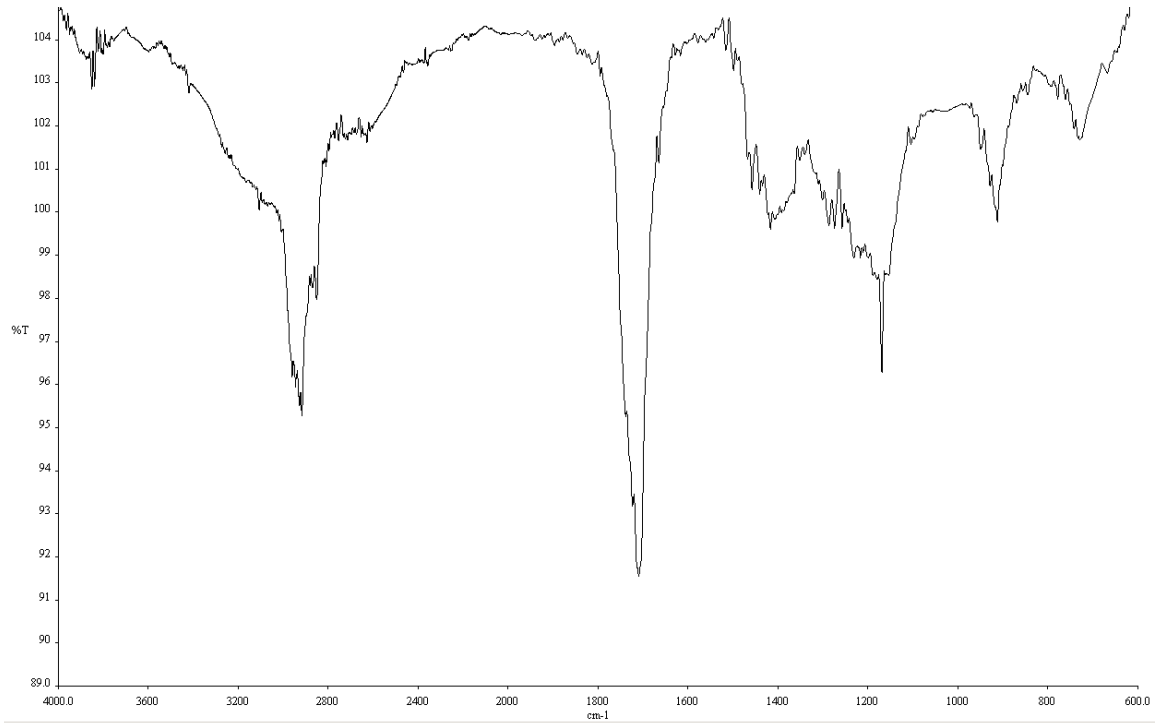


Figure A11.41. Infrared spectrum (Thin Film, NaCl) of compound **376**.

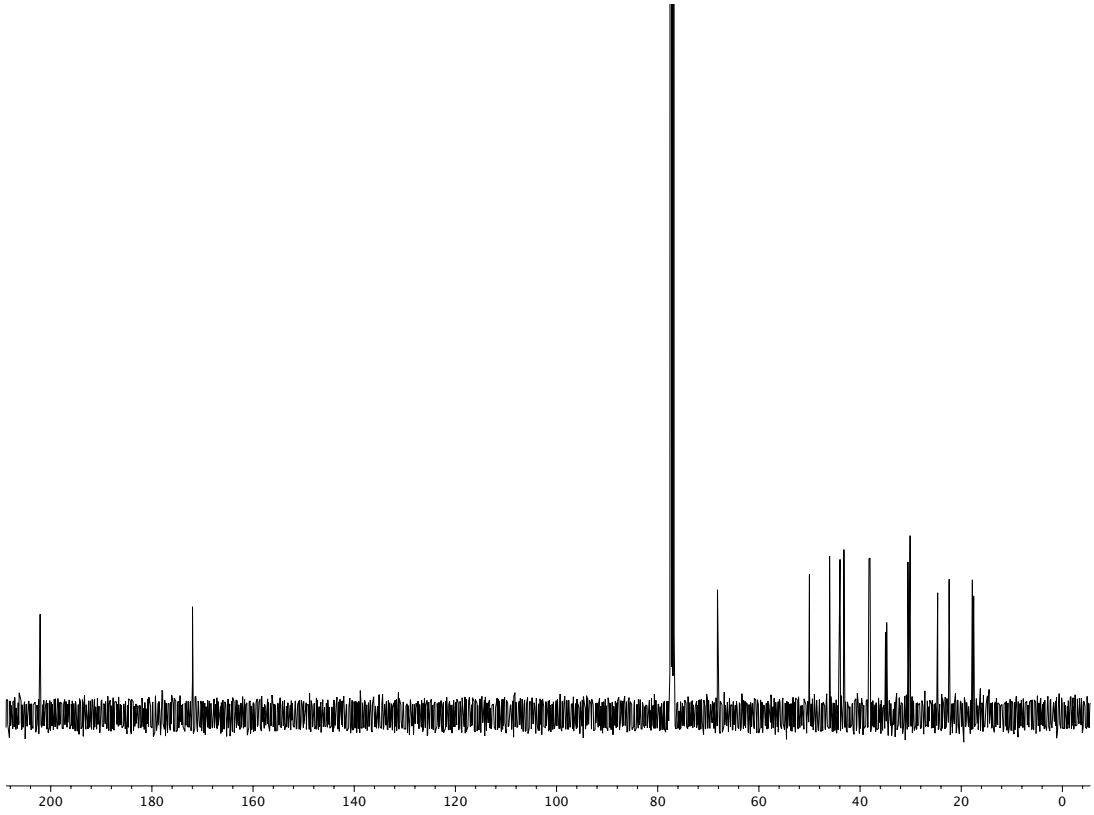


Figure A11.42. ^{13}C NMR (100 MHz, $CDCl_3$) of compound **376**.

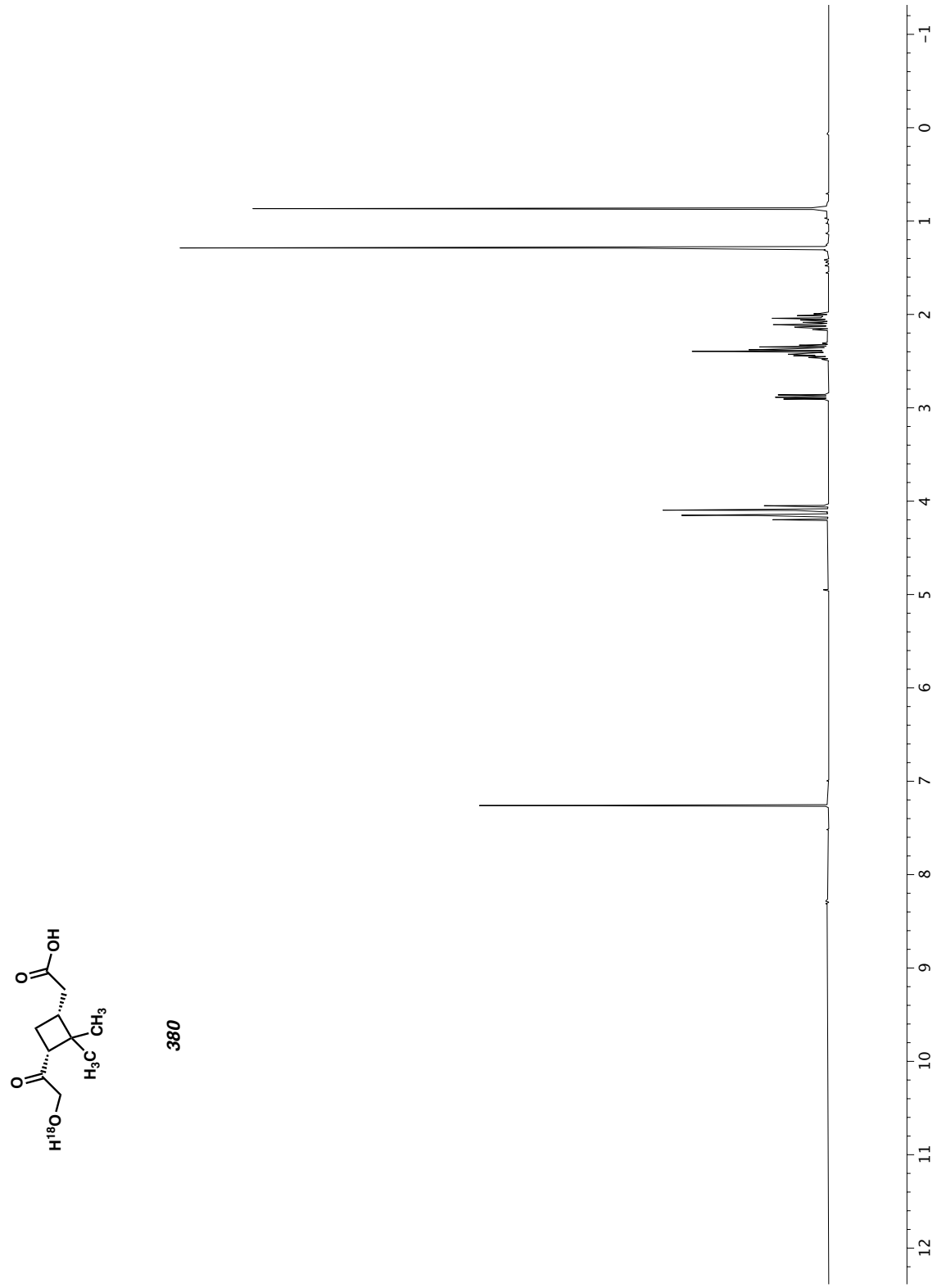


Figure A11.43. ^{1}H NMR (400 MHz, $CDCl_3$) of compound **380**.

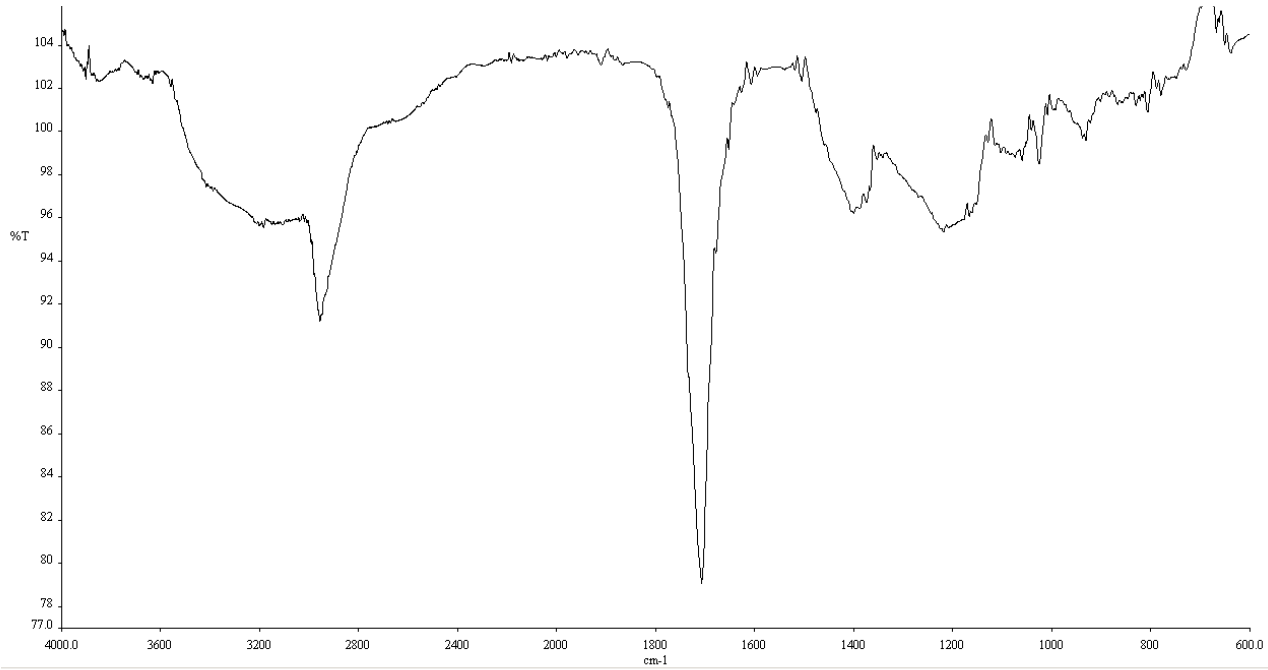


Figure A11.44. Infrared spectrum (Thin Film, NaCl) of compound **380**.

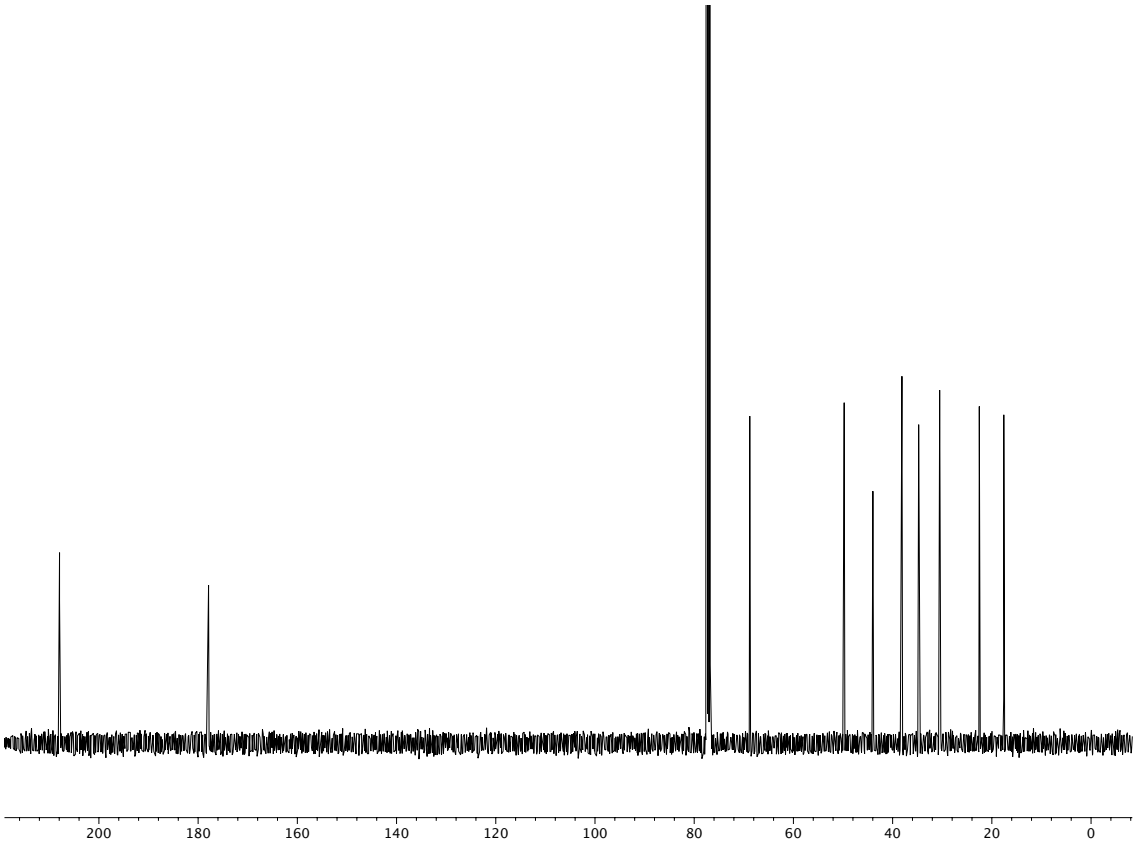


Figure A11.45. ^{13}C NMR (100 MHz, $CDCl_3$) of compound **380**.

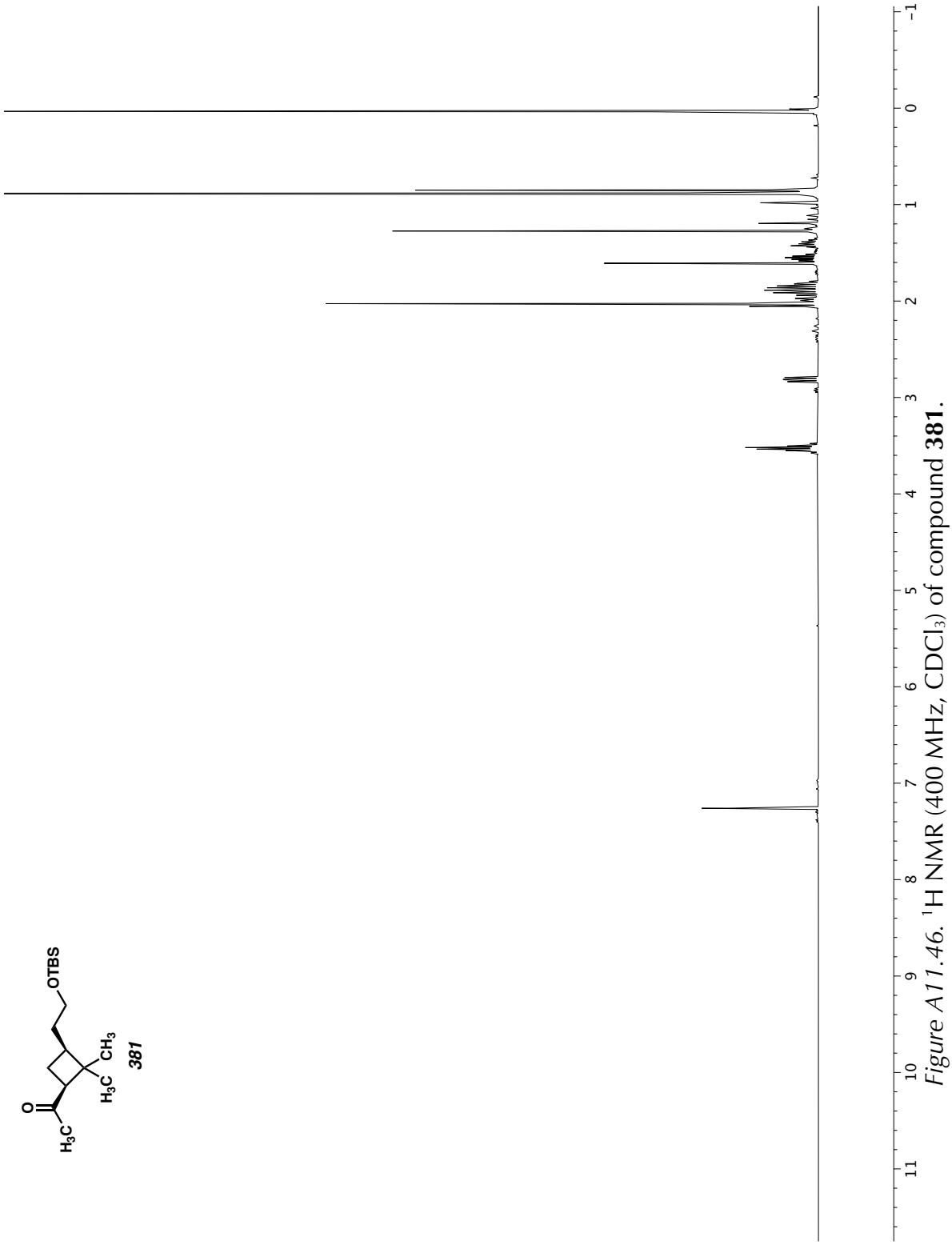


Figure A11.46. ^{1}H NMR (400 MHz, $CDCl_3$) of compound **381**.

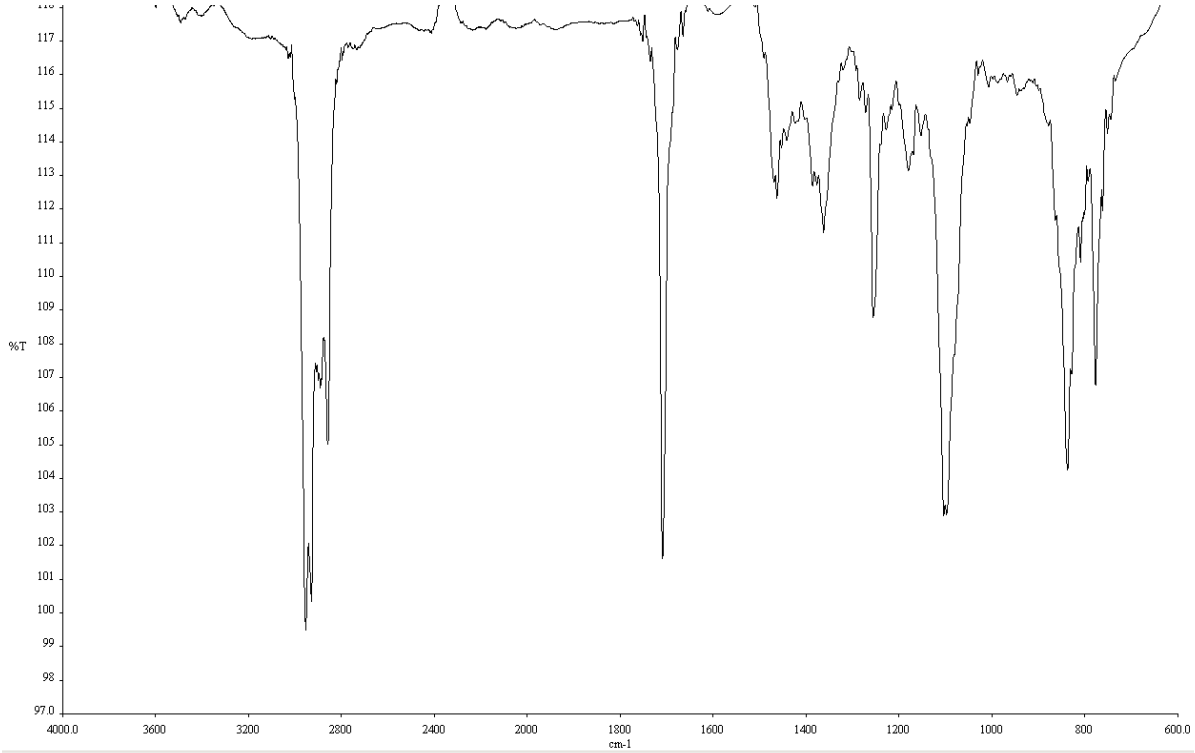


Figure A11.47. Infrared spectrum (Thin Film, NaCl) of compound **381**.

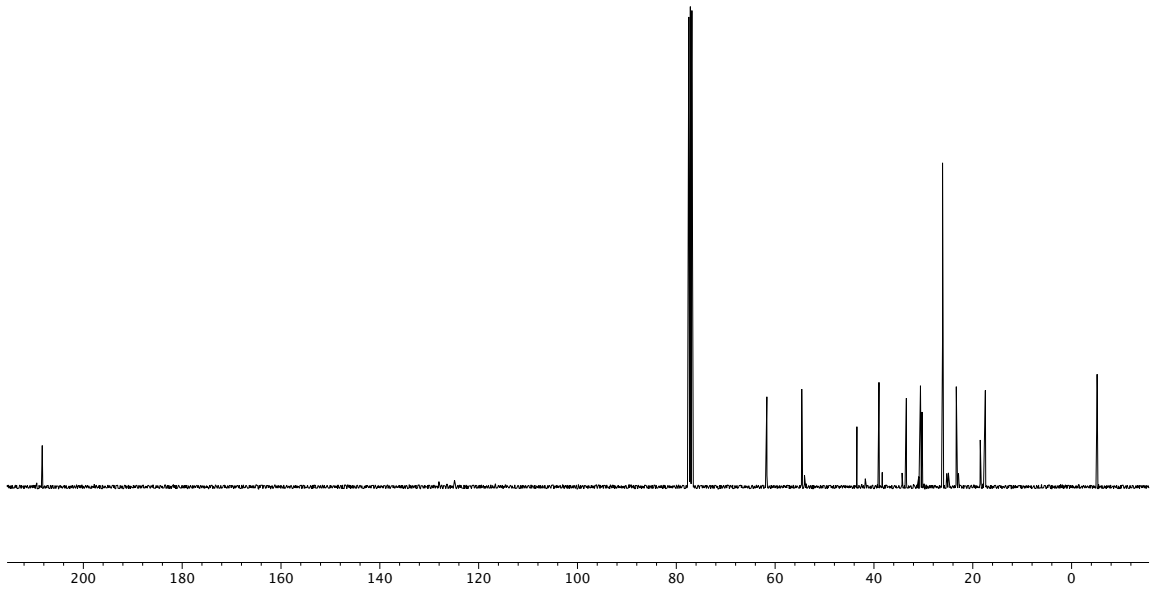


Figure A11.48. ^{13}C NMR (100 MHz, $CDCl_3$) of compound **381**.

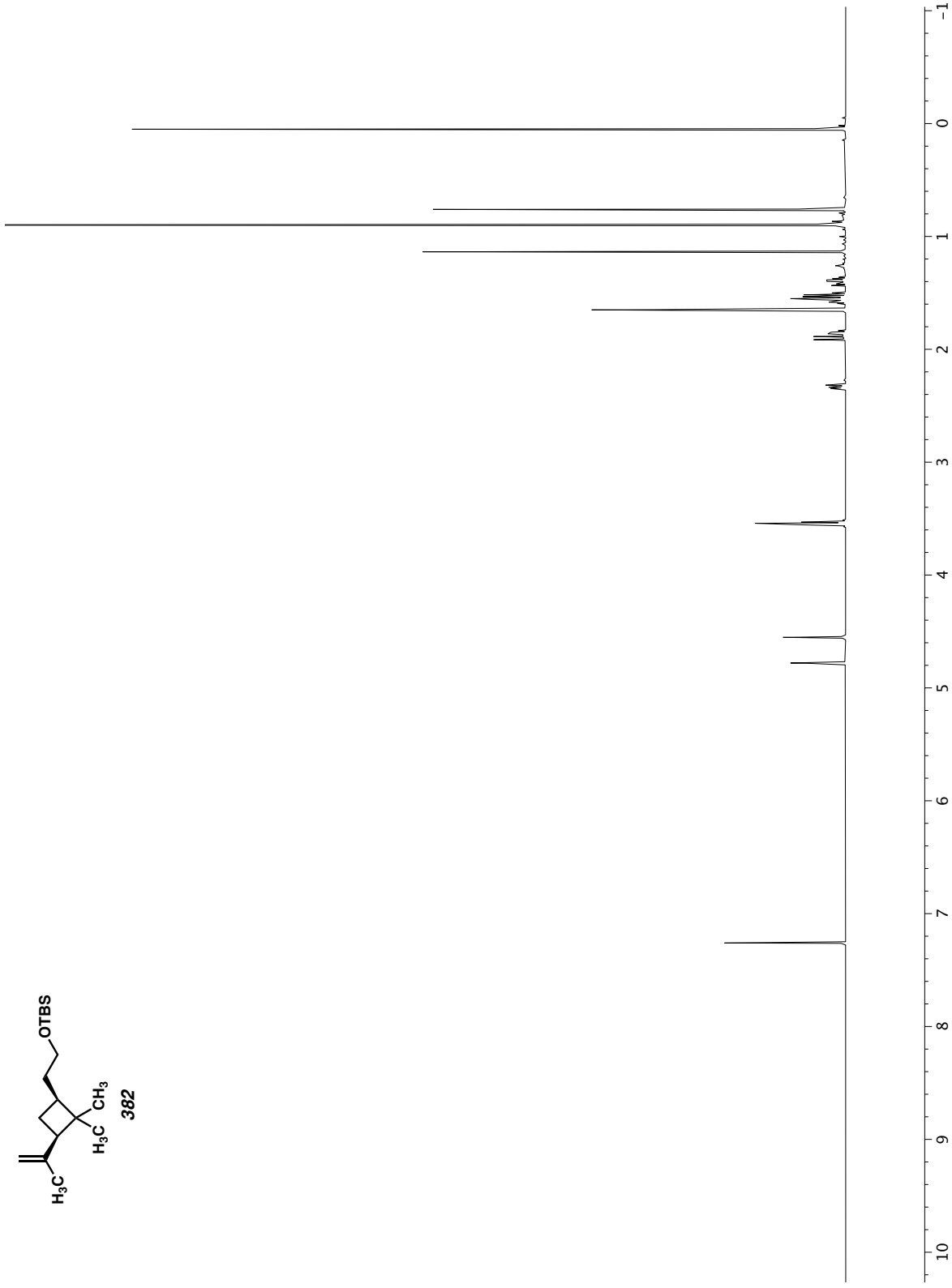


Figure A11.49. ^{1}H NMR (400 MHz, $CDCl_3$) of compound **382**.

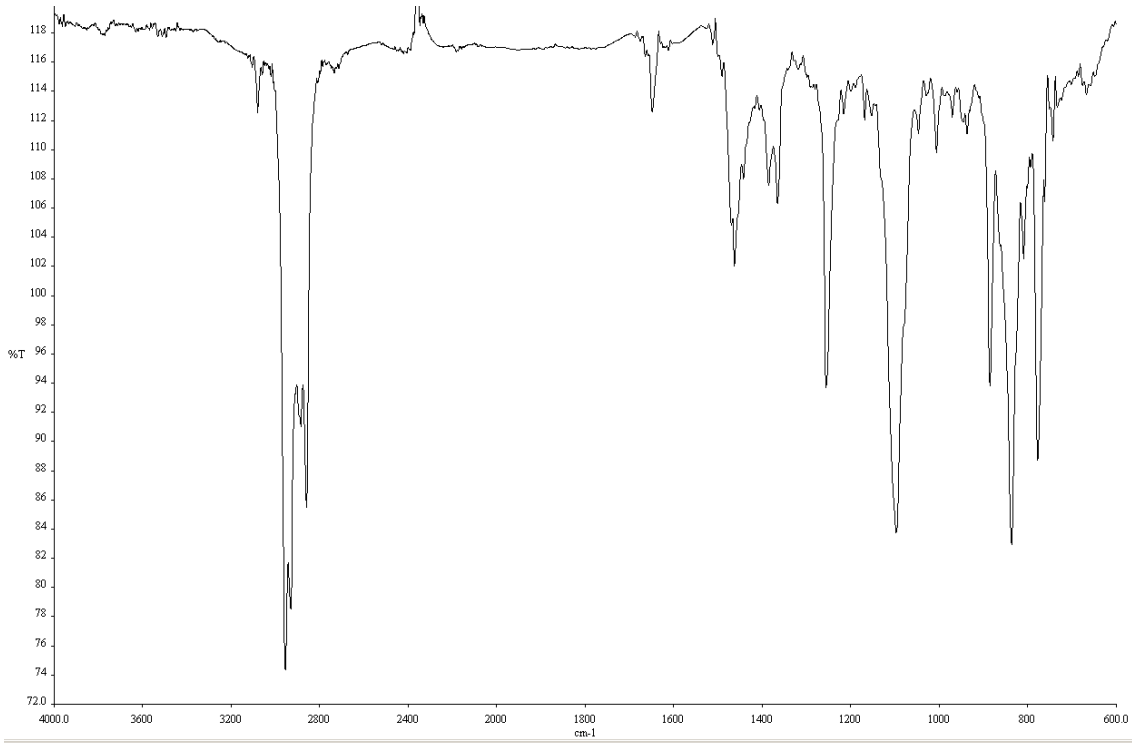


Figure A11.50. Infrared spectrum (Thin Film, NaCl) of compound **382**.

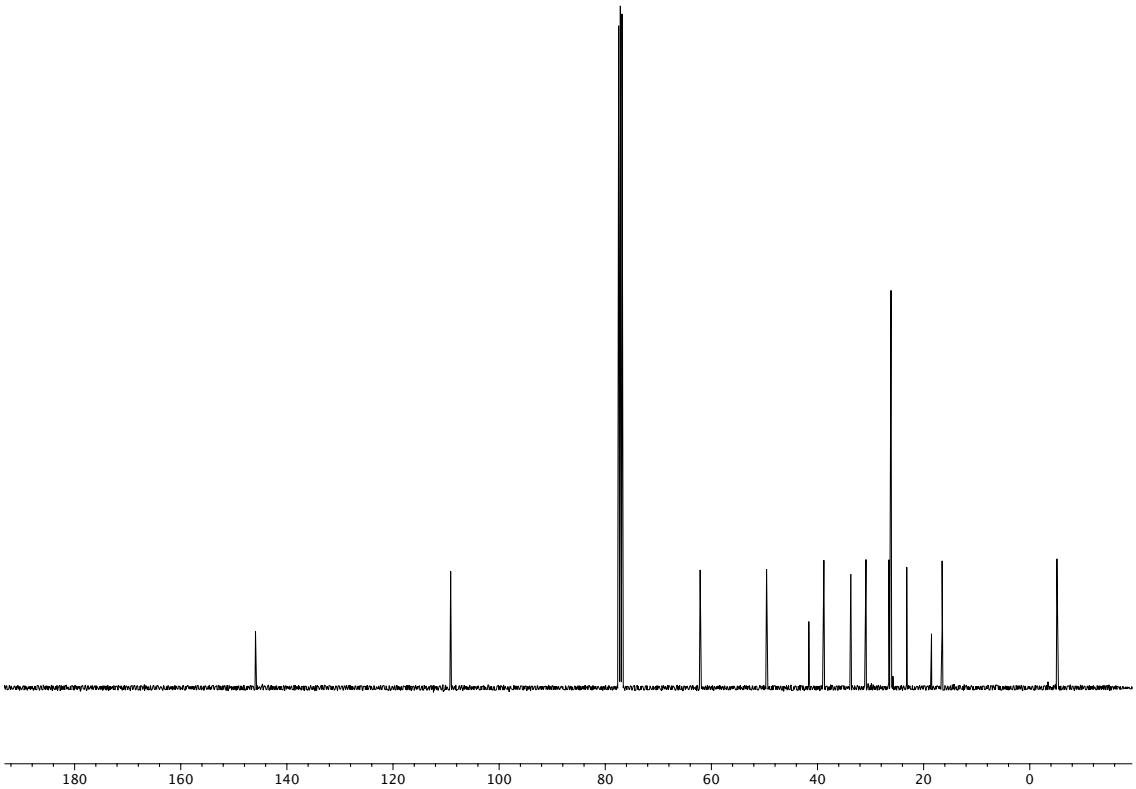


Figure A11.51. ^{13}C NMR (100 MHz, $CDCl_3$) of compound **382**.

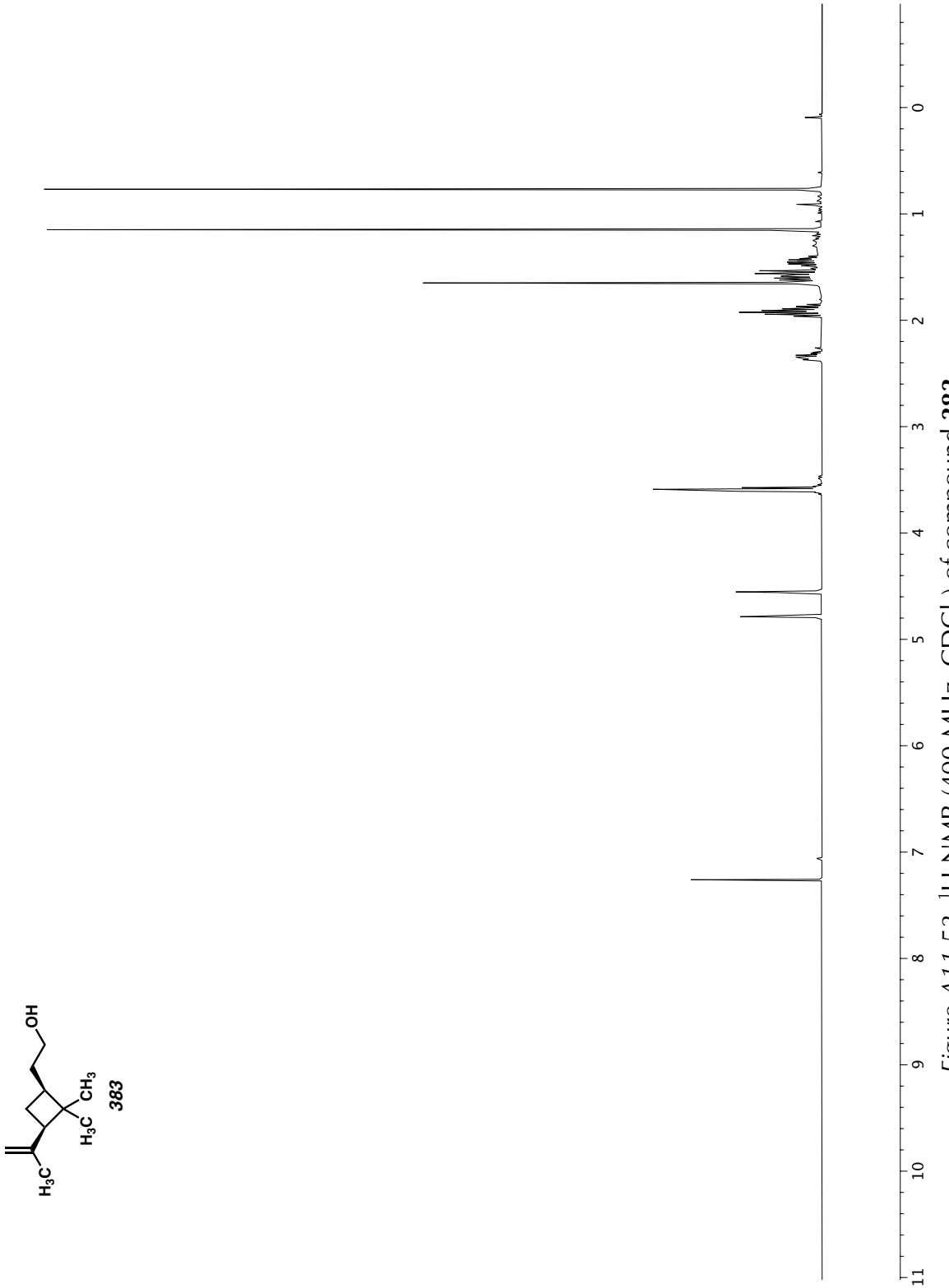


Figure A11.52. ^{1}H NMR (400 MHz, $CDCl_3$) of compound **383**.

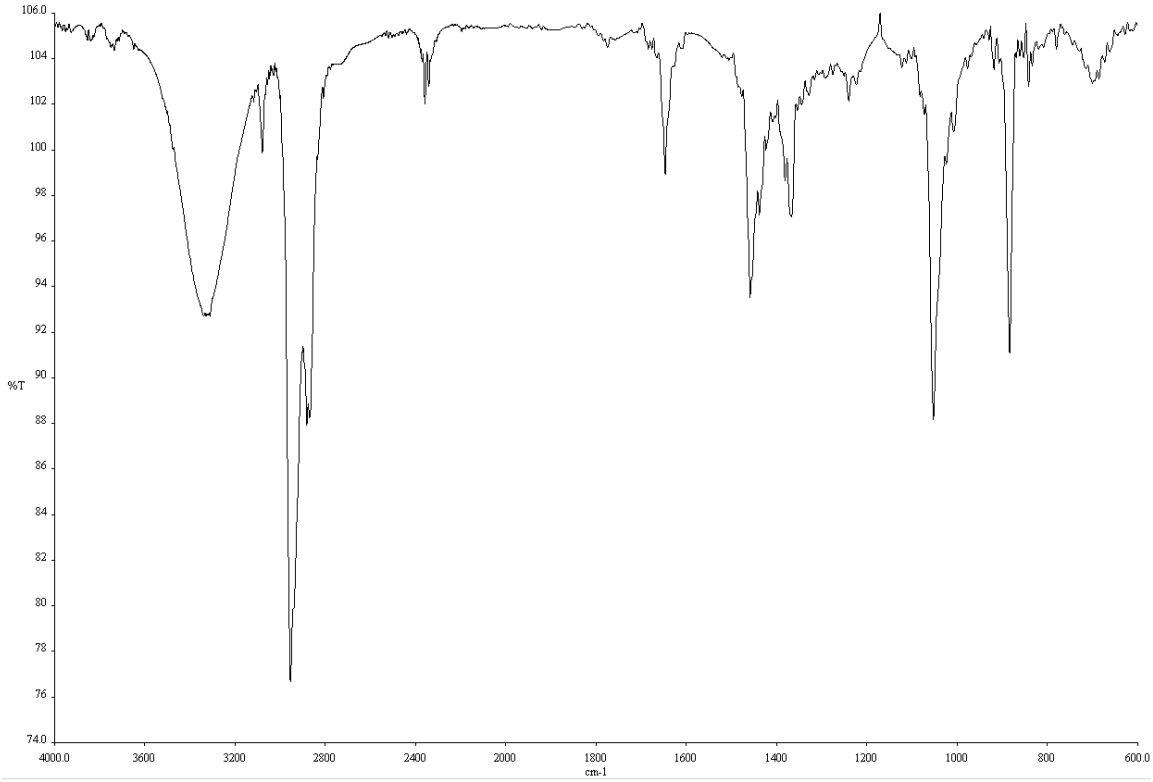


Figure A11.53. Infrared spectrum (Thin Film, NaCl) of compound **383**.

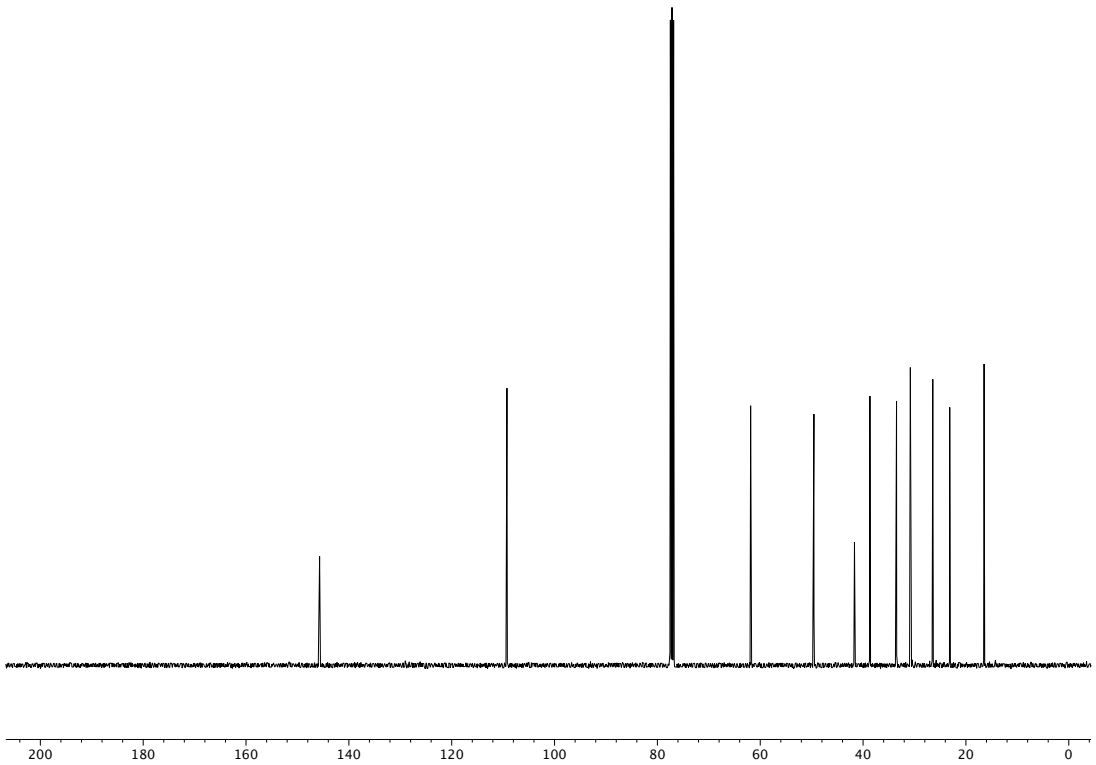


Figure A11.54. ^{13}C NMR (100 MHz, $CDCl_3$) of compound **383**.

ABOUT THE AUTHOR

Samir Peter Rezgui was born to Leslie Pfieffer and Mohammed Ali Rezgui in Paris, France in 1998. Two months after his birth, his parents, and older brother Alexander, moved him to Colorado Springs, Colorado, where he was raised. He attended Rampart high school in Colorado Springs, from which he graduated in 2016. Throughout his adolescence and and early young adult years, Samir's main focus was athletics; one of Samir's main sports was boxing, in which he was trained by his father Ali beginning at the age of two.

He then moved to Denver, Colorado in 2016, where he attended the University of Denver, initially as an international business major. However, at the beginning of college, he decided to instead pursue a pre-med track. In his first year, Samir excelled in his chemistry classes— perhaps the first time he was truly engaged in an academic subject. At this point, Samir switched his major to chemistry and at the end of his freshman year joined the atmospheric chemistry lab of Prof. Alex Huffman, where he studied pollen classification using a single particle fluorescence spectroscopy technique. Samir became deeply interested in organic chemistry after taking the first sophomore organic chemistry course, largely thanks to Prof. Verl. At the end of his sophomore year, Samir joined the lab of Prof. Brian Michel, where he synthesized olefin metathesis-based fluorescent probes for the selective detection of ethylene in live cells. Prof. Alex Huffman and Prof. Brian Michel were the main motivators for Samir to continue the study or organic synthesis in graduate school after completing his bachelor's degree in 2020.

In the summer of 2020, Samir moved to Pasadena to pursue graduate studies at the California Institute of Technology under the guidance of Prof. Brian Stoltz. In the Stoltz group, he has focused on natural product synthesis, particularly the total synthesis of pyrroloiminoquinone

alkaloids. In August of 2025, Samir will begin his professional career as a process chemist at Gilead in San Francisco and will be joined in the move by his girlfriend Sydney, who is pursuing a masters in social work at San Jose State University.